AD NUMBER

ADB002822

LIMITATION CHANGES

TO:

Approved for public release; distribution is unlimited.

FROM:

Distribution authorized to U.S. Gov't. agencies only; Test and Evaluation; JUL 1974. Other requests shall be referred to Air Force Flight Dynamics Laboratory, Attn: FBS, Wright-Patterson AFB, OH 45433.

AUTHORITY

AFFDL per DTIC form 55

AFML-TR-74-179
AFFDL-TR-74-106

WELDBOND FLIGHT COMPONENT DESIGN/MANUFACTURING PROGRAM

Lockheed-Georgia Company

TECHNICAL REPORT AFML-TR-74-179
TECHNICAL REPORT AFFDL-TR-74-106
DECEMBER 1974

Air Force Flight Dynamics Laboratory
and
Air Force Materials Laboratory
Air Force Systems Command
Wright-Patterson Air Force Base, Ohio 45433

NOTICE

When Government drawings, specifications, or other data are used for any purpose other than in connection with a definitely related Government procurement operation, the United States Government thereby incurs no responsibility nor any obligation whatsoever; and the fact that the government may have formulated, furnished, or in any way supplied the said drawings, specifications, or other data, is not to be regarded by implication or otherwise as in any manner licensing the holder or any other person or corporation, or conveying any rights or permission to manufacture, use, or sell any patented invention that may in any way be related thereto.

Copies of this report should not be returned unless return is required by security considerations, contractual obligations, or notice on a specific document.

WELDBOND FLIGHT COMPONENT DESIGN/MANUFACTURING PROGRAM

J.J. GROSKO
J.A. KIZER

FOREWORD

This Final Technical Report was prepared by Lockheed-Georgia Company, a Division of Lockheed Aircraft Corporation, Marietta, Georgia, under contract No. F33615-71-C-1716, entitled "Weldbond Flight Component Design/Manufacturing Program". The report presents results of the contract during the period from July 1971 through July 1974. The contract work consisted of development of an optimized weldbond process to installation of a weldbonded fuselage component on an operational C-130 aircraft for flight demonstration and evaluation. The contract was accomplished in five tasks and was conducted under co-sponsorship of the Air Force Flight Dynamics Laboratory and the Air Force Materials Laboratory, Wright-Patterson Air Force Base, Ohio. Work was initiated under AFFDL Project 1368, Task 136802 and AFML Project 834-1. Installation of the weldbonded fuselage component on a C-130H aircraft was accomplished through an engineering change proposal approved by the C-130 Systems Project Office, Aeronautical Systems Division, Wright-Patterson Air Force Base, Ohio.

Mr. Fred R. Miller (AFML/LTM) was the Air Force Materials Laboratory Project Manager and Mr. Charles L. Ramsey (AFFDL/FBS) was the Air Force Flight Dynamics Laboratory Project Manager. Mr. J. A. Kizer was the Lockheed-Georgia Program Manager.

Major contributions to the developmental efforts described herein were provided by the following Lockheed-Georgia Company personnel:

Associate Program Manager: and Analysis of Test Data	J. J. Grosko
Surface Treatment Development:	Dr. R. N. Miller
Materials and Processes:	G. E. Davis J.C. Tomlinson
Manufacturing/Fabrication:	D. Fields M. Foston
Quality Assurance:	W. H. Thompson
Design and Analysis:	J. H. Brown S. K. Brown V. F. Gardener R. C. Reynolds
Structural Testing:	G. J. Gilbert H. F. Ortwein

Automated Application: Methods and Cost Analysis	K. M. Barre'
Sonic Fatigue Development:	H. W. Bartel
Internal Joint Stress Analysis:	R. F. Wilkinson

The Lockheed-Georgia Company report identification for this AFFDL/AFML Document is LG74ER0178.

This report was submitted by the authors on 20 December, 1974.

This technical report has been reviewed and is approved for publication.

C. L. Ramsey

Charles Ramsey
Proj. Engr., Structural Dev. Branch
Structures Division

Frederick Miller

Frederick Miller
Proj. Engr., Metals Branch
Manufacturing Technology Division

Francis J. Janik, Jr., Chief
Structural Development Branch
Structures Division
Air Force Flight Dynamics Laboratory

H. A. Johnson, Chief
Metals Branch
Manufacturing Technology Division
Air Force Materials Laboratory

ABSTRACT

This report describes the weldbond process developments, component analyses, and tests that led to the design and manufacture of a C-130H weldbonded fuselage component. The weldbonded fuselage component was installed on C-130H Serial No. AF73-01592 for flight evaluation. This development program was accomplished in five tasks; namely, process development, engineering data development and component design, component fabrication, structural testing and qualification, and component installation. During the course of the program, fourteen surface preparations and seventeen candidate adhesives were evaluated for selection of the weldbond process used in fabrication of the test specimens, test components, and the flight component. Weldbonded elemental specimens and sub-scale components were fabricated and tested for static strength, fatigue strength, strength after environmental exposures, crippling strength, shear and compression stability, and sonic fatigue. In addition, a full-scale weldbonded fuselage component assembled into a test specimen in conjunction with two standard production fuselage components was comparative strength tested. Also, nondestructive inspection methods for weldbonded joints and cost data were developed.

TABLE OF CONTENTS

TABLE OF CONTENTS (Cont'd)

TABLE OF CONTENTS (Cont'd)

TABLE OF CONTENTS (Cont'd)

TABLE OF CONTENTS (Cont'd)

TABLE OF CONTENTS (Cont'd)

LIST OF FIGURES

LIST OF FIGURES (Cont'd)

LIST OF FIGURES (Cont'd)

LIST OF FIGURES (Cont'd)

LIST OF FIGURES (Cont'd)

LIST OF FIGURES (Cont'd)

LIST OF FIGURES (Cont'd)

LIST OF FIGURES (Cont'd)

LIST OF FIGURES (Cont'd)

LIST OF FIGURES (Cont'd)

LIST OF TABLES

LIST OF TABLES (Cont'd)

LIST OF TABLES (Cont'd)

LIST OF TABLES (Cont'd)

SUMMARY

The Weldbond Flight Component Design/Manufacturing development program conducted by the Lockheed-Georgia Company for the Air Force under Contract F33615-71-C-1716, has demonstrated that the weldbond process can be applied effectively in the design and fabrication of primary aircraft structural components. The program constituted the first application of the weldbond process in the design and fabrication of a major (approximately 9 feet by 10 feet) primary fuselage component.

The major program goals have been achieved. Static and fatigue tests in conjunction with theoretical analyses have demonstrated adequate structural integrity and endurance for evaluation of the weldbonded fuselage component in an operational aircraft. Compressive stability, shear stability, and sonic fatigue tests of sub-scale weldbonded components have given results that are equivalent to or better than comparable riveted component tests.

This development program included the design, fabrication and test of a C-130 weldbonded fuselage component, and the fabrication and installation of a second weldbonded fuselage for installation on a production C-130H aircraft. Installation of the weldbonded fuselage component was accomplished by modification of a larger production fuselage side panel followed by installation of the modified fuselage side panel on the C-130 production line. The modified fuselage side panel was installed on C-130H serial number 4557.

During the course of the program, several tasks were accomplished in support of the design of the C-130 weldbonded fuselage components. These tasks included preparation of materials and process specifications, engineering design data including static and fatigue joint strengths, development of internal joint stress distributions, and cost comparison investigations. In the early portion of the program, efforts were directed toward development of an optimum weldbond process which would satisfy weldability, corrosion, and mechanical property requirements. Those efforts culminated in the selection of an epoxy paste adhesive applied to a spot-weld etch prepared aluminum alloy. During the process development tasks, various adhesive forms, surface preparation processes, and adhesive application methods were evaluated.

Several inspection techniques were investigated for use in inspection of weldbonded joints. The basic techniques investigated were radiography for the spot-welds and ultrasonics for the adhesive bondlines. It was demonstrated that TV x-rays could be applied in a production environment for rapid assessment of spot-weld quality in weldbonded joints and contact ultrasonics was the best inspection technique for the adhesive bondlines.

The successful completion of this program has demonstrated that the weldbond process can be applied in the design and fabrication of selected airframe assemblies for operational military aircraft. The following conclusions can be drawn.

- o Adequate structural design data are available for weldbonded structures having adherends thicknesses varying from 0.020 inches to 0.090 inches.
- o Fabrication costs are competitive with automatic riveting and significant savings can be realized over adhesive bonding and hand riveting.
- o Production applications can be achieved and schedule milestones accomplished.
- o Sealing of joints is automatically achieved in weldbonded joints while in mechanically fastened joints sealing is an additional operation.
- o Adherend stresses in weldbonded joints are lower and more uniform than comparable spot-welded or mechanically fastened joints.
- o Weldbonding also provides a human factor advantage over drilling and riveting operations in a production facility because of the much lesser noise levels.

This report summarizes the work accomplished under Contract F33615-71-C-1716 during the period from July 1971 to July 1974.

SECTION I

INTRODUCTION AND BACKGROUND

1.1. Introduction

Resistance spot-welding has long been recognized as a means of low-cost metal joining. In addition to being a readily automated process, this joining method eliminates valuable small parts procurement and inventory attendant to conventional fastening methods. However, its relatively poor joint fatigue characteristics have seriously limited its structural application. A modification of spot-welding, that was initially used in Europe and Russia, makes use of an adhesive in the joint through which the spot-welds are formed. This process has been termed "weldbond" and typically consists of a fabrication sequence involving part detail pre-fit and surface preparation, adhesive application to the faying surfaces, spot-welding through the uncured adhesive and adhesive cure. This process results in a joint exhibiting many of the load transfer advantages of adhesive bonded joints while reducing the fabrication costs incurred through the tooling requirements of bonded structure.

1.2 Background

Although originally conceived and applied by European and Russian aircraft fabricators, weldbond has been under evaluation as a metal joining process in this country since the middle 1960's. Developmental work conducted since that time has proceeded successfully through feasibility studies to establish weldbonding as a potentially reliable manufacturing process. This early work also established the potential structural advantages of weldbonding over conventional metal joining methods. Specifically, it was demonstrated that weldbonded joints show both high and low cycle fatigue endurance in excess of many fastening systems and static strength superior to most fastening systems. The fatigue and static strength of weldbond joints was shown significantly superior to spot-welded joints in this early development.

1.2.1 Program Overview

At this point, the further development of the weldbond joining method pointed in the direction of process refinement and possible improvement, the establishment of pertinent engineering data for weldbonding, and the development of weldbond-related non-destructive inspection (NDI) techniques. The final goal of these advancements was the actual design, fabrication, structural test, installation and planned in-service flight evaluation of a significant aircraft component using weldbonding as the primary joining medium. Related areas, such as weldbond cost projections and comparisons, weldbond joint internal stress

studies, potential adhesive application methods, and weldbond joint repair considerations were also considered essential to a complete understanding of the weldbond joining method. In order to accomplish these objectives, Lockheed-Georgia Company has performed a five (5) task program covering the above areas. This program addressed 2000 and 7000 series aluminum alloy and progressed generally through process development, the establishment of engineering data, NDI method development, and component design, fabrication, test and installation on an operational aircraft.

Initial efforts conducted under this contract were concerned primarily with the development of improved surface preparations and adhesives for weldbonding. The first step to this end was to conduct two concurrent evaluations – one involving a constant surface preparation and various adhesives and the other holding a constant adhesive while varying surface preparations – to initially screen candidate improvements. As candidate surface preparations and adhesives satisfied requirements during these studies, they were combined for further evaluation. The areas addressed during this testing were weld quality, initial bondline strength and bondline strength retention after exposure to aggressive environment. After adjustments necessitated by adaptations to production line facilities, the results of these evaluations were used during the remainder of the program. This was accomplished through material and process specifications generated under this contract. Although not implemented within this program, various automated adhesive application methods were studied and are discussed within this report.

The second task conducted under this program primarily addressed the generation of engineering design data and the C-130 fuselage panel design and stress analysis. A photograph showing the location and relative size of this component is shown in Figure I. Weldbond design data in the form of static and fatigue joint properties, engineering design limits, panel stability data and sonic fatigue properties were developed. These data concentrated on structure in the adherend thickness range 0.020" to 0.090". The C-130 fuselage panel was designed during this task to take advantage of weldbonding. Certain part configuration, attach point and spot-weld machine throat depth limitations restricted, to some degree, the full realization of weldbonding advantages. However, within these restrictions, weldbonding was effectively used on this panel. Stress analyses conducted during this task indicated all positive margins for the weldbonded fuselage panel. Internal weldbond joint stress analysis were conducted to provide a better understanding of the weld/adhesive bond roles in joint load transfer and to further substantiate weldbond fuselage joint designs.

The third task of this program covered the fabrication of the weldbond panel static test, fatigue test and flight evaluation articles. Qualification of these articles demanded the satisfaction of weldbond process specification requirements. This included non-destructive

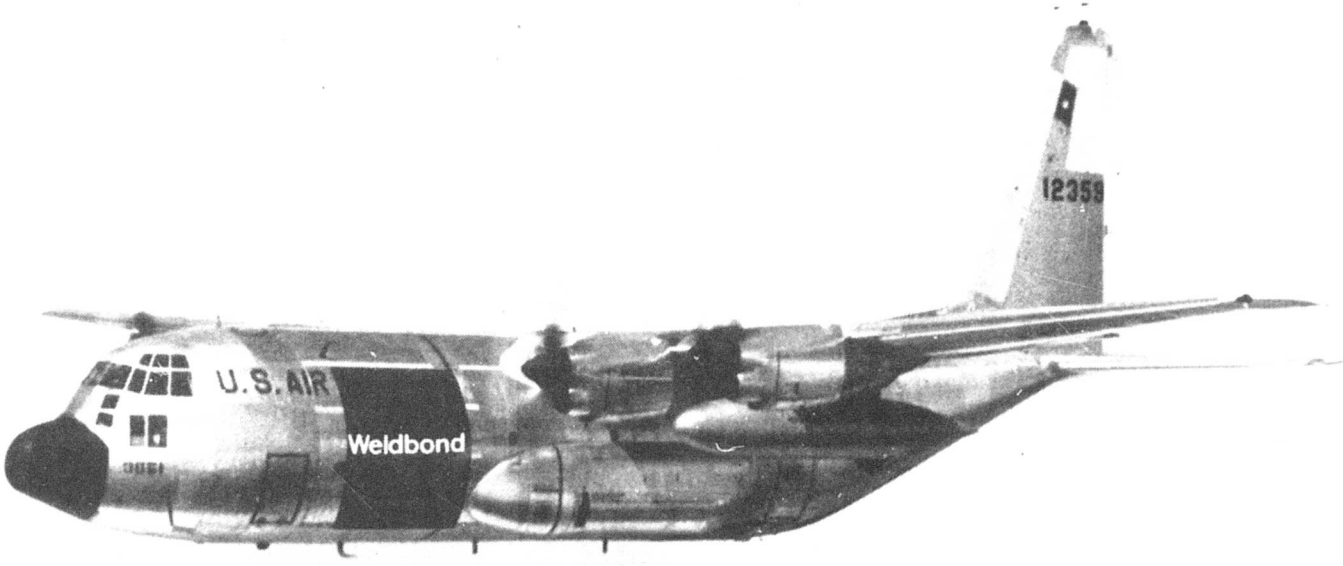

FIGURE 1 – WELDBOND COMPONENT LOCATION

inspection (NDI) of the weldbonded panels through the NDT methods assigned to weldbonded structure under this program. During this and previous tasks, cost analyses for weldbond fabrication and comparisons with riveted structure were performed. In addition, under this task, two (2) panels of conventional riveted construction were modified for use in the static test arrangement.

The next task involved the actual testing of the static and fatigue test articles. These tests were conducted to structurally qualify the flight evaluation panel for installation on an operational aircraft. Additional supporting internal weldbond joint stress analyses were conducted to substantiate the fatigue test arrangement and external loading.

The fifth and last task on this program addressed the development of a flight demonstration plan and the installation of the flight article on an operational C-130 aircraft. Included in the demonstration plan were repair procedures for weldbonded joints. The installation of the in-flight article concluded the program.

Lockheed-Georgia Company has successfully completed the five (5) task program outlined above. Details of the accomplishments of this program and insights into the weldbond process gained through conducting these evaluations are given in the following sections.

SECTION II

WELDBOND PROCESS DEVELOPMENT

2.1 Adhesive Evaluations

Four[4] general forms of modified epoxy adhesive were investigated under this contract. These were semisolid bulk, paste, liquid and powder adhesives. The bulk systems were actually tested in an unsupported film form to approximate the final adhesive state, prior to welding and bonding, in a hot spread adhesive application sequence for weldbonding. In addition, with the intention of later combining them with adhesive systems, liquid primer systems were included in the early sequences of this testing. A summary of systems evaluated for weldbonding under this contract along with their suppliers and form is tabulated in Table I. All initial adhesive evaluations were performed using the standard spot-weld etch surface preparation for bare aluminum alloys (See Table I).

2.1.1 Initial Weld Strength Tests-Adhesives

For three of these systems – semisolid bulk, paste and powder –, the initial evaluation performed was a weld feasibility check. Candidate adhesive primer systems were also checked for welding compatibility. This was conducted by cleaning the adherend surface and applying the adhesive or primer and then welding a six-specimen panel. Upon apparent successful welding, these specimens were tested, with the adhesive uncured, in the conventional tensile shear mode and visually inspected after test. The liquid adhesive systems were considered only for the capillary adhesive application technique in which the adhesive is applied to the joint after welding. Therefore, no weld tests were conducted on liquid systems.

The results of these weld tests showed that the powdered system, both with and without primer, was unweldable, as no welds could be formed through this system. The unsupported films, representing the semi-solid bulk systems, were weldable but only after application of local heat to flow the adhesive in the weld area. The paste systems were found to be weldable as applied. The results of the weld strength tests for paste systems ranged from 715 pounds to 1020 pounds while the results from room temperature tests on the unsupported films, heated for welding, ranged from 910 pounds to 1085 pounds. On visual inspection of the failed unsupported film weld test specimens, bond failures indicating a contribution from the adhesive toward specimen strength were found. Since the objective of these tests was to isolate and assess the weld, further tests above the adhesive flow temperature were conducted at 200°F. This reduced the indicated weld strength range to 730-760 pounds and eliminated the significant adhesive strength contribution.

TABLE I – SUMMARY OF ADHESIVE SYSTEMS

SYSTEM	SUPPLIER	FORM
XA3435	3M Company	Paste
XA3435 with XC3924	3M Company	Paste with Primer
M6800	Whittaker Corp.	Paste
A1340B	B.F. Goodrich	Paste
CS4742	B.F. Goodrich	Paste
CS4740	B.F. Goodrich	Paste (high viscosity)
A1357B	B.F. Goodrich	Unsupported Film (.045 psf)
XB66	3M Company	Unsupported Film (.030 psf)
XB66	3M Company	Unsupported Film (.045 psf)
XB66	3M Company	Unsupported Film (.060 psf)
XB66 with XC3924	3M Company	Unsupported Film (.060 psf) with Primer
XC3700	3M Company	Powder
XC3700 with XC3924	3M Company	Powder with Primer
ADX-59	Hysol	Liquid
PA3921	3M Company	Liquid Primer
0500PE28	B.F. Goodrich	Liquid Primer

The two corrosion inhibiting primer systems listed in Table I were also checked for weld process compatibility. Welding through one of these (PA3921) produced low strength, non-uniform weld nuggets and caused primer wash-out in the nugget area. It was dropped from further consideration. The second of these (0500PE28) was indicated to be compatible with welding operation exhibiting weld strength of from 855 pounds to 930 pounds. This system was retained on a welding compatibility basis but subsequently dropped when further corrosion resistance evaluations conducted by the supplier showed no significant advantage to the inclusion of this system.

2.1.2 Adhesive Bond Strength Tests

Out of a total of fifteen (15) initial systems evaluated for weld quality, seven (7) candidates were retained for further evaluation of adhesive properties. Tests specimens used to evaluate each system included both "adhesive only" and weldbonded coupons. As mentioned earlier, "adhesive only" coupons were machined from weldbonded test panels by eliminating the spot-welds from the test section. The test specimens and conditions included in this evaluation were:

(1) "Adhesive only" lap shear specimens with overlaps of one inch tested at -67°F, room temperature and 160°F,

(2) "Adhesive only" lap shear specimens with overlaps of two inches tested at -67°F and room temperature,

(3) Weldbonded lap shear specimens with overlaps of one inch tested at room temperature and 160°F,

(4) "Adhesive only" lap shear specimens with overlaps of one inch tested for creep rupture at room temperature and 160°F, and

(5) "Adhesive only" metal-to-metal peel specimens tested at -67°F, room temperature and 160°F.

The seven (7) adhesive systems retained from weld feasibility checks are listed below:

(1) Unsupported film (.045 psf) A1357B (B.F. Goodrich)

(2) Unsupported film (.030 psf) XB66 (3M Company)

(3) Paste XA3435 (3M Company)

(4) Paste XA3435 with primer XC3924 (3M Company)

(5) Paste M6800 (Whittaker Corporation)

(6) Paste A1340B (B.F. Goodrich)

(7) Paste CS4742 (B.F. Goodrich)

The eighth and last system under evaluation at this time in the program was the liquid adhesive (ADX-59) intended for the capillary adhesive application technique. Under evaluation, this system exhibited unacceptable handling characteristics which resulted in its elimination from the program early in the adhesive evaluation. It was found, however, that one of the seven (7) above systems, CS4742, could be used as a capillary application system. As a result, some tests were conducted on both chromic anodized and non-anodized surfaces with this adhesive applied through the capillary method.

Test panels were fabricated using 7075-76 bare aluminum alloy sheets. After surface treatment, each adhesive system was hand applied to its panel details and then welded with its established weld schedule. The capillary application candidate adhesive was also applied subsequent to spot-welding. The adhesives were all cured for 60 minutes minimum at 250 ± 10°F. After the panels were cured, test specimens were then machined from the panels and tested in accordance with their prescribed schedule. The results of these tests are shown in Figure 2 through Figure 8 and in Tables II, III, and IV. Based on the data generated from adhesive mechanical property tests, three (3) of the above seven (7) systems were eliminated leaving the following systems:

(a) Whittaker Corp. – M6800 Adhesive
(b) B.F. Goodrich – A1357B Adhesive
(c) 3M – XB66 Adhesive
(d) B. F. Goodrich – CS 4742 Adhesive

This selection resulted in two semi-solid bulk (unsupported film) epoxy adhesive systems and two epoxy paste systems (one of which could be used in capillary applications) retained for further evaluation after combining these with improved surface preparations.

2.1.3 Adhesive Application Method Studies

Within the forms of epoxy adhesives evaluated, a variety of potential automated application methods were found to be possible. Specifically, the semi-solid bulk system may use a roller coater, may be extruded and spread over the bond area or may even be considered in a film form and employ a tape laying machine for adhesive application. Similarly, the paste systems may be applied through roller coating or the extrude/spread method and may also be applied through capillary action after welding. Electrostatic spray was considered as the applicable method for the powder adhesive system. Liquids were limited to application by post-welding capillary action.

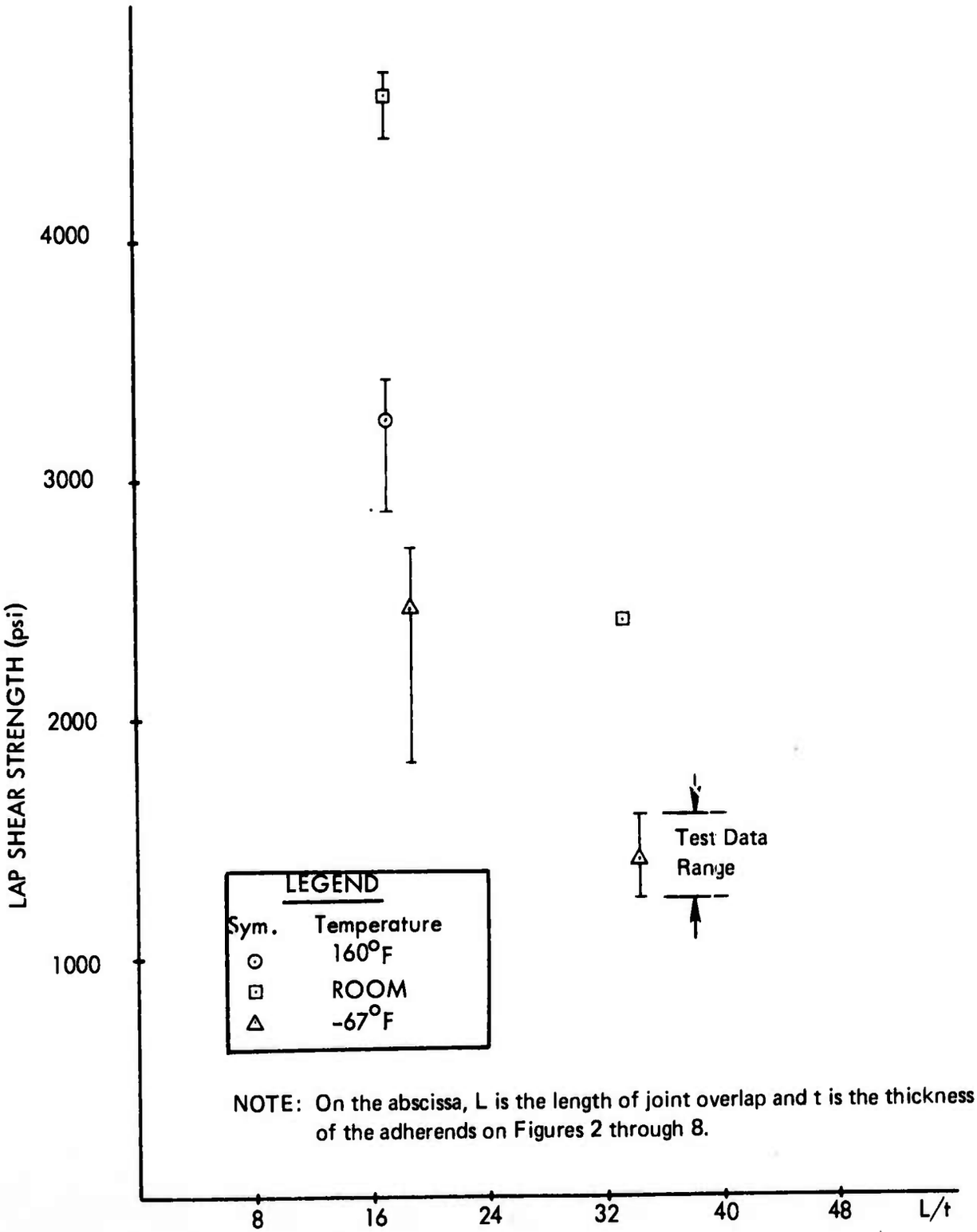

NOTE: On the abscissa, L is the length of joint overlap and t is the thickness of the adherends on Figures 2 through 8.

FIGURE 2 – LAP SHEAR STRENGTH VS L/t (A1357B ADHESIVE)

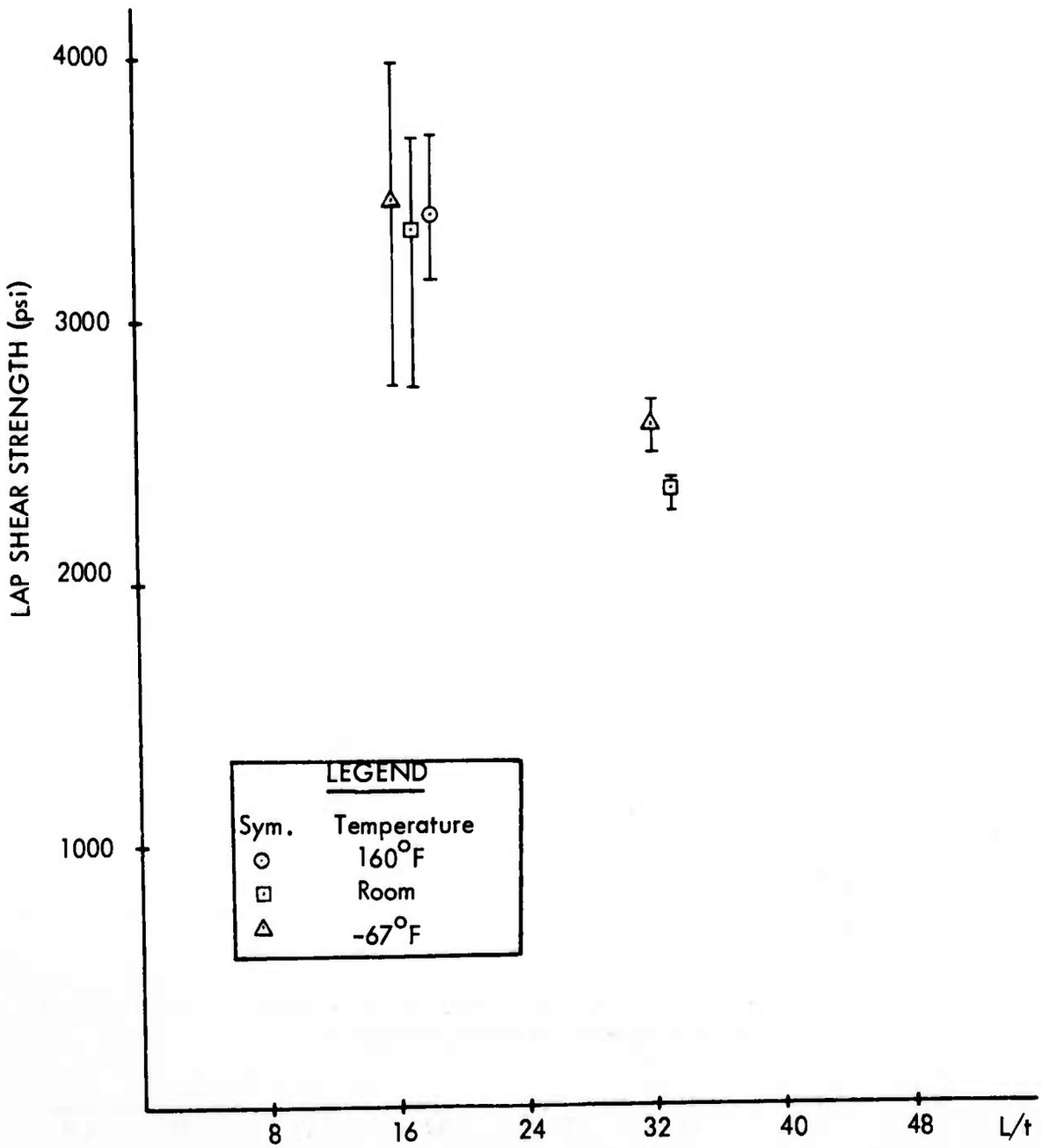

FIGURE 3 – LAP SHEAR STRENGTH VS L/t (XB66, 0.030 psf ADHESIVE)

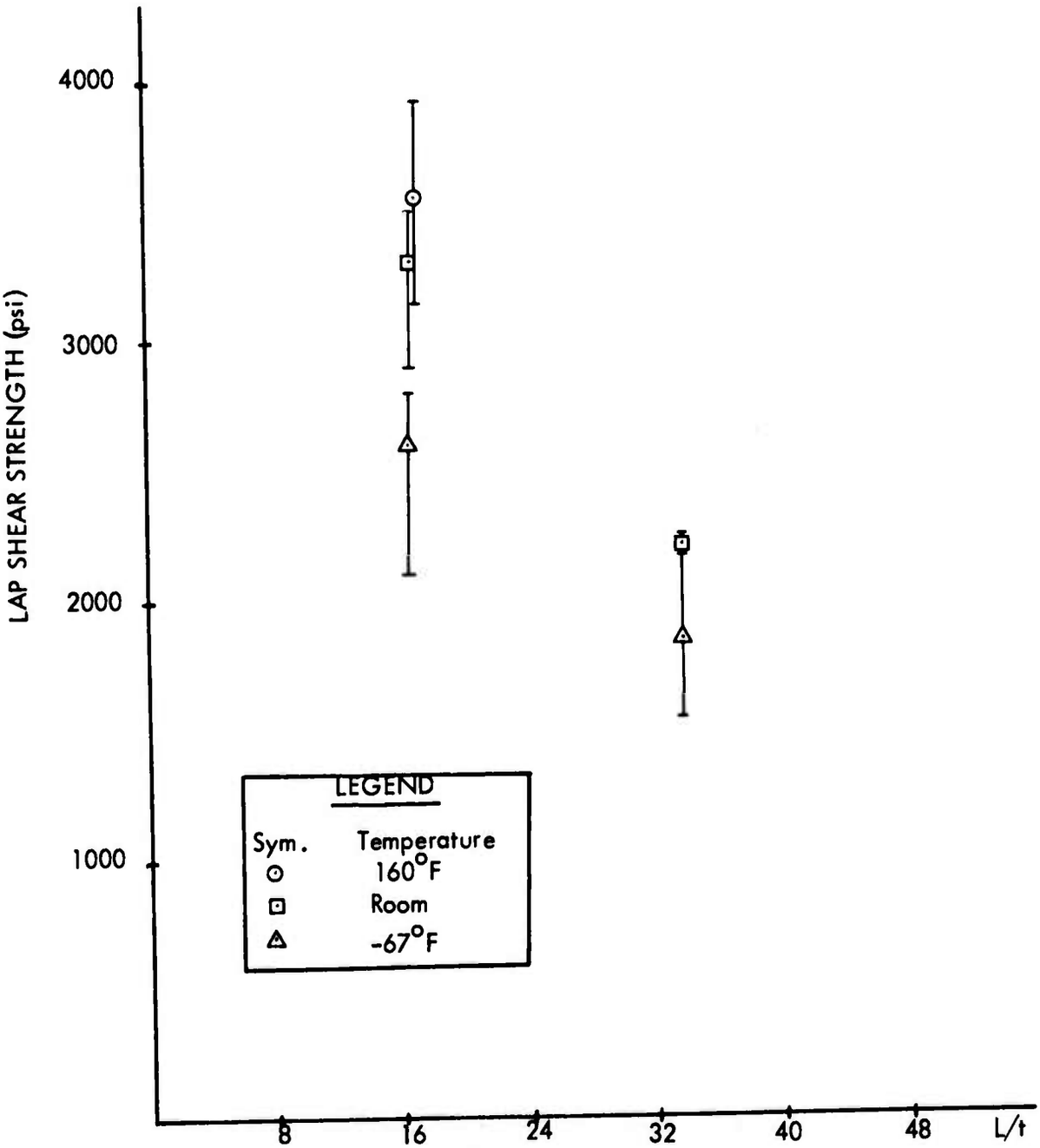

FIGURE 4 – LAP SHEAR STRENGTH VS L/t (XA3435 ADHESIVE)

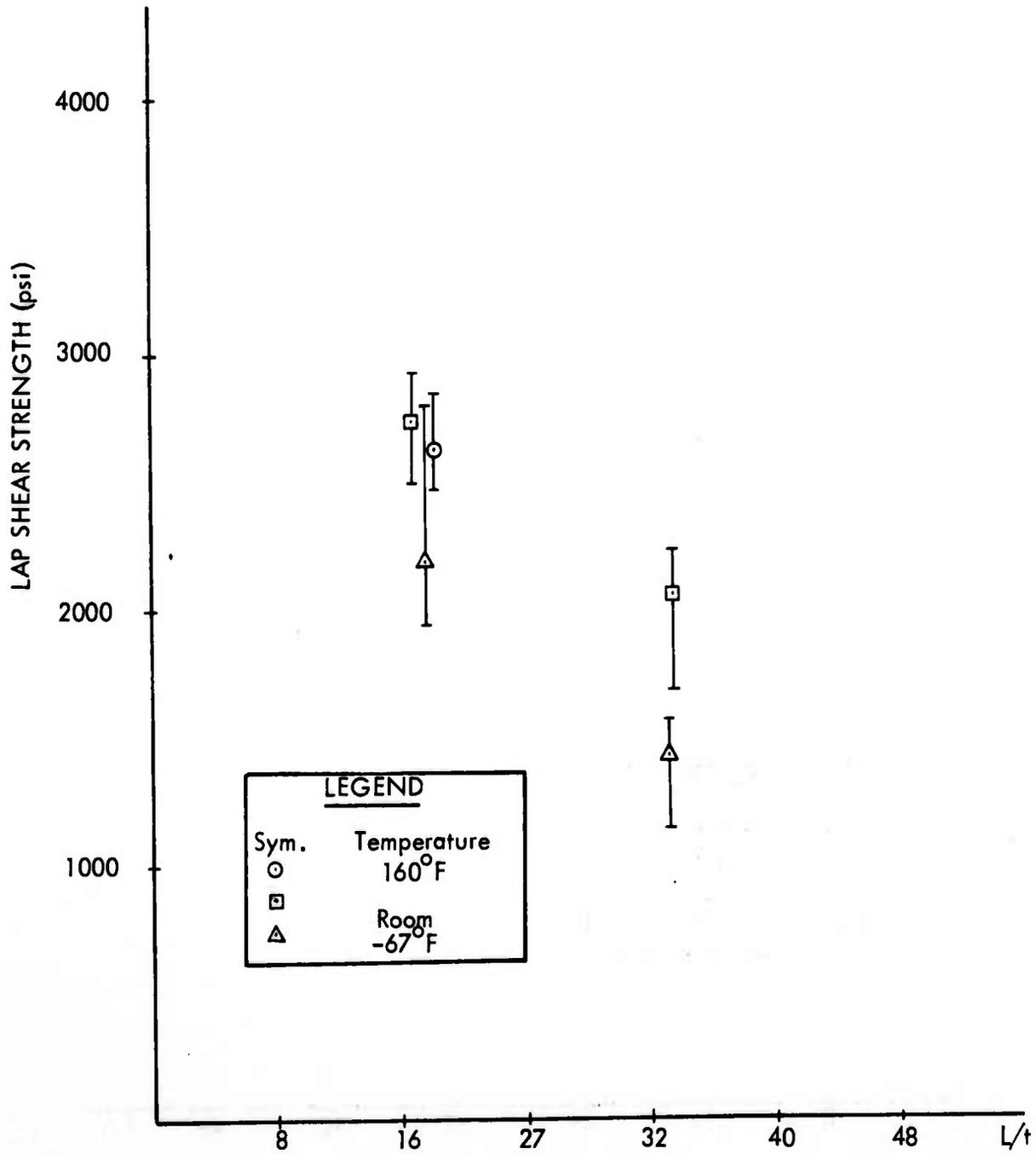

FIGURE 5 – LAP SHEAR STRENGTH VS L/t (XA3435 ADHESIVE WITH XC3924 PRIMER)

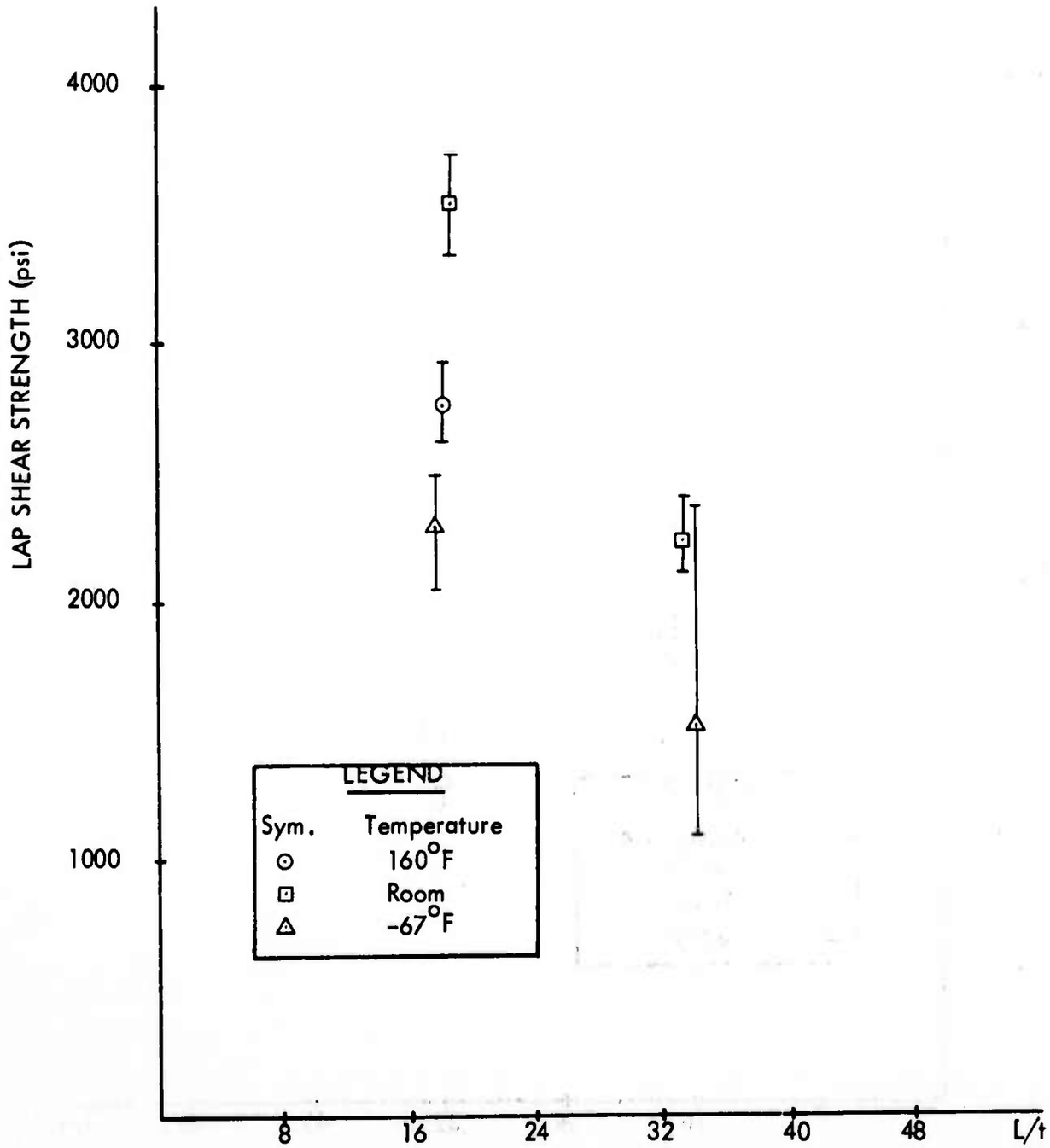

FIGURE 6 – LAP SHEAR STRENGTH VS L/t (X6800 ADHESIVE)

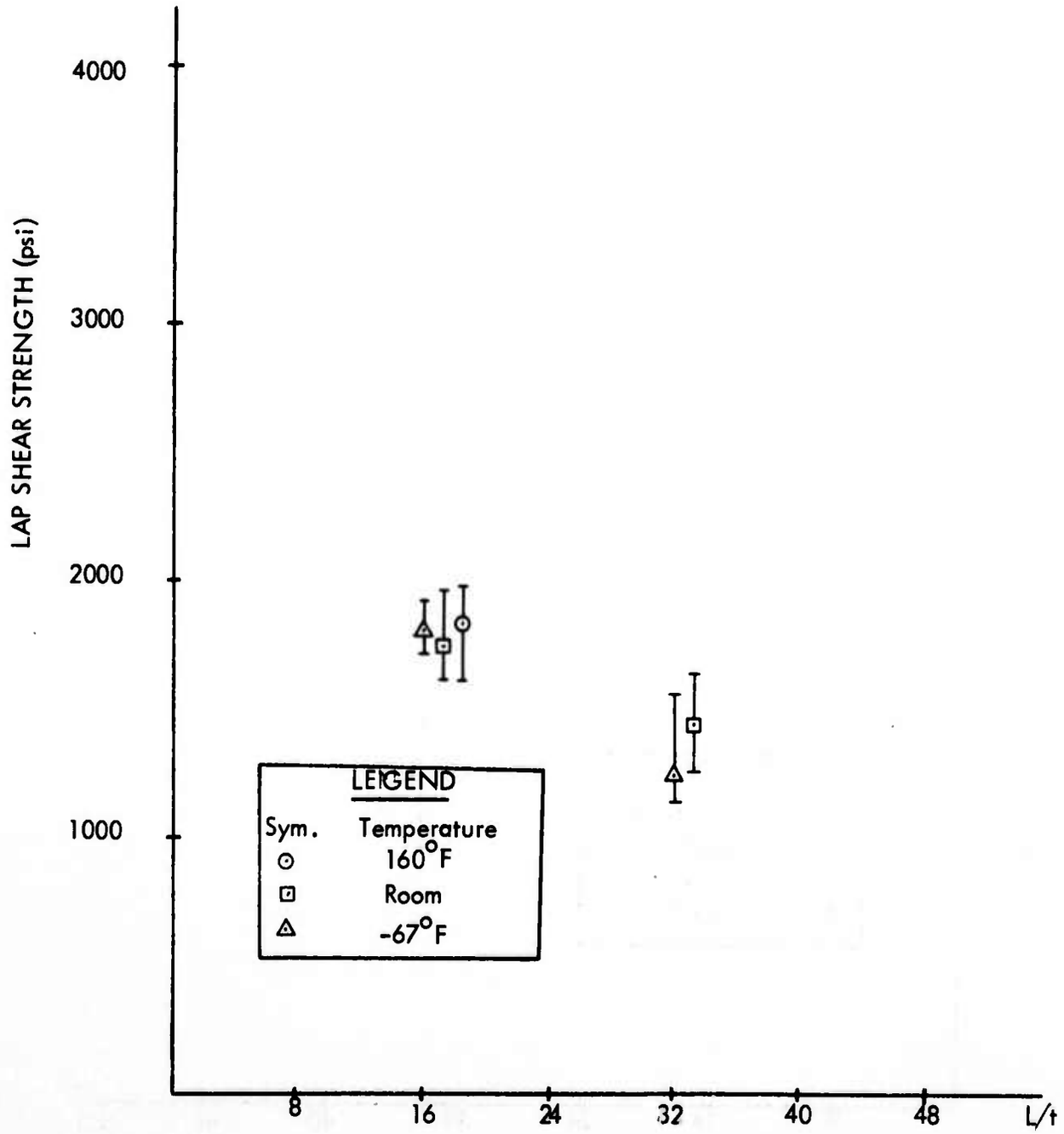

FIGURE 7 – LAP SHEAR STRENGTH VS L/t (A1340B ADHESIVE)

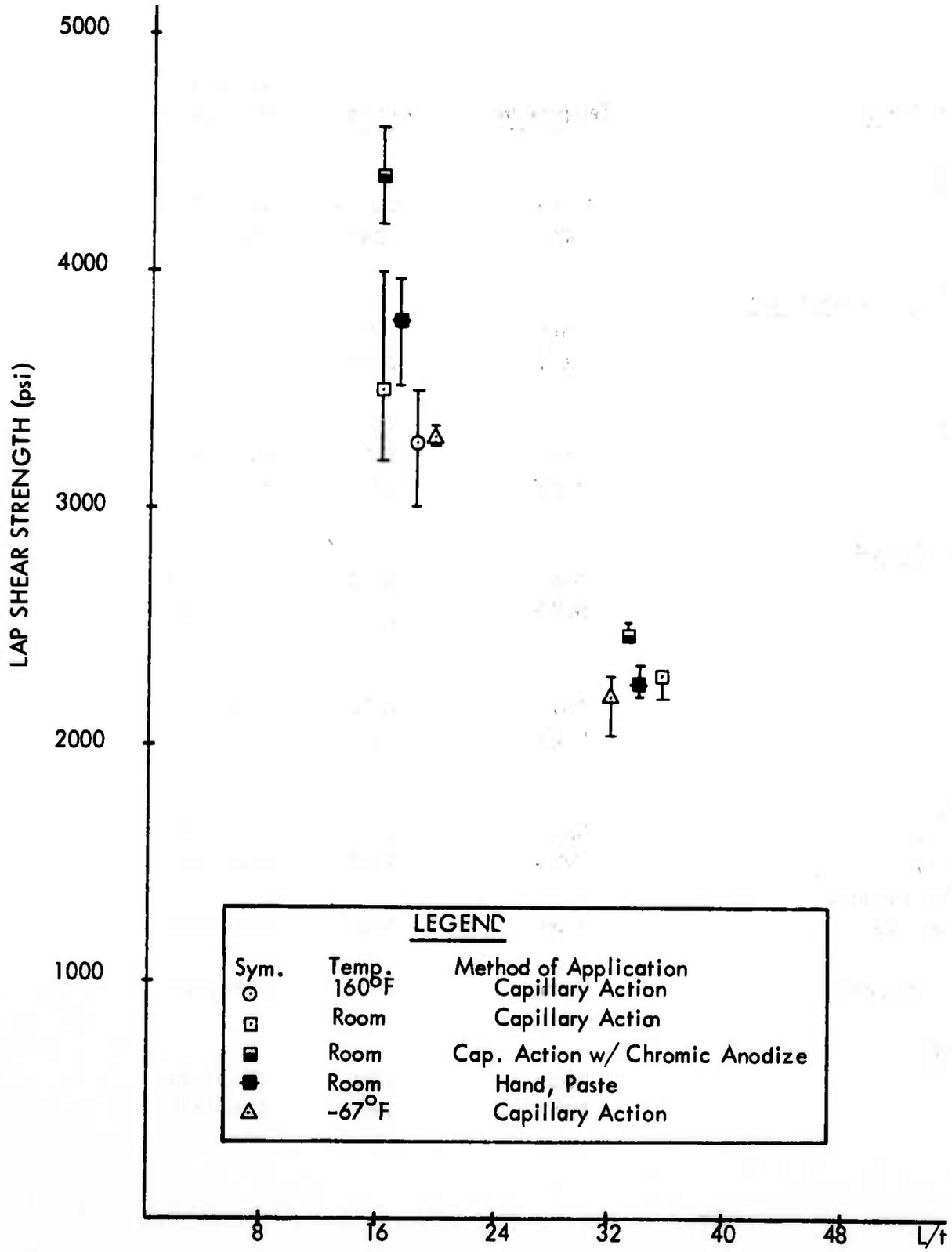

FIGURE 8 – LAP SHEAR STRENGTH VS L/t (CS4742 ADHESIVE)

TABLE II – WELDBOND TEST RESULTS – LAP SHEAR (psi)
(Adhesive Evaluation)

Adhesive Systems	Temperature	Average	Maximum/ Minimum
A1357B			
	Room	4600	4800/4500
	160°F	3850	4000/3740
XA3435 W/XC3924 Primer			
	Room	2800	2960/2570
	160°F	2090	2400/1620
XA3435			
	Room	3300	3600/3000
	160°F	3620	3840/3470
XB66, 0.030 psf			
	Room	4030	4330/3030
	160°F	3490	4100/2200
M6800			
	Room	2800	2900/2710
	160°F	3050	3400/2490
CS4742			
(Capillary)	Room	3300	3800/2700
(Capillary)	160°F	3100	3370/2850
(Capillary-Chromic Anodize)	Room	4300	4500/4100
(Hand Application)	Room	3500	3900/2200
A1340B			
	Room	1660	1880/1440
	160°F	1880	3300/1410

TABLE III – CREEP DATA (mils)

Adhesive Systems	Temperature	Average	Maximum/ Minimum
A 1357B			
	Room	0.4	0.6/0
	160°F	0.6	1.9/0.1
XA3435/XC3924 Primer			
	Room	0.6	1.0/0.5
	160°F	1.0	1.6/0.4
XA3435			
	Room	0.4	0.8/0
	160°F	0.3	0.6/0
XB66, 0.030 psf			
	Room	1.3	1.3/1.2
	160°F	0.7	1.1/0.4
M6800			
	Room	0.7	1.7/0.2
	160°F	0.7	1.5/0.2
CS4742 (Capillary)			
	Room	0.5	0.9/0
	160°F	1.0	2.0/0.4
A1340B			
	Room	0.4	0.5/0.4
	160°F	0.1	0.4/0

TABLE IV – METAL-TO-METAL PEEL TEST RESULTS (piw)

Adhesive Systems	Temperature	Average	Maximum/ Minimum
A1357B			
	-67°F	10.6	16.6/4.8
	Room	10.8	14.8/6.8
	160°F	9.6	10.4/8.6
XA3435 W/XC 3924 Primer			
	-67°F	5.1	6.9/2.7
	Room	5.5	6.6/4.8
	160°F	4.6	7.2/2.6
XA3435			
	-67°F	4.4	10.6/0.6
	Room	5.5	7.2/1.6
	160°F	5.4	7.3/4.4
XB66, 0.030 psf			
	-67°F	5.1	6.8/2.8
	Room	32.0	35.1/28.4
	160°F	15.8	23.0/5.1
X6800			
	-67°F	3.9	5.4/3.1
	Room	7.8	9.8/5.5
	160°F	10.6	14.6/7.8
CS4742			
(Capillary)	-67°F	6.3	7.7/3.8
(Capillary)	Room	14.0	17.6/8.8
(Capillary)	160°F	10.4	14.8/7.0
(Capillary—Chromic Anodize)	Room	29.1	32.1/24.6
(Hand Application)	Room	10.0	10.8/9.4
A1340B			
	-67°F	4.9	5.9/3.4
	Room	3.5	4.7/1.8
	160°F	3.9	5.6/2.4

For specific applications, such as long floor panels involving continuous bondlines, the automated roller coating and capillary action methods show some advantages. However, these are severely limited in the most common structural configurations, where stringer-rib-intersections, variable bondline widths and changes in joining media are frequent. For the purpose of selecting the most universal application method, the extrusion/spread method was isolated for further study. The electrostatic spray method involved powder adhesive systems was dropped from further consideration when the adhesive proved to be unweldable. Although not evaluated in detail as an automated method, the capillary application method for paste adhesives and the roller coating method and direct film lay-up for semi-solid bulk systems were considered logical alternatives for certain structural configurations. An optimum fabrication plan for weldbonding would probably use combinations of these methods.

The extrusion/spread application method may use either paste or hot spread adhesive. Extruding heads may dispense adhesive in a single bead or in several beads. The equipment would be stationary and part conveyance would be required. The extruding heads may be solonoid controlled to dispense and stop as desired. These would be heated for the hot spread systems. Varying bondline widths present some problems, but these can be overcome using tandem beads of varying widths. The applied adhesive beads would be followed by a hot "knife" or spreader to spread the beads into a full film coating. Currently available hot spread adhesive application systems demonstrate the feasibility of such a system. However, equipment capable of handling the structural adhesives under consideration, would have to be designed. Features such as cartridge loading, would be required to prevent over age of the adhesive at temperature, and to avoid major clean up problems of unused adhesive.

2.2 Surface Preparation Evaluation

Within the program, fourteen (14) surface treatments methods intended for the preparation of aluminum alloy for weldbonding were evaluated. As in the parallel adhesive evaluation under which the surface treatment was held constant, in order to minimize adhesive effects, a common adhesive was used throughout this initial testing. The adhesive used was EC2214 Hi-Flex (3M Company) epoxy paste which had been proved feasible for weldbonding under previous contracts. This evaluation proceeded through initial weld strength tests into adhesive bond strength determinations at low temperature and at room temperature after exposure to aggressive environments.

2.2.1 Candidate Surface Preparation Definitions

The fourteen (14) surface treatment methods evaluated for use in weldbonding are defined in Table V. The individual steps within these sequences are defined as follows:

TABLE V – CANDIDATE SURFACE PREPARATION SEQUENCES

(Time in Solution in Minutes)

SURFACE PREPARATION STEP	(01)- Spot-Weld Etch For Bare Aluminum Alloys	(02)- Metal Bond Etch For Bare and Clad Aluminum Alloys	(03)- Russian Surface Preparation Method (Reference	(04)- Modified Russian Surface Preparation Method	(05)- Spot-Weld Etch For Bare Aluminum Alloys With A-1100 Bath	(06)- Metal Bond Etch For Bare and Clad Aluminum Alloys With A-1100 Bath	(07)- Phosphoric Chromic Acid Etch With A-1100 Bath	(08)- Spot-Weld Etch For Clad Aluminum Alloys	(09)- Spot-Weld Etch For Clad Aluminum Alloys With A-1100 Bath	(10)- Chromic Acid Anodize After Welding Spot-Weld Etch For Bare Aluminum Alloys	(11)- Spot-Weld Etch For Bare Aluminum Alloys With L-10 Bath	(12)- Spot-Weld Etch For Clad Aluminum Alloys With L-10 Bath	(13)- Metal Bond Etch For Bare and Clad Aluminum Alloys With L-10 Bath	(14)- Metal Bond Etch For Bare and Clad Aluminum Alloys With L-10 Bath (Reduced Time)
Akaline Clean	15													
Spray Rinse	3-5													
Spot-Weld Acid Etch	3-5				3-5			10-20	10-20	3-5	3-5	10-20		
Metal Bond Etch		8-10				8-10							8-10	8-10
Nitric Acid Etch			60-90	10										
Phosphoric-Dischromate Etch			10											
Phosphoric-Chromic Acid Etch							8-10							
Spray Rinse	3-5				3-5	3-5	3-5		3-5	3-5	3-5	3-5	3-5	3-5
Akaline Etch	5-10			8-10	5-10					5-10	5-10			
Nitric Acid Etch				5										
Spray Rinse	3-5			3-5	3-5					3-5	3-5			
Spot-Weld Acid Etch	5-10				5-10					5-10	5-10			
Phosphoric-Dischromate Etch				8-10										
Spray Rinse					3-5						3-5			
Coupling Agent Bath (L-10)											8-10	8-10	8-10	4-6
Coupling Agent Bath (A-1100)					8-10	8-10	8-10		8-10					
Spray Rinse	3-5													
Hot Air Day	Until Dry													
Spot-Weld Panel										X				
Chromic Acid Anodize										X				
Cold Water Spray into Bondline										6 (min.)				
Hot Air Dry										Until Dry				

Aklaline Clean –	6-8 oz. of Wyandotte Altrex Cleaner per gallon of tap water Solution temperature, $170^{\pm}$ $10^{o}F$
Spray Rinse –	Tap water Temperature, ambient
Spot-weld Acid Etch –	9-12 oz. of Suluric Acid (1.828 Specify Gravity), 5.3 – 7.4 oz. of Sodium Dichromate and 0.14 – 0.28 oz. of Ammonium Bifluoride per gallon of tap water Solution temperature, ambient
Metal Bond Etch –	29-37 oz. of Sulfuric Acid (1.828 Specific Gravity), and 3.4 – 12.7 oz. of Sodium Dichromate per gallon of tap water Solution temperature , $145^{o}F$ to $160^{o}F$
Nitric Acid Etch –	12 oz. of 25% Nitric Acid per gallon of tap water Solution temperature, ambient
Phosphoric – Dichromate Etch –	12 oz. of 85% Phosphoric Acid and 0.2 oz. of Potassium Dichromate per gallon of tap water Note: This process step is electrochemical and was conducted in this program using a stainless steel container in electrical contact with the specimens being treated. Solution temperature, ambient
Phosphoric - Chromic Acid Etch –	7.7 oz. of 85% Phosphoric Acid and 2.7 oz. of Chromic Oxide per gallon of tap water Solution temperature, $180^{o}F$
Alkaline Etch –	1-6 oz. of Sodium Hydroxide per gallon of tap water with Sodium Gluconate added as an inhibitor. The Sodium Gluconate concentration was 1 part to every 100 parts of Sodium Hydroxide. The aluminum build-up in this solution was kept to 1 oz./gal. below that of the Sodium Hydroxide. Solution temperature, ambient

Coupling Agent Bath –	L-10(½ oz./gal. of soluble chromates and 1% by volume of A-1100) or A-1100 (1% by volume), as noted, in tap water solution. Solution temperature, ambient.
Chromic Acid Anodize –	Anodize at a minimum current density of 1 ampere per square foot and a minimum steady voltage of 38 volts in a Federal Specification O-C-303 Chromic Acid and Tap water solution. The time in solution was 45 to 50 minutes. No Sodium Dichromate or Nickel Acetate Seal. Solution temperature, 90 to 95°F
Cold Water Spray into Bondline –	High pressure spray into bondline in order to flush chromic acid solution out of bondline.

2.2.2 Initial Weld Strength Tests - Surface Preparations

The last surface preparation evaluated (metal bond etch with the reduced time L-10 coupling agent bath) was an adjustment to the metal bond etch with ten (10) minute L-10 bath method conceived later in the program to alleviate welding problems. As such, it was not investigated in the initial studies. With the exception of this and of the treatment method intended for capillary action adhesive application (spot-weld etch for bare alloys and chromic acid anodize after spot-welding), the remaining twelve (12) surface preparation methods were initially tested for weld feasibility. These tests were conducted to determine spot-weld strengths on single overlap, .063-inch thick aluminum alloy adherends by testing in a tensile shear mode with the adhesive in the uncured condition.

The results of the initial spot-weld strength testing are shown in Table VI. Using the MIL-W-6858C average and minimum (840 pounds and 670 pounds, respectively) weld strength requirements for .063-inch thick adherends, a review of these results showed that the metal bond etch with A-1100 coupling agent, the phosphoric-chromic acid etch with A-1100 coupling agent and the spot-weld etch for clad aluminum alloy with both A-1100 and L-10 coupling agents failed to meet these requirements for at least one data set. In addition, in these cases, the corresponding standard deviations for these data sets are relatively high. Weld strength data for the remaining surface treatments were considered adequate to show weld feasibility.

TABLE VI – INITIAL SPOT-WELD STRENGTH RESULTS VS. CANDIDATE SURFACE TREATMENTS

Surface Treatment	Aluminum Alloy	Specimen Quantity	Spot-weld Strength (pounds)			
			Max	Ave.	Min.	Std. Dev.
Spot-weld Etch for Bare Aluminum Alloy	7075-T6 Bare	42	1240	1114	980	71.6
Metal Bond Etch for Bare or Clad Aluminum Alloy	7075-T6 Bare	30	1030	948	740	79.1
	7075-T6 Bare	12	1060	922	730	129.7
	7075-T6 Clad	10	950	903	810	39.5
	2024-T3 Clad	10	920	869	805	39.4
Russian Procedure	7075-T6 Bare	30	1070	982	810	69.9
Modified Russian Procedure	7075-T6 Bare	30	1030	961	880	36.1
Spot-weld Etch for Bare Aluminum Alloy with A-1100 Coupling Agent Bath	7075-T6 Bare	41	1150	1068	1000	34.0
Metal Bond Etch for Bare or Clad Aluminum Alloy with A-1100 Coupling Agent Bath	7075-T6 Bare	30	1010	973	920	21.9
	7075-T6 Bare	12	1060	1021	930	25.0
	7075-T6 Clad	10	990	960	930	23.6
	2024-T3 Clad	12	985	832	665	92.2

TABLE VI – INITIAL SPOT-WELD STRENGTH RESULTS VS. CANDIDATE SURFACE TREATMENTS (CONT'D.)

Surface Treatment	Aluminum Alloy	Specimen Quantity	Spot-weld Strength (pounds)			
			Max.	Ave.	Min.	Std. Dev.
Phosphoric-Chromic Acid Etch with A-100 Coupling Agent Bath	7075-T6 Bare	30	995	859	475	167.5
Spot-weld Etch for Clad Aluminum Alloy	2024-T3 Clad	12	995	905	830	40.9
Spot-weld Etch for Clad Aluminum Alloy with A-1100 Coupling Agent Bath	7075-T6 Clad	15	975	876	655	100.9
Spot-weld Etch for Bare Aluminum Alloy with L-10 Coupling Agent Bath	7075-T6 Bare	24	1090	1033	950	41.8
	7075-T6 Bare	30	1070	1005	930	34.2
Spot-weld Etch for Clad Aluminum Alloy with L-10 Coupling Agent Bath	7075-T6 Clad	24	995	795	530	118.6
Metal Bond Etch for Bare or Clad Aluminum Alloy with L-10 Coupling Agent Bath	7075-T6 Bare	29	1020	947	870	38.5
	7075-T6 Clad	30	965	903	730	50.7

2.2.3 Adhesive Bond Strength Tests

Through conventional lap shear, metal-to-metal peel and environmental wedge specimen testing, eight (8) candidate surface treatments were further evaluated for bond strength and permanence. These consisted of the following:

- o Spot-weld Etch for Bare Aluminum Alloys
- o Metal Bond Etch for Bare or Clad Aluminum Alloys
- o Russian Surface Preparation Method
- o Modified Russian Surface Preparation Method
- o Spot-weld Etch for Bare Aluminum Alloys with A-1100 Coupling Agent Bath
- o Metal Bond Etch for Bare or Clad Aluminum Alloys with A-1100 Coupling Agent Bath
- o Phosphoric – Chromic Acid Etch with A-1100 Coupling Agent Bath
- o Spot-weld Etch for Bare Aluminum Alloys with L-10 Coupling Agent Bath

This selection permitted the evaluation of the totally new surface treatments defined under this program, i.e.,

- o Russian Surface Preparation Method
- o Modified Russian Surface Preparation Method
- o Phosphoric – Chromic Acid Etch with A-1100 Coupling Agent Bath

and the Spot-weld Etch for Bare Aluminum Alloy and the Metal Bond Etch for Bare or Clad Aluminum Alloy and their derivatives involving the A-1100 and L-10 coupling agents. Throughout these tests, both strength and failure mode were recorded and, in frequent instances, the failure mode was the overriding factor in determining the acceptability of surface preparation response to test.

For instance, as shown in Figure 9, average initial bond strength on specimens without spot-welds ranged in room temperature strength from 2950 psi (for Spot-weld Etch for Bare Aluminum Alloys with L-10 Coupling Agent Bath) to 3780 psi (for Metal Bond Etch for Bare and Clad Aluminum Alloys). These closely approximated typical bond strengths for similar one inch overlap specimens with .063-inch thick 7075-T6 bare adherends experienced in earlier programs. Furthermore, the mode of failure for these specimens was

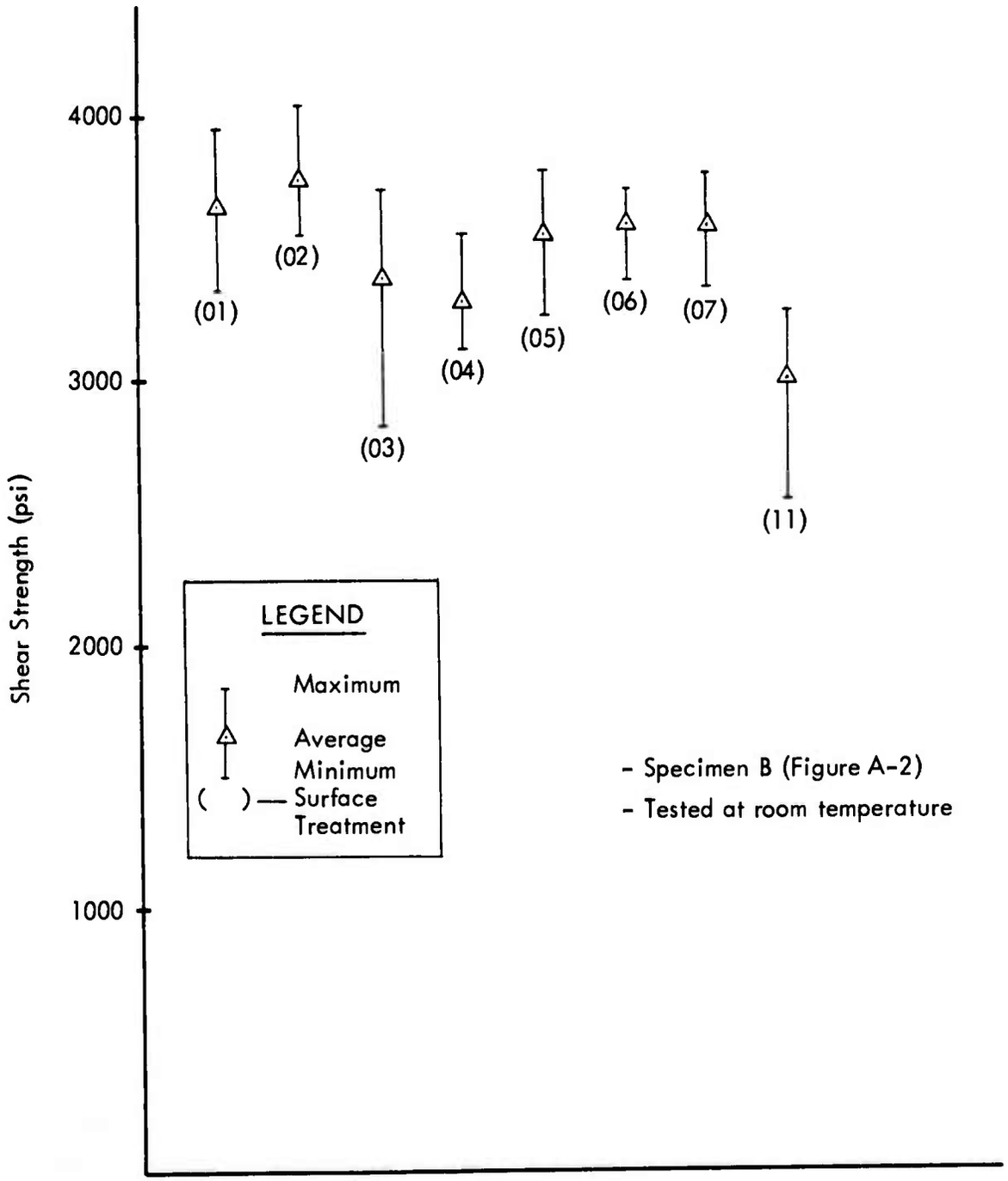

FIGURE 9 – ADHESIVE LAP SHEAR TEST RESULTS (ROOM TEMPERATURE)

essentially cohesive so that it was concluded that all candidate treatments were at least initially capable of developing the strength of the bondline adhesive at room temperature.

Environmental test data in the form of results from lap shear tests after fifteen (15) temperature – humidity cycles and the results from wedge tests in a high humidity environment are shown in Figure 10 and Table VII, respectively. In general, these two (2) sets of data correlated well with the exception of the phosphoric-chromic acid etch with A-1100 coupling agent prepared specimen results. These data show that the spot-weld etch for bare aluminum alloys without coupling agent and with both A-1100 and L-10 coupling agents and the metal bond etch for bare and clad aluminum alloys without coupling agent and with A-1100 coupling agent resisted environmental degradation to a satisfactory degree.

Temperature-humidity lap shear specimen test results were greater than ninety-three (93) percent of the control values, and wedge test durations exceeded twenty (20) days with the exception of one (1) specimen for these surface treatments. These tests also concurrently showed excessive environmental degradation of the Russian procedure and the modified Russian procedure prepared specimens with greater than twenty-five (25) percent reduction from control in temperature-humidity lap shear specimen tests and wedge test durations of less than one (1) day.

Further tests of "adhesive only" lap shear specimens at -67°F, of weldbonded lap shear specimens at room temperature and of "adhesive only" metal-to-metal peel specimens at -67°F and room temperature were conducted. In general, the specimen failure modes exhibited in these tests were cohesive and the strength values were sufficient to preclude elimination of candidate surface preparations through these tests. A summary of data for this testing is shown in Figures 11, 12, 13 and 14.

After review of the above mechanical test data, especially with respect to weld quality and environmental testing, it was apparent that the best of the candidate systems was to be from among the spot-weld etch for bare aluminum alloys or the metal bond etch for bare or clad aluminum alloys or their derivatives involving coupling agents.

2.2.4 Surface Preparation-Salt Spray Evaluation

The candidate coupling agents were further evaluated for their effectiveness in protecting the metal surface against salt spray corrosion. 7075-T6 aluminum panels were cleaned by the metal bond etch procedure and were then given the following surface treatments:

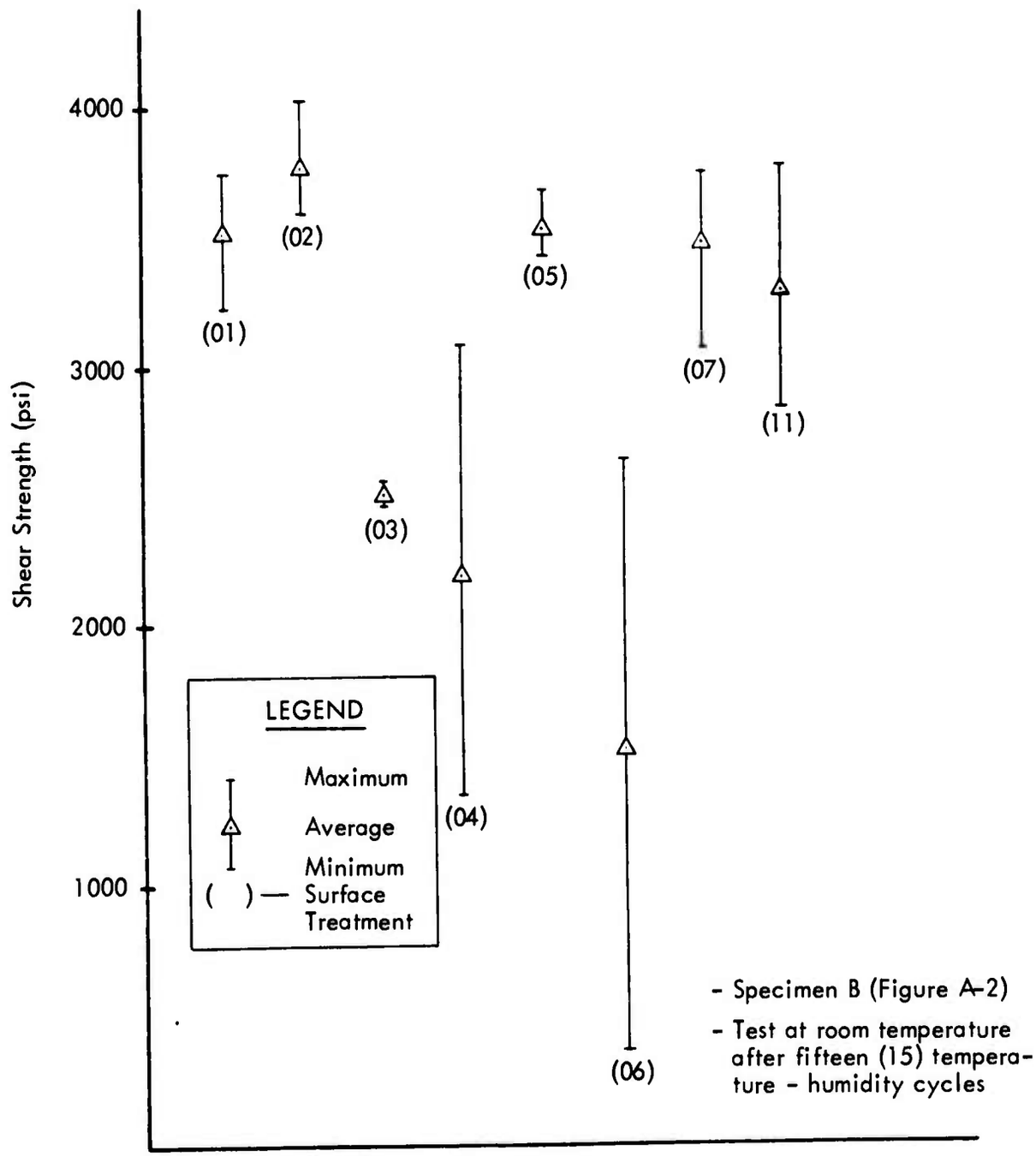

FIGURE 10 – ADHESIVE LAP SHEAR TEST RESULTS (WEATHERED SPECIMENS)

TABLE VII – WEDGE TEST DATA

Surface Preparation	Duration in High Humidity (Days)			
	Specimen No.	1	2	3
Spot-weld Etch for Bare Aluminum Alloys		20	23	27
Metal Bond Etch for Bare and Clad Aluminum Alloys		50	56	62
Russian Surface Preparation Method	All less than 1 day			
Modified Russian Surface Preparation Method	All less than 1 day			
Spot-weld Etch for Bare Aluminum Alloys with A-1100 Coupling Agent Bath		9	21	56
Metal Bond Etch for Bare and Clad Aluminum Alloys with A-1100 Coupling Agent Bath		35	36	42
Phosphoric-Chromic Acid Etch with A-1100 Coupling Agent Bath	All less than 1 day			
Spot-weld Etch for Bare Aluminum Alloys with L-10 Coupling Agent Bath		22	36	64

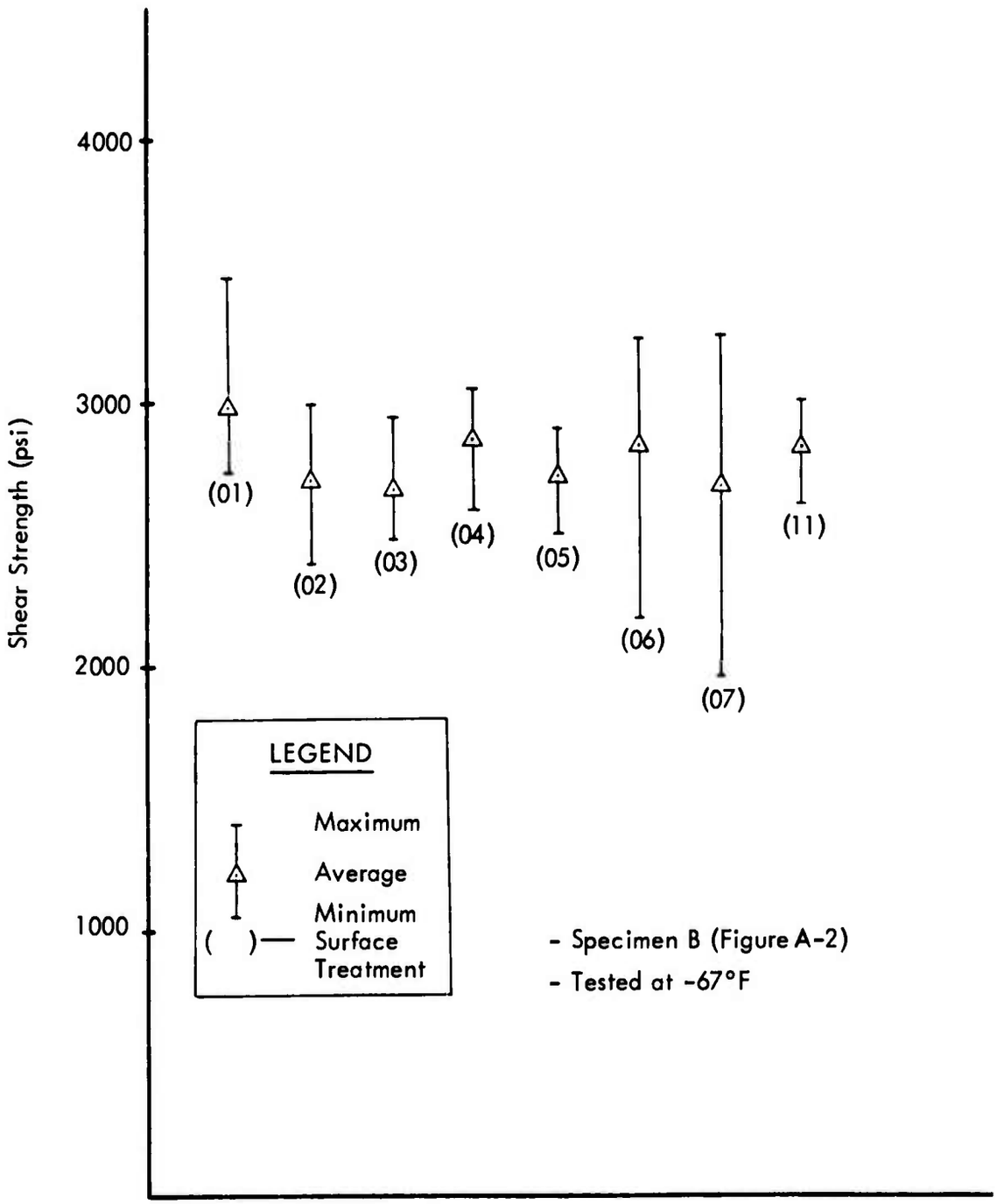

FIGURE 11 – ADHESIVE LAP SHEAR TEST RESULTS (-67°F)

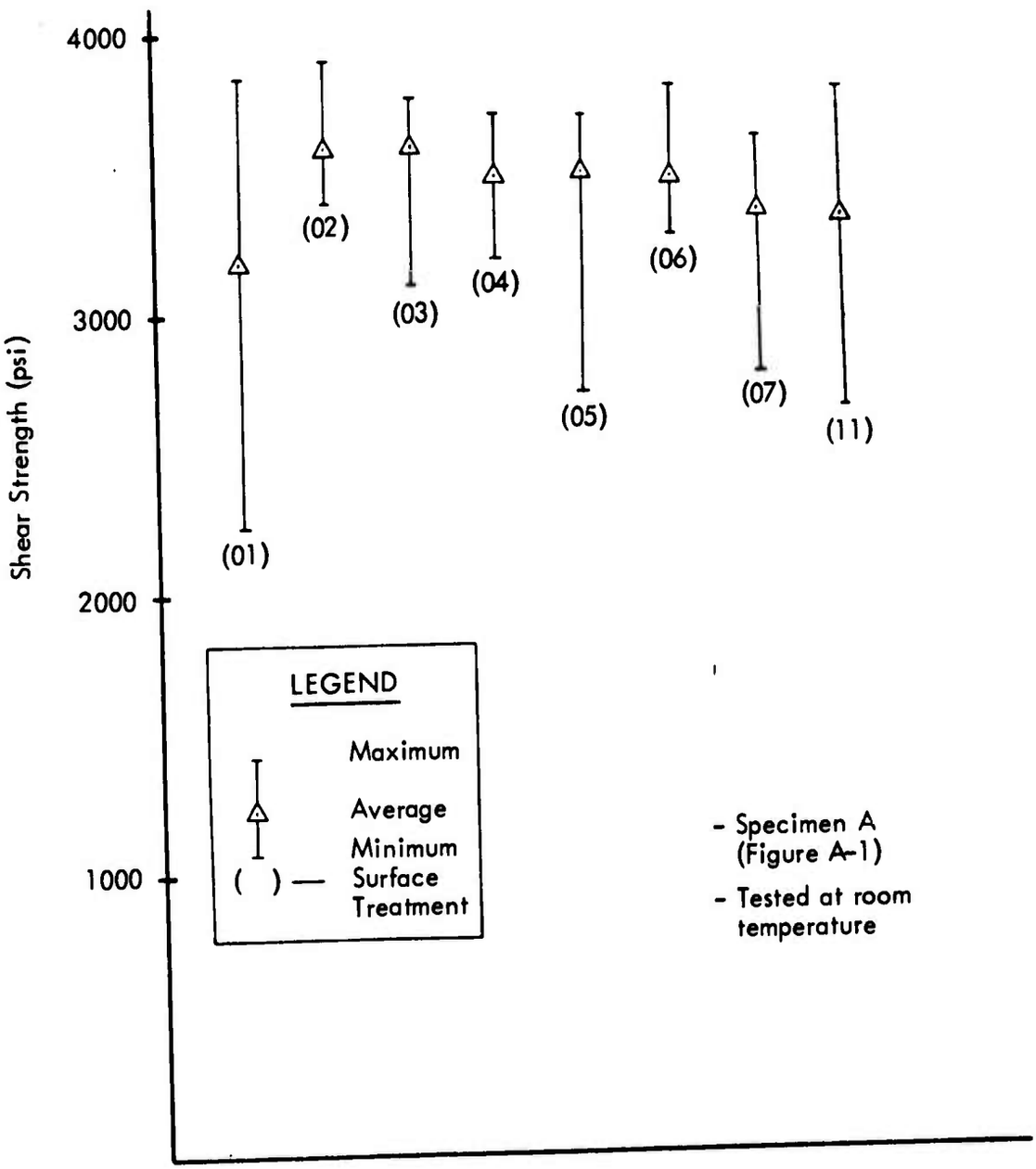

FIGURE 12 – WELDBOND LAP SHEAR TEST RESULTS

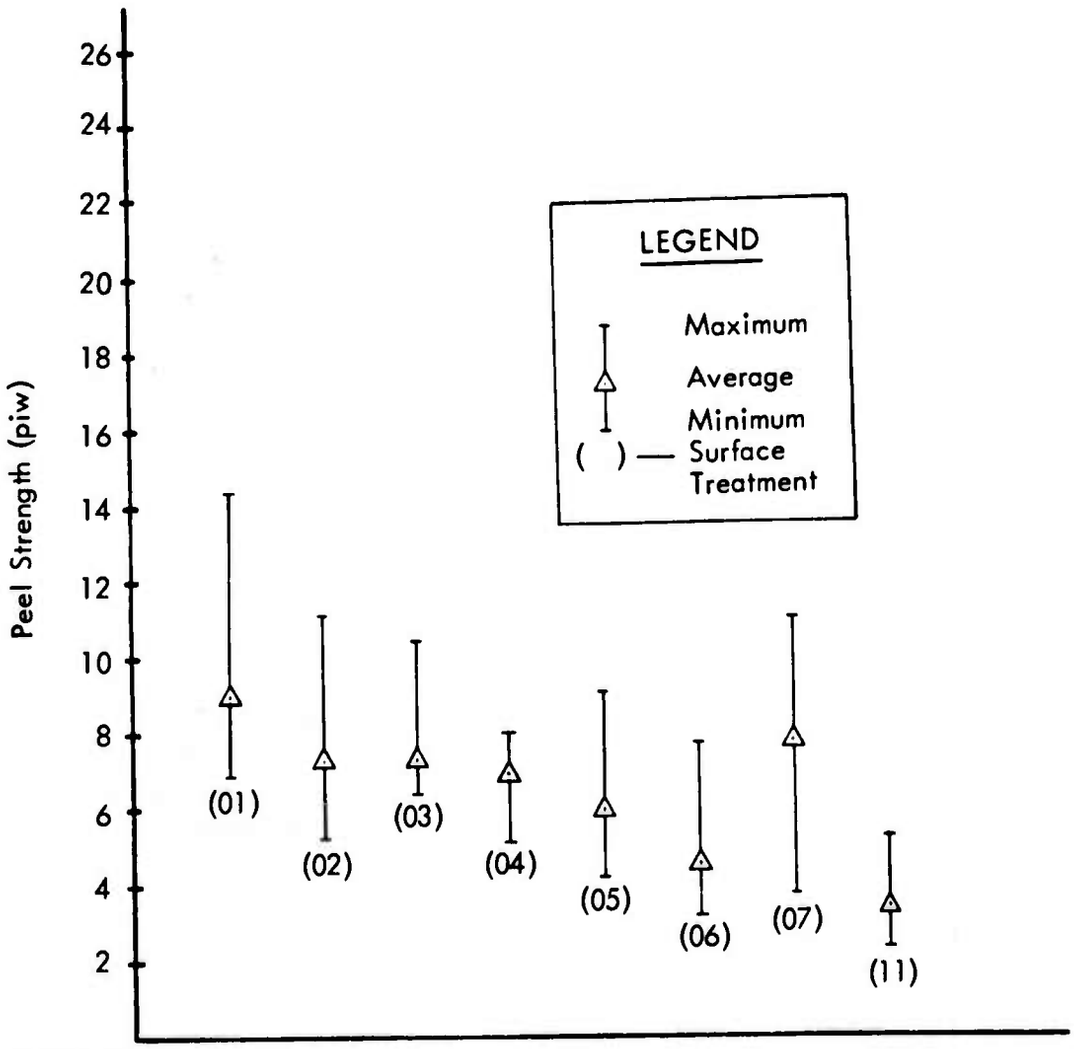

FIGURE 13 -- ADHESIVE PEEL TEST RESULTS (-67°F)

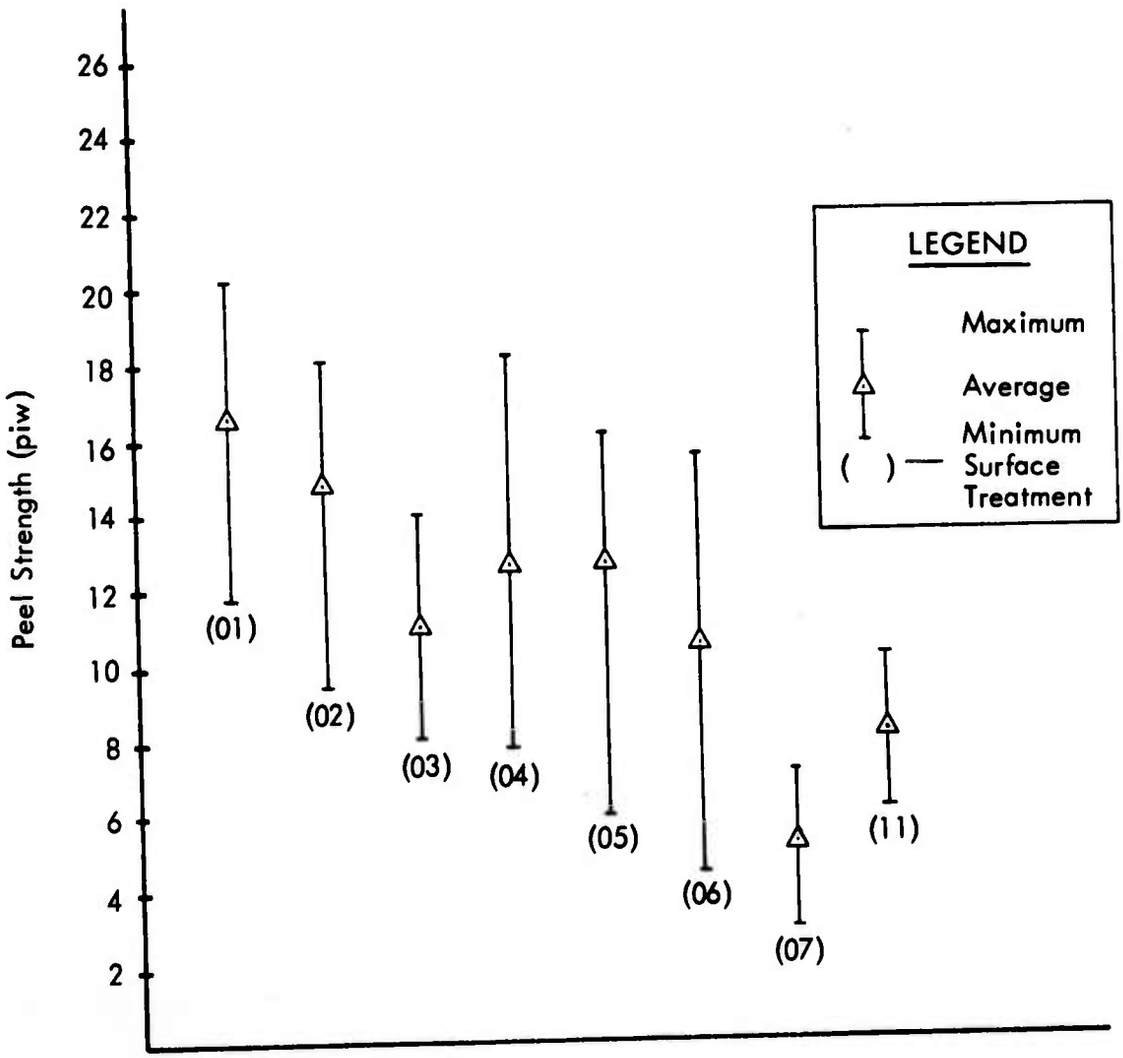

FIGURE 14 – ADHESIVE PEEL TEST RESULTS (ROOM TEMPERATURE)

(1) Alodine 1200
(2) A-1100 Coupling Agent
(3) L-10 Coupling Agent (10 minute immersion)
(4) L-10 Coupling Agent (5 minute immersion)
(5) EC3926 Adhesive Primer

The test panels were scribed to increase the susceptibility to corrosion and were placed in a salt fog cabinet for 88 hours. Figure 15 is a photograph made of the panels after the environmental exposure. The control panel and the panel with A-1100 were badly corroded. The panels treated with L-10 were just beginning to show signs of corrosion with only slight differences between the 10-minute immersion panel and the 5-minute immersion panel. The panels treated with Alodine 1200 and EC3926 showed no signs of corrosion. However, Alodine 1200 and EC3926 form high resistance films which are not compatible with the welding process. With these and earlier results, it was apparent that the L-10 treatment gave the best available balance of corrosion resistance and compatibility with the welding process.

Using the results of the previous weld, adhesive bond and surface corrosion tests, the candidate systems were reduced to

- Spot-weld Etch for Bare Aluminum Alloys with L-10 Coupling Agent Bath, and
- Spot-weld Etch for Clad Aluminum Alloys with L-10 Coupling Agent Bath, or
- Metal Bond Etch for Bare or Clad Aluminum Alloys with L-10 Coupling Agent Bath

2.3 Initial Weldbond Adhesive/Surface Preparation Selection

With the adhesive candidate systems reduced to two (2) epoxy paste systems and two (2) epoxy semi-solid bulk (or unsupported film) systems, i.e.,

- M6800 paste, Whitaker,
- CS4742 paste, B.F. Goodrich,
- A1357B film, B.F. Goodrich, or
- XB66 film, 3M Company,

and the surface preparation candidates reduced to

- Spot-weld Etch for Bare Aluminum Alloys with L-10 Coupling Agent Bath, and
- Spot-weld Etch for Clad Aluminum Alloys with L-10 Coupling Agent Bath, or

FIGURE 15 – 7075-T6 ALUMINUM SPECIMENS WITH VARIOUS SURFACE TREATMENTS AFTER 88 HOURS IN SALT FOG CABINET

- o Metal Bond Etch for Bare or Clad Aluminum Alloys with L-10 Coupling Agent Bath.

further weld quality tests involving combinations of these three (3) candidate surface preparations and four (4) adhesives were conducted. These involved lap shear tests of both cured and uncured specimens, and x-ray and visual inspection for spot-weld porosity, metal expulsion and cracks, and for small or irregular spot-welds. Generally, forty-eight (48) specimens per combination were fabricated and tested.

The results of these tests, particularly the x-ray inspection, showed a substantial increase in weld defects in clad specimens relative to those found in bare specimens. Moreover, greater difficulties were encountered in welding the spot-weld etched with L-10 coupling agent prepared clad specimens than with the metal bond etched with L-10 coupling agent prepared clad specimens. As a result of these tests, the metal bond etch plus L-10 coupling agent surface preparation was selected for further investigation. Further testing on specimens prepared with variable L-10 bath times indicated an advantage in reducing this time from ten (10) minutes to five(5) minutes. At this time in the program, the selected weldbond surface preparation was defined as:

Surface Preparation Step	Nominal Time in Solution (min.)
Alkaline Clean	15
Spray Rinse	3-5
Metal Bond Etch	8-10
Spray Rinse	3-5
Coupling Agent (L-10)	4-6
Spray Rinse	3-5
Hot Air Dry	Until Dry

At this point, a test program was defined to evaluate combinations of the four (4) remaining adhesive candidates and the selected surface preparation. Additional weld quality tests, adhesive lap shear tests both after and prior to exposure to aggressive environment and

metal-to-metal adhesive peel tests at -67°F and room temperature were conducted. Adherends .063 inch thick of 7075-T6 and 2024-T3 aluminum alloys both bare and clad were used during this testing. Additional adhesive tests were included using the chromic acid anodize – capillary fabrication method and CS 4742 adhesive with 7075-T6 bare adherends.

On the four primary systems, weld evaluations were conducted which included weld strength tests following x-ray inspection. The results of the x-ray inspection are shown in Table VIII.

Table VIII – X-Ray Inspection Results

Adherend	Adhesive	N	Number of Defects	
			Cracks & Metal Expulsion	Cracks
7075-T6 bare	A1357B	30	–	15
7075-T6 clad	A1357B	30	19	–
2024-T3 bare	A1357B	20	–	2
2024-T3 clad	A1357B	20	–	20
7075-T6 bare	XB66	30	–	11
7075-T6 bare	M6800	30	1	–
2024-T3 clad	CS4742	20	5	–
2024-T3 bare	CS4742	20	–	–
7075-T6 clad	CS4742	30	9	–
7075-T6 bare	CS4742	30	1	–

Weld strength data on these specimens are given in Table IX.

Table IX – Weld Strength Results

Adherend	Adhesive	N	Weld Strength (lb.)		
			Minimum	Average	Maximum
7075-T6 bare	A1357B	30	895	1020	1150
7075-T6 clad	A1357B	30	615	960	1750
2024-T3 bare	A1357B	20	805	936	1085
2024-T3 clad	A1357B	20	460	870	1080
7075-T6 bare	XB66	30	725	1006	1180
7075-T6 bare	M6800	30	815	1023	1285
2024-T3 clad	CS4742	20	525	886	1050
2024-T3 bare	CS4742	20	805	870	995
7075-T6 clad	CS4742	30	630	988	1225
7075-T6 bare	CS4742	30	605	929	1175

The subsequent adhesive tests on 7075-T6 bare adherends consisted of lap shear control, lap shear tests after exposure to aggressive environments such as JP-4 fuel, hydraulic oil, temperature — humidity cycling and salt spray, and metal-to-metal peel tests at room temperature and at -67°F.

The results of these tests are given in Tables XI, XII, XIII, and XIV.

Additional testing of panels which were treated with the conventional spot-weld etch procedure, welded, and chromic acid anodized and cold water rinsed after welding was conducted. After this surface preparation, CS4742 epoxy paste adhesive was applied to the bondline through capillary action and cured. These tests consisted of lap shear controls and after exposure to salt spray and to temperature-humidity cycling and metal-to-metal peel at -67°F and at room temperature. As in the previous tests, the substrate adherends were 7075-T6 bare aluminum alloy. These results are shown in Table X.

Table X — CS4742 Adhesive Bond Test Results (Capillary Application)

Test	Prior Environment	Strength (Lap Shear in psi, Peel in lb./inch width)			Typical Failure Mode
		Maximum	Average	Minimum	
Lap Shear (Room Temperature)	None	4100	3300	2500	0% Coh., 100% A
	30 day salt spray	2200	1500	1000	0-5% Coh., 95-100% A
	15 Temp.-humidity cycles	2700	2300	1500	0% Coh., 100% A
Metal-to-Metal Peel (Room Temperature)	None	2.7	2.2	1.8	0% Coh., 100% A
Metal-to-Metal Peel (-67°F)	None	3.7	3.2	3.1	0% Coh., 100% A

Coh. – Cohesive

A – Adhesive-to-Anodize

Table XI – A1357B Adhesive Bond Test Results

Test	Prior Environment	Strength (Lap Shear in psi, Peel in lb/inch width)			Typical Failure Mode
		Maximum	Average	Minimum	
Lap Shear	None	4800	4760	4700	60-70% Coh., 30-40% Am
(Room Temp.)	30 day salt spray	4900	4700	4400	60-80% Coh., 20-40% Am
	15 temp.-humidity cycles	4600	4500	4400	60-70% Coh., 30-40%Am
	7 day hydraulic oil	4600	4500	4300	80-90% Coh., 10-20% Am
	7 day JP-4 fuel	4600	4600	4600	80% Coh., 20% Am
Metal-to-Metal Peel (Room Temp.)	None	52.7	48.6	42.5	100% Coh., 0% Am
Metal-to-Metal Peel (-67°F)	None	50.7	44.8	36.9	90-100% Coh., 0-10% Am

Coh. – Cohesive

Am – Adhesive-to-Metal

Table XII – XB66 Adhesive Bond Test Results

Test	Prior Environment	Strength (Lap Shear in psi, Peel in lb/inch width)			Typical Failure Mode
		Maximum	Average	Minimum	
Lap Shear (Room Temp.)	None	4900	4400	3700	40-80% Coh., 20-30%Am
	30 day salt spray	4700	4600	4500	50-40% Coh., 60-95%Am
	15 temp.-humidity cycles	4600	4200	3900	40-80% Coh., 20-60%Am
	7 day hydraulic oil	4700	4560	4500	80% Coh., 20%Am
	7 day JP-4 fuel	4900	4700	4500	70-80% Coh., 20-30%Am
Metal-to-Metal Peel (Room Temp.)	None	50.3	45.8	41.3	100% Coh., 0%Am
Metal-to-Metal Peel (-67°F)	None	23.8	20.5	15.2	100% Coh., 0%Am

Coh. – Cohesive

Am – Adhesive-to-Metal

Table XIII – M6800 Adhesive Bond Test Results

Test	Prior Environment	Strength (Lap Shear in psi, Peel in lb/inch width)			Typical Failure Mode
		Maximum	Average	Minimum	
Lap Shear (Room Temp.)	None	4300	3900	3200	80-95% Coh., 5-20%Am
	30 day salt spray	4700	4200	3600	90-95% Coh., 5-10% Am
	15 temp-humidity cycles	4400	3900	3400	70-100% Coh., 0-30% Am
	7 day hydraulic oil	3900	3700	3000	100% Coh., 0% Am
	7 day JP-4 fuel	4100	3760	3100	100% Coh., 0% Am
Metal-to-Metal Peel (Room Temp.)	None	11.8	9.7	7.8	100% Coh., 0% Am
Metal-to-Metal Peel (-67°F)	None	13.0	7.9	3.6	100% Coh., 0% Am

Coh. – Cohesive

Am – Adhesive-to-Metal

Table XIV – -CS4742 Adhesive Bond Test Results

Test	Prior Environment	Strength (Lap Shear in psi, Peel in lb/inch width)			Typical Failure Mode
		Maximum	Average	Minimum	
Lap Shear	None	3600	3300	3000	80-90% Coh., 10-20% Am
(Room Temp.)	30 day salt spray	3500	3100	2800	0-5% Coh., 95-100% Am
	15 temp.-humidity cycles	3400	3280	3000	10% Coh., 90% Am
	7 day hydraulic oil	3900	3300	2700	0% Coh., 100% Am
	7 day JP-4 fuel	3700	3000	2700	0-10% Coh., 90-100% Am
Metal-to-Metal Peel (Room Temp.)	None	9.2	5.6	3.7	0% Coh., 100% Am
Metal-to-metal Peel (-67°F)	None	14.5	10.3	7.6	0% Coh., 100% Am

Coh. – Cohesive

Am – Adhesive-to-Metal

Since preliminary tests indicated that consistent, acceptable quality, welds could not be formed through two of the candidate adhesive (A1357B. and XB66) without heating the bondline prior to welding, these adhesives were manually heated to 200°F before welding. The remaining candidates were welded without prior heating. The x-ray inspection results of these tests as shown in Table VIII indicate a distinct advantage in welding the two paste systems (M6800 and CS4742). Specifically, out of thirty (30) tests on .063, 7075-T6 bare specimens, the paste systems had one (1) defect each while the hot spread systems showed fifteen (15) and eleven (11) defects for a 1357B and XB66, respectively. The minimization of these defects, in the form of cracks and metal expulsion, for the final process was considered essential. In addition to yielding the above comparison, this data shows the increased difficulty in welding clad materials over that encountered in the welding of bare alloys.

A review of the weld strength data in Table IX is not as conclusive as the above NDI data. No real advantage in static weld strength is indicated for pastes over hot spread systems. However, it should be noted that the M6800 adhesive data showed the highest average weld strength. Comparison of this mechanical test data and the previous NDI evaluation shows the absence of a relationship between static weld strength and the presence of cracks and metal expulsion in the weld.

Reviewing the weld-through weldbond systems results, all adhesives tested showed acceptable initial lap shear strength values and only slight (nine (9) percent maximum) reductions in lap shear strength due to aggressive environments. The average initial strengths of the two hot spread systems were greater than 4000 psi while the average initial strength of the M6800 paste was 3900 psi and the average initial strength of the CS 4742 paste was 3300 psi. The failure modes on the first three of these systems (A1357B, XB66 and M6800) were predominantly cohesive while the failure mode on the CS 4742 system was mostly adhesive-to-metal.

The metal-to-metal peel results showed high strength with cohesive failures for the A1357B system, high-room temperature strength and intermediate -67°F strength with cohesive failure for the XB66 system, low strength with cohesive failure for the M6800 system, and low strength with adhesive-to-metal failures for the CS 4742 system. Considering these along with the previous lap shear data, a ranking of candidate systems based solely on adhesive properties was (1) A1357B, (2) XB66, (3) M6800 and (4) CS 4742.

In order to select the primary system for weldbonding, considerations of both weld quality and adhesive characteristics were made. Although the two hot spread systems showed superior adhesive characteristics, the weld data, specifically the NDI results, showed excessive weld defects for these systems. In future weldbond developments, this may be at

least partially correctable through the use of a pre-heat control built into the welding machine and controlled through the weld schedule. This was not attempted on this program and, as a result of the poor weld quality, these systems were eliminated from further evaluation on this program.

Eliminating the hot spread systems left the two paste systems for further consideration. Both of these systems were considered equivalent with respect to weld quality. When the adhesive characteristics of each were considered, it was seen that the M6800 paste system was the better of the two. The essential undesirable characteristic of the CS 4742 system was the predominance of adhesive-to-metal failure, especially in the peel tests conducted.

With this reasoning, the primary weldbond system was, at this time, defined as the metal bond etch and L-10 coupling agent surface preparation with M6800 paste adhesive cured at 250°F for one hour.

Due to the limitations of a capillary system regarding improbable universal usage for all structural configurations such as bondline width limitations and general fay surface inaccessibility, the capillary action method of adhesive application was considered as a possible secondary method to complement the primary system chosen above. With this method, weld quality was not an area for investigation since welding was done through a spot-weld etch prepared surface with no adhesive in the bondline at the time of welding. Historically, this has been an acceptable surface for spot-welding. Adhesive test data on this system is shown in Table X. These data show a problem with this system in that the failure modes were typically one hundred (100) percent adhesive-to-anodize. This is an undesirable system characteristic and different from test results previously obtained on this system. The problem may be traceable to either the particular adhesive batch used or some change in the method of anodizing. In any event, no further work was performed relative to the capillary application method on this contract.

2.4 Subsequent Weldbond Revisions and Adjustments

After conducting weldbond process development per contract requirements as defined earlier, further weld quality tests on specimens prepared using production solutions and equipment were conducted. The tests addressed adherends with thicknesses over the 0.020 inch to 0.090 inch thickness range and showed a high frequency of weld defects at the extreme thicknesses. Specifically, welding through the 0.020 inch to 0.020 inch 7075-T6 bare aluminum alloy combination resulted in low inconsistent weld strengths with approximately ten (10) percent of the results showing a "no weld" or "dud" condition. Meanwhile, welding through the 0.090 inch to 0.090 inch 7075-T6 bare combination resulted in more than one-half of thirty (30) welds cracked. Since the ability to consistently produce high-quality welds at these thicknesses was necessary to the performance of this contract, adjustments and revisions to the previously defined surface preparation were made.

2.4.1 Elimination of the L-10 Coupling Agent-Metal Bond Etch Evaluation

In order to alleviate the weld defect problem, the initial adjustment made was to eliminate the L-10 coupling agent. At this point, with the weldbond surface preparation redefined as the metal bond etch process, further problems involving weld cracking and metal expulsion into the adhesive bondline were encountered. In the light of previous successes involving welding through surfaces prepared by the metal bond etch procedure with and without the L-10 coupling agent, the coincident change from laboratory to the production line became a prime area of concern.

The metal bond etch tank used in the fabrication of these weldbonded specimens was maintained by production control and it was chemically analyzed at a standard frequency for sulfuric acid and sodium dichromate contents, and the resulting data was recorded. A review of these data indicated a steady increase in the sodium dichromate content over the time period that it was in use by this program for preparation of weldbond test specimens. However, this increase was well within the specified control limits for the process tank. At this stage of the spot-weld expulsion problem, no correlation was achieved between increased dichromate content and frequency of occurrence of spot-weld expulsions. This investigation prompted the initiation of an experimental program for determination of surface resistivity measurements of test specimen details cleaned in the production metal bond etch tank. The high surface resistance measurements and accompanying spot-weld expulsions experienced with aluminum alloy test specimen details prepared in the production metal bond etch tank led to the conclusion that the metal bond etch tank solution could be contaminated. This conclusion further led to investigations for trivalent chrome content in the etch tank, an independent investigation by the Lockheed Missiles and Space Company (LMSC), and a chemical analysis of the expelled material.

Upon investigation, no correlation could be established relative to trivalent chrome content in the production metal bond etch solution and the occurrence of spot-weld expulsions.

In order to eliminate any possible equipment or instrumentation problems, an independent investigation was conducted at LMSC. All test specimen details in this investigation were prepared by the metal bond etch procedure using a newly prepared solution in a volume of twenty-two (22) gallons. Test specimens were fabricated from both 7075-T6 bare and clad aluminum alloy sheet materials using the M6800 epoxy adhesive. The aluminum alloy sheet thicknesses used ranged from 0.020 inches to 0.090 inches. Test panels were weldbonded in four inch widths and then individual one inch wide test specimens were machined from each panel. Each individual test specimen contained a single spot-weld. Electrical surface resistance measurements were made on each pair of test panels prior to adhesive application. The results from the test specimens in this program are shown in Table XV.

Table XV - Summary of Spot-Weld Expulsion Investigation Results from LMSC Program

Material Thickness and Alloy	Cleaning Procedure	Percentage of Defective Welds	Electrical Surface Resistivity
0.020" 7075-T6 Bare	MBE, 10 Min. Etch	8.0	18 to 56
0.050" 7075-T6 Bare	MBE, 10 Min. Etch	8.0	32 to 132
0.050" 7075-T6 Bare	MBE, 5 Min. Etch	12.0	20 to 220
0.050" 7075-T6 Clad	MBE, 10 Min. Etch	12.0	25 to 52
0.050" 7075-T6 Clad	MBE, 5 Min. Etch	40.0	26 to 180
0.090" 7075-T6 Bare	MBE, 10 Min. Etch	72.0	33 to 47

NOTE:

MBE in the above table is the abbreviation for metal bond etch, and the time specified immediately following MBE is the time that the aluminum details are immersed in the etchant solution.

Again, no definite conclusion could be drawn relative to the specific cause of spot-weld expulsion and a method for its elimination. This program did reflect, for the first time, that the metal bond etch solution would reduce the surface resistivity to levels comparable to those gained by cleaning with the spot-weld etch surface preparation procedure.

In order to gain a further insight into the spot-weld expulsion problem, a chemical analysis was performed on a sample of the expelled material from a failed test specimen. An emission analysis confirmed that the expelled material contained aluminum and magnesium. Optical emission, infrared and microscopic analyses indicated that the sample of expelled material contained fine aluminum particles dispersed in the epoxy adhesive. Also, no carbon was present which indicated an absence of charring. Furthermore, infrared analysis indicated that the adhesive had not been degraded.

An additional investigation whose aim was establishing the source(s) of the spot-weld expulsion problem was initiated. The variables considered were adherend thickness, etch time, surface preparation procedures, and adhesives. Lap shear tests were conducted on butt lap shear specimens which were fabricated considering the aforementioned variables.

The test panels were fabricated in two thicknesses, 0.050 inches and 0.071 inches. Each panel consisted of two (2) butt lap shear specimens. After weldbonding, the specimens were machined from the panel resulting in two specimens 3 inches wide and 12 inches long. Forth-five (45) panels were fabricated for each of the two thicknesses. Following the spot-weld machine weld schedule development, in-process inspections were performed during the test specimen fabrication including surface resistivity measurements prior to applying the adhesive. All test specimens were radiographically inspected prior to structural testing. The test specimens were tested to failure and visual inspections made on the failed specimens. The results of this investigation are listed in Table XVI.

Table XVI – Summary of Spot-Weld Expulsion Investigation Results

Material Thickness	Cleaning Procedure	Adhesive	Percentage of Defective Welds	Electrical Surface Resistivity - (Micro-OHMS)
0.050	MBE, 5 Min. Etch	M6800, Lot 107	37.5	1200
0.050	MBE, 8 Min. Etch	M6800, Lot 107	45.0	2500
0.050	MBE, 10 Min. Etch	M6800, Lot 107	55.0	1200
0.071	MBE, 5 Min. Etch	M6800, Lot 107	37.5	1250
0.071	MBE, 8 Min. Etch	M6800, Lot 107	40.0	1500
0.071	MBE, 10 Min. Etch	M6800, Lot 107	37.5	1500
0.050	DMBE, 5 Min. Etch	M6800, Lot 107	60.0	1600
0.050	DMBE, B Min. Etch	M6800, Lot 107	60.0	2000
0.050	DMBE, 10 Min. Etch	M6B00, Lot 107	77.5	1700
0.071	DMBE, 5 Min. Etch	M6800, Lot 107	45.0	1300
0.071	DMBE, B Min. Etch	M6800, Lot 107	42.5	1600
0.071	DMBE, 10 Min. Etch	M6800, Lot 107	37.5	1400
0.050	Spot-Weld Etch	M6B00, Lot 107	0	B0
0.050	Spot-Weld Etch	M6B00, Lot 106	0	80
0.050	Spot-Weld Etch	EC 2214	0	60
0.071	Spot-Weld Etch	M6800, Lot 107	0	B0
0.071	Spot-Weld Etch	M6800, Lot 106	0	40
0.071	Spot-Weld Etch	EC 2214	0	75

NOTE:
MBE in the above table is the abbreviation for metal bond etch and DMBE is the abbreviation for the metal bond etch procedure with a deoxidizer step added to the processing sequence prior to the MBE acid etch step.

Upon analyzing the results of spot-weld expulsions listed in Table XVI, none of the variables introduced into the weldbond systems study could be singled out as the contributing factor for high surface resistivity and high frequency of spot-weld expulsions except the metal bond etch tank solution.

The next phase of the spot-weld expulsion investigation was to determine the effect of the variation of both sulfuric acid and sodium dichromate concentration within the tank control limits. Electrical surface resistivity measurements were made on 7075-T6 bare aluminum test panels that were prepared using the metal bond etch solution which had varying concentrations of sulfuric acid and sodium dichromate dihydrate. Electrical surface resistivity measurements corresponding to sulfuric acid and dichromate concentrations are given below. Three sets of test panels were prepared for each sulfuric acid to sodium dichromate dihydrate ratio.

Panel No.	Sulfuric Acid Conc.	Dichromate Concentration	Electrical Surface Resistivity
L-1	34	3.0	78-56-70
L-2	34	4.8	140-180-192
L-3	34	7.2	290-390-850
L-4	34	9.6	200-270-290
L-5	36	3.0	96-56-30
L-6	36	4.8	96-110-124
L-7	36	7.2	220-480-560
L-8	36	9.6	465-480-485
L-9	38	3.0	20-40-82
L-10	38	4.8	220-240-240
L-11	38	7.2	140-120-250
L-12	38	9.6	500-480-625

The above sulfuric acid and sodium dichromate concentrations are in ounces per gallon of solution with balance of solution being clean water. The electrical surface resistivity is recorded in micro-ohms for 36 panels.

A sample of the production metal bond etch solution was used to clean three test panels. A portion of the sample solution was adjusted (by adding sulfuric acid to achieve an acid/sodium dichromate ratio of 10) and three panels were cleaned with this solution. Surface resistivity was measured on each with the following results.

Panel	Etch Solution	Electrical Surface Resistivity
P-1	Production Solution	500-620-340
P-2	Adjusted Solution	47-17-127

These data indicate that the electrical surface resistivity of cleaned aluminum parts is directly related to the sodium dichromate content. Also, these data indicate that the etch solution can be brought into tolerance with respect to electrical surface resistance by adjustment of the sulfuric acid/sodium dichromate ratio.

Earlier investigations indicated that low electrical surface resistivities (less than 200 micro-ohms) yielded quality spot-welds. Furthermore, surface films containing chromate resulted in poor quality spot-welds. In order to establish the metal bond etch cleaning procedure as a workable surface preparation, the ratio of the sulfuric acid content to sodium dichromate content was varied from 7 to 50. The lower ratios had given high percentages of spot-weld expulsions. It was reasoned that higher ratios might yield acceptable quality welds and yet maintain a corrosion resistance level nearly that of the metal bond etch. Evaluations of the metal bond etch solution with sulfuric acid content to sodium dichromate content ratios of 7, 10, 15, 30, and 50 were performed. Over 2000 electrical surface resistivity measurements were made on the aforementioned metal bond etch solutions and two spot-weld etch solutions. The scatter in the resistivity measurements of surfaces prepared by the metal bond etch surface preparations evaluated was high. Surfaces of specimens prepared by the spot-weld etch cleaning procedures resulted in average measurements that were lower than the average measurements of the specimens prepared by the metal bond etch solutions.

Weldbonded lap shear specimens were fabricated and tested in three thicknesses of aluminum alloy sheet material. Each specimen thickness was prepared by two metal bond etch solutions, ratios of 15 and 50. Examination of the failed specimens did not reveal any significant improvement of one metal bond etch cleaning procedure over the other. Also, after analyzing the results of this investigation, it was concluded that a source other than surface resistivity was the principal contributing factor for spot-weld expulsions.

As part of the continued effort directed toward resolving the spot-weld expulsion problem, a special weld schedule program was initiated. This program was directed toward developing weld schedules without regard to maintaining specification nugget quality relative to size and strength. The results of this effort are as follows:

1. The initial work involved establishing a weld schedule for both 0.050 and 0.020 inch thick bare 7075-T6 aluminum sheet materials cleaned in a modified metal bond etch solution containing sulfuric acid to sodium dichromate ratio of 50:1. Successful schedules were established for these two adherend thicknesses bonded with M6800 paste adhesive. Approximately 12-15 expulsion free nuggets were made on each

thickness. Only the nuggets in the 0.020 inch sheet were sectioned and those were found to be free of cracks. The successful schedules were accomplished only after the weld area was heated to lower the adhesive's viscosity to encourage its removal from the weld area during the welding operation. Analysis of the anticipated results with incorporation of a heating step in the weldbond cycle discounted its feasibility. The impracticality of a heating step is due to: (1) reduction of adhesive open time; (2) difficulty in controlling spot-weld location heating and (3) increased production time/cost. Other methods of viscosity reduction such as solvating with removal prior to adhesive cure, incorporation of a reactive diluent, and development of a new low viscosity adhesive were also rejected as being impractical, at this time.

2. Previous weldbond developments indicated that 3-M's EC2214 Hi-Flex paste adhesive was easier to weld through than Whittaker M6800 adhesive. Since the most obvious difference between the two adhesives was the content of aluminum powder in EC 2214, it was surmised that the same modification to M6800 might improve its weldability on a metal bond etch prepared surface. The addition of 1 percent by weight of TT-P-320A, Type I, Class A aluminum powder to the M6800 did improve the weldability of M6800. The sulfuric acid to sodium dichromate ratio was lowered to 15:1 in lieu of 50:1 for this effort.

The results of the two investigations are listed in Table XVII. As shown in the table, it is concluded that weld quality on 0.020 and 0.032 inch thicknesses of aluminum alloy sheet was unacceptable, for the 0.050 and 0.090 inch thicknesses it was acceptable, and for the 0.063 thickness it was marginal. Although the aforementioned results show promise in solving the weld quality problem, time did not permit continued development in this program. Thus, the decision was rendered to substitute the spot-weld etch cleaning procedure for the metal bond etch cleaning procedure for the remainder of the program.

2.5 Welding Schedules for Weldbonding

During the course of weldbond process development spot-welding schedules were established. These schedules varied with the adhesive in the joint, material thickness and material alloy. Table XVIII shows several typical welding schedules used in weldbonding test specimens and components.

TABLE XVII – Weldability Program Results

Thickness (in.)	No. of Welds	Etch (1)	Adhesive	Expulsions	Cracks
.050(2)	12	MBE-50	M6800	None	--------
.020(2)	12	MBE-50	M6800	None	--------
.054	30	MBE-15	M6800/AL.	None	None
.020	20	MBE-15	M6800/AL.	7	3
.090	25	MBE-15	M6800/AL.	None	1
.063	25	MBE-15	M6800/AL.	3	1
.020	25	MBE-15	M6800/AL.	24	2
.054	20	MBE-15	M6800/AL.	None	N.A.
.032	25	MBE-15	M6800/AL.	14	None
.032	40	MBE-15	M6800/AL.	None	26

Note:

(1) MBE-50 is metal bond etch solution with sulfuric acid to sodium dichromate ratio of 50:1; MBE-15 has a ratio of 15:1.

(2) Heated Material

2.6 Material and Process Specifications

Specifications for adhesives, surface preparation and weldbond processing were completed and are included in Appendix B.

The adhesive material specification contains both qualification and acceptance requirements for weldbond adhesives. The qualification requirements are those which a material must meet to be considered a source for weldbond adhesive. The acceptance requirements are those which all incoming adhesive lots must meet in order to ensure a maintenance of the qualification standards.

The weldbond process and surface preparation specifications contain the engineering, manufacturing, and quality assurance requirements essential to the process. For example, these requirements include welding machine performance and qualification, certified weld schedules, material controls, controls for auxiliary equipment, part assembly, weld and adhesive bond mechanical properties, acceptance criteria, and inspection methods. In light of the total process development and adhesive evaluation program, these specifications reflect the M6800 paste epoxy adhesive system and the conventional spot-weld etch surface preparation.

TABLE XVIII – TYPICAL ALUMINUM WELDBONDING SCHEDULES

ADHEREND ALLOY	GAGE, UPPER – in. LOWER – in.	ELECTRODE DIMENSIONS		HEAT CYCLES	WELD IMPULSES	NET ELECTRODE FORCE (lb)	AVG. SHEAR STRENGTH (lb)	WELDING MACHINE RATING (kva)
		UPPER	LOWER					
7075-T6 Clad 2024-T6 Clad	.032 .032	.45"D & 4"R	.45"D & 4"R	2	1	800	422	90
7075-T6 Bare 7075-T6 Bare	.050 .050	.50"D & 4"R	.50" & 4"R	2	1	1300	678	90
7075-T6 Bare 7075-T6 Bare	.071 .071	.50"D & 4"R	.50"D & 4"R	2	1	1700	1048	90

SECTION III

GENERAL DESIGN DATA

3.1 Engineering Design Limits

Specific design limitations for weldbonding established through testing conducted under this program address approved aluminum alloys and tempers, adherend material thickness and thickness ratio limits, spot-weld spacing and edge distance requirements and operational temperature extremes for weldbonding. The following sections define these limitations.

3.1.1 Adherend Material and Temper

Weldbonding may be performed on any combination of material compositions in the 2000 and 7000 series aluminum alloys. Sheet material may be weldbonded to extrusions, and clad-one-side to bare surface combinations may be weldbonded provided that clad surfaces are not present in the faying surface of joints. All materials shall be in the solution treated and hardened condition. Basic temper designations -T3, -T4, -T6, -T7, and -T8 satisfy the hardness requirements.

3.1.2 Adherend Material Thickness and Thickness Ratios

The following thickness limits and thickness ratios are established for weldbonded assemblies:

(a) Single sheet thickness shall be in the range of 0.020 to 0.125 inches.

(b) The maximum combined joint thickness shall not exceed 0.180 inches or four (4) times the thickness of the thinner outer sheet of the joint, whichever is less.

(c) The maximum thickness ratio for two-sheet combinations is 3:1.

(d) The maximum thickness ratio requirements for three-sheet combinations are defined as follows:

(1) All sheets of equal thickness, the ratio is 1:1.

(2) Outer sheets in the joint which are equal in thickness but thicker than the middle sheet, the maximum ratio is 2.5:1.

(3) Outer sheets in the joint which are equal in thickness but thinner than middle sheet, the maximum ratio is 3:1.

(4) When all sheets in the joint are unequal in thickness, maximum ratio between adjacent sheets is 2:1 and the maximum ratio of the thickest to thinnest sheet is 2.5:1.

3.1.3 Spot-Weld Spacing and Edge Distance

The spot-weld spacing and edge distances are as follows:

(a) Spot-weld spacing shall be derived from Table XIX.

(b) The minimum edge distance, as measured from the center of the electrode impression shall not be less than 2.5t plus 0.1 inches (t = thickness of the thinner outer sheet).

TABLE XIX – SPOT-WELD SPACING – INCHES(2)

THICKNESS(1) (IN.)	STANDARD SPOT-WELD SPACING (IN.)	MINIMUM SPOT-WELD SPACING (IN.)	MAXIMUM SPOT-WELD SPACING (IN.)
.020	0.62	0.50	0.65
.025	0.65	0.55	0.70
.032	0.80	0.65	0.85
.040	0.90	0.85	1.20
.050	1.00	0.90	1.25
.063	1.25	1.00	1.40
.071	1.30	1.10	1.40
.080	1.40	1.20	1.50
.090	1.50	1.25	1.55
.100	1.60	1.30	1.60
.112	1.65	1.35	1.65
.125	1.70	1.40	1.70

(1) Thickness of thinnest outer sheet in the joint.

(2) Measured from center of electrode impression.

3.1.4 Operational Temperature

A maximum operational temperature range of -67°F to 200°F is established for the 250°F curing epoxy paste adhesives used in weldbonded joints.

3.2 Joint Design Properties

Under this program, thirty-six (36) weldbond joints with distinct combinations of adherend thickness, overlap length and weld pattern were tested for static and fatigue properties. These specimens were single overlap butt splice joints and were tested in a tensile shear mode. These included adherend thicknesses from 0.020 inch to 0.090 inch, splice overlaps from 0.50 inch to 2.50 inch and various weld patterns. Figures 16, 17, 18 and 19 and Table XX further define individual configuration geometries. Adherend aluminum alloy is typically 7075-T6 bare but some straps are 2024-T3 clad one-side (Configurations 3, 5, 6 and 8) to simulate the weldbonded C-130 joint design. In Figures 16 through 19 and Table XX, $ed^{(1)}$ and $ed^{(2)}$ identify the edge distance from the center of spot-weld to edge of joint strap and the edge distance from the center of spot-weld to the length wise edge of the adherend, respectively.

All specimens fabricated for joint static and fatigue testing were made with M6300 (Whittaker) epoxy paste adhesive cured for one (1) hour at 250°F. The surface preparation of the adherends for static test specimens of joint configurations 1 through 4 (except 160°F test specimens for Configurations 1 and 2) was the standard metal bond etch for bonding. Due to welding difficulties involving metal expulsion around weld nuggets, the standard spot-weld etch procedure was used for preparing the surfaces of the remaining specimens.

3.2.1 Joint Static Properties

Static strength properties for joint geometries defined above were determined in the temperature range -67°F to 160°F. Further testing of specimens with selected geometries was conducted at 200°F. The number of specimens fabricated and tested with no prior exposures to hostile environments is shown in Table XXI.

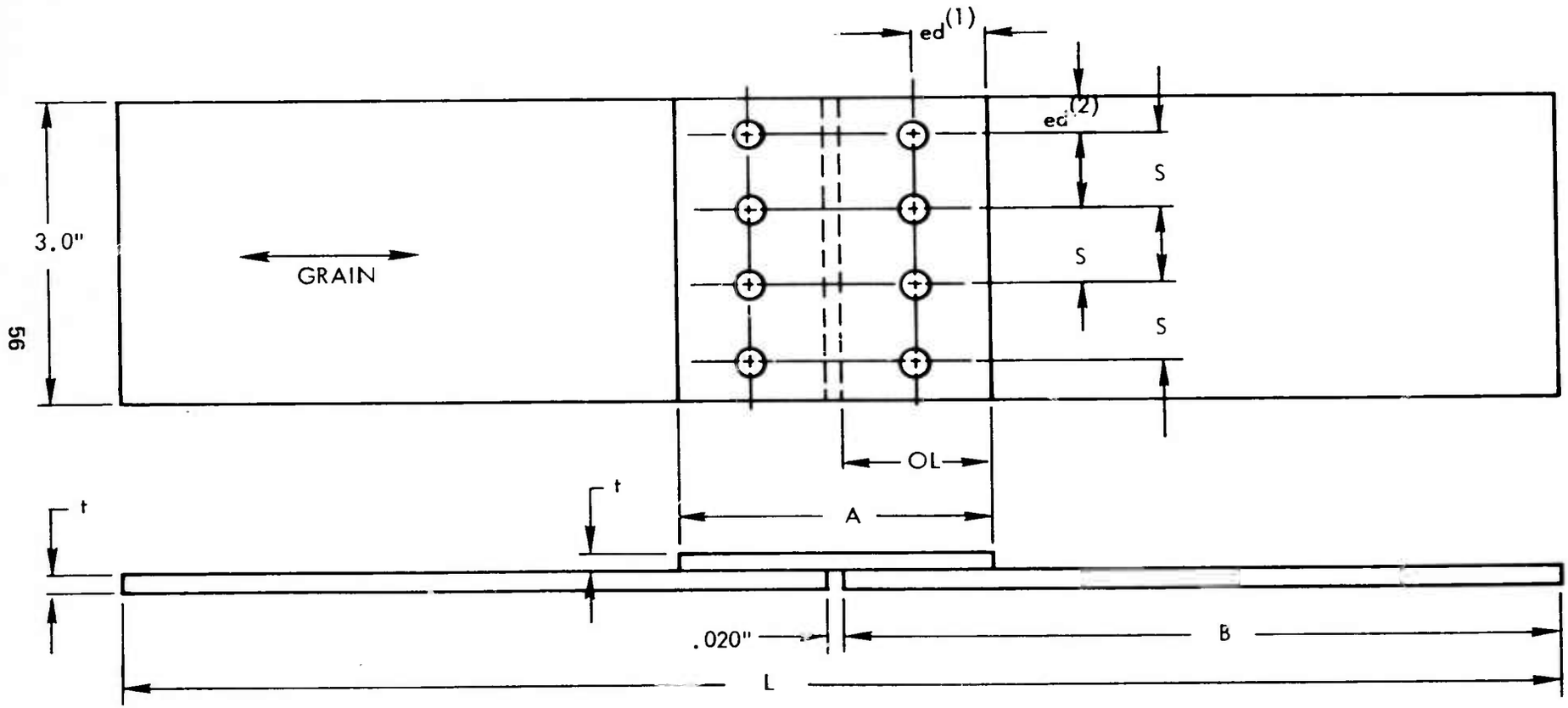

FIGURE 16 – CENTERED ROW WELD PATTERN SPECIMEN (4 WELD SPACING)

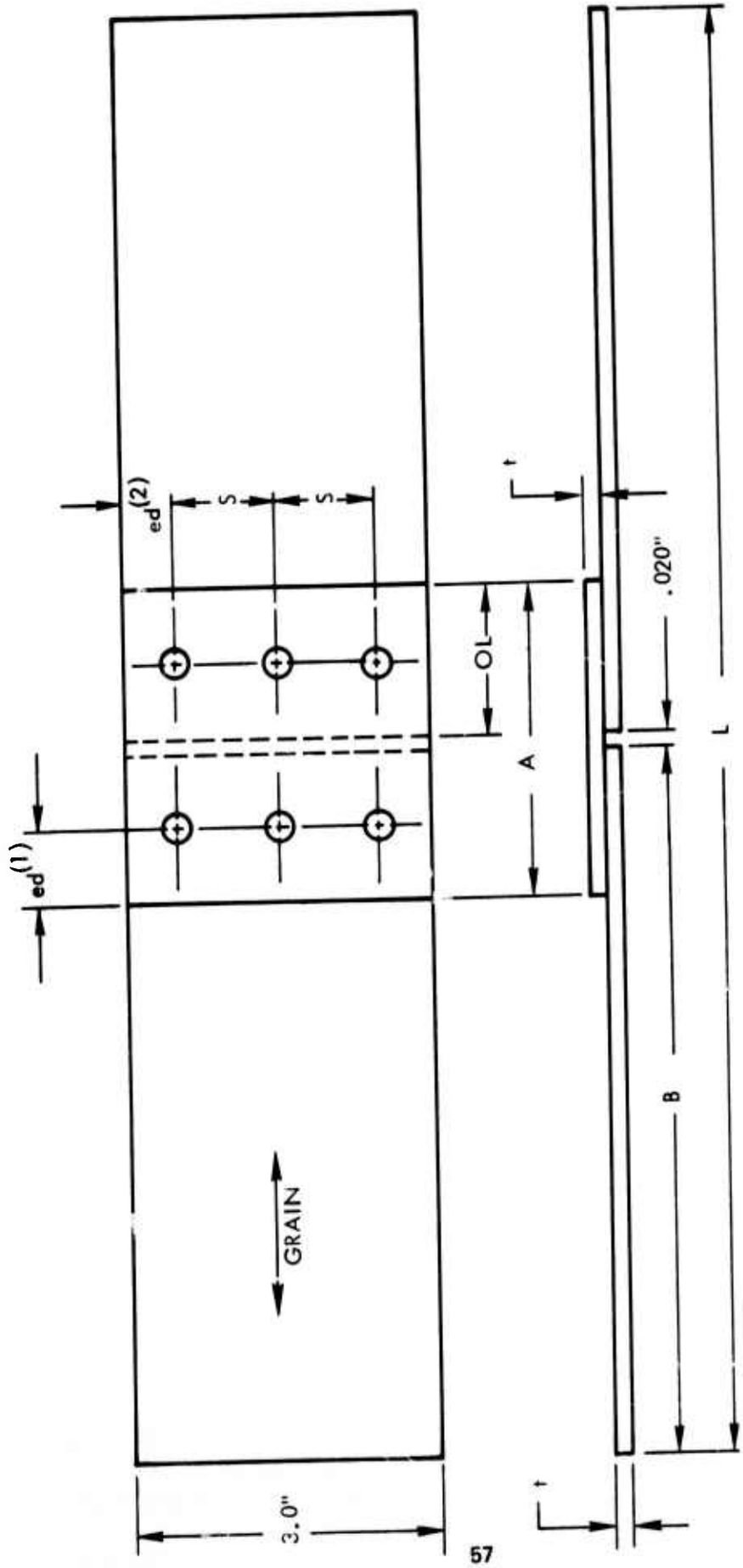

FIGURE 17 – CENTERED ROW WELD PATTERN SPECIMEN (3 WELD SPACING)

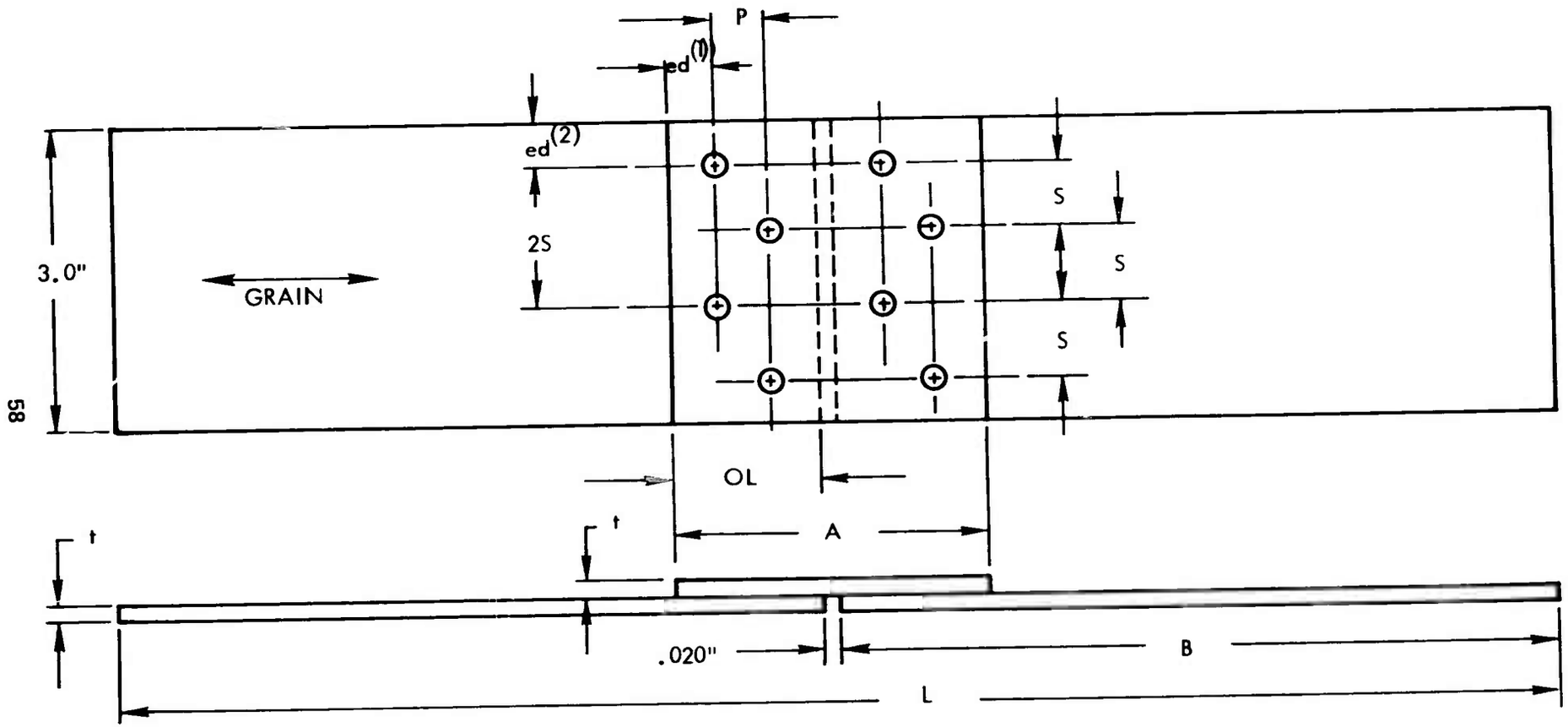

FIGURE 18 – STAGGERED ROW WELD PATTERN SPECIMEN

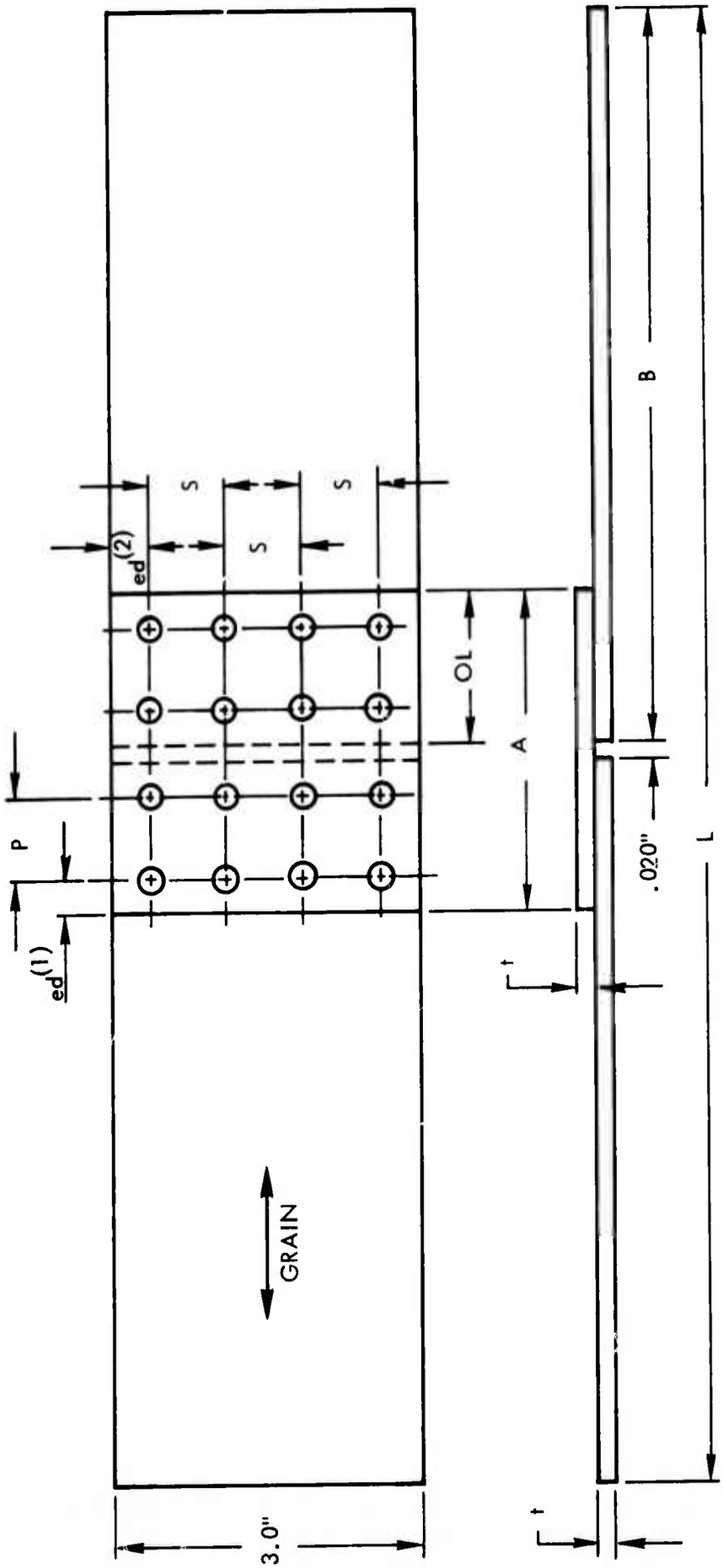

FIGURE 19 – DOUBLE ROW WELD PATTERN SPECIMEN

TABLE XX – JOINT SPECIMEN GEOMETRY

Config. Number	t (in.)	OL (in.)	Weld Pattern (Figure No.)	S (in.)	P (in.)	$ed^{(1)}$ (in.)	$ed^{(2)}$ (in.)	A (in.)
1	.050	1.00	16	0.75	–	0.50	0.375	2.02
2	.050	1.00	18	0.75	0.30	0.35	0.375	2.02
3	.050	0.62	16	0.75	–	0.31	0.375	1.26
4	.071	1.00	18	0.75	0.30	0.35	0.375	2.02
5	.050	0.62	17	1.25	–	0.31	0.25	1.26
6	.050	0.62	17	1.00	–	0.31	0.50	1.26
7	.032	0.64	16	0.75	–	0.32	0.375	1.30
8	.050	1.30	19	0.75	0.70	0.30	0.375	2.62
9	.032	0.90	18	0.75	0.20	0.35	0.375	1.82
10	.050	0.80	17	1.00	–	0.40	0.50	1.62
11	.071	0.80	17	1.00	–	0.40	0.50	1.62
12	.090	1.00	17	1.00	–	0.50	0.50	2.02
13	.050	0.80	16	0.75	–	0.40	0.375	1.62
14	.090	1.30	17	1.00	–	0.65	0.50	2.62
15	.050	1.20	18	0.75	0.50	0.35	0.375	2.42
16	.071	1.20	18	0.75	0.50	0.35	0.375	2.42
17	.032	1.10	18	0.75	0.40	0.35	0.375	2.22
18	.071	1.00	16	0.75	–	0.50	0.375	2.02
19	.025	0.50	16	0.75	–	0.25	0.375	1.02
20	.025	0.80	18	0.75	0.30	0.25	0.375	1.62
21	.040	0.80	16	0.75	–	0.40	0.375	1.62
22	.063	1.25	18	0.75	0.55	0.35	0.375	2.52
23	.080	1.60	18	0.75	0.80	0.40	0.375	3.22
24	.090	1.80	18	0.75	0.90	0.45	0.375	3.62
25	.080	1.00	16	0.75	–	0.50	0.375	2.02
26	.040	1.00	18	0.75	0.30	0.35	0.375	2.02
27	.063	1.60	18	0.75	0.90	0.35	0.375	3.22
28	.071	1.80	18	0.75	1.10	0.35	0.375	3.62
29	.080	2.00	18	0.75	1.20	0.40	0.375	4.02
30	.090	2.25	18	0.75	1.35	0.45	0.375	4.52
31	.063	0.90	16	0.75	–	0.45	0.375	1.82
32	.071	2.00	18	0.75	1.30	0.35	0.375	4.02
33	.063	1.50	18	0.75	0.80	0.35	0.375	3.02
34	.020	0.64	18	0.75	0.20	0.22	0.375	1.30
35	.080	2.25	18	0.75	1.45	0.40	0.375	4.52
36	.090	2.50	18	0.75	1.60	0.45	0.375	5.02

All Specimens –

B = 6.00", L = 12.02" (Static Test Specimens)

B = 9.00", L = 18.02" (Fatigue Test Specimens)

Adherend Alloy – 7075-T6 Bare except for Configurations 3, 5, 6, and 8 which had 2024-T3 clad one side straps (bare side bonded) and 7075-T6 bare splices.

TABLE XXI – JOINT STATIC TESTING

Configuration Number	Test Temperature		
	-67^{o}	Room Temperature	$160^{o}F$
1	30	30	30*
2	30	30	30
3	30	30	30*
4	30	30	30
5	3	30	3
6	3	30	3
7	3	30	3
8	3	30	3
9	3	10	3
10	3	10	3
11	3	10	3
12	3	10	3
13	3	10	3
14	3	10	3
15	3	10	3
16	3	10	3
17	3	10	3
18	3	10	3
19	3	10	3
20	3	10	3
21	3	10	3
22	3	10	3
23	3	10	3
24	3	10	3
25	3	10	3
26	3	10	3
27	3	10	3
28	3	10	3
29	3	10	3
30	3	10	3
31	3	10	3
32	3	10	3
33	3	10	3
34	3	10	3
35	3	10	3
36	3	10	3

* Ten (10) additional specimens tested at $200^{o}F$

In addition, specimens for both short term and long-term exposures to aggressive environments were fabricated under this program. All joint specimens subjected to aggressive environment under this program were sealed along their cut bondline edges with MIL-S-8802 sealant. In these design oriented tests, this was done to simulate actual weldbond aircraft structure usage where no cut bondline would remain unsealed. Testing of the short-term environment specimens as shown in Table XXII was completed. Long term on-site exposures of specimens as shown in Table XXIII are presently being conducted.

The average strengths of specimens tested at -67°F, room temperatures, 160°F and 200°F are shown in Table XXIV. Joint strengths are given in pounds per inch width. In Figure 20, the room temperature average joint strength data is repeated on an adherend stress at joint failure basis. Table XXV shows minimum values for the same data and Table XXVI presents "B" values for test sets in which the population is adequate for "B" value calculation. The predominant mode of failure for all weldbond static joint specimens was a mixture of cohesive and adhesive-to-metal failure in the bondline with shear failures of the welds. The typical joint failure mode was 75 percent cohesive and 25 percent adhesive-to-metal. For specimens prepared using the metal bond etch surface preparation, the prevailing failure mode was cohesive. In certain joints, the predominent failure mode was metal failure in the adherends through the welds. The joint configurations which exhibited this type of failure are indicated in Figure 20. Failure stresses indicated in this figure were calculated on a simple load/area basis while the effect of eccentricities in the test specimens are accounted for by considering the data for each adherend thickness separately. The superimposed curves are a "best fit" family of curves representing typical joint failure stresses for various overlaps and thicknesses for 7075-T6 adherends. A redundant cross-plot of common overlap length/thickness (L/t) ratios is presented to further clarify the presentation.

The results of short-term exposure to either salt spray or high humidity of specimens as defined in Table XXII are shown in Figures 21, 22, 23 and 24. As indicated by these figures, no reduction of strength values resulted from exposure up to ninety days in these environments. Similarly, degrading effects of ninety-day exposure to JP-4 fuel, hydraulic oil and temperature-humidity cycling on weldbond joint specimens were not indicated by the test results reported in Table XXVII.

TABLE XXII – JOINT STATIC TESTING AFTER SHORT-TERM AGGRESSIVE ENVIRONMENT EXPOSURES

Configuration Number	Salt Spray 30 days	Salt Spray 60-90 days		High Humidity 30 days	High Humidity 60-90 days		JP-4 Fuel 90 days	Hydraulic Oil 90 days	Temperature - Humidity 90 cycles
1	10	5	5	10	5	5	5	5	10
2	10	5	5	10	5	5	5	5	10
3	10	5	5	10	5	5	5	5	10
4	10	5	5	10	5	5	5	5	10

TABLE XXIII – JOINT TESTING AFTER LONG-TERM AGGRESSIVE ENVIRONMENT EXPOSURE

Configuration Number	McCook, Illinois				Patrick AFB, Florida			
	18 Months		36 Months		18 Months		36 Months	
	Fillet Sealed	Fillet Unsealed	Fillet Sealed	Fillet Unsealed	Fillet Sealed	Fillet Unsealed	Fillet Sealed	Fillet Unsealed
3	3	3	3	3	3	3	3	3

NOTE: (1) Three (3) additional specimens were fabricated along with the above twenty-four (24) specimens and tested as controls.

TABLE XXIV – JOINT STATIC TEST RESULTS, AVERAGE STRENGTH

Configuration	–67°F	Room Temp.	160°F	200°F
1	3223	3375	2739	2500
2	3400	3457	2704	–
3	2201	1885	1933	1735
4	2910	2784	3006	
5	1473	1805	1535	
6	1471	1602	1698	
7	1440	1915	1877	
8	2802	2735	2751	
9	2320	2235	2244	
10	2198	2474	2462	
11	1915	2267	2400	
12	1953	2457	2553	
13	2122	2450	2373	
14	2102	2944	2980	
15	2702	3305	3109	
16	2260	3139	2907	
17	2353	2264	2229	
18	2020	2694	2682	
19	1476	1653	1653	
20	1851	1783	1771	
21	1815	2149	2378	
22	2431	3465	3822	
23	3122	4339	4467	
24	3011	4245	4300	
25	2247	2715	2895	
26	1969	2879	2751	
27	3011	4298	4367	
28	3778	4437	4533	
29	3922	4923	4822	
30	3944	5033	5255	
31	2147	2678	2500	
32	4444	4840	4377	
33	3078	4156	3844	
34	–	1404	–	
35	4622	5353	4955	
36	5978	6018	5733	

NOTE: All strengths listed above are in pounds per inch of width. The metal bond etch surface preparation was used in fabrication of specimen joint configurations 1 through 4 (except 160°F for configurations 1 and 2) while all others were prepared with the spot-weld etch surface preparation.

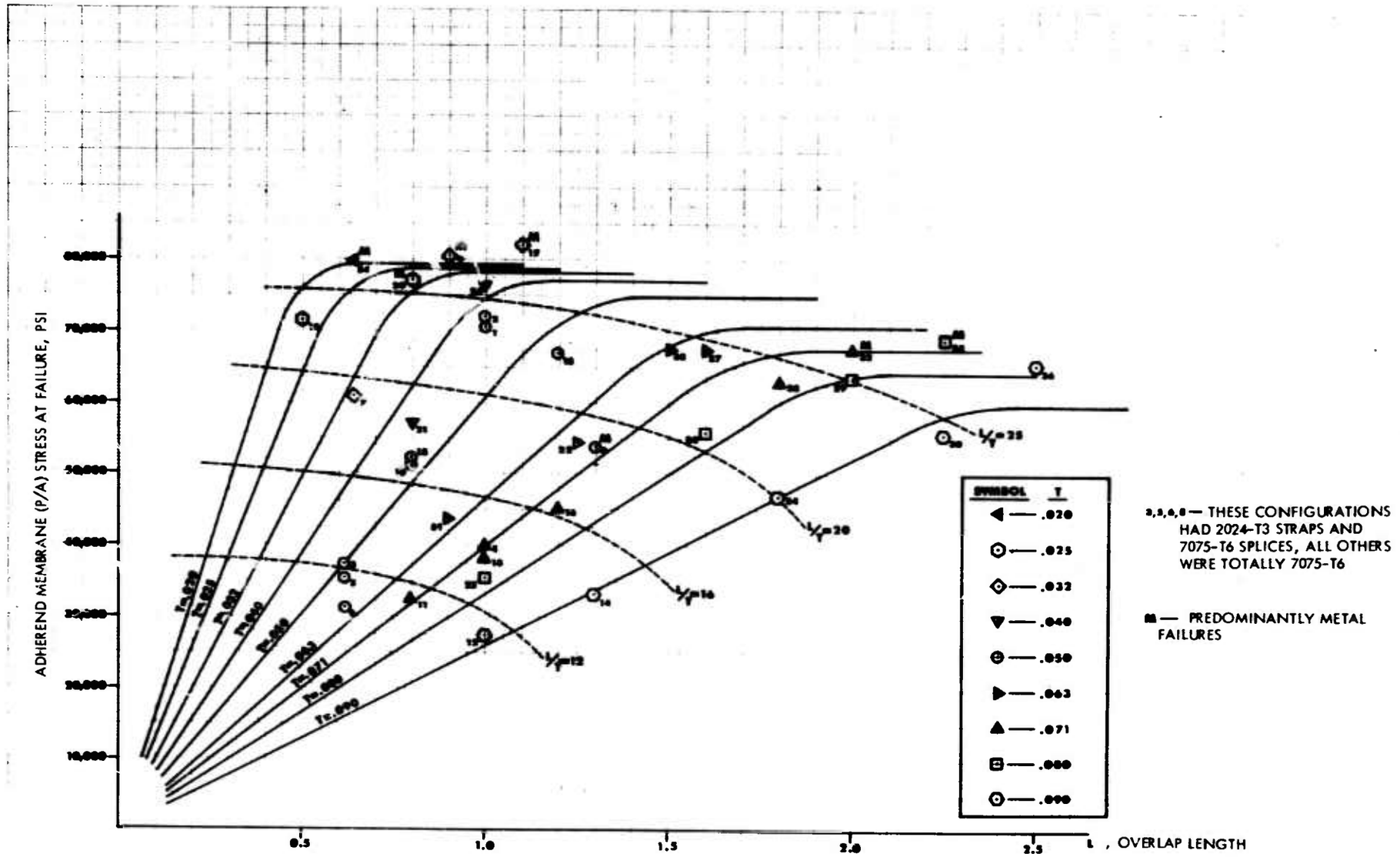

FIGURE 20 – ADHEREND STRESS AT FAILURE VS OVERLAP LENGTH -7075-T6 ADHEREND

TABLE XXV – JOINT STATIC TEST RESULTS, MINIMUM STRENGTH

Configuration	–67°F	Room Temp.	160°F	200°F
1	2800	3000	2333	2300
2	2900	3000	2166	–
3	2000	1667	1547	1550
4	2540	2433	2533	
5	1467	1567	1453	
6	1407	1500	1640	
7	1333	1408	1833	
8	2727	2608	2733	
9	2287	2216	2207	
10	2160	2283	2200	
11	1880	2133	2240	
12	1927	2275	2467	
13	2027	2133	2293	
14	2027	2500	2947	
15	2380	2950	2933	
16	2120	2858	2427	
17	2347	2216	2187	
18	1960	2491	2613	
19	1433	1592	1627	
20	1753	1725	1747	
21	1733	1933	2248	
22	2333	2925	3600	
23	2867	3808	4300	
24	2900	4016	4167	
25	2196	2933	2787	
26	1927	2750	2633	
27	2933	4117	4300	
28	3600	4183	4400	
29	3833	4800	4567	
30	3600	4333	5066	
31	2086	2467	2360	
32	4300	4683	4233	
33	2733	3925	3700	
34	--	1342	–	
35	4567	4850	4933	
36	5900	5866	5533	

NOTE: All strengths listed above are in pounds per inch of width. The metal bond etch surface preparation was used in fabrication of specimen joint configurations 1 through 4 (except 160°F for configurations 1 and 2) while all others were prepared with the spot-weld etch surface preparation.

TABLE XXVI – JOINT STATIC TEST RESULTS, "B" VALUES

Configuration	–67°F	Room Temp.	160°F
1	2828	2842	2297
2	2842	3081	2116
3	1950	1675	1681
4	2610	2436	2583
5	–	1519	–
6	–	1471	–
7	–	1591	–
8	–	2606	–

NOTE: All strengths listed above are in pounds per inch of width. The "B" values in this table and elsewhere in this report are statistically computed. The "B" value is the value above which 90 percent of the population of test specimen values is expected to fall, with a confidence level of 95 percent.

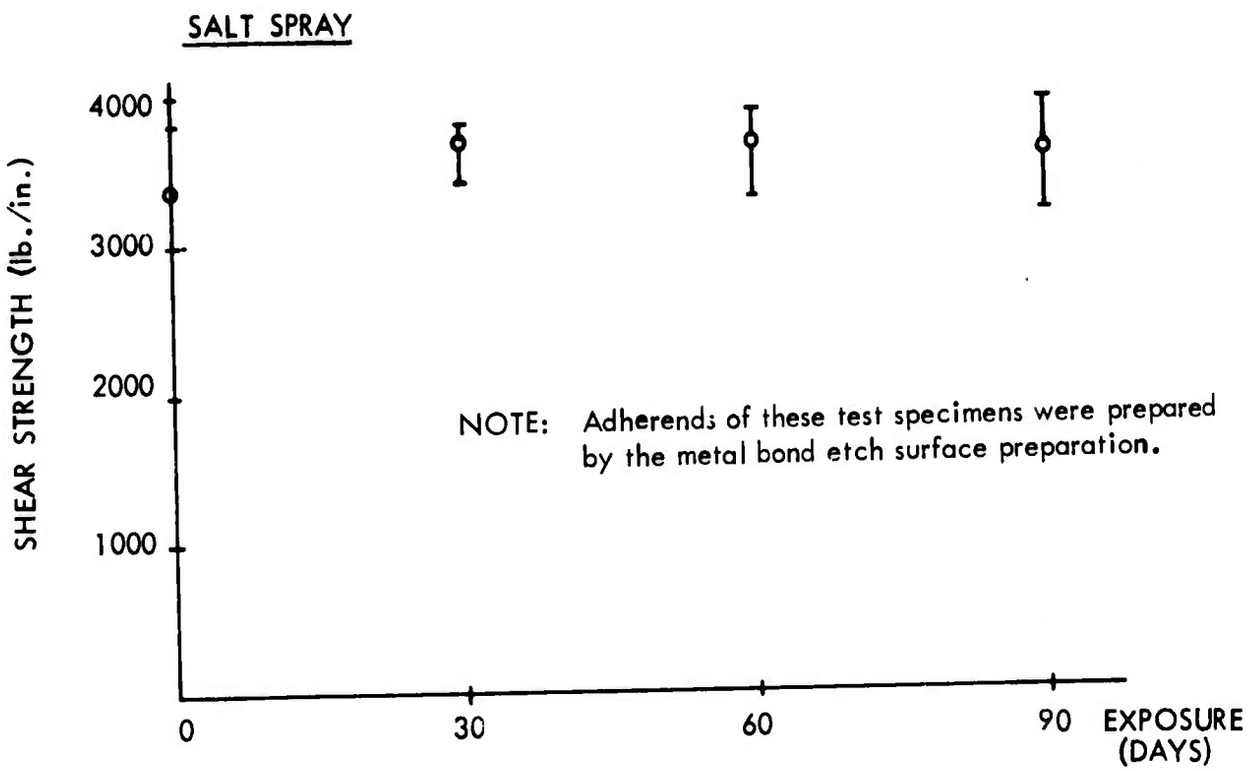

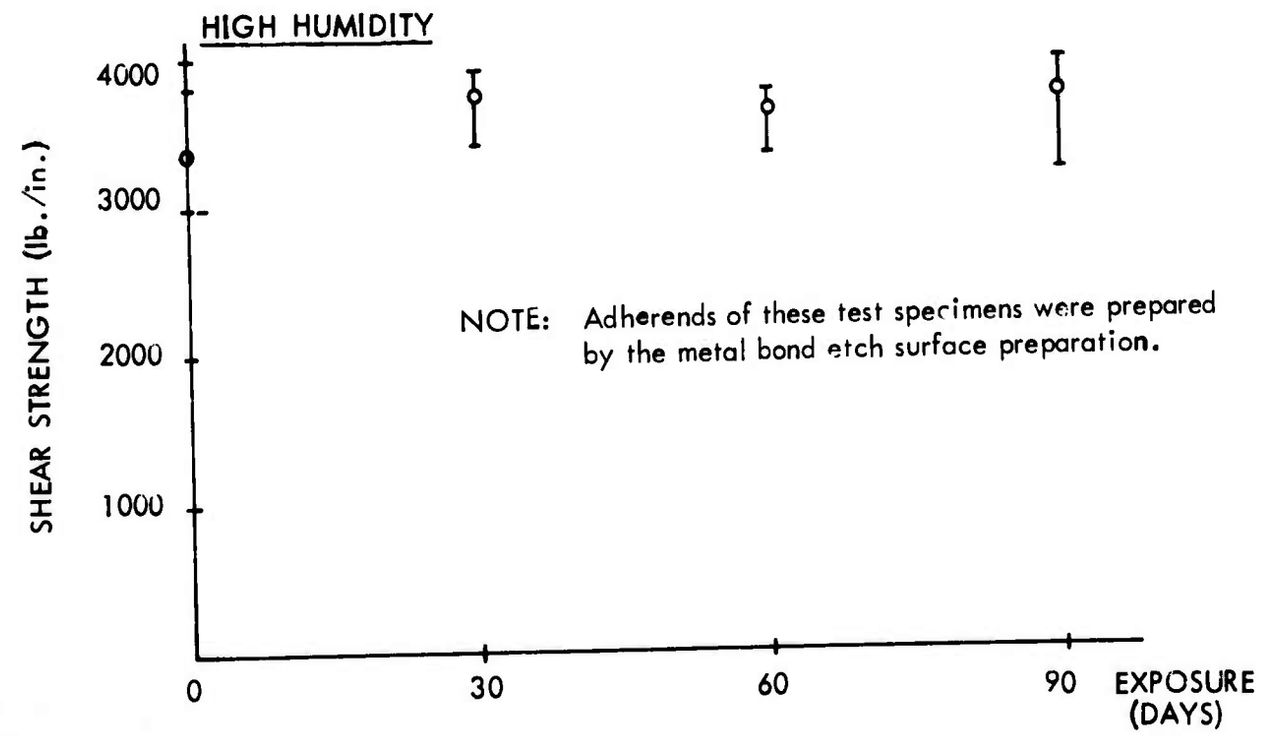

FIGURE 21 – SALT SPRAY AND HIGH HUMIDITY EXPOSURE DATA – CONFIGURATION 1

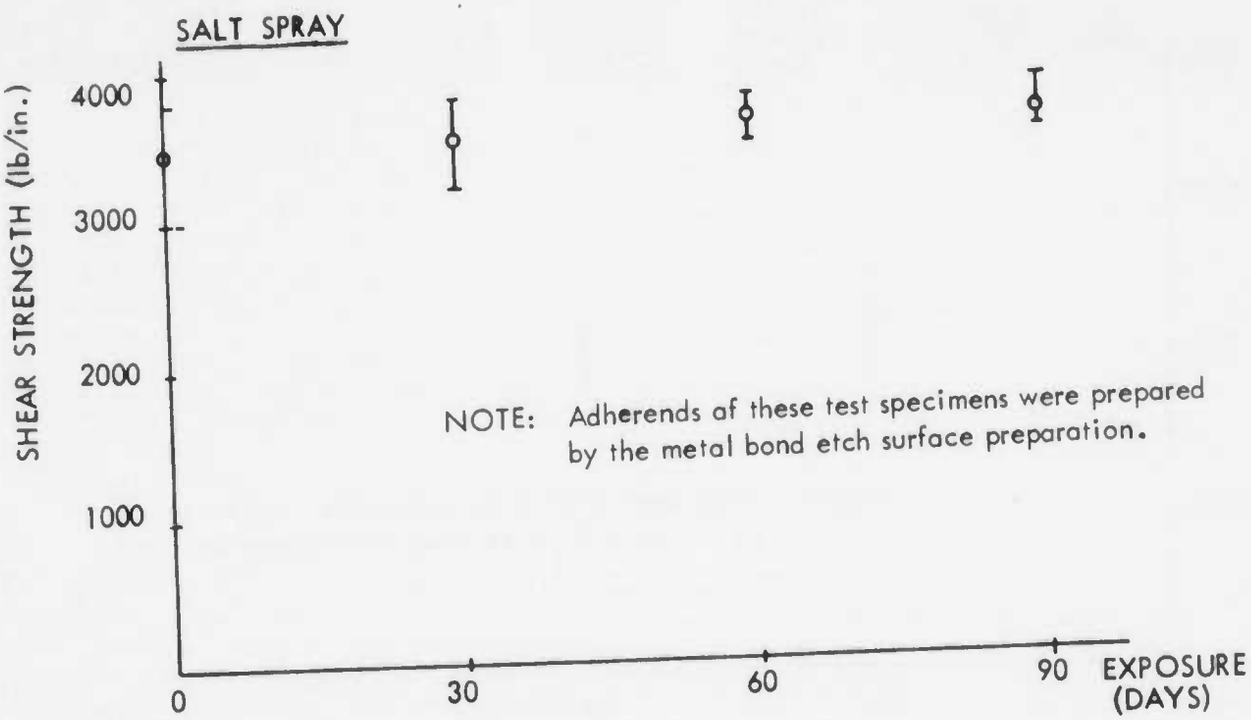

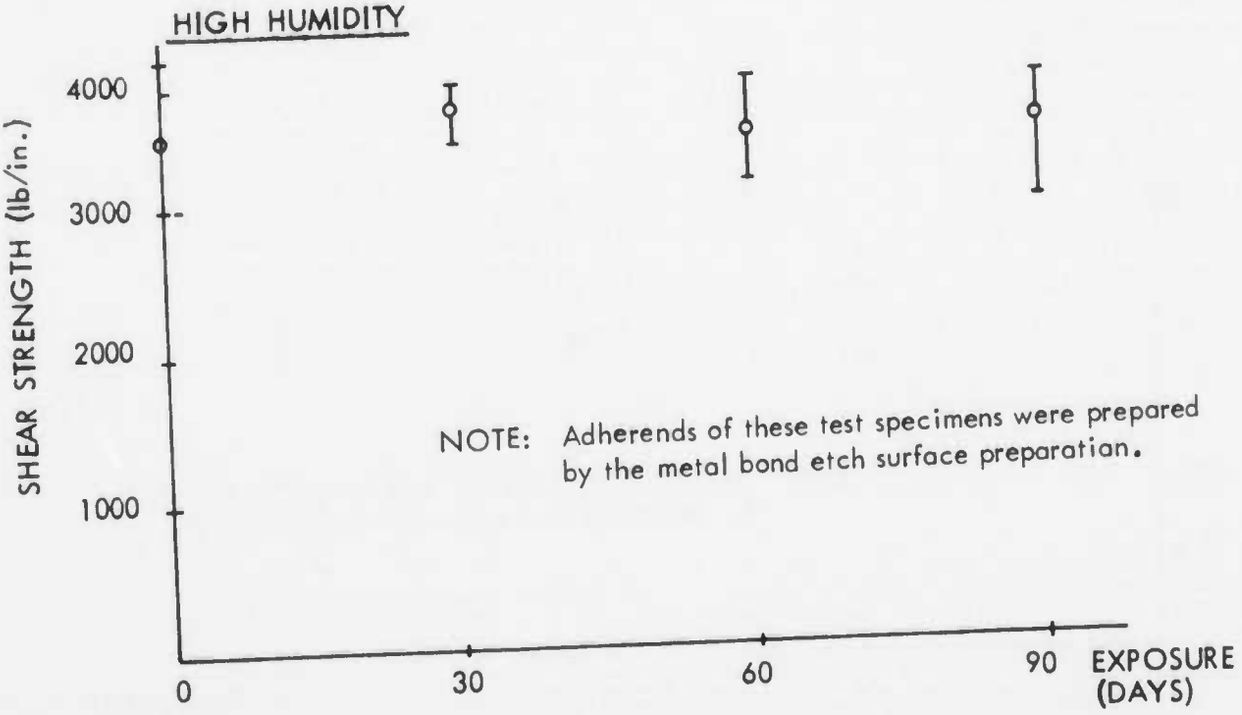

FIGURE 22 – SALT SPRAY AND HIGH HUMIDITY EXPOSURE DATA – CONFIGURATION 2

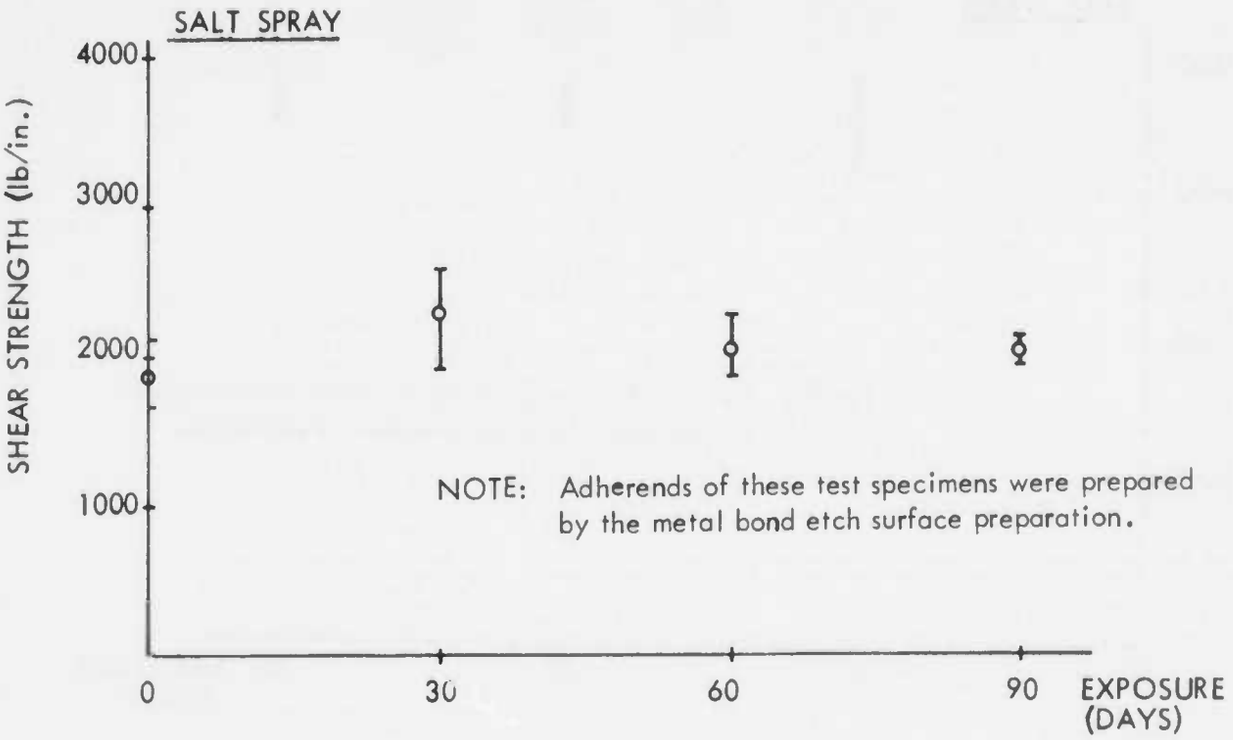

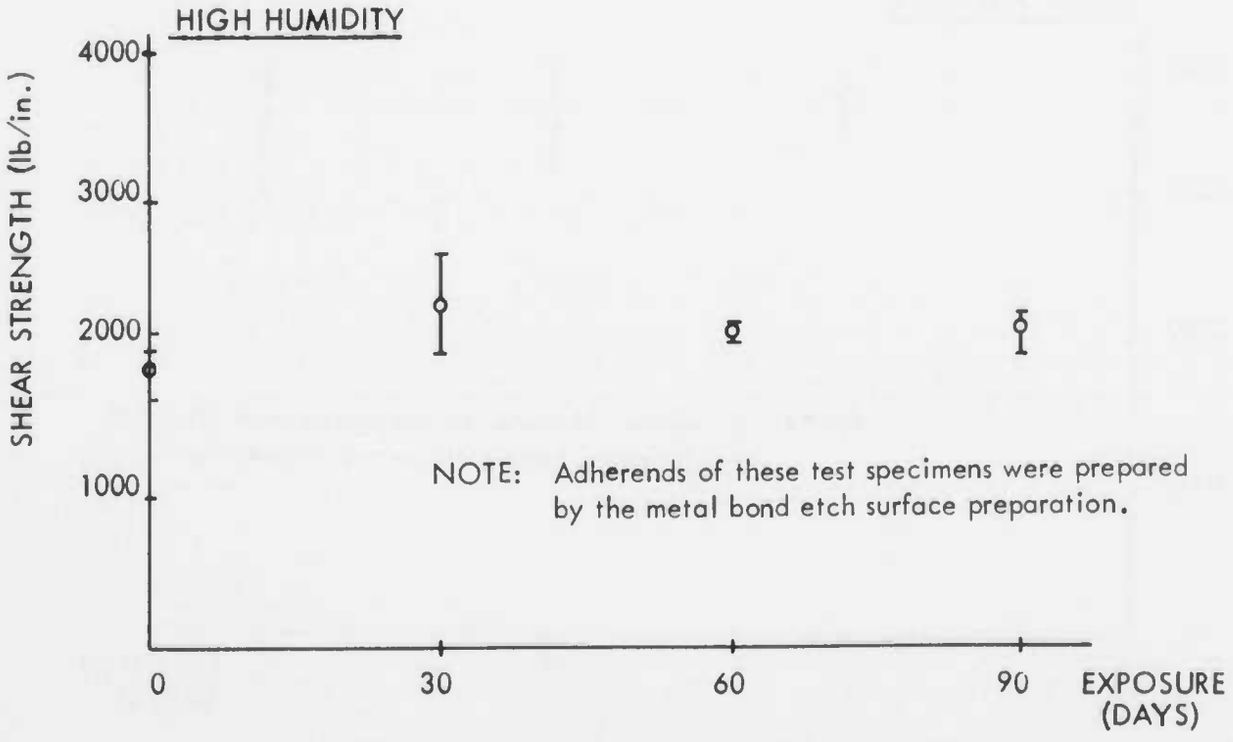

FIGURE 23 – SALT SPRAY AND HIGH HUMIDITY EXPOSURE DATA – CONFIGURATION 3

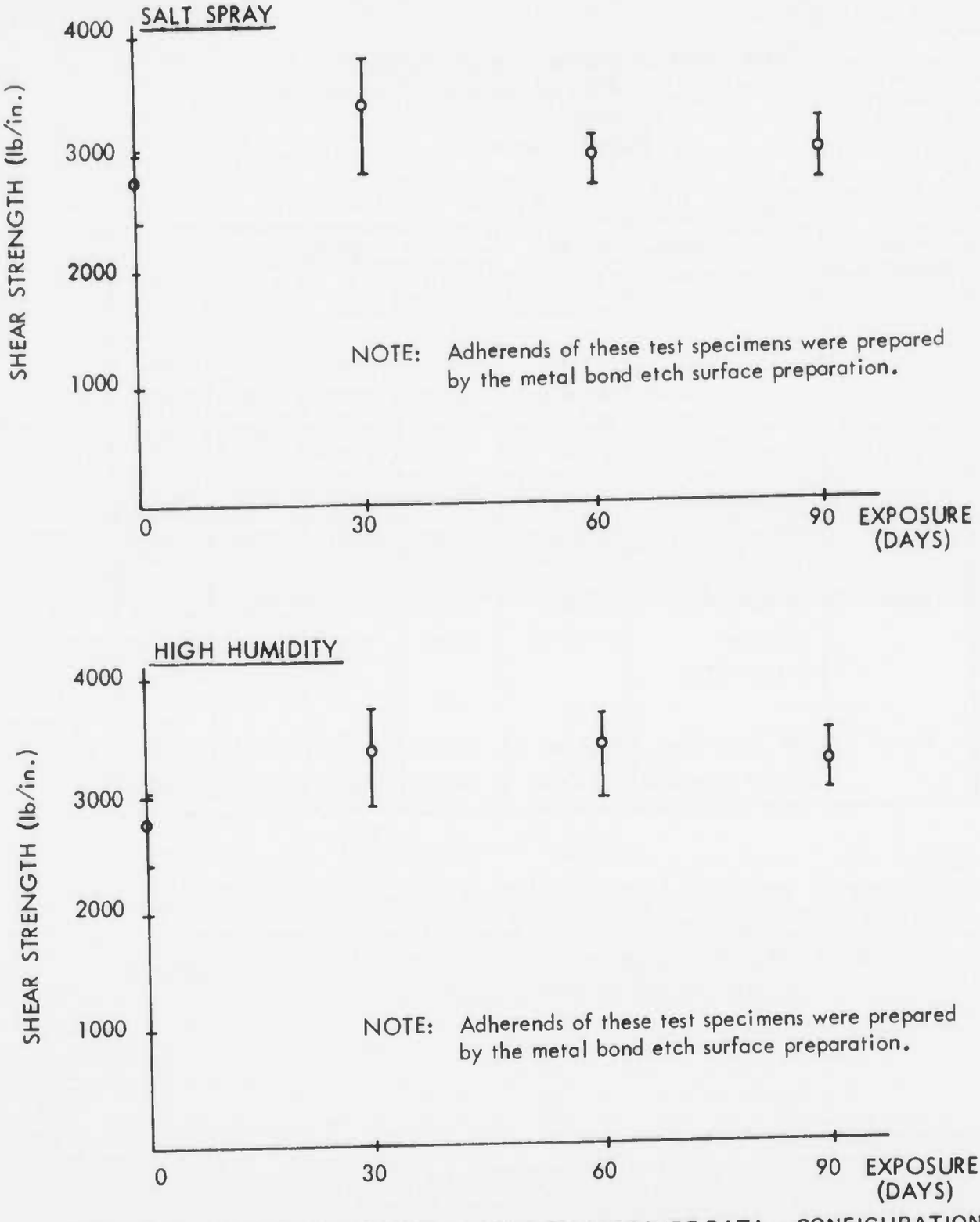

FIGURE 24 – SALT SPRAY AND HIGH HUMIDITY EXPOSURE DATA – CONFIGURATION 4

Table XXVII – Joint Shear Strength After Exposure to JP-4 Fuel, Hydraulic Oil or Temperature Humidity Cycling. (lb/inch of width)

Test Temperature	Prior Exposure	Strength Value	Configuration			
			1	2	3	4
	–	Average	3374	3475	1885	2784
		Minimum	3000	3000	1667	2433
		"B" Value	2842	3081	1675	2436
Room	JP-4 (90 Days) (MIL-J5624)	Average	3637	3527	2185	3180
		Minimum	3325	3233	1950	2766
Room	Hydraulic Oil (90 Days) (MIL-H-5606)	Average	3725	3630	2200	3193
		Minimum	3583	3275	2083	2650
Room	(90 Cycle, Temp.-Humidity Cycling)	Average	3750	3770	2250	3144
		Minimum	3200	3400	1950	2667

NOTE:

(1) Adherends of these test specimens were prepared by the metal bond etch surface preparation.

(2) The "B" strength values given in the above table are statistically computed as defined on Table XXVI.

Through these tests on four (4) specimen configurations, the most frequent mode of failure was 100% cohesive (79.7% of all specimens) while the next most frequent mode was net section of either the splice plate or the adherend (14.7% of all specimens). Adhesive-to-metal failures were reported over 10-25% of the failure surface in twenty (20) specimens. These occurred on Configuration 3 specimens subjected to 90 day or cycle exposure to either high humidity, JP-4 fuel, hydraulic oil or temperature-humidity cycles. Failure mode frequency is broken down by configuration, exposure and mode in Table XXVIII through XXXI.

The long-term environmental test specimens per Table XXIII were shipped to the Air Force Materials Laboratory Project Manager for disposition on or about 1 September 1973. These specimens were subjected to and passed both radiographic and ultrasonic inspection prior to delivery to the Air Force Project Manager. As noted, half of these specimens received fillet sealant while the other half received only sealing along cut edges.

Both sealed and unsealed test specimens are finished with systems representative of the interior and exterior surfaces of the C-130E fuselage. The "joint strap" side of each test specimen represents the interior surface while the opposite side is typical of the exterior surface. Three control specimens were tested directly after fabrication and the results are shown in Table XXXII.

TABLE XXVIII – SUMMARY OF FAILURE MODE DATA – CONFIGURATION 1

Environment	Days	Total Tests	Cohesive Failures	Cohesive w/Some Adhesive to Metal	Net Section of Metal
Control	–	30	30	0	0
Salt Spray	30	10	6		4
Salt Spray	60	5	5		0
Salt Spray	90	5	4		1
High Humidity	30	10	9		1
High Humidity	60	5	3		2
High Humidity	90	5	4		1
JP-4 Fuel	90	5	4		1
Hydraulic Oil	90	5	5		0
Temperature-Humidity 90 (Cycles)	90 (Cycles)	10	6	0	4

TABLE XXIX – SUMMARY OF FAILURE MODE DATA – CONFIGURATION 2

Environment	Days	Total Tests	Cohesive Failures	Cohesive w/Some Adhesive to Metal	Net Section of Metal
Control	–	30	25	0	5
Salt Spray	30	10	4		6
Salt Spray	60	5	4		1
Salt Spray	90	5	2		3
High Humidity	30	10	5		5
High Humidity	60	5	3		2
High Humidity	90	5	2		3
JP-4 Fuel	90	5	1		4
Hydraulic Oil	90	5	3		2
Temperature-Humidity	90 (Cycles)	10	2	0	8

TABLE XXX – SUMMARY OF FAILURE MODE DATA – CONFIGURATION 3

Environment	Days	Total Tests	Cohesive Failures	Cohesive w/Some Adhesive to Metal	Net Section of Metal
Control	–	30	30	0	0
Salt Spray	30	10	10	0	
Salt Spray	60	5	5	0	
Salt Spray	90	5	5	0	
High Humidity	30	10	10	0	
High Humidity	60	5	5	0	
High Humidity	90	5	1	4	
JP-4 Fuel	90	5	0	5	
Hydraulic Oil	90	5	4	1	
Temperature Humidity	90 (Cycles)	10	0	10	0

TABLE XXXI – SUMMARY OF FAILURE MODE DATA – CONFIGURATION 4

Environment	Days	Total Tests	Cohesive Failures	Cohesive w/Some Adhesive to Metal	Net Section of Metal
Control	–	30	30	0	0
Salt Spray	30	10	10		
Salt Spray	60	5	5		
Salt Spray	90	5	5		
High Humidity	30	10	10		
High Humidity	60	5	5		
High Humidity	90	5	5		
JP-4 Fuel	90	5	5		
Hydraulic Oil	90	5	5		
Temperature-Humidity	90 (Cycles)	10	10	0	0

TABLE XXXII – LONG-TERM ENVIRONMENTAL CONTROL SPECIMEN TEST RESULTS

Specimen No.	Failure Load (lb./in.)	Failure Mode
LG-C-1	1700	70% Cohesive; 30% Adhesive to Metal
LG-C-2	1750	70% Cohesive; 30% Adhesive to Metal
LG-C-3	1690	80% Cohesive; 20% Adhesive to Metal
	Avg. = 1713	

3.2.2 Fatigue Properties

Fatigue properties of specimens with weldbond joint configuration as defined earlier were determined according to the following schedule:

TABLE XXXIII – JOINT FATIGUE TESTING

Joint Configuration	Test Temperature	Maximum Adherend Stress Level (KSI)												
		30	26	22	20	18	16	15	14	13	12	11	10	9	7
1	Room	5	5	5		5		5							
1*	Room							3					3		
1	160°F	5		5		5		5		5					
2	Room	5	5	5		5		5							
2	160°F		5	5		5		5			5				
3	Room					5		5		5		5		5	
3	160°F							5		5		5		5	5
4	Room					5		5		5		5		5	
4	160°F							5		5		5		5	5
5	Room							3				3			
6	Room							3				3			
7	Room		3			3									
8	Room					3				3					
9	Room		3			3									
10	Room				3				3						
11	Room							3				3			
12	Room									3				3	
13	Room				3				3						
14	Room							3				3			
15	Room		3			3									
16	Room				3				3						
17	Room		3			3									
18	Room					3					3				
19	Room		3						3						
20	Room		3			3									
21	Room				3				3						
22	Room				3				3						
23	Room				3				3						
24	Room				3				3						
25	Room							3				3			
26	Room		3			3									
27	Room		3			3									
28	Room		3			3									
29	Room		3			3									
30	Room			3			3								
31	Room					3					3				
32	Room		3			3									
33	Room		3			3									
34	Room		3			3									
35	Room		3			3									
36	Room		3			3									

* Stress Ratio, R = -1.0. All other tests conducted at R = +0.1

As noted in this table, fatigue testing was conducted at room temperature and at 160°F. All of the fatigue tests, except as noted, were conducted at a stress ratio of +0.1. These specimens were stabilized to restrict lateral deflection through the use of support plates.

Figures 25 through 45 present individual specimen data for joint fatigue tests conducted under this program. Where two or more data sets are presented in a single figure, the configurations addressed have approximately the same overlap/adherend thickness (L/t) ratios. Figures 25 through 36 are arranged in the order of ascending L/t ratio. As expected, a general trend for similar weld patterns at a given stress level is that as L/t increases cycles to failure also increases and the frequency of metal failure through the spot-weld increases. Figures 37 and 38 compare staggered and centered weld patterns with all other joint parameters held constant. These figures show the effect of weld edge distance and relate to some of the internal joint stress distribution analysis results reported in Section IV of this report. The next two figures (Figure 39 and 40) show data and curves for specimens with 2024-T3 bare splice plates and 7075-T6 bare straps. All others were entirely 7075-T6 bare aluminum alloy.

Figure 39 indicates no significant effect on joint fatigue endurance resulting from spot-weld spacings in the range of 0.75 to 1.25 inches. Figures 41 through 44 compare elevated temperature fatigue test results with room temperature test results. This group of figures is arranged in their order of descending L/t ratio and indicate that as L/t ratio is decreased the effect of temperature is less pronounced. Referring to Figures 41 and 42, the effect of temperature on fatigue endurance of test specimens having a centered spot-weld pattern is greater at the higher stress levels than comparable tests on specimens having a staggered spot-weld pattern. Figure 45 shows the effect of stress reversal on fatigue endurance for the configuration 1 weldbonded test specimen.

Further general observations of these fatigue data results are that within a given overlap length versus adherend thickness (L/t) ratio, there is no further apparent effect of thickness on joint fatigue endurance and specimens tested at lower stress levels had a higher frequency of metal failures. Within the figures presenting weldbond joint fatigue data, metal failures are indicated by closed (shaded) data points while shear failure through the bondline is indicated by open points. Typical metal failures were through the spot-welds in either the adherend or the splice as shown in Figure 46. Bondline failures were typically mixed adhesive/cohesive failures ranging from 80% cohesive and 30% adhesive to 20% cohesive and 80% adhesive. Weld failures in these specimens were usually through shear in the bondline plane. Examples of these are shown in Figure 47.

LEGEND

SYMBOL	CONFIG. NO.	ADHEREND THICKNESS (IN.)	OVERLAP (IN.)	ACTUAL L/t	WELD PATTERN (FIGURE NO.)	S (IN.)	$ed^{(1)}$ (IN.)	$ed^{(2)}$ (IN.)	A (IN.)
◇	11	.071	0.80	11.3	17	1.00	0.40	0.50	1.62
⊙	12	.090	1.00	11.1	17	1.00	0.50	0.50	2.02

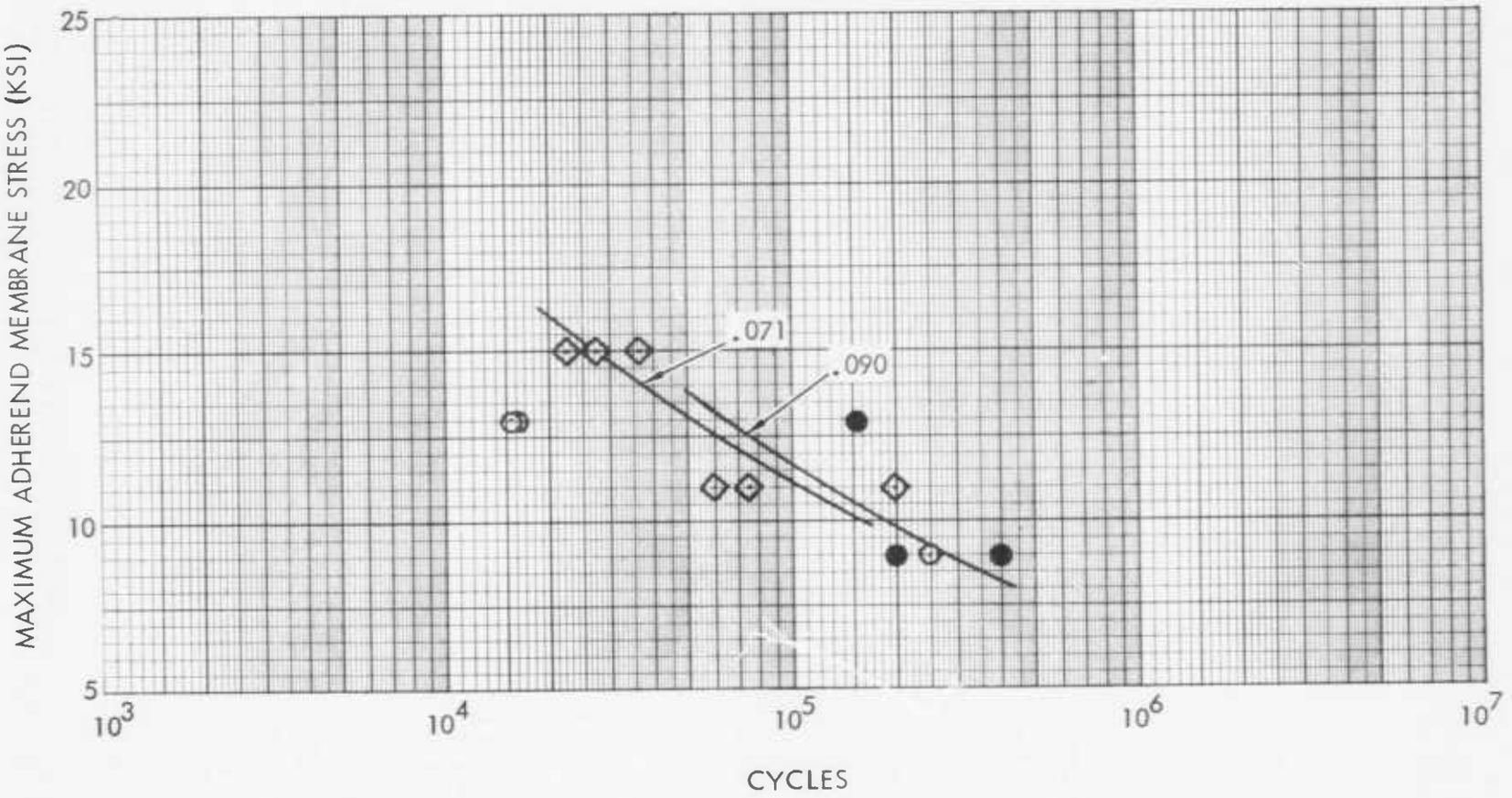

FIGURE 25 – WELDBOND JOINT S-N DATA, L/t = 11, R = 0.1

LEGEND

SYMBOL	CONFIG. NO.	ADHEREND THICKNESS (IN.)	OVERLAP (IN.)	ACTUAL L/t	WELD PATTERN (FIGURE NO.)	S (IN.)	$ed^{(1)}$ (IN.)	$ed^{(2)}$ (IN.)	A (IN.)
⊙	25	.080	1.00	12.5	16	0.75	0.50	0.375	2.02

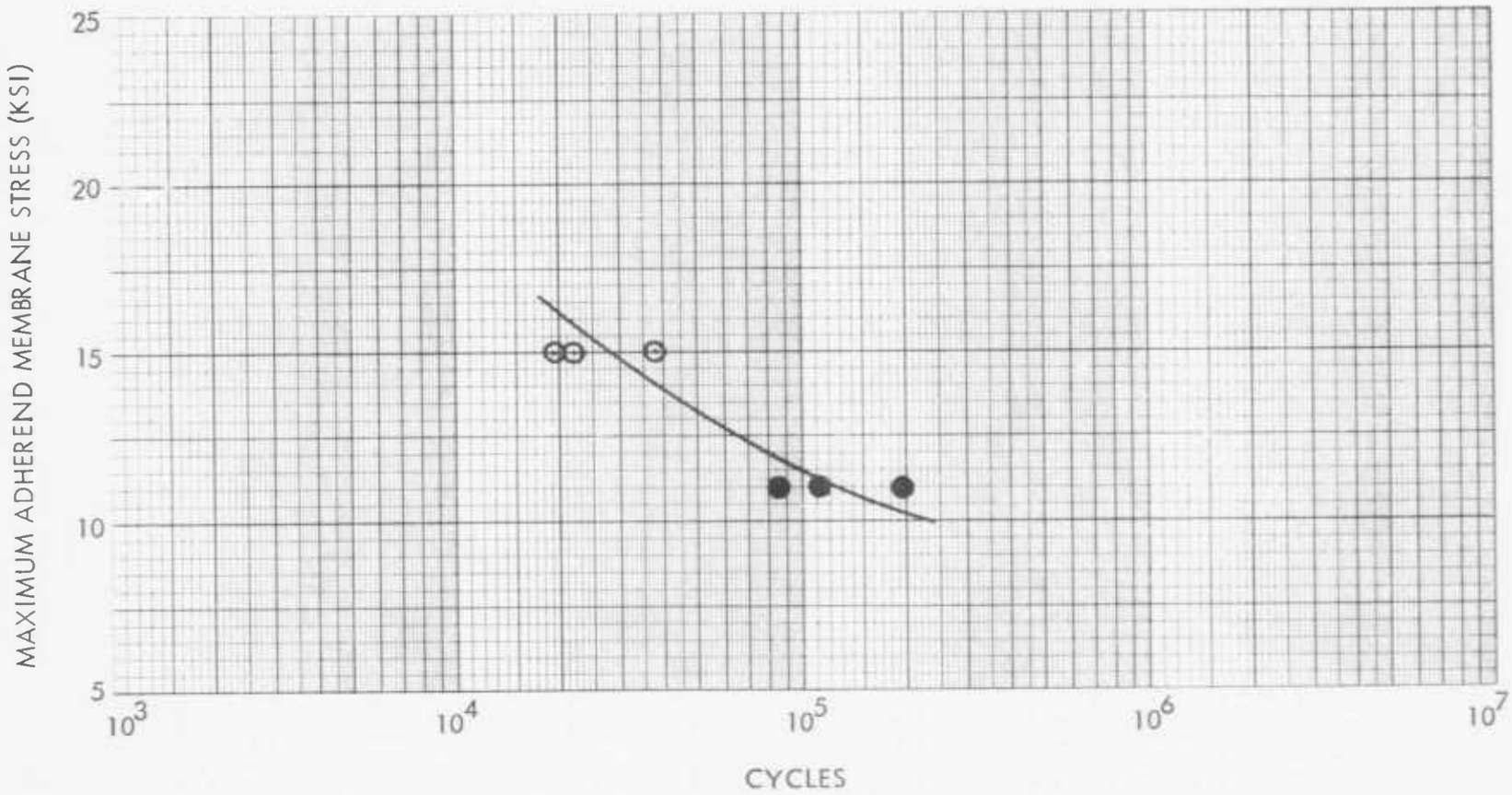

FIGURE 26 – WELDBOND JOINT S-N DATA, L/t = 12.5, R = 0.1

LEGEND

SYMBOL	CONFIG. NO.	ADHEREND THICKNESS (IN.)	OVERLAP (IN.)	ACTUAL L/t	WELD PATTERN (FIGURE NO.)	S (IN.)	$ed^{(1)}$ (IN.)	$ed^{(2)}$ (IN.)	A (IN.)
◇	31	.063	0.90	14.3	16	0.75	0.45	0.375	1.82
⬡	18	.071	1.00	14.1	16	0.75	0.50	0.375	2.02
△	14	.090	1.30	14.4	17	1.00	0.65	0.50	2.62

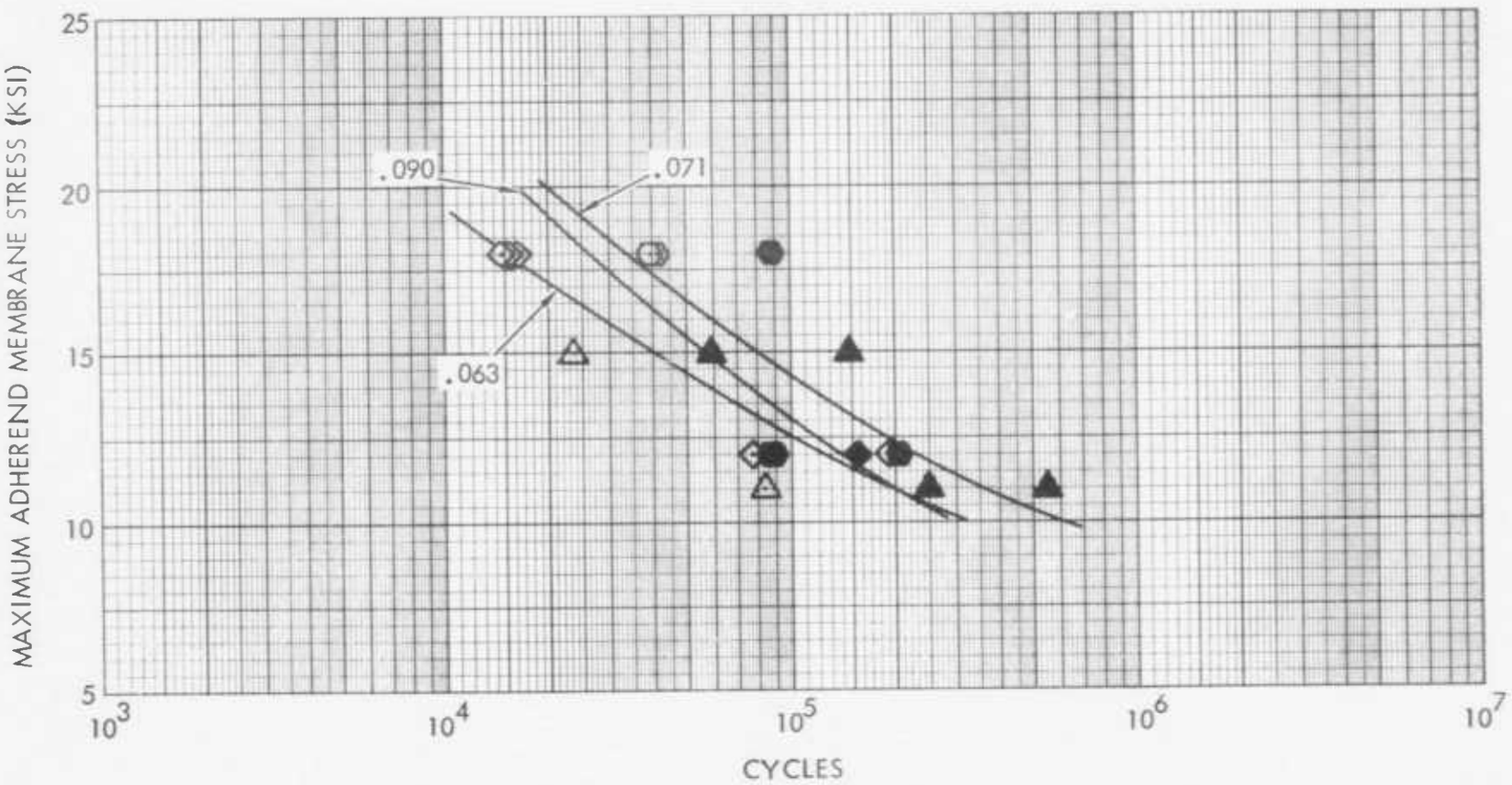

FIGURE 27 – WELDBOND JOINT S-N DATA, L/t = 14, R = 0.1 (CENTERED WELD)

LEGEND

SYMBOL	CONFIG. NO.	ADHEREND THICKNESS (IN.)	OVERLAP (IN.)	ACTUAL L/t	WELD PATTERN (FIGURE NO.)	S (IN.)	P (IN.)	$ed^{(1)}$ (IN.)	$ed^{(2)}$ (IN.)	A (IN.)
⊙	4	.071	1.00	14.1	18	0.75	0.30	0.35	0.375	2.02

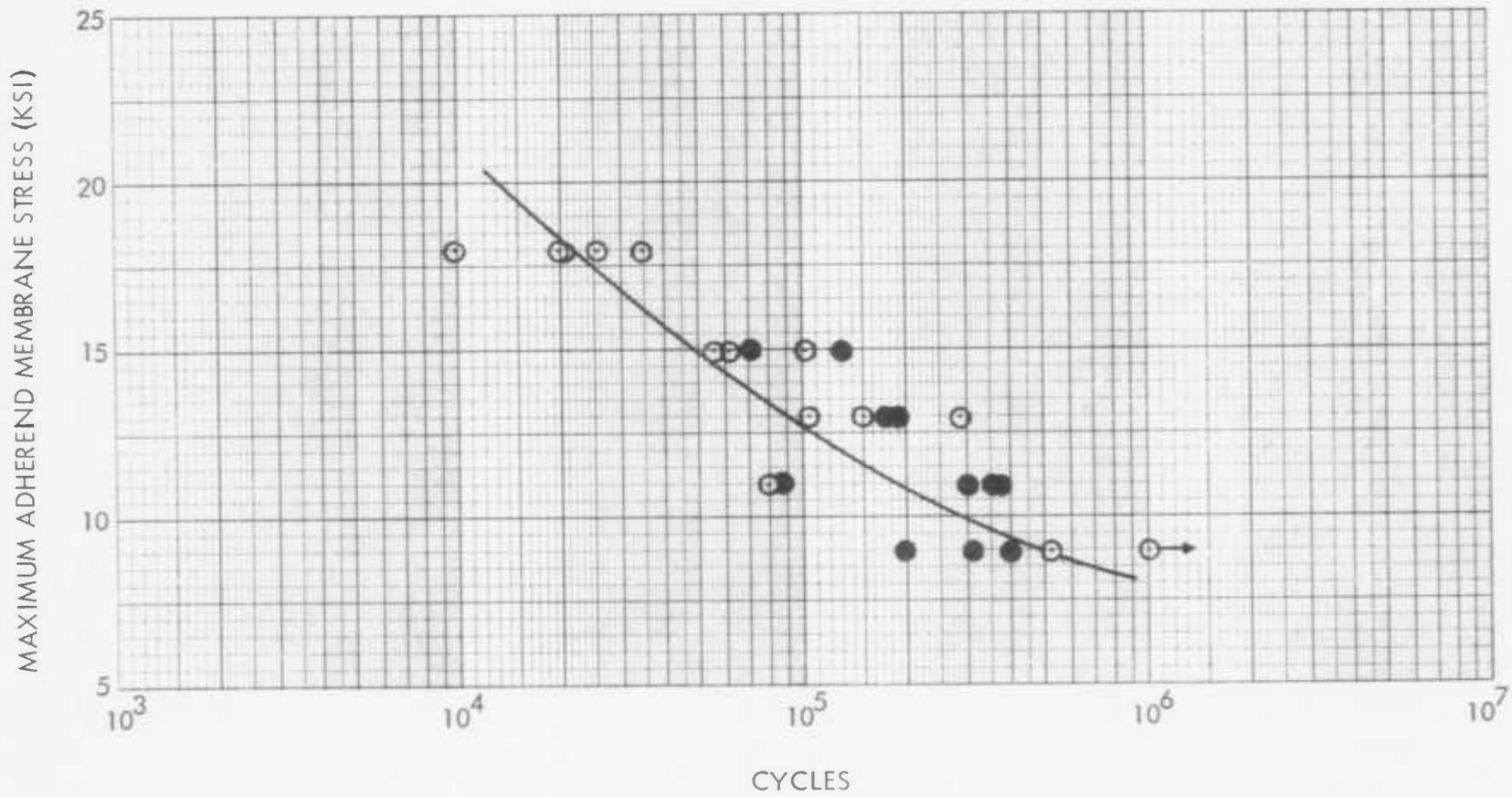

FIGURE 28 – WELDBOND JOINT S-N DATA, L/t = 14, R = 0.1 (STAGGERED WELD)

LEGEND

SYMBOL	CONFIG. NO.	ADHEREND THICKNESS (IN.)	OVERLAP (IN.)	ACTUAL L/t	WELD PATTERN (FIGURE NO.)	S (IN.)	$ed^{(1)}$ (IN.)	$ed^{(2)}$ (IN.)	A (IN.)
◇	10	.050	0.80	16	17	1.00	0.40	0.50	1.62
⊡	13	.050	0.80	16	16	0.75	0.40	0.375	1.62

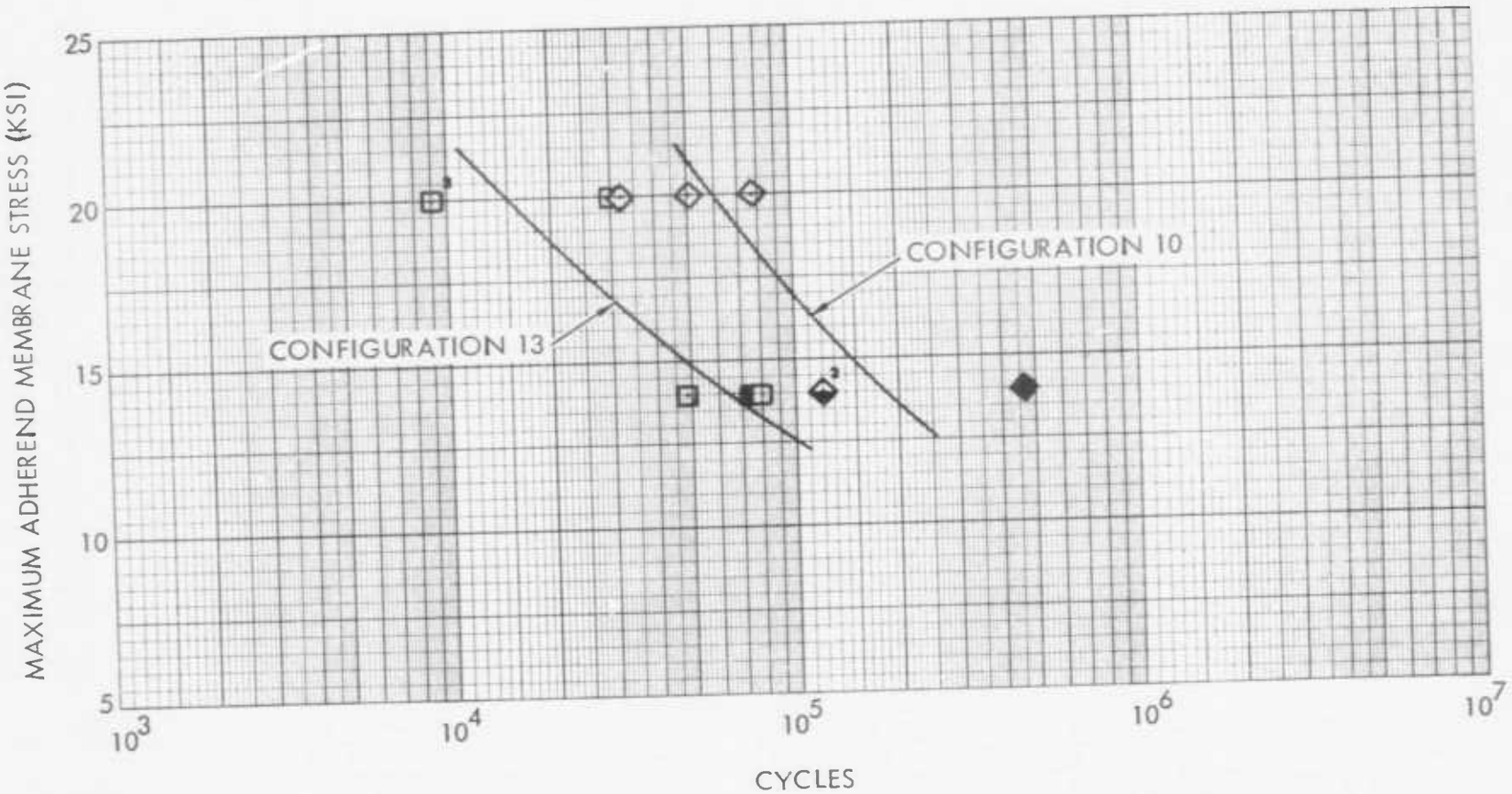

FIGURE 29 – WELDBOND JOINT S-N DATA, L/t = 16, R = 0.1

LEGEND

SYMBOL	CONFIG. NO.	ADHEREND THICKNESS (IN.)	OVERLAP (IN.)	ACTUAL L/t	WELD PATTERN (FIGURE NO.)	S (IN.)	P (IN.)	$ed^{(1)}$ (IN.)	$ed^{(2)}$ (IN.)	A (IN.)
△	16	.071	1.00	17.0	18	0.75	0.50	0.35	0.375	2.42

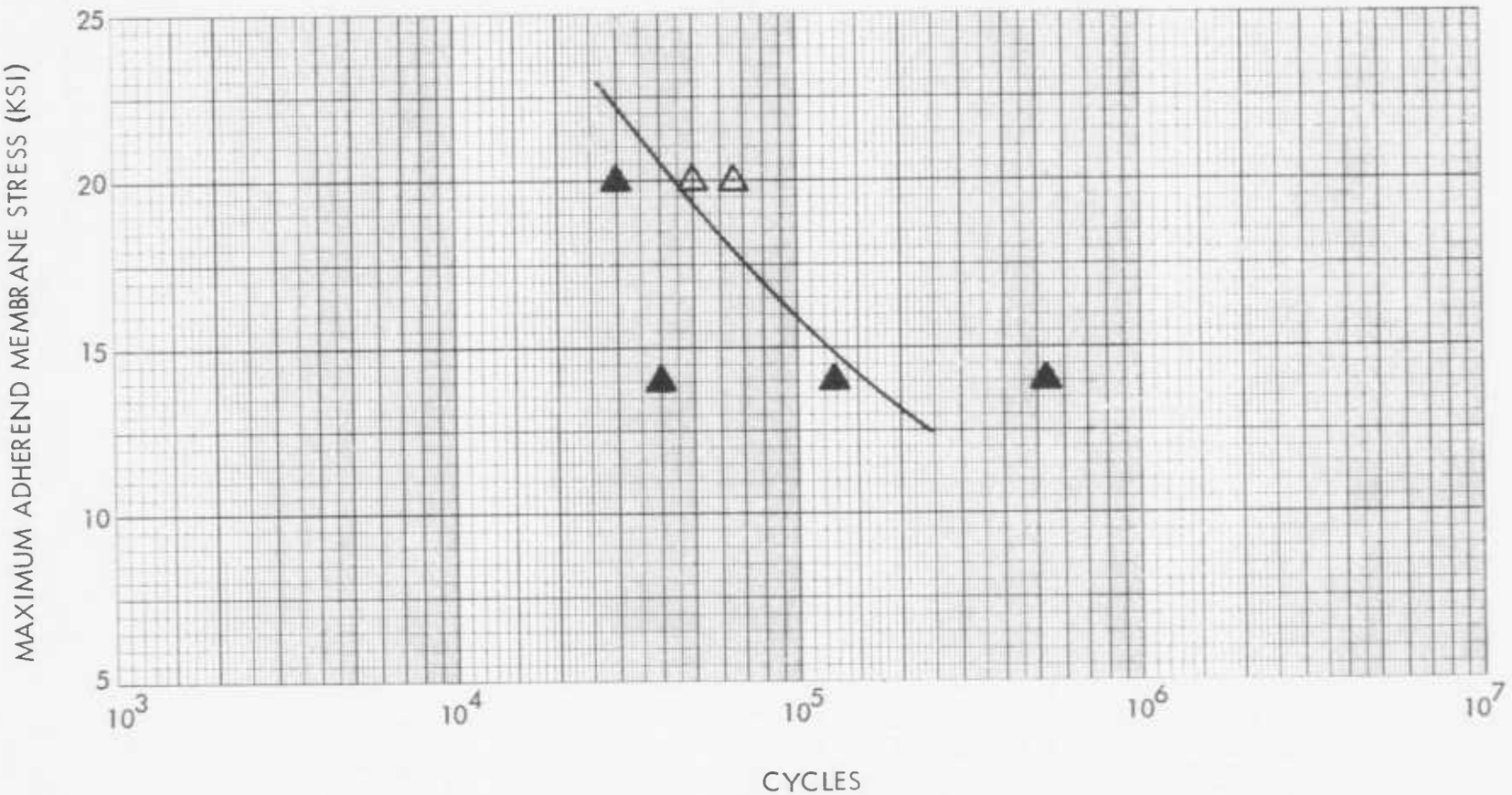

FIGURE 30 – WELDBOND JOINT S-N DATA, L/t = 17, R = 0.1

LEGEND

SYMBOL	CONFIG. NO.	ADHEREND THICKNESS (IN.)	OVERLAP (IN.)	ACTUAL L/t	WELD PATTERN (FIGURE NO.)	S (IN.)	$ed^{(1)}$ (IN.)	$ed^{(2)}$ (IN.)	A (IN.)
⊡	19	.025	0.50	20	16	0.75	0.25	0.375	1.02
△	7	.032	0.64	20	16	0.75	0.32	0.375	1.30
◇	21	.040	0.80	20	16	0.75	0.40	0.375	1.62
⊙	1	.050	1.00	20	16	0.75	0.50	0.375	2.02

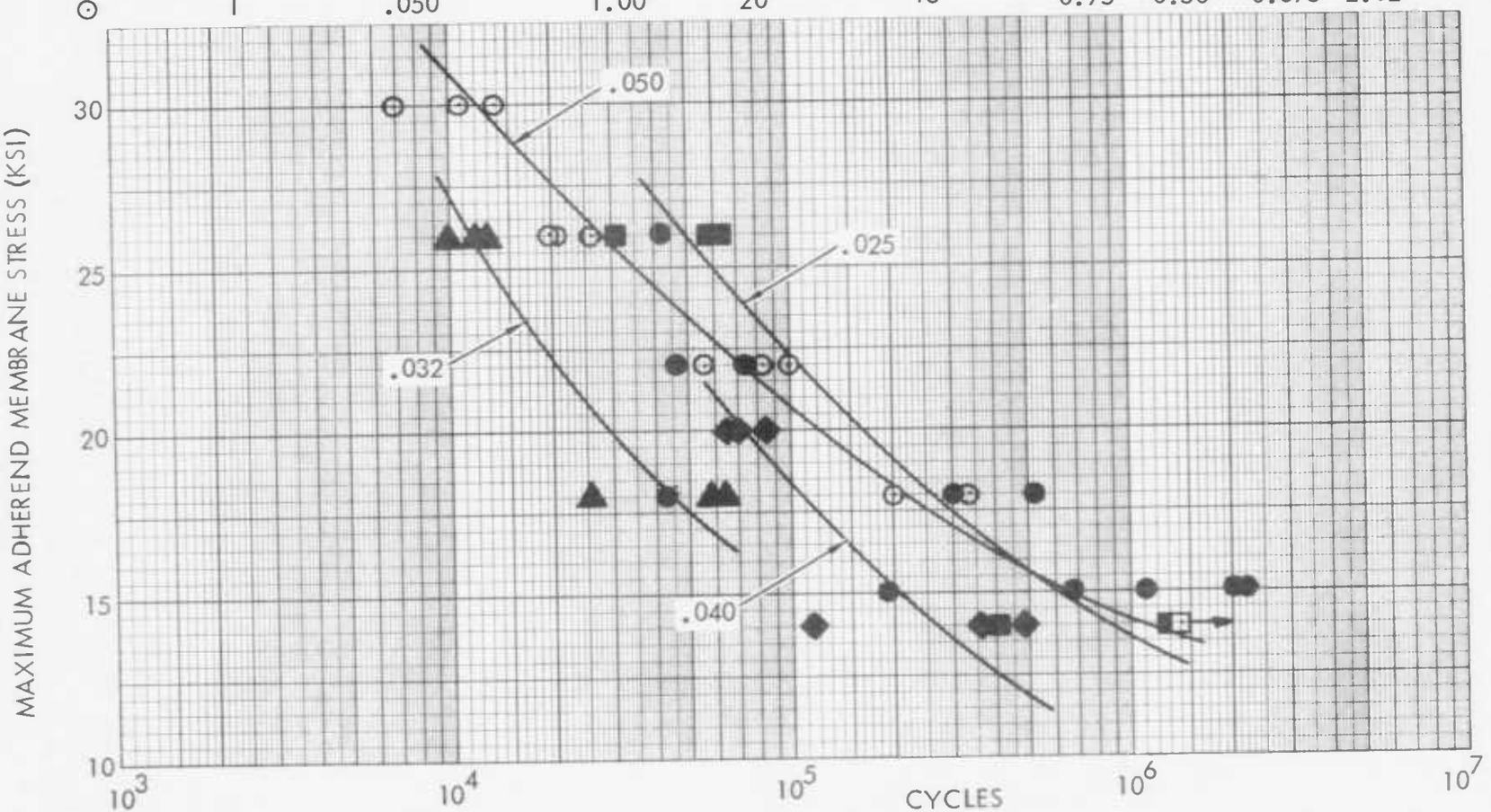

FIGURE 31 – WELDBOND JOINT S-N DATA, L/t = 20, R = 0.1 (CENTERED WELD)

LEGEND

SYMBOL	CONFIG. NO.	ADHEREND THICKNESS (IN.)	OVERLAP (IN.)	ACTUAL L/t	WELD PATTERN (FIGURE NO.)	S (IN.)	P (IN.)	$ed^{(1)}$ (IN.)	$ed^{(2)}$ (IN.)	A (IN.)
⊙	2	.050	1.00	20	18	0.75	0.30	0.35	0.375	2.02
△	22	.063	1.25	19.9	18	0.75	0.55	0.35	0.375	2.52
⊡	23	.080	1.60	20	18	0.75	0.80	0.40	0.375	3.22
▽	24	.090	1.80	20	18	0.75	0.90	0.45	0.375	3.62

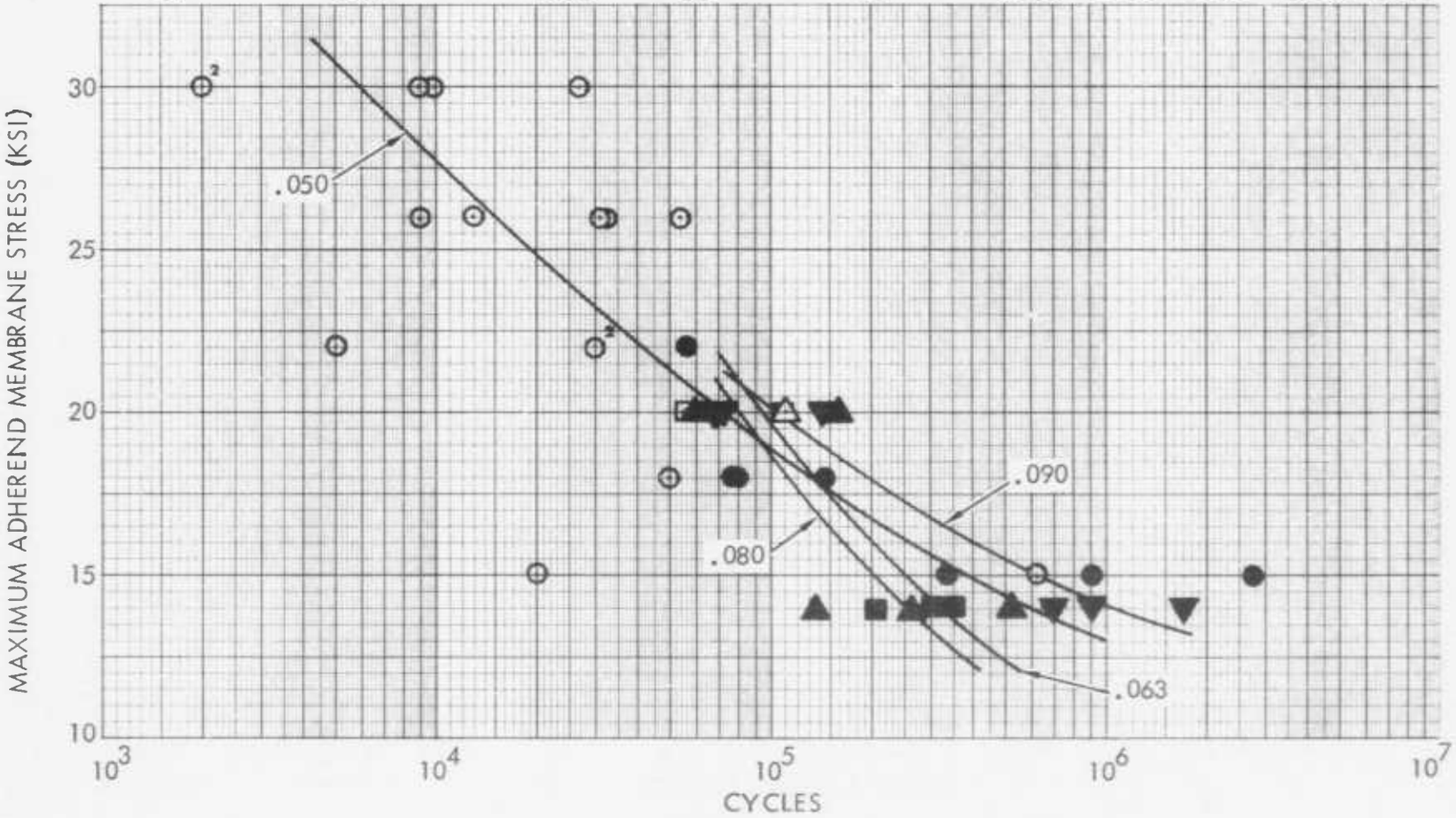

FIGURE 32 – WELDBOND JOINT S-N DATA, L/t = 20, R = 0.1 (STAGGERED WELD)

LEGEND

SYMBOL	CONFIG. NO.	ADHEREND THICKNESS (IN.)	OVERLAP (IN.)	ACTUAL L/t	WELD PATTERN (FIGURE NO.)	S (IN.)	P (IN.)	$ed^{(1)}$ (IN.)	$ed^{(2)}$ (IN.)	A (IN.)
△	15	.050	1.20	24	18	0.75	0.50	0.35	0.375	2.42
▽	33	.063	1.50	23.8	18	0.75	0.80	0.35	0.375	3.02

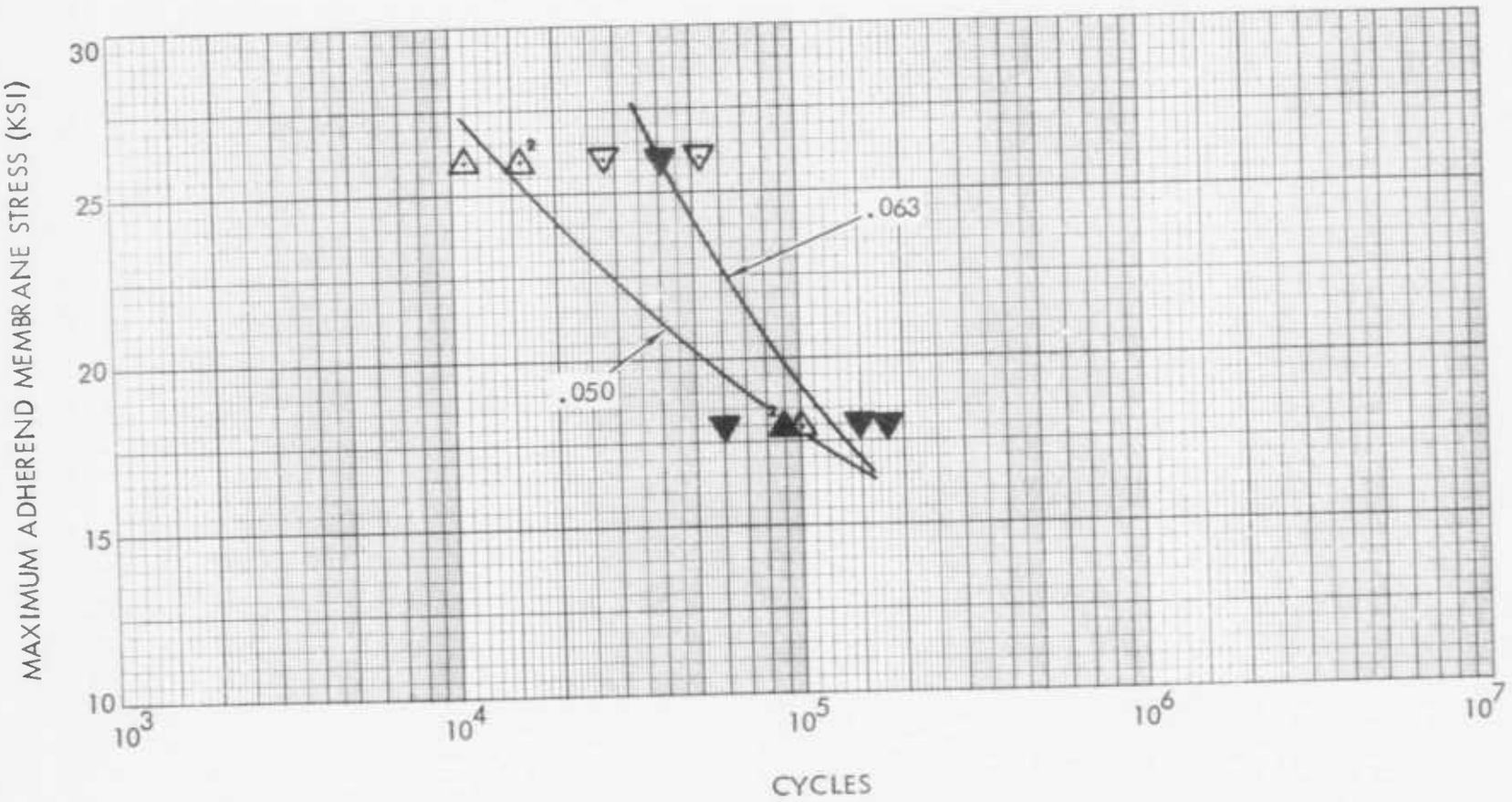

FIGURE 33 – WELDBOND JOINT S-N DATA, L/t = 24, R = 0.1

LEGEND

SYMBOL	CONFIG. NO.	ADHEREND THICKNESS (IN.)	OVERLAP (IN.)	ACTUAL L/t	WELD PATTERN (FIGURE NO.)	S (IN.)	P (IN.)	$ed^{(1)}$ (IN.)	$ed^{(2)}$ (IN.)	A (IN.)
⊙	26	.040	1.00	25	18	0.75	0.30	0.35	0.375	2.02
⊡	27	.063	1.60	25.4	18	0.75	0.90	0.35	0.375	3.22
△	28	.071	1.80	25.4	18	0.75	1.10	0.35	0.375	3.62
▽	29	.080	2.00	25	18	0.75	1.20	0.40	0.375	4.02
⊙	30	.090	2.25	25	18	0.75	1.35	0.45	0.375	4.52

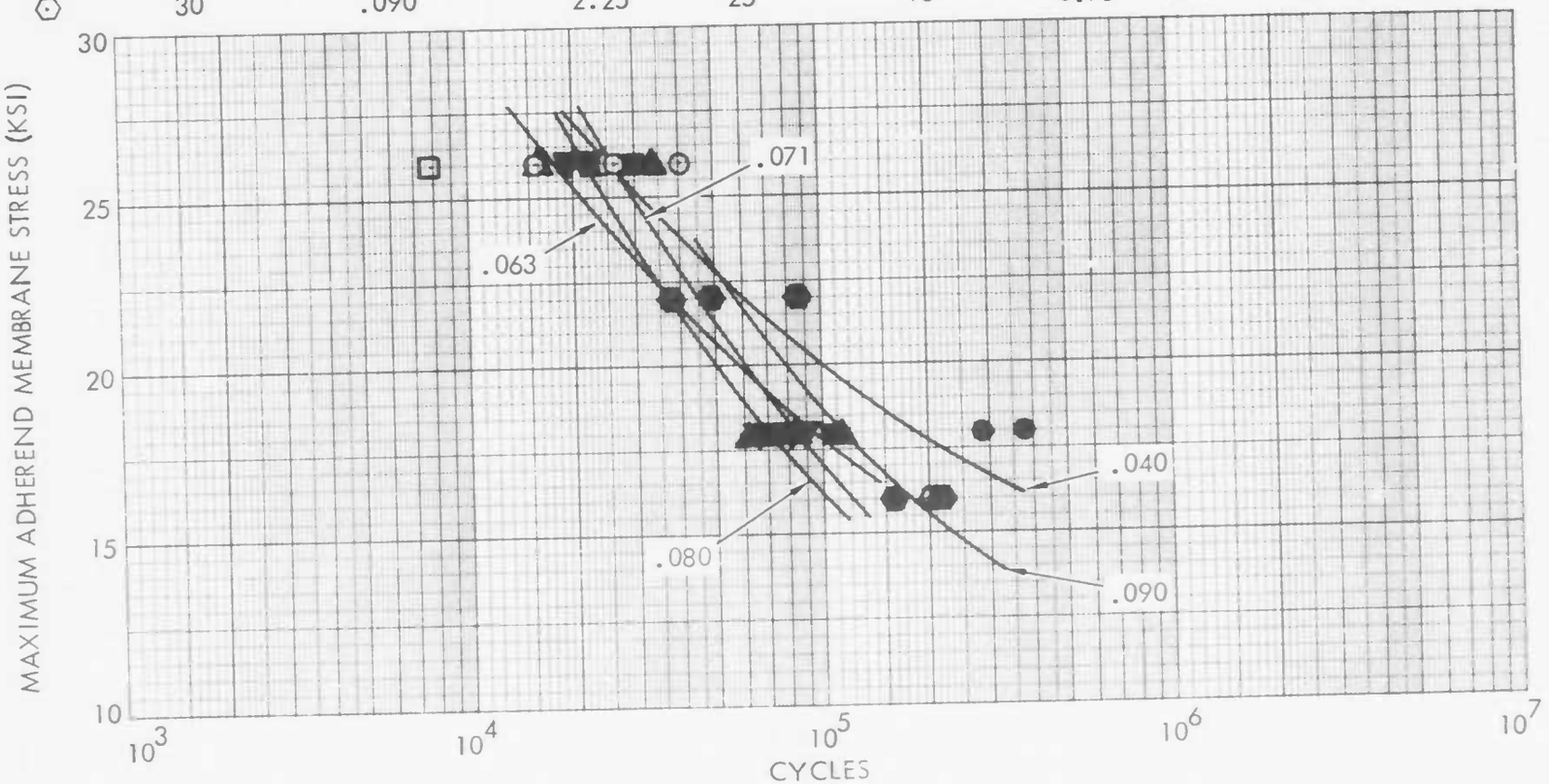

FIGURE 34 – WELDBOND JOINT S-N DATA, L/t = 25, R = 0.1

LEGEND

SYMBOL	CONFIG. NO.	ADHEREND THICKNESS (IN.)	OVERLAP (IN.)	ACTUAL L/t	WELD PATTERN (FIGURE NO.)	S (IN.)	P (IN.)	$ed^{(1)}$ (IN.)	$ed^{(2)}$ (IN.)	A (IN.)
◇	9	.032	0.90	28.1	18	0.75	0.20	0.35	0.375	1.82
▽	32	.071	2.00	28.2	18	0.75	1.30	0.35	0.375	4.02
△	35	.080	2.25	28.1	18	0.75	1.45	0.40	0.375	4.52
⊙	36	.090	2.50	27.8	18	0.75	1.60	0.45	0.375	5.02

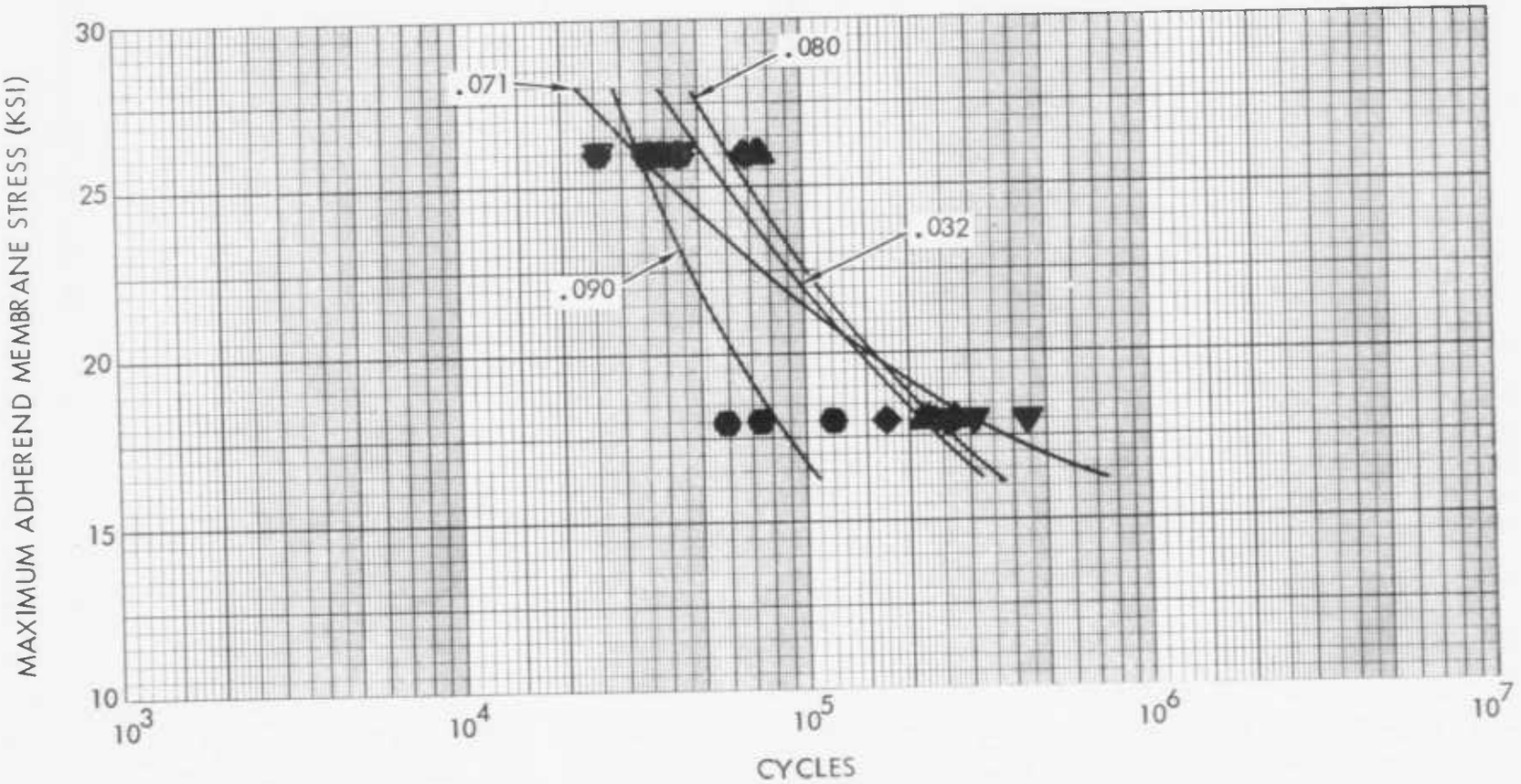

FIGURE 35 – WELDBOND JOINT S-N DATA, L/t = 28, R = 0.1

LEGEND

SYMBOL	CONFIG. NO.	ADHEREND THICKNESS (IN.)	OVERLAP (IN.)	ACTUAL L/t	WELD PATTERN (FIGURE NO.)	S (IN.)	P (IN.)	$ed^{(1)}$ (IN.)	$ed^{(2)}$ (IN.)	A (IN.)
⊙	34	.020	0.64	32	18	0.75	0.20	0.22	0.375	1.30
⊡	20	.025	0.80	32	18	0.75	0.30	0.25	0.375	1.62
△	17	.032	1.10	34.4	18	0.75	0.40	0.35	0.375	2.22

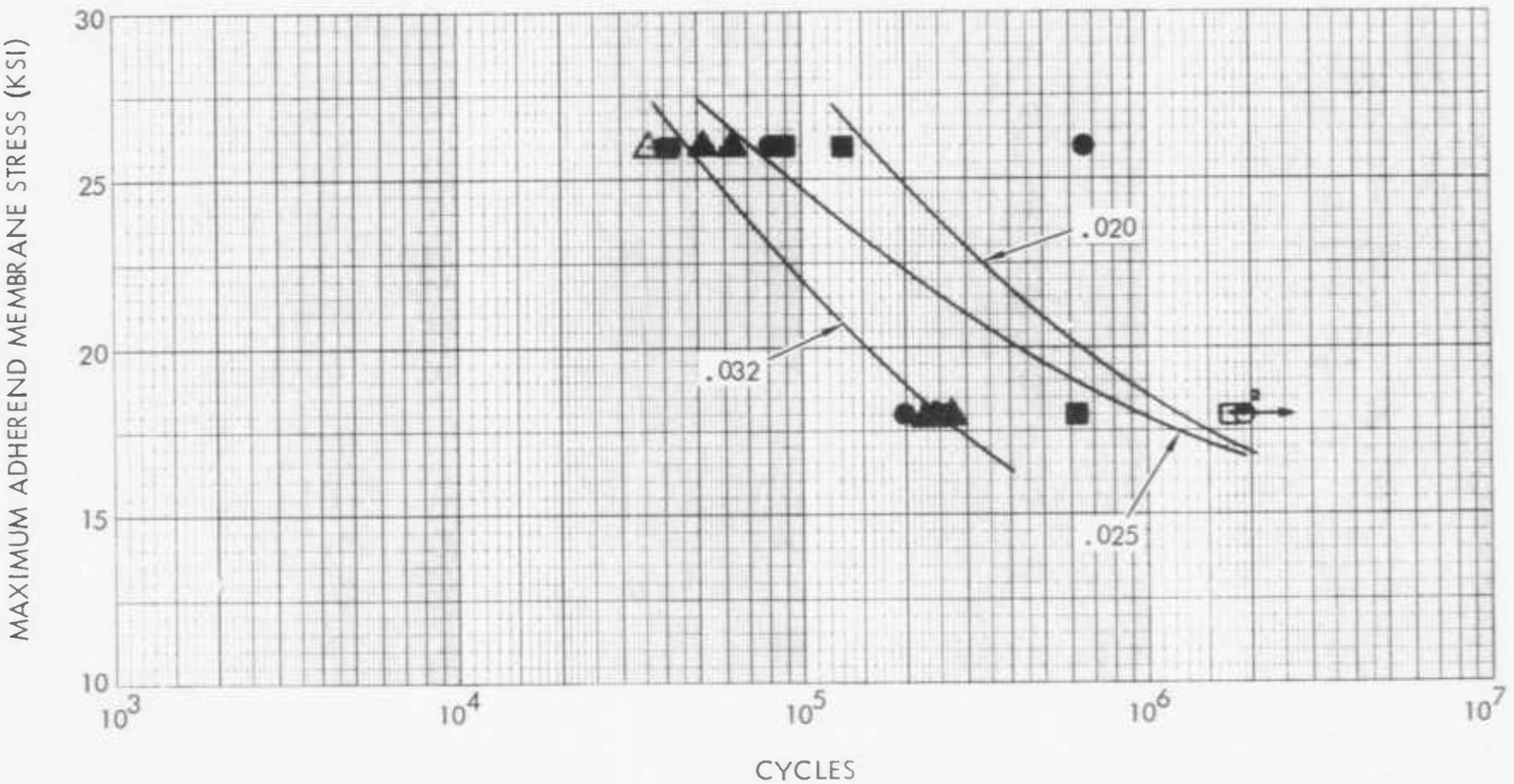

FIGURE 36 – WELDBOND JOINT S-N DATA, L/t = 32, R = 0.1

LEGEND

SYMBOL	CONFIG. NO.	ADHEREND THICKNESS (IN.)	OVERLAP (IN.)	ACTUAL L/t	WELD PATTERN (FIGURE NO.)	S (IN.)	P (IN.)	e_d(1) (IN.)	e_d(2) (IN.)	A (IN.)
⊙	1	.050	1.00	20	16	0.75	-	0.50	0.375	2.02
⊡	2	.050	1.00	20	18	0.75	0.30	0.35	0.375	2.02

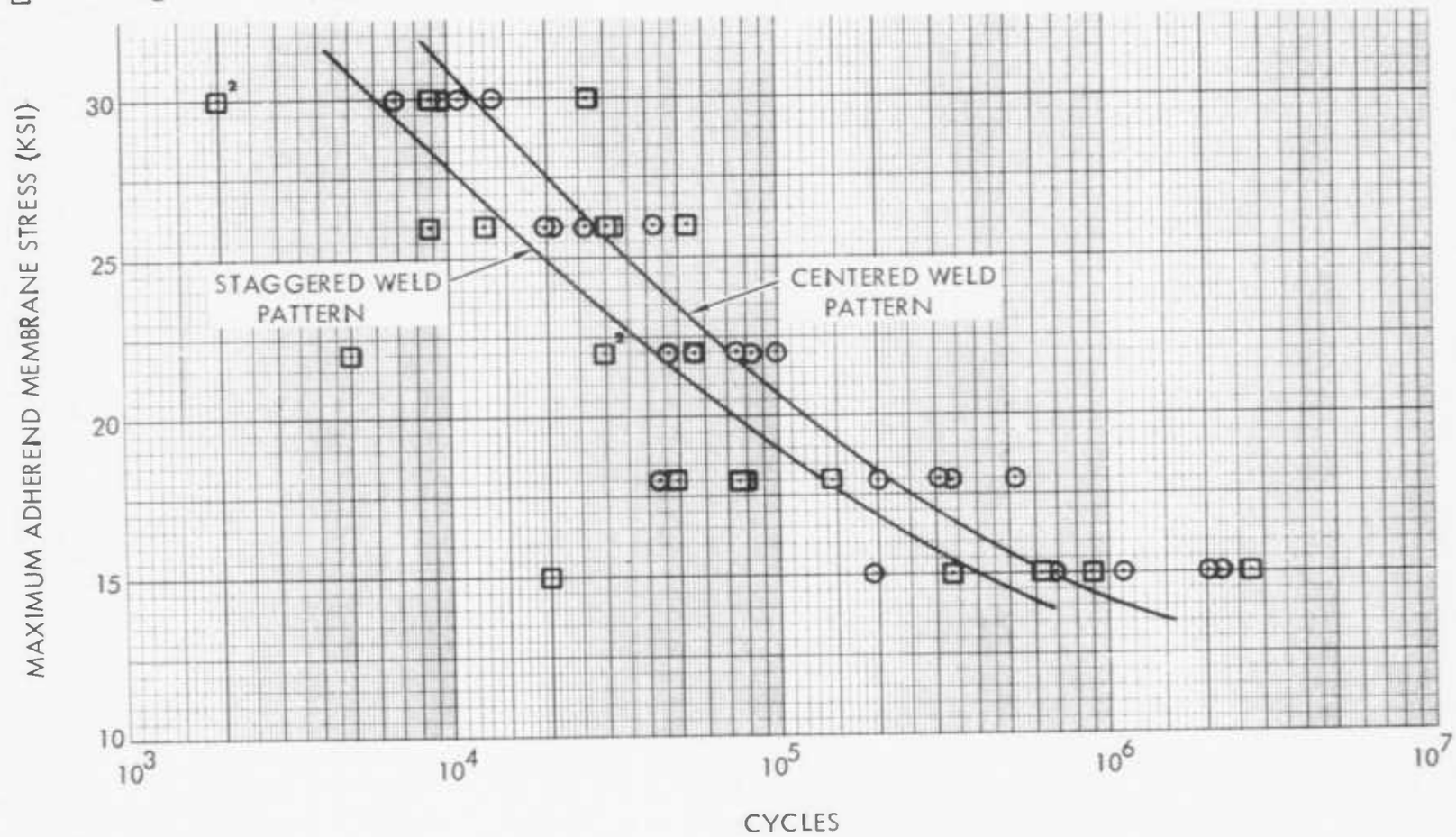

FIGURE 37 – S-N DATA COMPARISON OF CENTERED AND STAGGERED WELD PATTERNS (0.050 ADHERENDS, L/t = 20, R = 0.1)

LEGEND

SYMBOL	CONFIG. NO.	ADHEREND THICKNESS (IN.)	OVERLAP (IN.)	ACTUAL L/t	WELD PATTERN (FIGURE NO.)	S (IN.)	P (IN.)	$e_d^{(1)}$ (IN.)	$e_d^{(2)}$ (IN.)	A (IN.)
⊙	18	.071	1.00	14.1	16	0.75	-	0.50	0.375	2.02
⊙	4	.071	1.00	14.1	18	0.75	0.30	0.35	0.375	2.02

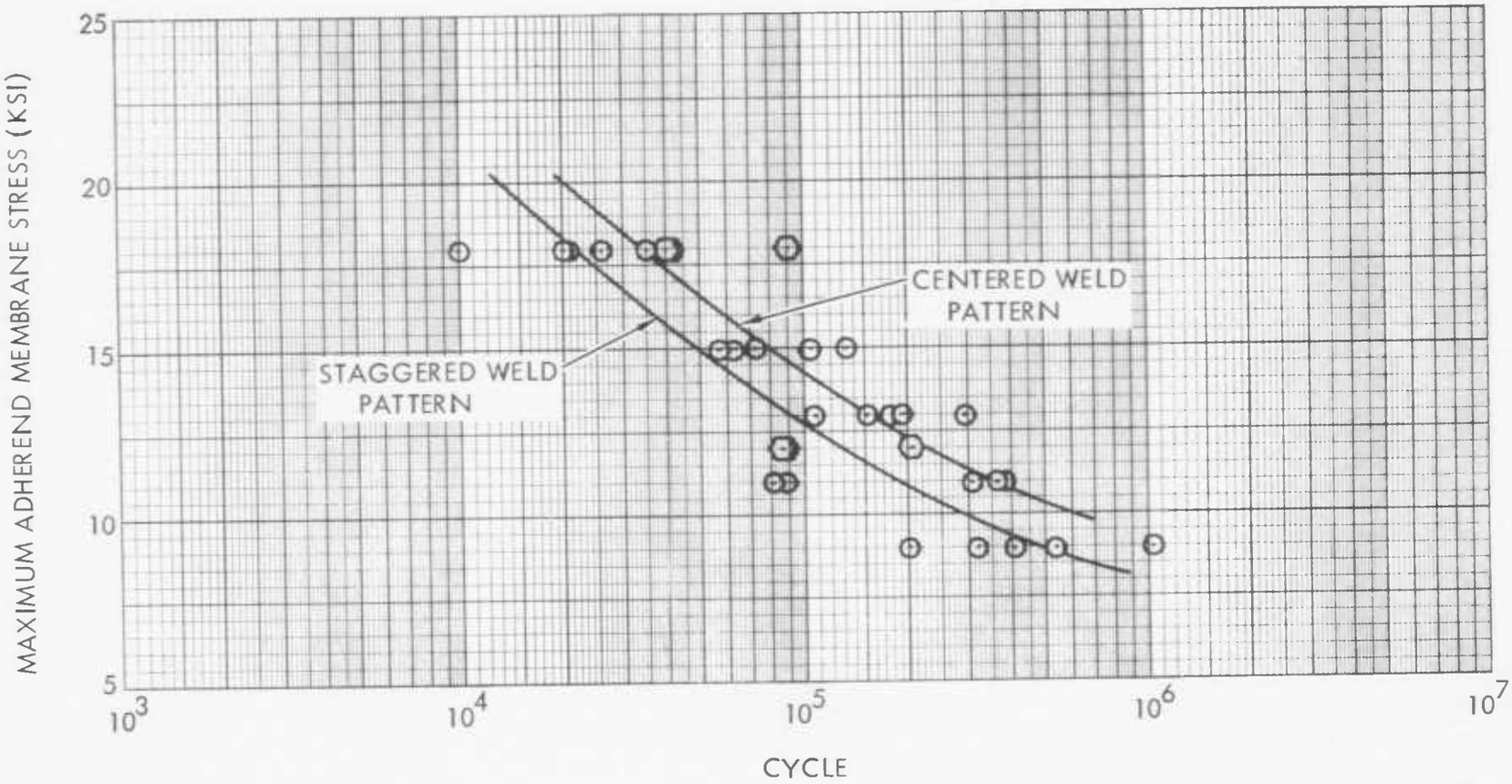

FIGURE 38 – S-N DATA COMPARISON OF CENTERED AND STAGGERED WELD PATTERNS (0.071 ADHERENDS, L/t = 14, R = 0.1)

LEGEND

SYMBOL	CONFIG. NO.	ADHEREND THICKNESS (IN.)	OVERLAP (IN.)	ACTUAL L/t	WELD PATTERN (FIGURE NO.)	S (IN.)	$ed^{(1)}$ (IN.)	$ed^{(2)}$ (IN.)	A (IN.)
⊙	3	.050	0.62	12.4	16	0.75	0.31	0.375	1.26
△	5	.050	0.62	12.4	17	1.25	0.31	0.25	1.26
◇	6	.050	0.62	12.4	17	1.00	0.31	0.50	1.26

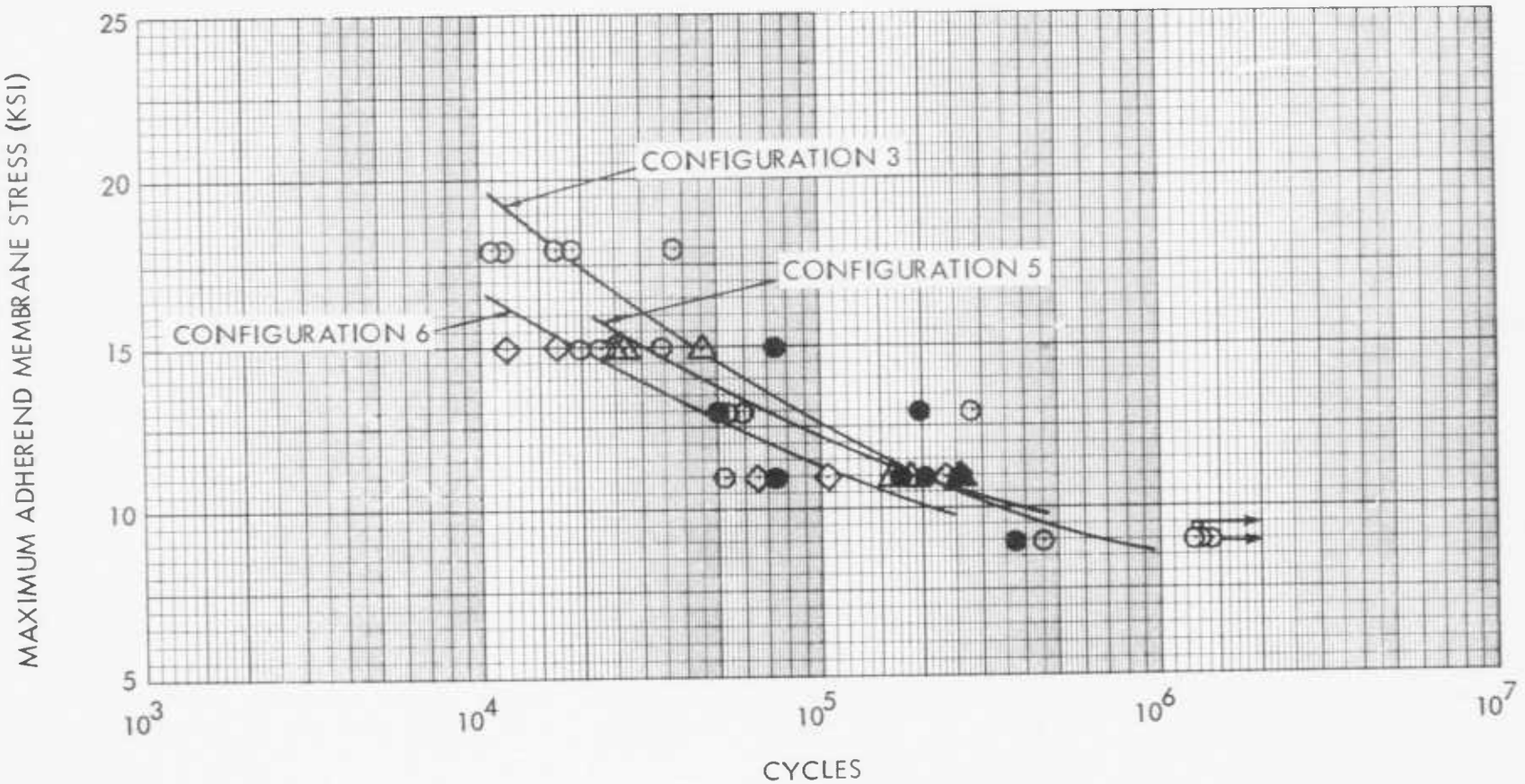

FIGURE 39 – WELDBOND JOINT S-N DATA, L/t = 12, R = 0.1

SYMBOL	CONFIG. NO.	ADHEREND THICKNESS (IN.)	OVERLAP (IN.)	ACTUAL L/t	WELD PATTERN (FIGURE NO.)	S (IN.)	P (IN.)	$ed^{(1)}$ (IN.)	$ed^{(2)}$ (IN.)	A (IN.)
⊙	8	.050	1.30	26	19	0.75	0.70	0.30	0.375	2.62

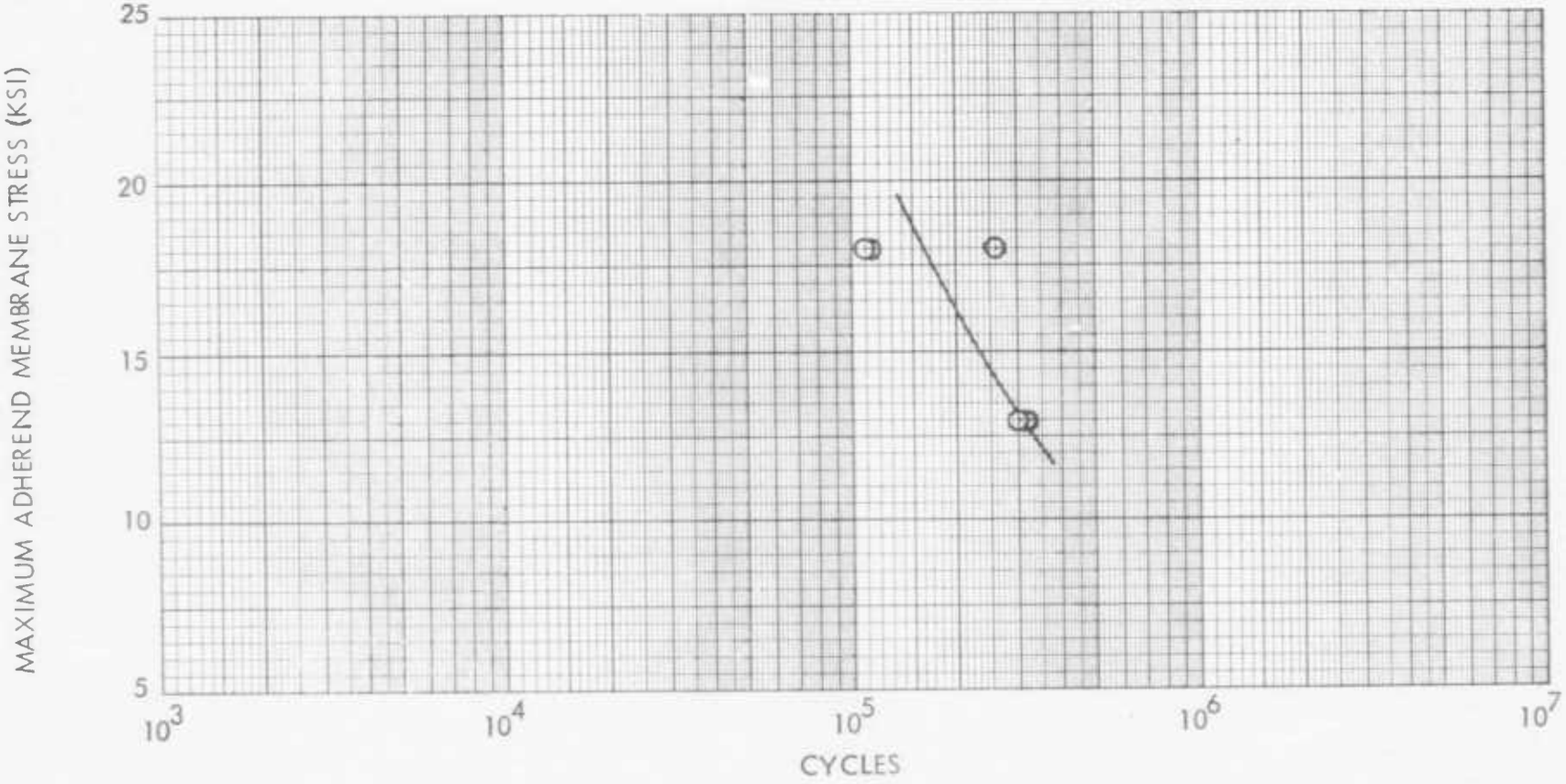

FIGURE 40 – WELDBOND JOINT S-N DATA, L/t = 26, R = 0.1 (DOUBLE ROW)

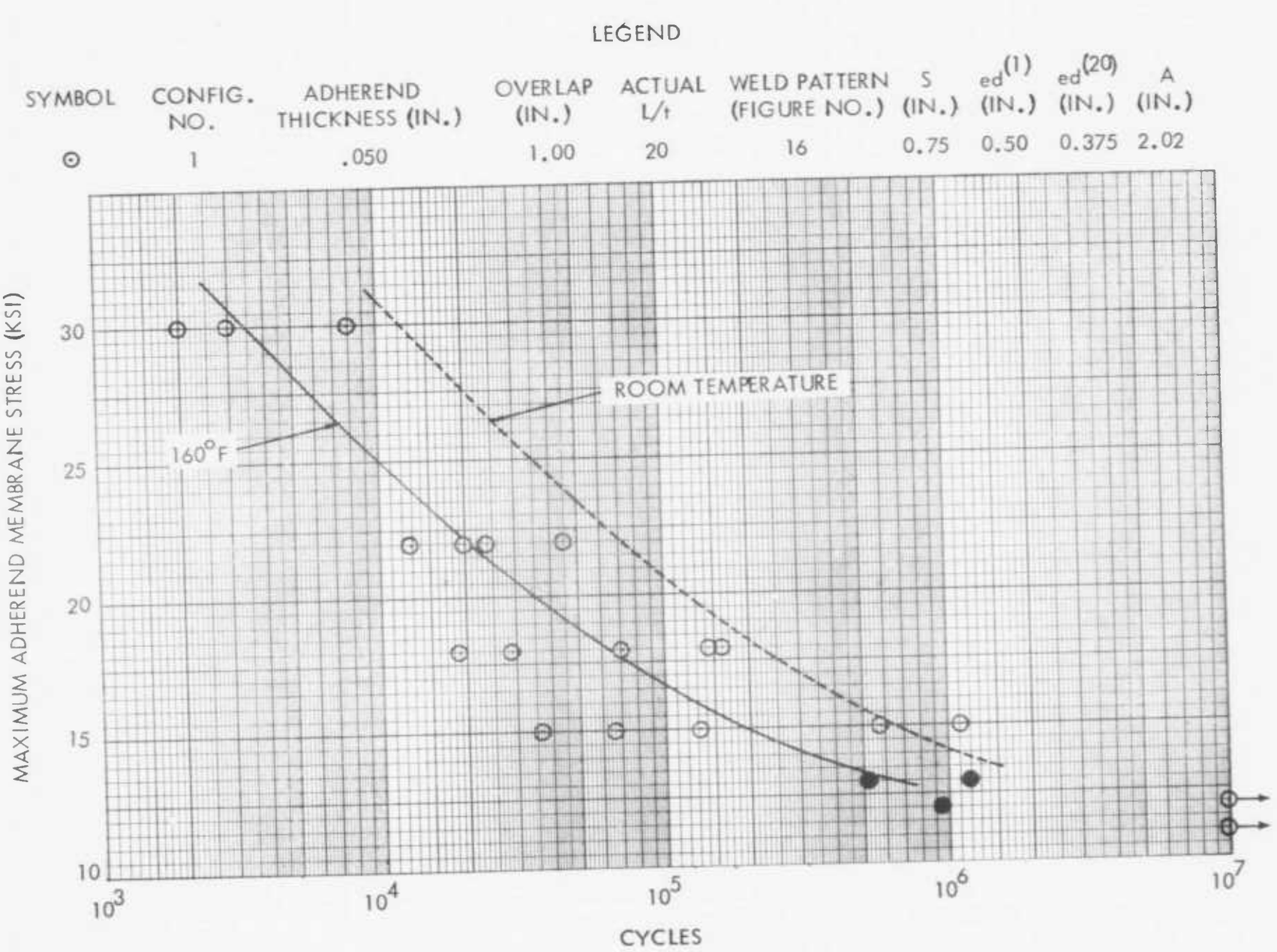

FIGURE 41 – 160°F WELDBOND JOINT S-N DATA, L/t = 20, R = 0.1 (CENTERED WELD)

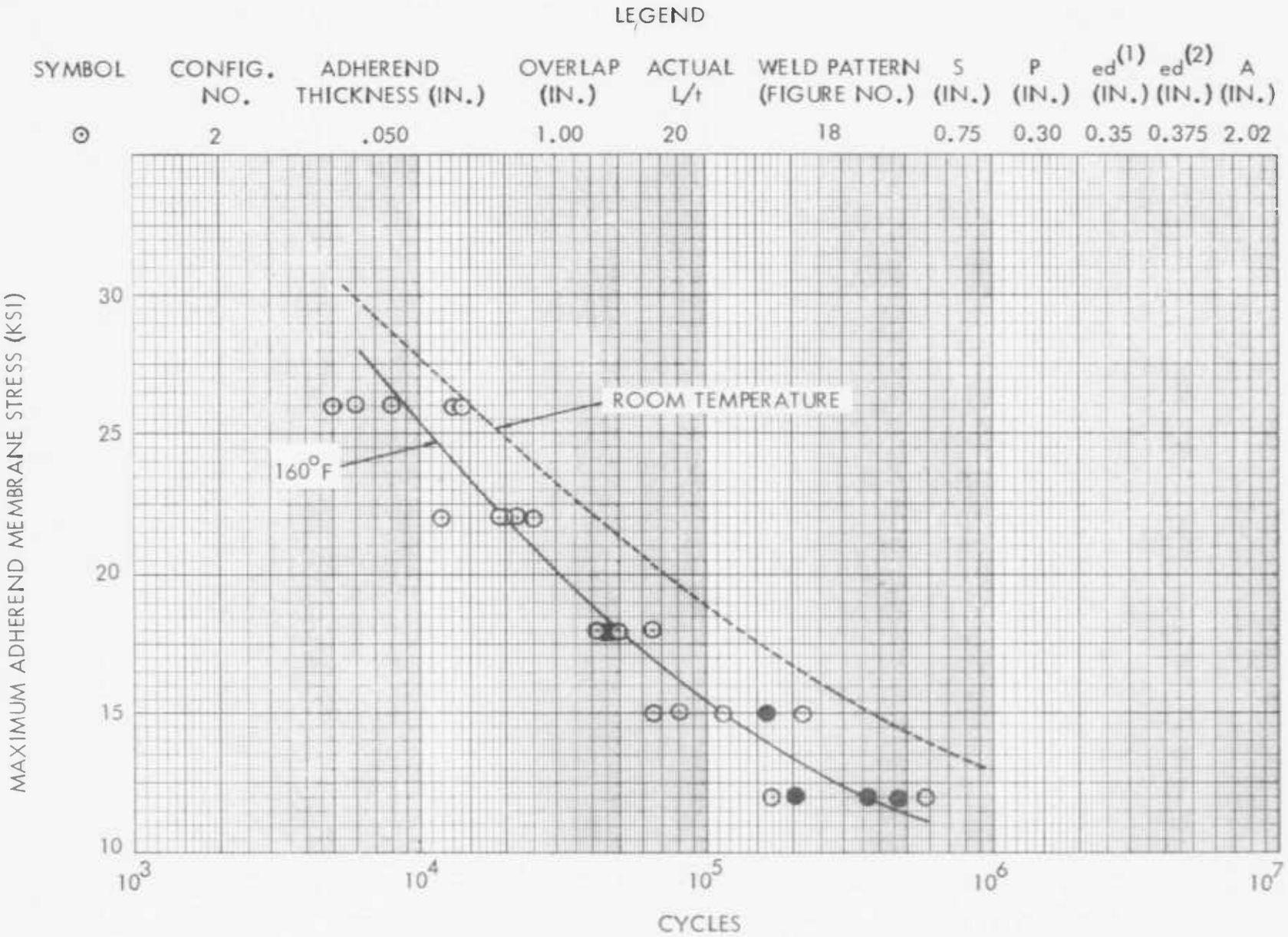

FIGURE 42 – 160°F WELDBOND JOINT S-N DATA, L/t = 20, R = 0.1 (STAGGERED WELD)

LEGEND

SYMBOL	CONFIG. NO.	ADHEREND THICKNESS (IN.)	OVERLAP (IN.)	ACTUAL L/t	WELD PATTERN (FIGURE NO.)	S (IN.)	P (IN.)	$ed^{(1)}$ (IN.)	$ed^{(2)}$ (IN.)	A (IN.)
⊙	4	.071	1.00	14.1	18	0.75	0.30	0.35	0.375	2.02

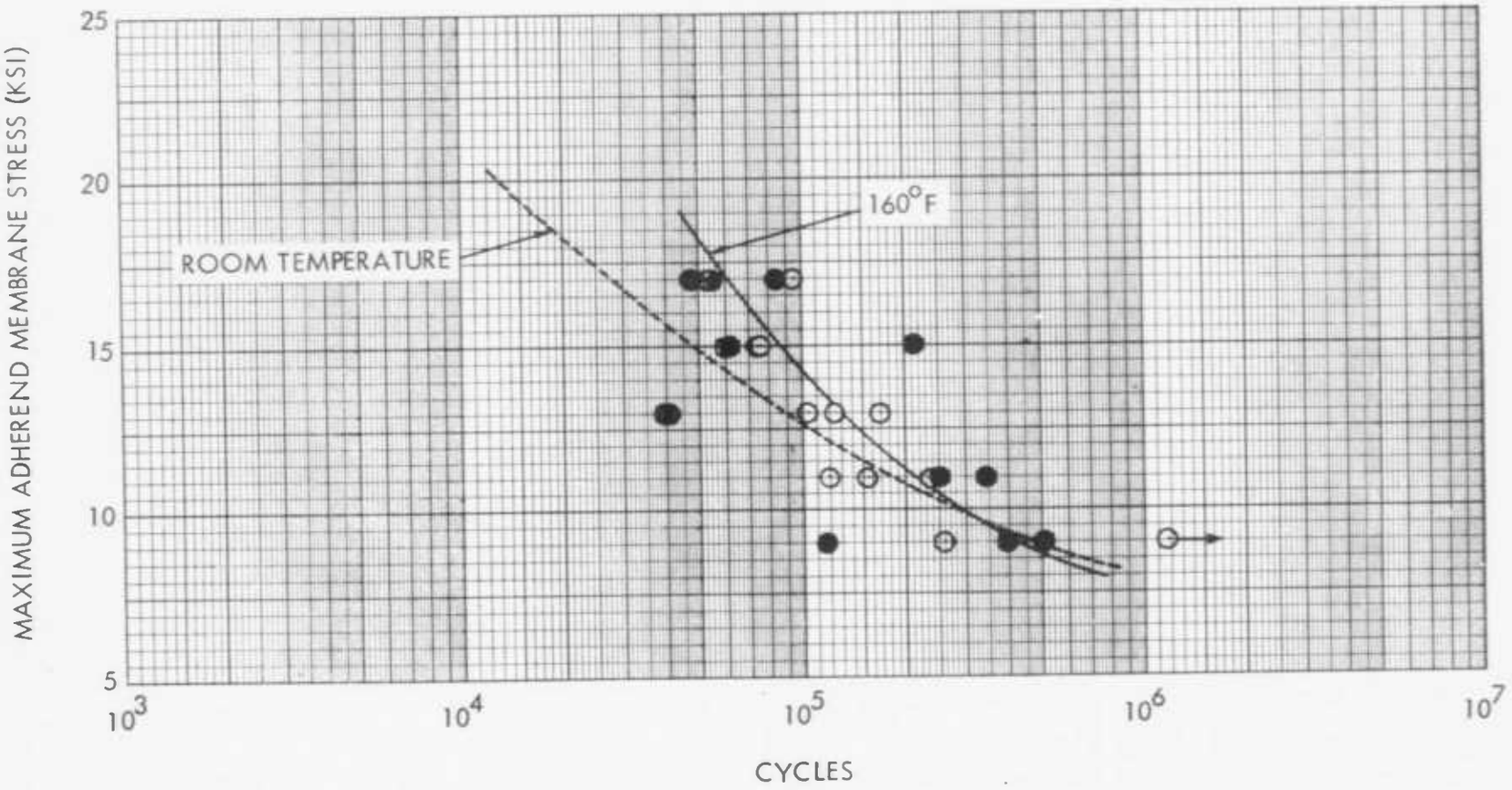

FIGURE 43 – 160°F WELDBOND JOINT S-N DATA, L/t = 14, R = 0.1 (STAGGERED WELD)

LEGEND

SYMBOL	CONFIG. NO.	ADHEREND THICKNESS (IN.)	OVERLAP (IN.)	ACTUAL L/t	WELD PATTERN (FIGURE NO.)	S (IN.)	$ed^{(1)}$ (IN.)	$ed^{(2)}$ (IN.)	A (IN.)
⊙	3	.050	0.62	12.4	16	0.75	0.31	0.375	1.26

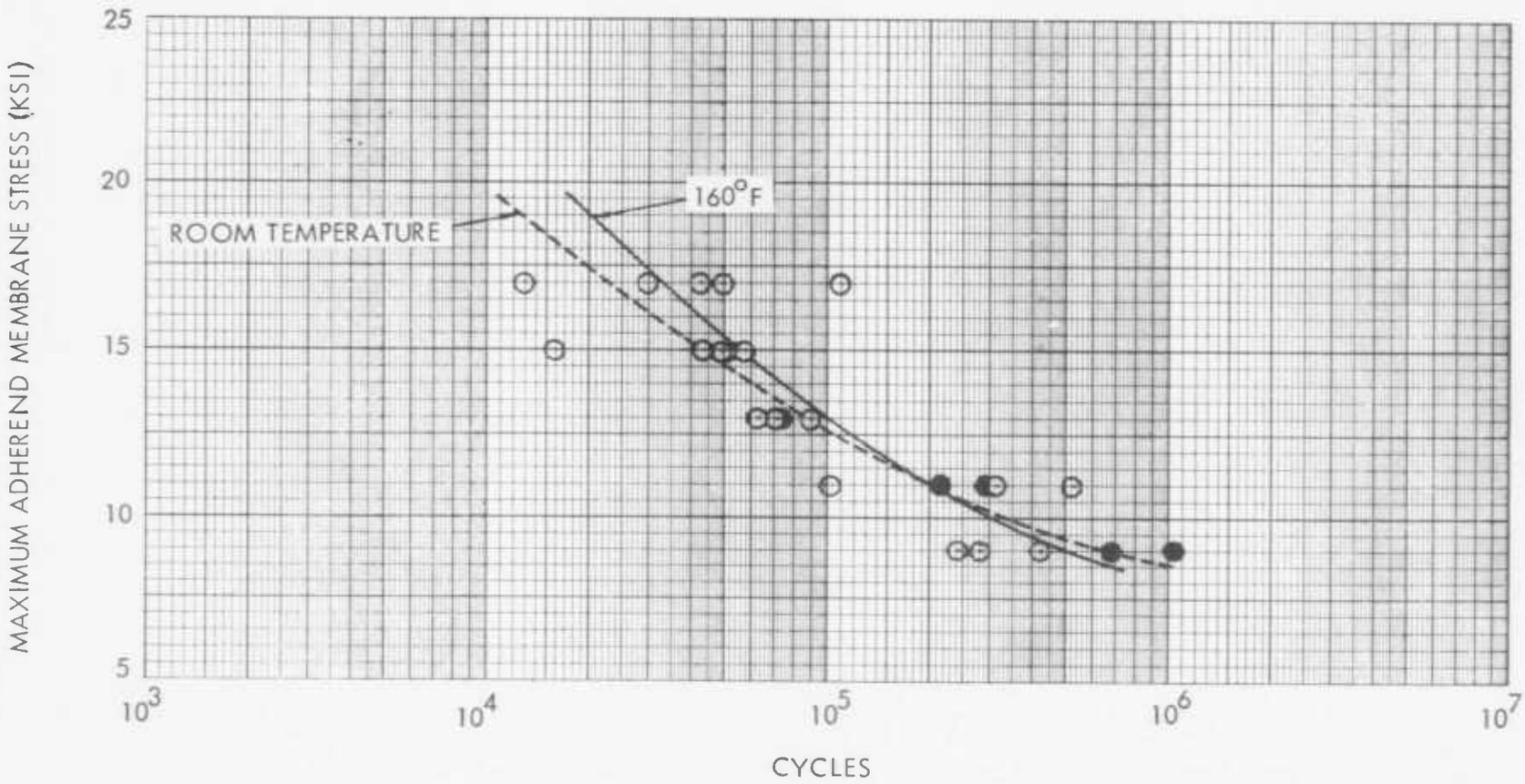

FIGURE 44 – 160°F WELDBOND JOINT S-N DATA, L/t = 12, R = 0.1

LEGEND

SYMBOL	CONFIG. NO.	ADHEREND THICKNESS (IN.)	OVERLAP (IN.)	ACTUAL L/t	WELD PATTERN (FIGURE NO.)	S (IN.)	$ed^{(1)}$ (IN.)	$ed^{(2)}$ (IN.)	A (IN.)
⊙	1	.050	1.00	20	16	0.75	0.50	0.375	2.02

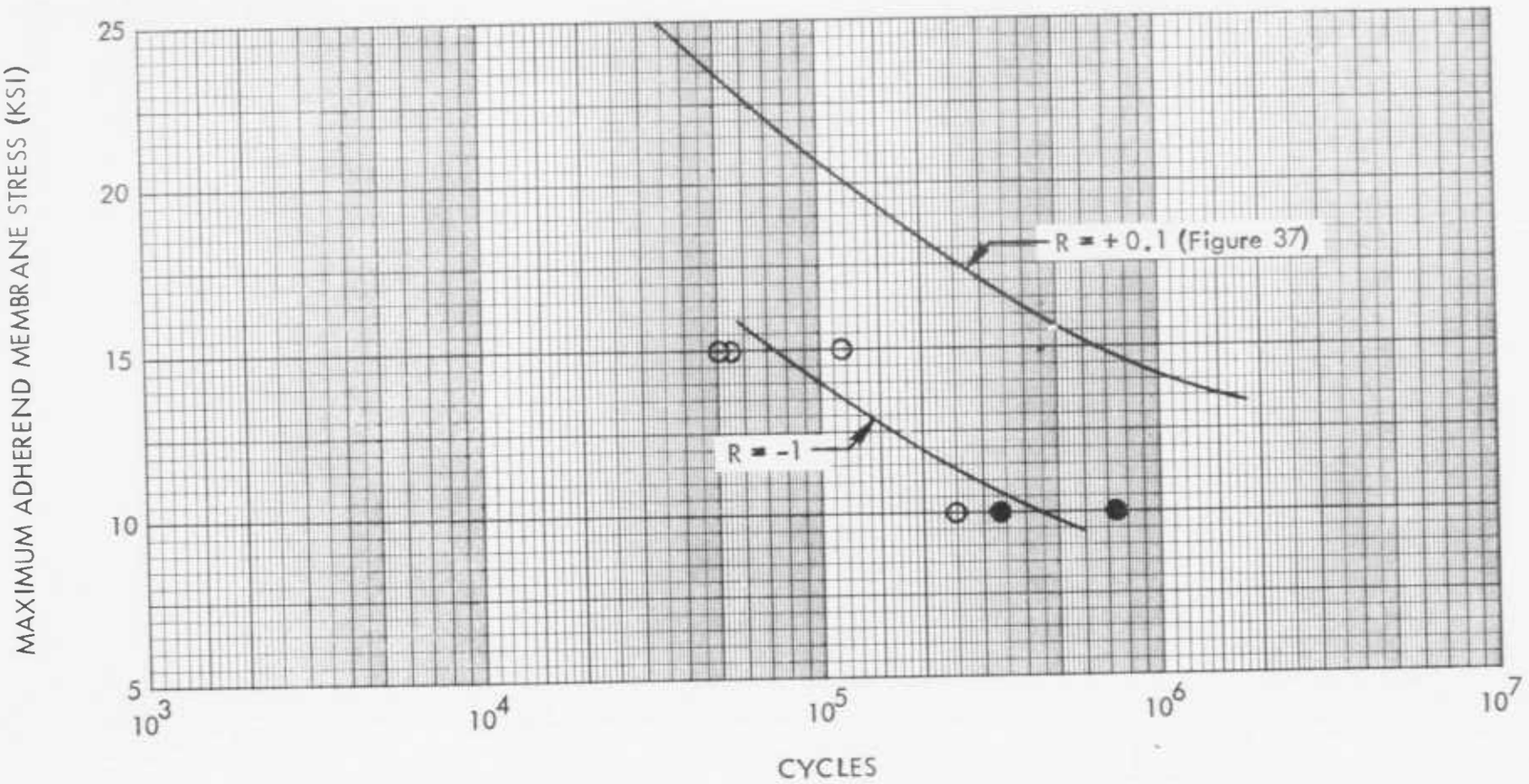

FIGURE 45 - WELDBOND JOINT S-N DATA, L/t = 20, R = -1 & R = +0.1 (CENTERED WELD)

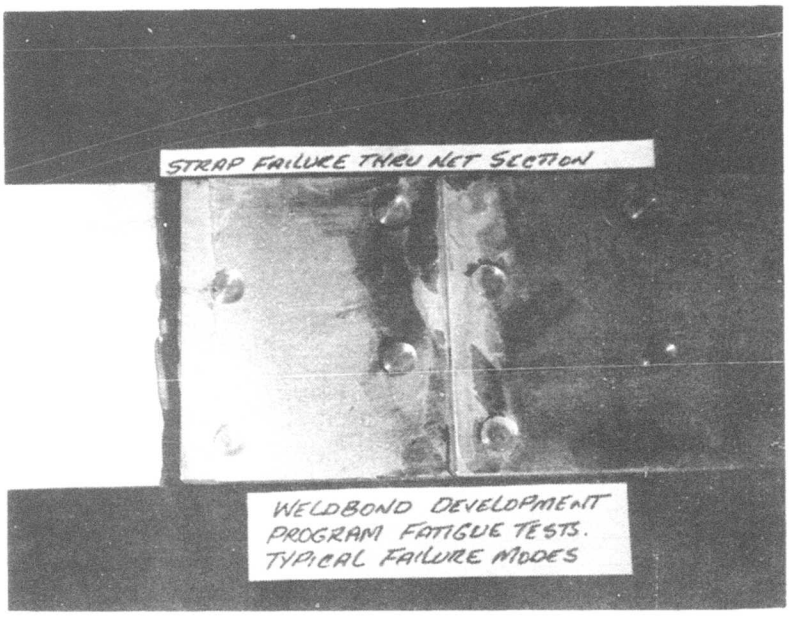

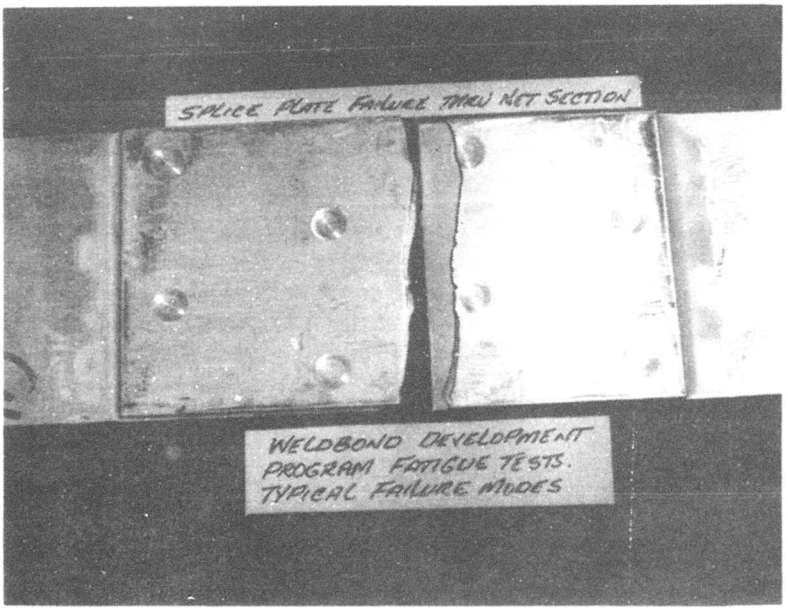

FIGURE 46 – TYPICAL FATIGUE SPECIMEN METAL FAILURES

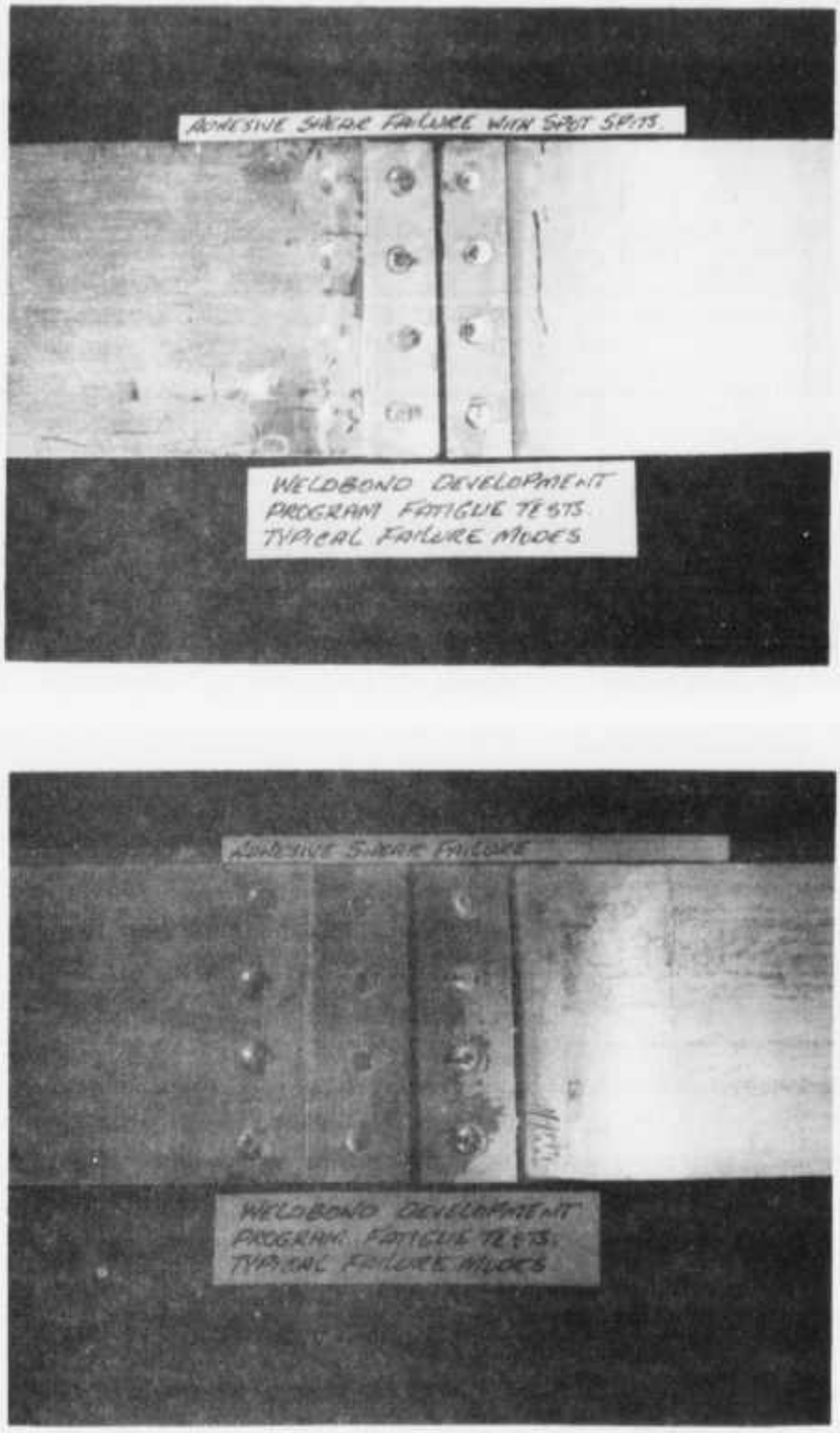

FIGURE 47 – TYPICAL FATIGUE SPECIMEN COHESIVE/ADHESIVE FAILURES

3.2.3 Tension-Shear Interaction Properties

Weldbonded joint "out-of-plane" loading characteristics have been evaluated through the testing of tension-shear interaction specimens as shown in Figure A8. Both static and fatigue tests were conducted and the results are shown in Table 34. All failure modes of test specimens presented in this table are 80-100 percent cohesive. Static failing loads and cycles to failure are the average of five (5) test specimens per test point except where noted.

Table XXXIV – Tension-Shear Interaction Test Results

Load Angle (Degrees)	Static	Fatigue = (R = +0.1)			
	Failing Load (lb.)	Max. Load (lb.)	Cycles to Failure	Max. Load (lb.)	Cycles to Failure
90	2060	1030	1,670	620	352,530
67.5	1820	910	59,050	–	–
45	1710	850	7,230	684**	256,063
22.5	2440	1220*	25,010	–	–

* Average of four (4) tests

** Average of three (3) tests

3.2.4 Metal-to-Metal Peel Properties

Metal-to-metal peel tests have been conducted using weldbonded panels and specimens shown in Figure A9. A total of thirty individual specimen tests were conducted at room temperature; fifteen (15) with one inch spot-weld spacings and fifteen (15) with one-half inch spot-weld spacings. Tests were conducted using a test fixture as shown in Figure A5. The test results show no significant effect of spot-weld spacing. For both spot-weld spacings, maximum peel load across spot-welds was in the 40 to 70 pound range while the average peel load was in the 20 to 30 pound range. All failure modes were described as "adhesive-to-metal with a slight amount of cohesive between welds". In all tests, the final failure was by tearing of the thinner aluminum strap either between the first and second welds or the second and third welds.

3.3 Sonic Fatigue Design Data

Two types of evaluation were performed under this contract in order to determine the sonic fatigue properties of weldbonded structure as compared to conventionally fastened structure. These involved vibratory fatigue beam coupon specimen tests and larger sub-scale

sonic fatigue panels. All of the sonic fatigue evaluation specimens were fabricated using Whittaker's M6800 epoxy paste adhesive and cured for one(1) hour at 250°F. The surface preparation for the vibratory fatigue specimens was the standard metal bond etch for bonding while the surface treatment for the sub-scale sonic fatigue panels was the standard spot-weld etch.

3.3.1 Vibratory Fatigue Specimens and Tests

Double cantilever beam coupon specimens of four separate configurations were designed, fabricated and tested. The specimen details are presented in Figures 48, 49 and 50. The test consisted of clamping the midspan stiffener of each coupon specimen to a vibration exciter and vibrating at resonance to generate alternating stresses in the beam. The quantities of specimens fabricated and tested for each configuration are shown in Table 35. Each specimen was inspected prior to testing by radiographics for weld defects and by ultrasonics for bondline voids and delaminations. The first four (4) specimens of Configuration 1 were instrumented with three (3) strain gages on each specimen in order to establish the region of highes stress in a vibratory environment. Upon this determination, the remaining specimens were instrumented at the high-stress location using only one (1) gage per specimen.

Table XXXV – Vibratory Fatigue Testing

Configuration	Number of Specimens	Figure Number
1	13	7
1a	7	7 (except adhesive bonded only)
2	7	8
3	13	9

The response tests on the first four specimens showed the fundamental resonance to be at about 17 Hz., and the second mode to be at 103 Hz. Further experiments revealed that it was impractical to conduct the fatigue tests at the second mode; that all testing would be at the fundamental resonance. Therefore, it became desirable to increase this frequency in order to accumulate cycles at a faster rate. For this reason, all specimens were reduced to a total length of 10 inches, as opposed to the original 20 inches. This increased the range of fundamental resonances to 70 to 100 Hz.

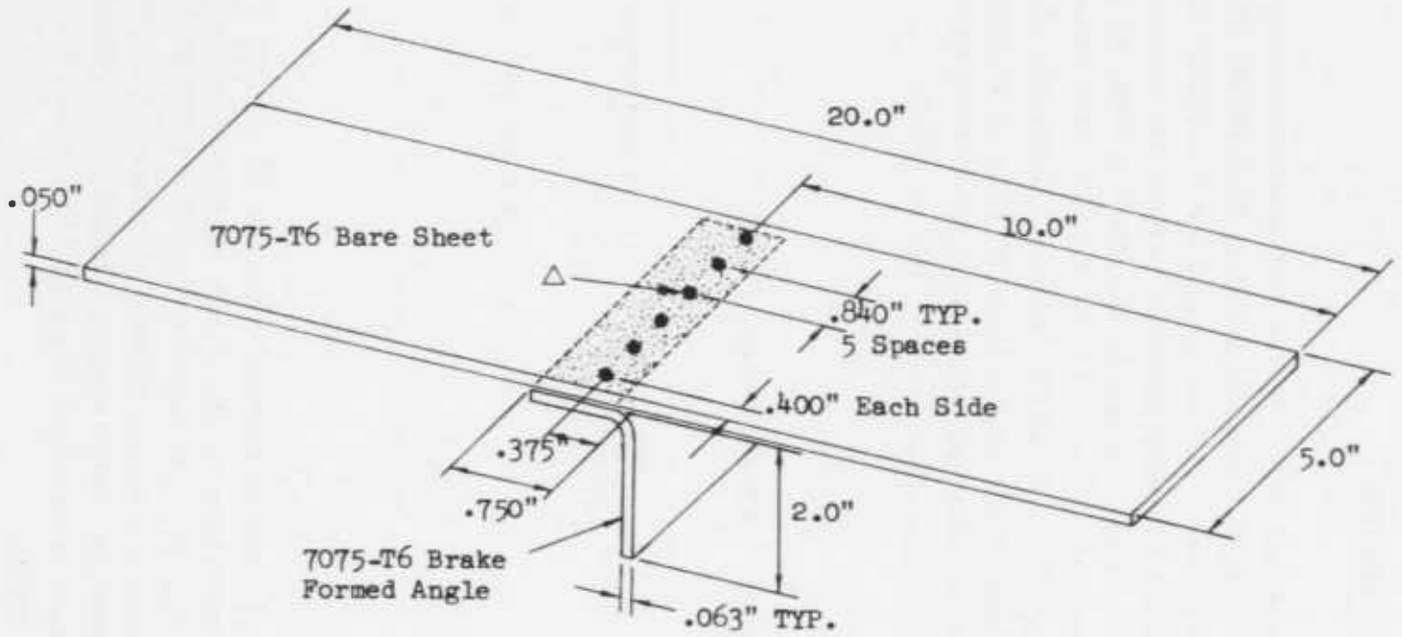

NOTES:

△ - Weldbond per Reference 1

1 - Panel & Rib Dimensions ± .005"

2 - X-Ray Inspect All Welds

3 - Ultrasonic Inspect All Bonds

FIGURE 48 – WELDBOND VIBRATORY FATIGUE SPECIMEN – CONFIGURATIONS 1 AND 1a

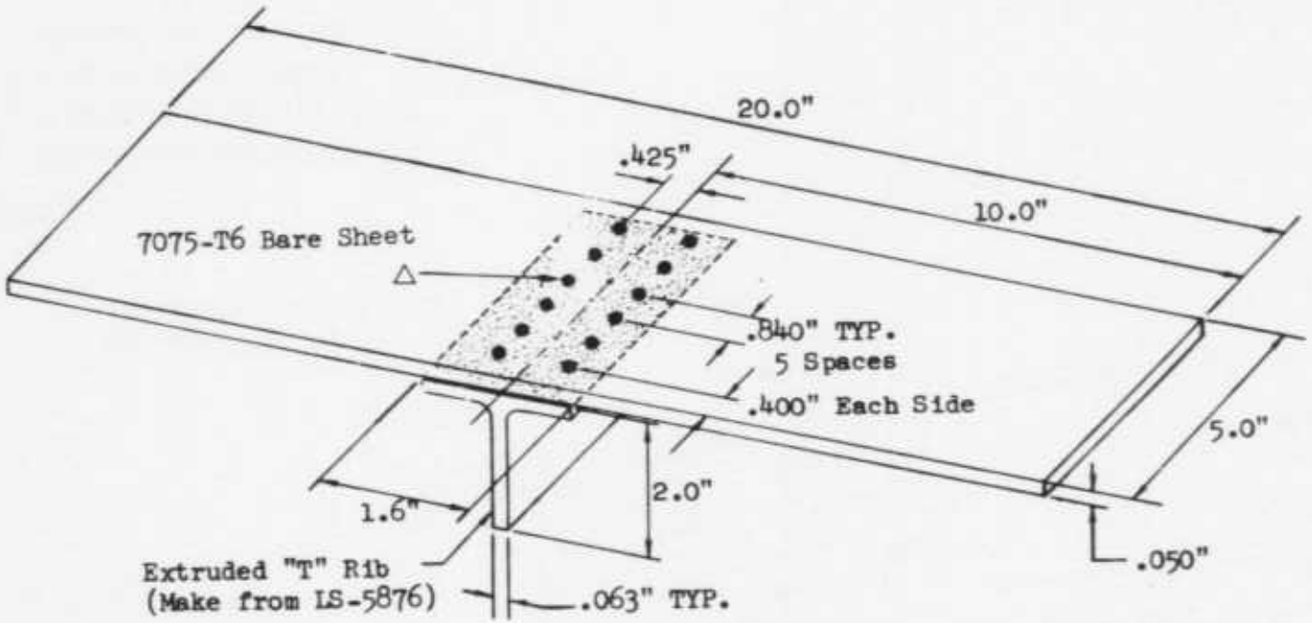

NOTES:

△ - Weldbond per Reference 1
1 - Panel & Rib Dimensions ± .005"
2 - X-Ray Inspect All Welds
3 - Ultrasonic Inspect All Bonds

FIGURE 49 – WELDBOND VIBRATORY FATIGUE SPECIMEN – CONFIGURATION 2

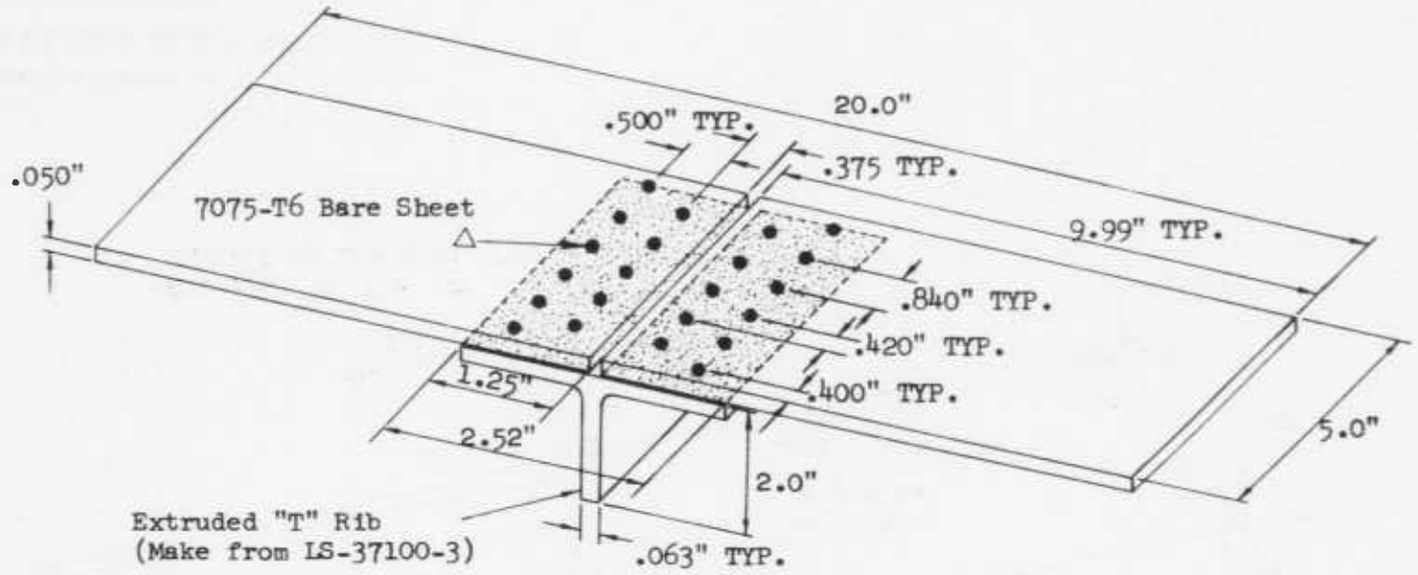

NOTES:

△ - Weldbond per Reference 1

1 - Panel & Rib Dimensions ±.005"

2 - X-Ray Inspect All Welds

3 - Ultrasonic Inspect All Bonds

FIGURE 50 – WELDBOND VIBRATORY FATIGUE SPECIMEN – CONFIGURATION 3

All of the vibration fatigue tests were accomplished by vibrating four specimens at resonance simultaneously using narrow band random excitation. The excitation spectrum was 30 Hz wide and centered on the average specimen resonance frequency. During testing, the resonant frequency was checked at frequent intervals at which time each specimen was carefully inspected. The random excitation was continued until failure.

After completion of testing, all of the resulting stress-life data were plotted on a log-log scale and fitted with a straight line using the method of least squares. After careful study of various individual plots and correlations, the data for all angle-stiffened specimens were combined as were the results of all tee-stiffened specimen tests. These results are shown in Figures 51 and 52.

Riveted skin fatigue data for clamped cantilever specimens of the same material were obtained from Reference 2, and are also shown in Figures 51 and 52.

Both Figures 51 and 52 show fatigue life of weldbonded structure as a function of bending stress in the skin at the edge of the stiffener. In the case of the angle stiffener, the skin stress is considerably higher over the bend in the stiffener than over the free edge of the flange, so the strain gages were located there, as shown in Figure 51. Thus, for a given bond or spot-weld fatigue life, the skin stress for the angle stiffener will be higher than for the tee stiffener. In riveted skin structure, the highest stress occurs at or near the rivet row. The riveted skin fatigue curves included for comparison in Figures 51 and 52 are therefore for stress at the rivet row midway between rivets.

These results show weldbonding to be as good, or better than, conventional countersunk rivets for joining skins and stiffeners whose design is governed by sonic fatigue considerations. In a typical structural application, where the sonic fatigue design life is on the order of 10^9 cycles, angle-stiffeners weldbonded with a single row of spot-welds are superior to a single row of rivets. Tee-stiffeners weldbonded with two or more spot-weld rows are as good as tees with two or more rivet rows.

From these vibratory fatigue tests, it became evident that in flexural bending across typical weldbonded joints, the weakest element in the joint is the adhesive bond; the next strongest element is the spot-weld; and the parent skin and stiffener material is the strongest. In other words, at a given level of bending stress in in the skin, the bond will fail first, then the spot-weld, and finally the skin. Because of this characteristic, two S-N curves are being provided for each type of skin stiffener, one for the bond and one for the spot-weld.

Although it would be poor general design practice if applied to significant load transfer structural joints, it is envisioned that, for some structures such as fairings assemblies and other secondary structure, joint designs may be based on spot-weld strength above. In these

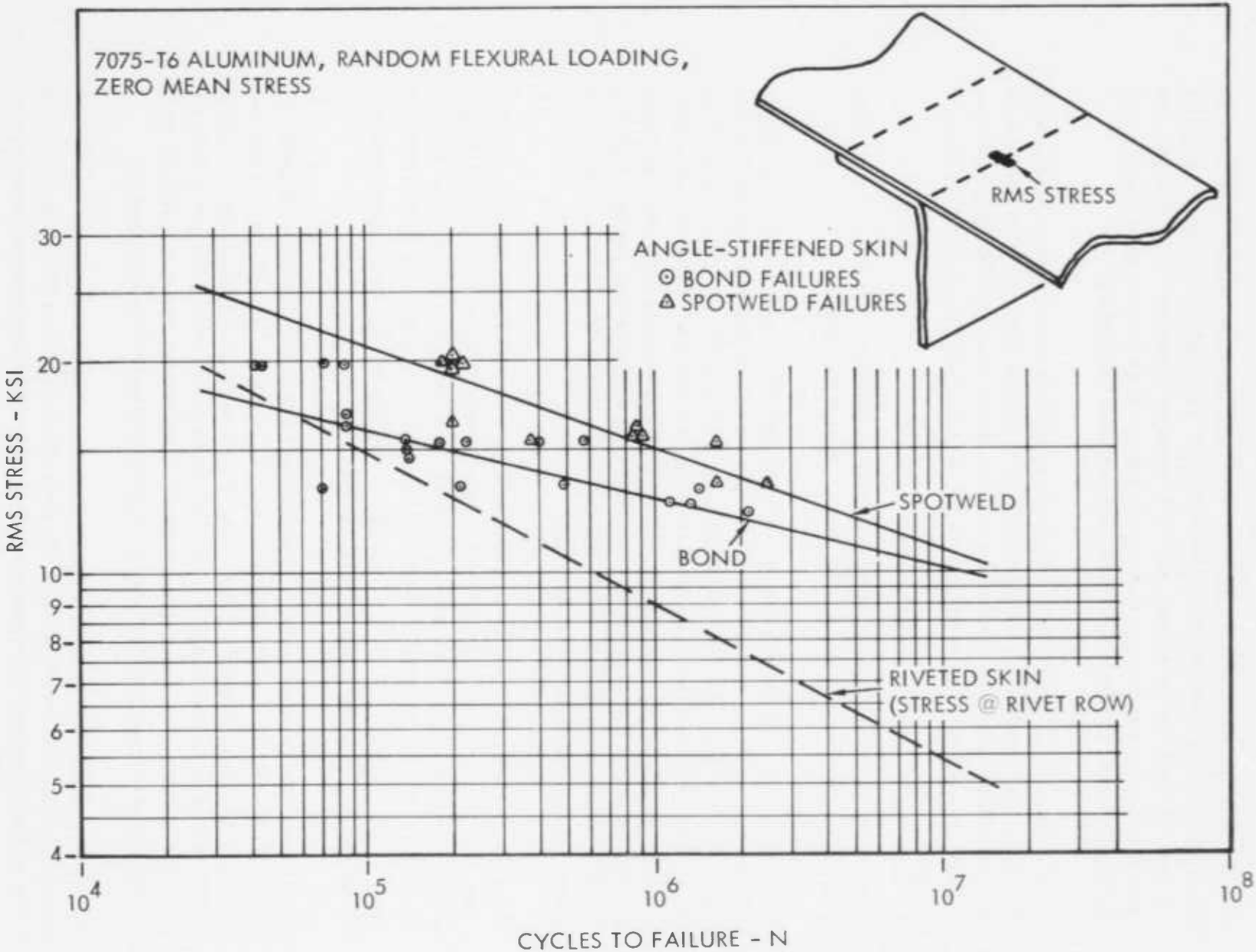

FIGURE 51. VIBRATORY FATIGUE OF WELDBOND STRUCTURE

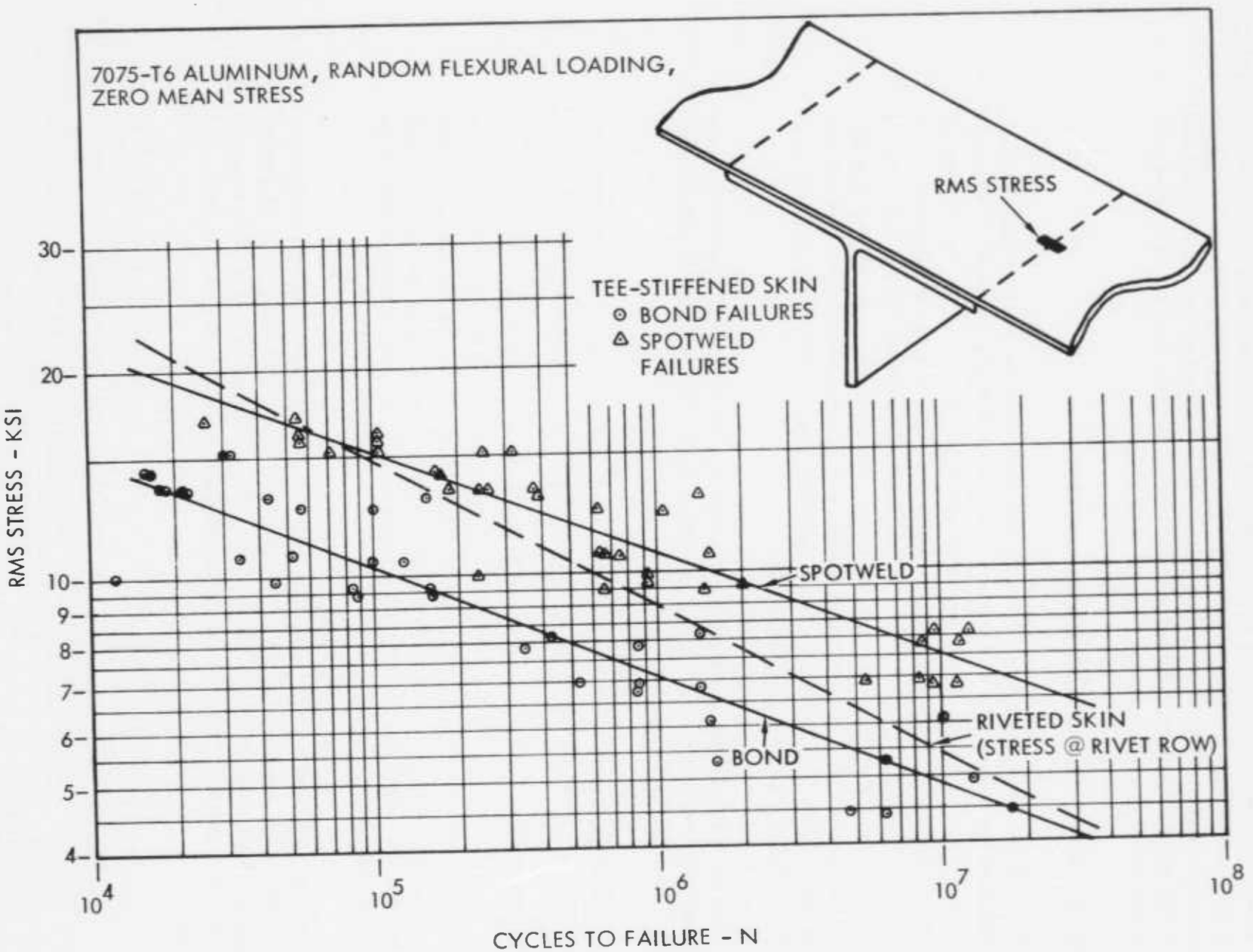

FIGURE 52. VIBRATORY FATIGUE OF WELDBONDED STRUCTURE

cases, the initial effect of the bond would be to increase the static strength of the joint and overall effect would be to enhance the fatigue strength of the spot-welds. In such applications, sonic fatigue failure of the bond would not constitute joint failure, and only the spot-weld fatigue curve would be used in designing for sonic fatigue. In other structural applications where the bond is loaded and an allowance for bond strength has been included in the design of the joint, failure of the bond would constitute joint failure, and the bond fatigue curve would be used in designing for sonic fatigue.

3.3.2 Sonic Fatigue Sub-Scale Specimens and Tests

Both flat and curved sub-scale sonic fatigue cover skin-rib-stringer specimens were designed, fabricated and tested under this program. The specimen details are shown on Figures 53 through 57. A total of six (6) specimens were fabricated – four (4) flat and two (2) curved. All specimens have nine (9) bays with the center bay size being approximately seven (7) inches by fourteen (14) inches. Overall sub-scale specimen size was approximately twenty-one (21) inches by thirty-one (31) inches. Two of the flat specimens had cover skin thicknesses of 0.050 inches and the remaining two flat specimens had cover skin thickness of 0.063 inches. The curved sub-scale specimens had cover skin thicknesses of 0.050 inches and the radius of curvature was 85.0 inches.

These sonic fatigue test specimens were designed to be similar to conventional riveted specimens which were evaluated in a previous program. This was done in order to make direct comparisons with test results from the riveted specimens.

All components were radiographically and ultrasonically inspected, and the number of defects were within acceptable limits allowed by the weldbond process specification.

After fabrication and inspection, the six (6) specimens were instrumented with strain gages, fitted into fixtures and then mounted in the acoustic test facility with monitoring microphones located at strategic locations. Figure 55 shows two (2) flat test components ready for testing with the strain gages and microphones installed. The rigid mounting frame and test component attachments are also visible. Figures 56 and 57 show the interior and exterior surfaces of the curved panels.

The flat components were tested first and the tests of the two curved components followed. The sonic fatigue tests were conducted on pairs of components at a sound pressure level of approximately 160 db overall. The test spectrum level at the first two (2) response modes was 135 db. Random excitation was used which ranged from 200 to 500 Hz.

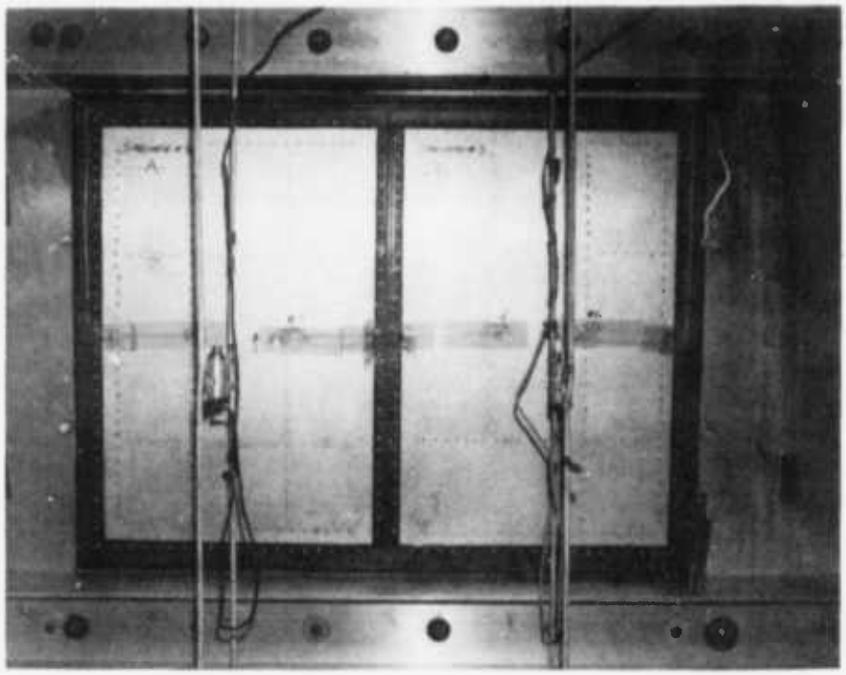

FIGURE 53 – FLAT WELDBONDED SUB-SCALE SONIC FATIGUE COMPONENTS INSTALLED IN TEST FIXTURE

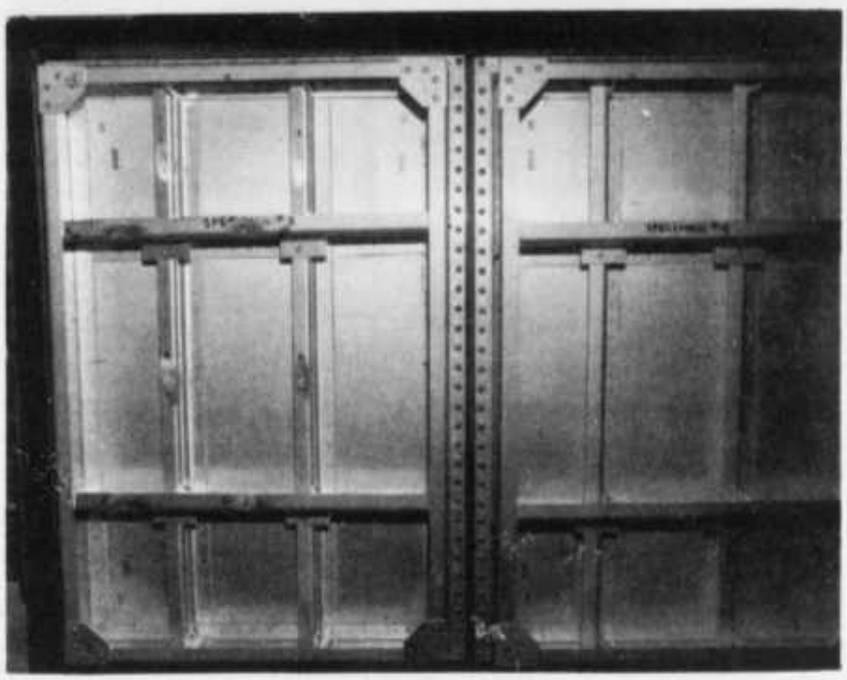

FIGURE 54 – FLAT WELDBONDED SUB-SCALE SONIC FATIGUE COMPONENTS INSTALLED IN ACOUSTIC FACILITY

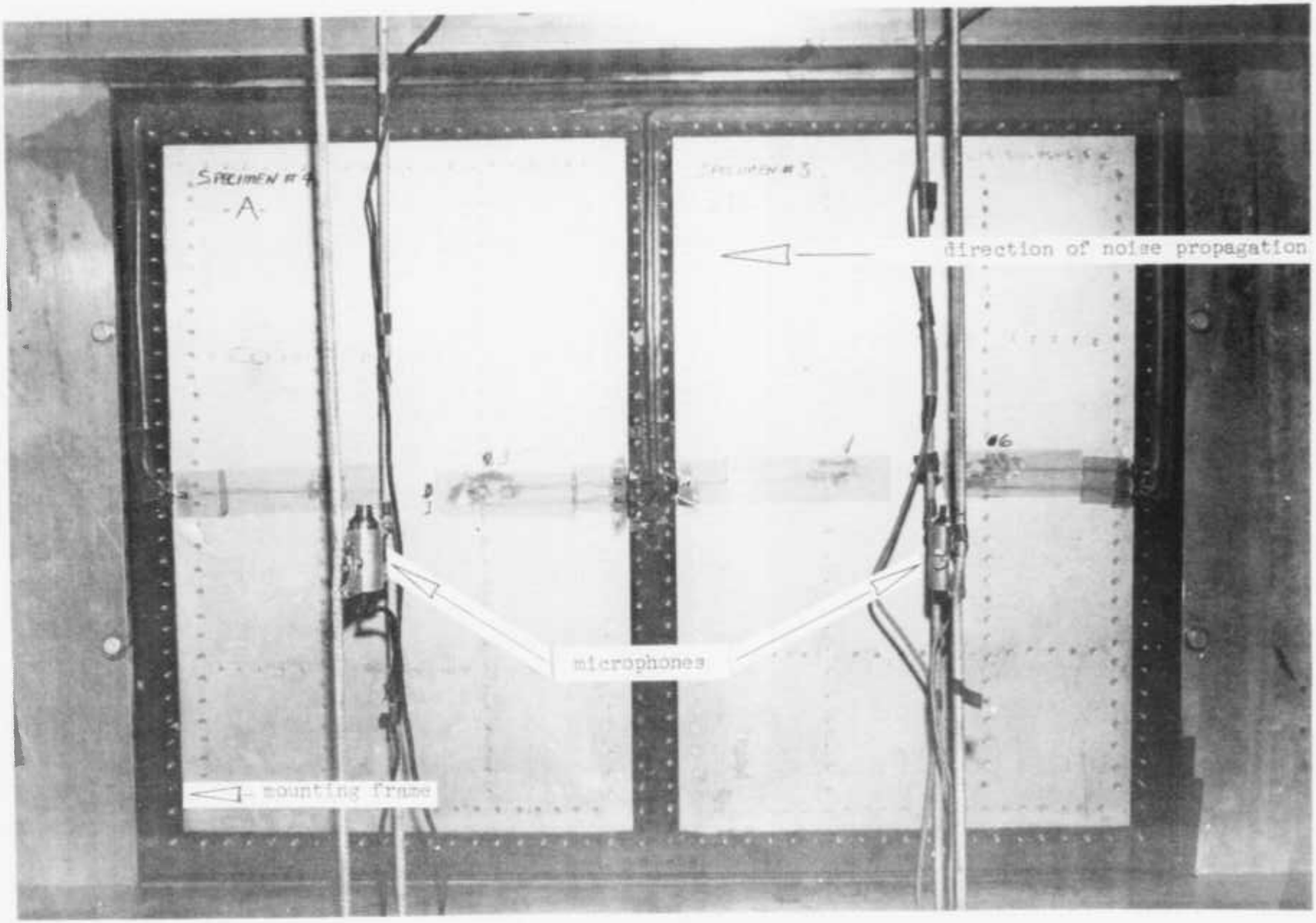

FIGURE 55 – FLAT TEST COMPONENT WITH STRAIN GAGES AND MICROPHONES INSTALLED

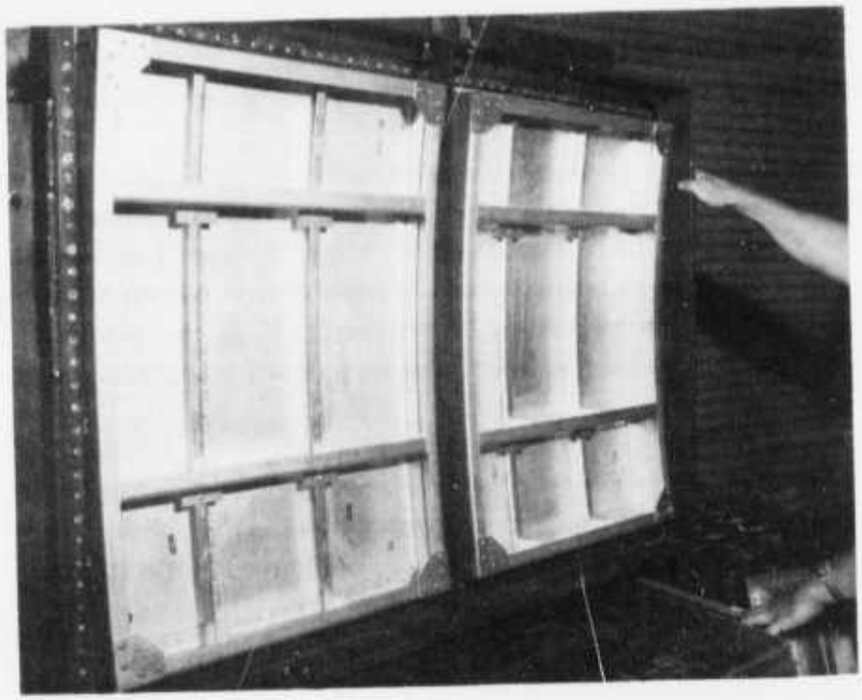

FIGURE 56 – CURVED SONIC FATIGUE COMPONENTS
VIEWED FROM THE INTERIOR SURFACE

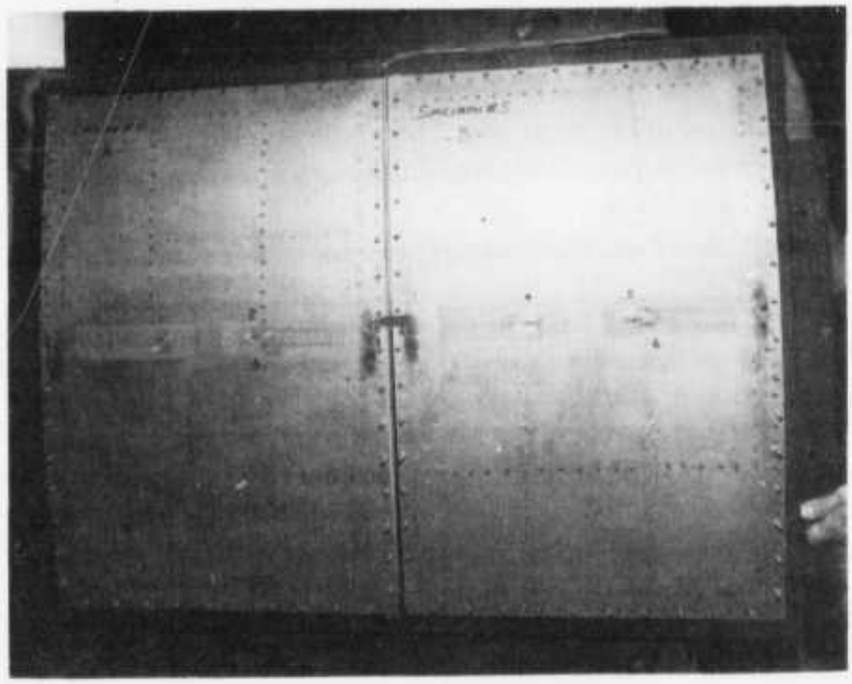

FIGURE 57 – CURVED SONIC FATIGUE COMPONENTS
VIEWED FROM THE EXTERIOR SURFACE

A resonance survey was conducted prior to fatigue testing to determine the damping and frequency range of the test spectrum. All of the weldbonded components were fatigue tested in pairs in a grazing incidence acoustic test facility. The components were tested using narrow band random noise with spectrum levels varying from 132 to 135 db.

In all tests, the first failure to appear was delamination of the adhesive bondline along the bondline fillet. The bondline failures would then progress along the edge of the stiffener or frame and penetrate into the weldbonded joint toward the row of spot-welds. Continued testing would result in small isolated cracks in the spot-weld nuggets in the region of the delaminated bondline. Further testing caused the cracks in the spot-welds to progress outward into the skin toward adjacent spot-welds until the cracks would ultimately interconnect.

Ultimately, some of the cracks that had originated in spot-welds had interconnected or progressed through several adjacent spot-welds resulting in sheet cracks extending approximately one-half the length of the sheet panels formed by the stiffeners as shown in Figure 58.

The resonant response of the weldbonded components was recorded throughout the fatigue tests to quantify resonance frequency. Total cycles to failure was based on the product of frequency and test time, and then summed for all of the test intervals.

The cycles to failure for each component are tabulated in Table XXXVI, along with test sound pressure level. The failure data shown in Table shows the first bondline failures and first spot-weld failures in the tests, and they occurred in the center bays of the components. In virtually every case these failures originated at the heel of the length-wise stiffener whose heel formed a boundary of the center bay. These failures duplicated the failures observed in the tests of the weldbonded angle-stiffened coupons which were reported previously.

Table XXXVI – Sub-Scale Weldbonded Component Sonic Fatigue Test Results

Component Ident. No.	Sound Pressure Spectrum Level (dB)	Bondline Cycles to Fail.	Spotwelds Cycles to Fail.
1	134.5	6.05×10^4	4.66×10^5
2	135.0	5.72×10^4	2.86×10^5
3	134.5	2.05×10^5	3.14×10^6
4	135.0	6.72×10^4	6.43×10^6
5	132.0	1.1×10^5	1.2×10^5
6	134.0	4.1×10^4	3.7×10^5

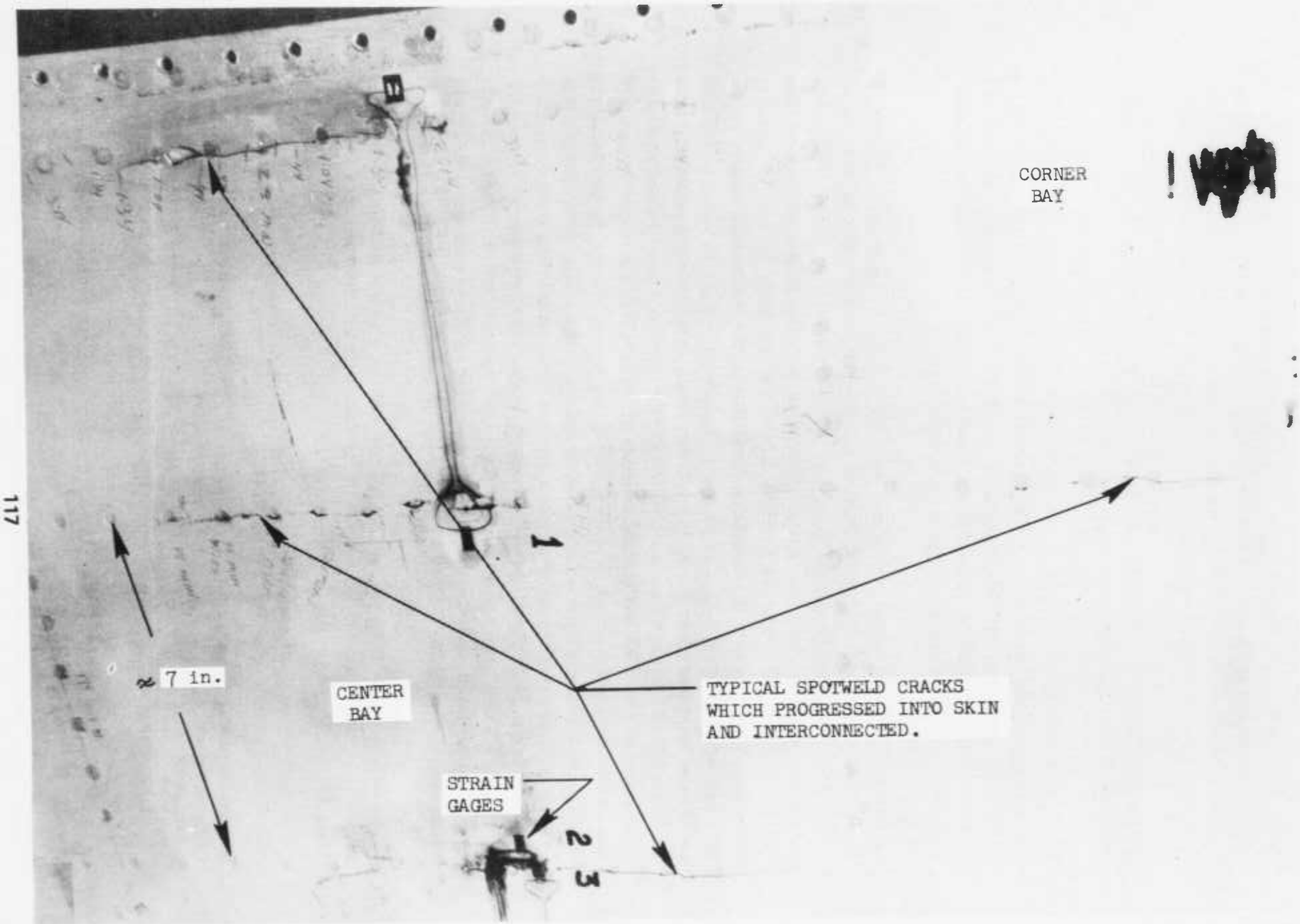

FIGURE 58 – FAILURES IN ONE OF THE FLAT TEST COMPONENTS

The curved weldbonded components, identified as numbers 5 and 6 in the above table, are identical to the flat components, 1 and 2 in the above table, except for the 85 inch radius. Examination of the data in Table XXXVI shows the curved component cycles to failure falling within the same general scatter band as the flat components. Thus, the effect of the 85 inch curvature is minor, and furthermore is much the same for comparative riveted structure. In general, the scatter in cycles to failure was larger than that experienced in riveted components and the weldbonded coupon specimens.

The sonic fatigue strength of riveted joints in flexural loading is principally established by the strength of the sheet and stiffener material in the vicinity of the rivet hole. In weldbonded joints that are similarly loaded, the strength of the adhesive bondline, the spot-weld nugget, and the heat-affected zone in the parent material are additional variables. A greater number of variables naturally leads to higher scatter.

Conventional sub-scale riveted components were tested in a previous program. The six (6) weldbonded components that were tested in this program were identical to these riveted components except for the method of joining. Both weldbonded and riveted components were tested similarly under identical conditions and both sets of test results have been plotted in Figure 59. Adhesive bondline failure and spot-weld failures are indicated separately. S-N curves with the same slope established by the weldbonded coupon fatigue tests (i.e., angle stiffeners with a single row of spot-welds that are the same as sub-scale weldbonded component joints) were fitted through these data points as depicted on Figure 59. These S-N curves may be compared directly to the regression line for riveted structure. As is shown on Figure 59, weldbonded structure of the type tested shows an improvement over riveted structure at service lives above 10^8 or 10^9 cycles. Also, at longer design life, weldbonding becomes progressively more advantageous over riveting. When design life is less than approximately 10^7 cycles to failure, weldbonding does not show an advantage, and below 10^6 cycles, weldbonding is clearly at a disadvantage. However, airplane structures are rarely designed for a sonic fatigue life of less than 10^8 cycles to failure. Thus, in the large majority of designs, it would be advantageous to use the weldbond joining method instead of conventional riveting.

Cycles to failure for riveted and weldbonded structures of identical configuration and test environment have been read from Figure 59 for typical service lives, and are tabulated in Table XXXVII.

Table XXXVII – Sonic Fatigue Service Life Comparison

Riveted Structure	Weldbonded Structure	
Cycles to Failure for Rivets or Sheet	Cycles to Failure For Adhesive Bondlines	Cycles to Failure For Spot-Welds
1×10^8	4.0×10^8	6.0×10^8
1×10^9	1.8×10^{10}	2.0×10^{10}

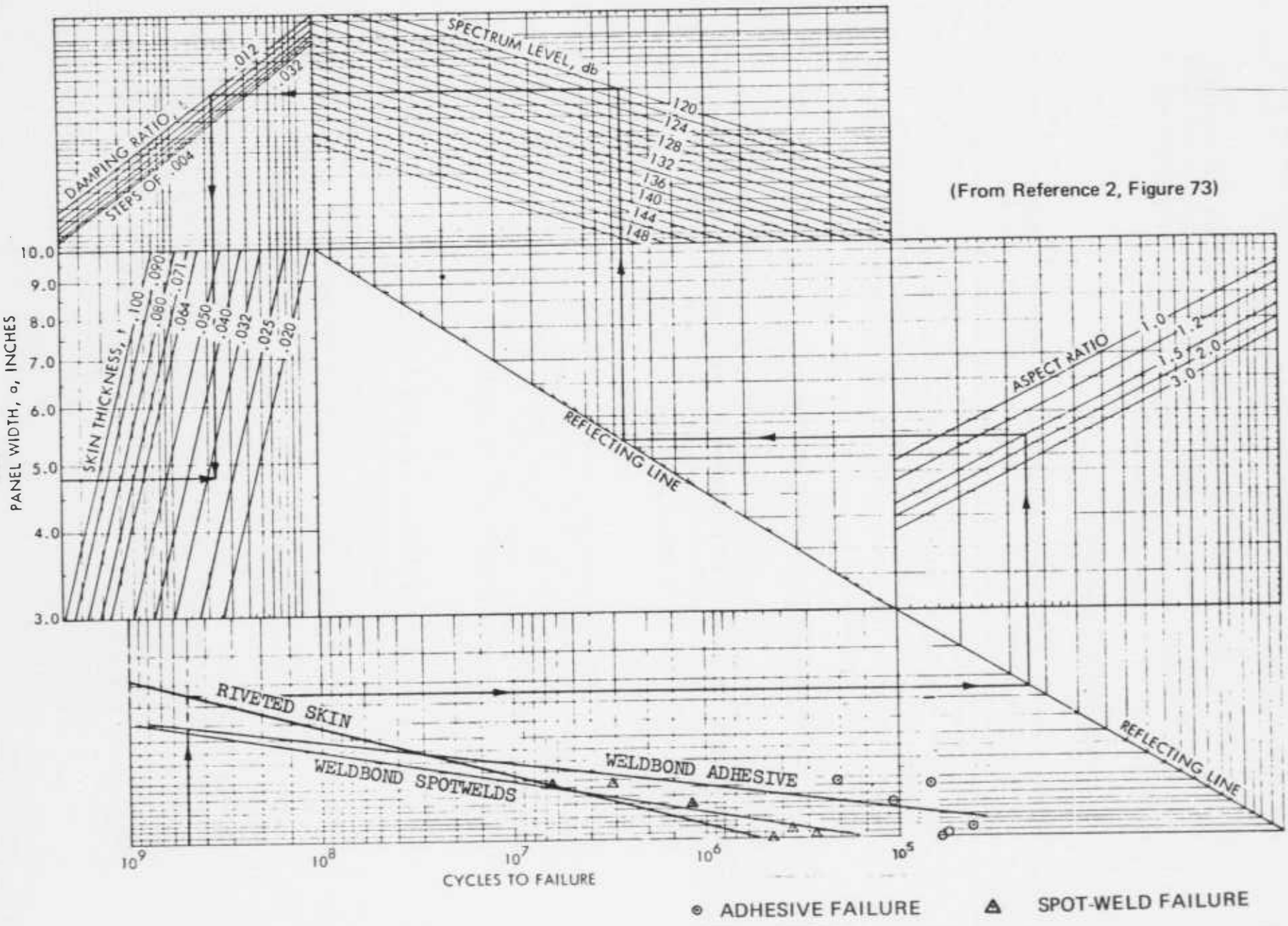

FIGURE 59 – STIFFENED-SKIN DESIGN-NOMOGRAPH 7075T6 ALUMINUM ALLOY

The data given in the above Table were based on 7075-T6 aluminum alloy flat stiffened-skin structure having angle stiffeners and single row rivets or spot-welds.

It was concluded from the results included herein that weldbonding is an acceptable substitute for riveting in the C-130 fuselage shell structure. The design of the C-130 weldbonded fuselage component was then reviewed for sonic fatigue requirements and it is approved for installation into an operational airplane.

3.4 Panel Stability Design Data

A series of stability tests were conducted under this program to determine the relative improvement of a weldbond connection between a skin and stringer over conventional riveted construction and to determining how closely a weldbond joint between skin and stringer approximates integral construction. Three (3) separate types of test were conducted to this purpose. These were compression crippling tests, shear panel tests and compression panel tests. All specimens surface treatments prior to weldbonding were the standard spot-weld etch. The adhesive used in specimen fabrication was M6800 (Whittaker) cured for one (1) hour at 250^{o}F.

3.4.1 Compression Crippling Specimens and Tests

The primary purpose for conducting crippling tests on weldbonded specimens was to determine the extent to which the weldbonded joint remainded intact as compression load was applied. The specimen configurations are defined by Figure 60 and Table XXXVIII. As indicated by Table XXXVIII, a total of twenty-seven (27) tests of this type were conducted under this program.

In preparing the specimens for testing, the end of each specimen were cast in Cerrobend to provide support during machining. Then the ends of each specimens were machined to form surfaces which were normal to the specimen load axis. Each specimen was instrumented with two axial strain gages as shown on Figure 61. The strain gage readings were used as a guide in aligning the specimens in the test machine for achieving a uniform strain distribution in the specimen.

Disbonding of the weldbonded joints was observed in the majority of the twenty-seven (27) specimens tested. The disbonding occurred well into the post buckling range for the flat sheet and Z-section stiffener, but prior to the yielding of the 7075-T6 Z-section stiffeners. Disbonding was accompanied by a sharp decrease in load even though the spot-welds remained intact. Visual examination of failed specimens revealed permanent buckles (crippling) limited to the vicinity of disbonding. A typical crippling specimen failure is shown in Figure 62. Apparently, the peeling loads in the bondline became quite large when the field strength of the 2024-T3 flat sheet was exceeded. The crippling specimen failure loads for the twenty-seven (27) tests are given in Table XXXIX. Other data given in Table XXXIX include the sheet and stiffener thicknesses and widths as well as stiffener heights. Also, the sheet and stiffener Rockwell"B" hardness are given as an average of three readings from each test specimen.

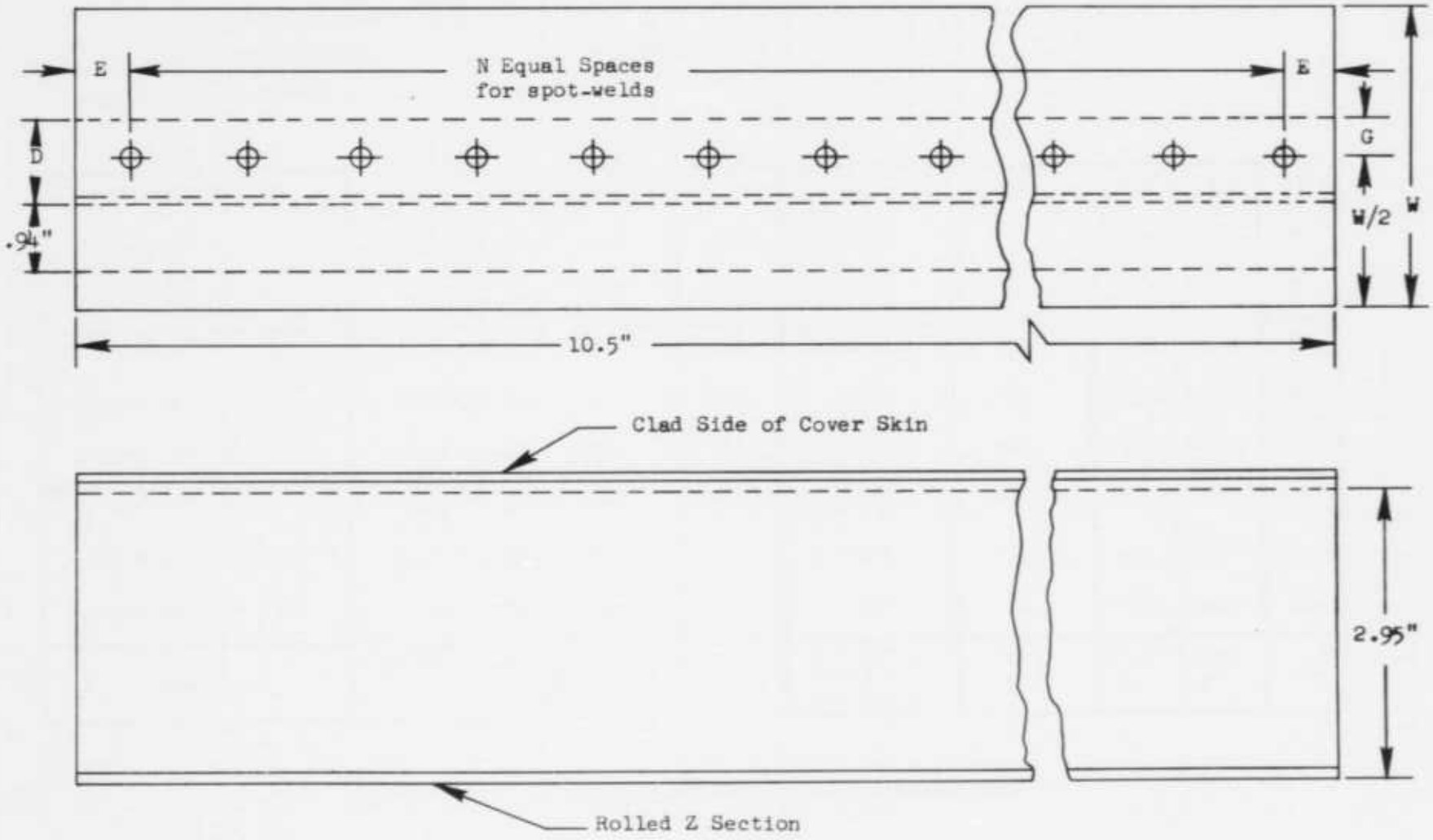

FIGURE 60 – WELDBOND CRIPPLING SPECIMEN

Table XXXVIII – Weldbond Crippling Specimen Geometrical Data

Specimen Code	Cover Skin Material & Thickness	W (in)	Rolled Z Section Thickness	D (in)	E (in)	G (in)	N
1-CR-1-1, -2, -3	2024-T3 Bare, .040	1.55	.040	.70	.375	.270	13
1-CR-2-1, -2, -3	2024-T3 Bare, .040	1.55	.050	.75	.400	.290	12
1-CR-3-1, -2, -3	2024-T3 Bare, .040	1.55	.063	.80	.438	.310	11
2-CR-1-1, -2, -3	2024-T3 (1), .050	1.75	.040	.70	.375	.270	13
2-CR-2-1, -2, -3	2024-T3 (1), .050	1.75	.050	.75	.400	.290	12
2-CR-3-1, -2, -3	2024-T3 (1), .050	1.75	.063	.80	.438	.310	11
3-CR-1-1, -2, -3	2024-T3 Bare, .063	2.00	.040	.70	.375	.270	13
3-CR-2-1, -2, -3	2024-T3 Bare, .063	2.00	.050	.75	.400	.290	12
3-CR-3-1, -2, -3	2024-T3 Bare, .063	2.00	.063	.80	.438	.310	11

NOTES: (1) This material is clad one side only

(2) Make Rolled Z Section from the dimensions in the above table and Figure 60

(3) Weldbond per Reference 1

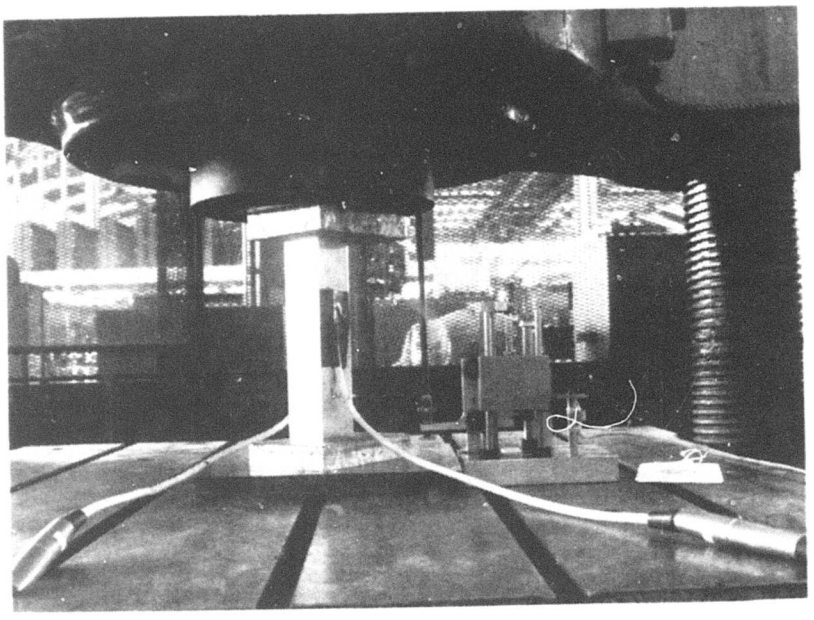

FIGURE 61 – TYPICAL TEST ARRANGEMENT FOR CRIPPLING SPECIMENS

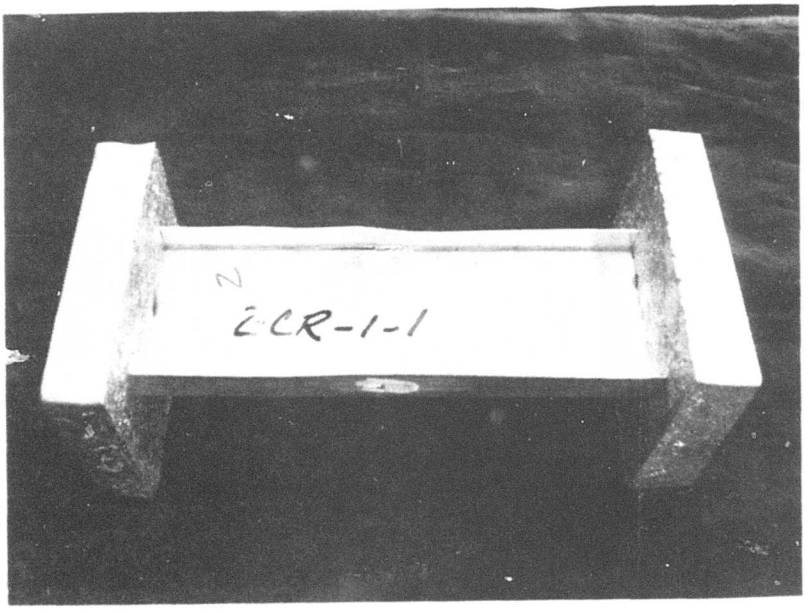

FIGURE 62 – TYPICAL CRIPPLING SPECIMEN FAILURE

TABLE XXXIX – SUMMARY OF CRIPPLING FAILURE LOAD DATA

SPECIMEN CODE	SHEET THICK. (IN.)	Z-STIFF. THICK. (IN.)	Z-STIFF. HEIGHT (IN.)	Z-STIFF. FLANGE WIDTH (IN.)	SHEET OVERHANG WIDTH (IN.)	AVG. SHEET HARDNESS (RB)	AVG. STIFF. HARDNESS (RB)	FAILURE LOAD (LBS.)
1-CR-1-1	.039	.037	2.97	.70	.27	64.2	88.5	5,420
1-CR-1-2	.039	.037	2.97	.70	.27	66.3	89.0	5,280
1-CR-1-3	.039	.037	2.96	.70	.27	66.8	88.0	5,760
1-CR-2-1	.039	.050	2.98	.74	.32	65.0	89.7	8,400
1-CR-2-2	.039	.049	2.96	.77	.34	66.2	90.0	8,140
1-CR-2-3	.039	.050	2.93	.76	.28	64.0	90.0	8,880
1-CR-3-1	.039	.059	2.97	.82	.34	65.7	91.0	10,720
1-CR-3-2	.039	.057	2.95	.80	.35	66.8	88.2	10,525
1-CR-3-3	.039	.057	2.99	.80	.35	65.3	91.0	10,450
2-CR-1-1	.050*	.039	2.99	.69	.27	66.8	91.0	6,700
2-CR-1-2	.050*	.037	2.96	.70	.28	64.3	88.0	5,580
2-CR-1-3	.050*	.038	2.98	.65	.28	66.0	88.3	6,400
2-CR-2-1	.050*	.050	2.96	.74	.29	65.8	89.2	8,800
2-CR-2-2	.050*	.050	2.94	.75	.33	65.7	89.8	9,040
2-CR-2-3	.050*	.050	2.96	.74	.30	66.0	89.0	8,900
2-CR-3-1	.050*	.057	2.99	.77	.29	65.2	88.7	11,480
2-CR-3-2	.050*	.058	2.95	.80	.30	66.8	91.0	11,040
2-CR-3-3	.050*	.058	2.95	.83	.33	65.7	90.0	11,350

TABLE XXXIX – SUMMARY OF CRIPPLING FAILURE LOAD DATA (CONT'D.)

SPECIMEN CODE	SHEET THICK. (IN.)	Z-STIFF. THICK. (IN.)	Z-STIFF. HEIGHT (IN.)	Z-STIFF. FLANG WIDTH (IN.)	SHEET OVERHANG WIDTH (IN.)	AVG. SHEET HARDNESS (RB)	AVG. STIFF. HARDNESS	FAILURE LOAD (LBS.)
3-CR-1-1	.062	.037	2.98	.65	.30	65.5	88.7	7,900
3-CR-1-2	.062	.037	2.98	.67	.30	77.0	88.2	8,250
3-CR-1-3	.062	.037	2.96	.67	.27	76.0	88.0	8,120
3-CR-2-1	.062	.050	2.94	.74	.34	72.2	88.3	10,880
2-CR-2-2	.063	.049	2.95	.76	.32	72.3	88.7	11,020
3-CR-2-3	.062	.050	2.92	.77	.32	77.3	88.3	11,100
3-CR-3-1	.062	.057	3.00	.82	.35	76.7	90.2	11,810
3-CR-3-2	.062	.057	3.00	.82	.34	76.7	91.0	13,040
3-CR-3-3	.062	.056	2.94	.81	.34	77.0	90.7	12,620

NOTES:

(1) All sheet material was 2024-T3 bare except where noted by asterisk (*) where clad one side only 2024-T3 was used.

(2) All z-section sitffeners were 7075-T6 bare aluminum alloy sheet.

(3) All thicknesses, heights, and widths are measured values.

(4) The average sheet and stiffener hardnesses are averages of three individual measurements.

Correlation of predictions and test results from the weldbonded crippling specimens is shown in Figure 63. It is noted that only one test result from a total of twenty-seven (27) tests is shown to lie on the unconservative side of the plot in Figure 63.

3.4.2 Sub-Scale Shear Panel Specimens and Tests.

Three (3) weldbonded shear panels with configurations as defined in Figure 64 through 66 and Table XL were tested to failure in a "picture frame" test jig. Location and type of instrumentation are shown in Figure 65. A tensile load was applied to the "picture frame" test jig which resulted in a shear load in the panel. After installing each test panel in the "picture frame" test jig, it was instrumented with electrical resistance strain gages. The first of the shear panels was instrumented with fifteen (15) axial-type strain gages while the other two (2) shear panels were instrumented with eight (8) strain gages each. In each test, incremental loading was applied and strain data recorded at each load increment. The first condition observed during all tests was the on-set of buckling of the flat sheet of the shear panel as shown in Figure 66. Continued increase in loading caused the buckles in the flat sheet to become deeper. The next occurrence as the applied load was increased was a delamination of the flat sheet-to-Z-section stiffener bondline. The delamination was accompanied by an audible "cracking" noise. The first delamination occured between the heel of the radius of the Z-section stiffener and the flat sheet, where the bondline was comparatively thick due to the radius. In the weldbonded panel tests, the next observed failure was the "tear through" of a spot-weld through the thinner of the structural elements, i.e., the flat sheet or the weldbonded flange of the rolled Z-section stiffener. The location of the spot-weld that failed first was near the middle of the weldbonded joint of one of the Z-section stiffeners where the buckles in the flat sheet appeared to be the deepest. Finally, as the load was increased, bondline delaminations and spot-weld failures continued, the flat sheet failed in tension on a line approximately normal to the direction of the applied load.

Table XL – Weldbond Shear Stability Panels

Specimen Code	Skin Material and Size in.	7075-T6 Sheet Rolled Z Sect. Thickness (3) in.	D in:	E in.	G in.	N (4) spaces
1-SP-1	2024-T3 (1), .063	.040	.92	.375	.270	26
2-SP-1	(2) .050	.050	.88	.400	.290	24
3-SP-1	(1) .040	.063	.85	.438	.310	22

NOTES:

(1) 2024-T3 sheet, bare

(2) 2024-T-3 sheet, clad one side only

(3) Make rolled Z-section as shown in Figure 65

(4) "N" equal spaces for spot-welds

(5) Dimensions D, E, and G have same definition as those on Figure 60.

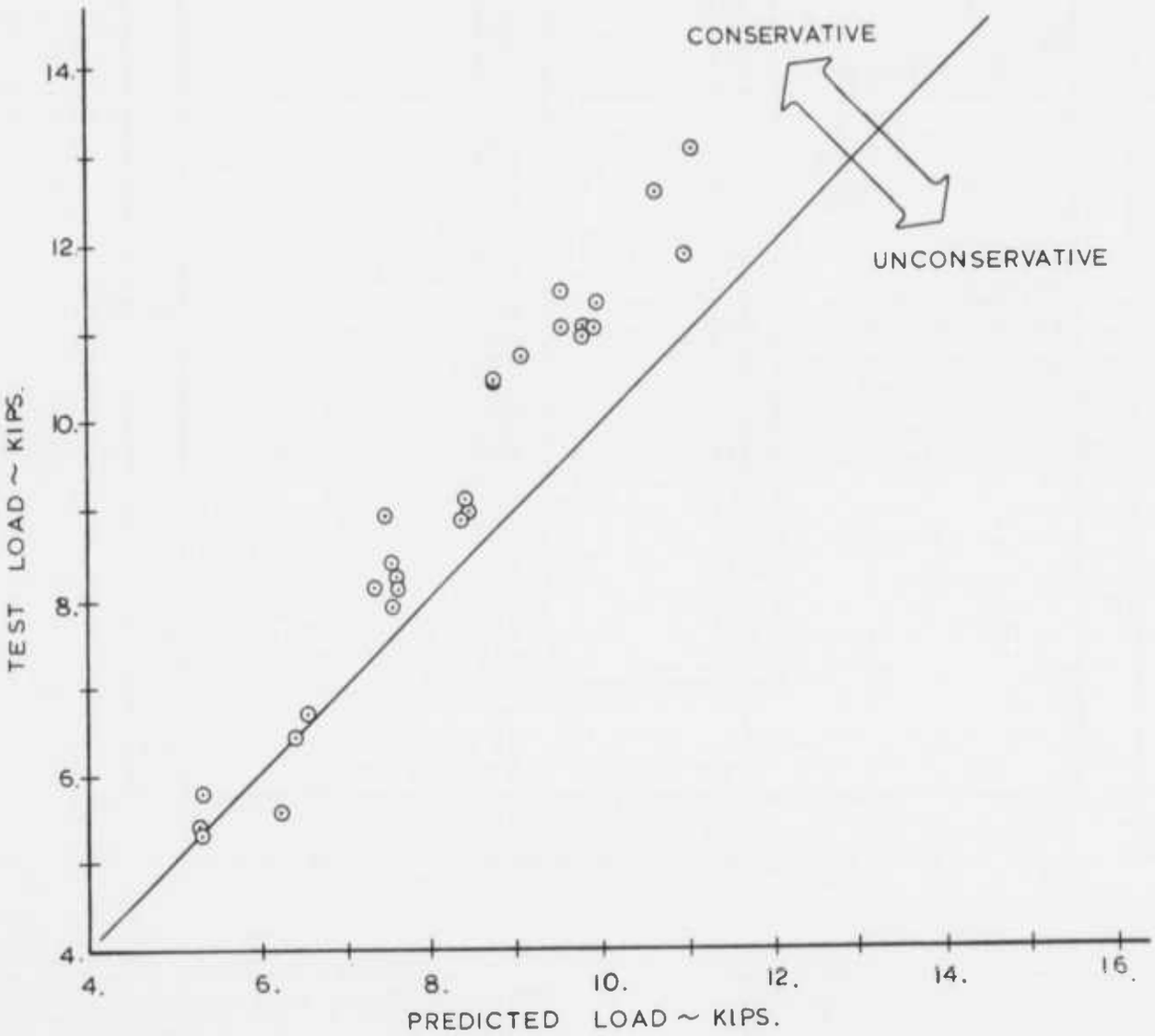

FIGURE 63 – CORRELATION OF THE WELDBONDED CRIPPLING SPECIMEN TESTS

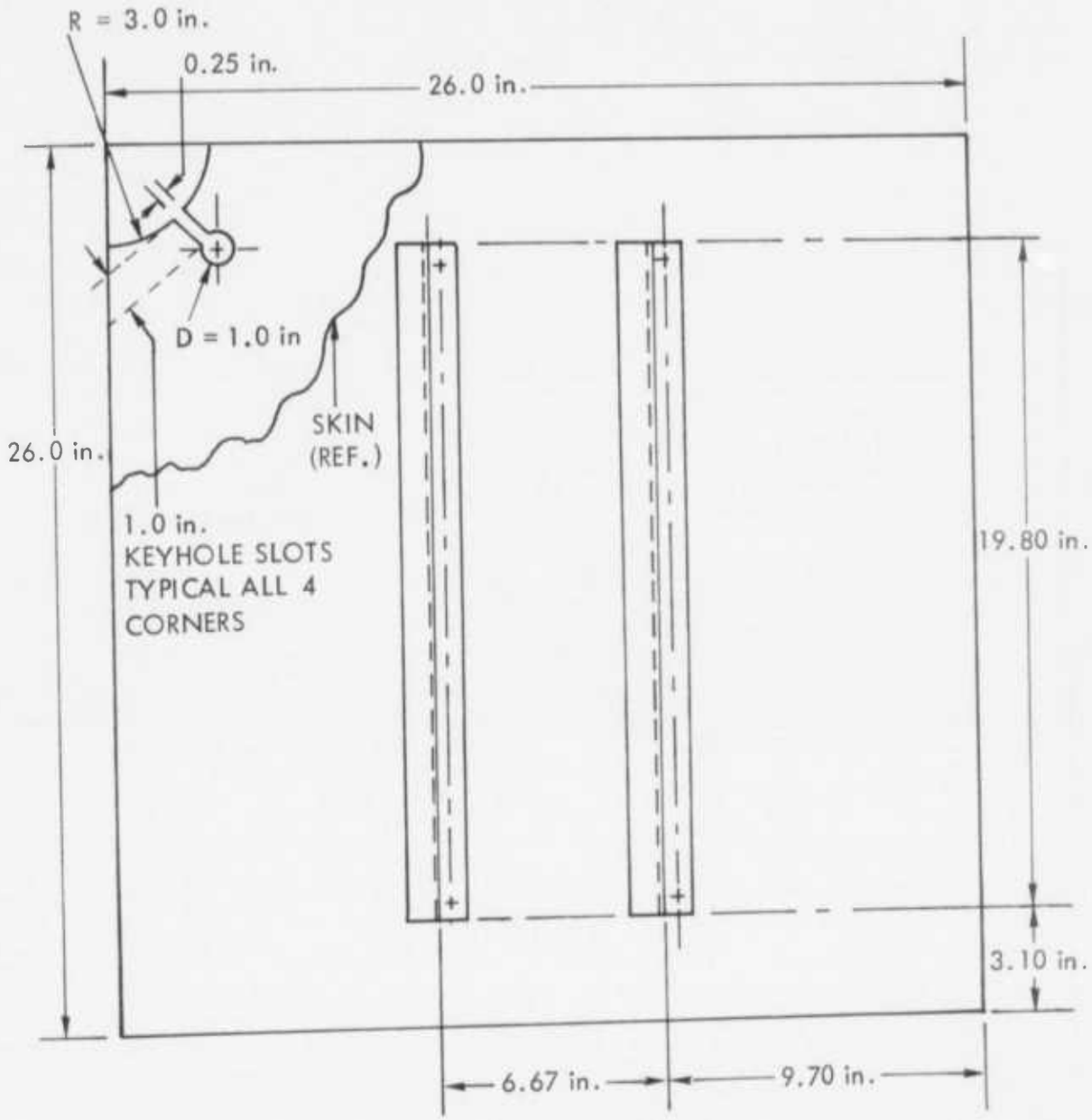

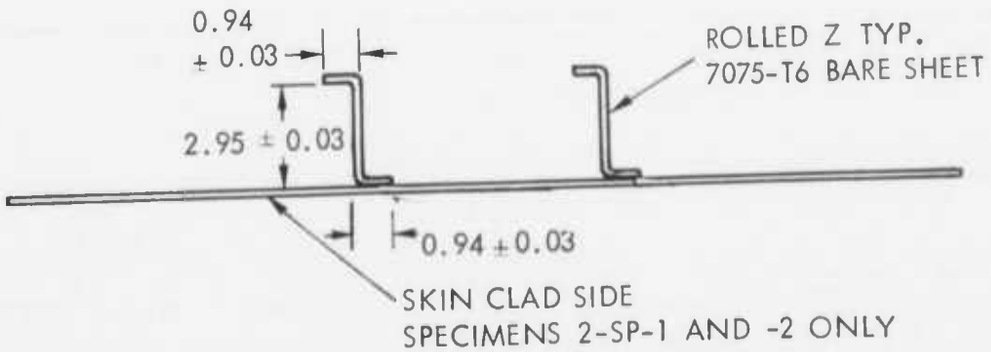

FIGURE 64. - WELDBOND SHEAR PANELS

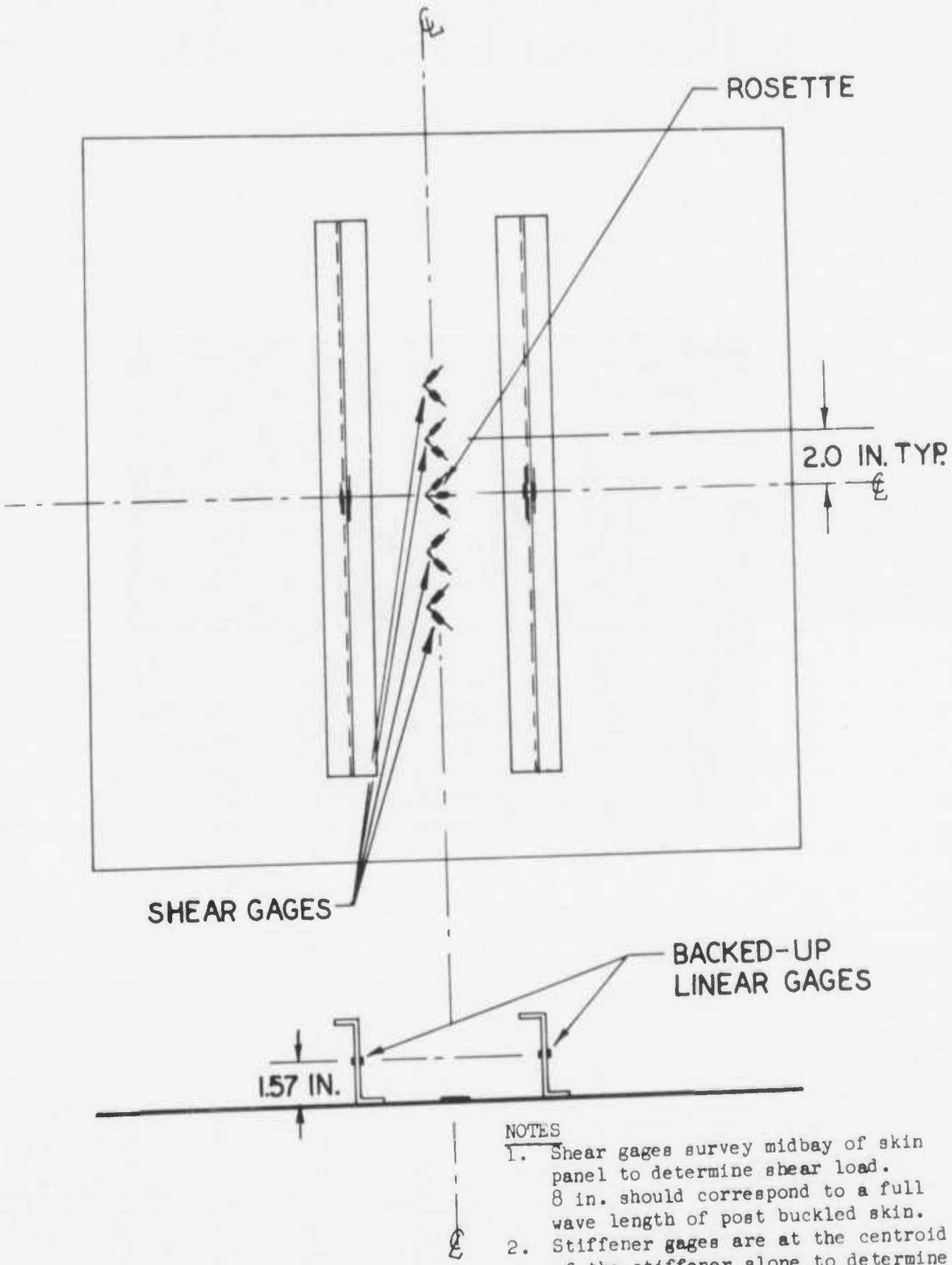

NOTES

1. Shear gages survey midbay of skin panel to determine shear load. 8 in. should correspond to a full wave length of post buckled skin.
2. Stiffener gages are at the centroid of the stiffener alone to determine stiffener load at midlength.

FIGURE 65 – STRAIN GAGES – WELDBOND SUB-SCALE SHEAR PANEL

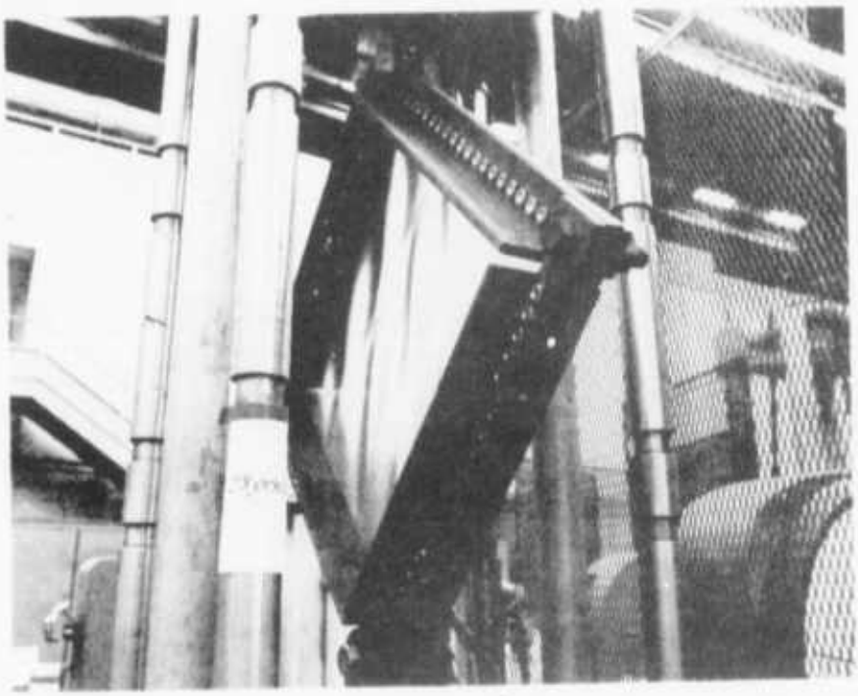

FIGURE 66 – TYPICAL BUCKLED CONDITION OF SHEAR PANEL, 3 SP 2

In addition to the weldbonded shear panels, three panels which substituted adhesive bonding for weldbonding were tested. These were fabricated with M6800 adhesive cured for one (1) hour at 250°F. Pressure was applied through mechanical clamping. The specimen surfaces were prepared for bonding through the standard spot-weld etch.

In the adhesive bonded panel tests, buckling of the flat sheet was followed by bondline delamination between the heel of the radius of the Z-section stiffener and the flat sheet as in the weldbonded panel tests. Continued increase in loading caused the buckles in the flat sheet to become deeper accompanied by further disbonding of the bondlines; however, disbonds did not occur at the crests of the waves in the flat where the stiffener pushed against the sheet. Disbonding in the valleys of the buckled sheet was complete at lower load levels than for the weldbonded panels. Finally, as was the case for the weldbonded panels, the buckled sheet failed in a tensile mode.

The initial delamination and final failure loads are shown in Table XLI for both weldbonded and adhesive bonded shear stability panels.

Table XLI – Summary of Shear Stability Panel Failure Load Data

Specimen Code	Sheet Thickness (in.)	Stiffener Thickness (in.)	Local Disbonding Load– lbs.	Final Failure Load– lbs.
1-SP-2	.058	.038	35,000	51,400
2-SP-1	.050*	.051	28,000	40,800
3-SP-2	.037	.061	26,000	31,400
1-SP-1A	.062	.037	30,000	55,700
2-SP-1A	.050*	.049	20,000	41,800
3-SP-1A	.038	.049	22,200	34,700

NOTES:

1. Shear stability panel codes containing "A" are adhesive bonded only panels
2. All sheet material was 2024-T3 bare except where noted by asterisk (*) where clad one side only 2024-T3 was used.
3. All Z-section stiffeners were 7075-T6 bare aluminum alloy sheet.

The local disbonding loads given in the above table are those loads at which distinct disbonds first became apparent. The final failure loads in Table XLI are maximum loads that were achievable in the tests and represent tensile failure modes in the panel sheets. The tensile failure loads in the panel sheets are not appropriate to use as ultimate design loads in weldbonded and adhesive bonded panels because complete local disbonding and spot-weld failures in the sheet-to-stiffener joints occur at lesser load levels. Thus, it is suggested that complete local disbonding loads be established as the allowable strengths for adhesive bonded shear panels and spot-weld failure loads be established as the allowable strengths for weldbonded shear panels. In applying these criteria, weldbonded shear panels would support applied loads that are 10 to 15 percent higher than comparable adhesive bonded panels.

3.4.3 Sub-Scale Compression Panel Specimens and Tests

As in the case of the sub-scale shear panels, compression stability tests were conducted on three (3) weldbonded and three (3) adhesive bonded flat test panels. Each test panel consisted of six (6) Z-section stiffeners joined to a flat aluminum alloy sheet. Both Z-section stiffeners and flat sheet were 0.063 inch 7075-T6 bare aluminum alloy. All test panels were 43 inches in length and approximately 18 inches wide.

In preparation for testing, the ends of each test panel were encased in Cerrobend to provide end support during machining. The first weldbonded and first adhesive bonded test panels were instrumented with 28 axial strain gages while the remaining test panels were instrumented with 21 axial strain gages. Twelve (12) strain gages were used to verify uniform load distribution across the test panel. Six (6) of the twelve (12) strain gages were located on a line six (6) inches from each end of each test panel. Figure 67 shows an instrumented test panel located in the test machine. In general, compression load was applied to each test panel in increments of 10,000 pounds for the initial part of each test and then in increments of 5000 pounds in the latter part of each test. The load rate was 5,000 pounds per minute.

Figures 68 and 69 show typical failed weldbonded and adhesive bonded compression panels. It is noted that the length of stiffener-sheet disbonds for the adhesive bonded panel were significantly longer than those of weldbonded panel.

The following results given in Table XLII were obtained from the six (6) compression stability tests of weldbonded and adhesive bonded panels. Also, a riveted panel test is included from Reference 3 for comparison with the weldbonded and adhesive bonded panel tests.

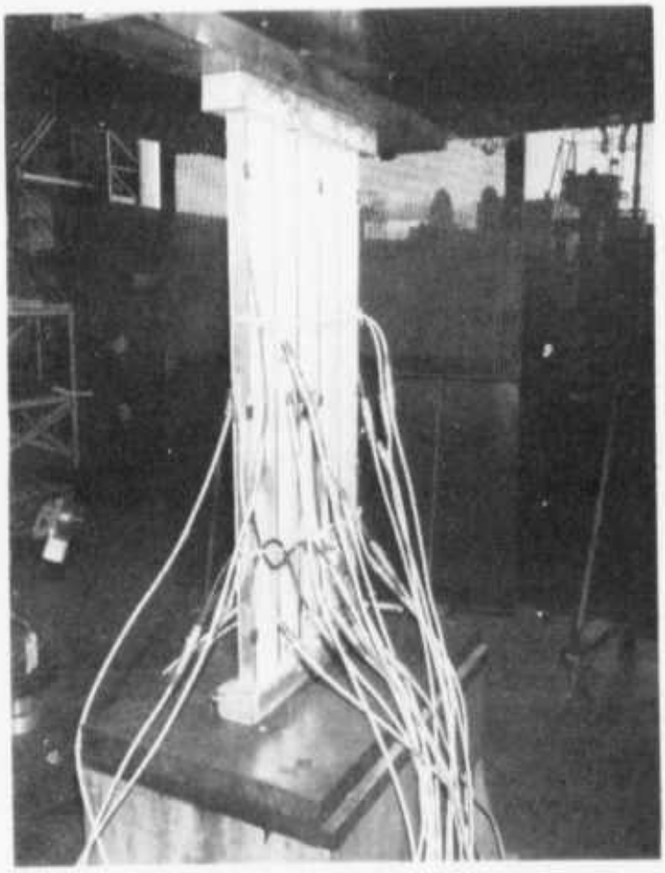

FIGURE 67 – TYPICAL INSTRUMENTED COMPRESSION STABILITY PANEL IN TEST MACHINE

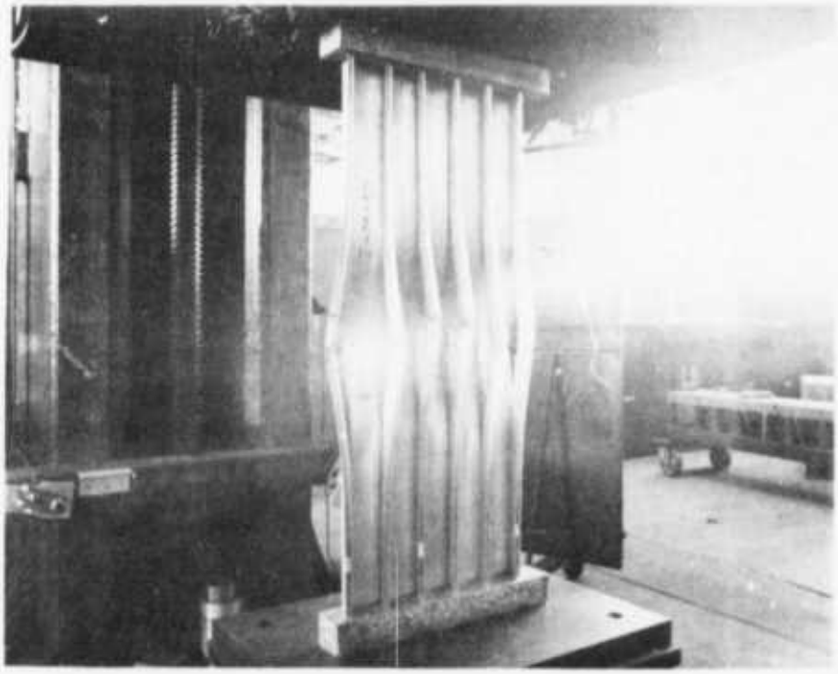

FIGURE 68 – TYPICAL FAILED WELDBONDED COMPRESSION STABILITY PANEL

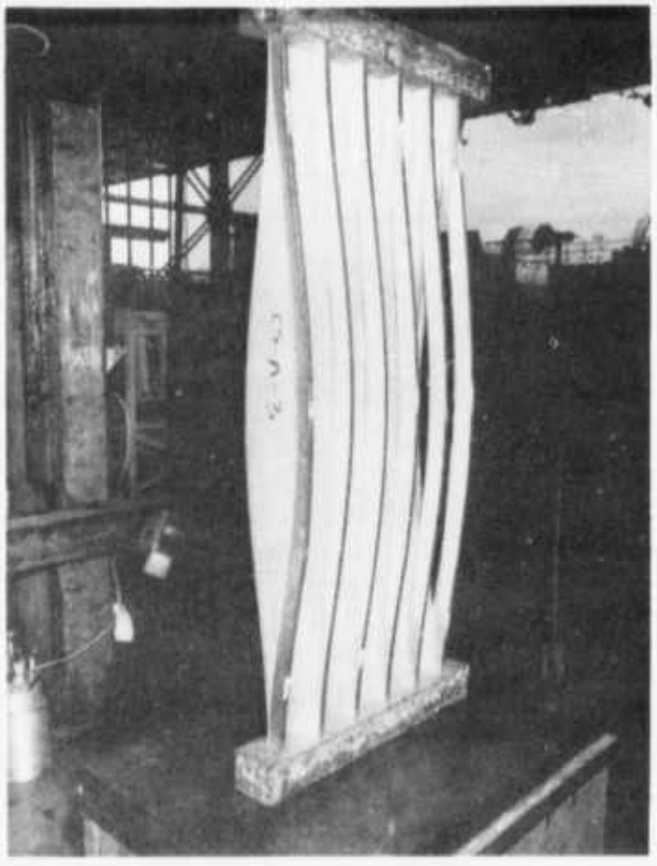

FIGURE 69 – TYPICAL FAILED ADHESIVE BONDED COMPRESSION STABILITY PANEL

TABLE XLII – SUMMARY OF COMPRESSION STABILITY PANEL FAILURE LOAD DATA

Type of Sheet-Stiffener Joint	Failure Load (Lbs.)	Failure Mode
Weldbonded	76,200	Torsional instability of edge stiffener
Weldbonded	76,100	Torsional instability of edge stiffener
Weldbonded	70,000	Torsional instability of edge stiffener
Adhesive Bonded	44,500	Total disbonding of stiffener-to-sheet joint
Adhesive Bonded	60,000	Total disbonding of stiffener-to-sheet joint
Adhesive Bonded	63,700	Total disbonding of stiffener-to-sheet joint
Riveted	75,000	Torsional instability of edge stiffener

Post failure examination of the first adhesive bonded test panel listed in Table XLII revealed that the Z-section stiffener flanges had become disbonded from the flat sheet at each end of the panel. Since traces of Cerrobend were found in the failed bondline, it was concluded that premature disbond occurred during the Cerrobending operation. Furthermore, it was assumed that this disbonding contributed to the relative low failure load (44,500 lbs.) of the first adhesive bonded test panel. In order to alleviate the disbonding condition in the second and third adhesive bonded test panels, two Hi-Lok steel fasteners were installed in the end of each stiffener through the bondline at both ends of each of the panels. As seen by the failure loads of the second and third adhesive bonded panels, this modification gave more reasonable failure loads compared to the weldbonded and riveted test panels. It is concluded from the limited data given in Table XLII that weldbonded panels are comparable to riveted panels when tested in a compression stability mode, and adhesive bonded panels develop failure loads of approximately 83 percent of weldbonded or riveted panels.

SECTION IV

INTERNAL WELDBOND JOINT STRESS DISTRIBUTION

4.1 Preliminary Analysis

In order to gain an early and general insight into the contributing roles of the weld and the adhesive bond in a weldbond joint, preliminary finite element and closed form analyses of a typical single overlap weldbond joint were performed. Both of these analyses considered only elastic deformations so that no plastic material conditions were considered. Since the analysis is linear, no stress redistribution was considered with increasing applied load and direct factoring or ratioing of the analysis results is valid within material elastic range limitations.

4.1.1 Preliminary Finite Element Analysis

Preliminary analysis of bondline stresses was performed using Lockheed-Georgia Company's Flutter and Matrix Algebra System (FAMAS) Program 97. The isotropic triangular membrane-translational spring fastener element model used in this analysis is shown in Figure 70 . The joint modeled is a single one-inch overlap with 0.05 aluminum adherends. The bondline thickness was set at five mils and the adhesive shear modulus, G, was assumed as 100,000 psi. The spotweld location is determined by varying the spring constants in the model to reflect the higher spot-weld shear modulus. Bondline thickness variations may be treated in the same manner.

Calculation of spring constants for bondline shear stress analysis proceeds by assuming that each spring is theoretically located at the geometric center of the top face of a material block of length, d; width, w; and height, t_a as shown in Figure 71.

If a shear stress, τ, is uniformly applied as shown in Figure 71, the elastic shear stress-strain relationship

$$\tau = G\gamma \qquad (1)$$

may be written where γ is the shear strain. The total force F, applied to this face is

$$F = \tau wd = G\gamma wd \qquad (2)$$

Now consider the deformation, δ , of a spring located at the center of the sheared face. The force resulting from this deformation is

$$F = K\delta \qquad (3)$$

where K is the spring constant. Further, the deformation, δ , and the shear strain, γ , may be related by

$$\delta = t_a\gamma \qquad (4)$$

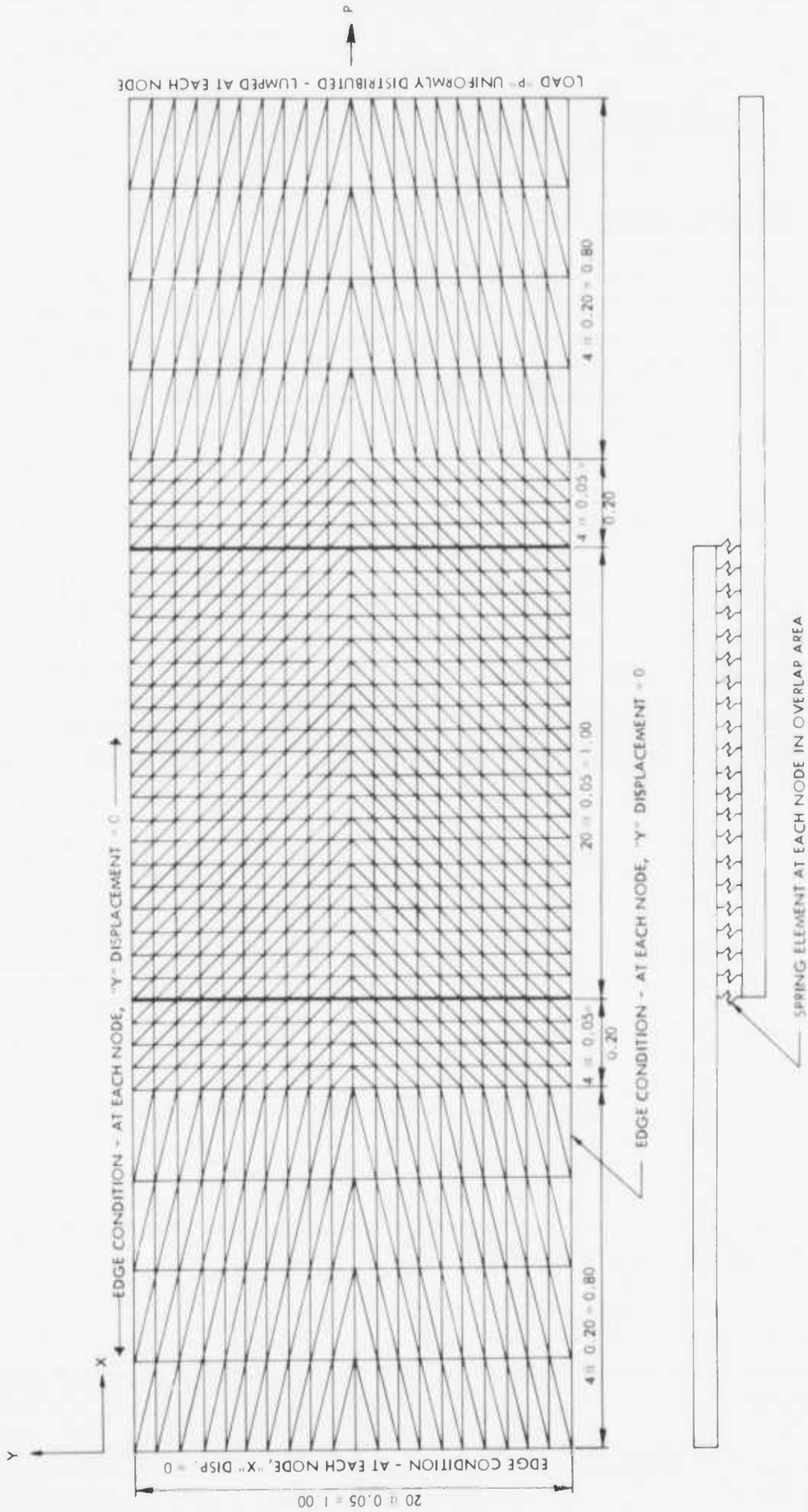

FIGURE 70 – SINGLE OVERLAP LAP SHEAR FINITE ELEMENT MODEL

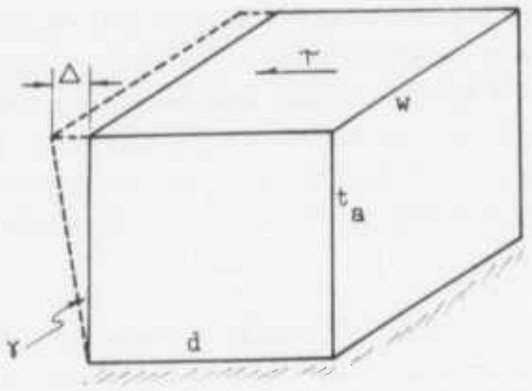

FIGURE 71 – MATERIAL BLOCK FOR SPRING CONSTANTS

for small deformations so that (3) may be written

$$F = K \gamma t_a \qquad (3a)$$

Equating the forces (2) and (3a)

$$G \gamma wd = K t_a \gamma$$

or

$$K = \frac{Gwd}{t_a} \qquad (5)$$

For the Figure 70 model grid spacing, both w and d were 0.05 inches. As stated earlier, the adhesive thickness used was 0.005 inches and the adhesive shear modulus, G, was 0.1×10^6 psi. The aluminum shear modulus used was 3.9×10^6 psi. Using these values, springs representing the bond were given constants of 0.5×10^5 pounds per inch while springs representing the weld were given constants of 1.95×10^6 pounds per inch.

While this model provided a two-dimensional solution of both joint shear stresses and adherend membrane stresses, it ignored joint normal stresses (out-of-plane stresses) and adherend bending stresses. In addition, the zero shear boundary conditions at X = 1.00 inch and X = 2.00 inches were not satisfied and the analysis resulted in a stress discontinuity at the adhesive-weld interface. With these limitations understood, analyses were conducted to gain a preliminary in-sight into the effect of weld location on weld and adhesive shear stresses.

To this end, analyses were conducted after modifying elements to represent four different bondline cases. The first represented an adhesive bondline without a weld while the last three represented bondlines with welds at various locations. The first of these had the weld located at the center of the joint area and the second two had the weld offset from center distances of 0.15 inches and 0.25 inches, respectively, in the X-direction. The X-direction shear stress distributions through the joint center-line for these for cases with and applied load of 1000 pounds per inch are shown in Figures 72, 73, 74 and 75. The diameter of the weld in each of the last three cases is 0.25 inches. A summary of maximum weld stresses and load carrying function in each of these cases is given below.

Case	Weld Offset From Center (In Load Direction)	Max. Shear Stress In Weld (PSI)	Percentage of Joint Load Carried by Weld
1	(No weld-adhesive only)	–	–
2	0.00 in.	950	2.1
3	0.15 in.	5300	4.1
4	0.25 in.	14600	8.4

The maximum shear stress in the adhesive in these cases ranged from 4200 to 5000 psi.

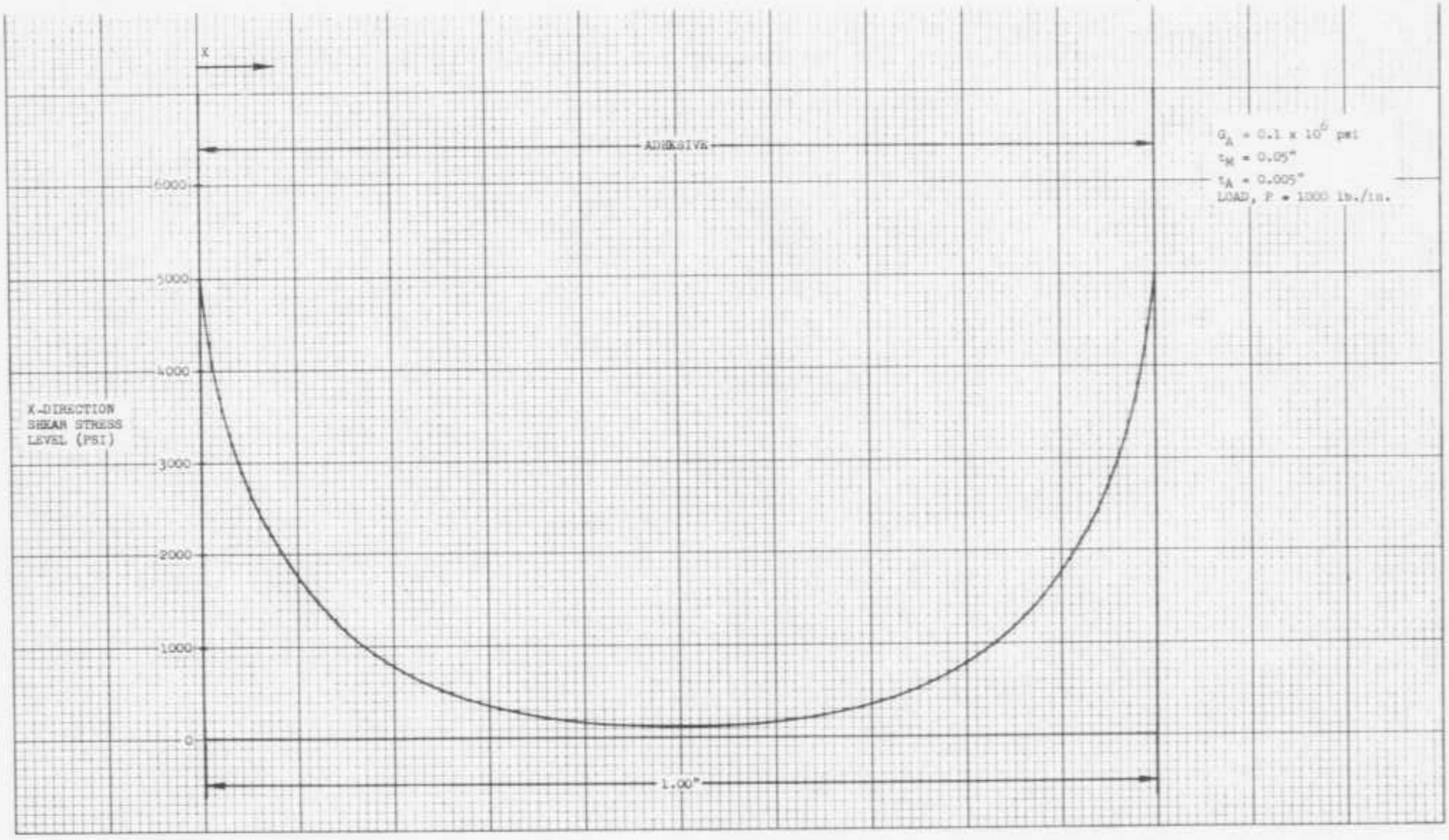

FIGURE 72 – FINITE ELEMENT, CASE 1 SHEAR STRESS DISTRIBUTION IN OVERLAP DIRECTION OF ADHESIVE BONDED SPECIMEN THROUGH THE CENTER-LINE OF THE SPECIMEN

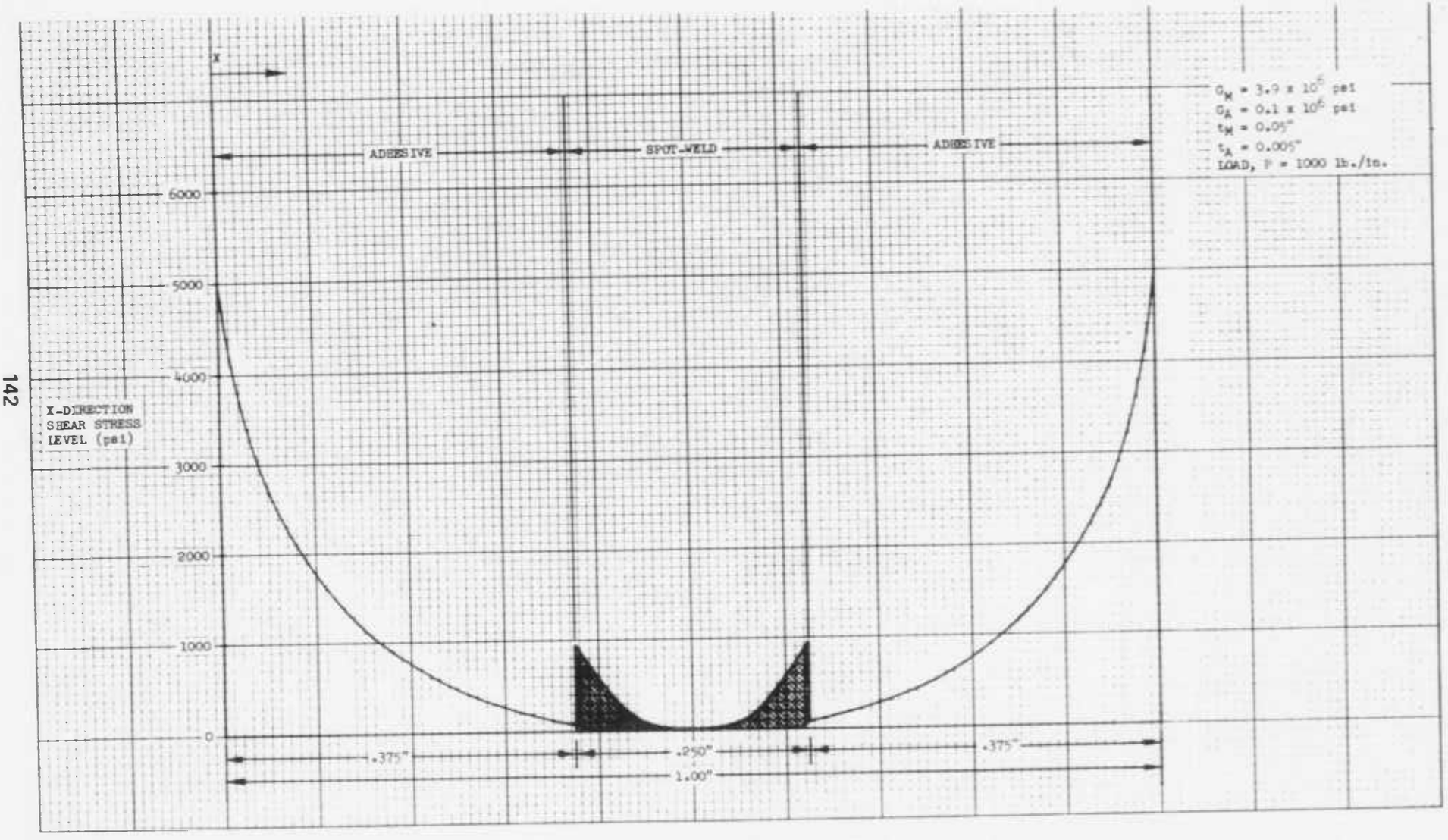

FIGURE 73 – FINITE ELEMENT, CASE 2 SHEAR STRESS DISTRIBUTION IN OVERLAP DIRECTION OF WELDBOND SPECIMEN THROUGH THE CENTER-LINE OF THE WELD-CENTERED WELD

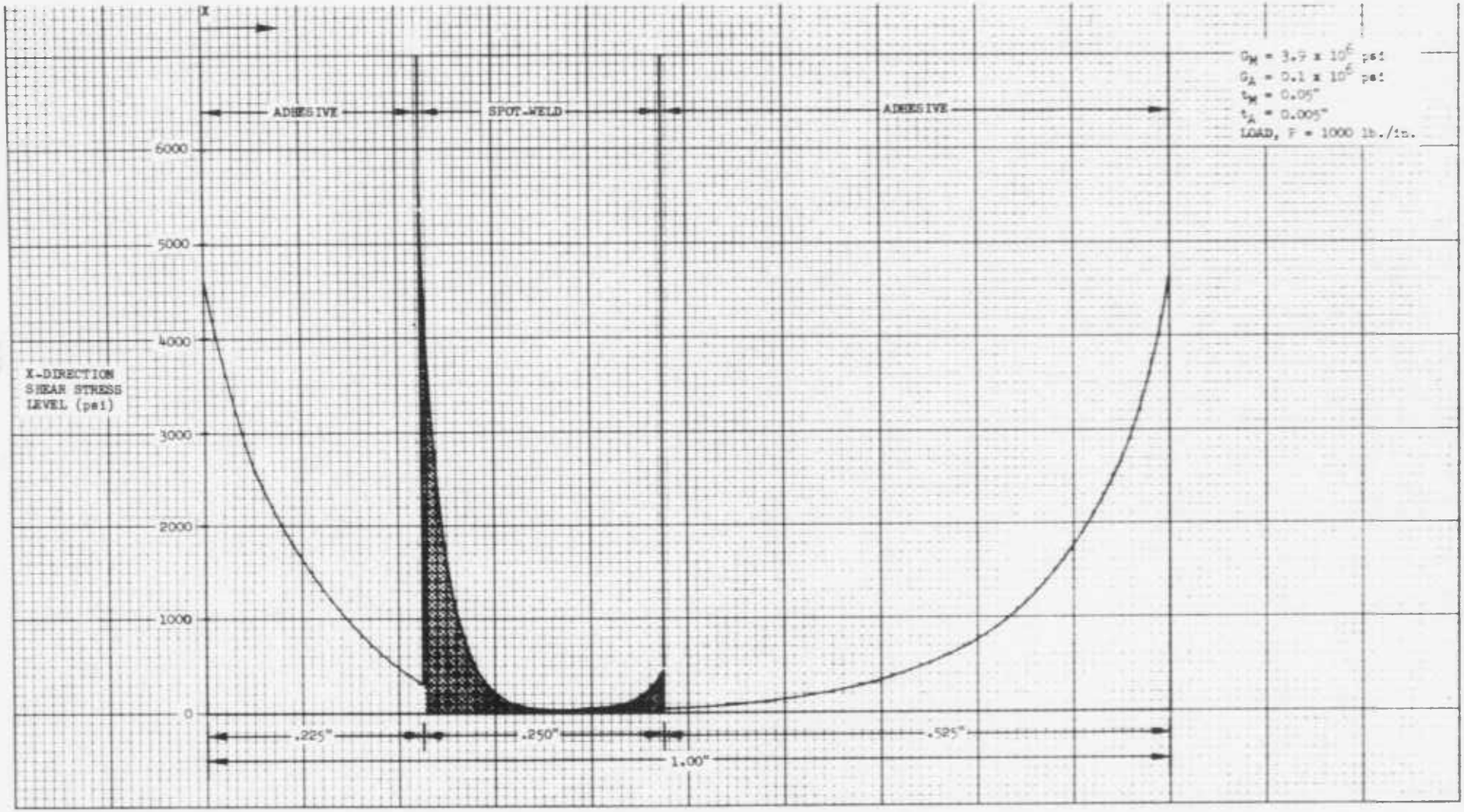

FIGURE 74 – FINITE ELEMENT, CASE 3 SHEAR STRESS DISTRIBUTION IN OVERLAP DIRECTION OF WELDBOND SPECIMEN THROUGH THE CENTER-LINE OF THE WELD-WELD SHIFTED 0.150 OFF-CENTER IN X-DIRECTION

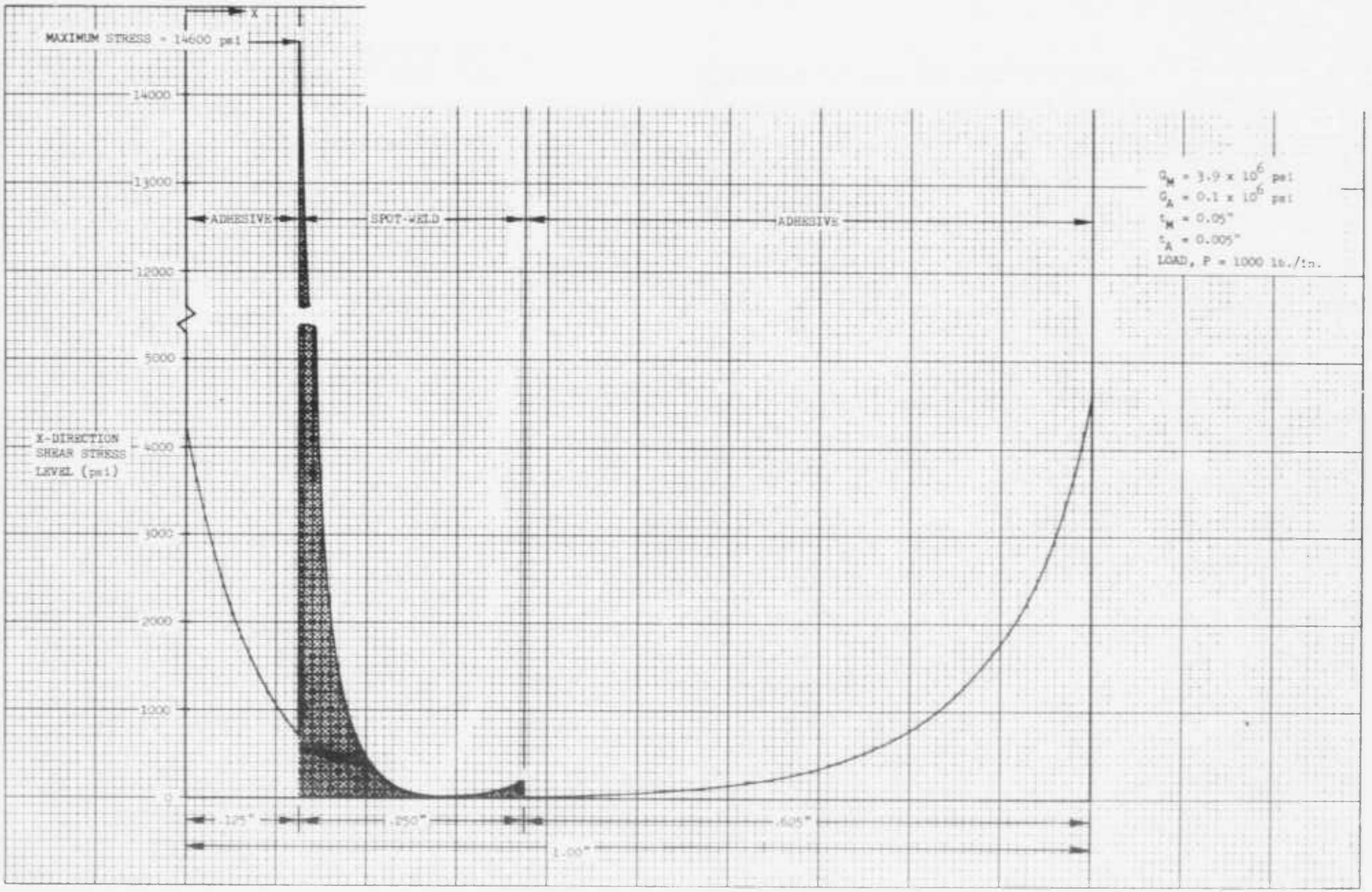

FIGURE 75 – FINITE ELEMENT, CASE 4 SHEAR STRESS DISTRIBUTION IN OVERLAP DIRECTION OF WELDBOND SPECIMEN THROUGH THE CENTER-LINE OF THE WELD-WELD SHIFTED 0.250 OFF-CENTER IN X-DIRECTION

4.1.2 Preliminary Closed Form Analysis

Using a digital computer program (BONJO I) developed for adhesive bonded joint analysis under Reference 4, comparisons were made between the previous finite element (open form) results and solutions reached through a closed form (or exact) approach. In addition to making this comparison, this particular program allowed the economical consideration of the effects of joint variables such as bondline thickness, adhesive material properties, adherend thickness, adherend material properties and joint overlap. Consideration of these effects through a finite element method was prohibited in this program by the cost of such an approach. Although this analysis did not allow for the presence of a spot-weld, it did include both bending and axial (membrane) forces which result in both shear and normal forces in the bondline. The zero shear boundary conditions at X = 1.00 inch and X = 2.00 inches in the finite element model were satisfied by this exact solution. These were not satisfied in the previous (finite element) analysis.

The general analysis proceeded through equilibrium considerations to the development of an eighth order differential equation. This, with eight boundary conditions on adhesive shear stresses and adherend transverse shear forces at the joint edge and applied loads at the specimen ends, formed the system for solution. Details of this method may be found in the final report for the above contract under Reference 4.

Figures 76 and 77 show the shear and normal bondline stresses for the single overlap adhesive only specimen analyzed earlier by the finite element method, i.e., 0.050 inch aluminum adherends with 5 mil thick adhesive (shear modulus = 0.1×10^6 psi) and 1.0 inch overlap. In addition, an adhesive Young's modulus of 0.26×10^6 psi was used. Maximum adhesive shear stresses by this method of analysis were 8200 psi as compared to 5000 psi for the finite element method. Further comparison of this shear stress distribution with that shown in Figure 72 revealed lower shear stresses toward the center of the joint than resulted from the finite element approach. This was considered the effect of recognizing the out-of-plane bending and normal stresses in the closed form method. An estimate of maximum 0.25 inch diameter weld shear stresses, given this change, is shown below.

Case	Weld Offset From Center (In Load Direction)	Estimated Max. Shear Stress In Weld (PSI)
2	0.00 in.	70
3	0.15 in.	880
4	0.25 in.	9400

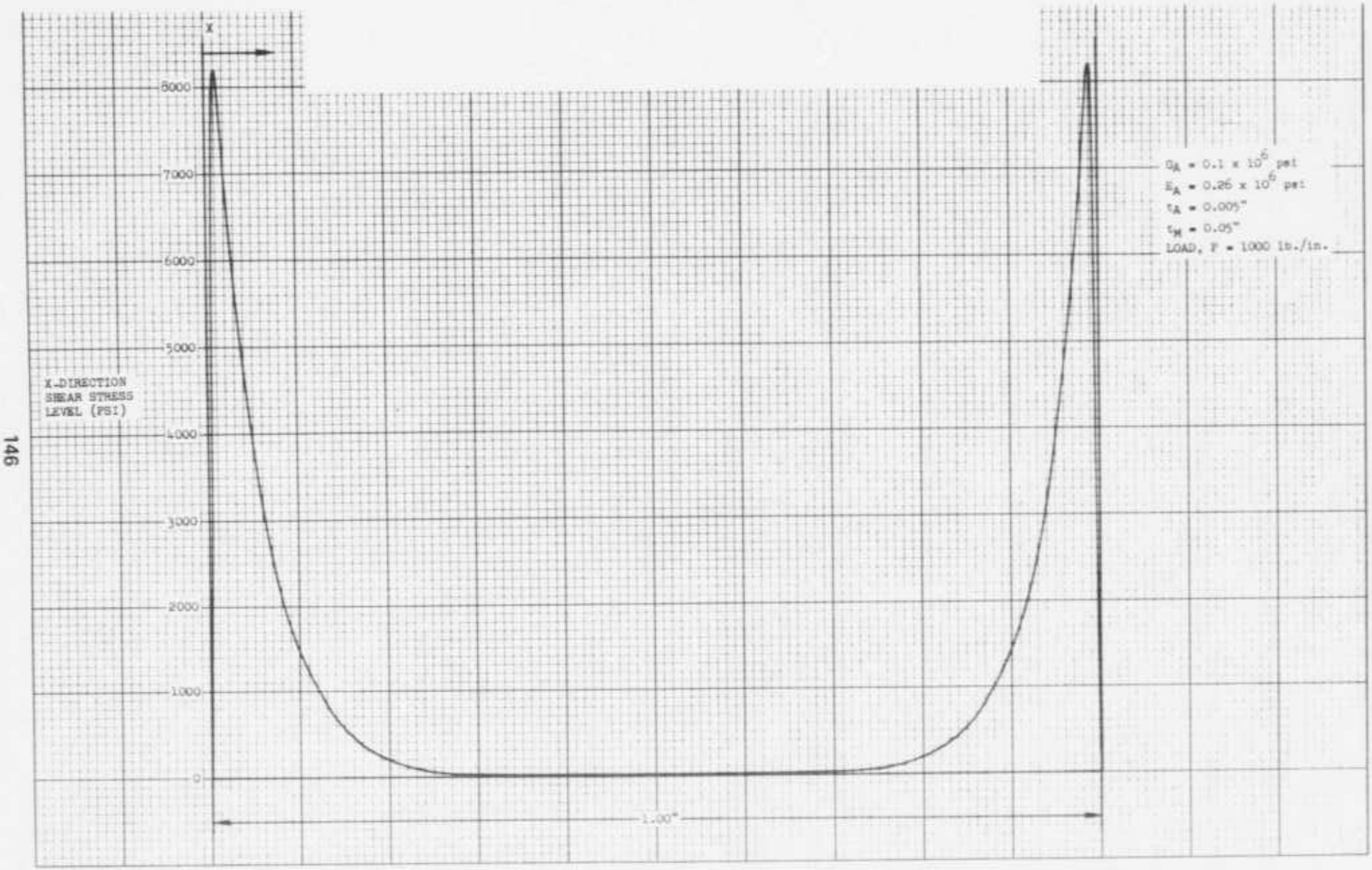

FIGURE 76 – CLOSED FORM SOLUTION, CASE 1 SHEAR STRESS DISTRIBUTION IN OVERLAP DIRECTION OF ADHESIVE BONDED SPECIMEN THROUGH THE CENTER-LINE OF THE SPECIMEN

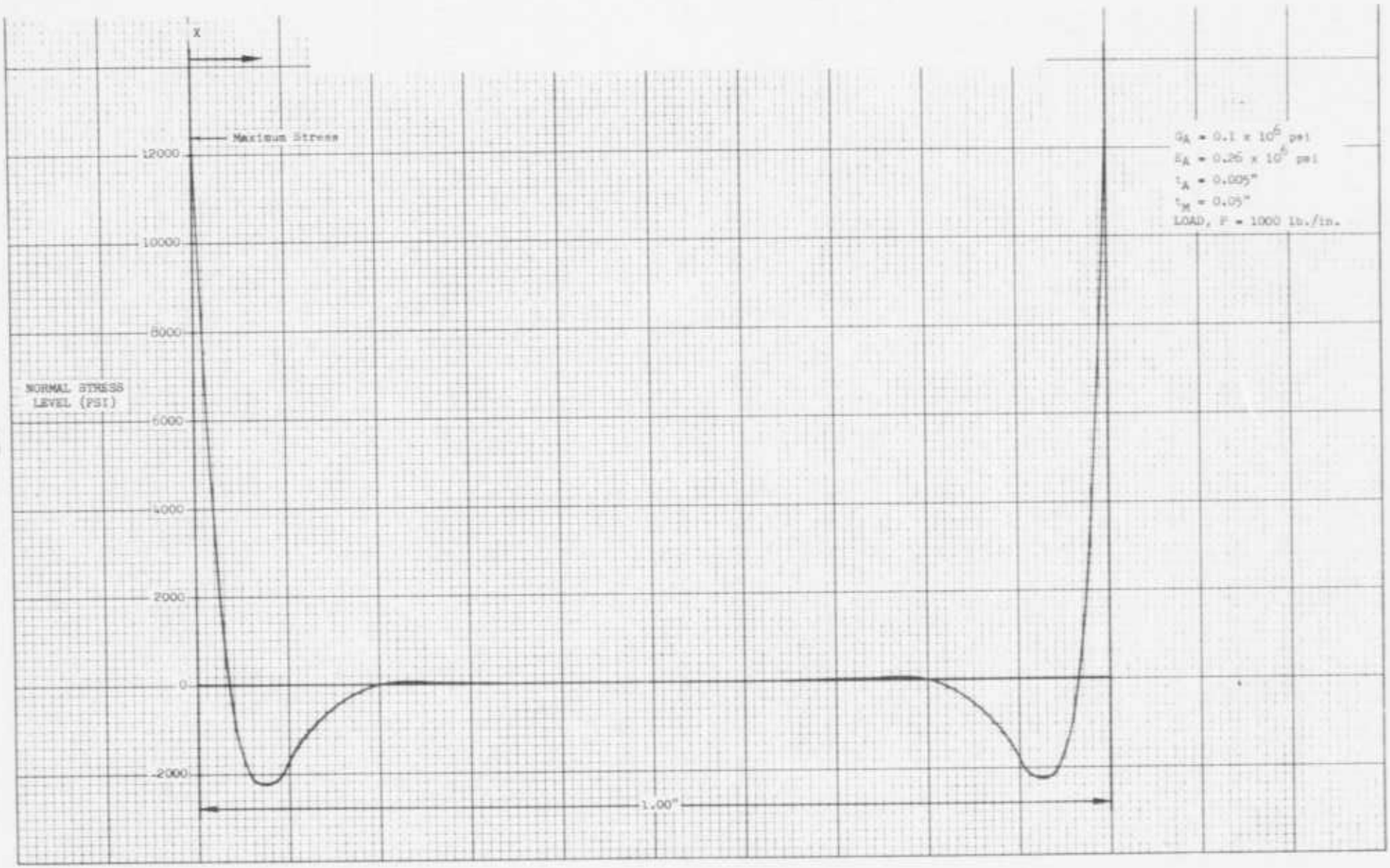

FIGURE 77 – CLOSE FORM SOLUTION, CASE 1 NORMAL STRESS DISTRIBUTION IN OVERLAP DIRECTION OF ADHESIVE BONDED SPECIMEN THROUGH THE CENTER-LINE OF THE SPECIMEN

Further BONJO I analysis addressing joints with various adherend thicknesses, adherend material, bondline thicknesses and overlaps were performed. The results showed that for a fixed spot-weld offset from the joint center at a location greater than one-tenth of the overlap length from the joint edge, the following qualitative statements may be drawn. Considering all other joint variables fixed including the applied load,

- a change in adherend material from aluminum ($E = 10.3 \times 10^6$ psi, $G = 3.9 \times 10^6$ psi) to titanium ($E = 16.0 \times 10^6$ psi, $G = 6.2 \times 10^6$ psi) will decrease the peak adhesive shear and normal stresses and increase the maximum weld stress and percentage of joint load carried by the weld,

- an increase in adherend thickness will decrease the peak adhesive shear and normal stresses and increase the maximum weld stress and percentage of joint load carried by the weld,

- an increase in adhesive moduli will increase the peak adhesive shear and normal stresses and decrease the maximum weld stresses and percentage of joint load carried by the weld, and

- a uniform increase in bondline thickness will decrease the peak adhesive shear and normal stresses and increase the maximum weld stresses and percentage of joint load carried by the weld.

4.2 Final Analysis – C-130 F.S. 377 Joint

A detailed stress analysis of a typical section of the C-130 aircraft fuselage station 377 frame-splice-skin joint was performed. NASA structural analysis program (NASTRAN) was used to implement the solution. This was a finite element displacement method program. The analysis solved for the normal and shear stresses in the weld and bond due to an internal fuselage pressure, an axial load transmitted through the joint, and a shear load transmitted through the joint.

After initial attempts resulted in an analysis which exceeded computer run time limitations, an approach involving two finite element models was implemented. This general approach is illustrated in Figure 78. As shown, a two-dimensional model of a beam on an elastic foundation was used to determine the average radial restraint offered by the curvature of the fuselage. A flat three-dimensional model representing a typical strip of the fuselage through the joint was constructed. The curvature of the fuselage was represented in this model by applying, as external forces, the restraint loads determined from the two-dimensional model. This model was then used to determine internal shear and normal stress distributions in the C-130 fuselage joint.

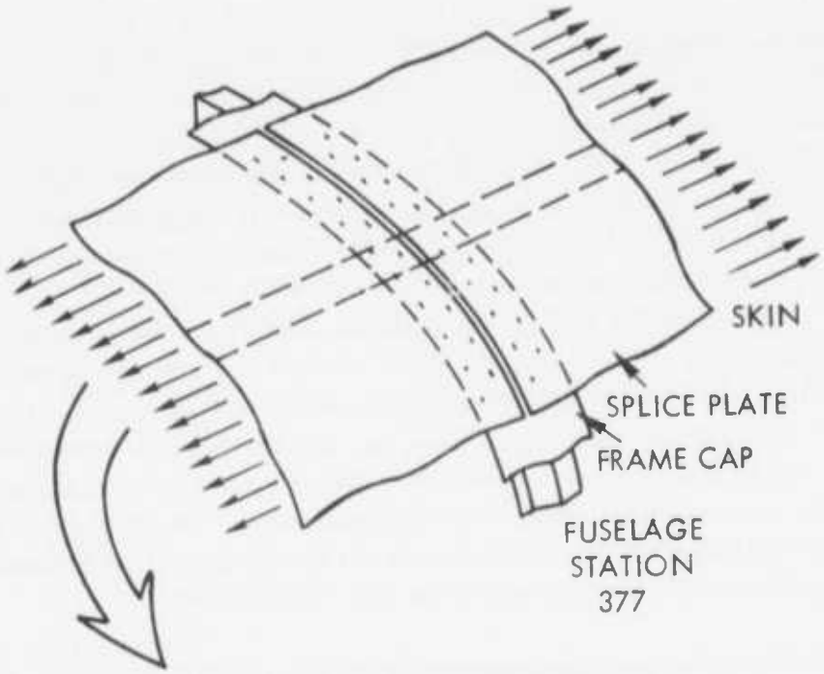

A MODEL OF A BEAM ON AN ELASTIC FOUNDATION IS USED TO OBTAIN THE EFFECT OF THE FUSELAGE CURVATURE

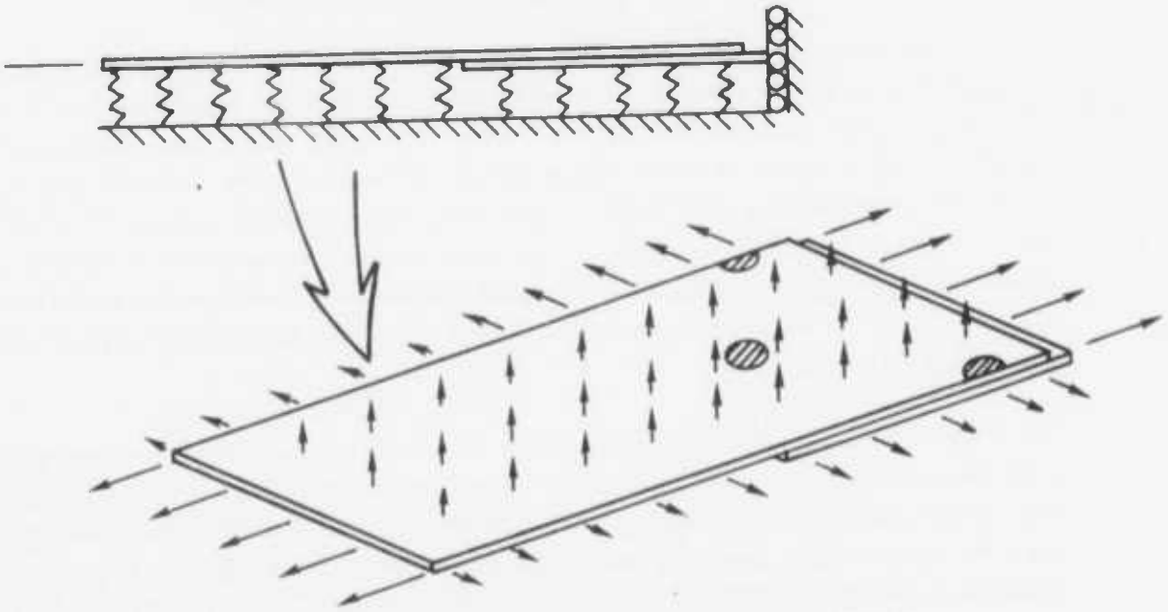

A FLAT PLATE MODEL OF THE SPLICE IS ANALYSED WHERE THE FRAME CURVATURE IS INCLUDED AS APPLIED FORCES

FIGURE 78 – FINITE ELEMENT MODELS

The two-dimensional model shown in Figure 79 represents a one-inch slice of the splice plate and fuselage skin running from the center-line of the frame web to the center-point between frames. The two-dimensional model geometry was constructed to match that of the three-dimensional model. The nodes were located at the center-line of the bond-line between the fuselage skin and splice plate. The fuselage skin and splice plate, both 0.05 inch thick aluminum, were represented by NASTRAN CBAR elements using an offset of ±.028 inches. The bending stiffness of the beams was taken as $t^3/12\ (1-\nu^2)$ to match the rigidity of the three-dimensional model plate elements. NASTRAN scalar spring elements (CELASI) represented the adhesive and spot-welds between the splice plate and fuselage skin. The bond-line thickness was .006 inches and the adhesive shear modulus, G, and the tensile modulus, E, were assumed to be 100,000 psi and 260,000 psi, respectively. The spot-weld shear modulus and tension modulus were assumed to be the same as aluminum. Each node of the two-dimensional splice model was supported in the radial direction by a scalar spring element (CELASI). The stiffnesses of these springs were chosen to simulate the radial restraining effect of the skin, the splice plate, and the frame ring.

The model was analyzed for two load conditions, a one psi internal pressure and a 1000 psi axial stress. The resulting spring forces in the radial direction were used as applied loads for the three-dimensional model. Also, the radial displacements were converted into equivalent circumferential stresses and applied to the three-dimensional model.

The three-dimensional model representing a typical strip of the fuselage skin-splice joint is shown in Figure 80. The length of the strip was the same as the two-dimensional model and the width was taken as one spot-weld pitch. The model nodes were located at the center-line of the fuselage skin and the center-line of the splice plate. The skin and splice plate were represented by NASTRAN plate bending and membrane elements (CQUADZ). The skin and splice plate were connected by scalar elements to represent the bonding and spot-welds. The stiffness matrix for these scalar elements was directly input on DMI cards and included in the NASTRAN system of analysis. The stiffness matrix for a typical scalar element is given in Figure 81.

The three-dimensional model was analyzed for three load cases, a unit internal pressure, a 1000 psi axial stress, and a unit shear stress. The applied loads for the unit pressure case and the 1000 psi axial stress case were symmetric about the model boundaries while the applied loads for the unit shear case were antisymmetric. It was therefore necessary to analyze the model with two sets of boundary conditions as shown in Figure 82. The external loads for the unit pressure case and the 1000 psi axial stress case were applied as nodal forces as derived from the two-dimensional model. The external loads for the unit shear stress case were induced by imposing a distortion to the boundary of the model as shown in Figure 82 .

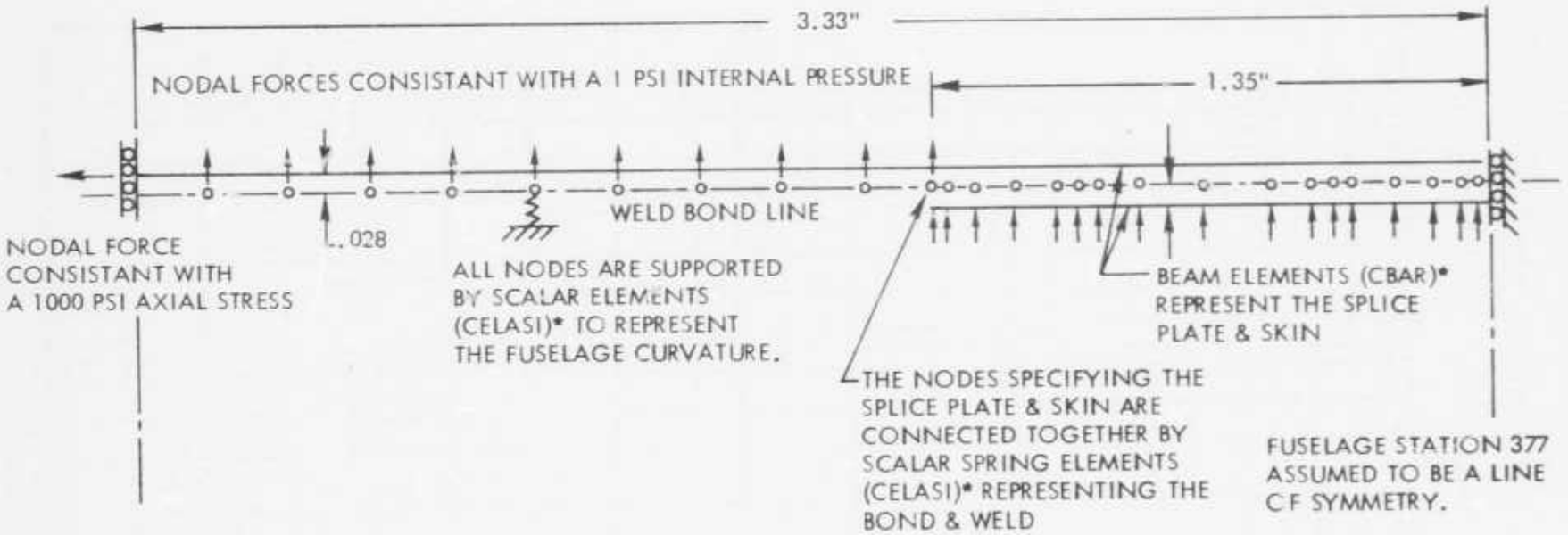

FIGURE 79 – TWO DIMENSIONAL FINITE ELEMENT MODEL

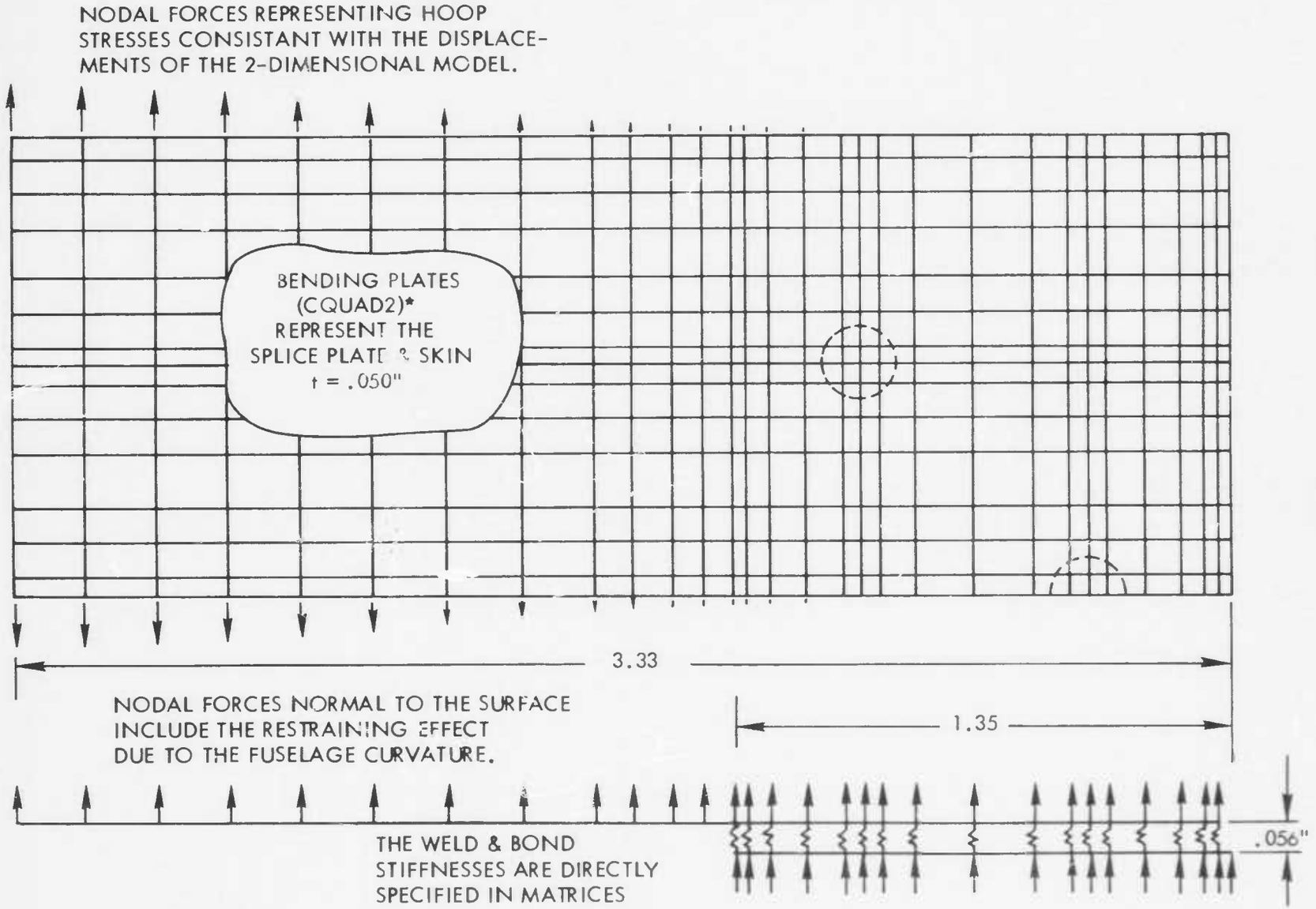

FIGURE 80 – THREE-DIMENSIONAL FINITE ELEMENT MODEL

SCALAR ELEMENT USED TO CONNECT SKIN & SPLICE PLATE

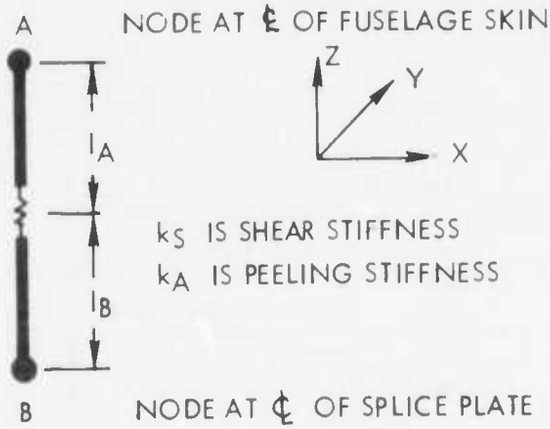

	F_x^A	F_y^A	F_z^A	M_x^A	M_y^A	F_x^B	F_y^B	F_z^B	M_x^B	M_y^B	
U_x^A	k_S				$-k_S l_A$	$-k_S$				$-k_S l_B$	
U_y^A		k_S		$k_S l_A$			$-k_S$		$k_S l_B$		
U_z^A			k_A					$-k_A$			
x^A		$k_S l_A$		$k_S l_A^2$			$-k_S l_A$		$k_S l_A l_B$		
y^A	$-k_S l_A$				$k_S l_A^2$	$k_S l_A$				$k_S l_A l_B$	
U_x^B	$-k_S$				$k_S l_A$	k_S				$k_S l_B$	
U_y^B		$-k_S$		$-k_S l_A$			k_S		$-k_S l_B$		
U_z^B			$-k_A$					k_A			
x^B		$k_S l_B$		$k_S l_A l_B$			$-k_S l_B$		$k_S l_B^2$		
y^B	$-k_S l_B$				$k_S l_A l_B$	$k_S l_B$				$k_S l_B^2$	

FIGURE 81 – STIFFNESS MATRIX FOR SCALAR ELEMENTS CONNECTING THE SKIN AND SPLICE PLATES

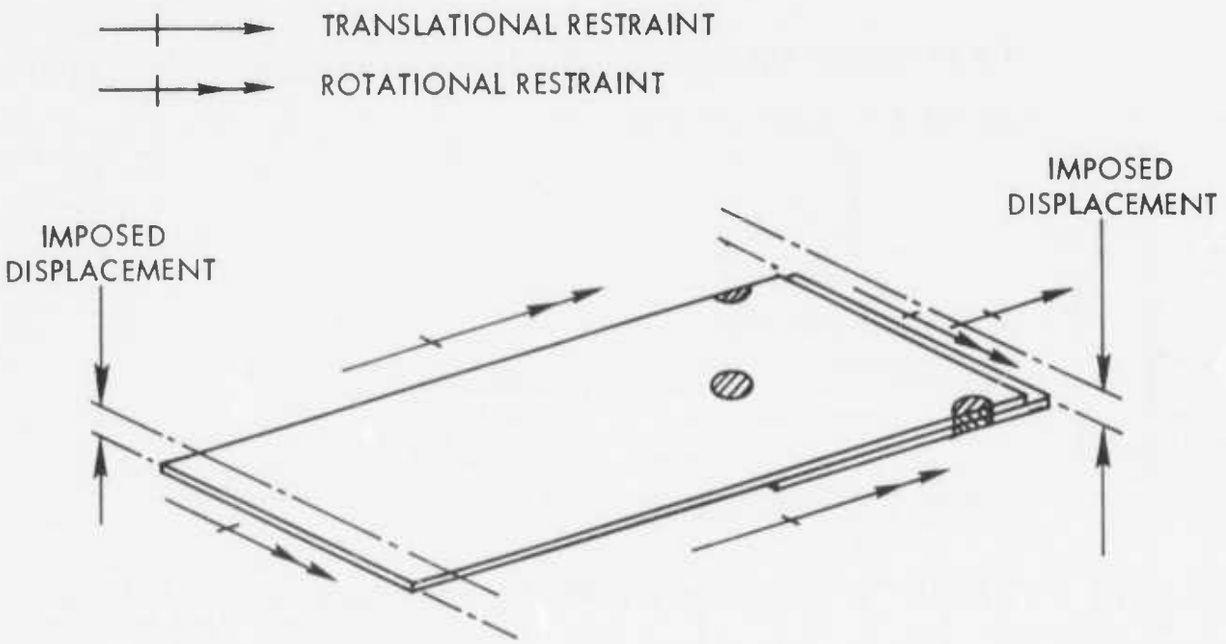

BOUNDARY CONDITIONS FOR THE AXIAL LOAD & PRESSURE CASES

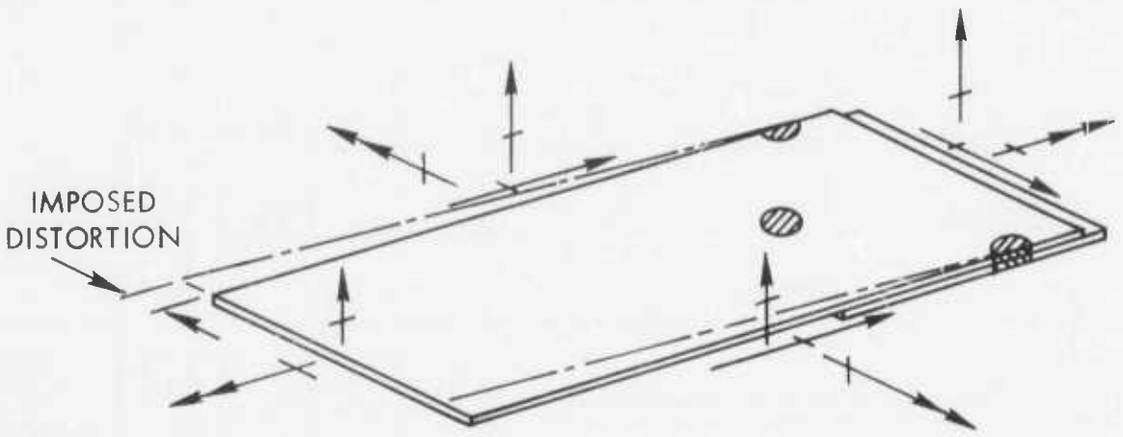

BOUNDARY CONDITIONS FOR THE SHEAR CASE

FIGURE 82 – BOUNDARY CONDITIONS FOR THE THREE-DIMENSIONAL MODEL

The results of the analysis showed that spot-welds carry very little load and have very little effect on the distribution of stresses in the bond. Figure 83 shows the circumferential distribution of the peak shear stress in the bond due to the 1000 psi axial stress case. The circumferential distributions of shear stresses and normal stresses for all conditions analyzed had a similar uniform trend. Figure 84 shows the longitudinal distribution of shearing stress in the bond and weld due to the 1000 psi axial stress case. Figure 85 shows the longitudinal distribution of normal stress in the bond and web due to the unit internal pressure case.

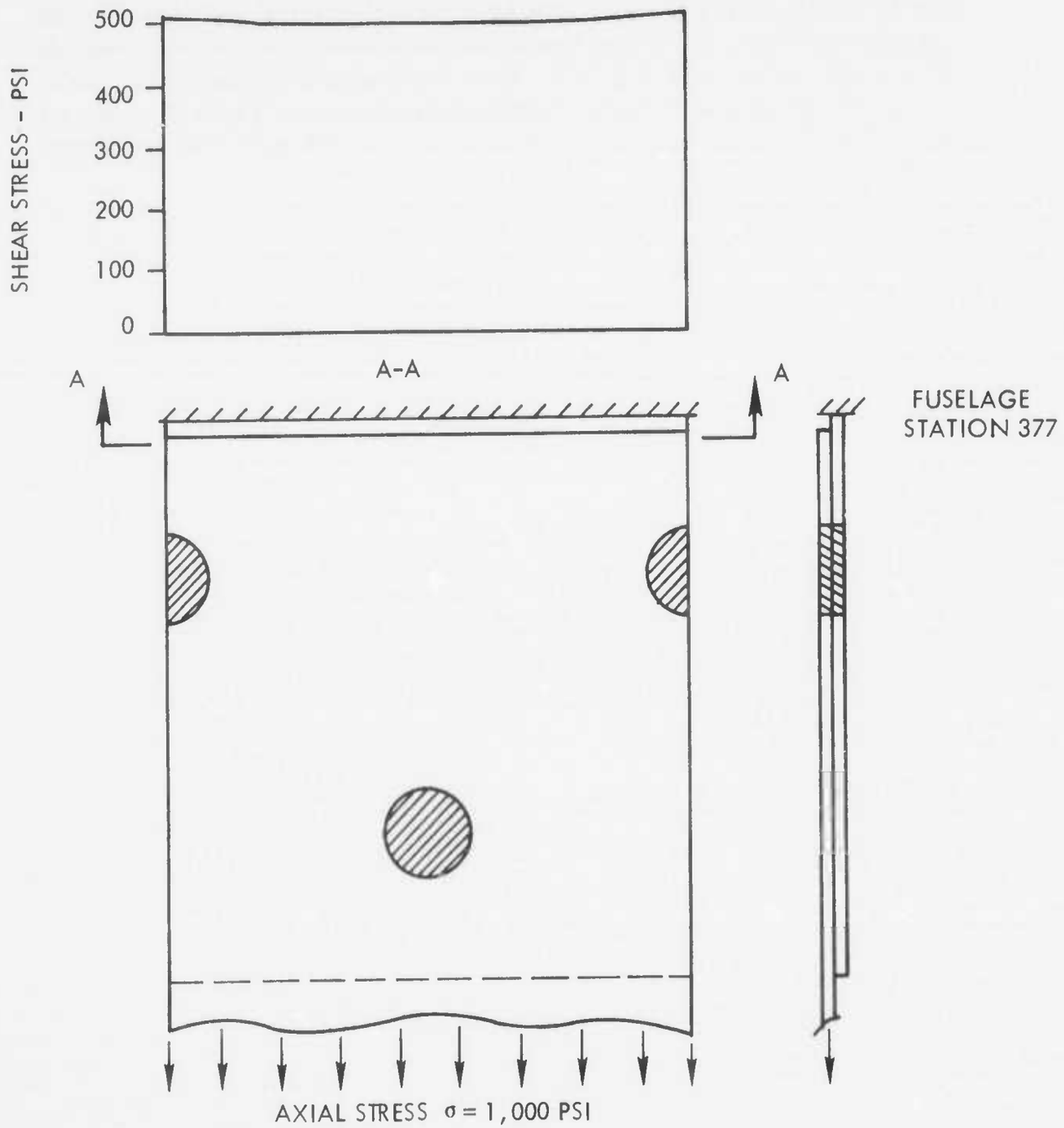

FIGURE 83 – CIRCUMFERENTIAL DISTRIBUTION OF PEAK SHEARING STRESS

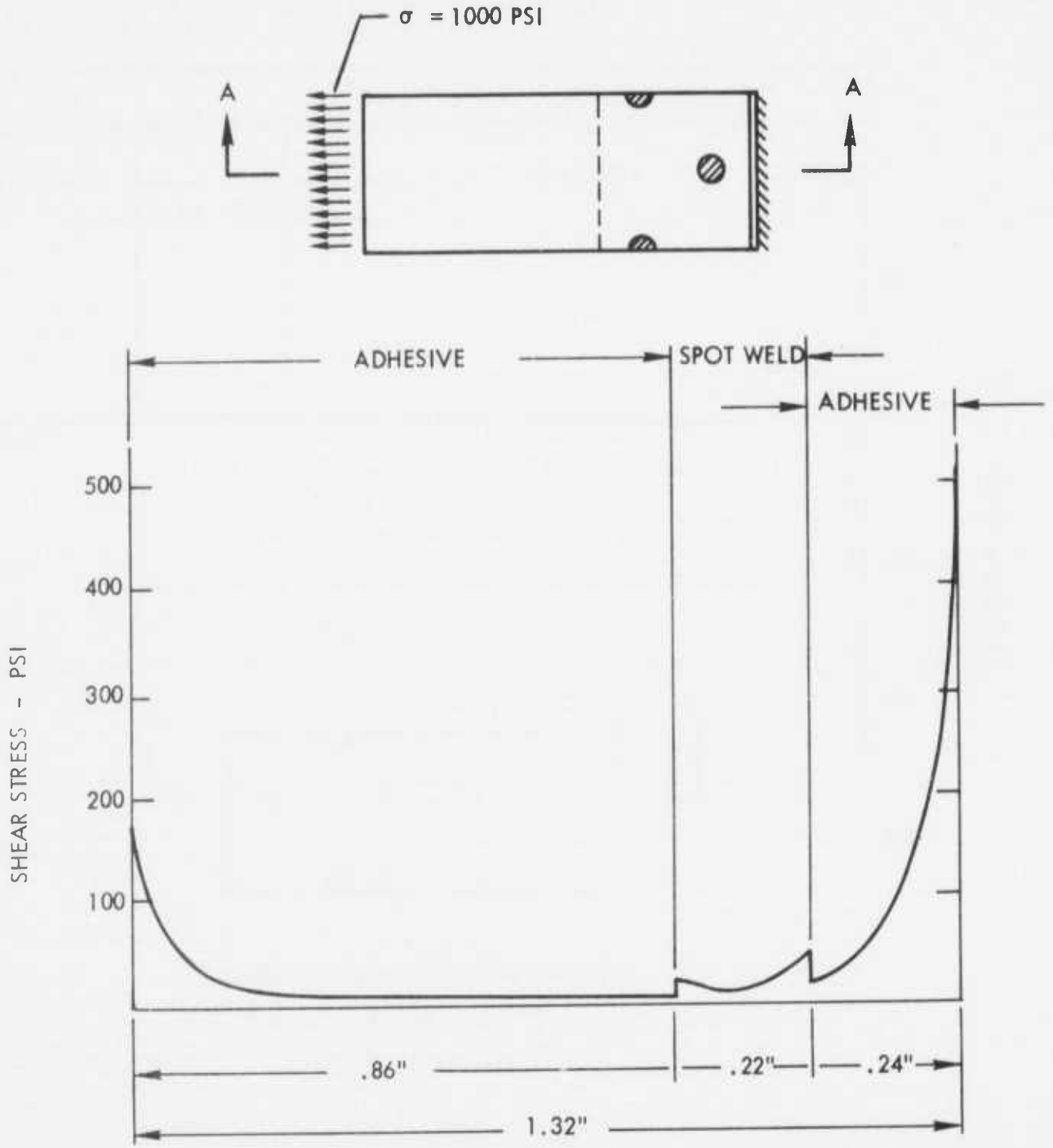

FIGURE 84 – LONGITUDINAL DISTRIBUTION OF SHEARING STRESS IN THE BONDLINE THRU A-A

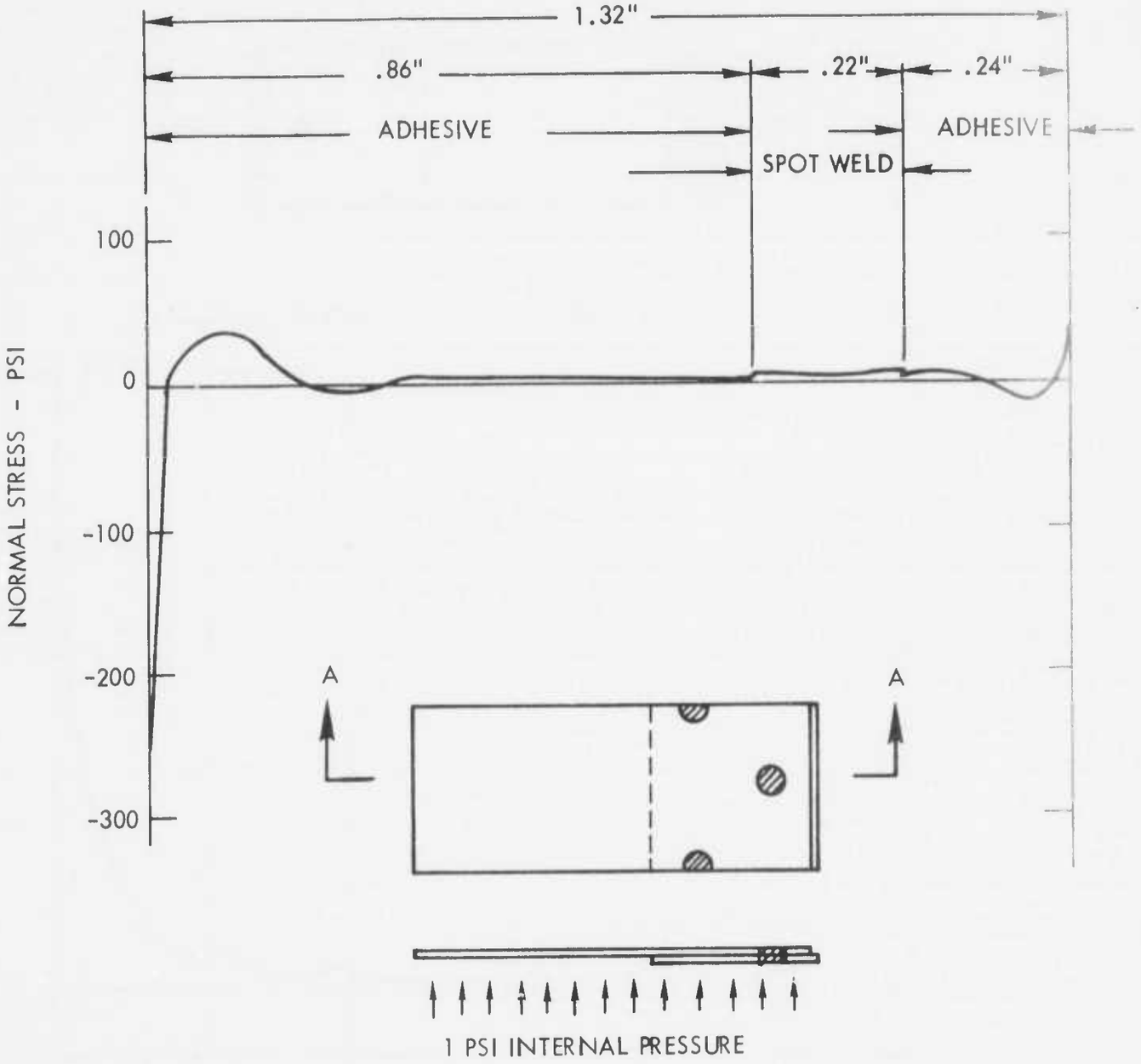

FIGURE 85 – LONGITUDINAL DISTRIBUTION OF NORMAL STRESS IN THE BONDLINE THRU A-A

SECTION V

WELDBOND NON-DESTRUCTIVE INSPECTION (NDI) DEVELOPMENTS

5.1 Infrared Nondestructive Inspection

The infrared nondestructive inspection technique was investigated for use in inspection of adhesive bondlines in weldbonded assemblies. It offered a non-contact, high-speed inspection method for detecting discontinuities and irregularities in adhesive bondlines; however, it is limited by material thickness. The infrared equipment used in developments of this program was developed by Lockheed and it is referred to as the Lockheed Traversing Infrared Inspection System, TIRIS. This equipment is capable of detecting voids and delaminations in metal-to-metal bonded joints as small as 0.30 inch in diameter in adherend thicknesses of up to 0.15 inch. Thicker adherends are limited to correspondingly larger defects.

A painted surface is mandatory in application of the infrared NDI technique to aluminum alloy specimens since the infrared reflectivity of aluminum is high and irregular. Almost any non-glossy paint is acceptable for this purpose. Aircraft zinc chromate primer has been tested and is a satisfactory coating. Also, sprayed, water removable or strippable emissivity coatings are commercially available and can be applied prior to inspection and then removed. A lineal inspection rate of eight feet per minute is a potential advantage in using the TIRIS infrared system for inspection of the adhesive bondline.

Weldbonded demonstration specimens were designed and fabricated for inspection by the infrared NDI technique. The first of the demonstration specimens was weldbonded with 0.051 inch thick 7075-T6 fare aluminum alloy sheets. Intentional voids were fabricated in the specimen and the results of the infrared inspection indicated bondline void areas. Although inspection of spot-welds in weldbonded joints by the infrared inspection technique was not planned, attempts to inspect the spot-welds in the first demonstration specimen yielded unsatisfactory results.

The second and third demonstration specimens were designed and fabricated. Both of these specimens included intentional bondline voids to determine the capability of inspecting the adhesive bondlines with TIRIS. The second demonstration specimen consisted of an 0.063 inch thick extruded angle weldbonded to an 0.050 inch thick sheet which was six (6) inches wide and fifty (50) inches long. This demonstration specimen was inspected by TIRIS and three (3) of the four (4) intentioanl bondline voids were detected. It was concluded that the undetected void was obscured during the adhesive curing process. The demonstration specimen was disassembled and the failed bondlines compared with TIRIS results. Comparison of TIRIS results with the disassembled specimen components gave only fair correlation. It was confirmed that repeatibility in inspection results from TIRIS could be established provided the demonstration specimen was allowed to return to the initial temperature between successive scans.

A third infrared demonstration specimen was designed and fabricated because of the difficulty of interpretation of isothermal patterns caused by the spot-welds and the relatively low thermal inertia of the first and second demonstration specimens. The third demonstration specimen had a sheet-stringer structural arrangement and was twenty-one (21) inches wide and forty-eight (48) inches in length. Three (3) equally spaced angle stringers were weldbonded to the sheet in the lengthwise direction. The adhesive used was M6800 (Whittaker) epoxy paste, the sheet was 0.050 inch thick bare aluminum alloy, and the angle stringers were 0.063 thick aluminum alloy extrusion. The TIRIS heat injection nozzles were modified to optimize temperature differentials across the void areas occurring in weldbond joints of this specimen. Infrared scanning of this demonstration specimen in the TIRIS facility yielded unacceptable results. It was concluded that interpretation of displayed temperature patterns recorded on thermograms was too difficult for production inspection. Interruption of the heat front normal distortion patterns caused by the overriding spot-weld to spot-weld thermal conductivity disallows infrared inspection for weldbond structures until a faster frame rate camera is available. Since this third demonstration specimen was closely representative of a typical aircraft structural component and acceptable inspection results could not be achieved, it was concluded that the infrared nondestructive inspection method is not acceptable for weldbonded structural assemblies.

5.2 Ultrasonic Nondestructive Inspection

Immersion and contact (longitudinal wave) ultrasonics have long been acceptable methods for inspecting metal-to-metal bonded assemblies. Investigations were accomplished for applying these techniques to adhesive bondlines in weldbonded assemblies. It is noted that the immersion ultrasonic technique could not be applied to large assemblies because of the size limitations of the available laboratory in immersion tank as well as not being applicable to field inspection. The immersion ultrasonic technique was applied to small engineering test specimens and the results correlated with contact ultrasonic findings and destructive test results in establishing quality standards for larger weldbonded assemblies. Contact ultrasonics was used to inspect the C-130 weldbonded fuselage components. Quality standards for use in calibration of the ultrasonic inspection equipment were designed and fabricated for use in inspecting several weldbonded joint configurations.

5.2.1 Immersion Ultrasonics

Weldbonded demonstration specimens were designed and fabricated for use in investigating the feasibility of applying the ultrasonic inspection technique to weldbonded assemblies. The first demonstration specimen was weldbonded and it contained intentional voids in the bondline to establish the merits of the inspection method. An ultrasonic C-scan was

developed for the demonstration specimen. The specimen was disassembled for comparison of the failed bondline conditions to those recorded on the ultrasonic C-scan. Excellent correlation was obtained between the C-scan and the actual void and disbond areas in the bondline. Comparative results are shown in Figures 86 and 87.

Eight (8) lap shear weldbonded panels containing five specimens per panel were fabricated for immersion ultrasonic inspection. Four (4) panels were fabricated with 7075-T6 clad aluminum alloy sheet and four (4) panels with 7075-T6 bare aluminum alloy sheet. Each of the panels was immersion ultrasonic inspected and C-scans developed. Upon completing the ultrasonic C-scans the eight (8) panels were machined into five (5) individual lap shear specimens each and all specimens were destructively tested. Good comparative results were achieved with the ultrasonic C-scan and the failed bondline surfaces.

5.2.2 Contact Ultrasonics

Contact ultrasonic inspection techniques for weldbonded assemblies were developed coincident with immersion ultrasonic techniques. This was accomplished by performing contact ultrasonic inspections on demonstration specimens that were immersion ultrasonic inspected. Contact ultrasonic equipment used in development of the inspection technique for weldbonded joints consisted of a Sperry UM-715 or UM-771 Reflectoscope with a 5 mHz transducer 0.187 inches in diameter. Room temperature tap water containing a detergent was applied to the specimen surface to act as a couplant during inspection operations. Calibration of the contact ultrasonic equipment begun with detection of very small bondline voids and porosity. As mechanical property data were developed and process requirements established, calibrations were varied. Quality standards were fabricated after the final bondline quality requirements were established. The quality standards were fabricated to replicate weldbonded joints having both single and double bondlines. Also, the standards included bondline areas that exhibited both acceptable and unacceptable bondline qualities for the purpose of calibrating the contact ultrasonic equipment. Typical scope presentations of the cathode ray tube signals of bondlines in the weldbonded joints of a sub-scale test panel are shown in Figures 88 through 91. Figure 88 is the display of a high quality bondline. A comparison of signals for a farside disbond, nearside disbond, and porosity in the bondline is shown in Figures 89, 90, and 91. Comparable techniques were developed for weldbonded joints with double bondlines. It is noted that in inspecting double bondline joints the defects can be detected from either inspection surface. However, if disbonds are present in the bondline nearer the inspection surface, disbonds in that region of the farther bondline cannot be detected. The disbonds in the farther bondline may be detected by using the opposite face of the weldbonded joint as the inspection surface.

During the course of development, a weldbonded shear panel was ultrasonically inspected prior to and after testing. The ultrasonic inspection was performed on the failed shear panel prior to removal of the two (2) Z-section stiffeners. Upon completing the ultrasonic inspection of the failed shear panel from the sheet side, the stiffeners were removed to

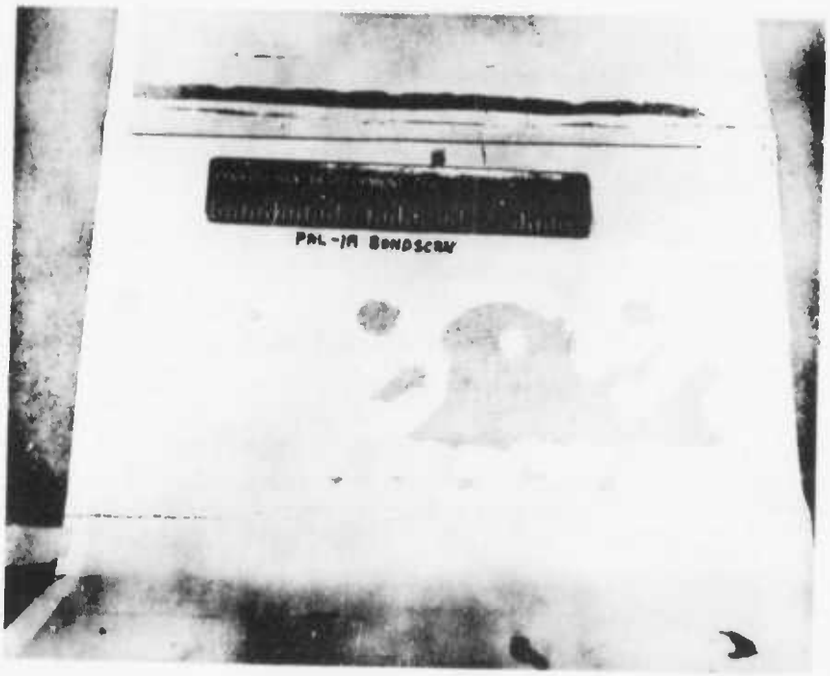

FIGURE 86 – C SCAN RECORDING OF FIRST DEMONSTRATION SPECIMEN

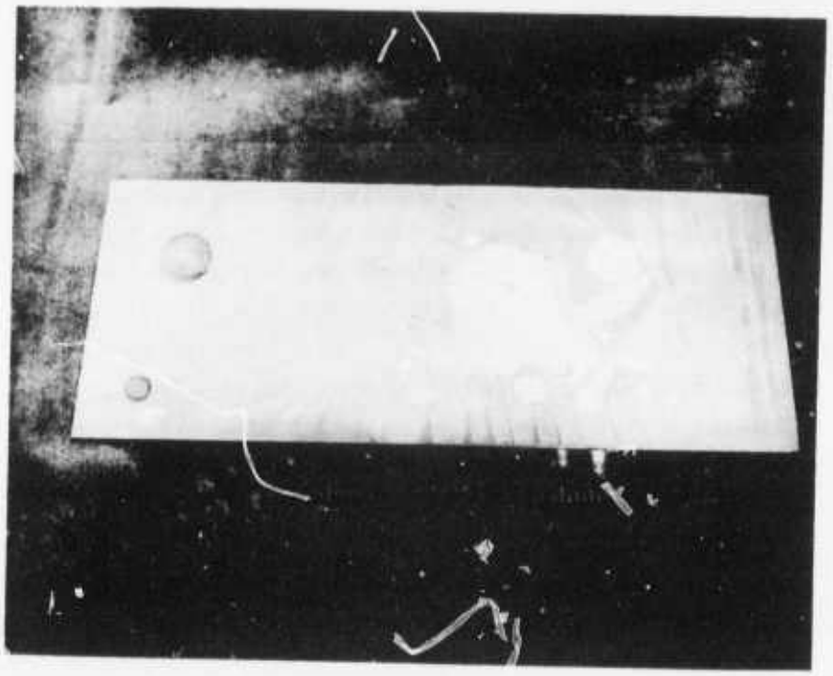

FIGURE 87 – FIRST DEMONSTRATION FAILED SPECIMEN

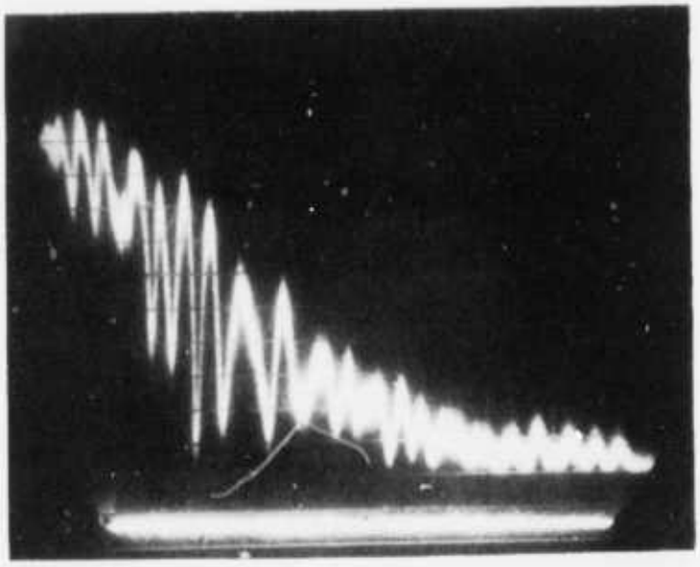

FIGURE 88 – SIGNAL OF QUALITY BONDLINE

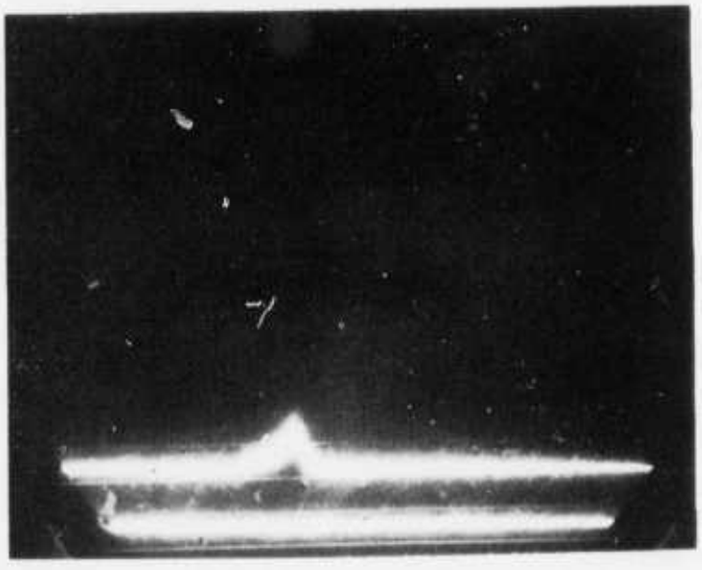

FIGURE 89 – SIGNAL OF FARSIDE DISBOND IN BONDLINE

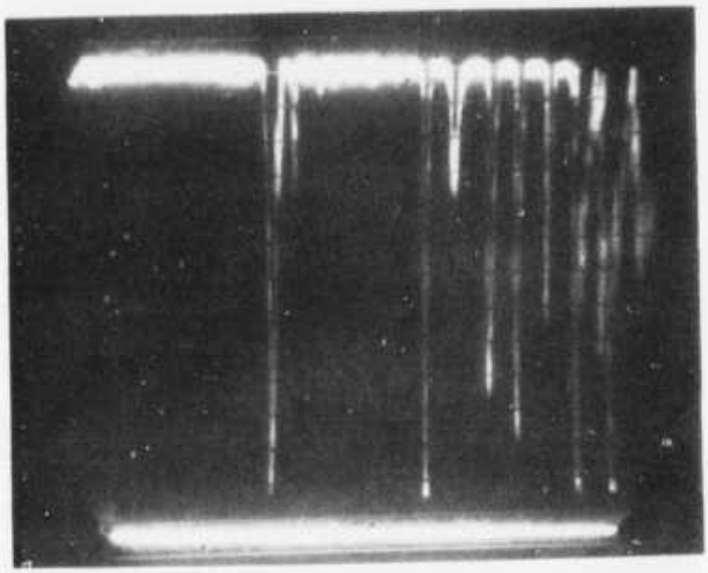

FIGURE 90 – SIGNAL OF NEARSIDE DISBOND IN BONDLINE

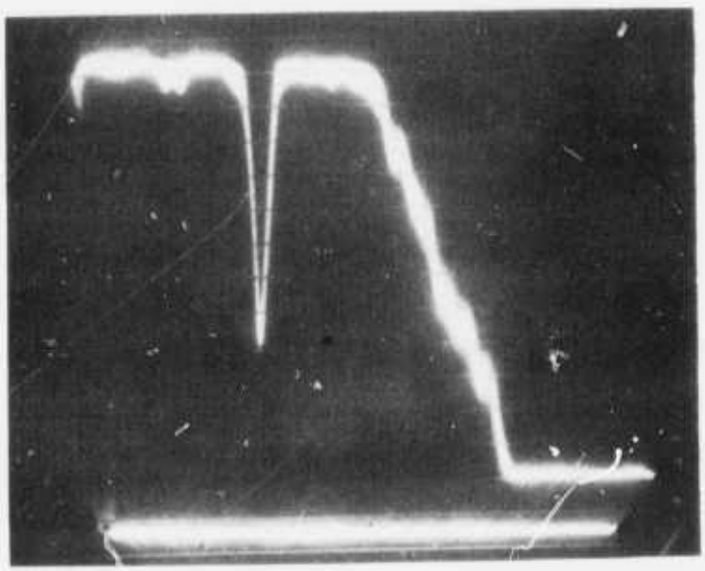

FIGURE 91 – SIGNAL OF POROSITY IN BONDLINE

verify the inspection findings visually. A good correlation was observed and it was concluded that the ultrasonic inspection technique was confirmed. Figure 92 shows the failed weldbonded shear panel and Figure 93 shows the failed weldbonded shear panel with inspection markings.

5.2.3 Development of Non-Destructive Inspection Standards

Non-destructive inspection standards were designed and fabricated for use in calibration of ultrasonic inspection equipment. The inspection standards were developed for assessing defects in weldbonded bondlines having quality areas that are defined as acceptable, marginal and unacceptable. It is noted that the marginal condition will not be included in standards released to production or in-service inspection personnel. The reason for not releasing such a standard is because a judgment would be required of the inspector that is generally reserved for a materials review board.

The degree of quality of bondlines in weldbonded joints is determined in part by the frequency of occurrence, size and location of the defects. Figure 94 depicts a typical inspection standard used in assessing three levels of bondline quality. In the original inspection standard, bondline porosity is simulated by 1/16 inch diameter flat bottom holes drilled through the lower adherend in the bonded joint of the standard. Three 1/16 inch diameter holes on 1/8 inch centers were drilled to the face sheet to simulate nearside disbonds and three 1/16 inch diameter holes on 1/8 inch centers were drilled to the bondline to simulate farside disbonds. The hole depth variations are necessary in order for the display on the cathode ray tube to be representative of the actual defect condition.

The simulated voids in the present standard occupy .16 square inch area. The size was increased to prevent any interpretation of data by the inspector which would occur using the 1/4 and 3/8 inch diameter simulated voids. The 1/4 and 3/8 inch diameter voids caused the inspection to be too sensitive as discovered when inspecting the flight article. A .250 or .187 inch diameter probe can be used interchangeably on the .40" x .40" defect standard and maintain the same inspection time and reliability. Either transducer can effectively "map" the size of the defect. The standard will also be painted to correlate with the panel installed on the aircraft.

5.3 Radiography of Spot-Welds in Weldbonded Joints

Early in the program it was established that the majority of quality sensing equipment used the density of the material as the basic sensing parameter. Since the density of the spot-weld nuggets in weldbonded joints is so much greater than the density of the adhesive in the bondline, it was concluded that it was improbable that a single inspection technique could be used. Thus, radiography was selected for inspection of the spot-weld nuggets.

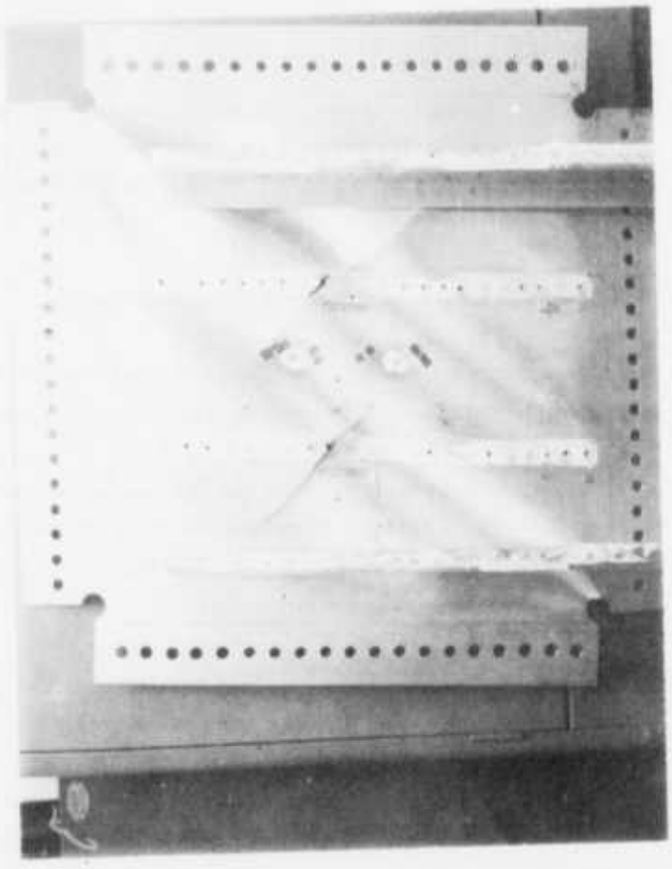

FIGURE 92 – FAILED WELDBONDED SHEAR PANEL

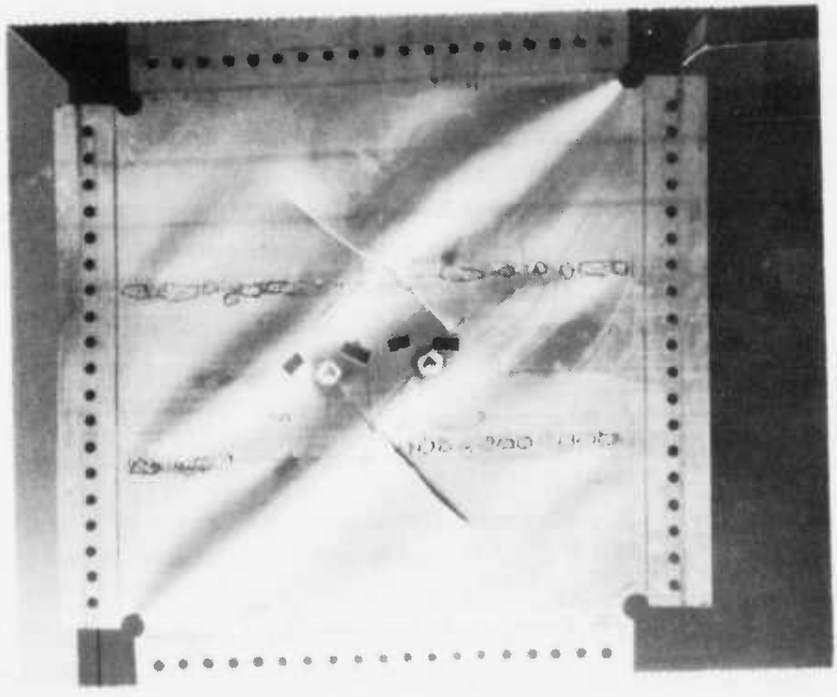

FIGURE 93 – FAILED WELDBONDED SHEAR PANEL SHOWING ULTRASONIC INSPECTION RESULTS

NOTE

1. .50 HOLE DRILLED TO ALUMINUM
2. .50 HOLE DRILLED TO ADHESIVE
3. PAINT ZONE 1 - FUS. STA. 280-337
4. PAINT ZONE 2 - FUS. STA. 337-387
5. UNPAINTED ZONE FOR COMPARATIVE PURPOSES AND USE AS NEARSIDE DISBOND BACK-UP
6. M6800 PASTE ADHESIVE
7. MYLAR SCRIM INSERT FOR HOLES DRILLED TO ALUMINUM ONLY

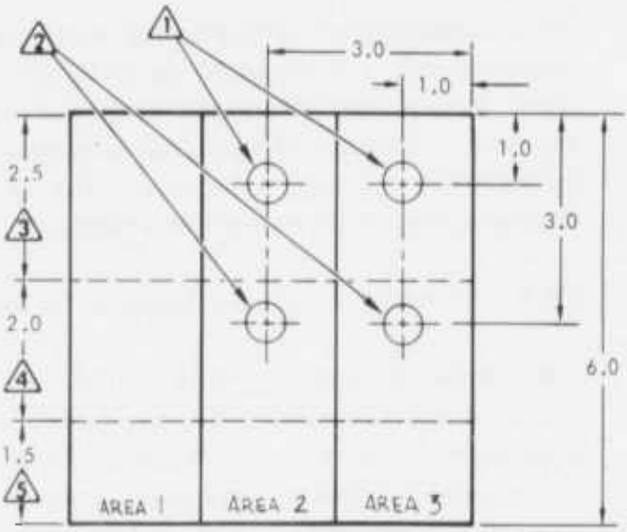

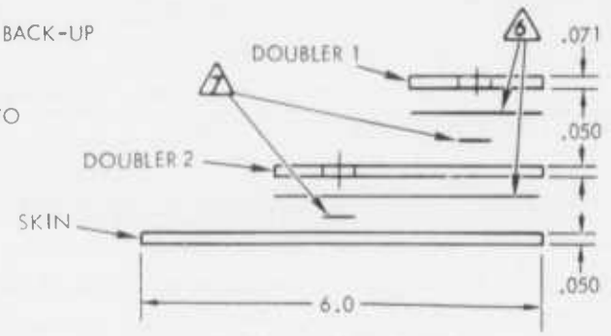

CALIBRATION STANDARD
MATL. 2024-T4 ALUMINUM

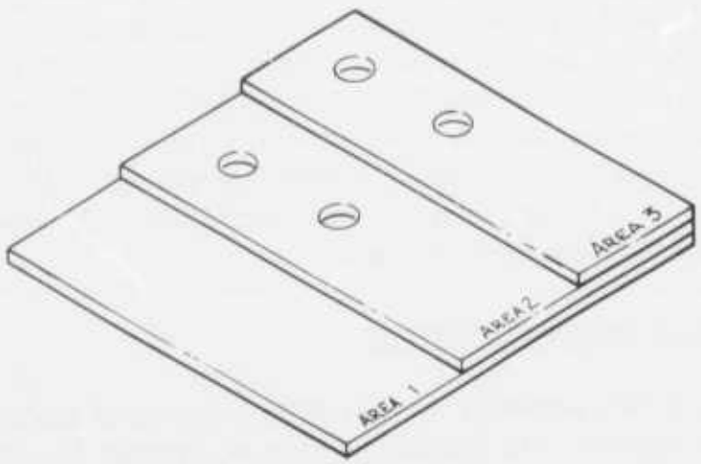

FIGURE 94 – CALIBRATION STANDARD FOR IN-SERVICE INSPECTION OF WELDBONDED C-130 FUSELAGE PANEL

5.3.1 Film Radiography

Film radiography has long been the most popular and reliable inspection technique for spotwelds, and it is acceptable as an inspection method for spot-welds in weldbonded joints. At best, film radiography is slow and costly for production assemblies. However, it was used in inspection of spot-welds in weldbonded joints of elemental test specimens, and sub-scale and full-scale components. Two other types of inspection equipment were investigated during the course of this program.

5.3.2 Ultrasonic Equipment Evaluation for Inspection of Spot–Welds

The Branson Company Model 101 Ultrasonic Digital Caliper was evaluated for spot-weld inspection and was determined to be unsatisfactory for this application. Normal spot-weld indentations in the sheet coupled with the relatively large diameter of the contacting surface of the caliper transducer gave poor ultrasonic response. The oval cross-section of the spot-weld nugget has an averaging effect on measurements and consistency of results was poor. Therefore, this instrument was dropped from consideration as a potential means for inspecting spot-welds in weldbonded joints.

5.3.3 Television X-Ray Investigations

The more recently developed television radiographic inspection method was investigated for application to production weldbonded assemblies. Television radiography has the advantages of real time response and elimination of film and film processing costs over film radiography. Evaluation of the television radiographic method was accomplished on weldbonded demonstration specimens. The weldbonded demonstration specimens were designed and fabricated and transmitted to the Phillips-Norelco Company for examination with a Searchray Television X-Ray System. Intentional defects were included in the spot-weld nuggets in the weldbonded demonstration specimens. The results from the examination of the demonstration specimens were recorded on Polaroid photographs. The Polaroid photographs of the television X-rays were compared with the film radiographs of the demonstration specimens, and excellent agreement in spot-weld quality was achieved. The intentional defects in the spot-welds were clearly exhibited on the Polaroid photographs as the result of the television screen magnification.

5.4 NDI Methods Development Summary

The current state of NDI technology necessitates the inspection of weldbonded joints by two (2) separate methods. The adhesive bondline is inspected by one method and spot-welds by a different method. Investigations in this program led to the conclusions that ultrasonics was the best technique for examining the adhesive bondlines and radiography was the best method for inspecting the spot-welds. Quality standards were developed for

calibrating ultrasonic equipment for use in inspecting adhesive bondlines in weldbonded joints. Film radiography was used throughout the program for inspecting spot-welds in weldbonded joints principally due to the unavailability of television radiographic equipment. However, it was concluded that television radiography can be applied in a production program as a cost effective technique for rapidly and reliably inspecting spot-welds in weldbonded assemblies.

SECTION VI

COST ANALYSIS OF WELDBONDED STRUCTURES

6.1 Cost Analysis Summary

The purpose of the cost analysis is to determine the relative recurring production cost of weldbonding compared to riveting and conventional bonding. Detail cost analysis of the C-130 side panel fabricated for flight evaluation, supported by program developments, shows that the weldbond process is the least costly of the processes evaluated. Weldbonding shows a cost savings of 37 percent over the baseline riveted structure and 18 percent over the adhesive bonded structure. Additional refinements of the weldbond process provides a good potential for the reduction of airframe manufacturing costs.

Additional cost studies conducted outside the scope of this program are included in this section of the report for a more complete assessment of the weldbond process cost potentials.

6.2 Structural Description

The design of the weldbonded fuselage component is described in Section VII and it consisted of four (4) fuselage skin sections, thirteen (13) roll formed Z-section ring frames, three (3) fuselage splices that include Z-section ring frames and splice plates, two (2) windows, and miscellaneous reinforcing doublers, clips, and stiffeners. The center fuselage skin splice was mechanically fastened for the weldbonded component and was considered mechanically fastened for alternative configurations. Materials used in all configurations evaluated were commonly used aluminum alloys and the mechanical fasteners were aluminum rivets.

6.3 Cost Methodology and Ground Rules for the Cost Analysis

Procedures normally used for cost estimating were reviewed and the industrial engineering detail method was selected over both the analogy method and the parametric method as the best method for projecting production costs for this program. The industrial engineering detail method uses time and motion study data to develop "standard" times for basic manufacturing operations required in the fabrication of detail parts and assemblies. The operations necessary to produce parts and assemblies were complete and well defined for a meaningful cost estimate. Historical performance and learning curve factors were applied in order to develop a total labor estimate. This method of estimating had the advantages of providing cost estimates that were sensitive to design configuration details, peculiar materials and/or processes, specific manufacturing techniques, and to advanced state-of-the-art technology.

The ground rules for estimating recurring costs were as follows:

1. All cost estimates were projected in 1974 rates.

2. A total labor rate of twenty (20) dollars per hour was used.

3. Costs were cumulative average for quantities of aircraft shown and include materials, labor, and inspection costs.

4. Material costs were projected on a ninety-five (95) percent learning curve; labor costs are projected on an eighty-two (82) percent learning curve except for metal bonding which was projected on an eighty-five (85) percent learning curve.

5. Material costs included aluminum alloys, sealant, adhesive, and fasteners.

6. Fabrication costs included the labor to produce detail parts; structural assembly costs for weldbonding, riveting, or metal bonding of the detail parts into a sub-assembly; and costs necessary for post assembly operations such as finishing and sealing.

6.4 Recurring Production Cost Estimates

In order to evaluate the relative cost of weldbonding, automatic riveting, metal bonding, and hand riveting, it was necessary to consider the basic manufacturing process steps for the respective processes. From these steps it can be seen that many of the detail operations were the same or similar.

6.4.1 Basic Process Steps

(a) Weldbond

- o fabricate detail parts
- o degrease detail parts
- o prefit parts in fixture
- o remove parts from fixture
- o clean detail parts
- o apply adhesive to faying surface
- o assemble parts, clamp, tack weld

- o set-up machine and load fixture into machine
- o spot-weld
- o clean adhesive "squeeze out"
- o unload fixture from machine
- o rig thermocouples and oven cure
- o unload assembly from fixture
- o clean assembly for anodize
- o anodize, paint

(b) Hand Rivet

- o fabricate detail parts
- o clean detail parts for anodizing
- o anodize and paint detail parts
- o prefit parts in fixture
- o pilot drill all holes
- o drill holes full size
- o countersink holes
- o disassemble parts and deburr
- o apply fay surface sealant
- o re-assemble parts and clamp in fixture
- o install fasteners "wet"
- o clean sealant "squeeze out"
- o unload assembly from fixture

(c) Automatic Rivet

- o fabricate detail parts
- o clean detail parts for anodizing
- o anodize and paint detail parts
- o prefit parts in fixture
- o remove parts from fixture
- o apply fay surface sealant
- o re-assemble parts, clamp, tack rivet
- o set-up machine and load fixture onto machine
- o install fastener "wet" automatically
- o clean sealant "squeeze out"
- o unload fixture from machine
- o unload assembly from fixture

(d) Metal Bond

- o fabricate detail parts
- o clean detail parts for anodizing
- o anodize detail parts
- o degrease detail parts
- o prefit parts in fixture
- o remove parts from fixture
- o clean detail parts
- o apply primary adhesive
- o apply secondary adhesive

- o re-assemble parts for bonding
- o bag assembly for curing
- o rig thermocouples and cure in autoclave
- o remove from autoclave and debag
- o unload assembly from fixture
- o clean assembly and paint

6.4.2 Actual Weldbond Costs of C-130 Weldbonded Fuselage Component

Table XLIII summarized the actual manhour costs which were recorded during the manufacturing development of the C-130 weldbonded fuselage component. Recorded hours represented actual productive work time and not span time. The basic process steps were representative of current technology and production methods except for the spot-welding. Spot-welding in a production environment with appropriate production tools will generally represent five (5) to fifteen (15) precent assembly cost rather than the thirty-nine (39) percent shown for the weldbonded fuselage component.

TABLE XLIII – C-130 WELDBONDED FUSELAGE COMPONENT PROCESS STEP COSTS

MANUFACTURING PROCESS STEPS	MANHOURS	PERCENT OF TOTAL MANHOURS
IDENTIFY	2.8	2.5
CLEANING	10.0	8.8
ADHESIVE	3.4	3.0
ASSEMBLY	19.4	17.0
SPOT-WELDING	44.1	38.8
CURING	8.5	7.5
ANODIZING	2.6	2.3
Q.A. TEST PANELS	8.0	7.0
SEALING	15.0	13.1
	113.8	100.0

6.4.3 Sealing Requirements

The weldbonded component requires environmental fillet sealing of all bonded joints after anodize due to the current state of the art. Through continued development of adhesives, surface preparation techniques and finish systems, post cure environmental sealing can be eliminated. Figure 95 shows the structural assembly cost of weldbonding with sealing compared to weldbonding without those environmental sealing requirements.

The current requirement to fillet seal all bondlines and spot-weld rates of 15 spots/min make automatic riveting competitive with weldbonding. Full automation of the process and elimination of sealing requirements results in weldbonding being the least costly joining process evaluated. This is further discussed in section 6.4.4.

6.4.4 Cost Effects of Improved Production Efficiency (Automation)

Within the basic process steps for weldbonding are manufacturing operations with potential for improved production efficiency through automation. As additional production experience is gained with weldbonding and more efficient tools and techniques are developed, improvements are possible in areas such as spot-welding, adhesive application and part preparation.

Improvements in spot-welding up to the equivalent of 50 spot-welds per minute are shown on Figure 96. Significant savings were indicated up to approximately ten (10) spot-welds per minute with diminishing returns thereafter. Increasing the spot-weld rate from sixteen (16) spot-welds per minute (current technology) to fifty (50) spot-welds per minute yields a thirteen (13) percent cost saving in structural assembly labor cost. Roll spot-welding would reduce welding cost significantly for suitable structures.

Figure 97 shows the potential cost savings for improvements in adhesive application. Cost analyses, with a high degree of confidence, were not possible at this time because of the lack of automated adhesive application methods and associated equipment. However, sufficient conceptual work has been performed to insure feasibility of applying adhesive by automated means and logical assumptions have been made for cost comparisons. Because of the relatively small area of weldbonded joints compared to the total area of the assembly, the cost of applying adhesive by hand was only approximately three (3) percent of the total cost and, therefore, the potential savings were small. Other structural assemblies may very well show greater potential for cost savings.

Automated cleaning by the spray-line method as described in "Processing for Adhesive Bonded Structures" from the conference held at Stevens Institute of Technology in August 23-25, 1972, was another basic process step applicable to weldbonding which had potential cost savings. Cleaning represented approximately eight (8) percent of the structural assembly cost. Cost savings using an automated cleaning spray line amounted to approximately two and a half (2 1/2) percent of the structural assembly cost.

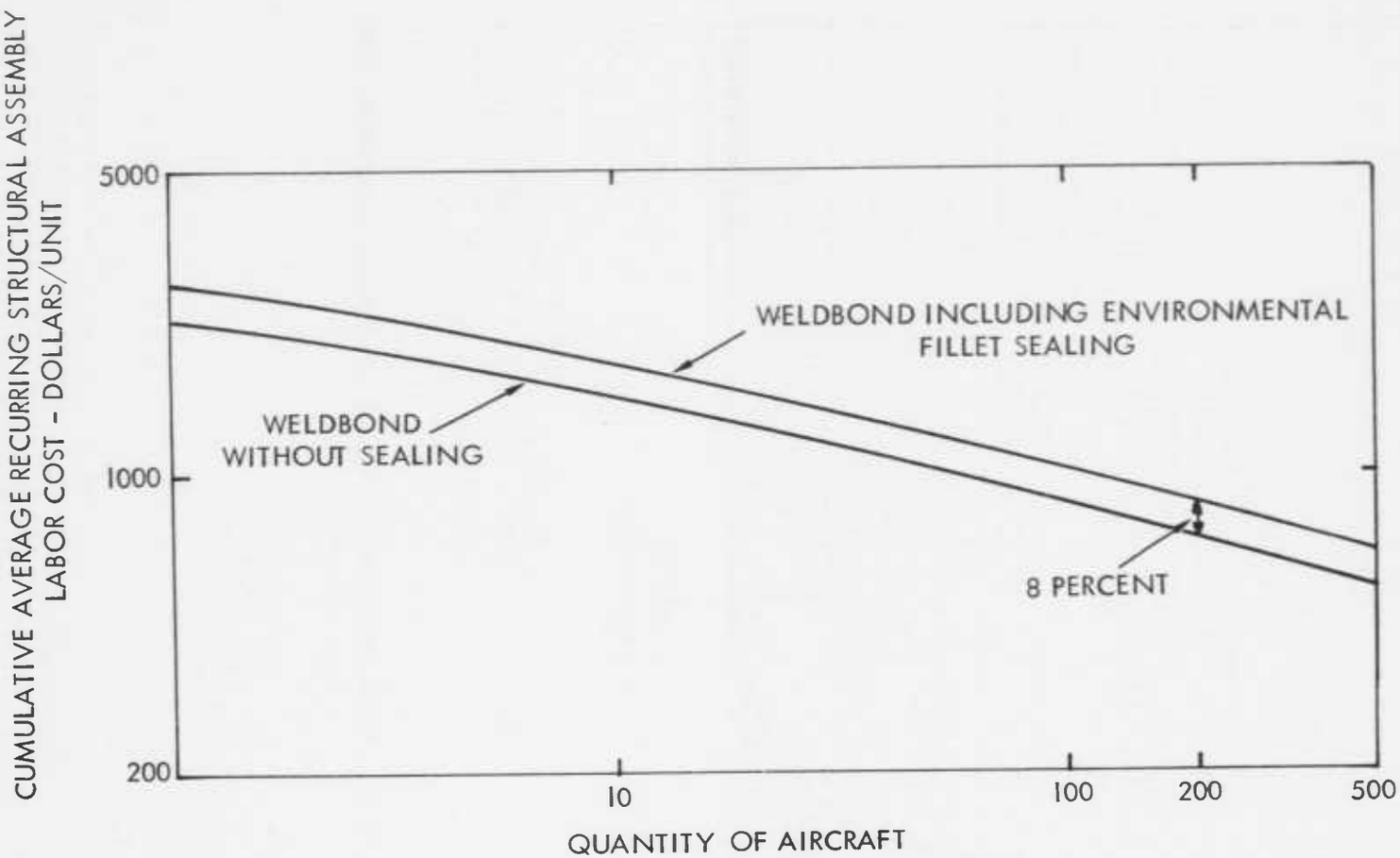

Figure 95. - Comparison of Recurring Labor Costs for Weldbonding

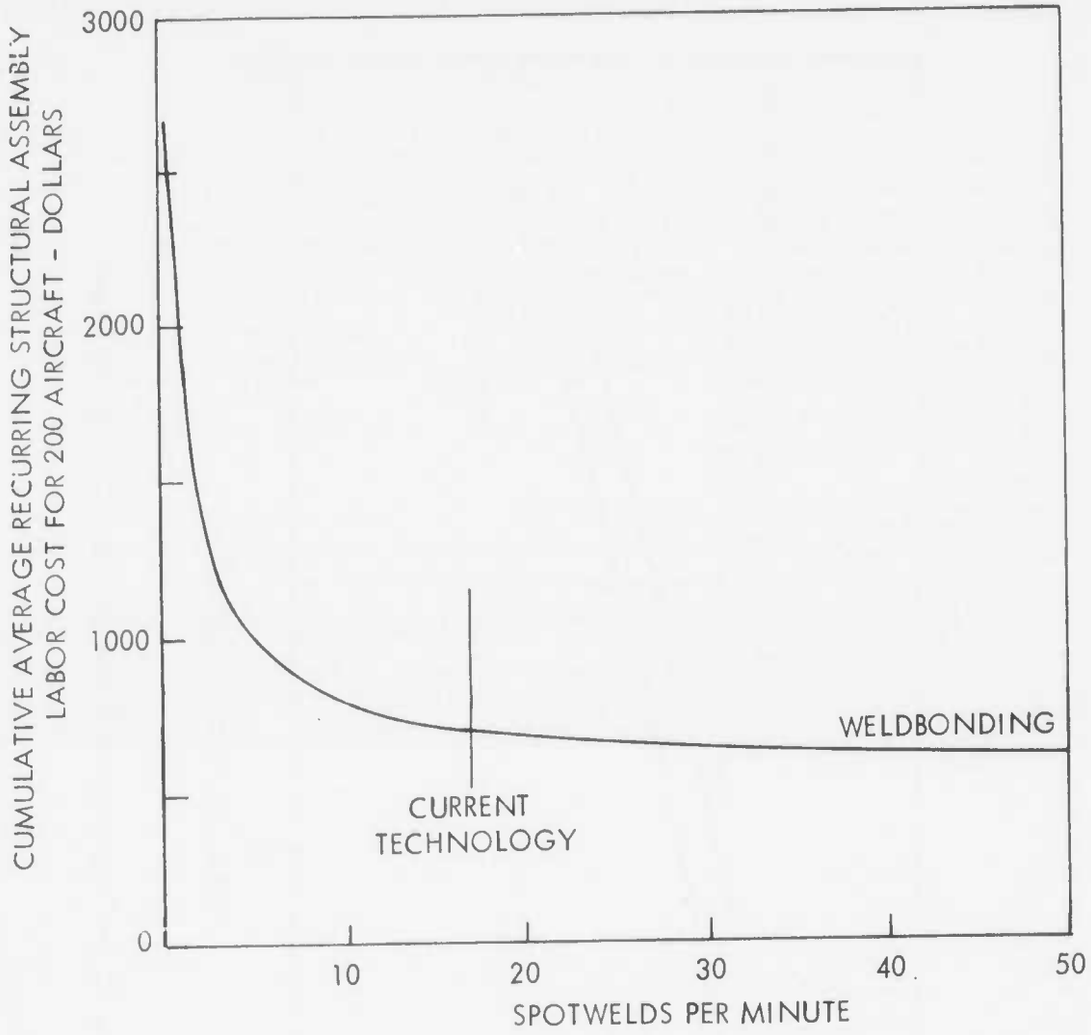

Figure 96. - Projected Labor Cost Based on Increased Spotwelding Rate

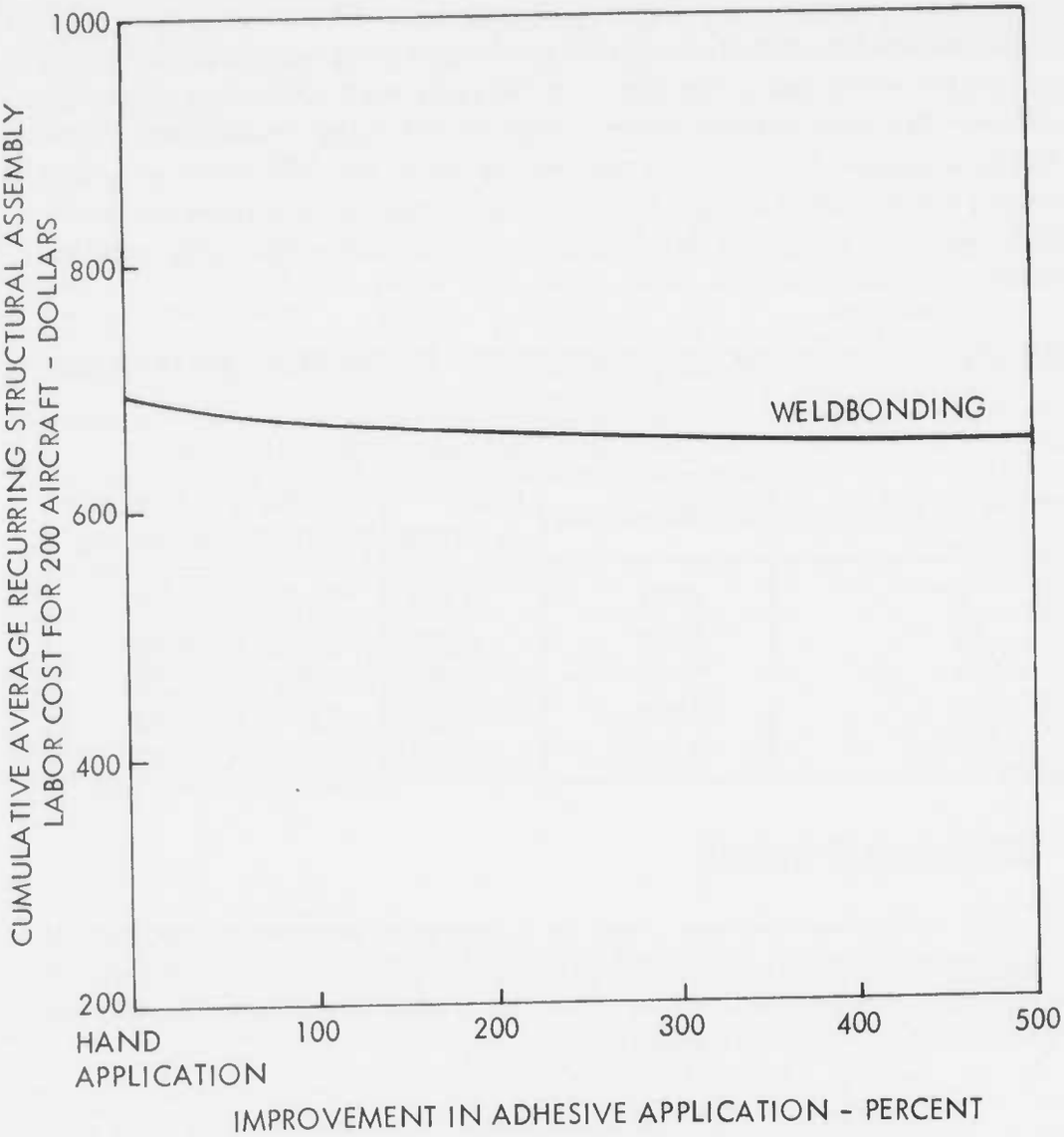

Figure 97. - Projected Labor Cost Based on Automating the Adhesive Application Operation.

Figure 98 and Table XLIV show the combined effects of improved production efficiency using automation in spot-welding, adhesive application, and cleaning and the elimination of environmental fillet sealing the bondlines. As seen on Figure 98 and Table XLIV at the 200th unit, weldbonding showed an eight (8) percent cost saving over automatic riveting, thirty-seven (37) percent cost savings over hand riveting for the C-130 fuselage component, and eighteen (18) percent cost savings over full structural bonding. Development of these cost savings were based on a projected spot-welding rate of fifty (50) welds per minute (possibly use of roll welding), a hundred (100) percent improvement in adhesive application, and thirty-three (33) percent in surface percent in surface preparation using spray line equipment.

TABLE XLIV – CUMULATIVE AVERAGE COST PER AIRCRAFT IN 1974 DOLLARS

QUANTITY OF AIRCRAFT	JOINING METHOD – DOLLARS/UNIT			
	WELDBONDING	HAND RIVETING	METAL BONDING	AUTOMATIC RIVETING
1	7,171	12,202	8,178	7,867
10	5,026	8,370	5,893	5,497
100	3,104	4,969	3,762	3,376
200	2,677	4,221	3,271	2,905
500	2,211	3,400	2,727	2,392

6.5 Non-Recurring Tooling Costs

Non-recurring tooling estimates were made for a production program for the four (4) configurations and are shown in Table XLV. Fabrication tooling was the same for all four (4) configurations. Weldbonding required the largest number of tools which resulted in a slightly higher tooling cost than automatic riveting.

TABLE XLV – PRODUCTION TOOLING ESTIMATES

WELDBOND	AUTOMATIC RIVET	METAL BOND	HAND RIVET
$116,000	$110,000	$84,000	$79,000
Fab Tools	Fab Tools	Fab Tools	Fab Tools
Weld Fixture	Automatic Rivet Fixture	Metal Bond Fixture	Assembly Fixture
Handling Equipment	Handling Equipment	Handling Equipment	Handling Equipment
Oven Dolly	NC Tape		
NC Tape			

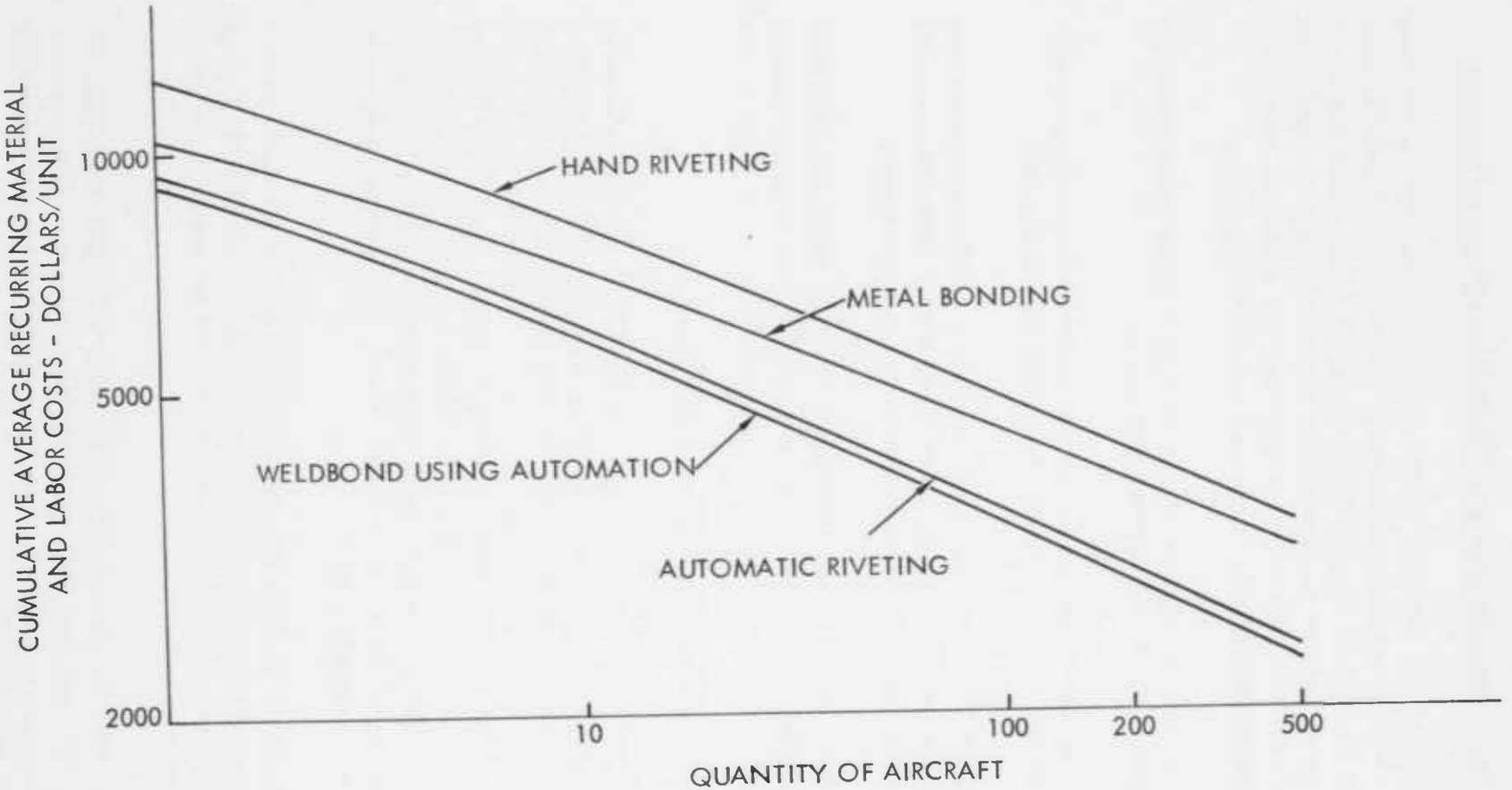

Figure 98. - Cost Comparison of Automated Weldbonding with other Joining Processes.

6.6 Additional Cost Analysis and Transition of the Weldbond Process to Production

Other programs utilizing the weldbond joining process that have been or are being conducted by the Manufacturing Research Department at the Lockheed-Georgia Cornpany (Gelac) that parallel the program described herein offered the opportunity to supplement and confirm cost data derived from the accomplishments performed under this development program (F33615-71-C-1716). This weldbond prototype and production development related programs consisted of separate but similar areas available for cost analysis.

1. Fabrication, delivery and cost analysis of a prototype Common Shelter (part of the SAM-D missile complex for the Raytheon Corporation).

2. Fabrication and cost analysis of work to date on 44 storage shelter containers for an ASD/SMB contract which will total 75 units on completion in early 1975.

3. IR&D studies involving cost analysis and fabrication of C-130 cargo floor and wing trailing edge experimental parts by the weldbond process. These assemblies were compared to the present process of joining by riveting and metal bonding.

The data discussed herein is a condensed description of the work, cost analysis, and results of development work performed at the Lockheed-Georgia Company outside the scope of this contract.

6.6.1 Background Methodology for Related Program Cost Analysis

During the past two years, Gelac has responded to several inquiries involving the use of weldbond as a production joining method. Two of the inquiries, one from the Raytheon Corporation, and the other from the ASD/SMB, Air Force Systems Command, resulted in contracts for production work. The Raytheon Corporation contacted the Manufacturing Research Department in an inquiry about the weldbond process during 1972. Further exchange between the two companies led to the fabrication of two weldbonded test assemblies. Subsequent testing of the assemblies at Raytheon led to the change of design for their SAM-D missile common shelter from a riveted structure to an essentially weldbonded structure, Contract No. 71-3876-BM-95407.

Concurrent development of the Bare Base Shelter contract for the Air Force led to a contract to build the General Purpose Shelter Container shown in Figure 99. The General Purpose Shelter Container utilizes resistance welding and/or weldbond joining in approximately 80 percent of its major structure.

Continued in-house effort for the utilization of the weldbond process has initiated the evaluation of the C-130 cargo floor, Figure 100, and the C-130 trailing edge assemblies, Figure 101, as candidates for change from riveted and bonded structure to weldbonded structure, Figure 102 and Figure 103.

FIGURE 99 – WELDBONDED GENERAL PURPOSE CONTAINER BUILT UNDER CONTRACT F33657-C-0167

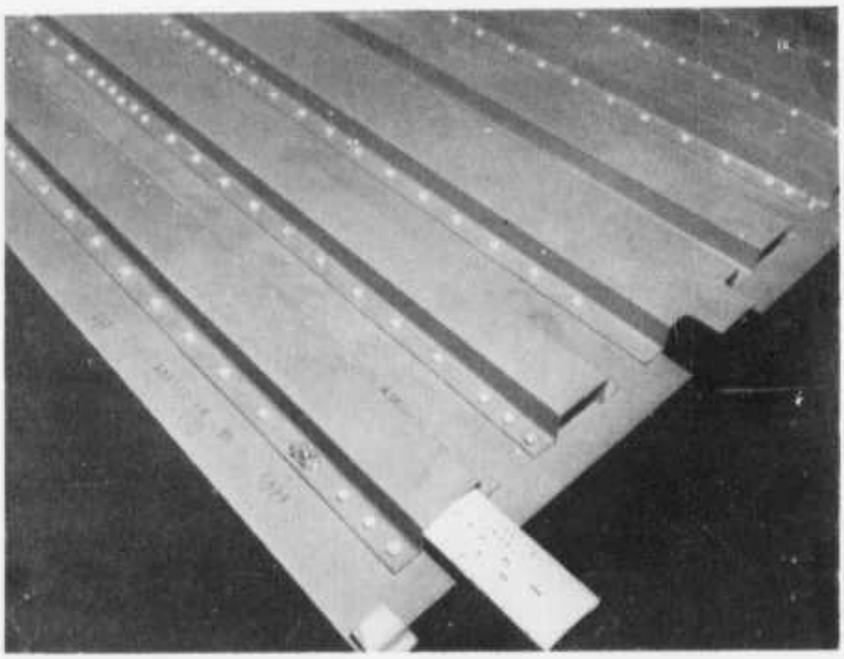

FIGURE 100 – C-130 CARGO FLOOR SECTION FABRICATED BY CONVENTIONAL RIVETING PROCESS

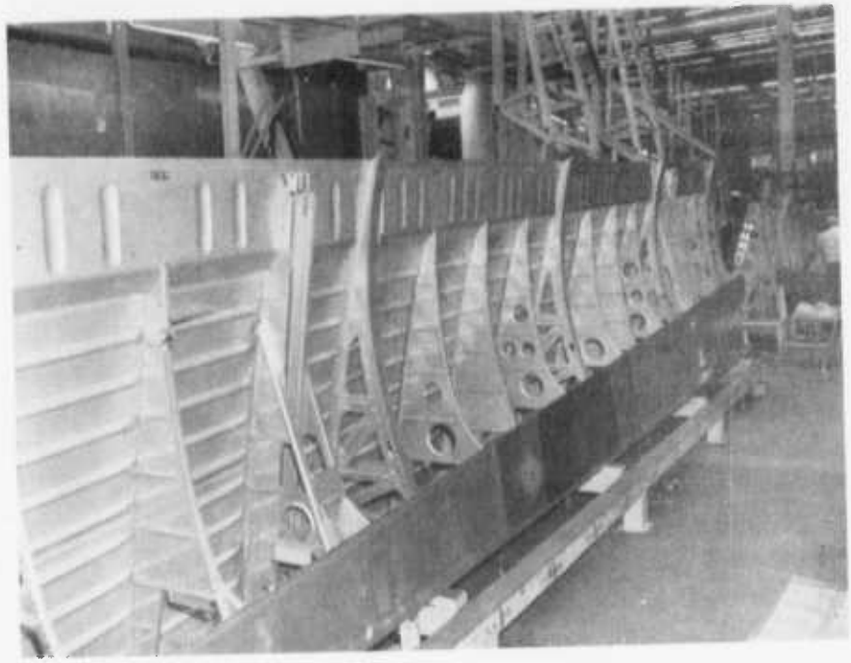

FIGURE 101 – A SECTION FO THE C-130 TRAILING EDGE JOINED BY AUTOCLAVE METAL BONDING

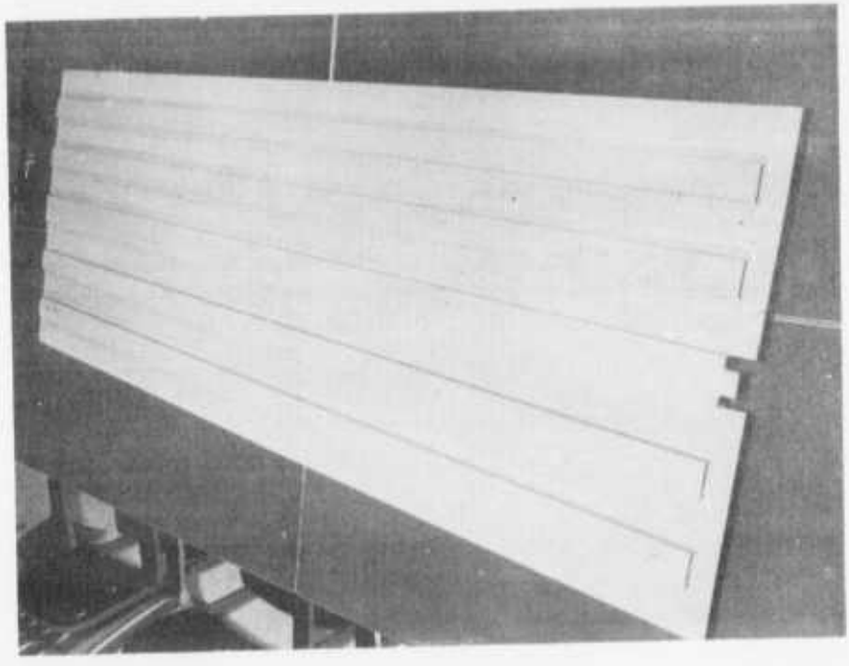

FIGURE 102 – A SECTION OF THE C-130 CARGO FLOOR JOINED BY ROLL SPOT WELDBONDING

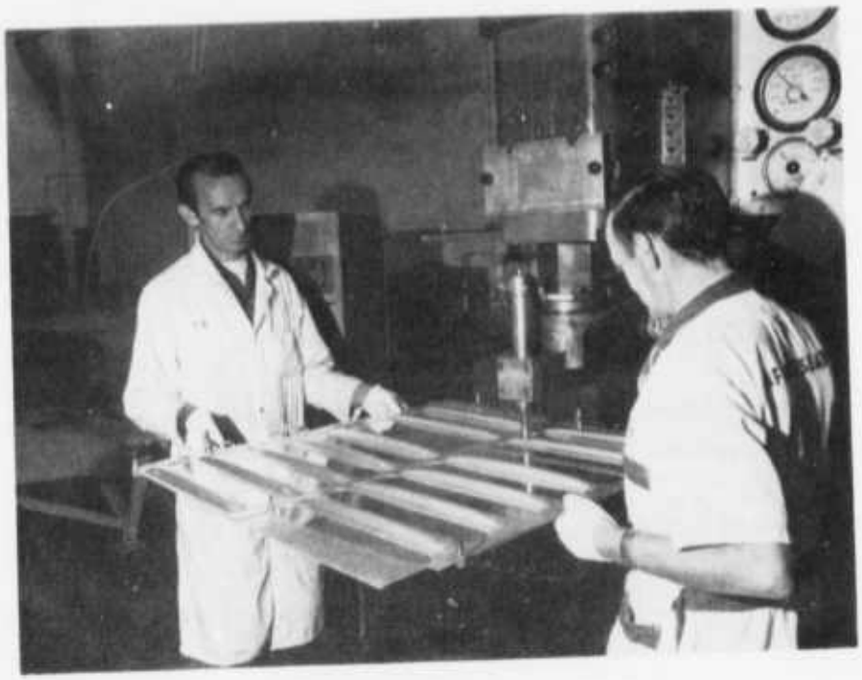

FIGURE 103 – TYPICAL SECTION OF THE C-130 TRAILING EDGE BEING JOINED BY WELDBONDING

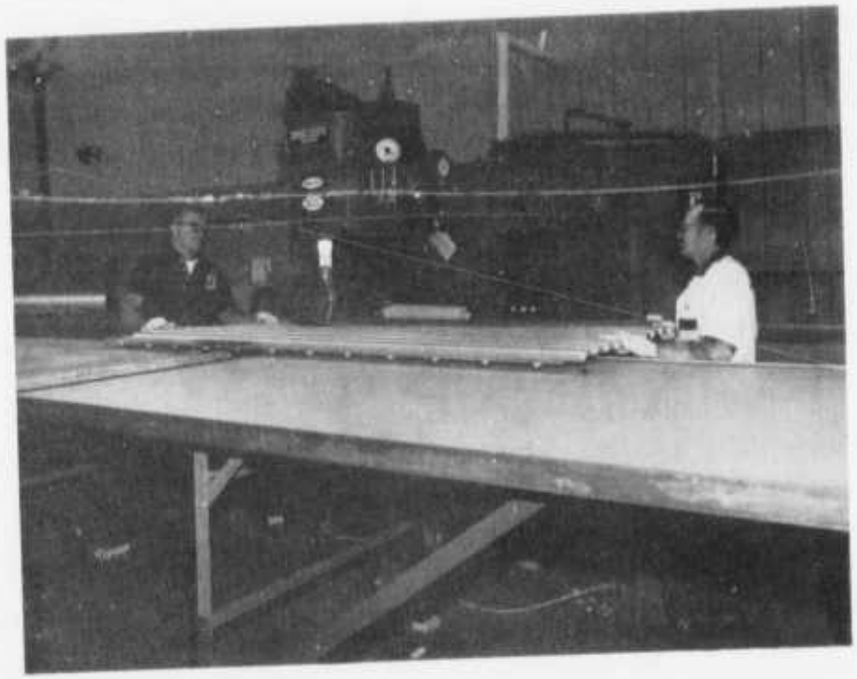

FIGURE 104 – SCIAKY ROLL SPOT WELDER SHOWN WITH BALL TRANSFER PALLETS BEING USED TO JOIN THE GENERAL PURPOSE SHELTER CONTAINER SUBASSEMBLIES

Transition from development to production of items of large size and/or quantity required several separate but interdependent efforts. These were as follows:

1. Acquisition and layout of a work area large enough to handle present and anticipated future weldbond work.

2. Movement and installation of machines and equipment.

3. Development and certification of weldbond schedules.

4. Training a combined production work force of Manufacturing Research and Production personnel.

5. Establishment of each process as a standard practice.

6. Phaseout of Manufacturing Research supervision and phasein of Production supervision.

A portion of the Production Bonding Clean Room in the B-1 Building was selected to house the layup and joining of the weldbonded structures. Additional floor space adjacent to the clean room was selected and laid out for build-up and final assembly of the Common Shelter and General Purpose Shelter Container.

Three resistance welders plus necessary fixtures as shown in Figures 104,105, and 106 were moved into position in the clean room. These three welders, plus the approximately 7000 square feet of clean room floor space have provided Gelac with an unmatched capability in weldbonding. An additional 8000 square feet of clean room area are available as required.

In addition to, and adjacent to, the clean room area is curing equipment adequate for the largest of aircraft assemblies.

6.6.2 Weldbonding the Raytheon SAM-D Shelters

Actual joining of the large Raytheon SAM-D panels was accomplished by roll spot welding as shown in Figure 104. Prior to the roll welding operation, adhesive had been applied to the hat sections and zee extrusions and tack welding had been accomplished on the Rocker Arm Welder as shown in Figure 105.

Weld schedules were developed and certification made for each type and joint thickness prior to the production operation.

After the cleaning, lay-up, welding, curing, and alodining operations, final assembly joining of the inner skins and final joining of the panels were done with mechanical fasteners. A view of the completed 84 inches x 170 inches shelter is shown in Figure 107.

FIGURE 105 – TACK WELDING A SIDE SECTION OF THE RAYTHEON SHELTER PRIOR TO ROLL SPOT WELDBONDING

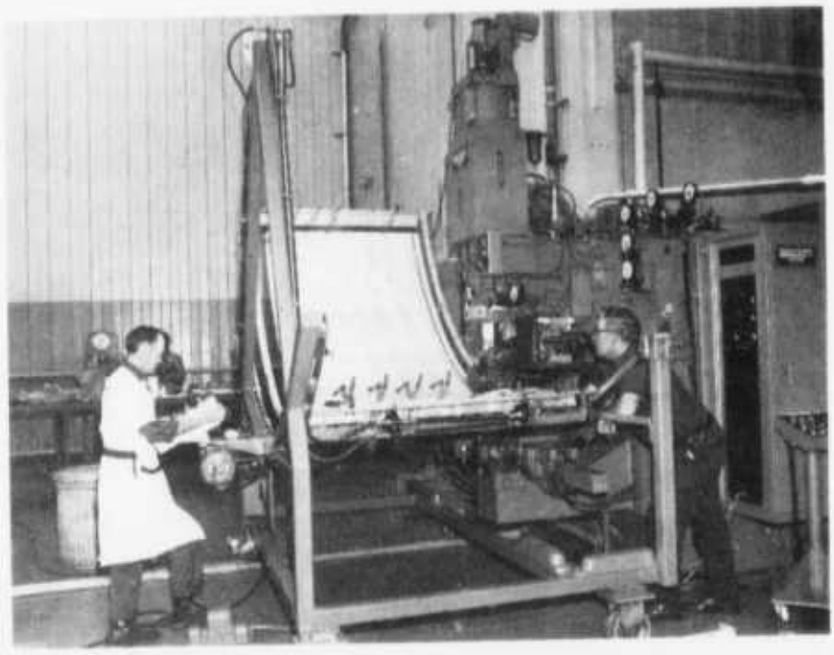

FIGURE 106– VIEW OF THE 3-AXIS SEMI-AUTOMATIC WELD POSITIONER USED TO JOIN THE C-130 FLIGHT AND TEST PANELS

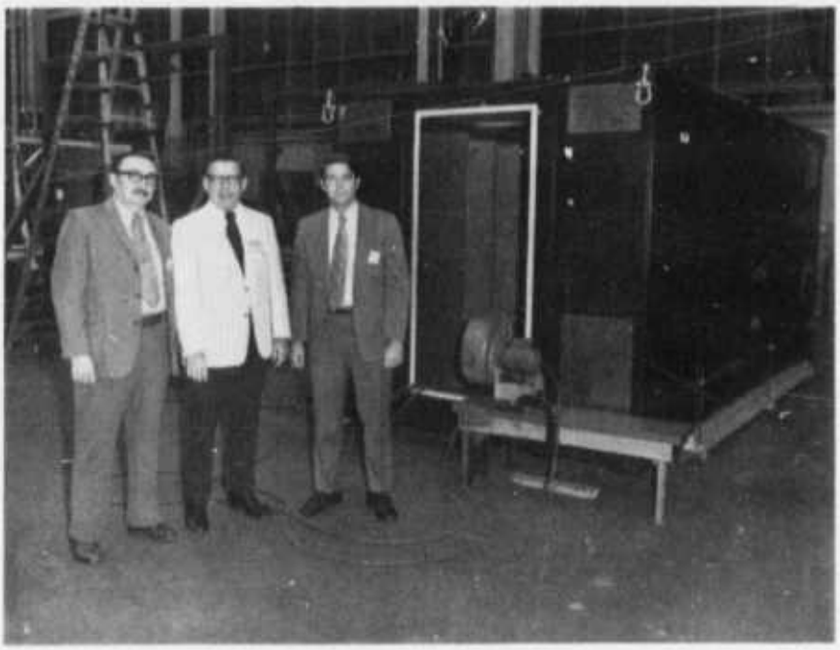

FIGURE 107 – THE COMPLETED RAYTHEON SAM-D COMMON SHELTER

6.6.3 Weldbonding the General Purpose Shelters

Successful completion of the Bare Base Shelter Program at Lockheed-Georgia Company led to an interest in, and finally resulted in, a General Purpose Shelter Container for storage and shipment of Bare Base type shelters. Final design of the General Purpose Container resulted in Approximately 80 percent of the structure being joined by spot-welding and/or weldbonding. The new weldbond facility was used essentially as it existed to join the embossed corrugated outer skins used in the fabrication of the General Purpose Shelter Container.

It was established that after cleaning the adhesive could be laid in a single bead on the corrugated skins and that the pressure and rolling action of the seam welder wheel would automatically spread the adhesive. This resulted in an extremely fast operation as shown in Figure 104. One completed hood section (one container) could be weldbonded per day using this technique. The completed container is shown in Figure 99. Final assembly joining of the Container was accomplished in three sections by a splice doubler after brake forming of the weldbonded assemblies. An average of 216 square feet of weldbond (one complete hood unit) is being produced daily on the 75-unit Container program. Two complete door units (240 square feet) can also be completed in one eight-hour shift. To date, a total of 35 hood units and 40 doors have been completed for an estimated grand total of 34,200 square feet of weldbonded structure. Table XLVI shows a breakdown of manhours versus square footage of structure. (Due to the use of doublers to stiffen the door corrugated skins, actual square feet of welding is double that of the door size.)

TABLE XLVI – ROLL SPOT WELDBONDING HOOD AND DOOR UNITS LABOR COSTS

MANHOURS BREAKDOWN BY SQUARE FEET/UNIT			
HOOD & DOOR UNIT AREA ($FT.^2$)	UNIT COST ($MH/FT.^2$)	HOOD & DOOR TOTAL LABOR COST (MH)	TOTAL SQUARE FOOTAGE MANUFACTURED TO DATE
456	.105	48	34,200

6.6.4 Development of Weldbond Joining for C-130 Trailing Edge and Cargo Floor

The C-130 aircraft trailing edge panels, which consists of approximately one-third of the upper wing surface area, or 468 square feet per aircraft, are presently autoclave bonded at Lockheed's Charleston, South Carolina, facility. In a proposal to return the work to Gelac, Manufacturing Research built two sections of the trailing edge (Dwg. No. 341239-36); one by conventional single point resistance spot weldbonding and one by roll spot weldbonding. Assembly No. 341239-36 is typical of the trailing edge sections and is 30 inches x 40 inches in size, made up of two subassemblies, -30 and -33, spliced together. A view of the panel is shown in Figure 103.

As in the case of the General Purpose Shelter Assembly, it was found that the adhesive could be applied to the beaded panels by air dispenser in a single bead form and that the spreading of the adhesive would be accomplished by electrode pressure. Again this resulted in a very fast lay-up and welding time.

In order to establish a base for cost analysis comparison of manhours for weldbonding versus autoclave bonding, standard shop paper was written and normal inspection procedures were followed for the weldbond process. Time comparison for this estimate was taken directly from standard hours on the shop order for Assembly No. 341239-36 and from time recorded for weldbonding the same assembly. Many of the operations required to produce the assembly by standard bond procedures at the Charleston facility were not required for weldbonding and because only total hours were listed for some operations on the shop orders, it was necessary to break down operations for commonality in order to determine comparative times.

Based on the estimated total of 468 square feet of trailing edge per aircraft, Table XLVII shows the breakdown in manhours for the two methods of joining and the resulting estimated manhours saved per 100 aircraft by weldbonding the trailing edges at Gelac.

TABLE XLVII – COMPARATIVE LABOR COSTS FOR WELDBONDING AND AUTOCLAVE BONDING C-130 TRAILING EDGE SECTIONS

MANHOURS BREAKDOWN BY SQUARE FEET/AIRCRAFT								
AUTOCLAVE BONDING AT CHARLESTON				WELDBONDING AT GELAC				
FT^2/SHIP	MH/FT^2	TOTAL MH/SHIP	TOTAL MANHOURS (100 SHIP)	FT^2/ SHIP	MH/ FT^2	TOTAL MH/SHIP	TOTAL MANHOURS (100 SHIP)	TOTAL SAVINGS (100 SHIP)
468	1.06	496	49,608	468	.69	323	32,292	17,316

As shown in Table XLVII, a 35 percent savings in manhours is realized by weldbonding the C-130 trailing edge. No learning curve factor has been applied to the 100 ship estimate in order to deliberately keep the estimate conservative. Also, no shipping charges for transporting the parts and assemblies to and from Charleston have been included in the savings estimate.

The C-130 main cargo floor is approximately 418 square feet in area and is made up of subassembly sections consisting of webs joined to hat section extrusions typical of the 31 inches x 80 inches section shown in Figure 100. The subsections are presently fabricated by automatic riveting. The Super Stretch model C-130 adds approximately 80 square feet to the total size; however, for this study only the standard floor was evaluated.

Because of the long uninterrupted attachment areas for the hat section to skins, the assembly is ideally suited to roll spot weldbonding. Width and length of all the subsections are compatible with present Gelac weldbond equipment and facilities. With cost savings as the predominant motivating factor, a section of the floor (Figure 102) was roll spot weldbonded and time studied to determine the feasibility of changing the joining method from automatic riveting to weldbonding.

Cargo floor panel (Dwg. No. 354123-2) has an area of approximately 17.5 square feet and, as was the case with the trailing edge section, this experimental panel was used to establish basic cost per square foot for weldbonding versus automatic riveting. A shop order was written and followed for weldbonding the assembly in order to establish authentic times per operation. A standard production shop order was obtained to establish sequence and time for the present method of joining. Only total operation time for set-up and joining had been established by Time Standards for the automatic riveting operation, whereas a specific breakdown of each weldbonding operation was obtained during the timing of the weldbond process.

Since the detail parts for the floor are chemically cleaned and anodized prior to rivet joining, and the same parts are chemically cleaned, weldbonded, and then anodized, this part of the cost was a trade-off and was, therefore, deleted from the study. Comparable operations are shown in Table XLVIII.

Considering the standard length C-130, there are approximately 418 square feet of cargo floor applicable to automatic riveting or roll spot weldbonding. Based on part number 354123-2, a typical center floor panel, Table XLVIII shows that the 17.5 square foot panel required 4.87 manhours to join by automatic riveting and 1.85 manhours to join by the weldbonding process. Again, as with the trailing edge panels, this better than two to one manhours saving was achieved on the first weldbond unit without benefit of either tooling or applied learning factor. A further breakdown in manhours comparison and cost saving is shown in Table XLIX.

TABLE XLVIII – COMPARATIVE UNIT LABOR COSTS FOR WELDBONDING AND AUTOMATIC RIVETING THE C-130 CARGO FLOOR

AUTOMATIC RIVETING			ROLL SPOT WELDBONDING		
OP. NO.	DESCRIPTION	MH/ UNIT	OP. NO.	DESCRIPTION	MH/ UNIT
1	Rivet wells to floor wells & C.S. (2) holes		1	Prepare test specimens	.01
2	Locate hat sections & floor web in rivet jig		2	Set up welder	.03
3	Back drill stiffeners through web		3	Apply adhesive	.30
4	Countersink and burr		4	Cleco	.10
5	Tack rivet web and stiffener		5	Weld	1.00
6	Rivet		6	Cure	.21
7	Identify		7	Solvent wipe	.15
			8	Identify	.05
		TOTAL = 4.87			TOTAL = 1.85

TABLE XLIX – COMPARATIVE LABOR COSTS FOR WELDBONDING AND AUTOMATIC RIVETING 100 C-130 CARGO FLOORS

MANHOURS BREAKDOWN BY SQUARE FT./AIRCRAFT							
AUTOMATIC RIVETING				ROLL SPOT WELDBONDING			
FT^2/ SHIP	MH/ FT^2	TOTAL MH/SHIP	TOTAL MH (100 SHIP)	FT^2/ SHIP	MH/ FT^2	TOTAL MH/SHIP	TOTAL MH (100 SHIP)
418	.28	117	11,704	418	.105	44	4,400

6.6.5 Summary Discussion of Related Weldbond Programs Cost Analyses

The weldbond clean room has been in continuous operation as a production facility for approximately 8 months with technical support from the Manufacturing Research. As noted within the body of this report, over 34,200 square feet of structural assemblies have been fabricated by weldbonding for the General Purpose Container alone. The time estimates made herein are supported by the factual data of having produced the stated square footage on a week by week basis.

It had been estimated previously that weldbond would prove to be economical when approached with both a design and facility suitable for production weldbonding. Even so, actual efficiency of day to day results has startled the technicians and supervision familiar with the speed of the process. Daily joining of the Container hood and door at 0.11 manhours/square foot has established a record low cost for joining conventional aluminum structures.

The very low cost joining is not peculiar to the General Purpose Shelter Container as is shown in Tables XLVII and XLVIII for the C-130 trailing edge assembly and the C-130 cargo floor assembly. The cargo floor assembly time study shows a 0.12 manhour/square foot cost, indicating and excellent cross check between a time study of one unit versus actual time for several thousand square feet of container assembly. Weldbonding of both assemblies shows a cost of less than half as compared to automatic riveting. When comparing weldbonding of the C-130 trailing edges versus autoclave metal bonding a one-third reduction in manhours favors the weldbond process. Most of this manhours reduction shows up as a result of eliminating the time consuming lay-up, bagging, vacuum leak checking, loading with shot for added pressure, and thermocouple attachments associated with massive tooling and temperature problems in the autoclave.

As is the case with any new process, the initial cost, and sometimes loss associated with first run prototype operations, tend to obscure the real long term value of a process. It can be proved that any problems that may have surfaced from the Raytheon and the General Purpose Shelter cost estimating involved that of materials, mechanical joining, or items other than weldbonding. These costs must and will be recognized in any future evaluation of the process.

Initially the General Purpose Shelter Container was designed to be joined by spot-welds and/or mechanical fasteners only. As a result of a required corner drop test, buckling of the embossed corrugations was noted. A preliminary fix was established using a 12-inch long double row of rivets on each side of the hood section. This fix proved to be so time consuming that the entire side sections were redesigned and changed from welded and riveted to a weldbonded structure. The weldbonded shelter passed all drop tests without failure.

As a result of this temporary use of manual riveting an excellent cost base was established for comparing manual riveting to roll spot weldbonding. In addition to the data obtained from the manual rivet fix, additional data have been obtained from weekly rates for manual riveting the hood close-out splices. Comparative data for roll spot weldbonding versus manual riveting are shown in Table L.

Initial manhours data for this report were computed in linear feet but because density of rows and pitch of spots for the cargo floor, trailing edge, and shelter container are similar and because comparison is made to bonded structure, all tabular data are reduced to square feet.

Cost evaluation of weldbonding the General Purpose Shelter, C-130 Cargo Floor, and C-130 Trailing Edge has provided hard comparative data not only of rivet and bonding versus weldbonding but has also provided data that can be later, (if factored by learning curves and other data), reduced to time standards. No attempt to do so has been made herein.

The following items have also become evident from roll spot weldbonding on a production basis:

1. Doubling the number of spots per row has no significant effect on rate per linear foot since both wheel speed and weld cycle time can be varied independently, thus maintaining a wheel speed governed only by guidance control factors.

2. Density of weld rows and interrupted runs caused from cross members are rate limiting factors when roll spot weldbonding.

3. Up to 4500 spots are made between manual (on machine) dressing of the wheel electrodes.

4. Up to 30,000 spots are made between re-contouring (lathe dressing) of the wheels.

5. Simple contour (non-compound) structure can be roll weldbonded at a rate equal to that of flat surfaces if runs are uninterrupted and adequate positioner tooling is assumed.

TABLE L – LABOR COST COMPARISON OF ROLL SPOT WELDBONDING VERSUS MANUAL RIVETING THE GENERAL PURPOSE SHELTER CONTAINER

MANUAL RIVETING				ROLL SPOT WELDBONDING				
FT^2/ CONT.	MH/ FT^2	MH/ CONT.	MH/74 CONT.	FT^2/ CONT.	MH/ FT^2	MH/ CONT.	MH/74 CONT.	MH SAVED
456	.58	264	19,572	456	.105	.48	3,543	16,029

A further graphic breakdown of manhours and cost data is shown in Figures 108 through 113. Even though these data have not been factored by learning curves which would over a 100 or 200 ship spread show even greater superiority of the weldbond process, the graphs show distinct savings when compared to old line operations such as mechanical fastener joining and metal bonding.

Tooling and fixturing costs for production weldbonding also proved to be surprisingly economical. By designing for use of Cleco type temporary clamps and using tack welding prior to the final roll welding operation, hard tooling for both the SAM-D Shelter and the General Purpose Shelter was kept to a minimum. Only shop aid tooling and one Final Assembly Jig for each of the shelters were required. Two additional assembly jigs were required for mechanical joining of the General Purpose Shelter.

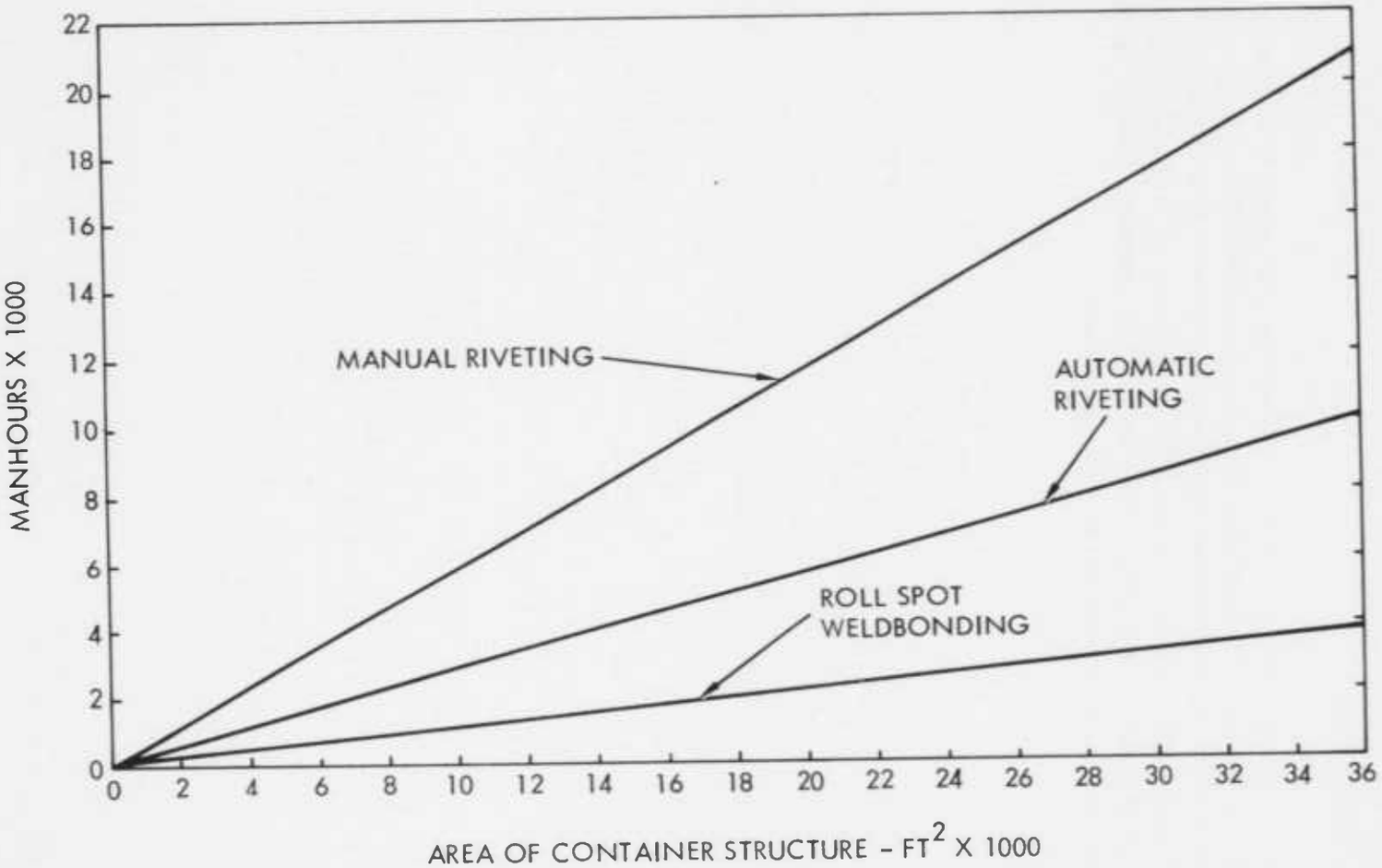

FIGURE 108 - COMPARISON OF MANHOURS/FT^2 REQUIRED FOR RIVETING VERSUS ROLL SPOT WELDBONDING - GENERAL PURPOSE SHELTER CONTAINER

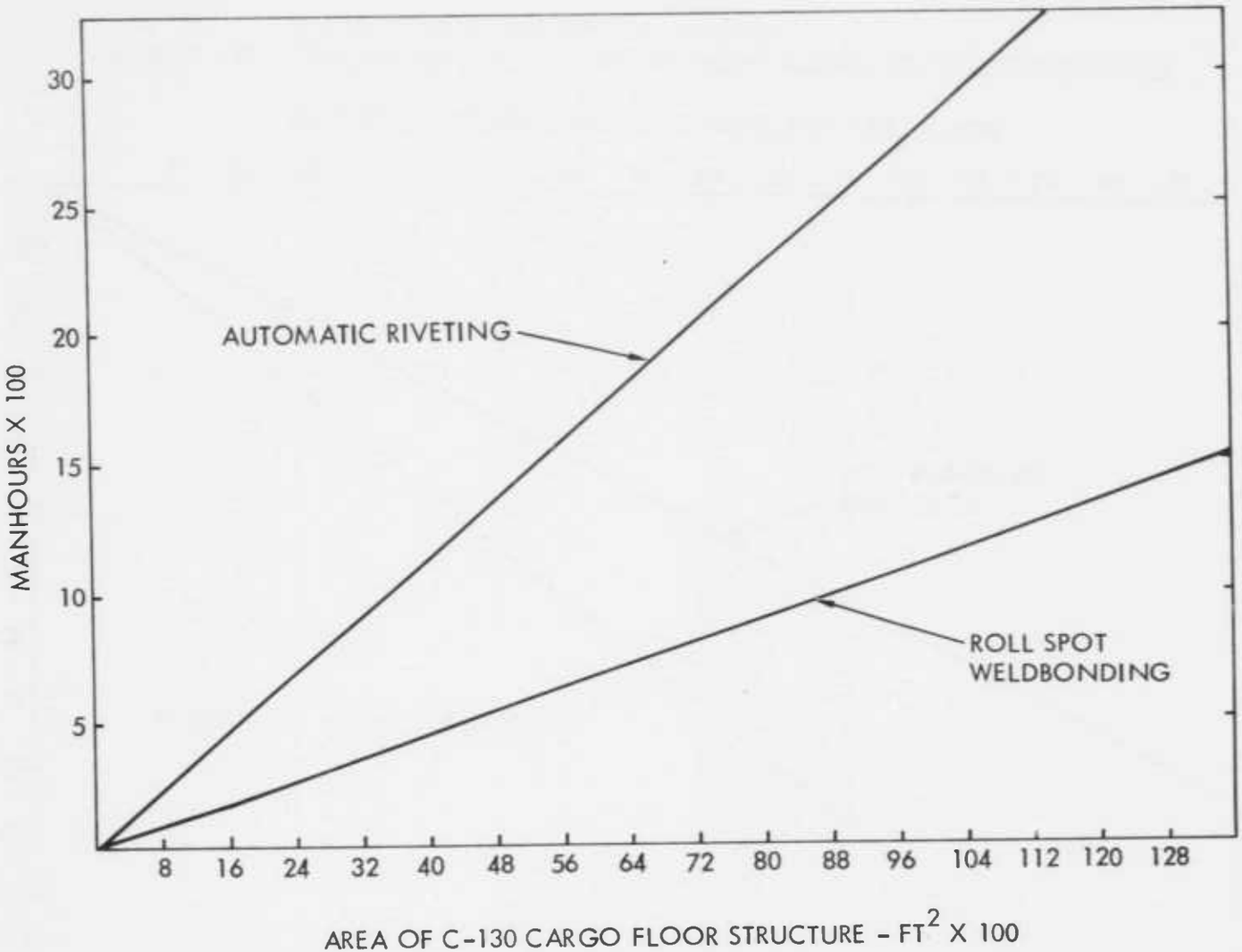

FIGURE 109 - COMPARISON OF MANHOURS/FT^2 REQUIRED FOR ROLL SPOT WELDBONDING VERSUS AUTOMATIC RIVETING THE C-130 FLOOR

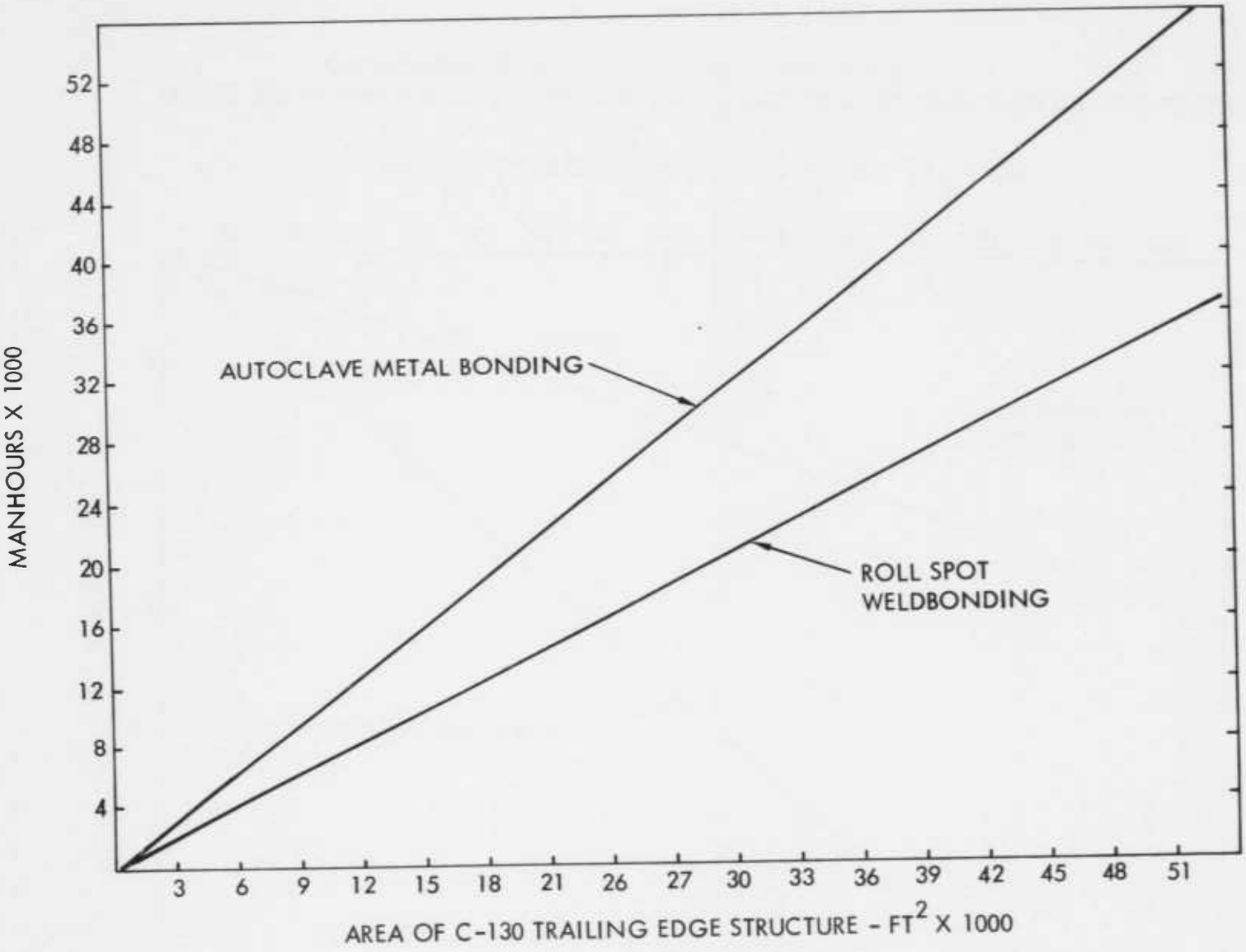

FIGURE 110 - COMPARISON OF AUTOCLAVE METAL BOND VERSUS WELDBONDING THE C-130 TRAILING EDGE ASSEMBLIES

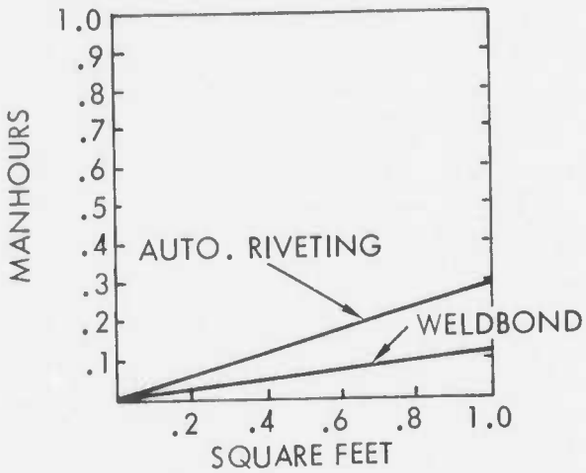

FIGURE 111 - CARGO FLOOR MH/FT^2 COMPARISON

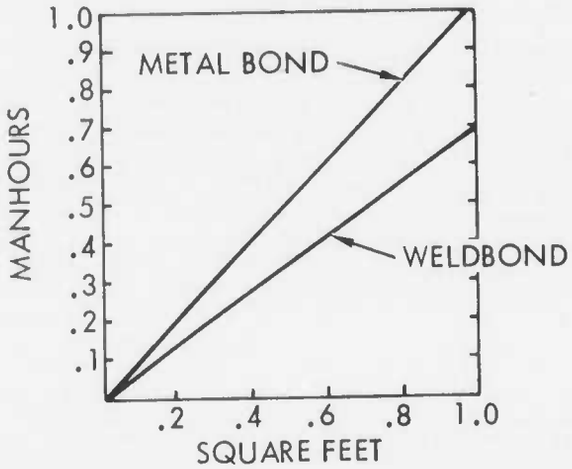

FIGURE 112 - TRAILING EDGE MH/FT^2 COMPARISON

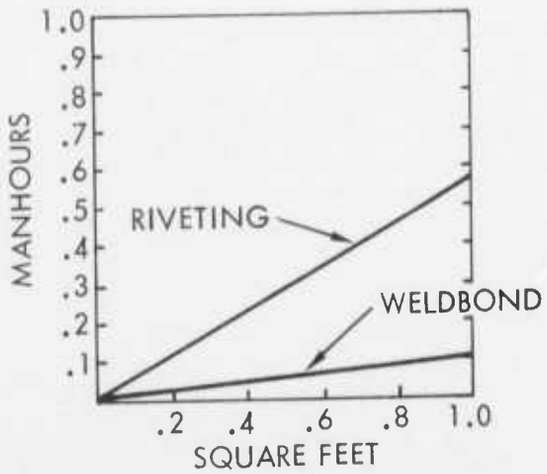

FIGURE 113 - SHELTER CONTAINER MH/FT^2 COMPARISON

SECTION VII

C-130 WELDBONDED FUSELAGE COMPONENT DESIGN

7.1 Component Selection

The rationale for selection of the subject component is based on achieving a thorough evaluation of the Weldbond process in an operational environment. Initially, an in-service C-130 aircraft fuselage was to be modified with the weldbonded component but this was later changed to a production line installation so that it could be installed on one of the two aircraft on which the experimental NASA boron reinforced center wing section is installed. In selecting the fuselage component, considerations were given to structural design limitations, finish requirements for environmental protection, sonic and mechanical fatigue endurances, and fabrication challenges.

The component selected was a left-hand side forward pressurized section of the C-130 fuselage. The length of the weldbonded fuselage component is 107 inches and extends from fuselage station 280 to 387. The height of the weldbonded fuselage is 117 inches and extends from the main cargo floor to the main fuselage upper longeron. Figure 114 shows a view of the weldbonded fuselage component installed on a C-130 airplane. The selection of the weldbonded fuselage component is considered representative of a typical structural configuration of the pressurized fuselage since it includes cutouts for windows, cargo tie-down support structure, intercostals, reinforcement doubler plates, frame to fuselage skin joints, and fuselage skin joints. Variable joint thicknesses and multi-layer joints are also included in the component.

7.2 Component Design

The selected fuselage component was designed and fabricated to utilize the weldbond process most advantageously; however, specific structural design requirements restricted complete freedom of redesign. These restrictions included fail-safe requirements, load path continuity in the ring frames, and stability of structural elements of the ring frames not affected by the joining process. The structural design philosophy employed in the design of the weldbonded fuselage component was to develop a structure whose strength capability is at least equivalent to that of the production mechanically fastened component. Also, joints were not designed to include both weldbonding and mechanical fasteners which is believed to be good design practice. Whenever possible, all joints envolving the fuselage skin were weldbonded. In several areas it was not possible to weldbond joints because of either the sequence of weldbonding operations or the inaccessibility of the spot-weld machine electrode.

The weldbonded fuselage component is a ring-stiffened structural configuration with a mechanical splice at fuselage station 337. The mechanically fastened splice was necessary because of the 39 inch throat depth limitation of the Sciaky Turret Head Spot-Welder. The

FIGURE 114 – WELDBONDED COMPONENT LOCATION ON C-130H AIRPLANE

weldbonded fuselage component has two (2) weldbonded fuselage skin splices at fuselage stations 290 and 377. The ring frame spacing dimension could not be changed from the production component since the frames had to mate with existing splice fittings at the cargo floor and the main upper fuselage longeron. Both extrusions and rolled formed rings having Z-section cross-sections were investigated for use in the weldbonded component. An extruded shape for the 0.050 inch frame was not available and an extrusion die would have had to be designed and fabricated to produce the extrusion. Such a task was not feasible from both the required lead time and costs for this development contract.

Since it was not desirous from structural considerations to have a mixed arrangment of rolled form rings and extrusions, it was decided to use only rolled formed ring frames in the weldbonded fuselage component. In order to develop the most efficient weldbonded joints as possible, the Z-section rolled formed ring frames were designed and fabricated with smaller bend radii and narrower flanges than the production ring frames. The reinforcing plate doublers around the window cutouts were weldbonded to the fuselage skin, but the windows themselves were installed with mechanical screws to accommodate removal in in-service operations as necessary.

Installation of the weldbonded fuselage component was accomplished in a longer production fuselage component (i.e., fuselage station 245 to 477) by two mechanically fastened splices. These splices at fuselage stations 280 and 387 were located between the ring frames and accomplished with a double row of rivets in each side of the splice through a splice plate. Upon completion of this installation, the component was delivered to the C-130 production line where it was installed in the aircraft exactly as a production component.

7.2.1 Component Alloy Selection

The C-130 weldbonded fuselage component was investigated relative to alloy selection during the course of design. One of the primary considerations in alloy selection was to have bare surfaces in the faying surfaces of weldbonded joints because a higher percentage of defect free spot-welds can be produced than with clad alloys. Also, bare surfaces in the weldbonded joints were desirable to provide the best surfaces for adhesive bonding. Tests have shown that strength properties of adhesive bonded joints of clad aluminum materials are degraded when the joints have been subjected to hostile environments. Another important consideration is that the exterior surfaces of pressurized fuselage skins must be clad material for satisfaction of the Air Force Handbook of Instructions for Aircraft Designers (HIAD) requirements. Thus, a clad one side only sheet material with the clad side positioned to the exterior was selected for the fuselage skin. Other important considerations in alloy selections included finish requirements for corrosion protection, fail-safe criteria, sonic and mechanical fatigue endurance, static strength, and service history of the component. Candidate materials considered for the design and fabrication of the weldbonded fuselage component were the 2000 and 7000 bare and clad series aluminum alloys. In consideration of all requirements, 2024-T3 clad one side only alloy was selected for the fuselage skin and 7075-T6 bare aluminum alloy was selected for the Z-section rolled formed ring frames. Other detail parts were fabricated of either 2000 or 7000 bare aluminum alloys depending upon design and fabrication requirements.

7.3 Finish System for the C-130 Weldbonded Fuselage Component

The finish system developed and applied to the subject weldbonded component is detailed as follows. This finish system was established from tests and consultation with both specialists from the Air Force and Lockheed.

I. Interior surfaces of the weldbonded component were finished and sealed as follows:

1. Chromic acid anodize the surfaces after weldbonding the assembly omitting the deoxidizing step in the anodize process

2. Fillet seal all weldbonded joints with STM 40-111 corrosion inhibiting sealant

3. Brush coat all sealed fillets with MIL-C-83019, clear flexible polyurethane, to prevent leaching of the chromates from the STM 40-111 sealant

4. Finish the forward section of the fuselage component, fuselage station 280 to 337, with a one mil coat of PR-1432GP inhibited primer followed by a one mil coat of MIL-C-83019 clear flexible polyurethane

5. Finish the aft section of the fuselage component, fuselage station 337 to 387, with two (2) coats of MIL-P-8585 zinc chromate primer.

Exterior surfaces of the weldbonded component were finished and sealed as follows.

1. Chromic acid anodize the surfaces coincident with anodizing the interior surfaces

2. Prime the groove in each of the fuselage skin splices with B. F. Goodrich's Plastilok 106 primer and fillet seal with STM 40-207 sealant (B. F. Goodrich's Plastilok 410)

3. Coat the exterior surfaces with Fabrifilm for protection during shop handling

4. After the aircraft is completed, remove the Fabrifilm with Fabrifilm Remover

5. Treat the surfaces with MIL-C-38334 metal conditioner and then treat with MIL-C-5541 color conversion coating

6. Apply one (1) coat of epoxy primer, MIL-P-23377

7. Finish surfaces with two (2) coats of polyurethane enamel, MIL-C-83286.

SECTION VIII

C-130 WELDBONDED FUSELAGE COMPONENT STRUCTURAL ANALYSIS

8.1 Structural Design Criteria

The C-130E airplane is a high wing, long range, cargo land plane powered by four Allison T56-A-7 prop-jet engines. These engines are equipped with Hamilton Standard 13.5 foot diameter, constant-speed, four-bladed propellers. The airplane is intended for missions including the transportation of personnel, and/or cargo, for delivery by landing or parachute as desired. The airplane is shown in a three view drawing in Figure 115.

The fuselage of the C-130E airplane was investigated for the loads impact by the wings, landing gear, empennage, power plants, and control systems in the various flight and ground handling conditions. A significant number of the design load cases were noncritical for the fuselage side panel region, fuselage station 280.0 to 387.0, the location of the weldbonded component. The critical design loads for this region were derived from fuselage inertia, air and cargo loading for various flight conditions.

A fuselage panel was defined as the fuselage structure between each pair of fuselage rings for analysis purposes. The fuselage panel loads consists of the weight assigned to each panel from the fuselage distributed weights, and included all items of fixed equipment. Panel weights did not include the mass of the wing structure outboard of the wing-fuselage juncture at B.L. 61.6, or any other similarly located items contained in or attached to the wing. The effect of these masses was brought into the buselage centerbody as net wing loads applied at the wing attach points, fuselage station 517.0 and fuselage station 597.0. The aerodynamic lift of the fuselage was included in the loads calculations. The fuselage airload distributions were applied in a rational manner.

An increase in airplane gross weight resulted in increased fuselage airloads; however, since fuselage airloads provide relief for the net fuselage loads, lower gross weight load cases were design critical. Also, for balanced maneuver load conditions, an increase in gross weight produced lower loads than lighter gross weight conditions primarily due to the airplane load factor reduction. Therefore, it was concluded that minimum fuel gross weight cases produced the highest loads for balanced maneuver conditions, and when combined with a total cargo weight of 25,000 pounds located in the region of fuselage being investigated, a total gross weight of 101,404 pounds produced the critical loading condition for the weldbonded component.

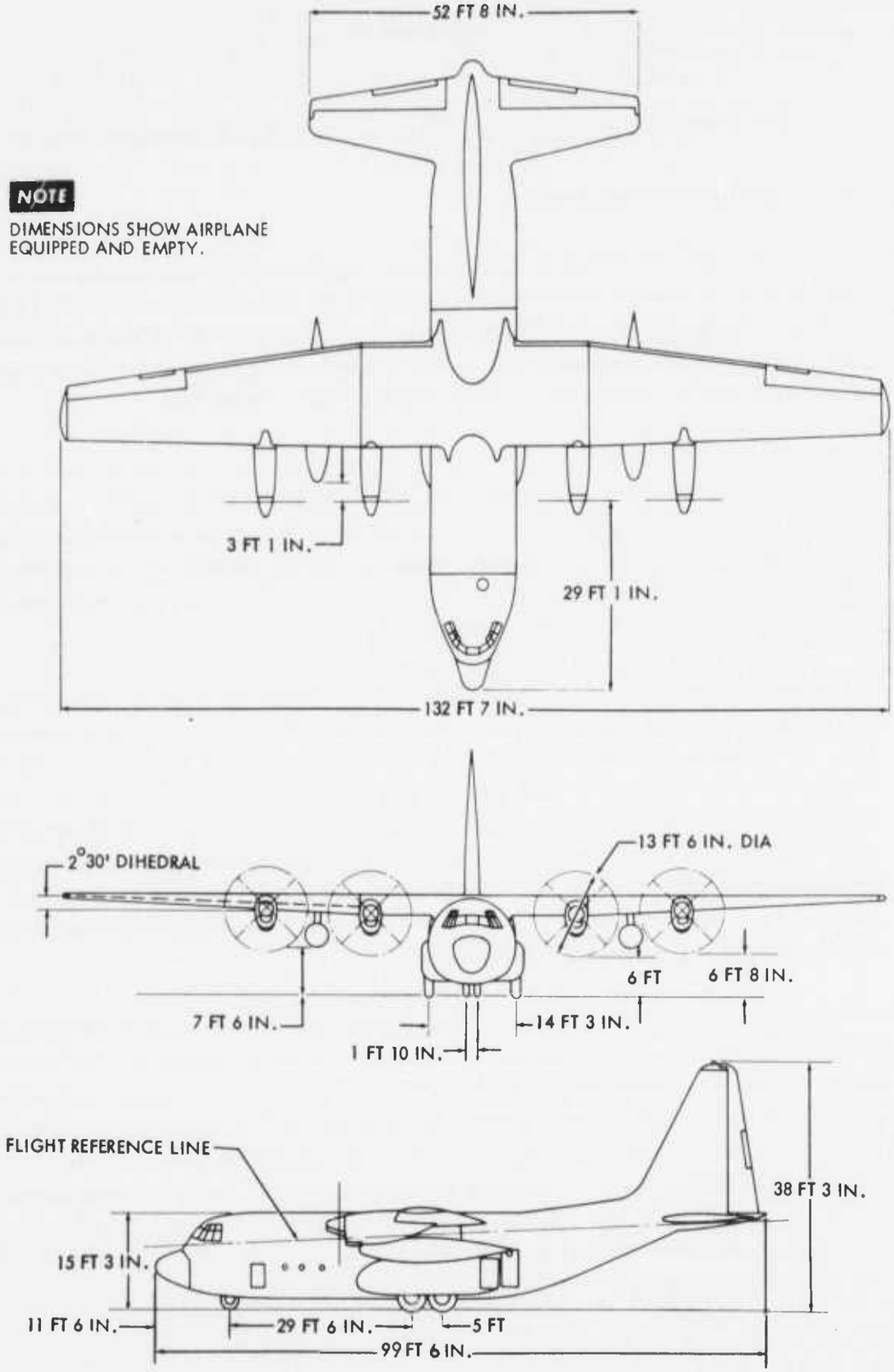

Figure 115 – THREE VIEW DRAWING, C-130E AIRPLANE

The weldbonded fuselage component is subjected to cabin pressurization loads and loads induced by the cargo loading. The cargo distribution and pressurization differentials are given in the following paragraphs.

The location of the payload in the airplane was determined by the center-of gravity range for the particular gross weight under consideration. The distribution of the load in the cargo compartment was in accordance with the maximum allowable load per foot and per axle as shown in Figure 116. Cargo to be air dropped are limited to a running load of 2400 pounds per foot. For design purposes, adjacent cargo loads were located at least 60 inches from axle loads heavier than 6000 pounds, or at least 36 inches from axle loads of 6000 pounds or less. Axle loads up to and including 13,000 pounds were considered for structural design. The cargo was considered loaded symmetrically with respect to the fuselage centerline. At each fuselage station in the cargo compartment, the strength of the floor is symmetrical with respect to the airplane centerline.

The pressurized portion of the aircraft was designed for a maximum pressure differential of 7.5 psi. Thereafter, the differential pressure is maintained at 7.5 psi to 35,000 feet. A graphic representation is given in Figure 117. All parts of the airplane that are subjected to both pressure differential and flight loads were designed for the maximum stress resulting from the combinations of stresses from any critical limit flight condition with those from any applicable limit differential pressure ranging from 0 to 7.5 psi, whichever was critical. All parts of the airplane affected principally by pressure differential were designed for a limit pressure differential of +10 psi, ignoring all other loads. Loads resulting from landing and pressurization were not combined.

Fuselage design shear and bending moments were computed for the critical load condition for the region of the fuselage in which the weldbonded component is located. As previously stated, the critical load condition was a balanced maneuver condition for an airplane gross weight of 101,404 pounds and a limit load factor of 3.0g's. The critical load condition was composed of combined fuselage air loads, fuselage shell inertia loads, and cargo axle loads. Unit inertia loads, shears and bending moments, were calculated for a unit translational load factor. The calculated weight change of the airplane considering the weldbonded component installed in lieu of the production component was negligible. Thus, the unit inertia loads used in the calculation of the combined loads for the critical load condition were not changed from that of the production airplane fuselage. The development of the design loads for the critical load condition is given in Table LI.

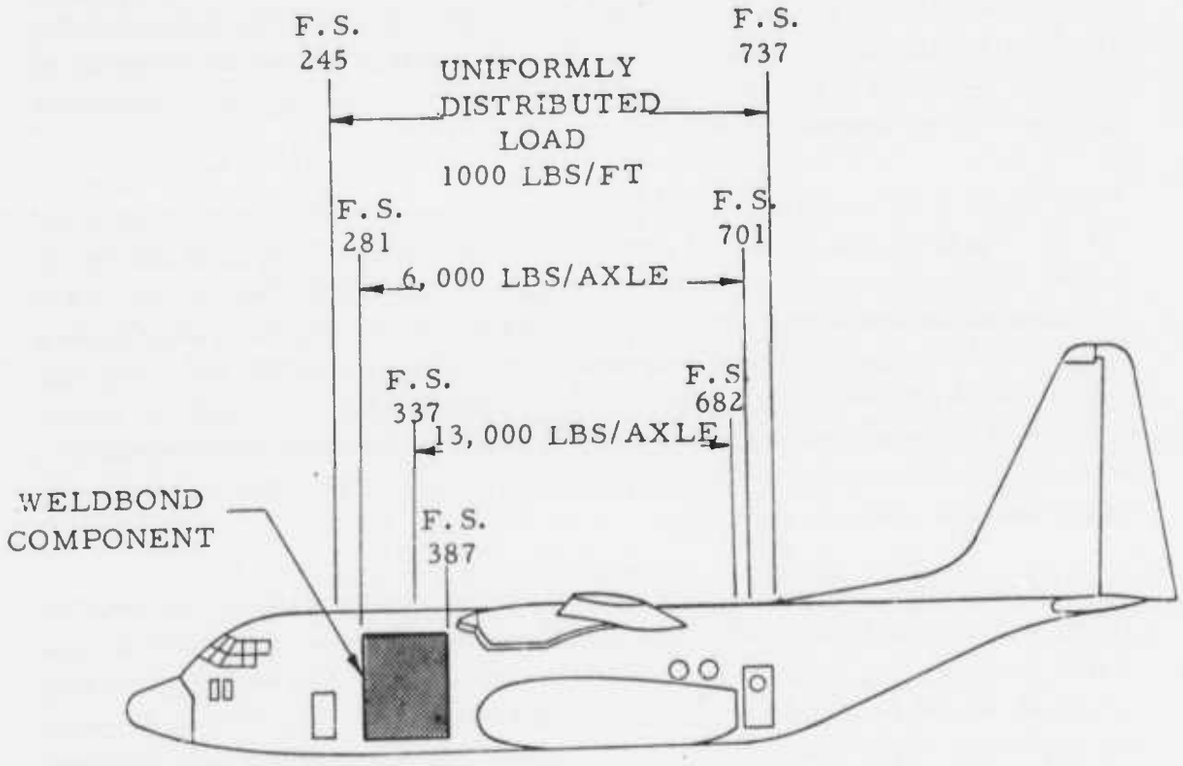

FIGURE 116 – PAYLOAD DISTRIBUTION FOR FORWARD FUSELAGE SHELL DESIGN LOADS

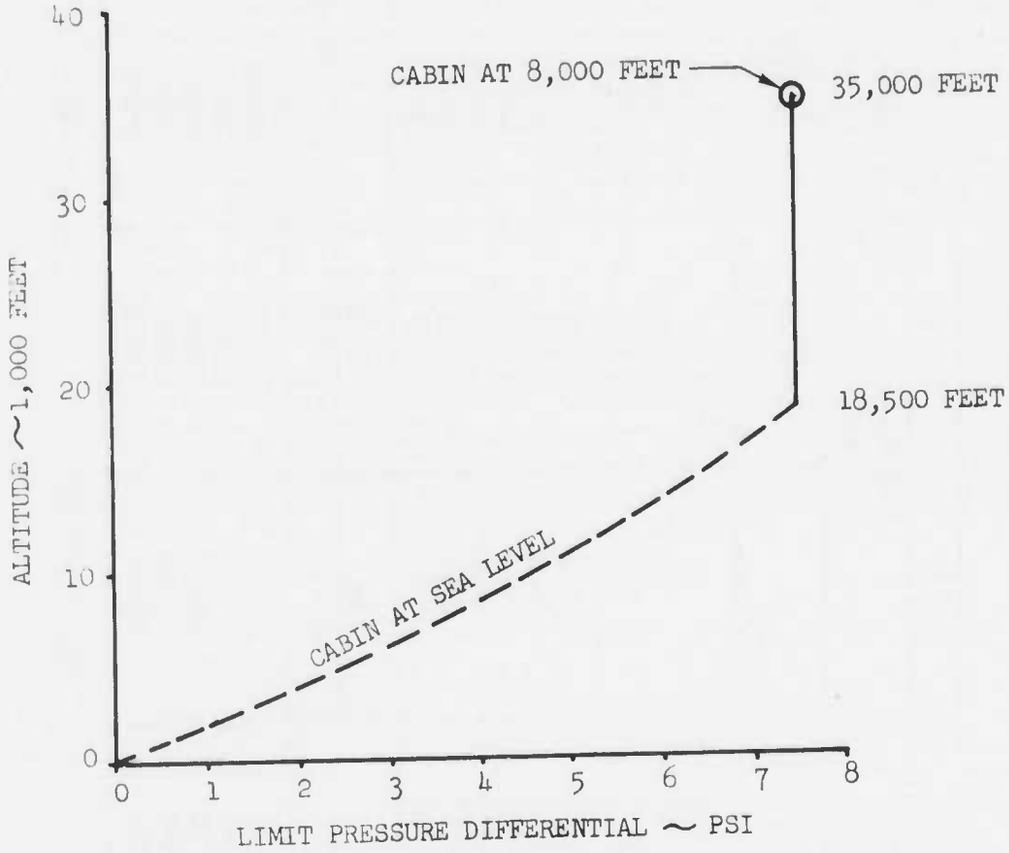

FIGURE 117 – C-130E FUSELAGE CABIN INTERNAL PRESSURE DIFFERENTIAL

TABLE LI – NET FUSELAGE FOREBODY LIMIT LOADS

1	2	3	6	7	S_z (LBS.)	$10^{-6}M_y$ (IN-LBS)
FUS. STA.	Unit Inertia Data for Fuselage Shell		Fuselage Air Loads		-3.0 (2) +1.0 (6)	-3.0 (3) +1.0 (7)
	S_z/n_z	$10^{-6}M_y/n_z$	S_z	$10^{-6}M_y$		
61	- 143	- .0032	0	0	429	.0096
125	- 1170	- .0391	- 201	- .006	3309	.1113
171	- 4204	- .1627	- 593	- .025	12019	.4631
200	- 6214	- .3138	- 899	- .046	17743	.8954
245	- 9119	- .6587	- 1343	- .097	26014	1.8764
300	-11134	-1.2157	- 1836	- .184	31566	3.4631
337	-12184	-1.6471	- 2137	- .258	34415	4.6833
400	-13751	-2.46 0	- 2593	- .407	38660	6.9850
457	-15424	-3.2955	- 9283	- .745	36989	9.1415
517	-18037	-4.2994	-20441	-1.637	33670	11.2612
Unit Inertia Data for Cargo Axle Loads			S_z -3.0 (2)	$10^{-6}M_y$ -3.0 (3)	Combined Loads	
300	- 6000	- .114	18010	.342	49566	3.8051
337	-12000	- .456	36000	1.368	70415	6.0513
400	-12000	-1.212	36000	3.636	74660	10.6210
457	-12000	-1.896	36000	5.688	72989	14.8295
517	-12000	-2.616	36000	7.848	69670	19.1092

Gross Weight = 101,404 Lbs.
Airplane C.G. = 16.5% MAC

V_e = 270 KEAS

n_z = 3.0g

8.2 Calculation of Fuselage Component Internal Loads

The weldbond joining technique used in assembly of the fuselage component did not affect the bending stiffness or the bending strength capability of the overall fuselage. Thus, only the design shear flows in the fuselage skin were required to be calculated. When fore-aft tension or compression loads are required in the analysis they are obtained by ratioing calculated bending loads from previous critical load conditions. The fuselage skin shear flows were derived from fuselage shell shear loads (inertia and air), cargo loading and pressure effects. The method used to calculate the applied shear flows for the weldbonded component was comparable to the method applied in calculating those shear flows used in the design of the C-130A airplane fuselage. The net applied shear flow, q, for the C-130A consisted of 1) q_o shear flow due to fuselage shell inertia and air loads, 2) q_p, shear flow due to the 11.25 lbs./in.^{2} cabin pressure, and 3) q_c, shear flow due to cargo loading. Since the shear flow due to the cabin pressure is relieving, it was neglected.

The fuselage shell shear flows due to fuselage inertia and air loads, q_o, were calculated for the C-130A airplane using a unit beam type solution of the applied external loads modified to correct for the forward cargo door cutout. The forward cargo door was deleted from the C-130E airplane; therefore, q_o were calculated in the following manner. It is conservatively assumed that all vertical shear loads, S_Z, were reacted by the fuselage side components between the upper and lower B.L. 61.6 longerons as shown in Figure 118. The q_o shear flow at a given fuselage station was calculated using the equation shown on Figure 118 and the shear flows are plotted in Figure 119 as the curve designated q_o.

The calculation of q_c, the shear due to cargo loads, was accomplished using the allowable cargo load distribution in the weldbonded component region as shown in Figure 116. It was noted that the distance between concentrated loads (i.e., vehicles with pneumatic tires) above 6000 pounds was limited to a minimum span of 60 inches (Reference 6). From previous analysis of various combinations of concentrated loads in the region of the weldbonded component, the critical condition was determined to be a 6000 pound concentrated load at fuselage station 821.0 and a 13000 pound load at fuselage station 337.0. For ease of calculations, it was conservatively assumed that the applied load at fuselage station 281.0 acts at the fuselage frame station 277.0.

Next in sequence, a concentrated vehicle wheel load applied at any cargo floor support bulkhead was considered. Since the footprint area of the tire under load extended approximately 10 inches on each side of the bulkhead station, the adjacent bulkheads reacted a portion of the wheel load. In previous the analysis, it was established that 78.2 percent of the total wheel load was reacted at the bulkhead where the load was applied and 10.9 percent was reacted at each adjacent bulkhead.

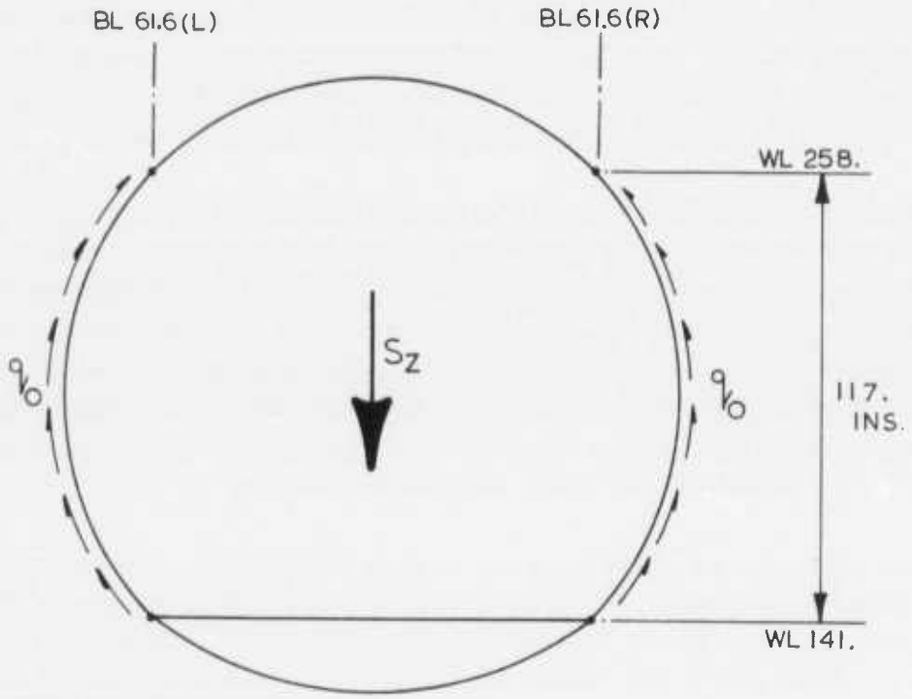

$$q_o = \frac{S_Z}{2 \times 117} \quad \text{LBS./IN.}$$

FIGURE 118 – FUSELAGE SHELL SHEAR FLOWS DUE TO FUSELAGE INERTIA AND AIR LOADS

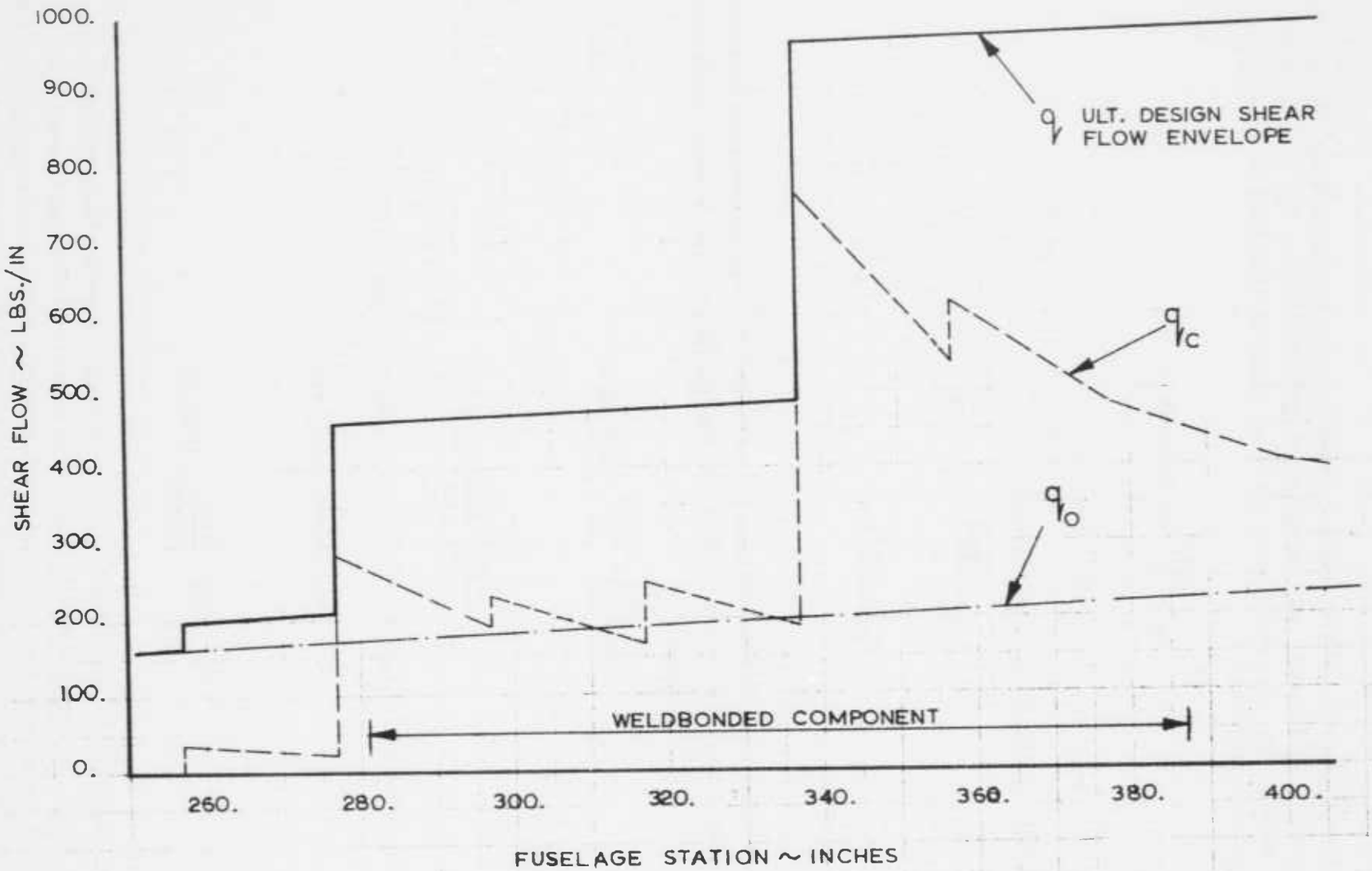

FIGURE 119 – ULTIMATE DESIGN SHEAR FLOWS IN FUSELAGE SKIN

The axle load of 13000 pounds was divided between two wheels and, according to cargo loading requirements, was symmetrically positioned about the airplane centerline. Therefore, the total wheel load using a load factor of 4.5g's (ult.) at the applied cargo bulkhead station was,

$$P_d = \frac{13000}{2} \times 4.5 \times 0.782$$

$$P_d = 22874 \text{ lbs.}$$

and the load at each adjacent bulkhead was

$$P_{adj} = \frac{13000}{2} \times 4.5 \times 0.109$$

$$P_{adj} = 3188 \text{ lbs.}$$

The above loads were assumed to be transferred from the cargo bulkheads into the fuselage frames which were in turn sheared into the fuselage skin over a length of 40 inches beginning at the cargo floor.

$$q_d = \frac{P_d}{40} = \frac{22874}{40} = 572 \text{ lbs./in.}$$

and

$$q_{adj} = \frac{P_{adj}}{40} = \frac{3188}{40} = 80 \text{ lbs./in.}$$

For the 6000 pound axle load, the fuselage skin shear flow was

$$q_d = 572 \times \frac{6000}{13000} = 264 \text{ lbs./in.}$$

and

$$q_{adj} = 80 \times \frac{6000}{13000} = 37 \text{ lbs./in.}$$

In computing a shear flow in the fuselage skin at a location other than the wheel location, it was assumed that the effective height of the fuselage skin reacting the wheel load increased aft toward the fuselage-wing intersection at an angle of 45^o. The shear lag angle of 45^o was slightly conservative. The shear flow in the fuselage skin at the point of load application was reacted over a height of 40 inches as previously stated. Thus, the shear flow in the fuselage skin at a distance "X" inches aft of the point of wheel load application is given by:

$$q_x = \frac{(40)\ (q_a)}{40 + X \tan 45^o}$$

where

q_a = shear flow at the shear force location - lbs./in.

and

X = distance aft of applied shear force - in.

The denominator of the above relation was limited to a value equal to the distance between the upper and lower B.L. 61.6 longerons of 117.0 inches. Table LII was prepared for calculating the composite shear flow curve for the critical load condition of a 6000 pound concentrated load at fuselage station 277.0 and a 13000 pound concentrated load at fuselage station 337.0.

The fuselage skin shear flows, q_c and q_o, are plotted in Figure 119 and added together to obtain the ultimate design shear flow envelope. As the peak shear flows resulting from the 6000 pound and 13000 pound axle loads can occur at any fuselage station aft of those shown, the design envelope is drawn for the most critical condition.

TABLE LII – CALCULATION OF TOTAL SHEAR FLOWS DUE TO CARGO LOADINGS, q_c

FUS. STA.	SHEAR FLOW DUE TO 6000 LBS. AT FS 277 (LBS./IN.)			SHEAR FLOW DUE TO 13000 LBS. AT FS 337 (LBS./IN.)			TOTAL SHEAR FLOW DUE TO CARGO LOADING (LBS./IN.)
257	37						37
277	25	264					25/289
297	19	176	37				195/232
317	15	130	25	80			170/250
337	13	106	19	53	572		191/763
357	13	90	15	40	381	80	539/619
377	13	90	13	32	286	53	487
397	13	90	13	27	229	40	412
417	13	90	13	27	196	32	371

8.3 Stress Analysis of the Weldbonded Fuselage Component

A detailed stress analysis of the C-130 weldbonded fuselage component was accomplished using the internal loads calculated in the previous sub-section and with the aid of the computer program developed for ring-stiffened fuselage structure which was furnished to the Air Force Project Managers. The major structural differences was emphasized in the analysis between the weldbonded fuselage component and the production mechanically fastened component. The computer program utilizes four subroutines for analyzing a ring-stiffened section of a curved fuselage structure and the fuselage skin shear panel associated with the ring-stiffened section. Input data to the computer program include the material designations, applied loads, and geometrical data of the section of structure being analyzed. A sketch of the weldbonded fuselage panel is shown in Figure 120 which depicts the locations that was analyzed. Figure 121 shows the geometrical data and applied loads required for input into the computer program. If there is no reinforcing angle or doubler in the ring-stiffened section being analyzed, the data associated with these structural elements were input as zero. For ease of reference the combination of the ring-stiffened section and associated fuselage skin shear panel was referred to as a shear panel. The two forward ring-stiffened sections are located at fuselage stations (F.S.) 290.0 and 330.0 at which the rolled Z-section ring-frame thickness is 0.050 inches. The aft ring-stiffened sections are located at F.S. 364.0 where the ring-frame thickness is 0.063 inches and F.S. 377.0 where the ring-frame thickness is 0.071 inches. One of the ring-stiffened locations in the forward half of the weldbonded component contains a circumferential weldbonded splice joint in the fuselage skin as well as one in the aft half of the weldbonded component. Each shear panel is analyzed with the aid of the aforementioned computer program using the geometries given in Figures 122 through 125 and applied loads from Figure 119. For clarity and sake of brevity, the detailed operations of 500 lines in the computer program are omitted.

The margins of safety were calculated for each of the shear panels considering stress distributions resulting from ultimate loads. A summary of margins of safety is given in Table LIII for all modes of failure considered in the computer program. However is is noted that all of the modes of failure are not applicable for the C-130H weldbonded fuselage component. The modes of failure included in the computer program are listed as follows:

1. Tensile rupture of free ring flange

2. Tensile rupture of fuselage skin, doubler, or angle

3. Yielding of the fuselage skin

4. Yielding of the doubler, angle, or attached flange

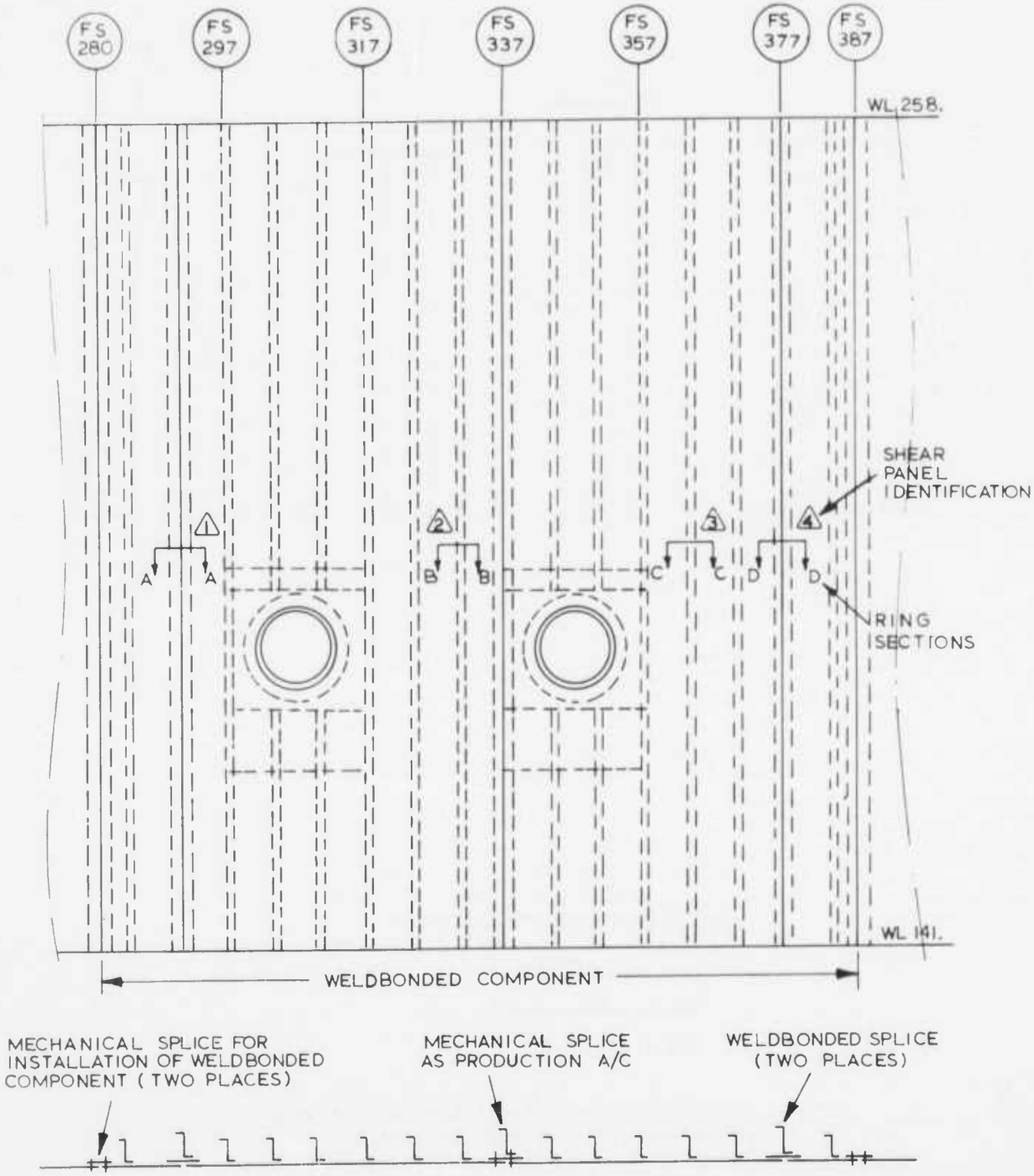

FIGURE 120– C-130E WELDBONDED FUSELAGE COMPONENT STRUCTURAL ARRANGEMENT

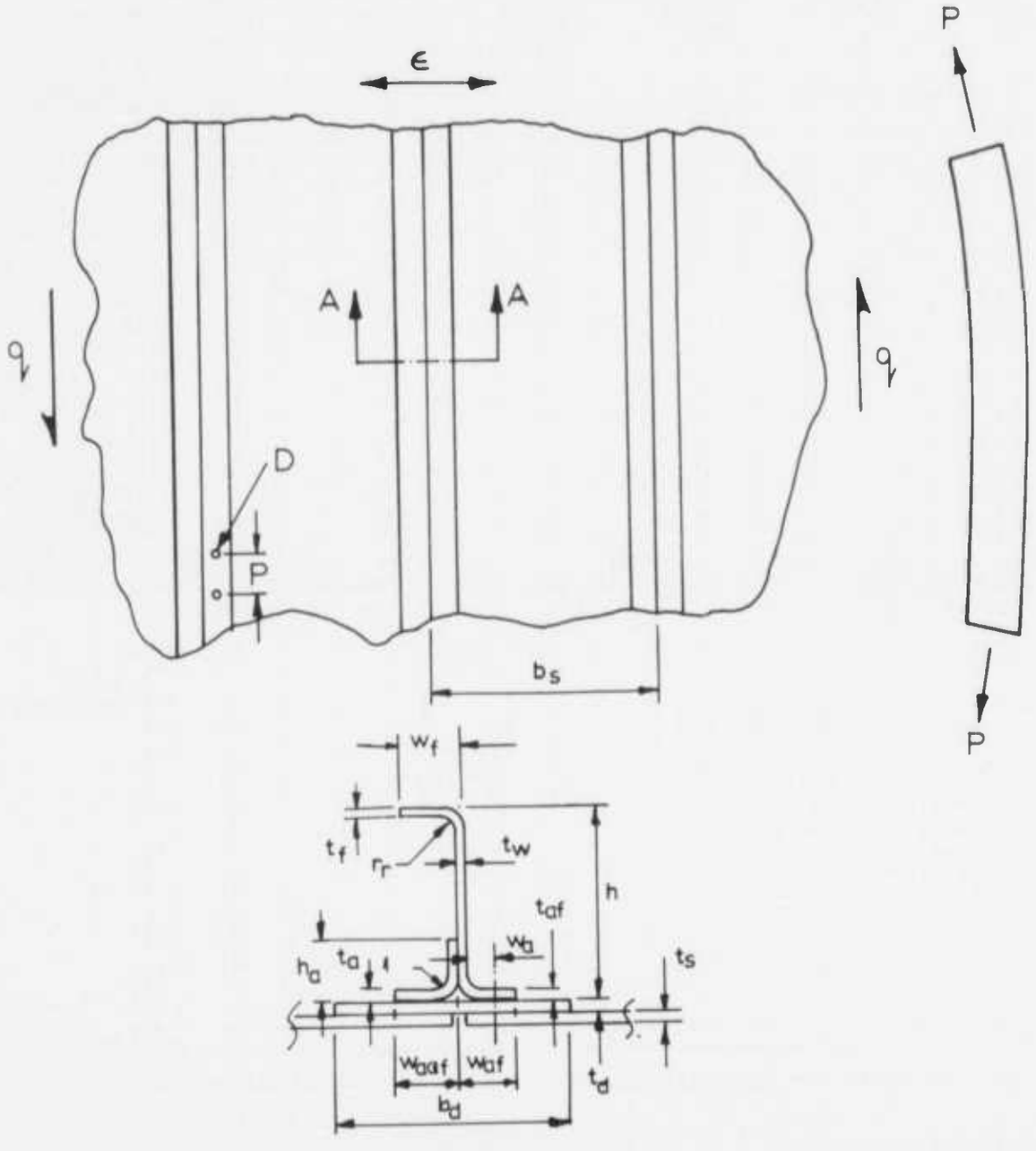

SECTION A-A

NOTE: Alternate attachments are rivets or weldbond. Angle and splice plate are optional.

FIGURE 121 – SECTION DATA FOR INPUT INTO COMPUTER PROGRAM

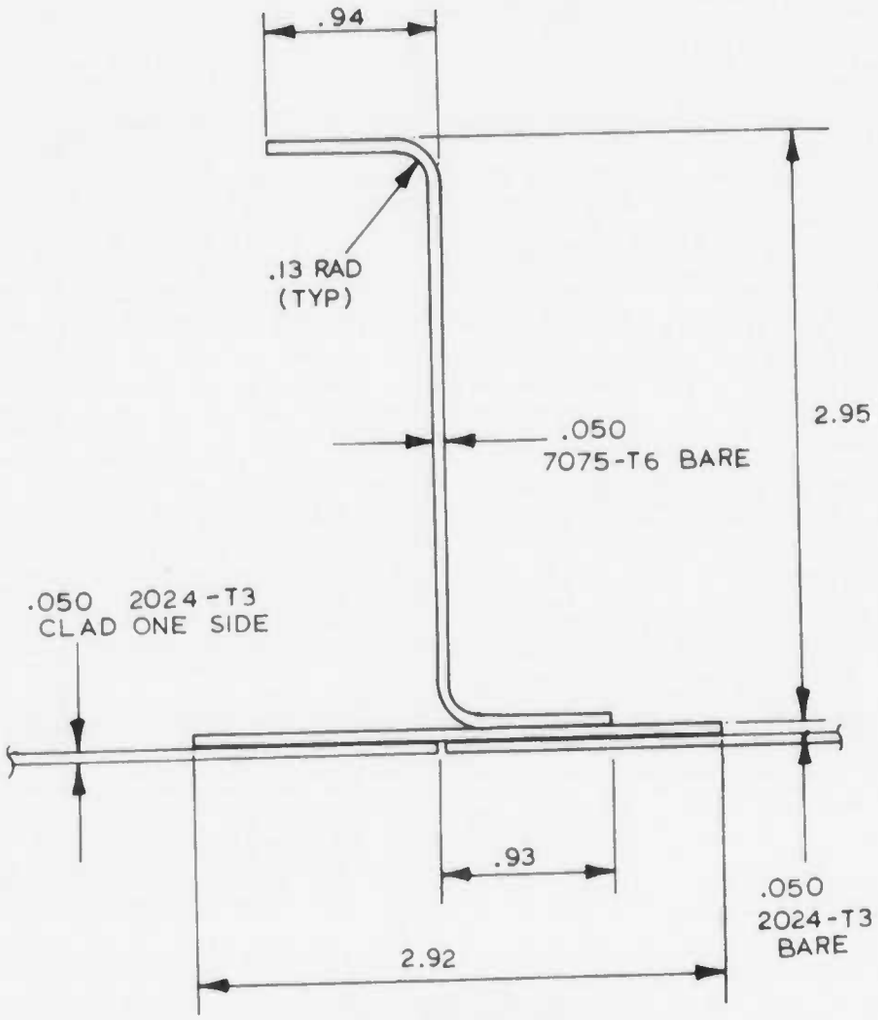

SECTION A-A (Ref. Fig. 120)

Shear panel (1) mid-bay location at F.S. 294.0

Panel width = 6.67 in. (Ring pitch)

Applied Loads:

Shear flow, q = 470 lbs/in. (Ref. Fig. 119)

Longitudinal Strain, ϵ = .001023 in./in.

Ring load, P = 6378 lbs. (Ref. page 223)

FIGURE 122 – SECTION DATA FOR COMPUTER PROGRAM INPUT FOR PANEL NO. 1

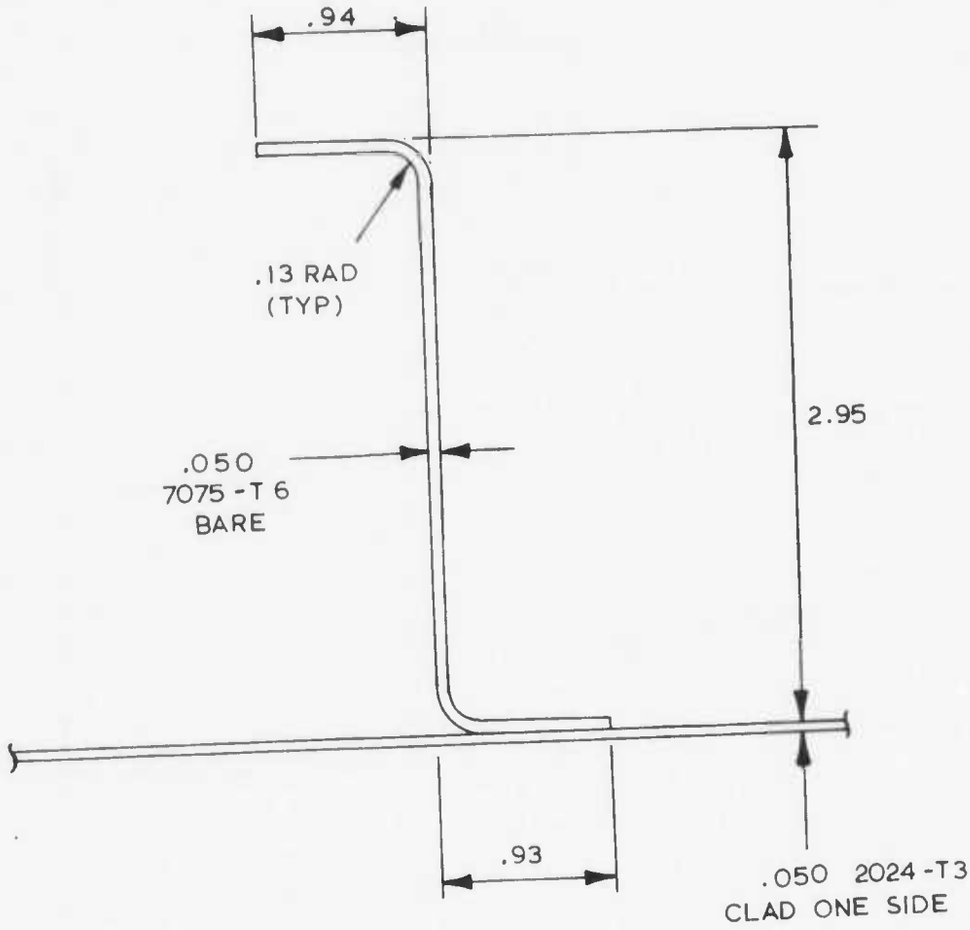

SECTION B-B (Ref. Fig. 120)

Shear panel (2) mid bay location at F.S. 327.0

Panel width = 6.67 in. (Ring Pitch)

Applied Loads:

Shear flow, q = 484 lbs/in. (Ref. Fig. 119)

Longitudinal Strain, ϵ = .001153 in/in.

Ring load, P = 6378 lbs. (Ref. page 223)

FIGURE 123 – SECTION DATA FOR COMPUTER PROGRAM INPUT FOR PANEL NO. 2

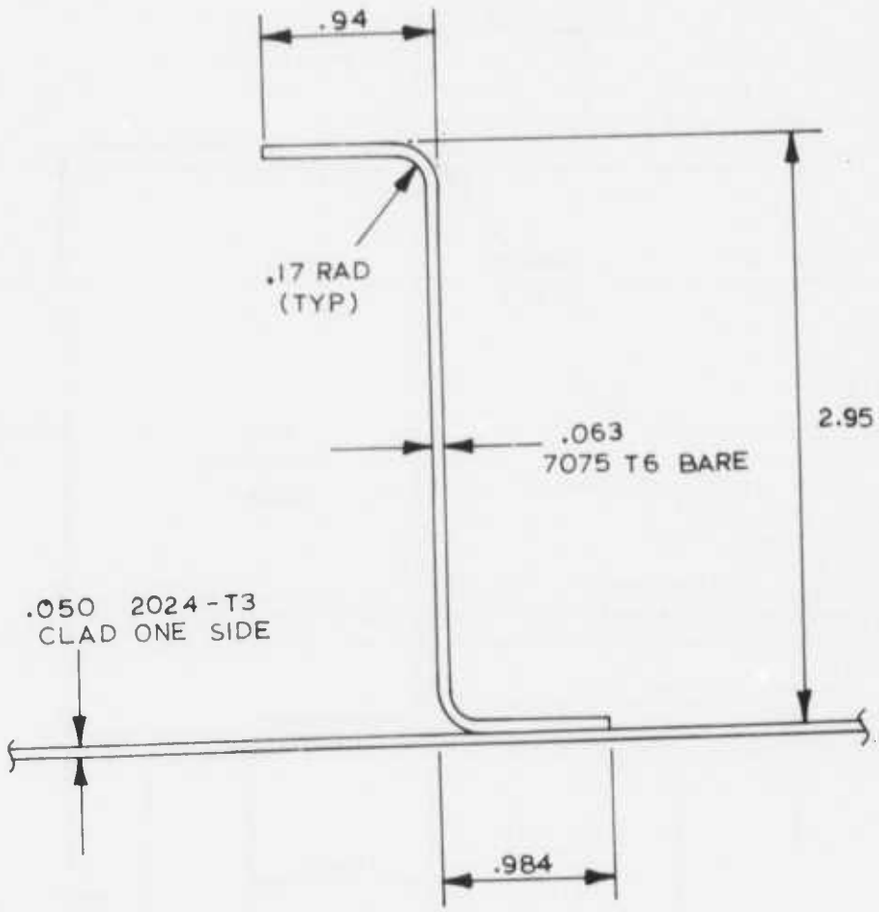

SECTION C-C (Ref. Fig. 120)

Shear panel (3) mid bay location at F.S. 367.0

Panel width = 6.67 in. (Ring Pitch)

Applied Loads:

Shear flow, q = 975 lbs/in. (Ref. Fig. 119)

Longitudinal Strain, ϵ = .0013 in/in.

Ring load, P = 6378 lbs. (Ref. page 223)

FIGURE 124 – SECTION DATA FOR COMPUTER PROGRAM INPUT FOR PANEL NO. 3

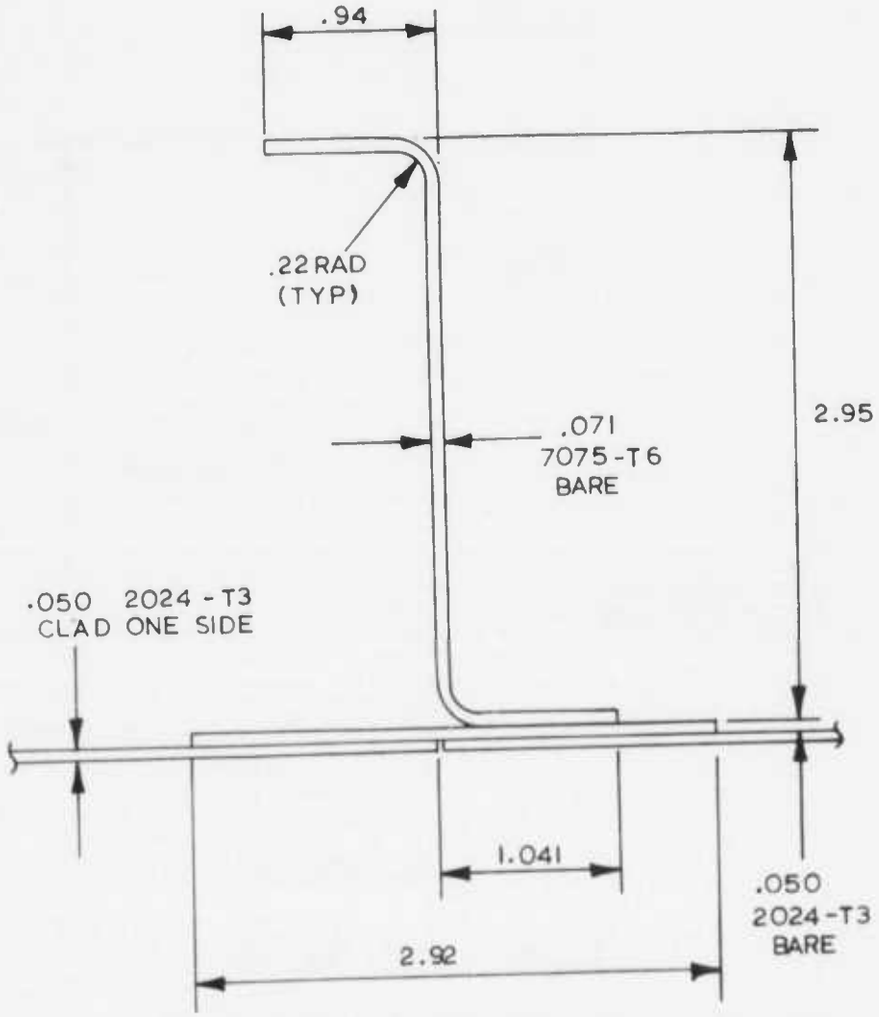

SECTION D-D (Ref. Fig. 120)

Shear panel (4) mid bay location F.S. 380.0

Panel width = 6.67 in. (Ring width)

Applied Loads:

Shear flow, q = 980 lbs/in. (Ref. Fig. 119)

Longitudinal Strain, ϵ = .0013 in/in.

Ring load, P = 6378 lbs. (Ref. page 223)

FIGURE 125 – SECTION DATA FOR COMPUTER PROGRAM INPUT FOR PANEL NO. 4

TABLE LIII – SUMMARY OF MARGINS OF SAFETY FOR THE C-130 WELDBONDED FUSELAGE COMPONENT

Failure Mode	Shear Panel No. 1	Shear Panel No. 2	Shear Panel No. 3	Shear Panel No. 4
1	7.881	6.051	6.613	8.671
2	8.371	7.025	8.450	10.808
3	.868	.740	.040	.043
4	***	***	***	***
5	11.078	***	***	4.574
6	2.831	2.727	.848	.838
7	***	***	***	***
8	***	***	***	***
9	***	***	***	***

NOTES: 1. The modes of failure are defined elsewhere in this subsection of the report.

2. Example of margin of safety: .040 indicates a positive 4 percent.

3. *** indicates that the margin of safety is not critical or not applicable for the C-130H weldbonded fuselage component.

5. Shear failure of weldbonded joint

6. Shear failure of fuselage skin, doubler, ring, or angle along weldbond joining media

7. Collapse of ring web

8. Crippling of free ring flange

9. Forced crippling.

Calculation of the margins of safety was based on the usual expression, F/f-1. However, as some peculiarities of some computations exist, an explanation is necessary. In cases where the analysis was not applicable, a row of asterisks was the program output. For example, this occurred if the tensile rupture of the free ring flange was considered as the failure mode and the flange was subjected to a compression loading.

The ultimate strength of the fuselage component was limited by the yielding in failure modes 3 and 4. The compressive yielding of the doubler angle or skin-attached flange led to crippling failure of riveted components. In the case of the weldbonded component, the failure expected shortly after yielding was disbonding which led to crippling of the resultant spot-welded only region with a sharp, but limited, load reduction and slow collapse. Yielding of the fuselage skin in mode 3 above meant that the Ramberg-Osgood yeild stress was reached in the skin mid-plane at a crucial location, the edge of the plate opposite the buckle crest. Yeilding in this region was used as a criterion for the failure of plates loaded in compression. However, the extension of this failure mode to shear requires an explanation. In the case of the "picture frame" shear stability tests, the skin did not fail at the yield stress. In that test considerable elongation occurred before the skin ruptures. When using the rigid test frame, the ultimate load was independent of whether or not the stiffener remained attached to the skin. However, in fuselage shells, the stability of the fuselage as a whole is dependent upon the stiffness of the skin. At that level of yielding, the stiffness reduced significantly. Also, the forced crippling analysis was based on an elastic buckled skin. Hence, the collapse of the fuselage shell followed yielding of the skin with forced crippling of the ring framed occurring before or during collapse.

In addition to the shear flows given in Table LII, both longitudinal strain at each of the four fuselage stations and a ring-fuselage skin panel axial load were required for input into the computer program. The applied loads are shown in the lower portion of Figures 122 through 125.

The longitudinal strains used in the weldbond computer program were obtained in the following manner for each of the four locations analyzed. A stress level at each location was obtained from a unit beam solution for a balanced maneuver case for the C-130E airplane

(Ref. 7, Appendix C, Case 4). The internal stress levels selected are for a load factor, n_z, of 2.5 (limit) at applicable stations for use in the analysis of the four shear panels. Since a balanced maneuver condition with an n_z equal to 3.0 was critical, the resulting strains calculated from the selected stress levels for a load factor of 2.5 were ratioed by a factor of 1.2.

The ring-frame axial load was assumed to be equal to the hoop tension load in the fuselage skin due to cabin pressure. For analysis purposes, the ringframe axial load was assumed to be distributed over the ring-frame-skin combination, i.e., the cross-section of the shear panel being analyzed. The ring-frame-skin axial load was computed as follows:

$$\text{Ring-frame-skin Load} = \left(\frac{PR}{t}\right) \times (d \times t) \times 1.5$$

$$= p \times R \times d \times 1.5$$

$$= 7.5 \times 85.0 \times 6.67 \times 1.5$$

$$= 6378 \text{ lbs.}$$

where p = Nominal operating pressure - psi

R = Fuselage radius - in.

d = Ring-frame pitch - in.

The above computed ring-frame-skin load was constant for all four fuselage locations.

8.4 Fatigue Analysis of the C-130 Weldbonded Fuselage Component

Fatigue analyses were performed on the fuselage circumferential splice at fuselage station 377.0 and the longitudinal splice at fuselage station 477.0. It is noted that longitudinal splices are not included within the boundaries of the weldbonded component, i.e., fuselage station 280.0 to 387.0; therefore, fuselage station 477.0 was selected for determination of fatigue endurance in the hoop direction. This selection was made because stress/loads data were known at this location and were higher in magnitude which led to conservative results. The fatigue damage as calculated in both analyses is dependent upon quality level, K_t, and the analyses were performed for a range of K_t's in order to bracket the K_t levels for the circumferential and longitudinal splice joints.

8.4.1 Fatigue Analysis of the Circumferential Splice at Fuselage Station 337.0

The circumferential splice at fuselage station 337.0 is approximately located at the mid-point of the weldbonded component in the fore and aft direction. The stresses contributing the major portion of fatigue damage to the circumferential splice are in the fore and aft direction. Since the fore and aft direction stresses were significantly lower than stresses in the hoop direction, the fatigue damage in the circumferential splice was less than in the longitudinal splices.

The fatigue analysis performed on the circumferential splice used the Damage Analysis in Rapid Time (DART) computer program. The DART Computer program has been used for analytically assessing fatigue damage in C-130 structural assemblies for several years. In subsequent paragraphs, the DART computer program is described in detail and results obtained from the analysis of the splice joint at fuselage station 337 were documented. Reference 8 provides a permanent record of the DART computer program and a detailed set of instructions for its use. The DART computer program was developed to perform fatigue analyses both rapidly and efficiently. The basic input ot the program consisted of various structural and operational parameters, and the program output were of fatigue damages at the selected locations on the aircraft structure. The analysis was accomplished by a series of internal program sub-routines which utilized stored and semi-permanent data tapes to describe environmental data, calculated internal loads, converted the internal loads to stresses, and computed fatigue damage using the calculated stresses and stored stress-cycle to failure (S-N) data. The following discussion outlines some of the capabilities and options of the DART program.

The basic unit or input to the computer program for calculations was the mission segment. A mission segment was a period of time during which operational parameters (altitude, velocity, runway roughness, cargo weight, and fuel weight) of the airplane were considered constant. As the name implies, mission segments were grouped to form missions. A mission consisted of any sequence of ground and flight segments, and there were no restrictions on the number of flight and taxis represented by a single mission. Each mission

segment was assigned by the user to a source, an arbitrary classification provided for the convenience of the user. One use of sources has been to assign mission segments to various typical aircraft operations such as climb, cruise, descent, etc.

In the DART program, calculations were performed for fatigue damage by mission and source. In order to explain the program printouts, the following notation was used.

D_{ij} = damage resulting from the i^{th} mission segment of the j^{th} mission

E_{ij} = 1 if the i^{th} mission segment of the j^{th} mission belongs to the k^{th} source

= 0 otherwise

U_j = utilization of the j^{th} mission

The computer performed the following calculations

1. Mission segment damage = D_{ij}
2. Mission damage, $m_j = \sum D_{ij}$
3. Total damage attributable to each mission, $M_j = U_j m_j = U_j \cdot \sum_i D_{ij}$
4. Total damage attributable to the k^{th} source, $S_k = \sum_j (U_j \cdot \sum_i D_{ij} \cdot E_{ijk})$

The DART program analysis was performed on the average Air Force usage, i.e., the nine mission profile. Table LIV describes the nine mission profiles and the utilizations for the average Air Force operational usage for the C-130 airplane. Mission utilization depends upon the user command as well as the base to which the aircraft is assigned.

Damage sources must also be known and assigned a code number in order to perform the fatigue analysis. Mission damage was compiled from the eight damage sources as illustrated in Table LV.

TABLE LIV – C-130 MISSION PROFILES, UTILIZATION, AND PRESSURE CYCLES

MISSION PROFILE	CRUISE ALTITUDE (FT.)	CABIN PRESSURE (PSI)	NUMBER OF PRESSURE CYCLES PER MISSION	UTILIZATION	PRESSURE CYCLES PER 10000 FL. HRS.	PRESSURE CYCLES PER 10000 FL. HRS.
PROFICIENCY TRAINING	17000	7.0	2	287.90	575.80	1047.7
BASIC TRAINING	17000	7.0	2	235.96	471.92	
S.R. LOGISTICS	20000	7.5	1	1018.79	1018.79	1329.2
L.R. LOGISTICS	22000	7.5	1	310.45	310.45	
LOW LEVEL	15000	6.3	1	118.53	118.53	118.53
SHUTTLE	10000	4.5	1	2664.87	2664.87	2718.8
STORM RECONNAISSANCE	10000	4.5	2	26.95	53.90	
AIR DROP	4000	1.9	2	84.57	169.14	169.1
COMBAT TRAINING	3000	1.4	1	106.70	106.70	106.7

NOTES:

1. UTILIZATION IS THE NO. OF TIMES THE MISSION WAS FLOWN IN 10,000 FLIGHT HOURS.

2. PRESSURE CYCLES/10000 FL. HRS. = $\left(\begin{matrix}\text{NUMBER OF PRESSURE} \\ \text{CYCLES PER MISSION}\end{matrix}\right)$ (UTILIZATION)

TABLE LV – FATIGUE DAMAGE SOURCES INPUT

Source Number	Source Nomenclature
01	Maneuver Less Than 500
02	Maneuver Above 500
03	Ground-Air-Ground
04	Roll-Out
05	Taxi
06	Take-Off
07	Gust
08	Landing Impact

Specific structural data were provided for the analysis. The surface (aircraft component) and station (location) on the surface that was analyzed was selected for which the data were inputted into the program. For each location analyzed, the structural performance parameters, stress-load ratio, and quality level, K_t, were provided as input data. The quality level was defined as the numerical value of an effective stress concentration factor which yielded a Miner's damage of unity. In addition to the geometry, a number of uncontrolled variables were included in the determination of the quality level of a specific area of a complex structure such as an aircraft fuselage structure. These uncontrolled variables included:

a. Material inconsistencies such as anisotropy, non-homogeneity, inelasticity, inclusions, voids, variations in physical properties, and grain size.

b. Manufacturing variables such as tolerances causing variations in part geometry and thickness, surface finish, fastener size, hole size, joint friction, and assembly errors.

c. Other variables such as non-linear slippage of joints, local plastic yielding at points of high stress concentration, complexity and redundancy of load paths, fretting of joints, fretting corrosion, design errors, irregularity of service usage, and external loadings.

When inputting the stress-load ratios at the location being analyzed, the sign convention must be observed. The sign convention used assigned positive loads in the direction of the positive airplane axes (i.e., up, aft and outboard to left). Bending moment signs were determined by the left hand rule, i.e., when the left thumb was pointed in the positive direction of an aircraft axis, the curve of the left fingers indicated the direction of the positive moment about that axis. When stress-load ratios were inputted, and a positive load produced tension, the stress-load ratio was positive. If the positive load produced

compression, the stress-load ratio was negative. Up to five stress-ratios and six quality levels may be inputted for each location selected for analysis.

The internal loads at a point on the periphery of the fuselage shell structure were computed through utilization of an independent high speed digital computer program which used the conventional engineering unit beam theory of bending. Generally, the internal stresses for a point on the periphery of the fuselage shell structure as obtained from flight bending loads were calculated by the equation:

$$\text{Stress} = \frac{\text{(Bending Moment) (Distance from Centroidal Axis)}}{\text{Effective Fuselage Moment of Inertia}}$$

$$\text{or} \quad f_b = \frac{Mc}{I}$$

Fuselage pressurization loads were converted into internal membrane stresses by the standard formula for cylindrical pressure vessel longitudinal stress equation:

$$\text{Stress} = \frac{\text{(Pressure) (Fuselage Radius)}}{\text{(2) (Cover Skin Thickness)}} = \frac{PR}{2t}$$

The tension stress-load ratios computed in the unit beam analysis for the fuselage station 337.0 location as depicted in Figure 126 and input into the DART computer program were as follows:

Unit Fuselage Up-Down Bending Moment, M_y = 1 in-lb converted to 0.000374 psi stress,

$$\frac{(My\ c_z)}{I_{yy}}$$

Unit Fuselage Side Bending Moment, M_z = 1 in-lb converted to 0.000374 psi stress,

$$\frac{(M_z\ c_y)}{I_{zz}}$$

Unit Fuselage Cabin Pressure Load, p = 1 psi converted to 555.10 psi stress, $\frac{(PR)}{2t}$

Operation data were input by missions, and for a given mission it were supplied in one of two methods. The first was to supply individual mission segment parameters. The second method was to supply mission profile parameters and to require the computer to segment the mission. Regardless of which method was used in supplying the operational data,

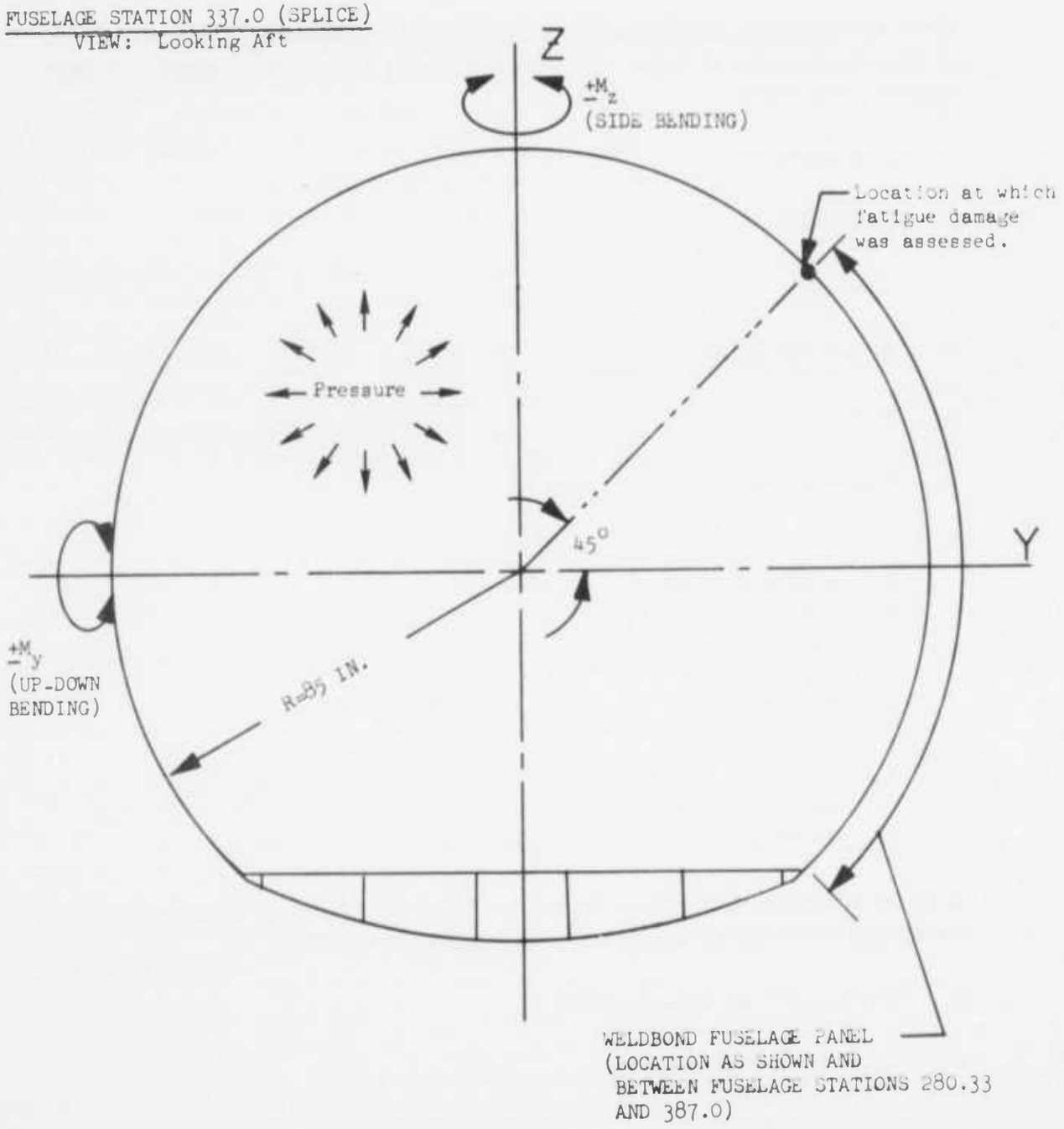

FIGURE 126 – TYPICAL FUSELAGE CROSS-SECTION FOR INTERNAL LOAD CALCULATIONS BY UNIT BEAM ANALYSIS

specific data about the mission had to be supplied. These data included the mission title, mission utilization, and ground-air-ground (G-A-G) option. The G-A-G option provided for the automatic calculation of G-A-G damage for each G-A-G cycle. The parametric use of this option pre-empted ordinary segment damage calculations.

When the operational data were supplied through mission segment parameters as was done in the weldbonded panel fatigue analysis, the following data had to be supplied for each segment of the mission:

a. Fuel weight

b. Cargo weight

c. Velocity

d. Altitude or runway

e. Time

f. Mission segment type identification

1. Vertical lateral air
2. Lateral air only
3. Taxi
4. Landing impact
5. Take off
6. Roll out
7. Braking
8. Turning
9. Transition

When the operational data were supplied through mission profile parameters, the following mission data had to be furnished as input to the computer program.

a. Cruise altitude and airplane velocity

b. Initial cargo and fuel weights

c. Mission time and distance

d. Takeoff and landing runway roughnesses

e. Climb and descent altitude increments

Unlike the structural and operational data inputs which change with each computer run, the environmental data input changed infrequently. The environmental data changed so infrequently that it was considered as "stored" data even though it was input in the computer card deck. These data consisted of eight (8) sets of data that contained specific information pertaining to the relationship of structural loads to the environment.

The procedures for manipulating the program input data in the DART program to provide the desired output quantities were rather involved. Figure 127 is an illustration of a flow diagram showing the fundamental DART program operations. As shown in Figure 127, the operational data for each mission segment were provided either directly by mission segment parameters or by mission profile parameters through the mission segmenting sub-routine. These data were processed through special checks to insure that they defined the operations which were possible. Mission segments which cleared the special checks were used to interpolate the loads and this operation provided the loads for the specific mission segment. The loads were selected for each input surface and were then interpolated for each station selected for analysis on each surface. Material S-N data were linearly interpolated between the input values of quality level, K_t, to provide S-N data for input for each station analyzed.

Material S-N data for ten separate materials including 7075-T6 and 2024-T3 aluminum alloys were stored in the DART computer program for a range of quality levels versus mean stress for several values of varying stress. The 7075-T6 aluminum alloy data were used in this analysis because the selected damage assessment location on the fuselage station 337.0 circumferential splice is in the near vicinity of the 7075-T6 upper fuselage main longeron. Furthermore, a range of mean stresses from -60 ksi to 60 ksi for quality levels ranging from 1.50 to 12.00 were provided. These data adequately spanned the required quality levels of 4.00, 5.00, and 6.00 applied in the fuselage station 337 damage analysis.

The fatigue damage is dependent upon quality level, K_t, and the analysis was performed for K_t's of 4.00, 5.00 and 6.00 in order to bracket the K_t levels that are expected to occur in both weldbonded and mechanically fastened splice joints. Using the stress-load ratios calculated previously for flight and pressure loads in conjunction with load sources, the following endurances were computed for the damage analysis location on the fuselage station 337.0 splice joint.

Quality Level, K_t	Flight Hrs. to Failure
4.00	1.2×10^{17}
5.00	4.1×10^{14}
6.00	2.0×10^{13}

The above fatigue endurances are illustrated graphically on Figure 128. In addition to the fatigue endurance, the DART program output included fatigue damage for the three input quality levels considering the load sources and profiles utilized. Tabulated fatigue damage data are given in Tables LVI and LVII.

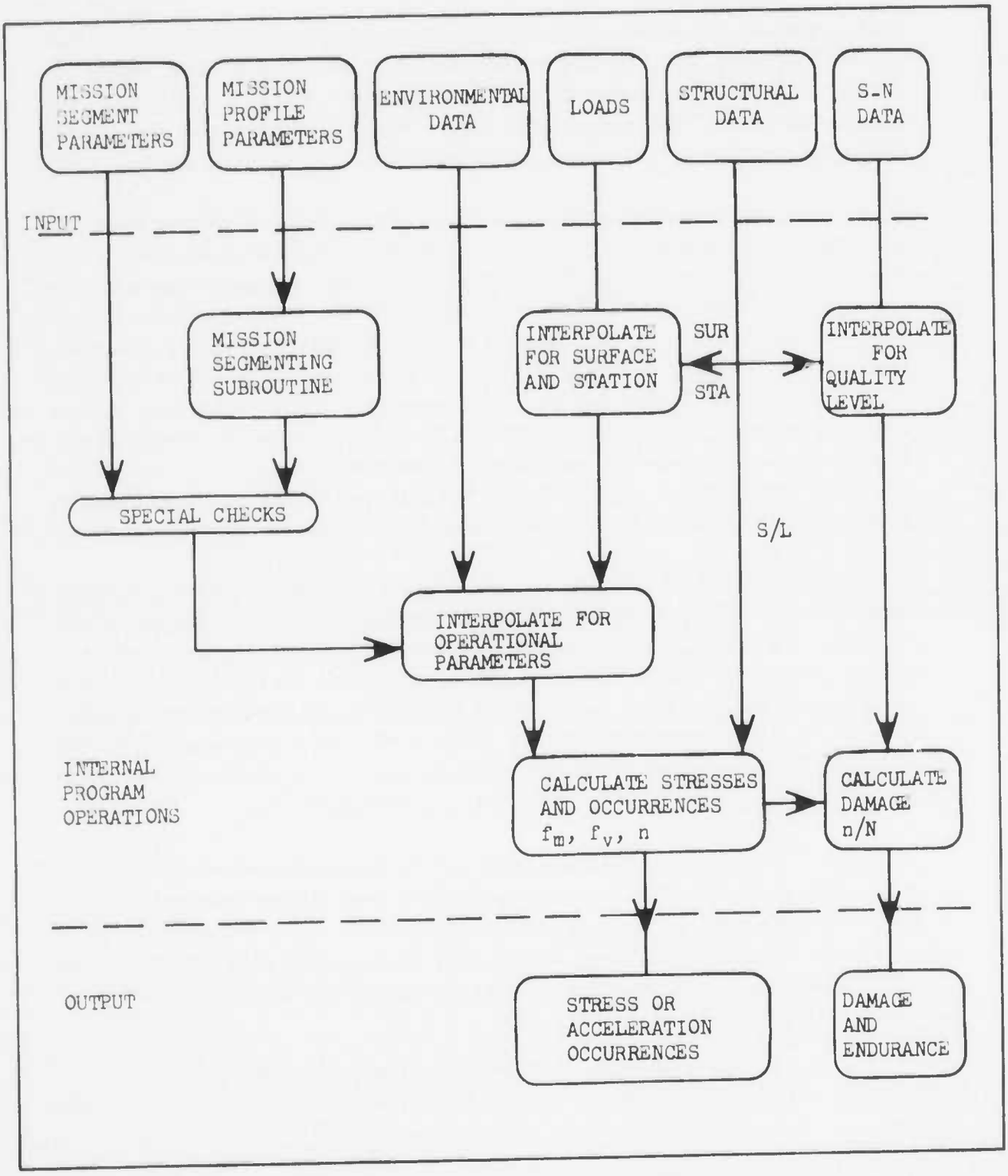

FIGURE 127 – DART COMPUTER PROGRAM FLOW CHART

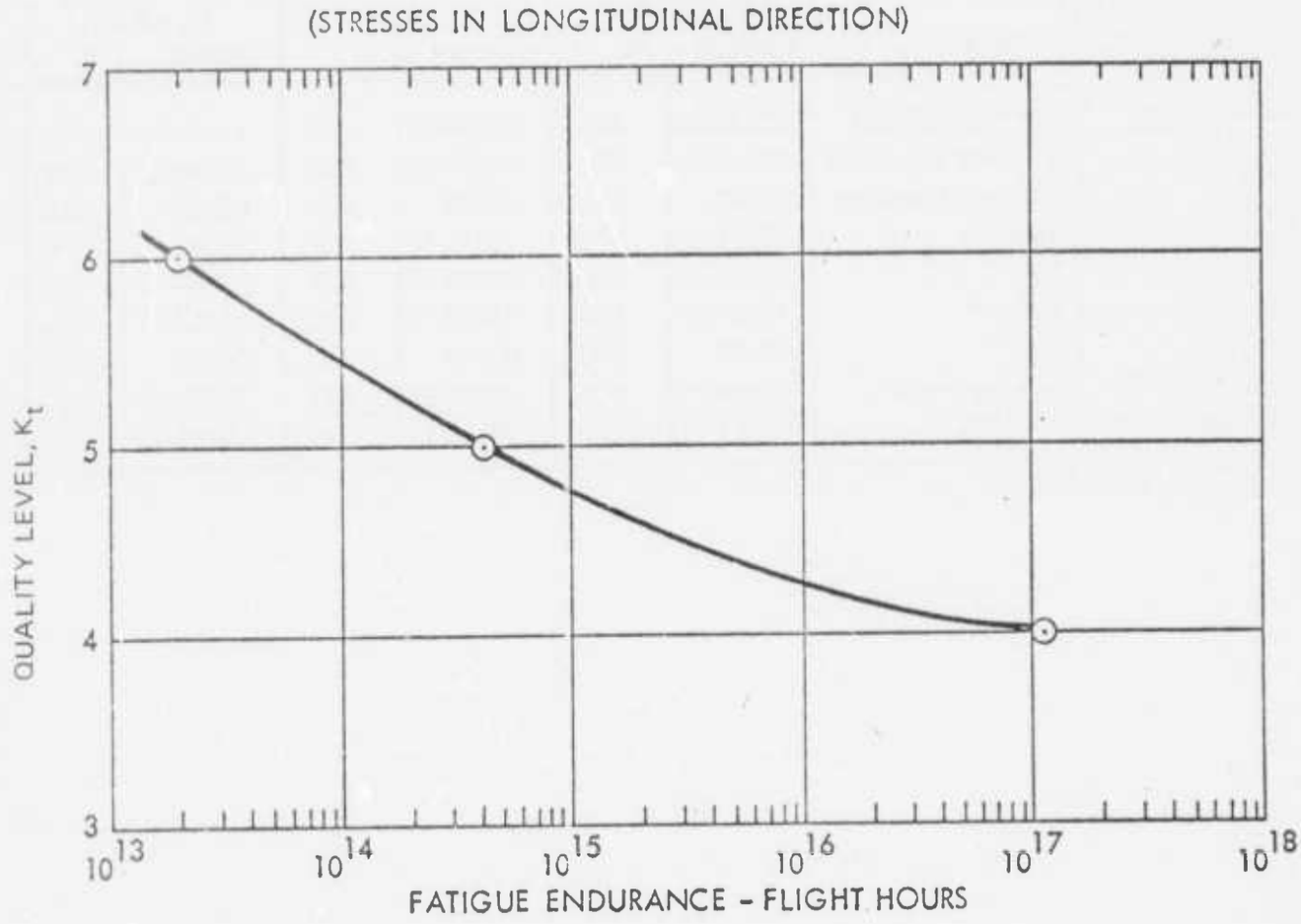

FIGURE 128 – FATIGUE ENDURANCE VERSUS QUALITY LEVEL, F.S. 337.0

TABLE LVI – CALCULATED FATIGUE DAMAGE BY LOAD SOURCE

Source Damage Per 1.0 Mission Station 337.0
Stress/Load Ratio = .000374

Source	K_t = 4.00 Damage	%	K_t = 5.00 Damage	%	K_t = 6.00 Damage	%
Maneuver LE. 500	.13838-35	.000	.12725-29	.000	.17643-26	.000
Maneuver above 500	.68065-34	.000	.64577-28	.000	.84358-25	.000
Ground-Air-Ground	.00000	.000	.00000	.000	.00000	.000
Roll-Out	.35577-17	.412	.10311-14	.427	.21943-13	.435
Taxi	.50694-17	.588	.13809-14	.573	.28460-13	.565
Take-off	.15059-27	.000	.22433-23	.000	.38457-21	.000
Gust	.00000	.000	.00000	.000	.00000	.000
Landing Impact	.18266-29	.000	.33206-23	.000	.22303-20	.000
Total =	.86271-17	1.000	.24120-14	1.000	5.0403-13	1.000

TABLE LVII– CALCULATED FATIGUE DAMAGE BY MISSION

Mission Damage Per 1.0 Mission Station 337.0
Stress/Load Ratio = .000374

Mission	K_t = 4.0 Damage	%	K_t = 5.00 Damage	%	K_t = 6.00 Damage	%
1	.36550-18	.042	.14408-15	.060	.37356-14	.074
2	.44947-20	.001	.28159-17	.001	.93953-16	.002
3	.73329-17	.850	.20385-14	.845	.42044-13	.834
4	.19573-18	.023	.63473-16	.026	.14307-14	.028
5	.77439-20	.001	.35220-17	.001	.94084-16	.002
6	.68645-18	.080	.14819-15	.061	.27428-14	.054
7	.89619-23	.000	.96872-20	.000	.40452-18	.000
8	.11098-28	.000	.43333-24	.000	.11559-21	.000
9	.34363-19	.004	.11435-16	.005	.26196-15	.005
Total =	.86271-17	1.000	.24120-14	1.000	.50403-13	1.000

It is noted that in Table LVI a zero fatigue damage resulted from the ground-air-ground cycle for all K_t values evaluated. Furthermore, it was concluded in the previous fatigue analysis reported in Reference 8 that the pressure cycle (G-A-G) was responsible for over 99 percent of the forward fuselage fatigue damage. The difference in the results from the two analyses was that the previous analysis assessed the damage in the hoop direction in the fuselage which had stresses that were twice the magnitude of those applied in fore and aft direction in the foregoing analysis. Also, the fatigue endurance calculated in the previous analysis was less than that computed in the foregoing analysis of fuselage station 337.0 splice joint. A detailed explanation of the basis for these differences are outlined in the following paragraphs.

The previous analysis reported in Reference 8 involved the hoop stresses due to cabin pressure and was calculated by:

$$\frac{PR}{t} = (7.50 \text{ psi} \times 85 \text{ in.})/0.050 \text{ in.} = 12{,}750 \text{ psi}$$

Since the pressure cycle range was from 0 to 7.50 psi, this condition translated into a mean stress of 12,750 psi/2 = 6,375 psi and a varying stress of 6,375 psi. The analysis of fuselage station 337.0 contained in this report involved a longitudinal pressure vessel stress of pR/2t. Thus,

$$pR/2t = (7.50 \text{ psi} \times 85 \text{ in.})/(2 \times 0.050 \text{ in.}) = 6375 \text{ psi}$$

which translated into a mean stress of 3190 psi and a varying stress of 3190 psi as graphically illustrated in Figure 129.

f_{mean} = 6375 psi - transverse
3190 psi - longitudinal

$f_{varying}$ = 6375 psi - transverse
3190 psi - longitudinal

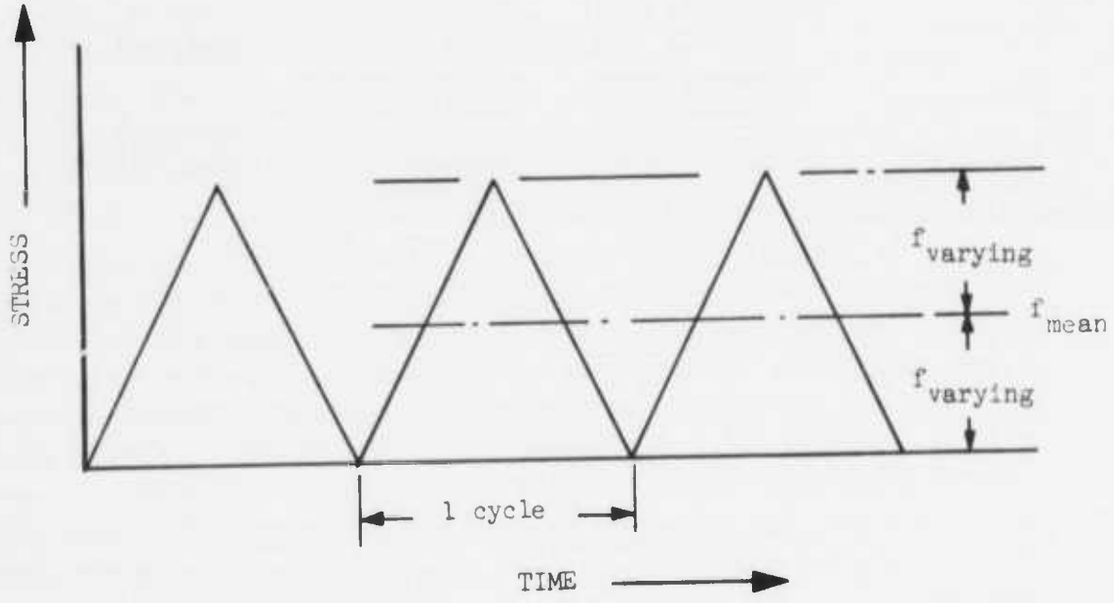

FIGURE 129 – STRESSES BASED ON PRESSURIZATION

The random flight loads can result in a wide variety of varying stresses which contribute different proportions of the total fatigue damage as illustrated in Figure 130. However, the discrete type of loading which was representative of the ground-air-ground cycle resulted in only one mean stress and one varying stress. The ground-air-ground cycle is illustrated in Figure 131. The important significance of Figures 130 and 131 was the fact that the flight loads were of a random or statistical nature such that they resulted in a spectrum of varying and mean stresses which in turn gave finite values of calculated fatigue damages. The ground-air-ground cycle resulted in a discrete spectrum of loads in the hoop (transverse) and fore and aft (longitudinal) directions for which each had only one mean stress and one varying stress. Figure 131 illustrated the point that the longitudinal stress in the ground-air-ground cycle had an allowable number of cycles to failure, N, greater than 10^7 cycles, the endurance limit for aluminum alloys. Therefore, the fatigue damage was zero (i.e., infinite endurance) for such a condition. This condition existed for the splice joint at fuselage station 337.0 which was the basis for the ground-air-ground cycle contributing zero fatigue damage in the splice joint as shown in Table LVI.

It was concluded on the basis of this fatigue analysis that the flight hours to failure for the mechanically fastened splice at fuselage station 337.0 and the weldbonded splices at fuselage stations 390.33 and 377.0 far exceeded the time to failure at other locations on the airplane structure, and that it was highly improbable that an in-service failure would occur as the result of low cycle fatigue.

8.4.2 Fatigue Analysis Showing Endurance in the Hoop Direction at Fuselage Station 477.0

Fatigue endurance in the hoop direction was not established within the boundaries of the weldbounded component because that region of the fuselage did not contain any longitudinal splices. A fatigue analysis previously performed on the C-130 forward fuselage structure established that the pressure cycle (hoop stresses) was virtually the only damaging load sustained by the fuselage structure. This analysis was reported in Reference 9 and was included herein for information purposes. In the referenced analysis, it was determined that the pressure cycle was responsible for over 99 percent of the forward fuselage fatigue damage for quality levels, K_t, ranging from 3.25 to 4.80 as shown in Table LVIII. The fatigue analysis was performed at fuselage station 477.0 using the Damage Analysis in Rapid Time (DART) computer program.

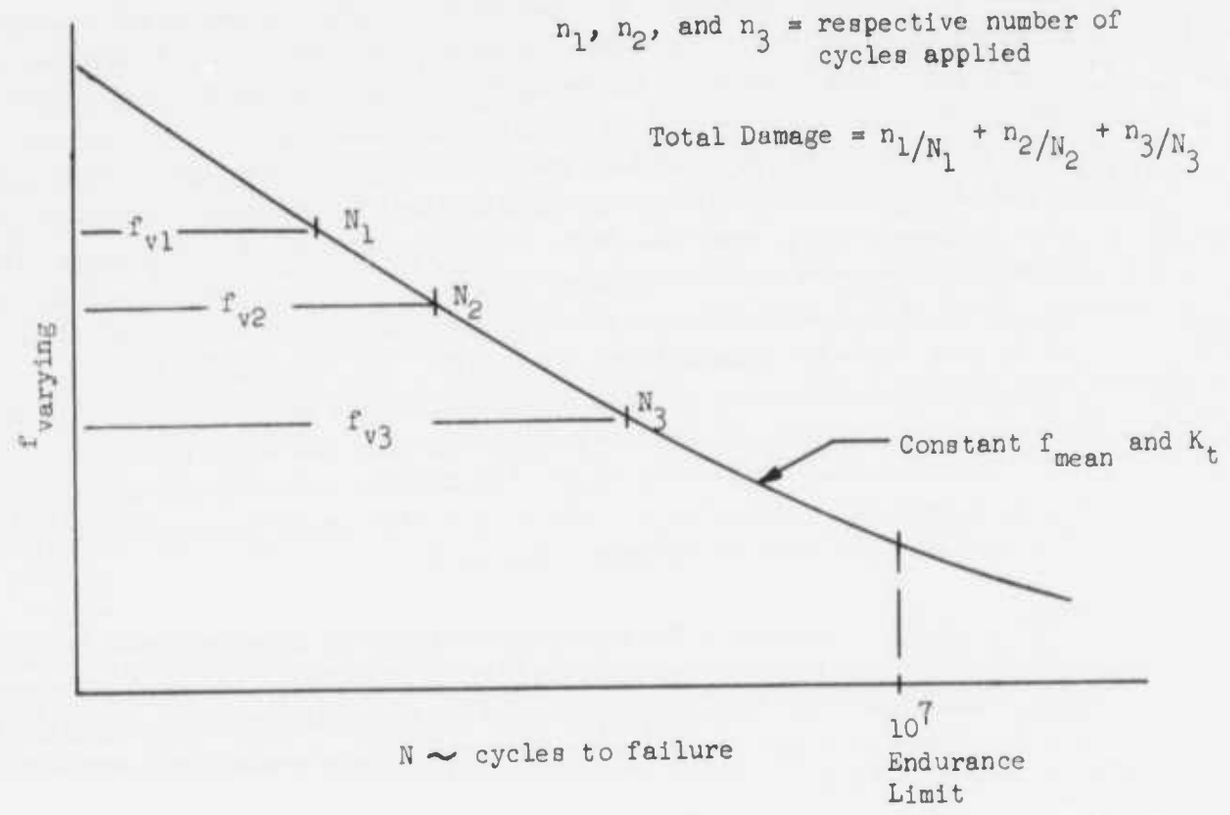

FIGURE 130 – RANDOM (STATISTICAL(FLIGHT LOADS))

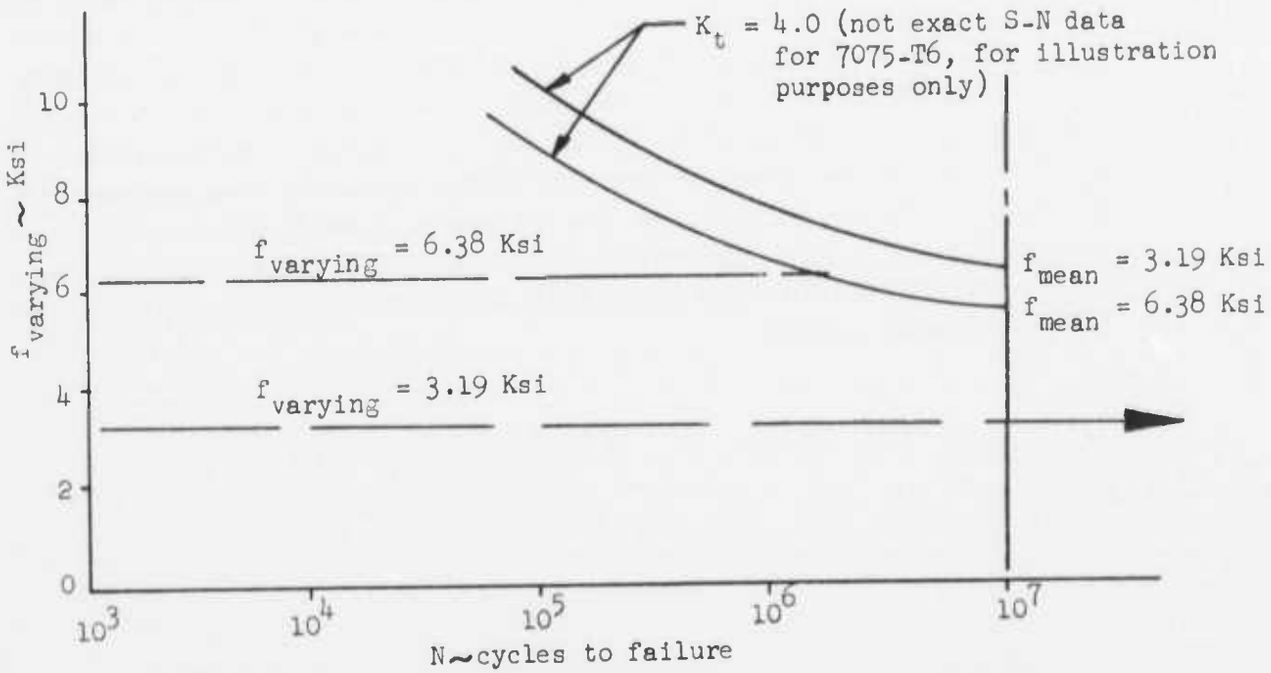

FIGURE 131 – DISCRETE LOADS - GROUND-AIR-GROUND CYCLE (PRESSURE)

TABLE LVIII – CALCULATED FATIGUE DAMAGE BY LOAD SOURCE

Source Damage per year, Mission Station 477

Source	K_t = 3.25 Damage	%	K_t = 4.00 Damage	%	K_t = 4.80 Damage	%
Climb	.13940-22	.000	.12904-18	.000	.46776-15	.000
Low Cruise	.10211-26	.000	.12513-21	.000	.25513-17	.000
High Cruise	.67530-23	.000	.76003-18	.000	.22913-12	.000
Descent	.11891-16	.000	.30978-13	.000	.52119-10	.000
Taxi In Phase	.00000	.000	.00000	.000	.12256-27	.000
Taxi Out of Phase	.00000	.000	.00000	.000	.00000	.000
Landing Impact	.00000	.000	.21601-22	.000	.10300-14	.000
Maneuver	.00000	.000	.00000	.000	.00000	.000
G-A-G Cycle	.49022-05	1.000	.21285-03	1.00	.10018-02	1.000
Total =	.49022-05	1.000	.21285-03	1.00	.10018-02	1.000

The fatigue damage was dependent upon quality level, K_t, and the analysis was performed for K_t's of 3.25, 4.00, and 4.80 in order to bracket the K_t levels for the longitudinal mechanically fastened splice joints. The average demonstrated K_t in the C-130 fuselage hydrostatic fatigue tests was 4.50.

Using the stress-load ratios calculated previously for flight and pressure loads in conjunction with the load sources shown in the above table, the following endurances were computed for the damage analysis location on the fuselage station 477.0 longitudinal splice joint.

Quality Level, K_t	Flight Hrs. to Failure
3.25	1.51×10^8
4.00	3.48×10^6
4.80	7.40×10^5

The above fatigue endurances were illustrated graphically in Figure 132.

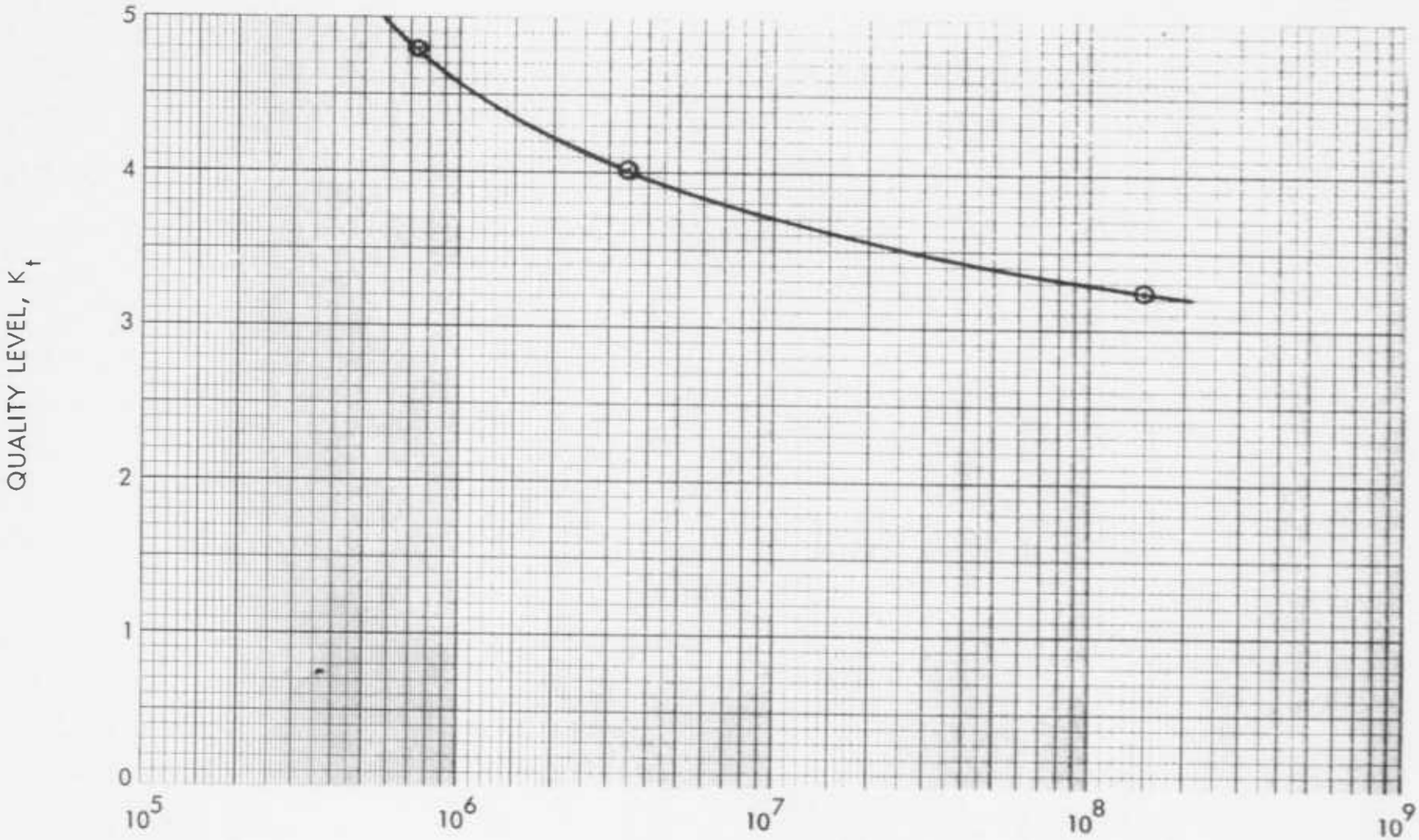

FIGURE 132 – FATIGUE ENDURANCE VERSUS QUALITY LEVEL, F.S. 447.0

8.5 Fail-Safe Analysis of the C-130 Weldbonded Fuselage Component

The following fail-safe analysis was performed on the weldbonded component. A conservative approach was taken in the analysis on the basis of the residual strength results given in Section X.

In the analysis, it was assumed that the load transfer around a crack in a curved panel subjected to internal pressure occurs over a much shorter distance than the flat panel with a crack perpendicular to the applied tension load or a flat panel with a crack perpendicular to the applied tension load with a lateral pressure superimposed. Previous developments have confirmed the assumption that the final crack length, X, and the effective width, W_e, were significantly smaller for curved panels than for flat panels. Figure 133 illustrates both flat and curved panels subjected to tension and pressure loads.

When deriving the fail-safe criterion for pressurized stiffened cylinders with longitudinal cracks, it was reasonable to assume that in the undamaged area of the structure the fuselage ring frames did not support an appreciable portion of the load due to pressurization. The fundamental equation for the damaged pressurized stiffened structure required at the time of failure that the load lost due to the damaged structure had to be offset by the reserve strength of the structural elements which supported the lost load.

$$Pcr\ R\ w = 2w_e t \left(F_{TU_s} - \frac{PcrR}{t}\right) + F_{TU_f} \left(\sum A_e\right)$$

where Pcr = Critical applied pressure, psi

R = Fuselage radius of curvature, in.

w = Width of crack at time equilibrium is assumed, in.

w_e = Width of effective zone in sheet ahead of tips of the crack, in.

F_{TU_s} = Ultimate tensile strength of fuselage skin, psi

t = Thickness of fuselage skin, in.

F_{TU_f} = Ultimate tensile strength of fuselage ring frame, psi

$\sum A_e$ = Total effective area of fuselage ring frame, $in.^2$

In the above equation it was assumed that failure of the fuselage skin (i.e., fast propagation of the crack) and ring frame occurred simultaneously. Also, it is noted that the term w_e was the width of the effective zone of the fuselage skin without consideration of any effects due to the ring frames but it was also dependent on the stringer on longeron spacing. Since the C-130 fuselage panel did not include stringers, and the longeron spacing, a, was 6.67 inches, $2w_e$ = 4.3 inches.

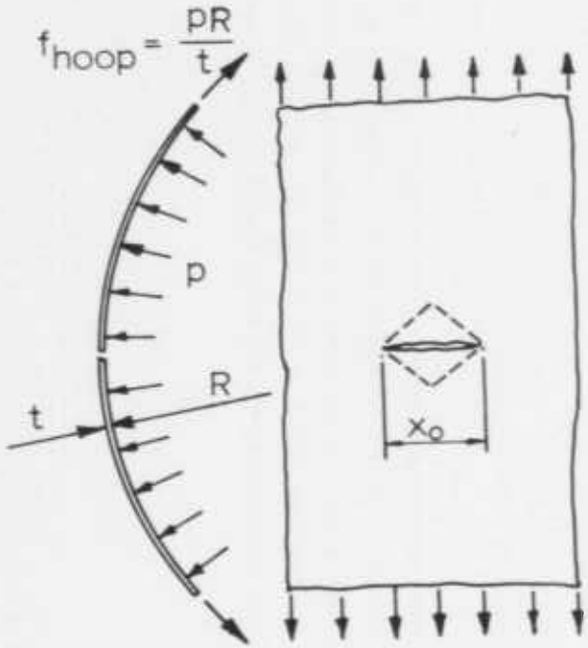

a) CURVED PANEL UNDER INTERNAL PRESSURE LOAD "p"

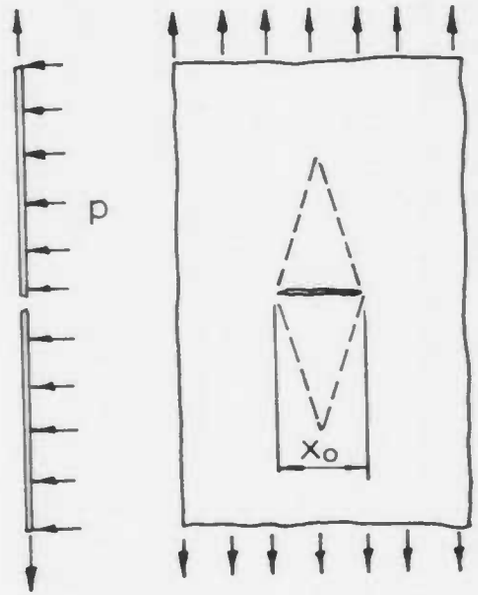

b) FLAT PANEL UNDER UNIAXIAL TENSION WITH ADDED LATERAL PRESSURE "p"

FIGURE 133 – FLAT AND CURVED PANELS SUBJECTED TO TENSION AND PRESSURE LOADS

The allowable hoop tension stress, F_{hoop}, of a pressurized fuselage with a longitudinal crack from the equilibrium equation above is,

$$F_{hoop} = \frac{PcrR}{t} = F_{TU_s} \left[\frac{2w_e + \frac{F_{tu_f}}{F_{TU_s}} \frac{\sum Ae}{t}}{X + 2w_e} \right]$$

where X = Final crack length before fast propagation, in.

For curved riveted aluminum panels, it has been established that $X = 1.15\ X_o$ where X_o was the initial crack length in inches.

It was concluded from the experimental results from the flat weldbonded panel fail-safe test that the determination of X for the flat weldbonded panel was essentially the same as for a flat riveted panel. Therefore, X for the C-130 weldbonded fuselage panel was taken as $X = 1.15\ X_o$.

The concept of allowable damage is that a readily perceptible crack will not propagate in an uncontrolled manner and cause explosive decompression. The arbitrary amount of damage chosen for the C-130 pressurized fuselage was the length of one ring frame pitch of 6.67 inches (Reference 10, page 33, Case 1), and as a conservative analysis the length of the damage was centered over a ring frame assuming that the right frame was totally severed. Applying this damage concept to the equilibrium equation immediately above and assuming the adjacent ring frames were not effective such that $\sum A_e = 0$,

$$F_{hoop} = F_{TU_s} \left[\frac{2w_e}{X + 2w_e} \right]$$

$X = 1.15\ X_o = (1.15)\ (6.67) = 7.67$ in.

F_{TU} for 2024 Bare aluminum sheet = 64,000 psi

F_{TU} for 2024 aluminum sheet, clad both sides = 62,000 psi.

$$F_{TU_s} = \frac{64{,}000 + 62{,}000}{2} = 63{,}000 \text{ psi for 2024 aluminum sheet, clad one side only.}$$

$$F_{hoop} = (63{,}000) \left[\frac{4.3}{7.67 + 4.3} \right] = 22{,}700 \text{ psi}$$

The fuselage hoop stress due to pressurization is,

$$f_{hoop} = \frac{PR}{t} = \frac{(7.5)(85)}{.050} = 12{,}750 \text{ psi}$$

Establishment of a positive margin of safety will give the conclusion that such a crack will not propagate. The equation for the margin of safety equation is,

$$M.S. = \frac{FG}{(fg)(1.15)} - 1.0 = \frac{F_{hoop}}{(f_{hoop})(1.15)} - 1.0$$

Where 1.15 is the dynamic factor for the fail-safe analysis.

$$M.S. = \frac{22700}{(12750)\ (1.15)} - 1.0 = +0.54$$

The above analysis has shown that for the assumed damage in the C-130 pressurized fuselage structure, the crack will not propagate.

8.6 Weight and Balance Evaluation

An investigation was conducted to determine the effect on the weight and balance of the airplane when the weldbonded fuselage component was substituted for the current mechanical fastened structure. The component is bounded by Fus. Stas. 280 and 387, the cargo floor, and the main fuselage upper longeron. Installing the weldbond component required forward (F.S. 280) and aft (F.S. 387) splices that were not present in the conventional structure. The weight analysis is as follows:

Item	Weight-lbs.
Conventional Fuselage Component (Removed)	−144.8
Weldbonded Fuselage Component (Added)	142.6
Splices at F.S. 280 and F.S. 387 (Added)	3.8
Net Airplane Weight Change (Increase)	+ 1.6

It is interesting to note that, even though weight savings was not a program requirement, the weldbonded fuselage component was calculated to be 2.2 pounds lighter than the comparable conventional riveted component. If the entire conventional riveted component had been weldbonded, rather than only a section of it, the splices at F.S. 280 and F.S. 387 would not be required. The splices, therefore, create an artificial weight penalty -- not due to weldbonding, but because of the selection of a section of an existing production assembly as the demonstration article. Even so, the difference in weight is so small as to fall within normal weighing accuracy and no change to the flight manual was necessary.

SECTION IX

FULL-SCALE WELDBONDED COMPONENT FABRICATION

9.1 C-130 Weldbonded Fuselage Component Tool Development

Development of tooling for use in fabrication of the C-130 weldbonded fuselage components included a mechanized spot-weld positioner for spot-welding the forward and aft sections of the components, a final assembly tool for mechanically splicing the weldbonded sections, and an oven fixture for supporting the weldbonded sections during cure of the adhesive.

9.1.1 Mechanized Spot-Weld Positioner

The spot-weld positioner was designed so that the fuselage component moved through the spot-welder throat with freedom of movement in three dimensions. Innovative design efforts resulted in a design of the spot-weld positioner that was mechanized in the normal and tangential panel directions as shown in Figure 134. Mechanization of the spot-weld positioner for two-axis motion was accomplished as follows. The system consists of a rack and pinion gear drive that was designed to move the C-130 fuselage components to be spot-welded along an arc corresponding to the 85 inch radius of the fuselage component. Also, air actuators were designed to lift the fuselage component in the direction normal to the panel at each spot-weld location in order to clear the spot-welder lower electrode when the component being spot-welded is rotated. The stepped rotation of the panel was accomplished by connecting an electronically controlled variable speed electric motor with the off-time control of the Sciaky turret head welder. Adjustment of the motor drive speed in relation to the spot-welder allowed a preset condition of the spot-weld pitch and results in a constant automated spot-weld spacing in the curvilinear direction of the fuselage component. Connecting the air actuator in conjunction with the motor drive and spot-welder time function allows synchronized movement of the spot-welder positioner in the two directions described above.

9.1.2 Final C-130 Weldbonded Fuselage Component Assembly Tool

The main assembly jig fixture used in the C-140 weldbonded fuselage barrel section under (Reference 5) was extensively modified for final assembly of the C-130 weld-bonded fuselage components. Figure 135 shows the partially completed final assembly fixture. This fixture provides dimensional control for the final weldbonded fuselage component and positioning of the mechanically fastened joint near the center of the component. The vertical ribs shown in the fixture will provide fuselage station dimensional control during the mechanical joining operation.

In addition to the joining of the weldbonded fuselage sections, other mechanically fastening operations were performed on the weldbonded fuselage component.

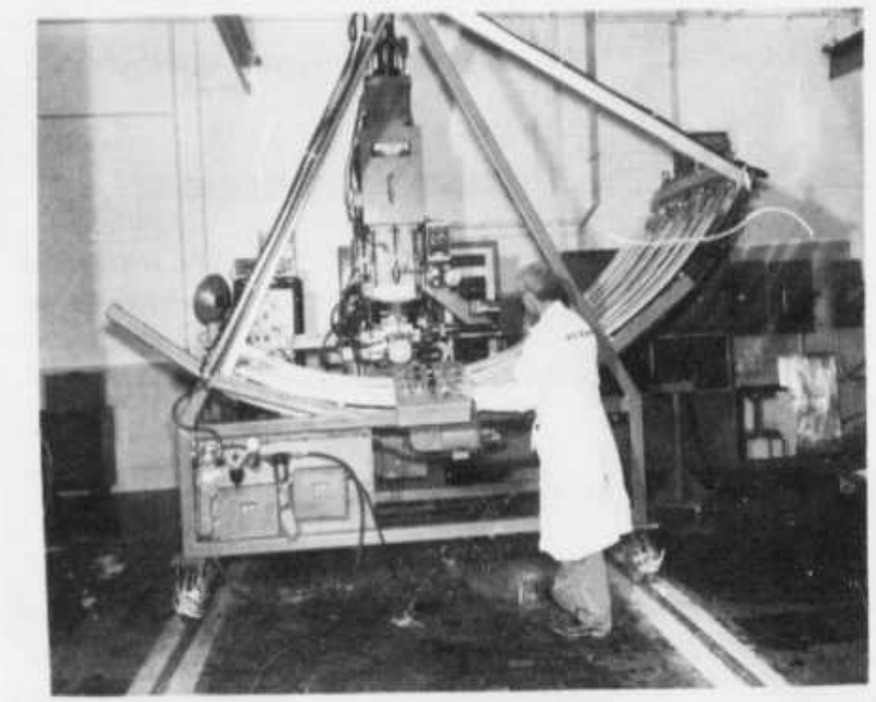

FIGURE 134 – SPOT-WELD POSITIONER IN OPERATION AT TURRET HEAD SCIAKY SPOT-WELDER

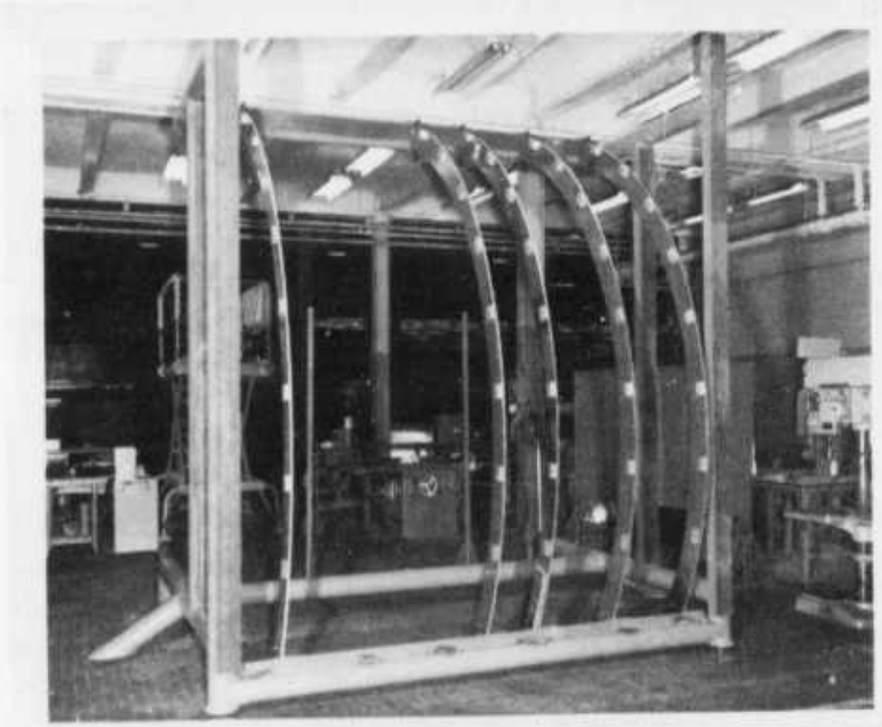

FIGURE 135 – FINAL ASSEMBLY TOOL PARTIALLY FABRICATED

9.1.3 Oven Curing Fixture for the C-130 Weldbonded Fuselage Components

An oven curring fixture for cradling the C-130 weldbonded fuselage components during cure of the adhesive bondlines in an oven was designed and fabricated. The curing fixture design is a simplified space framework structure whose upper surface forms the contour of the curved fuselage component as shown in Figure 136.

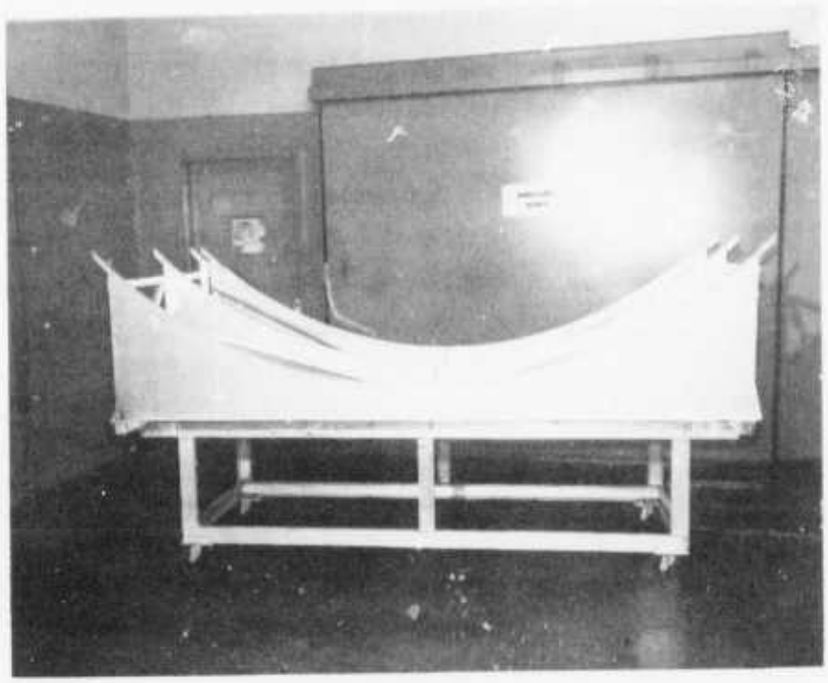

FIGURE 136 – OVEN CURING FIXTURE

The oven curing fixture also provides support to the weldbonded fuselage components during transportation to and from the curing oven.

9.2 C-130 Weldbonded Fuselage Component Drawing List

The following list of drawings are those required for fabrication of the subject component and modification of the production fuselage side panel assembly (Dwg. No. 388005 29).

Drawing No.	Drawing Title
3307700	Panel Assy-Center Fus Fwd (Mod)
3307701	Panel-Side Center Fus Fwd (Weldbond)
3307702	Doubler Instl L/E Light
3307703	Tiedown Instl-Sidewall
3307704	Angle Instl
3307705	Support-Static Pressure Fitting
3307706	Support Assy-Static Pressure Fitting
3307707	Ring Segment-Upper Assy of
3307708	Ring Segment-Assy of
3307709	Ring Segment-Lower Assy of
3307710	Skin Doubler-Static Pressure Port
3307711	Skin Doubler Instl-Fus Window
3307712	Ring Segment-Upper Assy of
3307713	Ring Segment-Upper Assy of
3307714	Ring Segment-Upper Assy of
3307715	Ring Segment-Lower Assy of
3307716	Ring Segment-Main Fwd Panel Assy of
3307717	Ring Segment-Assy of
3307718	Skin Doubler Instl-Fus Window
3307719	Track & Intercostal Instl-Litter
3307720	Beam-Lower Support, Litter Track
3307721	Beam-Lower Support, Litter Track
LS37668	Z-Section, Rolled

Several drawing changes were incorporated into the basic drawings to accommodate different assembly sequences and accessibility requirements during the weldbonding operations. The blind areas that existed beneath the cargo tie-down bracket assembly, Dwg. No. 3307703, required a local change in the bracket to permit installation of either blind or regular fasteners.

9.3 Manufacturing Planning and Inspection Procedures for the C-130 Weldbonded Fuselage Components

Manufacturing planning activities for fabrication of the weldbonded fuselage components included the qualification of the spot-welding machine, spot-weld schedule certifications for the appropriate weldbonded joint configurations, adhesive acceptance tests, and

procurement of materials. Shop orders giving sequenced operations for detail parts, sub-assemblies, and the weldbonded components were prepared. Inspection operations were included on the plans and an outline of those performed during fabrication of the C-130 weldbonded fuselage components follows:

1. Procured Parts and Material

   1.1 Inspect all raw stock for material type, hardness and conformance to specifications, QQ-A-250/4, /5, /12.

   1.2 Inspect new ring segment Z-sections for dimensional conformance, flatness and contour per LS 37668, Rev. A and QQ-A-250/12.

   1.3 Inspect weldbond adhesive on receipt for conformance to STM 30-106 (Material Specification; "Adhesive, Weldbond, Service Range -67°F to 160°F").

   1.4 Inspect windows and hardware for conformance to engineering requirements QQ-A-601 and QQ-A-362.

2. In-plant Fabricated Parts

   2.1 Inspect material for type and condition per QQ-A 250/4, /5, /12.

   2.2 Inspect forming, cutting, trimming, deburring operations for conformance to engineering drawings and specification LAC 1241.

   2.3 Inspect final hardness, identification, and finish. Parts subject to weldbond will be fabricated without finish. Finish applied after assembly per LAC 0471. See LAC G-14 for finish code.

3. Surface Preparation of Parts Per STP 57-005 (Process Specification; "Surface Preparation of Parts for Weldbonding")

   3.1 Inspect cleaning of detail parts, record time on Shop Order.

   3.2 Inspect process control test coupons, identified to each Shop Order.

   3.3 Verify that cleaned parts are protected from contamination during processing.

   3.4 Verify chemical balance of processing solutions prior to use daily.

4. Adhesive Application

4.1 Verify that parts to be welded are within the 48 hour limitation on cleaning and have not been exposed to contamination per STP 57-005.

4.2 Verify that adhesive is within certification, (168 hours since last test), per STP 55-001 (Process Specification; Weldbonding of 2000 and 7000 Series Aluminum Alloys).

4.3 Inspect adhesive bondline for fillet prior to cure per STP 55-001.

4.4 Verify date and time of adhesive application, record adhesive batch number.

5. Welding

5.1 Verify machine setting per weld schedule specified on Shop Order per STP 55-001.

5.2 Verify that adhesive is within one week time limitation on parts to be welded per STP 55-001.

5.3 Inspect process control test specimens at beginning of each production run, shift change, each time electrodes are changed, lot of adhesive is changed, control adjustments are changed, at intervals of two hours or less for production run (STP 57-005).

5.4 Inspect welds for external defects in accordance with weld quality requirements of STP 55-001.

5.5 Record results of all process control test specimens inspected.

6. Bonding

6.1 Verify cure cycle time and temperature, recorded on Shop Order.

6.2 Ultrasonically inspect all bondlines for voids, delaminations and in accordance with STP 55-001.

6.3 Inspect cleaning and anodizing per note 14, Dwg. 3307701.

6.4 Inspect "adhesive only" test specimens processed during bonding, route to Process Control Laboratory for testing. Record test results per STP 55-001.

6.5 Inspect all spotwelds radiographically for internal weld defects in accordance with STP 55-001.

6.6 Inspect adhesive bondline edges after curing for fillets per STP 55-001.

6.7 Inspect sealant application of bondlines per note 14 on Dwg. 3307701.

7. Weldbond Assembly Qualification

7.1 Both the test panel and flight article are inspected radio-graphically and ultrasonically per STP 55-001.

8. Weld Schedule Certification

8.1 Inspect test specimens for material and dimensions per STP 55-001.

8.2 Verify that test specimen have been cleaned in accordance with STP 57-005.

8.3 Verify that adhesive is proper material and is applied within time limits of cleaning and is within 168 hour certification limit per STP 55-001.

8.4 Verify that test specimens are welded within application time limits of the adhesive and identified to the weld schedule and weld machine per STP 55-001.

8.5 Verify that specimens are cured in accordance with STP 55-001. Record time and temperature.

8.6 Test specimens per STP 55-001.

8.7 Record results of test.

8.8 Approve the weld schedule when tests are acceptable.

9. Tool Inspection and Calibration

9.1 Tools and jigs used to control dimensional location of parts during assembly will be inspected and approved by Tool Inspection Department.

9.2 Welding equipment, recorders, and test machines are inspected and calibrated in accordance with approved schedules (STP 55-001).

10. Subassembly

10.1 Inspect fit-up of weldbond assemblies in fixture.

10.2 Inspect mechanical fastener installation and fay surface sealing.

10.3 Inspect installation of window details and miscellaneous hardware items.

10.4 Inspect cut-out side panel and fit-up of weldbond panel in side panel jig.

10.5 Inspect location of ring segments and skin trim lines to tool details.

10.6 Inspect finish touchup and identification.

9.4 Adhesive Acceptance and Process Control Tests

Lap shear, peel and adhesive bonded only specimens were fabricated and tested in accordance with Specification STM30-106. The adhesive bonded lap shear (L/t = 16) specimens were fabricated using two (2) 6-inch by 7.5-inch 0.063-inch-thick 7075-T6 bare aluminum alloy panels. The peel test panels were fabricated using 5-inch by 10-inch 0.025-inch-thick 7075-T6 bare aluminum alloy sheet and 5-inch by 8-inch 0.063-inch-thick 7075-T6 bare aluminum alloy sheet. The weldability specimens were fabricated using two (2) 5-inch by 6-inch 0.063-inch-thick 7075-T6 bare aluminum alloy panels. All of the test panels were assembled with Whittaker M6800 epoxy paste adhesive and cured at $270 \pm 10^{o}F$ for 60 minutes minimum. The test panels were machined into individual specimens and submitted to the Quality Assurance Laboratory where they were tested. The test results satisfied the requirements of STM30-106. Also, a sample of M6800 adhesive was tested for viscosity and solids content in accordance with the requirements of STM30-106.

Process control specimens was fabricated and tested during the several steps of weldbonding the C-130 static test and flight components. During the process control tests, it was determined that on one (1) three-sheet combination of the weldbonded joints had insufficient weld penetration depth. Review of the test results indicated no reduction in mechanical properties or joint quality. The spot-weld penetration requirements for three-sheet joint combinations having unequal outer sheet thicknesses were revised and incorporated in the weldbonded process specification, STP55-001.

9.5 Fabrication of the C-130 Weldbonded Fuselage Static Test Component

The forward and aft sections of the weldbonded fuselage component had to be weldbonded independently because of the 39-inch throat depth limitation of the spot-welding machine.

All detail parts for each section, including the Z-section ring segments and fuselage skins, were fabricated for assembly of the subject component. The detail parts and sub-assemblies to be weldbonded were prefitted in a shop aid jig to check fuselage station line dimensions, and the Z-section ring segments were checked for dimensional tolerances and mated to the fuselage skins. Upon completion of the prefit operation and rework as necessary, detail parts to be weldbonded were forwarded to the production spot-weld etch cleaning facility. After cleaning, the detail parts for each section that were to be weldbonded to the skin had the M6800 epoxy paste adhesive applied to their surfaces to be weldbonded, clamped to the fuselage skin in the spot-weld positioner tool, and then spot-welded. Figure 137 shows the spot-weld positioner with a portion of the forward fuselage section mounted for spot-welding. After spot-welding, the weldbonded sections were placed in the oven curing fixture and transported to the oven for curing. Each section was then cured at 270°F for 60 minutes minimum.

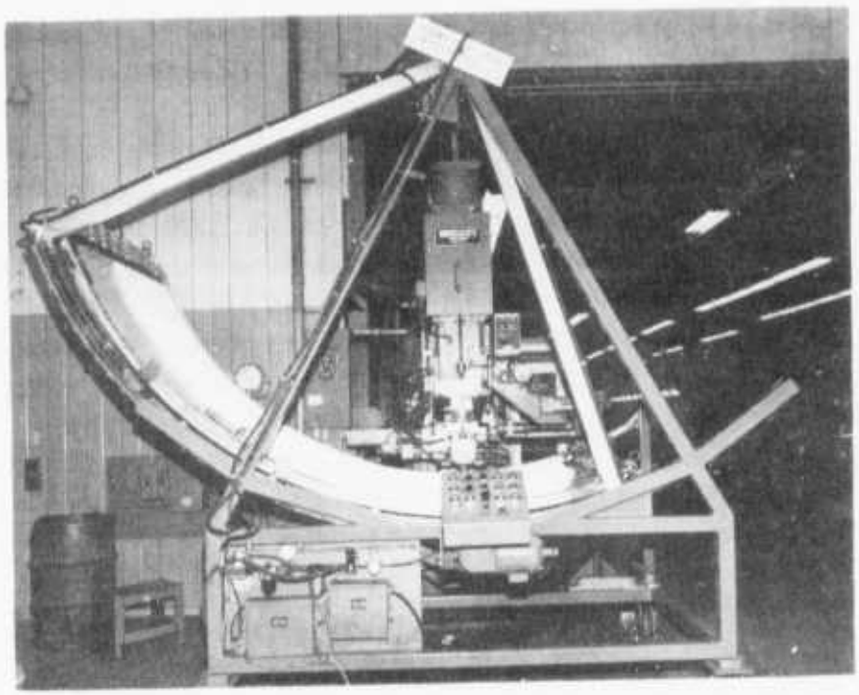

FIGURE 137 – PARTIAL WELDBONDED ASSEMBLY IN SPOT WELD POSITIONER

9.5.1 Inspection of the C-130 Weldbonded Fuselage Component

The forward and aft sections of the weldbonded fuselage component were inspected independently. All of the results from the process control specimen tests satisfied the requirements of STP 55-001 with the exception of spot-weld penetration requirements for one (1) joint thickness configuration described in Section 9.4. Results from the M6800 epoxy paste adhesive tests satisfied the requirements of the adhesive specification, STM 30-106.

Both forward and aft sections of the C-130 weldbonded fuselage components were radiographically and ultrasonically inspected. During the radiographic inspection of the forward section of the C-130 weldbonded fuselage component to be static tested, the first section to be weldbonded, nineteen (19) spot-weld defects that exceeded specification limits were detected out of a total of over 1200 spot-welds. All of the spot-weld defects detected appeared as small internal cracks within the spot-weld nuggets. This forward weldbonded section was visually inspected and squeeze-out of the adhesive in several of the joint fillets was not sufficient and repairs had to be accomplished after the section was cured. Small beads of adhesive were applied to the joint areas and cured. The Z-section heel-to-skin fillets were not uniform due to the radius at the heel of the Z-section stiffener.

After weldbonding the aft section of the C-130 weldbonded fuselage static test component, it was radiographically inspected and fourteen (14) spot-weld defects that exceeded specification limits were detected out of a total of over 1100 spot-welds. The type of defects detected were similar to those detected in the forward section. Also, the aft section of the weldbonded panel was ultrasonically inspected and several bondline voids were detected that exceeded the specification limits in the region extending approximately 5 to 8 inches from the ends of the section. It was decided not to repair these voids because in the fabrication of the static test article the tie-in brackets would extend over a length of 9 inches thus negating the need for repair. Also, vee-shaped longerons were to be mechanically fastened to the outside of the static test article and these would cover a significant percentage of the area in which the bondline voids occur. These longeron joints gave additional assurance of precluding any possible effect of the bondline voids during the static test.

Upon completing the inspections and adhesive repairs, both forward and aft weldbonded sections were mounted in the final weldbond component assembly tool shown in Figure 135 for mechanically splicing the sections. Also, other mechanical fastening operations were performed to complete the weldbonded fuselage component.

9.6 Fabrication of the C-130 Weldbonded Fuselage Flight Component

The detail parts, including the Z-section ring segments and skins, were fabricated for assembly of the flight component as they were for the static test component. Upon completing the weldbonding operations in fabrication of the static test component, the weldbonding operations were accomplished for the flight component in an identical seequence. Both forward and aft sections of the C-130 weldbonded fuselage flight component were radiographically and ultrasonically inspected after the weldbonded joints were cured. In the radiographic inspections, nine (9) spot-weld defects in the forward section and six (6) spot-weld defects in the aft section that exceeded specification limits were detected.

All of the spot-weld defects detected were internal cracks in the spot-weld nuggets very similar to those detected in the static test component. In the ultrasonic inspection of the forward weldbonded section, bondline voids on both ends of several of the weldbonded joints approximately five inches in length were detected. The cause of these bondline voids was attributed to the sharp angle (approximately 30 degrees) that the weldbonded joints at the ends of the sections make with the horizontal during cure causing run-out of the epoxy paste adhesive. In the ultrasonic inspection of the aft weldbonded section, bondline voids on both ends of several of the weldbonded joints approximately two to five inches in length were detected. Also, one of the aft weldbonded section Z-ring frame-to-skin joints contained two edge void approximately four inches in length. All bondline voids were repaired with a room temperature curing adhesive.

Upon completing the adhesive repairs, both forward and aft weldbonded sections were finished independently. Figure 138 shows the completed forward section (i.e., fuselage station 280 to 337) of the C-130 weldbonded flight component ready for finishing the interior surfaces prior to splicing to the aft section. Each section was finished as described in Section VII.

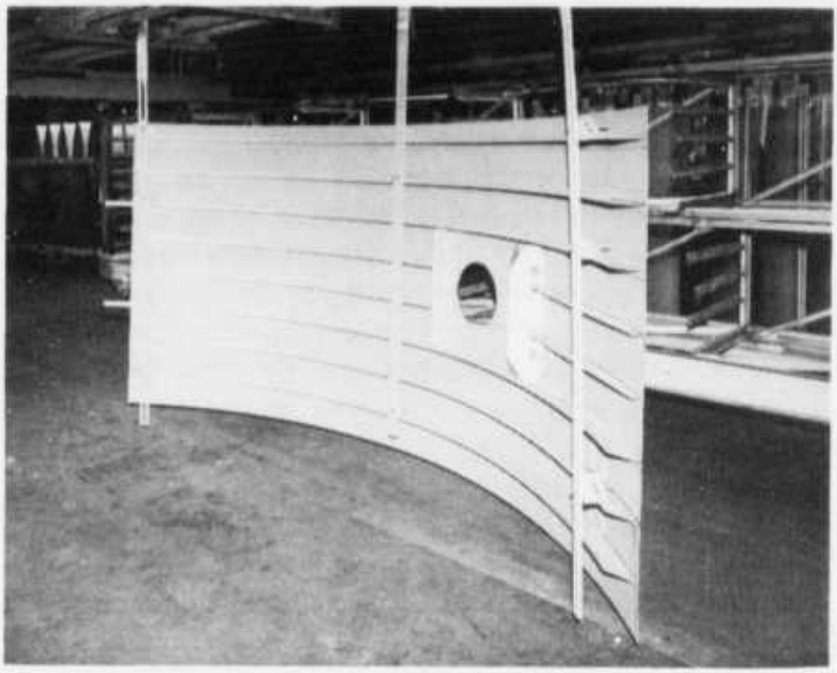

FIGURE 138 – WELDBONDED SECTION READY FOR FINISHING INTERIOR SURFACES

After finishing both forward and aft weldbonded sections, they were mechanically spliced to form the weldbonded flight component. Then the weldbonded flight component was assembled into a larger fuselage panel assembly to facilitate production line operations.

9.6.1 Assembly of Weldbonded Flight Component Into the Production Fuselage Panel

A production fuselage side panel was obtained from the C-130 inventory. This panel had been fabricated by Scottish Aviation Company, Ltd., and is identified as part number 388005-29. This panel was mounted in a special built jig fixture for incorporation of the weldbonded component. Figure 139 shows the production fuselage side panel mounted in the jig fixture. The center section of the production fuselage side panel was removed to accommodate the installation of the weldbonded flight component. Figure 140 shows the center section (i.e., fuselage station 280 to 387) of the production fuselage side panel being removed. Using the same jig fixture, the weldbonded flight component was mechanically spliced to the forward and aft sections of the production fuselage panel at fuselage stations 280 and 387.

This modified fuselage panel was installed into the C-130 fuselage in an identical manner as regular production fuselage side panel.

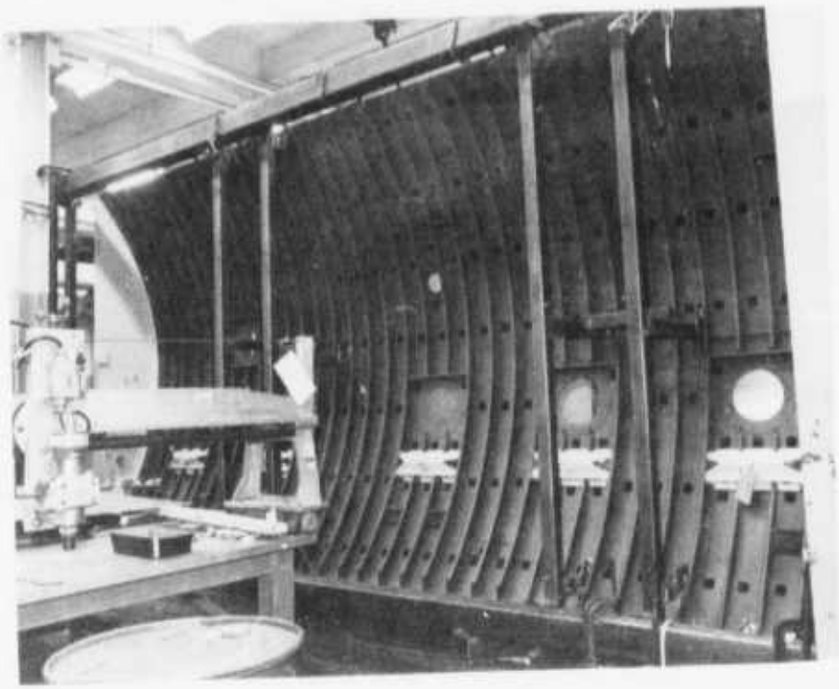

FIGURE 139 – FUSELAGE SIDE PANEL MOUNTED IN JIG FIXTURE

FIGURE 140 – CENTER SECTION OF FUSELAGE SIDE PANEL BEING REMOVED

SECTION X

STRUCTURAL TESTS

10.1 Structural Test Plan

A structural test plan that described the necessary component tests as part of the structural qualification requirements was prepared, reviewed and approved by the Air Force Project Managers. The plan principally consisted of a full-scale static test and a sub-scale fatigue test and was released as a separate document.

10.1.1 Sub-Scale Fatigue Test Plan

The purpose of the flat sub-scale fatigue test was to evaluate the effect of "pillowing deformation" on the weldbonded joints caused by cyclic pressure loads. The effect of "pillowing deformation" on the peel characteristics of weldbonded joints caused by cyclic pressure loads was the only loading condition not evaluated in other program tests. A sub-scale test panel could be used to evaluate the "pillowing deformation" effect as well as a full-scale test component. However, an adjustment in the peak cyclic pressure applied to the flat sub-scale test panel was necessary because the normal bondline stresses in the weldbonded joints are not relieved by hoop tension action as in the joints of the curved fuselage component. Thus, the peak cyclic pressure applied to the flat weldbonded test panel was reduced from that applied to the curved fuselage component to achieve comparable normal bondline stresses. The flat sub-scale weldbonded test panel was fabricated with weldbonded joint and splice configurations identical to the C-130 weldbonded fuselage component. Successful completion of the sub-scale fatigue test would give added confidence to successful in-service performance of the C-130 weldbonded fuselage component.

10.1.2 Full-Scale Static Test Plan

The objective of the full-scale static test was to compare the shear strength of the weldbonded fuselage component to the standard production riveted component. This type test was conservative and not representative of loads applied in the actual airplane; however, comparative strengths could be obtained from the shear test which would contribute toward qualifying the weldbonded component for flight evaluation.

The static test article was a triangular-shaped barrel section which consisted of three curved fuselage components joined together to form a closed structural assembly. One of the curved fuselage components was weldbonded and was designated the "test" component and the remaining two components were standard riveted components which served as "dummy" components. All three curved fuselage components were instrumented with back-to-back strain gages for collecting strain data during the course of the test.

10.2 Sub-Scale Flat Weldbonded Panel Fatigue Test

A flat weldbonded panel and test fixture were designed and fabricated for conducting the subject test. The goal of the fatigue test was for the test panel to sustain four (4) lifetimes of cyclic pressures without the weldbonded joints or splice suffering structural failure. The flat panel design and fabrication, test fixture, test apparatus, and test results are described in subsequent paragraphs.

10.2.1 Sub-Scale Weldbonded Fatigue Test Panel Design and Fabrication

A sub-scale weldbonded panel was designed and fabricated as required by the Structural Test Plan. The flat test panel consisted of three (3) Z-section stiffeners weldbonded to flat aluminum alloy sheet as shown in Figure 141. The sheet was spliced at the center stiffener and the spliced joint configuration was identical to that of one of the C-130 weldbonded fuselage component spliced joints. The -1 Z-section stiffener was formed from 0.063 inch 7075-T6 bare sheet, the -2 Z-section stiffener was formed from 0.071 inch 7075-T6 bare sheet, and the -3 Z-section stiffener was formed from 0.050 inch 7075-T6 bare sheet. The cross-sectional dimensions of the Z-section stiffeners were identical to the C-130 fuselage Z-section rings. All weldbonded joints were fabricated with M6800 epoxy paste adhesive. Upon completion of the weldbond operations, the side of the test panel on which the Z-section stiffeners were located was finished similarly to the interior surface of the aft section of the weldbonded fuselage panel to be flight evaluated. The finish system applied to the test panel was as follows:

1. After weldbonding the assembly, chromic acid anodize the entire test panel omitting the deoxidizing step in the anodize process,

2. All weldbonded joints were fillet sealed with STM 40-111 corrosion inhibiting sealant, and

3. The entire test panel was finished with two (2) coats of MIL-P-8585 zinc chromate primer.

10.2.2 Sub-Scale Fatigue Test Fixture and Control Equipment

A rectangular steel box fixture was fabricated so that the flat weldbonded test panel could be mechanically attached to the fixture with a pressure sealed joint. Figure 142 shows the test panel mounted in the fixture with the instrumentation installed. The side of the fixture opposite the test panel was removable in order to provide access for attachment of the Z-section stiffeners to the fixture. The center Z-section stiffener on the test panel was attached to a rigid steel angle that was welded to the test fixture frame. The vertical web of the center Z-section stiffener was sandwiched between a thick aluminum clamp bar and the rigid steel angle, and the sandwich joint was mechanically fastened for the full length of the stiffener. Each end of the two (2) outer Z-section stiffeners was attached to the test fixture by angle clips using mechanical fasteners.

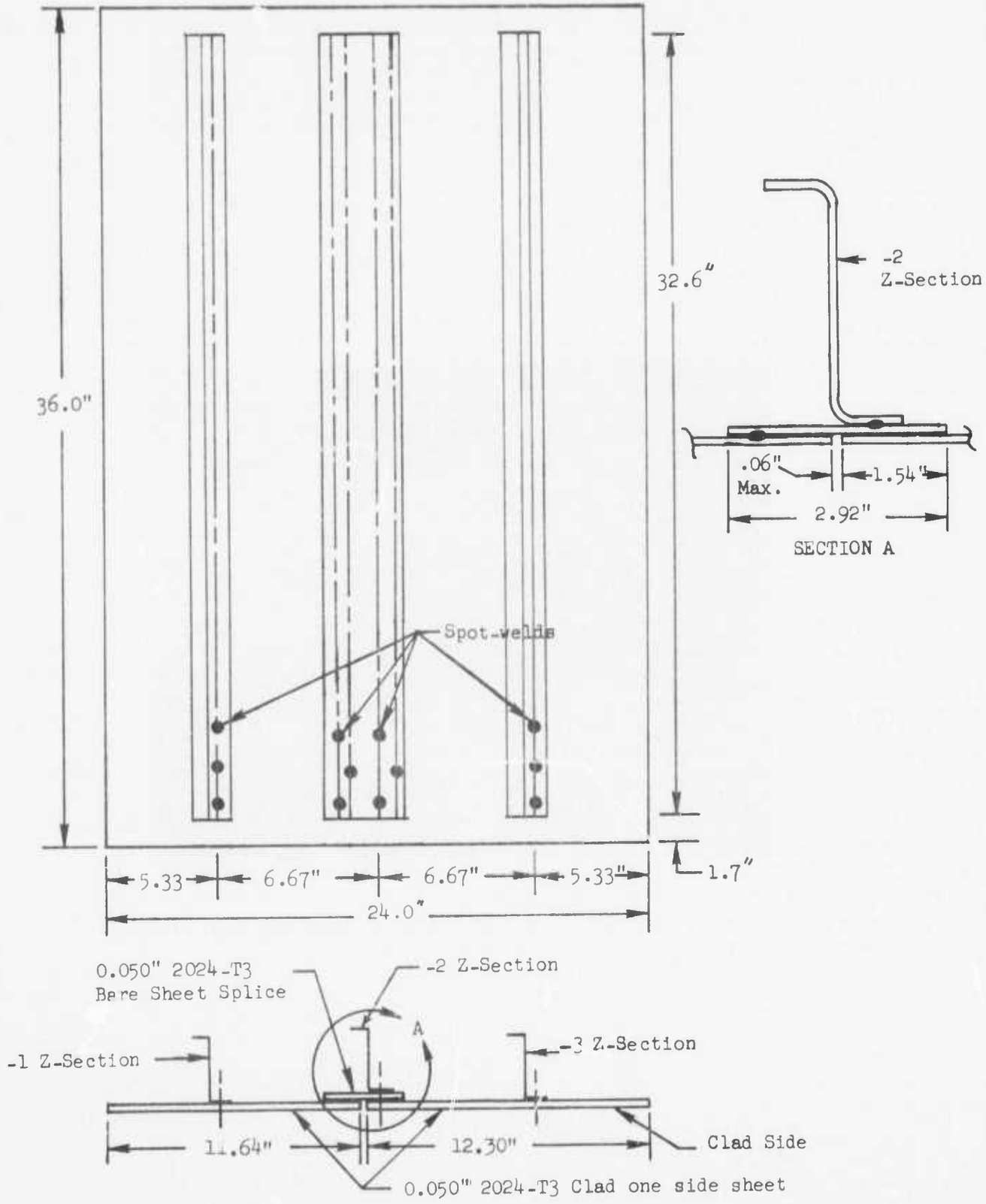

NOTE: Spot-weld spacing for all weldbonded joints, single row or double row, is 1.05 inches. End spot-weld edge distance is 0.30 inches.

FIGURE 141 – SUB-SCALE WELDBONDED FATIGUE TEST PANEL

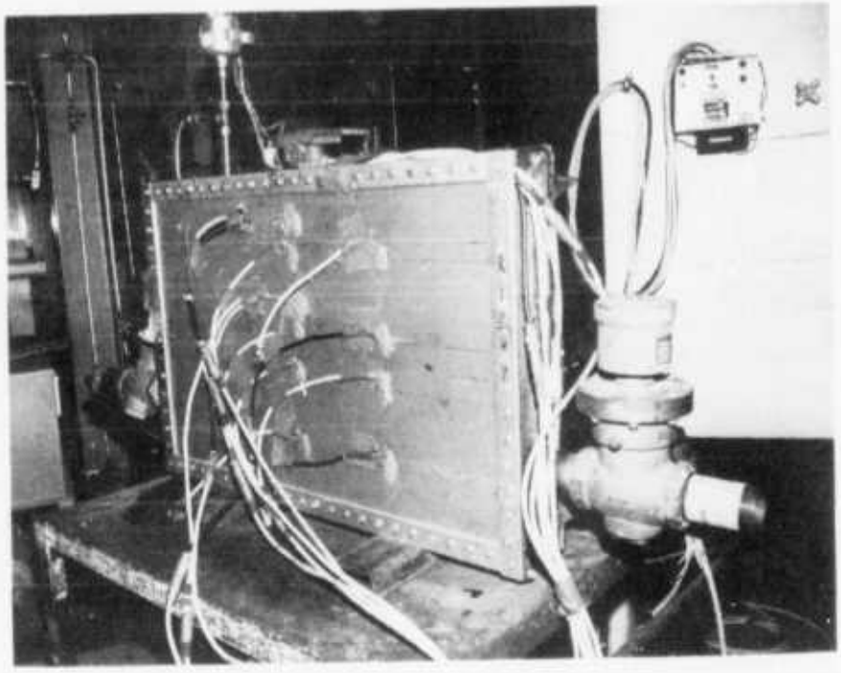

FIGURE 142 – INSTRUMENTED TEST PANEL IN PRESSURE TEST FIXTURE

The test fixture and associated control equipment are shown in Figure 143. Regulated air was used to cyclically apply pressure to the flat weldbonded test panel through a solenoid operated inlet valve located in one end of the test fixture. A solenoid operated dump valve was located in the end of the test fixture opposite the inlet valve. The maximum and minimum applied pressures were sensed by a pressure switch which in turn operated the inlet and dump valves through an electrical relay control system. The maximum and minimum applied pressures were mechanically adjustable through the pressure switch. A mercury manometer was used to establish the maximum and minimum applied test pressures and also to monitor the static pressure during the strain surveys. Cyclic pressure was monitored on a calibrated pressure gage and the number of applied pressure cycles was monitored on an electrically operated digital counter.

A mechanical safety valve was located at the top of the test fixture to relieve the pressure in the event of a system malfunction. Other safety precautions were taken relative to personnel safety in the test area to prevent injury from fragmentation damage in event of test panel failure.

Prior to installing the flat weldbonded test panel in the test fixture, it was instrumented with two (2) back-to-back strain rosettes and eight (8) axial strain gages. Strain recordings were made with a standard strain indicator.

10.2.3 Development of Peak Pressure to be Applied in Sub-Scale Fatigue Test

The development of a peak pressure to be applied to the sub-scale fatigue test panel was necessary. This pressure was chosen to match the normal bondline stresses in the test panel with comparable curved fuselage component stresses. A finite element analysis of the flat weldbonded fatigue test panel was accomplished along with a similar analysis of the curved weldbonded fuselage component. Finite element models were constructed for both the flat weldbonded test panel and the curved weldbonded airplane fuselage component. These models are shown on Figure 144 and 145.

Each model represented a unit width of each panel assembly. For analysis purposes, it was assumed that the flat test panel was symmetrical about the center Z-section stiffener. The splice plate located at the center Z-section stiffener and the skin was modeled as individual components connected by spring elements which represented the adhesive bond in the weldbonded joints. The Z-section stiffener flanges were modeled as individual components by beam elements and were connected to the skin and splice plate by spring elements which represented the adhesive bond. The pressure loading was applied to the finite element model as a running load and was coupled with an imposed displacement at the outer Z-section stiffener. The flat test panel was assumed to be rigidly supported at the center Z-section stiffener and the outer-most edge of the panel. The imposed displacement was calculated by considering the outer Z-section stiffener as a simply supported beam subjected to a uniform running load representing a strip of pressure loading six inches in width.

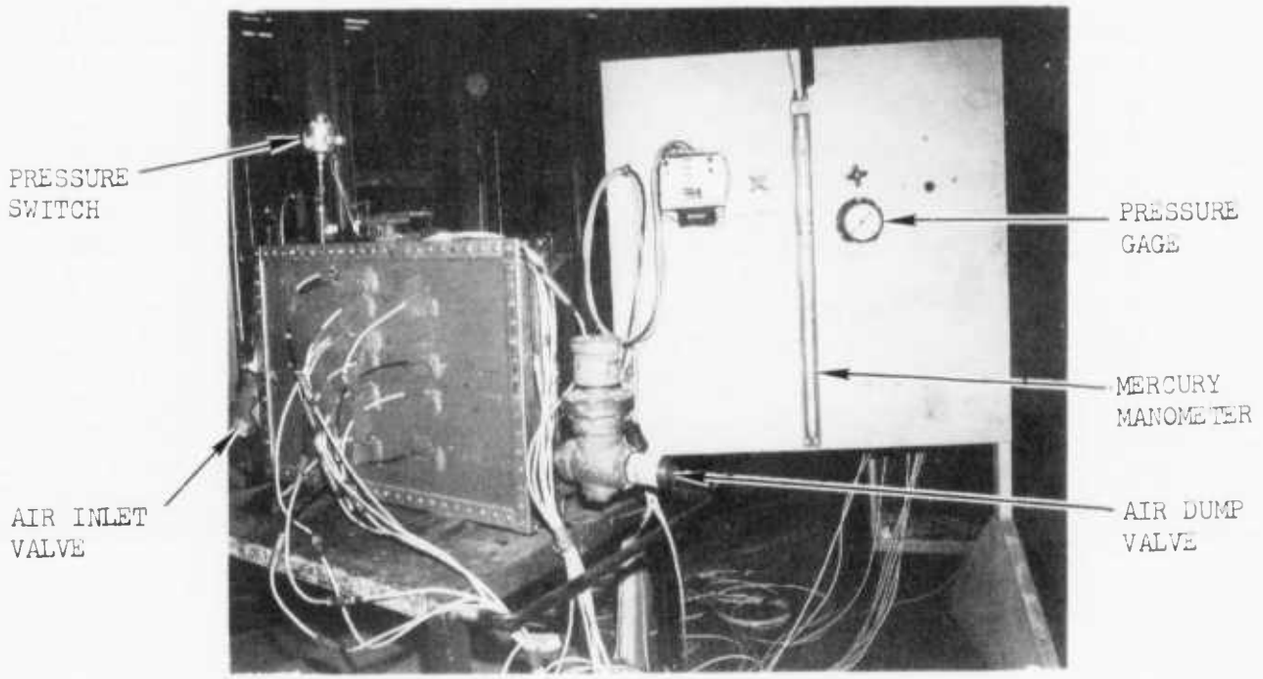

FIGURE 143 – GENERAL FATIGUE TEST ARRANGEMENT

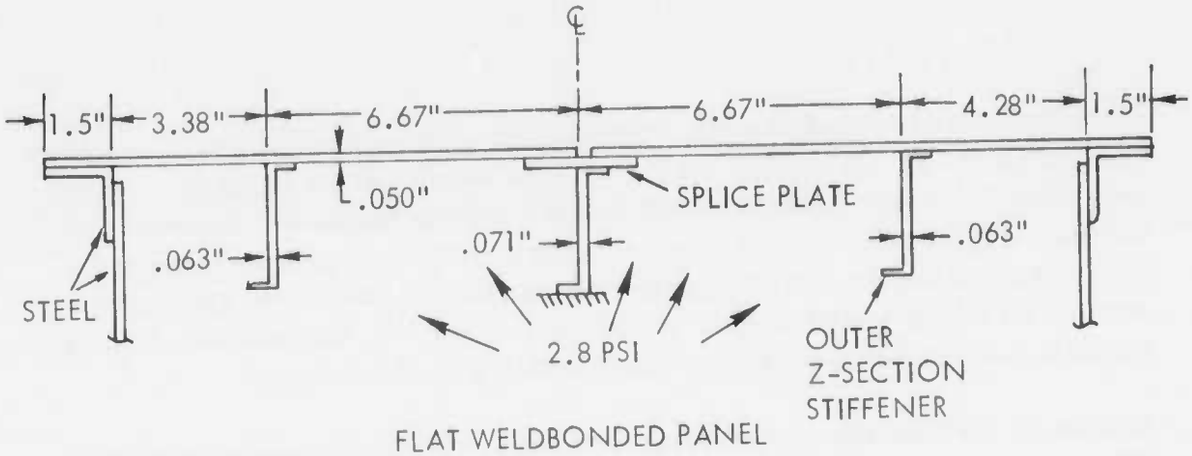

FLAT WELDBONDED PANEL

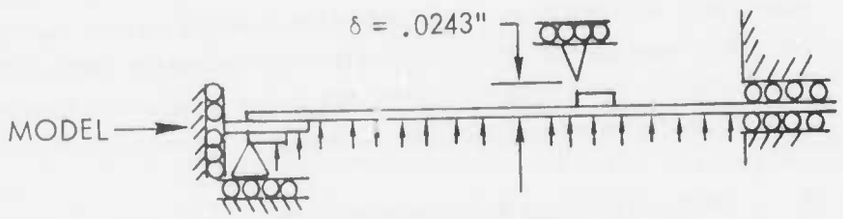

FIGURE 144. FINITE ELEMENT MODEL CONFIGURATION OF THE FLAT WELDBONDED TEST PANEL

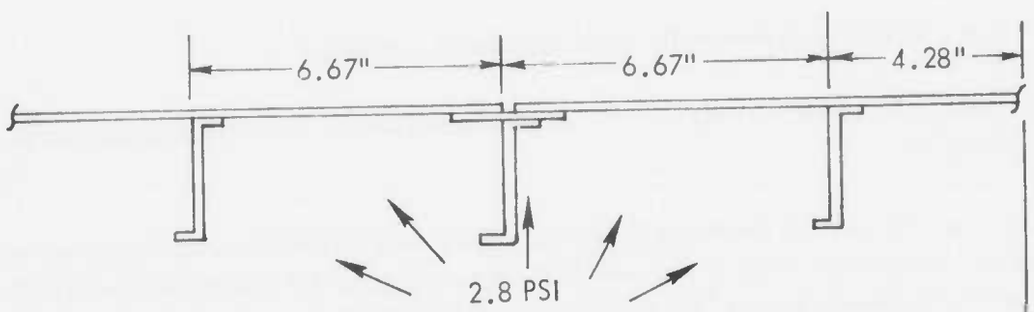

C-130 FUSELAGE PANEL

ELASTIC FOUNDATION
REPRESENTING CURVATURE

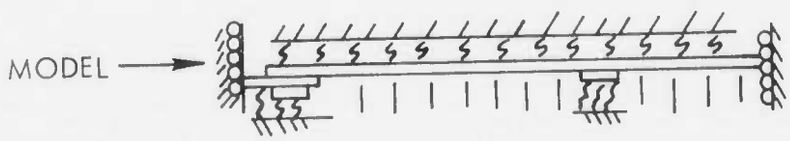

FIGURE 145. FINITE ELEMENT MODEL CONFIGURATION OF THE C-130 WELDBONDED FUSELAGE PANEL

The analysis of the curved weldbonded airplane fuselage component utilized a finite element model similar to the one used for the flat test panel except that the effects of curvature were included. The skin, splice plate and Z-section stiffener flanges were modeled in an identical manner to those elements in the flat test panel model. Spring elements representing the curvature of the skin and Z-section stiffeners were used to support the finite element model in the vertical (radial) direction as depicted on Figure 145. The pressure loading was applied as a running load in an identical manner to that for the flat test panel.

Solutions of the finite element models were performed on the digital computer from which stiffener reaction forces in pounds per inch and normal stresses in the bondlines were obtained. The development of the peak pressure that was applied in the sub-scale fatigue test culminated from results of the finite element model solutions. The approach in determining the peak pressure was to determine a factor which reduced the 7.5 pounds per square inch of pressure to a peak pressure that would develop normal stresses in the flat test panel that were comparable to those stresses in the curved weldbonded fuselage component. The factor was computed by ratioing the curved weldbonded fuselage component results to those of the flat test panel from the following:

a. Ratio of stiffener frame reaction forces,

b. Ratio of normal stresses in outer Z-section stiffener-to-skin bondline,

c. Ratio of normal stresses in the splice plate-to-skin bondline,

d. Ratio of normal stresses in the splice plate-to-center Z-section stiffener flange bondline,

The maximum ratios from the above are listed in Table LIX. The maximum ratios are given because a minimum reduction in the peak operation pressure of 7.5 pounds per square inch was required for development of the peak pressure to be applied to the flat weldbonded test panel.

Table LIX – Computed Factors for Development of Peak Pressure for Sub-Scale Fatigue Test

Bondline Location or Stiffener Load	Curved Aircraft Structure Load or Stress	Flat Test Panel Load or Stress	Factor to be Applied to Pressure
Outer Z-section Stiffener Load, lbs./in.	13.00	38.10	0.341
Center Z-section Stiffener Load, lbs./in.	8.08	28.97	0.279
Outer Stiffener-to-Skin Bondline Stress, psi	6,560	17,600	0.370
Splice Plate-to-Skin Bondline Stress, psi	2,380	7,150	0.333
Splice Plate-to-Stiffener Bondline Stress, psi	1,935	7,740	0.250

It is noted that compression stresses in the bondlines were not considered in computation of the factors given in the above table because compression stresses do not give rise to bondline delaminations.

The peak pressure that was applied in the sub-scale fatigue test was computed by multiplying the C-130 cabin peak operating pressure of 7.5 pounds per square inch by the maximum factor of 0.370 in the above table. The computation gave a peak test pressure of 2.8 pounds per square inch which was applied to the flat test panel. It was impractical to apply various factors at several locations on the flat test panel because the loading was normal pressure. Thus, the application of the peak pressure computed with the maximum factor from the above table assures development of a comparable normal stress in the bondline at one location in the flat-test panel to the normal stress in the curved weldbonded component, and at all other locations the normal stresses in test panel bondlines are greater than comparable stresses in the curved weldbonded fuselage component.

Figures 146, 147, and 148 show a comparison of normal bondline stresses in the test panel for an applied pressure of 2.8 pounds per square inch to normal bondline stresses in the aircraft structure which is subjected to 7.5 pounds per square inch. Figure 146 shows the normal stress distribution in the outer Z-section stiffener-to-skin bondline, Figure 147 shows the normal stress distribution in the splice plate-to-skin bondline, and Figure 148 shows the normal stress distribution in the splice plate-to-center Z-section stiffener bondline.

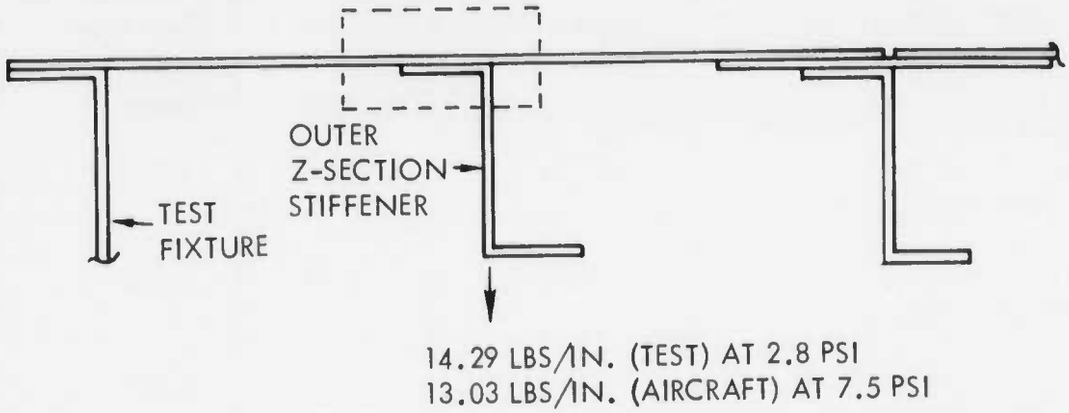

(NOTE: WHERE BROKEN LINE IS NOT SHOWN, "AIRCRAFT" AND "TEST" ARE COINCIDENT)

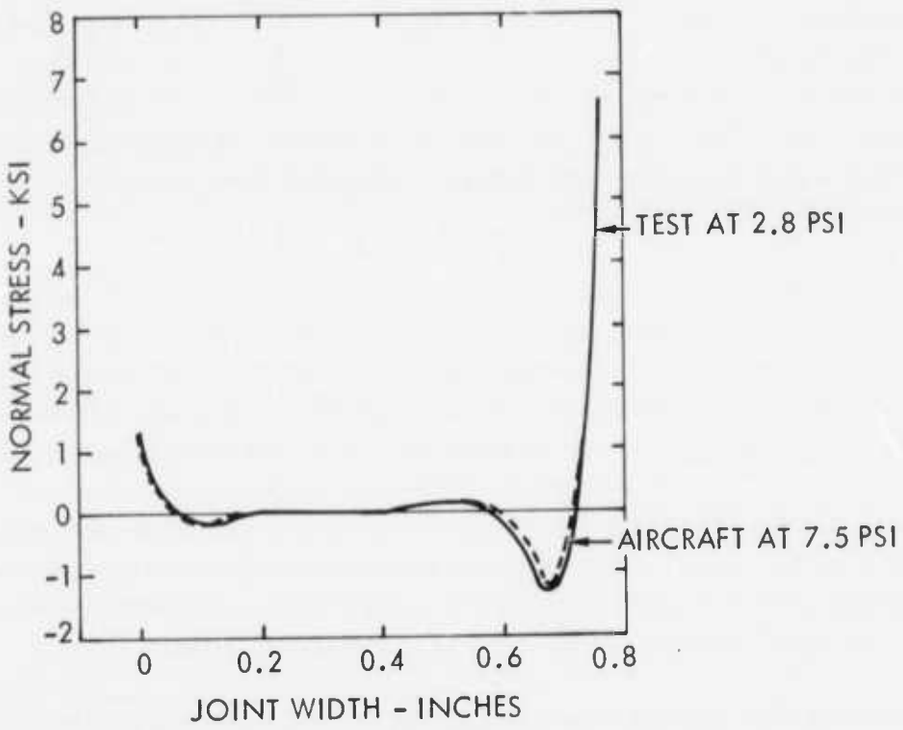

FIGURE 146. NORMAL STRESS DISTRIBUTION IN THE OUTER Z-SECTION STIFFENER-TO-SKIN BONDLINE

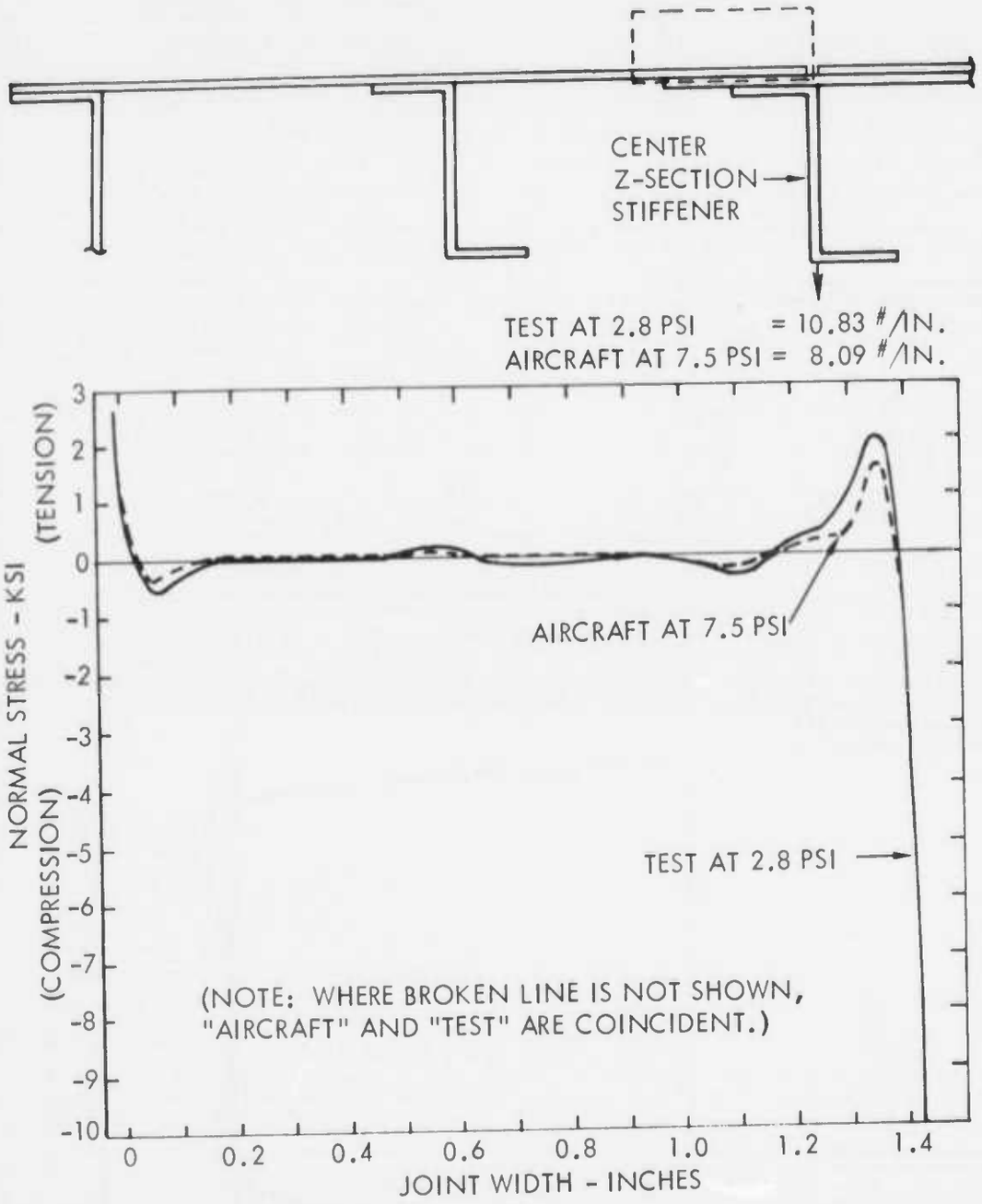

FIGURE 147. NORMAL STRESS DISTRIBUTION IN THE SPLICE PLATE-TO-SKIN BONDLINE

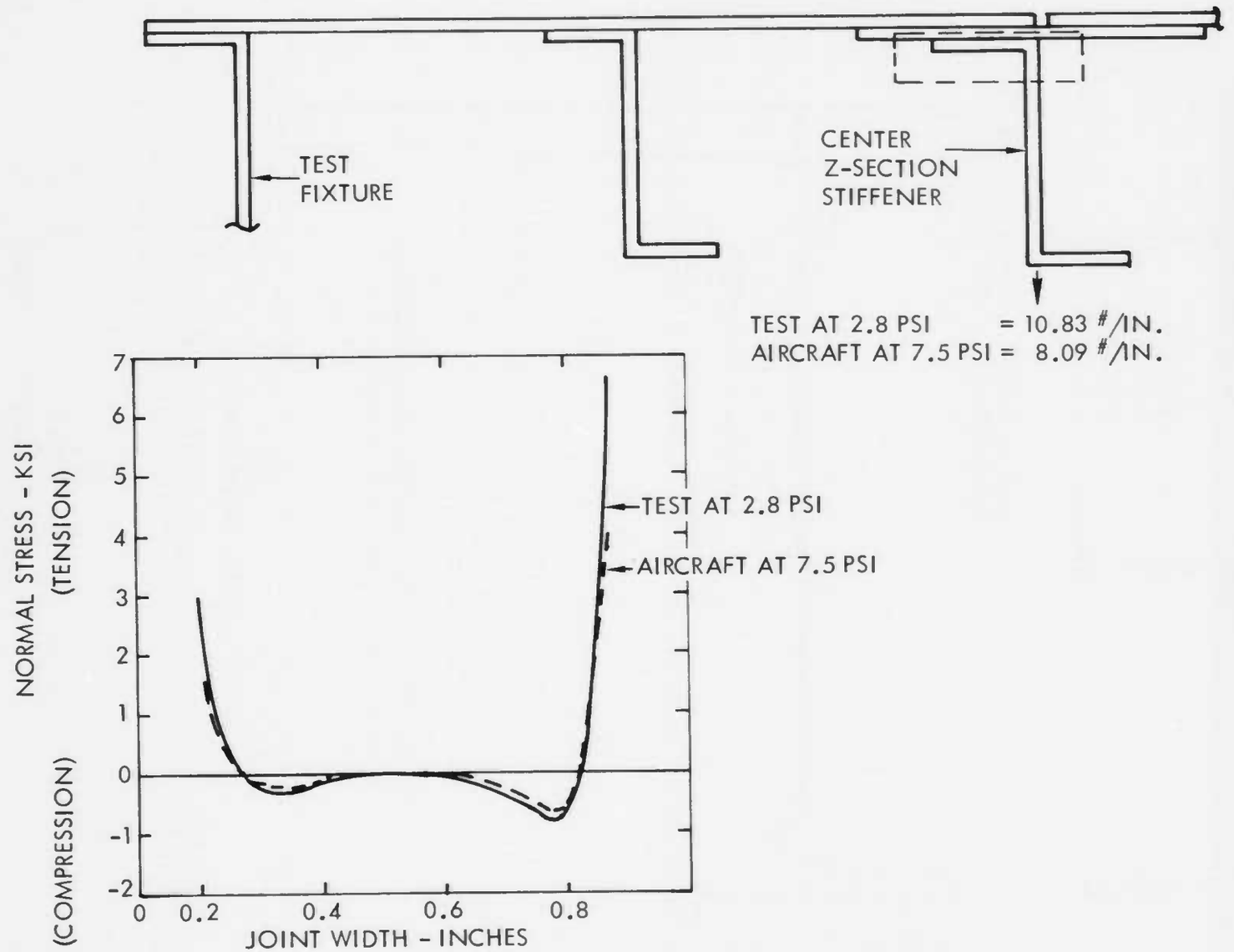

FIGURE 148. NORMAL STRESS DISTRIBUTION IN THE SPLICE PLATE-TO-CENTER Z-SECTION STIFFENER BONDLINE

10.2.4 Sub-Scale Flat Weldbonded Fatigue Test Results

The flat weldbonded test panel was installed in the test fixture and instrumentation installed as shown in Figure 149. The instrumentation consisted of two (2) backed-up strain rosettes and eight (8) axial strain gages. The strain rosettes were located on the panel skin while the axial gages were located at the heel of the stiffeners and splice plate edges. During the test, strain recordings for the strain gages and rosettes were accomplished with a standard strain indicator. The flat weldbonded test panel was pressure cycled from 0 to 2.8 pounds per square inch for four (4) lifetimes with each lifetime having 5,000 pressure cycles. Strain measurements were recorded at 0, 1/4, 1/2, 1, 1 1/2, 2, 3 and 4 lifetimes. All strain measurements were recorded with the test panel subjected to 2.8 pounds per square inch. Figure 150 shows plots of the strain measurements in micro inches per inch versus lifetime. This figure shows plots of the axial strains only since they were the only gages over the weldbonded joints. These strain data plots show no significant reductions over the four lifetimes, and it is concluded that the weldbonded joints in the test panel suffered no structural degradation at the gage locations.

During and prior to the fatigue test, the weldbonded joints in the flat test panel were inspected by the contact ultrasonic technique. The inspections were accomplished from the skin side of the test panel while it was installed in the test fixture as shown in Figure 143. The contact ultrasonic inspections were accomplished with equipment calibrations that were set to detect bondline defects less than the specification limit of 0.16 square inches.

Radiographic inspection of the spot-welds in the test panel's weldbonded joints revealed a total of thirteen (13) spot-welds that had internal cracks in the nuggets out of a total of 170 spot-welds. Seven (7) of the internal cracks were located in spot-welds in one of the outer Z-section stiffener-to-flat sheet weldbonded joints, and six (6) of the internal cracks were located in the center weldbonded splice.

Upon completing the four (4) lifetimes of cyclic pressure testing, the test panel was removed from the test fixture. It was disassembled into four (4) parts for immersion ultrasonic inspection. C-scans were developed on the weldbonded joints at a sensitivity level consistent with bondline specification requirements. The C-scans did not confirm the presence of many of the disbonds indicated by the contact ultrasonic inspections, but growth of some of the disbonds corroborated the contact ultrasonic inspection findings. Visual inspection of the filleted weldbonded joints revealed no cracks. The weldbonded joints in the four (4) parts of the flat test panel were disassembled and a visual inspection of the failed joint surfaces closely confirmed the C-scans developed during the immersion ultrasonic inspection.

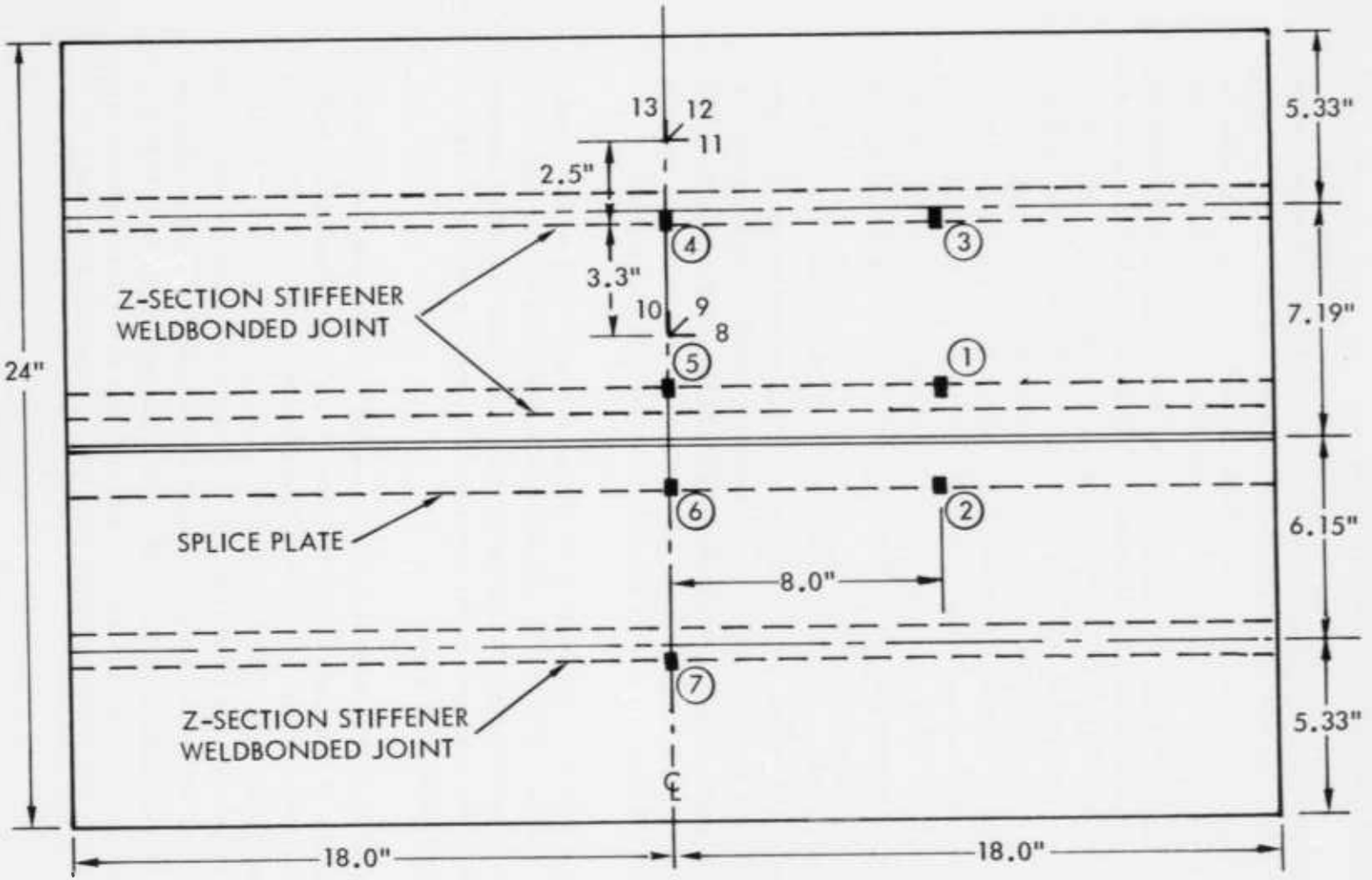

FIGURE 149. FLAT WELDBONDED TEST PANEL INSTRUMENTATION LAYOUT

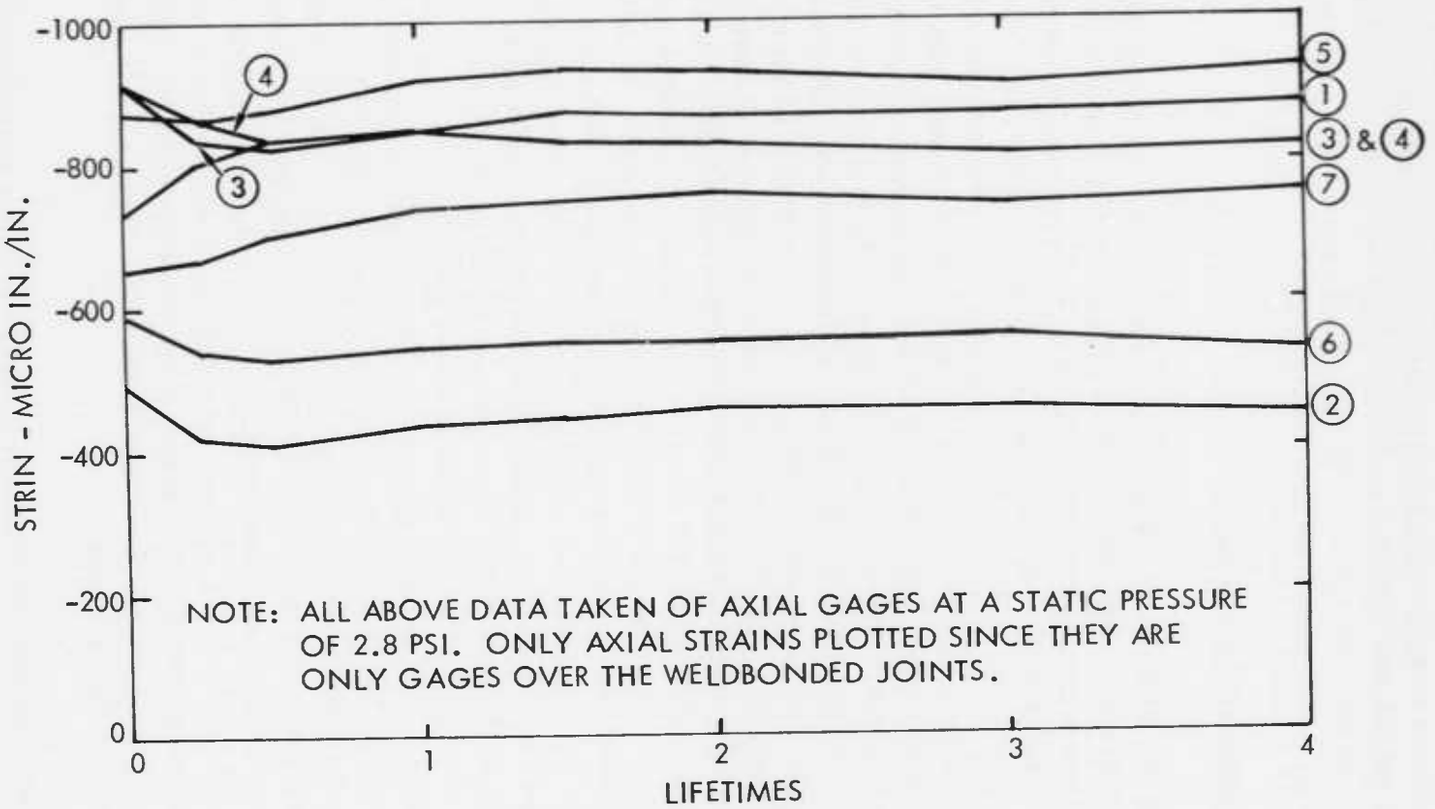

FIGURE 150. WELDBONDED SUB-SCALE FATIGUE TEST PANEL STRAIN SURVEY DATA

10.3 Full-Scale Weldbonded Component Static Test

A full-scale static test article containing a C-130 weldbonded fuselage component and associated test fixture were designed and fabricated for conducting the subject test. The primary objective of the static test was to determine the comparative shear strengths of the weldbonded and standard riveted C-130 fuselage components. As described in the Structural Test Plan, the full-scale static test article was located in a cubical universal test fixture and torsional shear loads introduced into the test article by two (2) large hydraulic jacks through a steel torque arm attached to the top of the test article.

10.3.1 Full-Scale Static Test Article

The static test article was a triangular-shaped barrel section comprising three (3) curved fuselage components which were joined by special gussets and splice plates. One of the threee (3) curved components was representative of the weldbonded fuselage component that was installed in the C-130 airplane and was designated the "test" component. The remaining two (2) curved components were standard riveted components and served as "dummy" components. The "dummy" components were removed from two (2) larger standard riveted fuselage side panels. One of the larger fuselage side panels was procured from the fabricator, Scottish Aviation Company, Ltd., as a separate item under this program. The second larger fuselage side panel was obtained from C-130 airplane inventory. A special steel jig fixture was fabricated for use in the removal of the standard riveted fuselage component using the first of the larger standard riveted fuselage panels as a dimensional guide. Figure 139 shows the larger standard riveted fuselage side panel mounted in the steel jig fixture. Figure 140 shows the center section of a riveted fuselage side panel being removed for use in assembly of the full-scale static test article. The weldbonded and two (2) standard riveted fuselage components were arranged to form the triangular barrel section with the ends connected by special gussets and splice plates. Figures 151 and 152 show the two (2) "dummy" components connected to form two-thirds of the static test article. The weldbonded fuselage component was similarly connected to the ends of the "dummy" components. Side plates that were nine (9) inches in width were mechanically fastened to the outside surface of the end of each component that was joined. A vee-shaped plate longeron was then mechanically installed over the side doubler plates at the three (3) static test article joints which completed the outside surface assembly of the static test article. The Z-section ring frames of the three (3) curved fuselage components were joined with special plate gussets that were mechanically fastened to the webs of the Z-section ring frames. A significant number of structural shims and filler plates had to be used when installing the plate gussets due to mismatch of the Z-section ring frames. Incorporation of the shims and fillers because of mismatch between the Z-section ring frames eliminated residual stresses in the ring frames.

The static test article was instrumented with back-to-back axial and shear strain gages prior to positioning the static test article in the test fixture. A total of 108 channels were provided for strain recordings with 57 channels located on the weldbonded fuselage component. Strain gage locations are shown on Figures 153, 154, and 155. All shear gages were installed on the fuselage skin midway between Z-section ring frames.

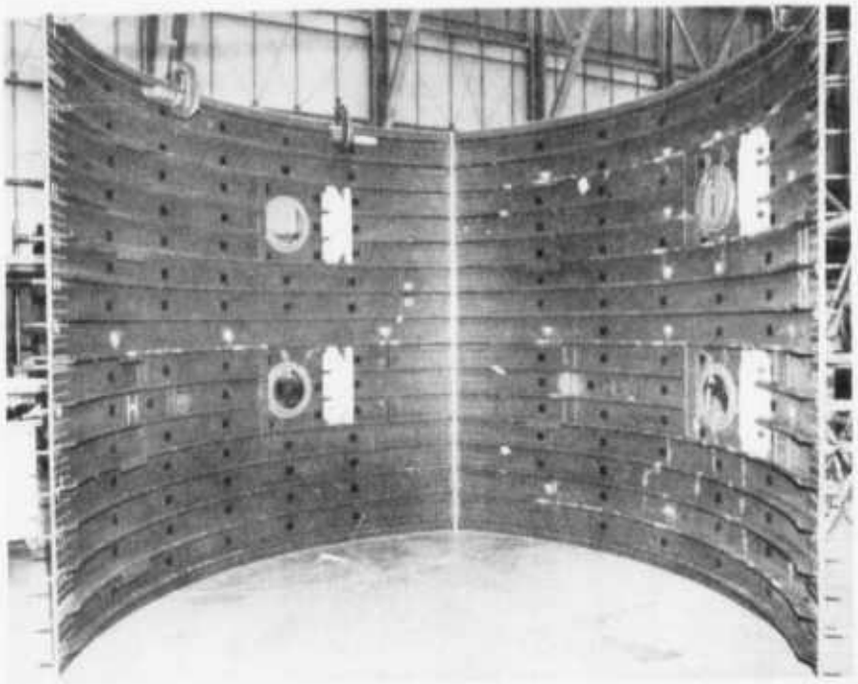

FIGURE 151 – INSIDE VIEW OF PARTIALLY ASSEMBLED TEST ARTICLE

FIGURE 152 – OUTSIDE VIEW OF PARTIALLY ASSEMBLED TEST ARTICLE

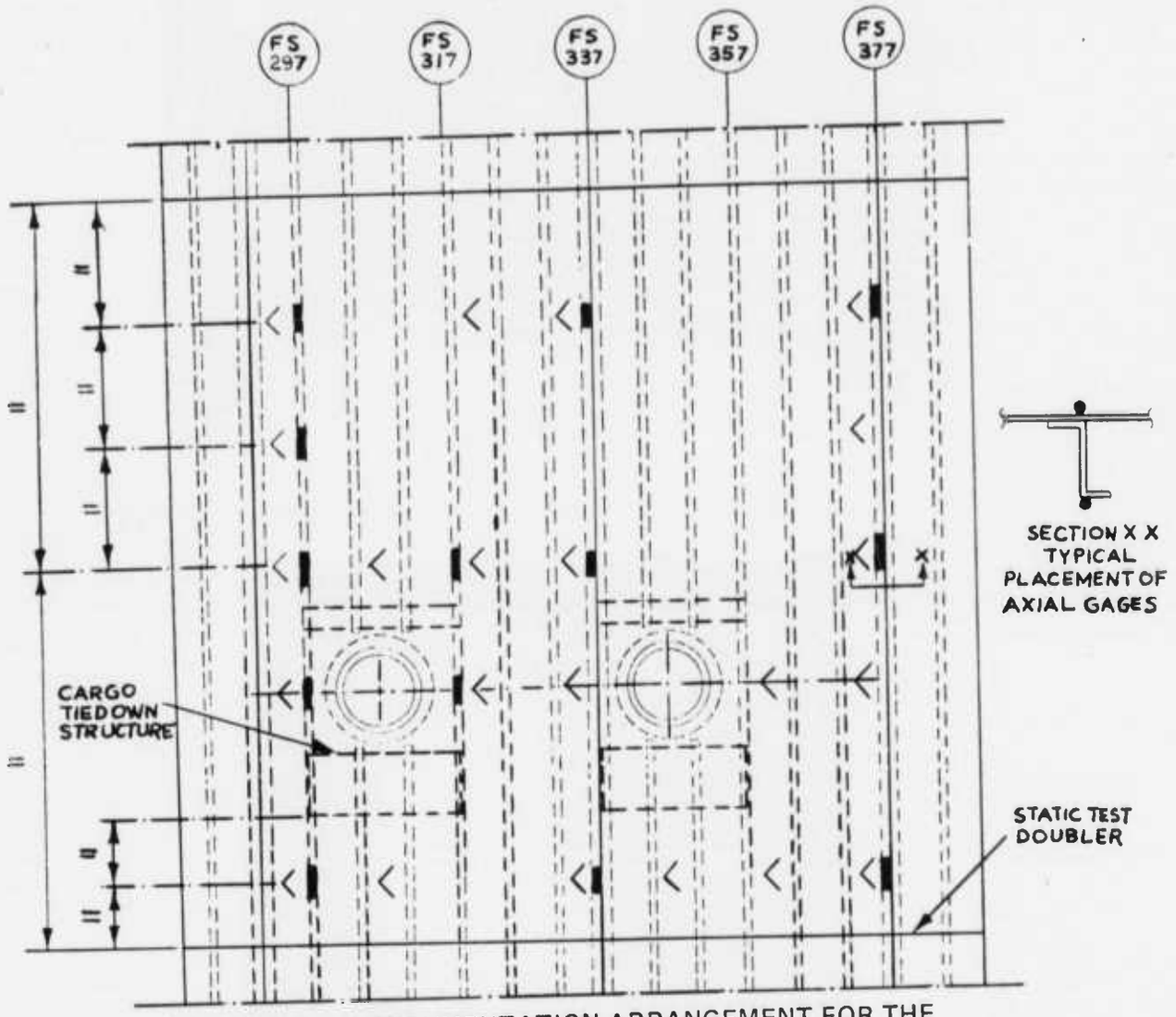

FIGURE 153 – INSTRUMENTATION ARRANGEMENT FOR THE WELDBONDED COMPONENT

NOTES: 1) < denotes shear type strain gage.
2) ▬ denotes axial type strain gage.
3) All shear gages mounted midway between frames.
4) Dimensions marked = means equally spaced.

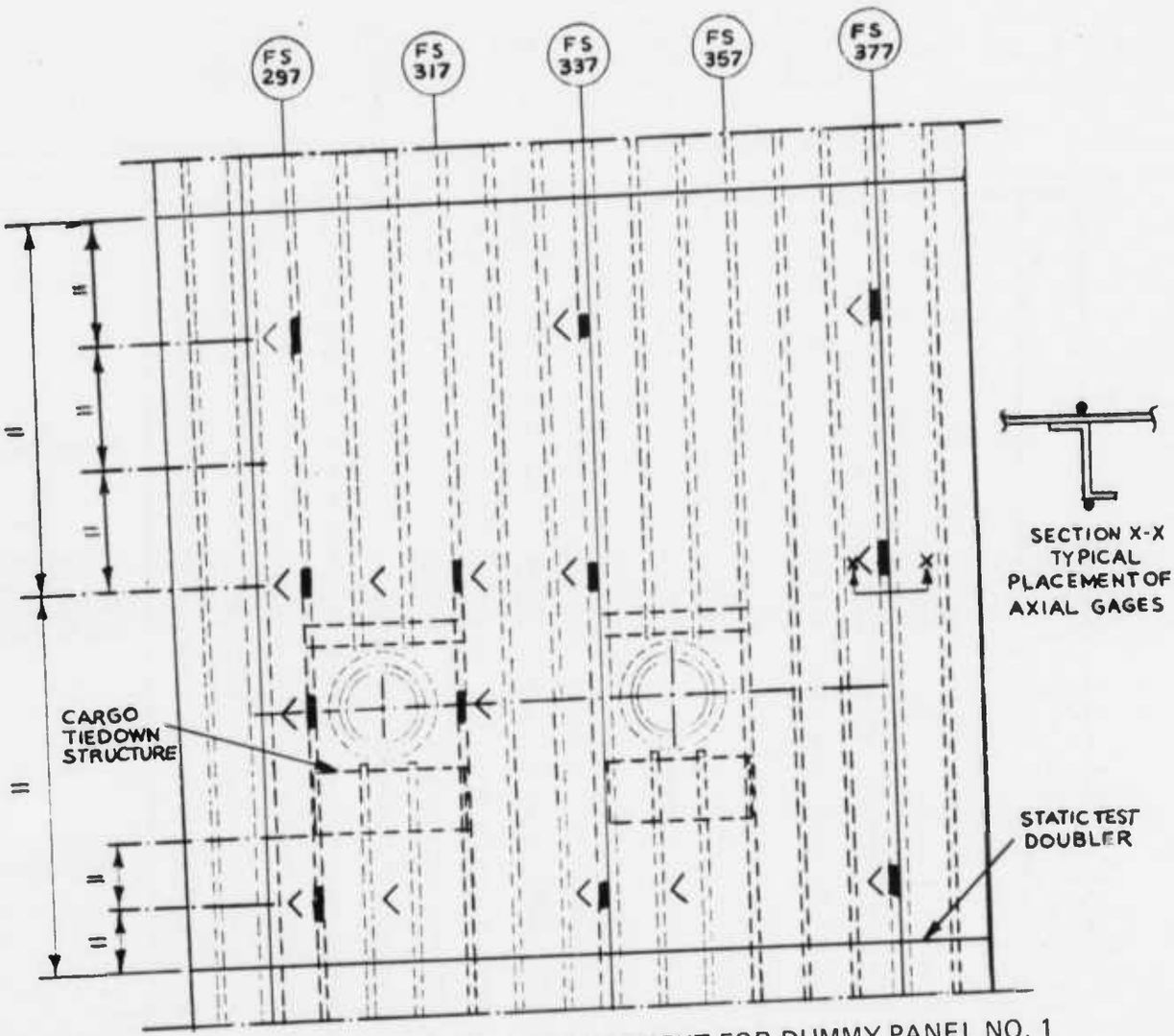

FIGURE 154 – INSTRUMENTATION ARRANGEMENT FOR DUMMY PANEL NO. 1

NOTES: 1) < denotes shear type strain gage.
2) ▬ denotes axial type strain gage.
3) All shear gages mounted midway between frames.
4) Dimensions marked = means equally spaced.

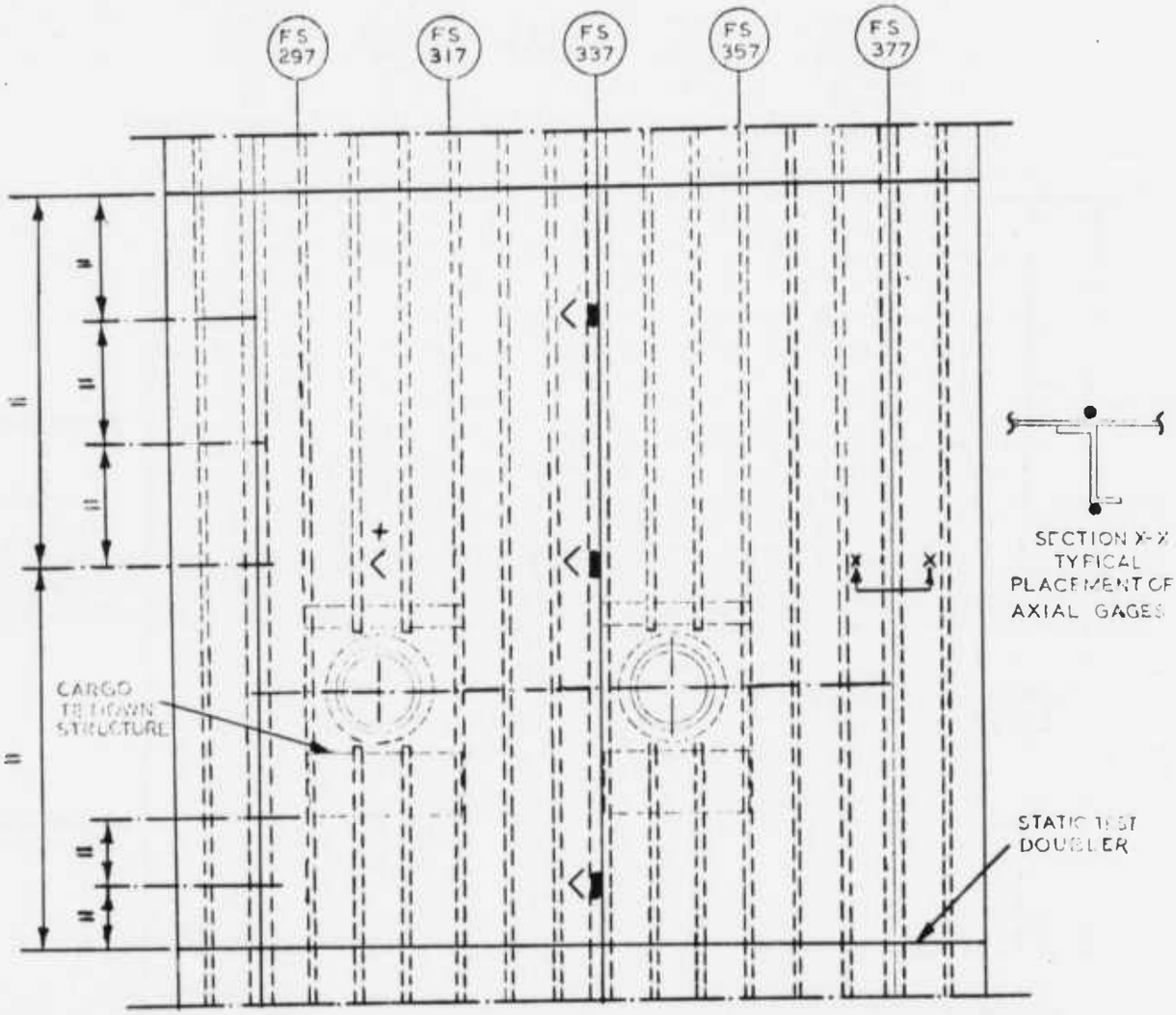

FIGURE 155 – INSTRUMENTATION ARRANGEMENT FOR DUMMY PANEL NO. 2

NOTES: 1) < denotes shear type strain gage.
2) ▬ denotes axial type strain gage.
3) All shear gages mounted midway between frames.
4) Dimensions marked = means equally spaced.

10.3.2 Static Test Fixture

The test fixture was designed and fabricated using a steel cubical universal test frame as a base structure. The static test article was tested in an upright position with torsional shear loads applied at the upper end and reacted at the lower end. The floor frame assembly to which the lower end of the test article was attached was fabricated with 14 inch by 14 inch steel I-beams, and then the assembly was attached to rigidly encased steel beams in the structural test laboratory floor within the cubical universal test fixture. Aluminum end plate assemblies consisting of three (3) individual plates contoured and assembled to match the cross-sectional configuration of the static test article were fabricated to serve as transition members for both upper and lower ends of the static test article. Figure 156 shows the partially completed test fixture being readied to accept the lower aluminum end-plate assembly. Steel angles formed to fit the contour of the cross-sectional configuration of the static test article were used to attach both ends of the static test article to the aluminum end-plate assemblies. Figure 157 shows the aluminum end-plate assemblies, some of the formed steel angles that were used to attach the ends of the static test article to the aluminum end-plate assemblies, and the steel torque arm fixture that was used to apply torsional shear loads to the upper end of the static test article in the cubical universal test fixture and attaching the lower end to the floor frame assembly, the steel torque arm was bolted to the aluminum end-plate assembly attached to the upper end of the static test article. The two (2) hydraulic jacks and load transducers were then connected between the ends of the steel torque arm and adaptor fittings on one side of the cubical test frame. The test set-up was completed by providing a counter-balancing system for the test hardware on top of the static test article. The strain gages were connected to a B & F Strain Data Acquisition System, Model SY156, for recording the strain data. Figure 158 shows the instrumented static test article installed in the test fixture prior to testing. Also, Figure 159 shows a view of the test article being installed in the test fixture from a location above the test setup.

10.3.3 Full-Scale Static Test and Results

Upon completing the hydraulic loading and instrumentation systems, loads were applied to the test article to check the uniformity of loads induced into test article components and verification of strain recordings. After reducing the check-out loads to zero, torsional loadings were applied to twenty (20) percent increments of the limit test torque. The torque applied to the test article was computed by multiplying the uniform shear flow by twice the cross-sectional area of the test article. The limit test torque was established using a uniform shear flow of 667 pounds per inch.

The test proceeded with application of the first twenty percent load increment. In applying the subsequent load increment, wrinkling of the fuselage skin on both of the standard riveted components was observed at approximately thirty-two (32) percent of the limit test torque. Similar type wrinkles did not occur in the fuselage skin of the weldbonded

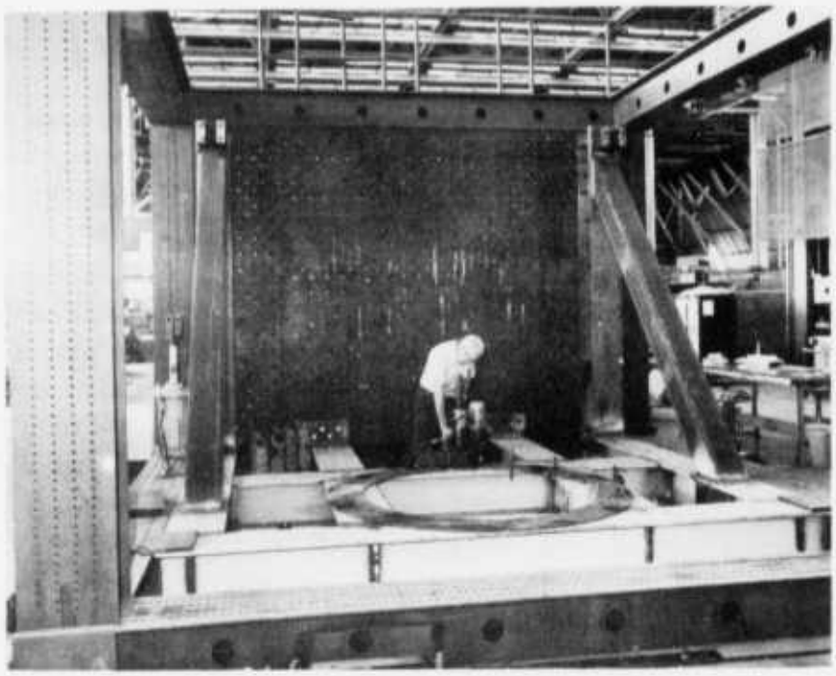

FIGURE 156 – UNIVERSAL TEST FIXTURE FRAME

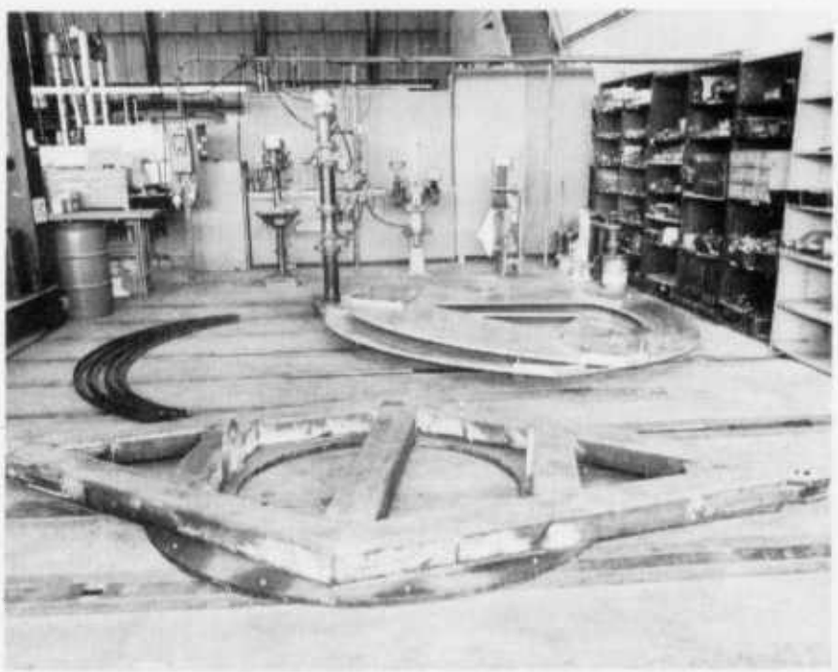

FIGURE 157 – STATIC TEST FIXTURE COMPONENTS

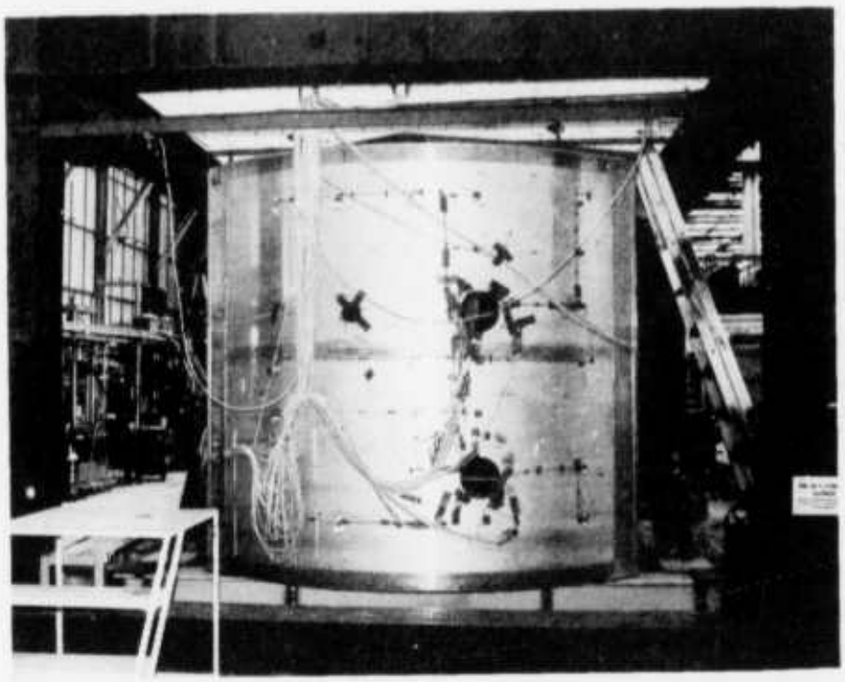

FIGURE 158 – INSTRUMENTED STATIC TEST ARTICLE INSTALLED IN THE TEST FIXTURE

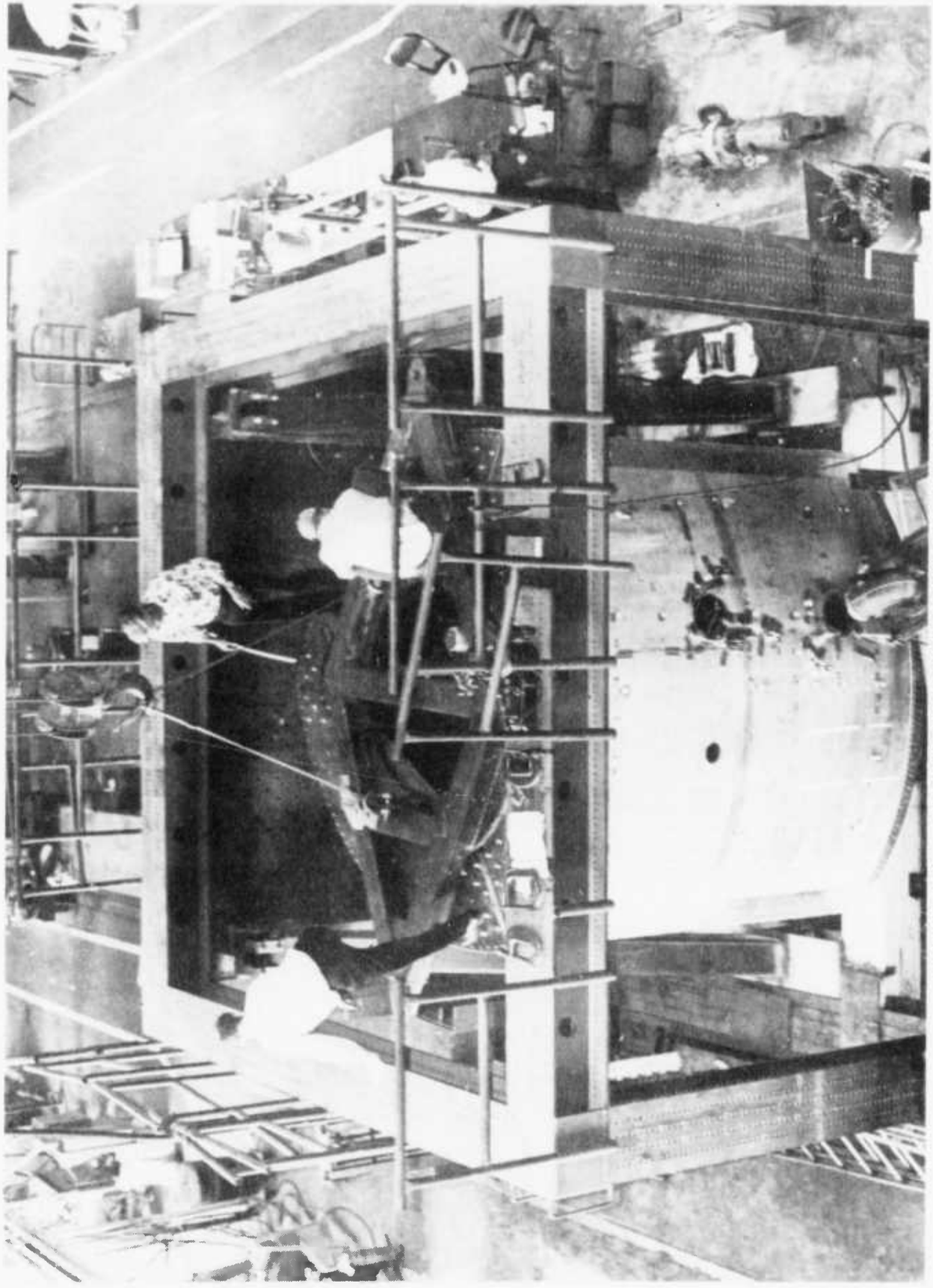

FIGURE 159 – TORQUE LOADING ARM BEING INSTALLED ON TOP OF TEST ARTICLE

component until forty (40) to sixty (60) percent of the limit test torque load was reached. The test continued with the application of the sixty (60) percent limit test torque which was accompanied by development of deeper buckles in the fuselage skin of the standard riveted components. After recording the strain data for the sixty (60) percent test load condition, loading was continued until failure occurred at 74.9 percent of limit test torque. Failure occurred in the standard riveted component designated as dummy panel No. 1. "Oil-canning" noises were evident prior to the failure, and a loud noise occurred with failure of the riveted component. Figure 160 shows an external view of the failed test article that occurred in the vicinity of one of the windows. Figure 161 shows a close-up view of the inside of the failed riveted component. The weldbonded test component did not fail in the static test; however, some wrinkling of the skin was apparent as shown in Figure 162. An inside view of the lower window vicinity of the weldbonded test component after the failure is shown in Figure 163 which also shows the fuselage skin wrinkles.

Strain data were recorded at 20, 40, and 60 percent limit test torque levels during the test and are reported in Table LX. All of the strains reported are given in micro-inches per inch. Figures 164 and 165 show shear flows (inset in each figure) in the riveted dummy panel No. 1 and the weldbonded component extrapolated to failure. These shear flows were calculated by converting the strains at failure taking into account plasticity effects. The strains at failure were obtained by plotting the strains given in Table LX and extrapolating the curves to the static test failure load. The theoretical shear flows in the weldbonded flight component for the ultimate design condition are shown on Figure 166. Comparison of the shear flows on Figures 164 and 165 with appropriate shear flows on Figure 166 shows the shear flows in both test panels at failure exceeding those for the ultimate design condition except for the region of the panel below the windows.

10.3.4 Post Analysis and Inspection of the Full-Scale Static Test Article

The weldbonded and riveted fuselage panels in the static test article were analyzed for both test load and design conditions utilizing the computer program that was developed for the design analysis. Subsequent to the test the fuselage skin thicknesses were measured on all components in the test article. The average thickness measurement for the weldbonded panel was 0.051 inches while the average thickness measurement for the riveted panels was 0.047 inches. These thickness measurements were used in the computer program in accomplishing the analysis of the weldbonded and riveted panels. The static test article joints connecting the weldbonded and riveted panels were not designed to represent the longitudinal stiffness comparable to the aircraft fuselage structure. Also, the hoop tension load in the panel when it is installed on the aircraft tends to increase the stress at which the fuselage panel buckles and the longitudinal strain produced by fuselage bending is carried by the extremely stiff upper longeron and the cargo floor in the area of high shear loads in the fuselage panel. Consideration of the aforementioned differences were accounted for in the computerized analyses. The results from the analyses accomplished with the computer program are presented in Table LXI.

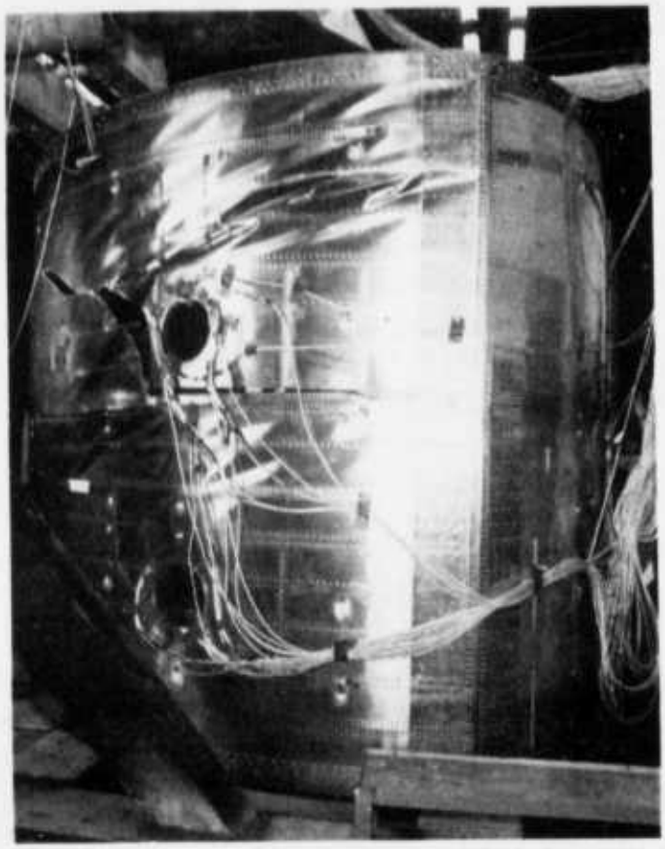

FIGURE 160 – FAILED STANDARD RIVETED DUMMY PANEL

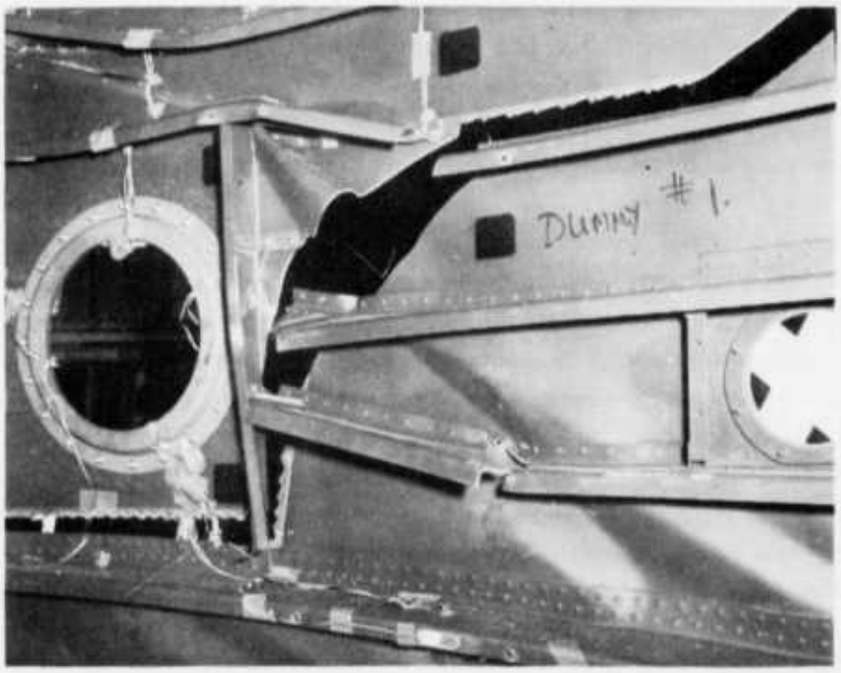

FIGURE 161 – INSIDE VIEW OF FAILED STANDARD RIVETED DUMMY PANEL

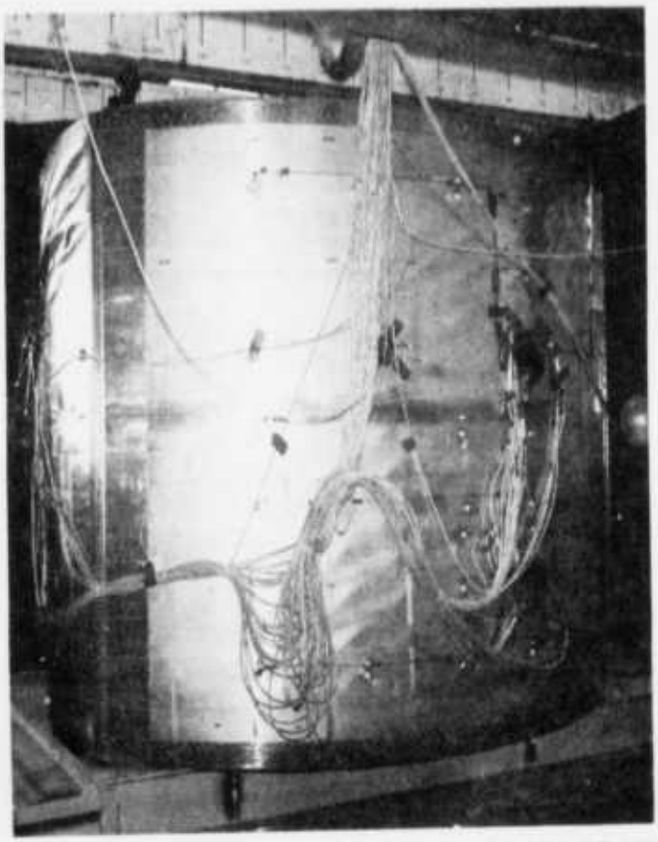

FIGURE 162 – WELDBONDED TEST PANEL AFTER STATIC TEST

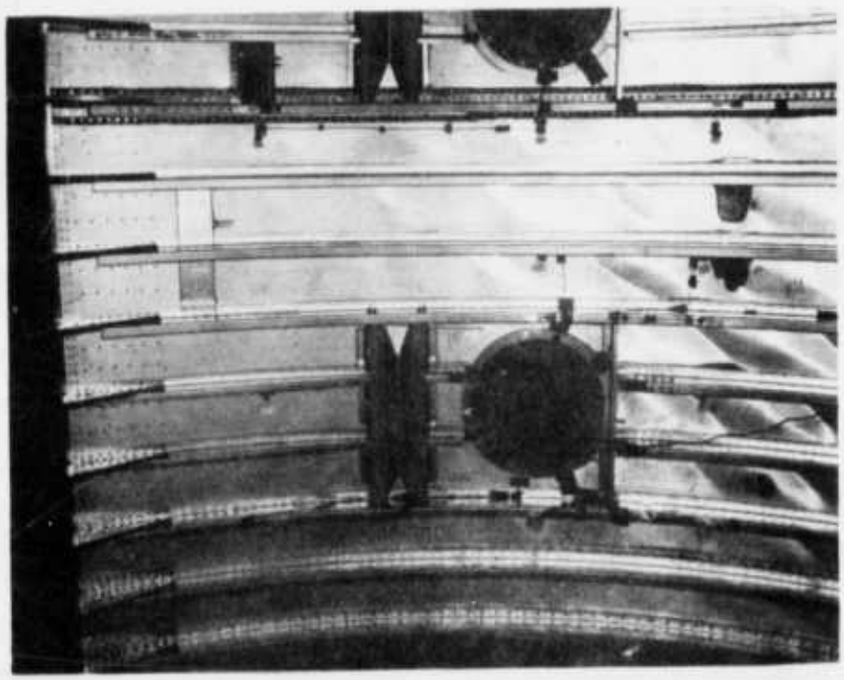

FIGURE 163 – INSIDE VIEW OF WELDBONDED TEST COMPONENT AFTER STATIC TEST

Table LX — Static Test Article Strain Data — Micro — in./in.

Strain Gage Number	Percent Limit Load			Strain Gage Number	Percent Limit Load		
	20	40	60		20	40	60
101	-20	- 10	+200	118	0	+30	- 80
102	0	+10	+10	119	0	0	- 420
103	+60	+140	- 260	120	- 10	+50	+70
104	+10	+20	- 60	121	- 50	- 280	- 510
105	- 30	0	- 1400	122	- 20	- 20	50
106	+10	- 10	+40	123	0	- 10	- 70
107	+70	+160	+190	124	0	- 10	- 130
108	+40	+70	+160	125	650	1290	1830
109	0	+30	- 270	126	0	0	- 30
110	+50	+110	+500	127	680	1550	2630
111	+30	+30	- 60	128	620	1240	1840
112	+50	+80	+30	129	720	1710	2560
113	- 30	- 30	- 230	130	590	1200	1830
114	+10	+40	- 130	131	790	1530	1890
115	+30	+50	- 90	132	640	1270	2160
116	+20	+30	- 70	133	690	1230	1810
117	0	0	+110	134	700	1330	1620

Table LX — Static Test Article Strain Data — Micro — in./in. (Cont'd)

Strain Gage Number	Percent Limit Load			Strain Gage Number	Percent Limit Load		
	20	40	60		20	40	60
135	740	1770	3600	152	630	1290	1770
146	580	1190	2150	153	740	1480	2170
137	730	1410	2370	154	610	1200	1730
138	710	1460	1490	155	740	1460	1860
139	540	840	1900	156	710	1540	3270
140	610	1290	2410	157	650	1300	1970
141	920	1430	1960	158	620	1260	1490
142	620	1280	1890	159	590	1310	2260
143	880	1900	3400	160	610	1210	2260
144	620	1290	2420	161	740	1490	2020
145	740	1300	1800	162	640	1300	1830
146	590	1140	1260	163	+20	+ 60	+ 60
147	660	1500	1750	164	−30	0	+620
148	700	1390	2340	165	− 10	− 40	− 370
149	680	1280	2570	166	640	1400	3330
150	620	1270	1760	167	610	1180	1620
151	910	1540	2100	168	670	1370	1700

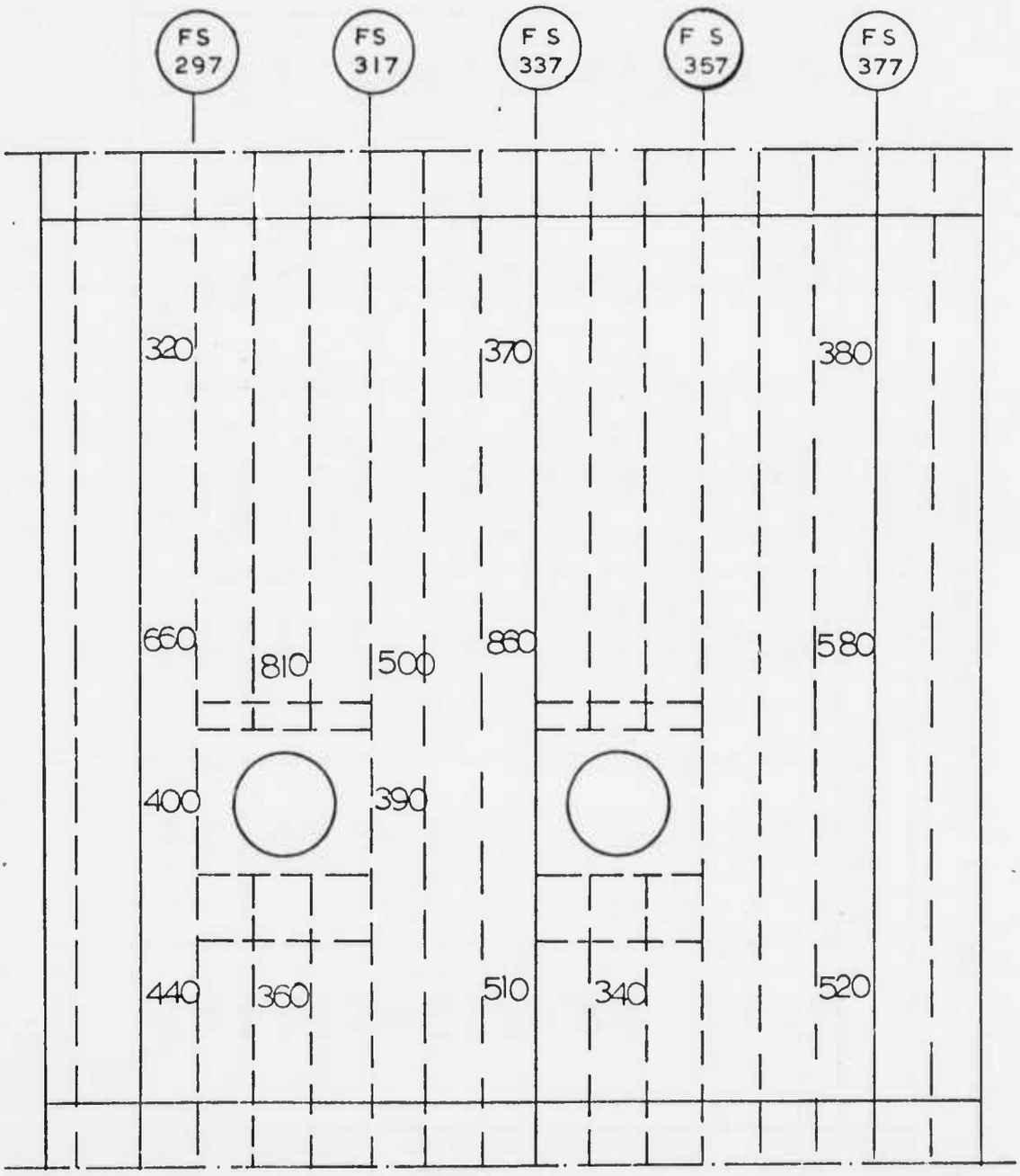

FIGURE 164 – SHEAR FLOWS IN DUMMY PANEL NO. 1
EXTRAPOLATED TO FAILURE

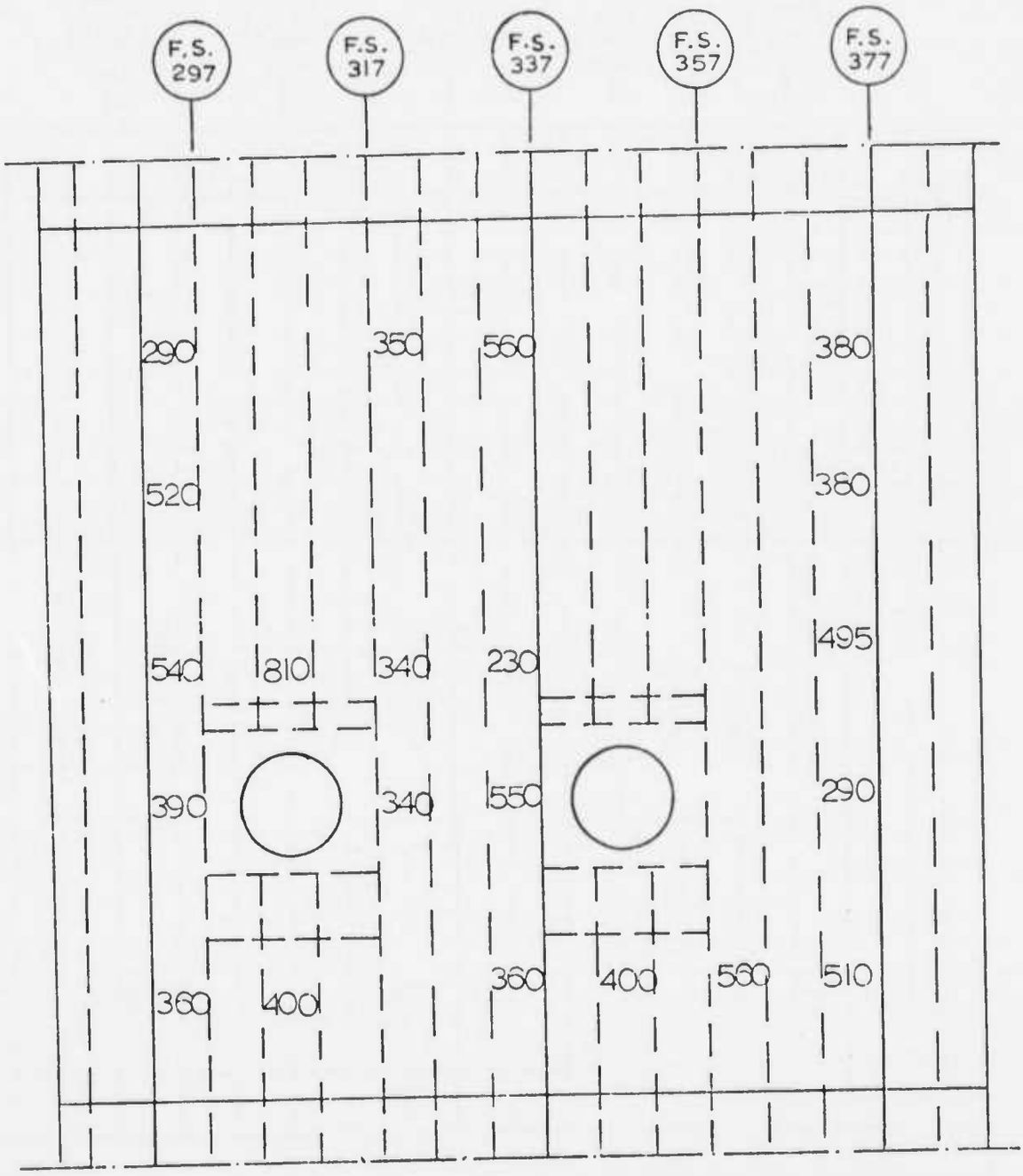

FIGURE 165 – SHEAR FLOWS IN WELDBONDED COMPONENT EXTRAPOLATED TO FAILURE

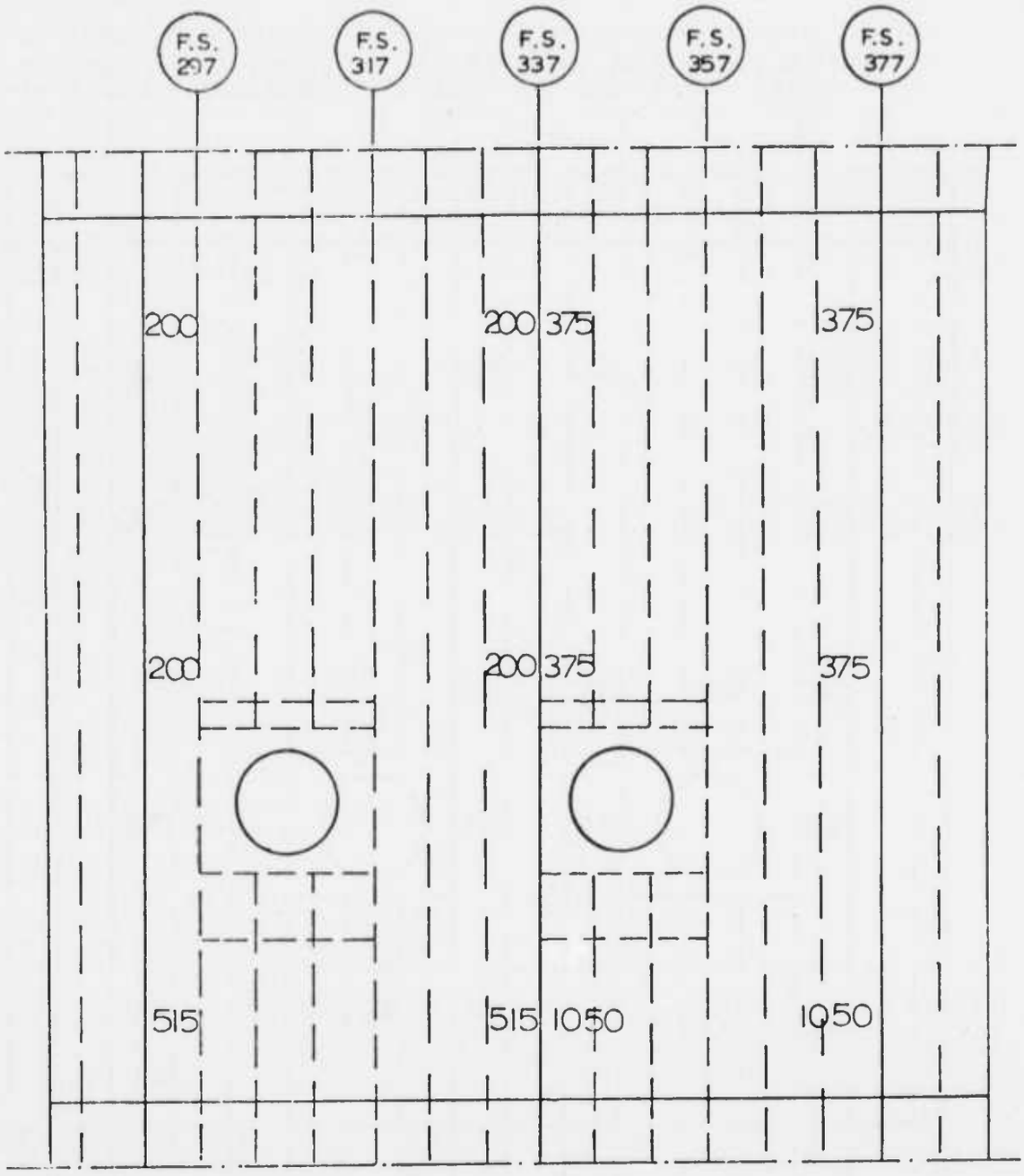

FIGURE 166 – THEORETICAL SHEAR FLOWS IN WELDBONDED FLIGHT COMPONENT FOR THE ULTIMATE DESIGN CONDITION

TABLE LXI – SUMMARY OF MARGINS OF SAFETY FOR THE WELDBONDED AND RIVETED PANELS FOR BOTH TEST AND FLIGHT LOAD CONDITIONS

Panel Analyzed	Allowable Shear Flow (lbs./in.)	Longitudinal Strain (in./in.)	Hoop Tension Load (lbs.)	Margin of Safety (%)
Riveted Test Panel	495	-0.00145	0	9.7
Weldbonded Test Panel	495	-0.00145	0	37.6
Riveted Flight Panel	975	+0.0013	6,387	0.2
Weldbonded Flight Panel	975	+0.0013	6,387	4.0

It is noted that an applied torsional load to the test article tended to shorten it due to the diagonal tension developed by buckles in each test panel in addition to the shear deflection of the test article. The shortening effect introduced a compressive strain in the test panels, whereas for the design condition, the longitudinal strain was a tensile strain. As seen from the above table, the longitudinal strain in both weldbonded and riveted panels has a significant effect on the margins of safety. In essence, the panels in the static test article were subjected to a compressive strain which yielded a lower allowable shear flow than the same panels subjected to a tensile strain and a hoop tension load in the critical design condition. Therefore, it is concluded that the test article configuration in conjunction with the loading method used in the test was more severe than the design load condition applied to either a weldbonded or riveted panel installed in the aircraft.

Upon completion of the static test, the weldbonded panel in the test article was visually and ultrasonically inspected. Visual examination of fillet areas of the weldbonded joints did not reveal any adhesive disbonds even through buckles were apparent in the skin. Also, the bondlines in the weldbonded joints were inspected by contact ultrasonics. Several suspected disbonds were detected during the inspection although no suspected disbonds were detected in the weldbonded joints prior to the test. The buckled fuselage skins could have been responsible for the several suspected disbonds.

In conclusion, the test condition was more severe than the condition for a panel installed in an aircraft. From the in-service operational viewpoint, the riveted fuselage panel has a history of trouble free service over a period of approximately 20 years. Thus, the failure of the riveted panel at a load level less than that of the test objective does not pose a problem relative to that type of structure being on operational aircraft. On the other hand, the weldbonded panel did not fail during the test. Also, there were no local failures in the weldbonded joints, and the fuselage buckles were not nearly as deep as those in the riveted panels. A theoretical assessment of the weldbonded panel showed it to have a strength of approximately 25 percent higher than the riveted panel.

10.4 Fail-Safe Weldbonded Panel Test

A flat stiffened-sheet weldbonded test panel was fabricated, artificial damage induced, and residual strength tested to failure. The test panel flat sheet was 2024-T3 clad one side aluminum alloy and it was weldbonded to five (5) Z-section 7075-T6 bare aluminum alloy stiffeners which were spaced 6.67 inches apart. A sheet splice similarly configured to the C-130 weldbonded fuselage component splices was incorporated in the second stiffener joint from the panel's edge as shown in Figure 167. Upon completing fabrication and inspection of the test panel, end loading plates were installed on both ends of the test panel as shown in Figures 168 and 169. The 7075-T6 aluminum alloy end plates attached to the sheet side of the test panel were 0.50 inches thick and the end plates attached to the stiffener side of the test panel were 0.31 inches thick. Prior to attaching the end plates to the test panel, attachment brackets were bonded to the stiffener flanges and sheet reinforcement doublers were bonded to the outer surface of the test panel sheet to assure uniform load distribution in the test panel. The test panel with the end plates installed is shown mounted in the test machine in Figures 168 and 169.

Artificial damage was induced into the test panel by locating a saw cut at the center-line of the test panel perpendicular to the load axis. The initial saw cut was 4.00 inches long and pierced the 0.051 inch thick sheet and the center Z-section stiffener. The final saw cut was lengthened to 4.30 inches by extending the initial saw cut 0.150 inches on each end using a jeweler's saw.

The test panel was strain gaged with eighteen (18) axial strain gages shown in Figure 167. Eight (8) of the strain gages were used to verify uniform load distribution across the test panel. The remaining ten (10) strain gages were strategically located in the near vicinity of the saw cut to assess the strains in that region of the test panel.

Upon instrumenting the test panel, it was mounted in the tension bay of the 1200 kip Baldwin Universal Testing Machine. Loads were introduced into the test panel through a 3.75 inch diameter pin installed in the end plates.

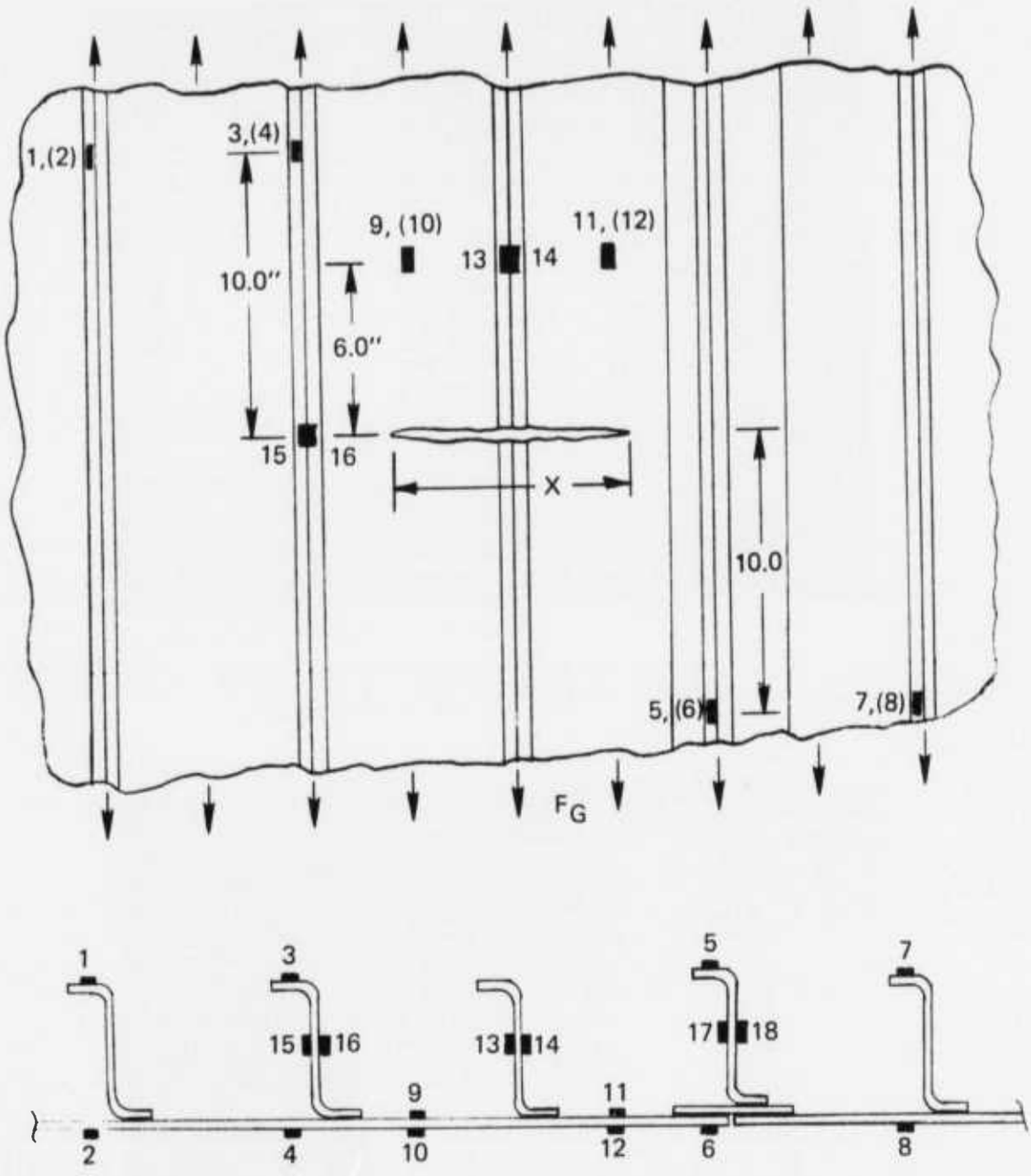

NOTES: 1. ALL STRAIN GAGES ARE AXIAL GAGES

2. STIFFENER SPACING = 6.67 INCHES

3. STIFFENERS ARE 7075-T6 BARE MATERIAL AND SHEET IS 2024-T3 CLAD ONE SIDE ONLY

FIGURE 167 – PANEL GEOMETRY AND STRAIN GAGE LOCATIONS

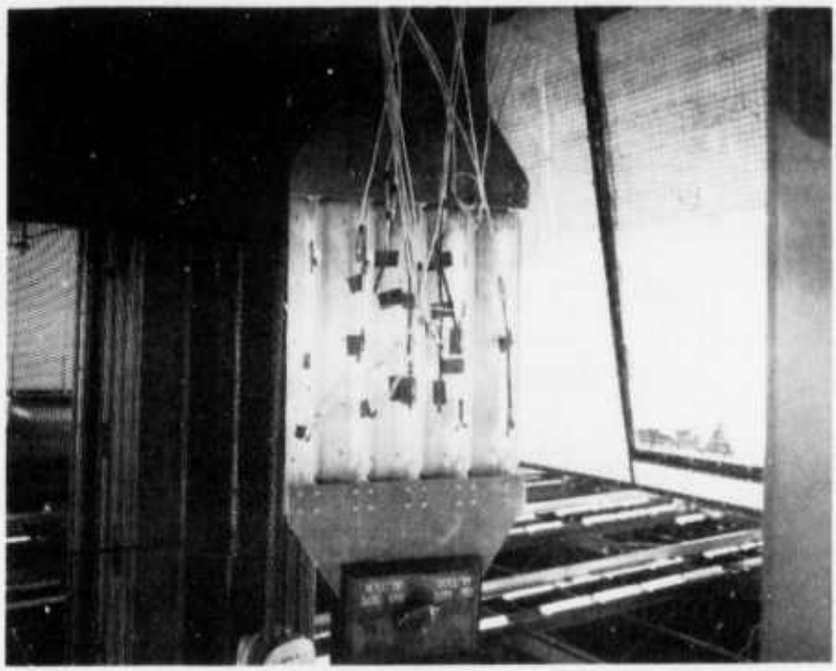

FIGURE 168 – STIFFENER SIDE OF FAIL-SAFE PANEL IN THE TEST MACHINE

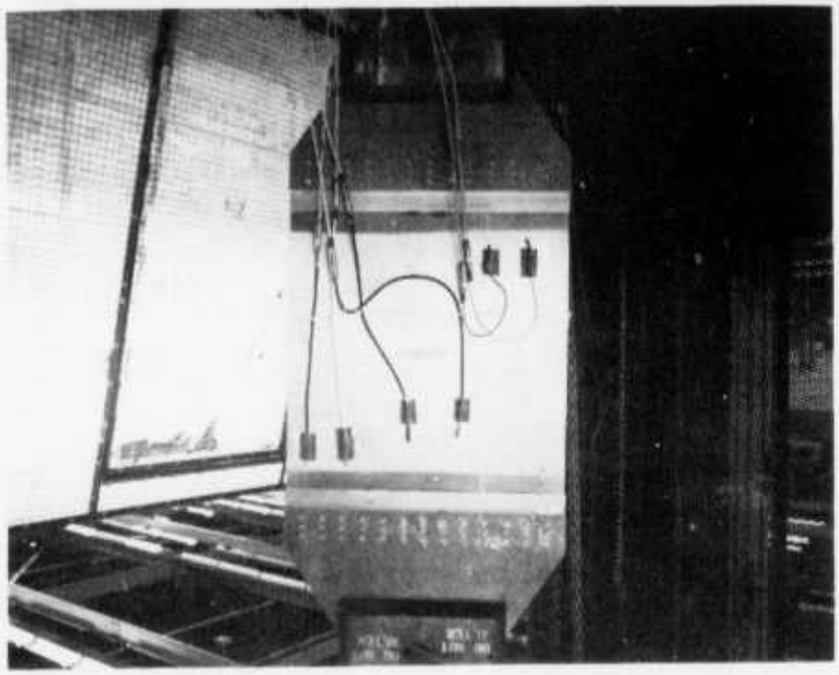

FIGURE 169– SHEET SIDE OF FAIL-SAFE PANEL IN THE TEST MACHINE

The crack front zone was lightly polished to assist observation of crack growth. A twenty-four (24) inch steel scale was taped to the sheet exterior surface of the test panel immediately above the saw-cut slot for measuring crack growth. A movie camera and a surveyor's transit were arranged to monitor crack growth. A remotely controlled light was located in the vicinity of the saw-cut region of the test panel and was used to indicate specific load levels on the film during the test. The load was applied to the test panel in increments and the strain gages were monitored to obtain the stress distribution in selected regions above and ahead of the crack front. Initially, tension load increments of 10,000 pounds were applied to the test panel at a loading rate of approximately 10,000 pounds per minute. In the range of 70,000 pounds to 100,000 pounds, the applied load increments were reduced to 5,000 pounds but the loading rate remained unchanged. From 100,000 pounds upward to the failure load, applied load increments of 1,000 pounds were used. The test panel failed at 122,000 pounds, and the failed test panel is shown in Figure 170.

During the test, strain data were collected at all load increments to panel failure. Table LXII shows a summary of strain measurements in micro inches per inch that span the test load spectrum including the failure load.

The stress analysis of the damaged panel was accomplished according to the residual strength methods established by Lockheed and documented in Reference 10. In the aforementioned reference, the gross area stress, F_G for a flat stiffened panel having a crack perpendicular to the load axis with the stiffeners acting as crack stoppers is defined as:

$$F_G = F_{TU} \frac{K_1 + K_2 \sum A_e/t}{CW + K_1 + K_2 \sum A_e/t}$$

Where = F_{TU} = Ultimate strength of the sheet
K_1 = Constant and K_2 = 0.75
$\sum A_e/t$ = Total effective section area
t = Sheet thickness
C = Ratio of critical crack length to initial crack length. For 2024-73 material, C = 1.35
w = stiffener spacing

Applying the above definitions to the gross area stress equation,

$$F_G = F_{TU} \frac{K_1 + 0.75 \sum A_e/t}{(1.35)(6.67) + K_1 + 0.75 \sum A_e/t}$$

The effective area of the undamaged stiffeners is generally defined as,

$$A_e = \frac{A}{1 + (y/\rho)^2}$$

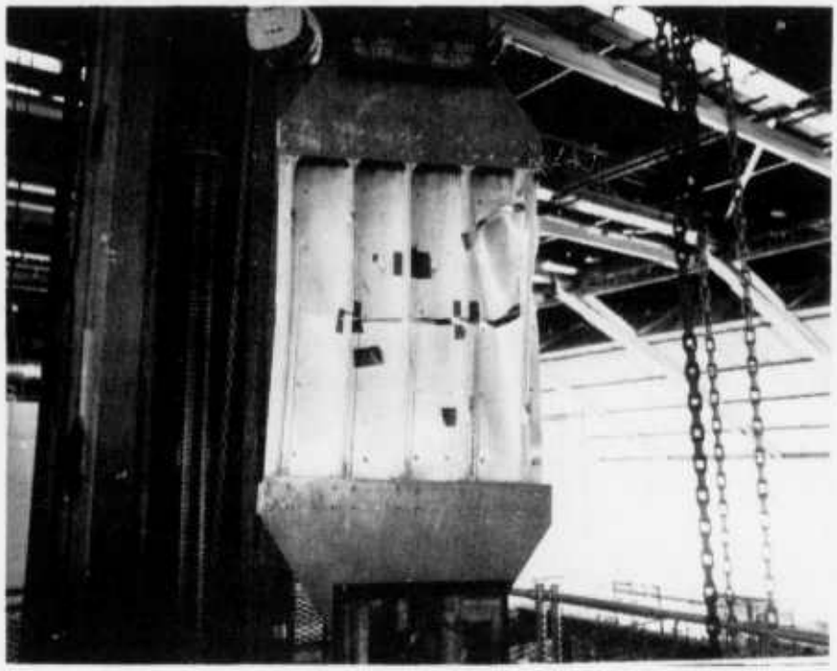

FIGURE 170 – FAILED FAIL-SAFE PANEL

Table LXII — Strain Measurements (Micro — in./in.) in Fail-Safe Test Panel

Strain Gage Number	Test Loads At Which Strain Measurements Recorded						
	10,000	20,000	40,000	60,000	80,000	100,000	122,000
1	323	613	1373	2039	2734	3529	5015
2	321	610	1224	1874	2518	3433	5942
3	470	868	1640	2418	3224	4166	6121
4	339	670	1350	2080	2852	3688	4294
5	404	710	1499	2250	3052	3985	5683
6	302	615	1247	1892	2513	3435	5022
7	449	814	1567	2356	3117	4109	5730
8	321	641	1298	1956	2617	3149	3686
9	281	590	1237	1919	2565	2931	1668
10	332	662	1334	2053	2769	3253	1869
11	215	571	1181	1800	2328	2484	1657
12	298	603	1207	1814	2355	2648	2194
13	81	160	303	423	487	415	110
14	70	141	273	394	473	453	105
15	460	860	1648	2450	3297	4349	10012
16	454	848	1628	2428	3277	4350	10133
17	443	834	1617	2385	3162	3392	1237
18	411	881	1690	2492	3348	4442	9170

where A is the cross-sectional area of the stiffener, y is the distance from the inside surface of the flat sheet to the centroid of the stiffener, and ρ is the radius of gyration of the stiffener. The effective area for a Z-section stiffener may be reduced to $A_e = A/5$. The cross-section area for the test panel Z-section stiffeners is 0.313 square inches which yields an effective area, A_e, of 0.313/5 = 0.0626 square inches. The total effective section area of the test panel is,

$$\sum A_e/t = \frac{0.0626 + 0.0626}{0.051} = 2.50$$

the relationship immediately above is valid if 24/2w is less than $\sum A_e/t$. Thus, making the appropriate substitution,

$\frac{24}{(2)\ (6.67)} = 1.79$ which is less than 2.50. Therefore, the relationship for determination of the total effective section area is valid.

The ultimate tensile strength, F_{tu}, of the flat test panel 2024-T3 clad one side sheet is defined as the average of 2024-T3 bare and 2024-T3 clad both sides sheet materials, and is equal to 63,000 pounds per square inch.

The gross area stress relationship was further refined by substituting the values for $\sum A_e/t$ and F_{tu}.

$$F_G = (63{,}000)\ \frac{K_1 + (0.75)\ (2.50)}{(1.35)\ (6.67) + K_1 + (0.75)\ (2.50)}$$

Thus,

$$F_G = (63{,}000)\ \frac{K_1 + 1.875}{K_1 + 10.88}$$

The constant, K_1 may be computed from the relationship immediately above if F_G is known. F_G is computed by dividing the test panel failure load of 122,000 pounds by the total cross-sectional area of the test panel. The total cross-sectional area of the panel includes the flat sheet, the splice plate, and five (5) Z-section stiffeners and is (30.68) (0.051) + (2.92) (0.051) + (5) (0.313) which equals 3.285 square inches. The gross area stress at failure is,

$$F_G = \frac{122{,}000}{3.285} = 37{,}200 \text{ lbs./in.}^2$$

Substituting the value of F_G into the gross area stress relationship, K_1 may be determined.

$$37,200 = (63,000)\ \frac{K_1 + 1.875}{K_1 + 10.88}\ ;\ K_1 = 11.1$$

The ultimate tensile strength to gross area stress ratio is defined as,

$$F_{TU}/F_G = 1 + \frac{X}{2\overline{W}_e}$$

where: X is the critical crack length

$$2\overline{W}_e = K_1 + K_2 \sum A_e/t$$

$$= 11.1 + (0.75)(2.50) = 12.98$$

Substituting $2\overline{W}_e$, F_{TU}, and F_G in the relationship immediately above and solving for X, the critical crack length,

$$\frac{63,000}{37,200} = 1 + \frac{X}{12.98} \quad ; \quad X = 8.95 \text{ inches}$$

The crack length measured by the movie camera at 108,000 pounds was 6.55 inches. The movie camera was not used to measure the crack length at failure because the lens was changed at the test load of 108,000 pounds to show a larger viewing area in order to follow rapid crack growth, but crack tip definition was not clear enough to continue the measurements. The crack length measured by the surveyors transit used readings from right and left sides of the taped scale. Readings on the left side of the scale were suspended at a test panel load of 111,000 pounds because the crack tip was obscured. The last reading taken by the surveyor's transit on the right side of the taped scale was at a test load of 118,000 pounds due to the rapid crack growth. The critical crack length estimated from the surveyor's transit readings is 8.20 inches.

Plots of F_{tu}/F_G ratio versus X are shown on Figure 171. The curves shown on that figure represent, an infinitely wide unstiffened flat sheet and a stiffened flat panel. The contribution of the stiffeners is shown by the difference in the curves on Figure 171. Furthermore, it is concluded that the large ratio of the C-130 fuselage radius to the critical crack length allowed the application of the method of analysis to stiffened curved panels as done in the fail-safe analysis of the C-130 weldbonded fuselage component in Section VIII of this report.

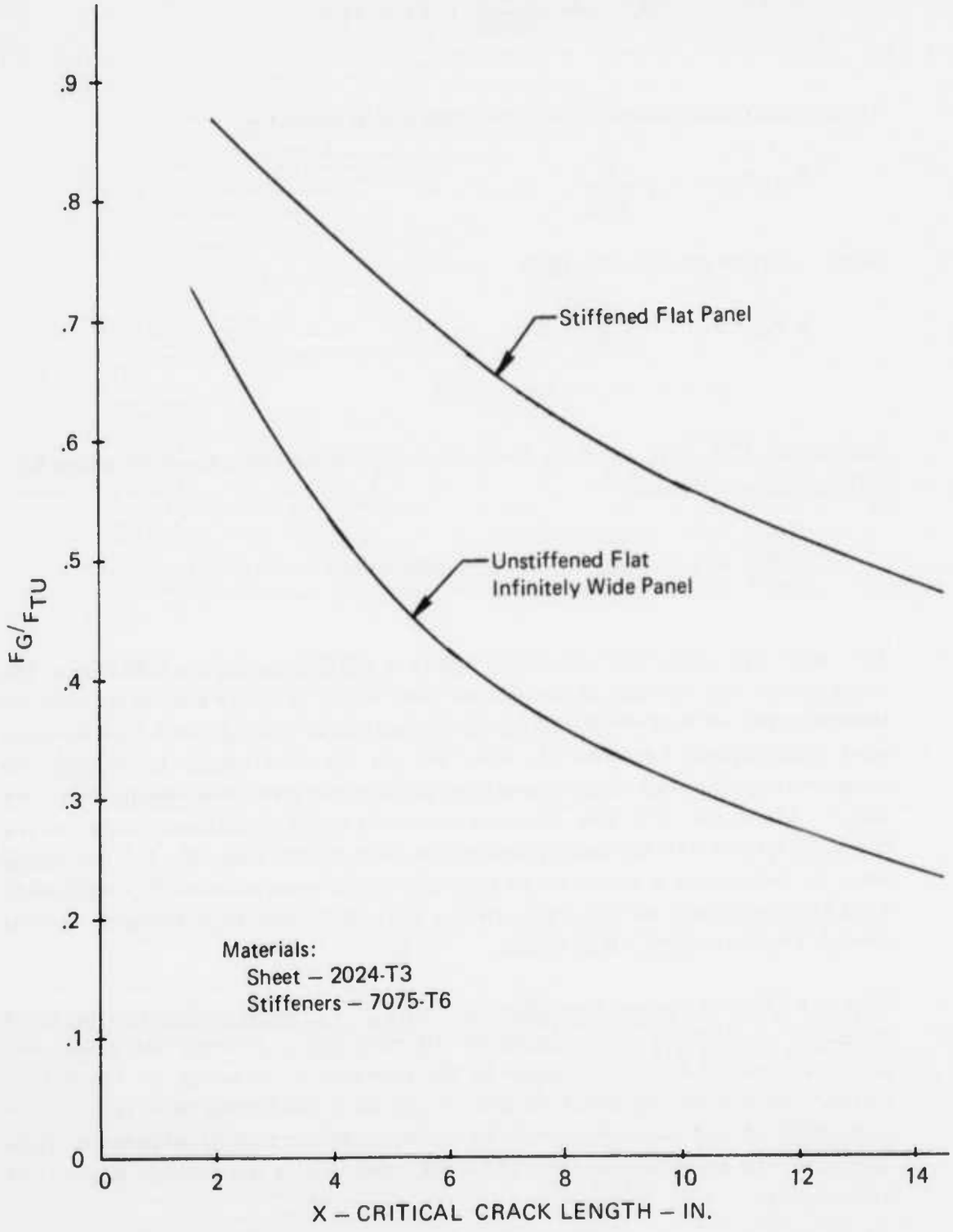

FIGURE 171 – ULTIMATE TENSILE STRENGTH/GROSS STRESS RATIO VS. CRITICAL CRACK LENGTH

SECTION XI

FLIGHT COMPONENT INSTALLATION

The weldbonded fuselage component was mechanically spliced into a larger production fuselage side panel at fuselage stations 280.0 and 387.0. The splices at both fuselage stations had an identical configuration as the splice at fuselage station 337.0. This larger modified production fuselage panel which extends from fuselage station 245.0 to 477.0 was installed on the C-130 production line in an identical manner as a standard fuselage panel. No special considerations had to be made in mechanically joining the weldbonded fuselage component to adjoining structure at the upper main longeron, B.L. 61.6, and the lower main longeron at the cargo floor, B.L. 61.6. Upon completion of the structural installation, the troop seat supports, electrical harnesses, and hydraulic tubing were attached to the weldbonded fuselage component identical to other production aircraft. Then a standard insulation blanket was attached to the interior surface of the weldbonded fuselage panel after installation of the interior equipment and furnishings. Figure 172 shows the C-130H aircraft with the weldbonded component installed. The dashed lines on the aircraft fuselage define the weldbonded fuselage component boundaries.

FIGURE 172 — C-130 AIRCRAFT WITH WELDBONDED FUSELAGE PANEL INSTALLED

SECTION XII

IN-SERVICE MONITORING PLAN

12.1 In-Service Monitoring Plan Development

An in-service monitoring plan was prepared for the weldbonded fuselage side panel installed on C-130H airplane Serial No. AF73-01592. The plan was published as an independent document and a Service Manual Publication Number, SMP 895, was assigned to the document in order that appropriate references and identification can be included in the airplane handbooks. The plan spans a period of forty months beginning with the delivery of the airplane. The contents of the plan include the following:

- Description of the C-130H Aircraft Modification and Usage
- Periodic Inspection Procedures and Schedule for the Installed Fuselage Side Panel
- Required Inspection Equipment for the Weldbonded Fuselage Side Panel
- Hazards and Levels of Risk Associated with the In-Service Evaluation of the Weldbonded Fuselage Side Panel
- Repair and Maintenance for the Installed Weldbonded Fuselage Side Panel
- Data Collection and Presentation of Results

The technical efforts outlined in the in-service monitoring plan, with the exception of repairs and maintenance activities, will be accomplished by the Lockheed-Georgia Company under separate contract. The Air Force user command or designated repair depot will accomplish all repairs and maintenance activities, as necessary, and provide assistance in preparing the weldbonded fuselage panel for inspection by Lockheed Quality Assurance personnel.

12.2 Periodic Inspections of Weldbonded Fuselage Side Panel

Periodic visual, ultrasonic and radiographic inspections will be accomplished on the weldbonded fuselage panel. Spot-welds in the weldbonded joints will be radiographic inspected and the bondlines in the weldbonded joints will be ultrasonically inspected. All inspections will be accomplished coincident with either Air Force phased or isocronal inspections. A total of seven periodic inspections is planned over the 40 month time period with the last inspection occurring concurrent with a programmed depot maintenance (PDM)

operation on the aircraft. Also, inspections are planned to coincide with inspections of the NASA boron-epoxy reinforced center wing.

12.3 Required Inspection Equipment for the Weldbonded Fuselage Side Panel

In-service inspections of the weldbonded joints necessitate the use of portable equipment. The equipment required for inspection of the spot-welds in the weldbonded joints using the standard radiographic inspection technique is:

1. X-ray Machine, Portable 160 KV, 40-Degree Tube Head, Sperry P/N 160E-8-C or equivalent.

2. X-ray film, GAF Type 400 or equivalent.

The equipment required for inspection of the adhesive bondlines in the weldbonded joints using the contact ultrasonic technique includes:

1. Reflectoscope, Sperry UM715 or equivalent.

2. Transducer, 5 mHz 0.250 inch diameter Type SFZ or equivalent.

3. Acoustic Couplant, tap water mixed with wetting agent.

4. Transducer Cable, 12-foot length, Microdot/UHF connector or equivalent.

5. Mylar overlay sheet.

6. Calibration standard as depicted in Figure 94.

12.4 Repair and Maintenance of the Installed Weldbonded Fuselage Side Panel

The repair and maintenance techniques described below are those specifically applicable to the weldbonded joints. All other areas of the weldbonded fuselage panel are to be repaired in accordance with the appropriate procedures contained in Air Force Technical Order 1C-130A-3. The following list is the major portion of applicable repairs contained in Air Force Technical Order 1C-130A-3.

1. Repair of pressurized fuselage skin scratches including the method of testing for penetration of the cladding on the exterior surface.

2. Repair for formed aluminum member flanges including the Z-section ring frame flanges, bracket flanges, and intercostal flanges not joined to the fuselage skin.

3. Repair for formed aluminum member webs including the Z-section ring frame webs, bracket webs, and intercostal webs.

4. Repair of fuselage rings and segments cracked at accessory clamp attachment points.

5. Repair of fuselage skin scratches that extend across the mechanically fastened splice at fuselage station 337 and the peripheral boundary splices of the weldbonded fuselage panel.

The following guidelines for repair of the weldbonded joints and splices in the weldbonded fuselage panel are presented for use by the user/repair activity. It is noted that all weldbonded joints and splices are common to the fuselage skin and recommended repairs take into consideration the pressurization effects on the fuselage skin.

12.4.1 Repair of Cracks in Spot-Welds in the Weldbonded joints and Splices

Internal cracks in spot-weld nuggets that are detected by radiographic inspection do not require repair. Test data developed in the current program in addition to other weldbond programs showed no degradation in joint structural performance for this type of defect.

Cracks in spot-weld nuggets that extend to the surface of the joint or splice may be repaired by drilling the cracked area out of the nugget and installing a protruding head MS20470AD5 aluminum alloy rivet. If the drilled hole for the MS20470AD5 rivet does not completely remove the cracked area, a larger (3/16-inch diameter) hole must be drilled for installation of a MS20470AD6 rivet. Prior to installation of the rivet, the drilled hole must be deburred and the rivet dipped in corrosion inhibiting sealant, MIL-S-81733. After installation of the rivet, the manufactured and bucked heads must be touched up with zinc chromate primer, MIL-P-8585, or other acceptable paint finish.

The above repair procedure is applicable to the weldbonded Z-section ring-to-skin joints and splices, weldbonded intercostal-to-skin joints, weldbonded window reinforcing doublers-to-skin joints, and weldbonded fuselage skin splices at fuselage stations 297 and 377.

12.4.2 Repair of Adhesive Disbonds in the Weldbonded Joints and Splices

An ultrasonic inspection of the adhesive bondlines in the weldbonded joints was accomplished prior to installation of the panel in the airplane. Several disbonds occurred on the lower end of the fuselage panel joints at fuselage stations 297 and 377. These disbonds occurred in the area of the panel that was repaired with room temperature curing adhesive, EC 2216, and were caused by run-out of the M6800 adhesive during the cure of the weldbonded panel adhesive. After detection of the disbonds in that area of the panel at fuselage stations 297 and 377, several protruding head Hi-Lok fasteners, Code HL18PB, were wet-installed between spot-welds to preclude further disbonding.

Previous experience with weldbonded joints indicate that adhesive disbonds can occur between spot-welds and not extend to the edge of the joint. Adhesive disbonds that occur between spot-welds in weldbonded joints that do not extend to the edge of the joints are to be repaired with 5/32-inch protruding head rivets (MS20470AD5). A rivet is to be installed through the disbonded area midway between spot-welds as shown on Figure 173. Also, the same size and type rivets are to be installed in adjacent spot-weld spaces midway between the spot-welds as shown on Figure 173. All rivets are to be installed wet with corrosion inhibiting sealant, MIL-S-81733. This repair is limited to three disbonds occurring in adjacent spot-weld spaces.

Adhesive disbonds in weldbonded joints that extend to the edge of the joint are to be repaired with 5/32-inch protruding head steel Hi-Lok fasteners (Code HL18PB). The Hi-Lok fasteners are to be installed midway between spot-welds with an edge distance of 0.400 inch from the edge of the joint as shown in Figure 174. All Hi-Lok fasteners are to be installed with corrosion inhibiting sealant, MIL-S-81733. This repair is limited to an edge disbond extending over a continguous length of four spot-weld spaces. This typical repair is applicable to edge disbonds for the splice plates and skin splices at fuselage stations 297 and 377.

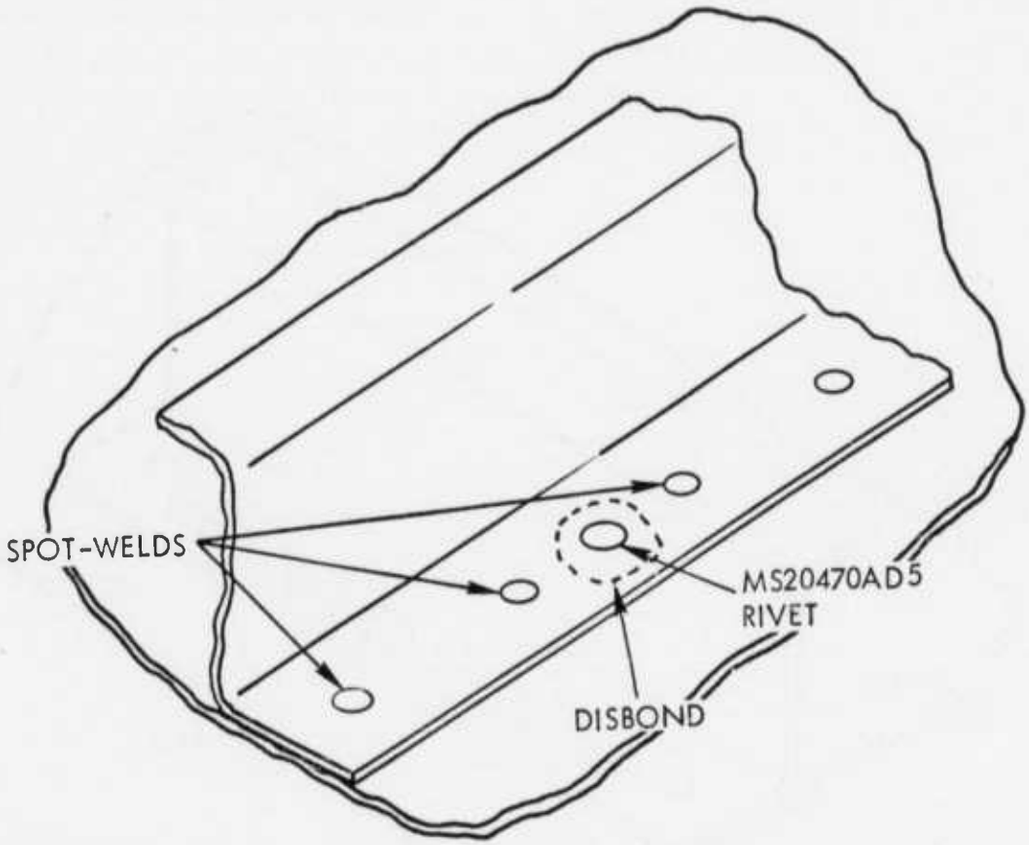

FIGURE 173 – TYPICAL REPAIR FOR ADHESIVE DISBOND BETWEEN SPOT-WELDS

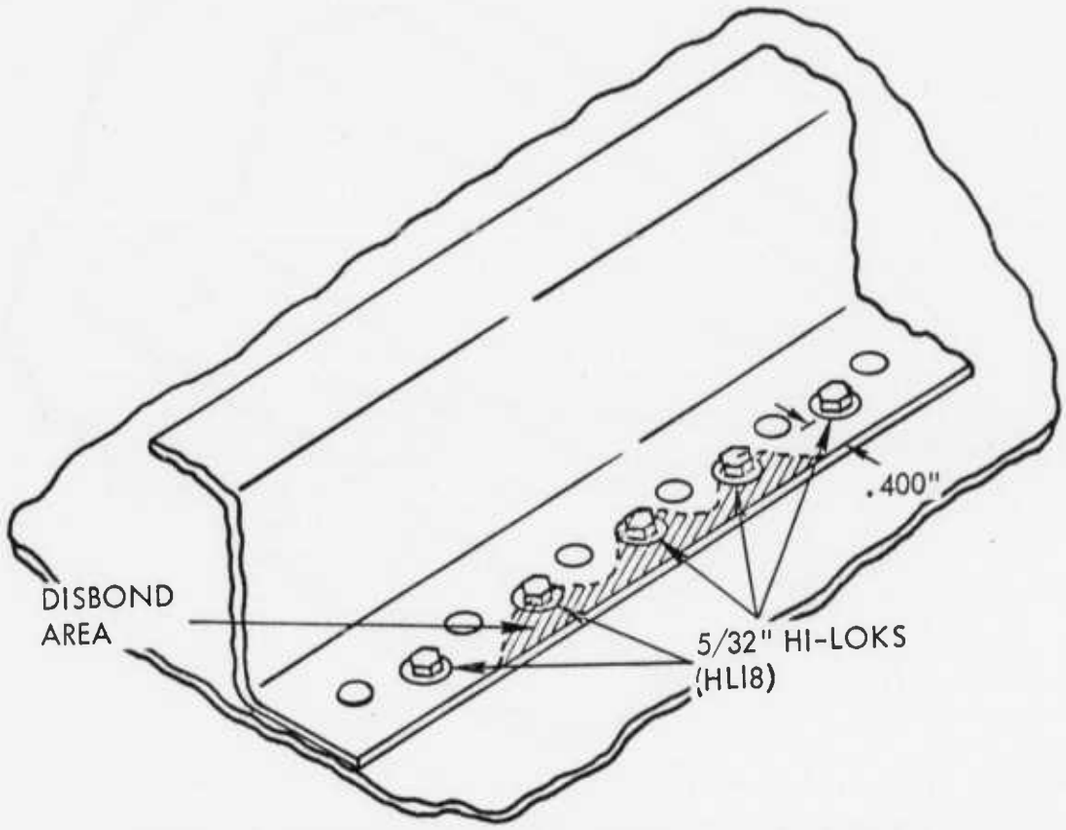

FIGURE 174 – TYPICAL REPAIR FOR ADHESIVE DISBONDS EXTENDING TO EDGE OF JOINT

SECTION XIII

CONCLUSIONS

The successful completion of this program has demonstrated that the weldbond process can be effectively used in the design and fabrication of flightworthy hardware for operational military aircraft. A weldbonded fuselage component approximately nine feet by ten feet was installed on a C-130H aircraft that became operational with the Air Force Tactical Air Command in November, 1974. In addition, other program objectives including process development, generation of engineering design data, design and fabrication of the full-scale weldbonded fuselage components, and structural tests on sub-scale and full-scale weldbonded components were successfully achieved.

Design and fabrication of the weldbonded fuselage component installed on the operational C-130H aircraft were accomplished with data and experience gained during this program and other weldbond assembly programs previously carried out at the Lockheed-Georgia Company. Design of the C-130 weldbonded fuselage component utilized joint strength data, sonic fatigue considerations and other engineering design data. Fabrication of the C-130 weldbonded component was accomplished in accordance with the material and process specifications developed in this program. The selected weldbond process used in the manufacturing operations was the epoxy paste adhesive, Whittaker's M6800, applied to the spot-weld etch prepared surfaces followed by spot-welding through the uncured adhesive. During the fabrication operations, in-process quality control tests were conducted in addition to 100 percent inspection of the weldbonded joints by radiographic and ultrasonic techniques for establishment of an airworthy structural component.

Detail cost analysis of the C-130 weldbonded fuselage component, supported by program developments, shows that assembly by the weldbond process is the least costly of the joining processes evaluated. Weldbonding shows a cost savings of 37 percent over the baseline riveted structure, and 18 percent over the adhesive bonded structure. Additional refinements of the weldbond process provides a good potential for the reduction of airframe manufacturing costs.

Technical developments proceeded with the selection of the best weldbond process after evaluating 14 surface preparations and 17 candidate adhesives. The selection was based on weldability characteristics, potential automated application of the adhesive, bondline permanence considerations and cost effectiveness. The selected process was the Whittaker M6800 epoxy adhesive applied to the spot-weld etch prepared surfaces. After weldbonding, the joint fillets were sealed with a corrosion inhibiting sealant.

Engineering data were developed for use in design of weldbonded aluminum alloy structures having adherend thicknesses ranging from 0.020 inches to 0.090 inches. Adhesive material and weldbond process specifications were concurrently developed for use in the assembly of aluminum alloy structures. Static and uniaxial fatigue strength data for 36 geometrical joint configurations were developed using elemental weldbonded test specimens. Crippling, shear and compression stability, and sonic fatigue sub-scale weldbonded components were fabricated and tested. Weldbonded and adhesive bonded shear stability tests resulted in local disbonding loads for the weldbonded components that were higher than comparable adhesive bonded components. Weldbonded compressive stability panel test results were equivalent to a riveted panel reported in Reference 3 and 20 percent higher than adhesive bonded panels of the identical configuration. Sonic fatigue sub-scale components were fabricated and tested for comparison with results from similar riveted component tests. The weldbonded components showed significantly higher design lives than the riveted components for the design life range greater than 10^7 cycles. Thus, in the large majority of structural assemblies, it would be advantageous to use the weldbond joining process instead of conventional aluminum riveting.

Structural tests and analyses were accomplished in structurally qualifying the C-130 weldbonded fuselage component prior to installation on an operational aircraft. A flat sub-scale weldbonded panel having two weldbonded joints and one weldbonded splice was cyclic pressure tested to an equivalent of four C-130 aircraft fuselage lifetimes without catastrophic failure. At the completion of each lifetime, the weldbonded joints were ultrasonically inspected. In the inspection after the first lifetime a suspected disbond was detected that exceeded the specification limit. During subsequent inspections the suspected disbond grew until it reached the edge of the weldbonded joint without any distinguishable effects on the cyclic pressure test.

A full-scale C-130 weldbonded fuselage component similar to the fuselage component installed on the C-130H operational aircraft was static strength tested. The static test article consisted of two standard riveted fuselage components and the weldbonded component joined together to form a triangular-shaped barrel section. A comparative strength test was conducted on the static test article with application of a pure torsional load. Failure occurred in one of the standard riveted fuselage components prior to reaching the test goal. A post analysis was performed on weldbonded and riveted fuselage components applying both test and design load conditions. It was concluded that the test article configuration in conjunction with the loading method used in the test was more severe than the design load condition applied to either a weldbonded or riveted component installed in the aircraft. In addition, visual examination of the fillet areas of the weldbonded joints in the weldbonded test component did not reveal any adhesive disbonds even though buckles were apparent in the skin. The failure of the riveted fuselage component at a load level less than the test goal does not pose a problem because it has a history of trouble-free service over a period of approximately 20 years and many thousands of flight hours. On the other hand, the weldbonded fuselage component did not fail during the test and it sustained significantly less damage than the standard riveted panel. A theoretical assessment of the weldbonded fuselage component showed it to be approximately 25 percent stronger than the standard riveted fuselage component.

During the course of the program a few of the technical areas investigated show need for further development to make the weldbond joining process more viable. In particular, improvement in bondline permanence of weldbonded joints without post-sealing the joint fillets. Subsequent programs are investigating this important area. Another technical area that deserves further investigation is chemical finishing of weldbonded joints after weldbonding. Application of the chromic acid anodize process omitting the deoxidize step resulted in a discoloration of the adhesive fillets of the weldbonded joints. It was established that the discoloration was not detrimental to the adhesive; however, improvement in the chemical finish system is advisable, if only for cosmetic appearances.

In summary, it is concluded that the major milestones of the program were accomplished. Furthermore, a successful history of in-service operational experience with the weldbonded fuselage component installed on the C-130H aircraft will be of considerable significance in selection of the joining processes for future aluminum alloy structural designs.

APPENDIX A

GENERAL TEST METHODS

A.1 Coupon Tests

During the initial task of this program, extensive small coupon testing was performed. These consisted of various forms of single overlap tensile shear, metal-to-metal peel and wedge tests. These were used primarily in investigations involving a particular element in the overall weldbond joining process. For this reason, it was desirable to segregate, in some instances, the welding and the bonding aspects of weldbonding. For instance, when performing weld quality evaluations and weld schedule certification, it was desirable to eliminate the effects of the adhesive on weld nugget lap shear strength test results by leaving the adhesive uncured through the test. This was consistent with the objectives of the program since the presence of the uncured adhesive at the time of welding influenced the weld nugget formation, and while the curing operation would not change nugget strength, it would result in a specimen useless for determining weld strength.

In the case of basic bond shear strength determinations which were used to assess various candidate surface preparations and adhesive, the reverse was true. The presence of the weld would only contribute an unnecessary variable – the strength of the weld nugget. This would tend to provide a variable strength "floor" which would confuse the results of initial bond strength and bond strength after environmental exposure testing.

Most of the first task coupon tests were either "spot-weld only" or "adhesive only" tests as described above. In both cases, the weldbond process was duplicated as closely as possible. For the weld only specimens, only the adhesive cure step was eliminated. For the "adhesive only " tests, specimens were fabricated by making a weldbonded panel and cutting the "adhesive only" specimens from between the welds.

During task 1, one set of weldbond specimens with the weld included along with the cured adhesive were tested. These were identical to the "adhesive only" specimens except for the presence of the weld.

Metal-to-metal peel and wedge tests were performed to evaluate bond strength resulting from various surface preparation/adhesive combinations. Following the reasoning presented above, these specimens were fabricated from cured weldbonded panels with the specimens removed from the panels so that the resulting specimens contained no welds.

A.1.1 Lap Shear – Spot-weld Only

Specimens as shown in Figure A1 were fabricated and tested in accordance with MIL-W-6858C. Some were built as panels and then removed while others were formed in their final dimensions from one (1) inch wide strips. These were fabricated by simulating the desired candidate process up to, but not including adhesive cure. At this point, these specimens were tested in the standard tensile shear mode at an approximate load rate of 1500 pounds per minute. Specimen geometry, weld dimensions, failing load and failure mode were recorded during this test.

A.1.2 Lap Shear – Adhesive Only

Panels as shown in Figure A2 were fabricated. Following adhesive cure, specimens were removed as shown in the same figure. Specimens with a one (1) inch overlap and with a two (2) inch overlap were tested during this program. Testing of these specimens was conducted according to the MMM-A-132 tensile shear method. Specimen geometry, failing load and failure mode were recorded during this test. In addition to standard static strength determination, these specimens were also used for creep testing per MMM-A-132.

A.1.3 Lap Shear – Weldbond

Panels as shown in Figure A3 were fabricated up to and including adhesive cure. At his point, specimens were removed as shown in the same figure. Testing of these specimens proceeded according to the corresponding MMM-A-132 tensile shear method. Specimen geometry, failing load and failure mode were recorded during this test.

A.1.4 Metal-to-Metal Peel – Adhesive Only

Panels as shown in Figure A4 were fabricated. Following adhesive cure, specimens were removed as shown in the same figure. Tests on these specimens were conducted in accordance with the ASTM-D14 Subcommittee test method. Specimen geometry, minimum, maximum and average load, and failure mode were recorded during this test. Figure A-5 shows the loading arrangement and jig.

A.1.5 Wedge Specimen and Test

Panels similar to those fabricated for the metal-to-metal peel specimens were fabricated with 7075-T6 bare aluminum alloy sheet. The spot-welds were located such that one (1) inch by four (4) inch adhesive bond specimens, as shown in Figure A6, could be removed. The bond in this specimen extended one (1) inch from the end giving a total bond area per specimen

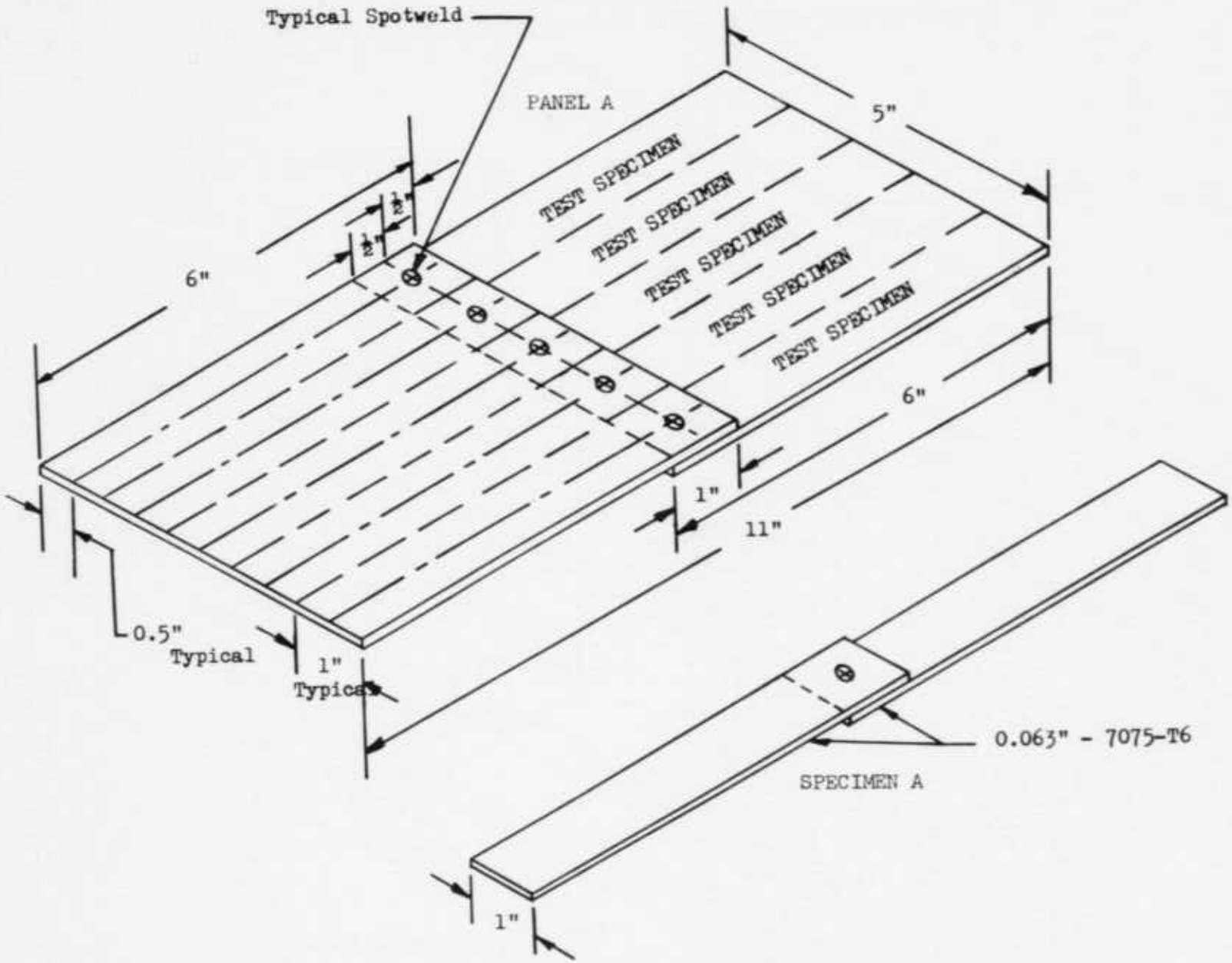

FIGURE A-1 – LAP SHEAR (W/SPOTWELDS) TEST PANEL AND TEST SPECIMEN FOR SPOTWELD-BOND PROGRAM – SPOT-WELD ONLY

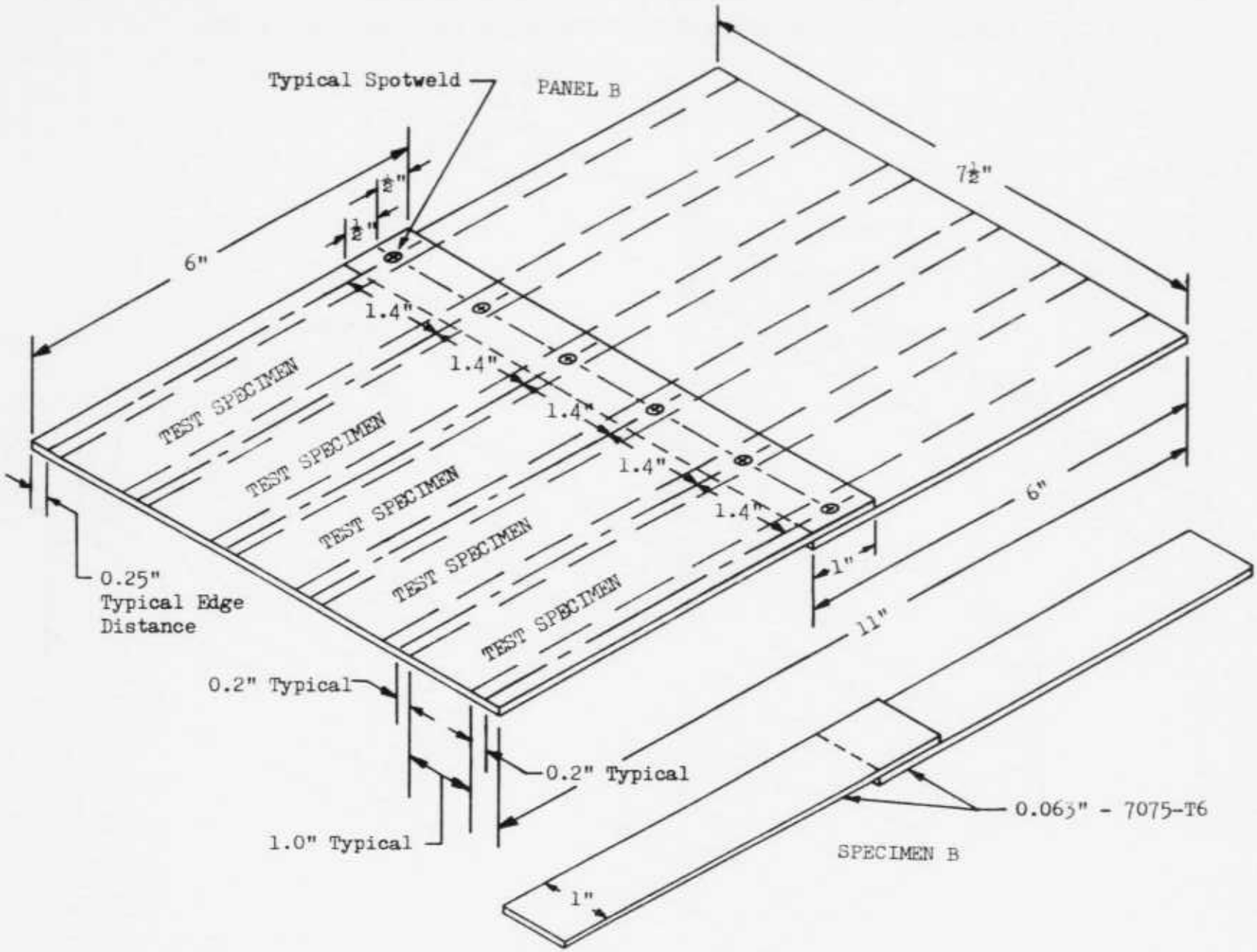

FIGURE A-2 – LAP SHEAR TEST PANEL AND TEST SPECIMEN FOR SPOTWELD – BOND PROGRAM – ADHESIVE ONLY

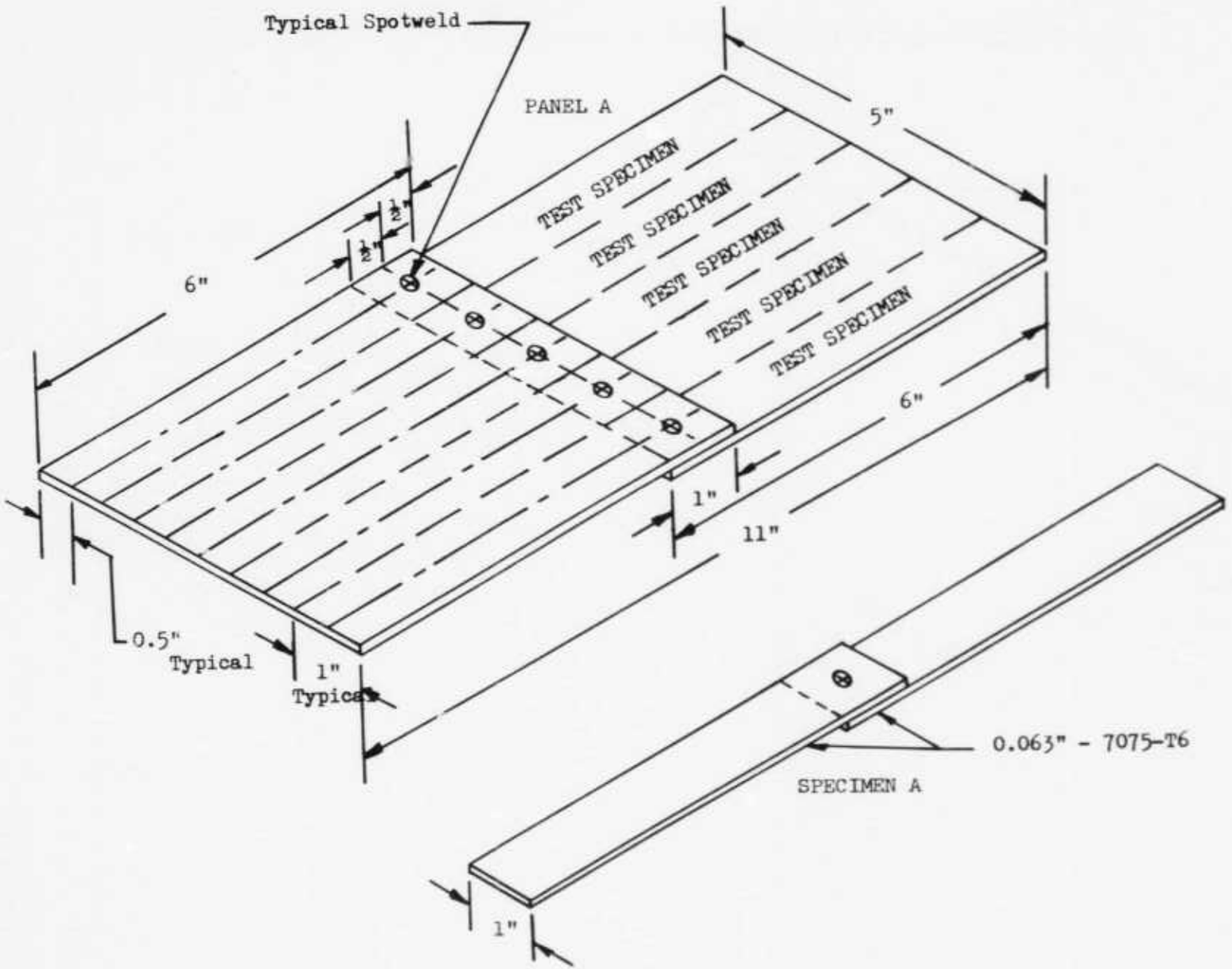

FIGURE A-3 – LAP SHEAR (W/SPOTWELDS) TEST PANEL AND TEST SPECIMEN FOR SPOTWELD – BOND PROGRAM – WELDBOND ONLY

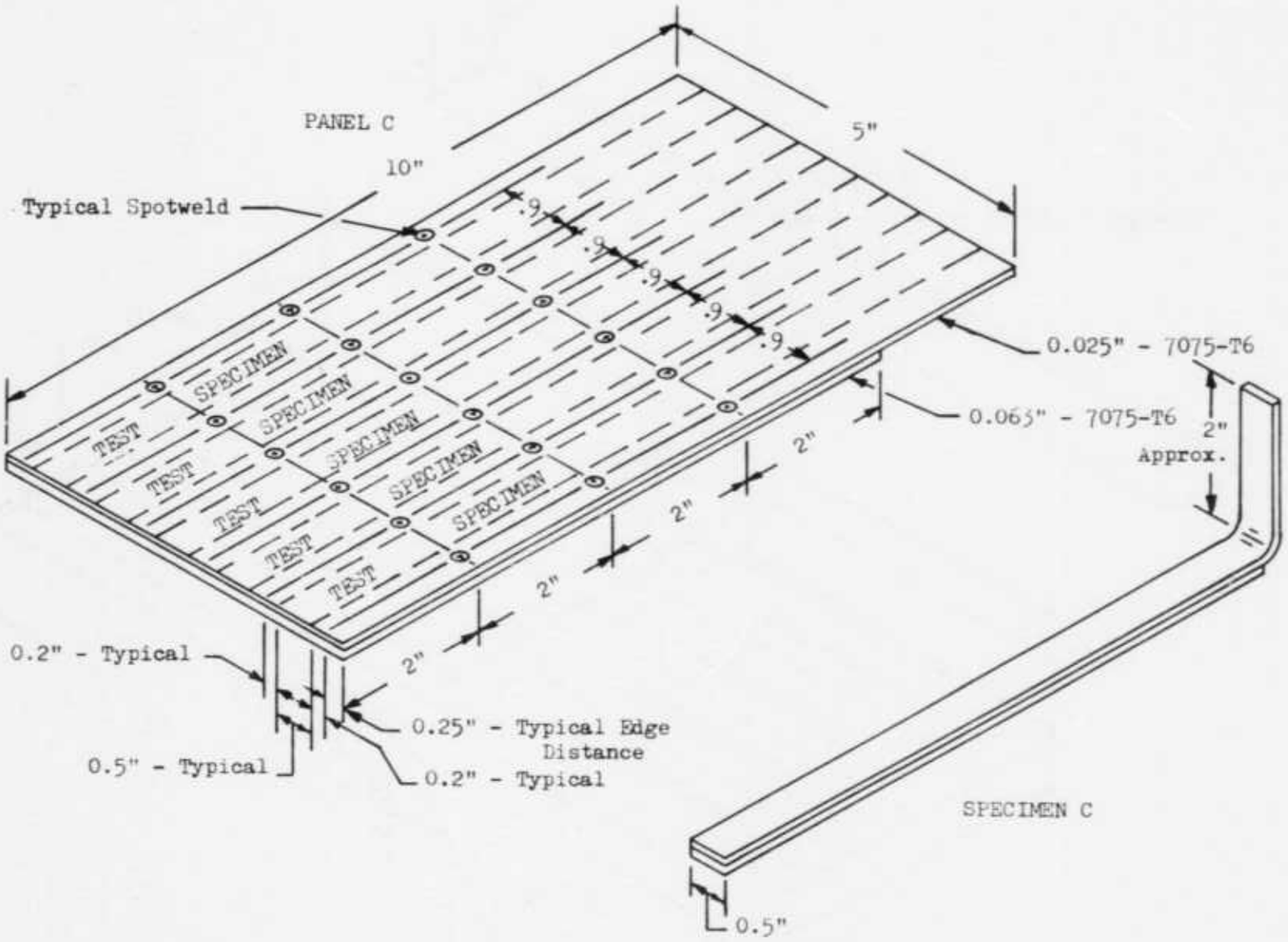

FIGURE A-4 – "BELL" PEEL TEST PANEL AND TEST SPECIMEN FOR SPOTWELD – BOND PROGRAM

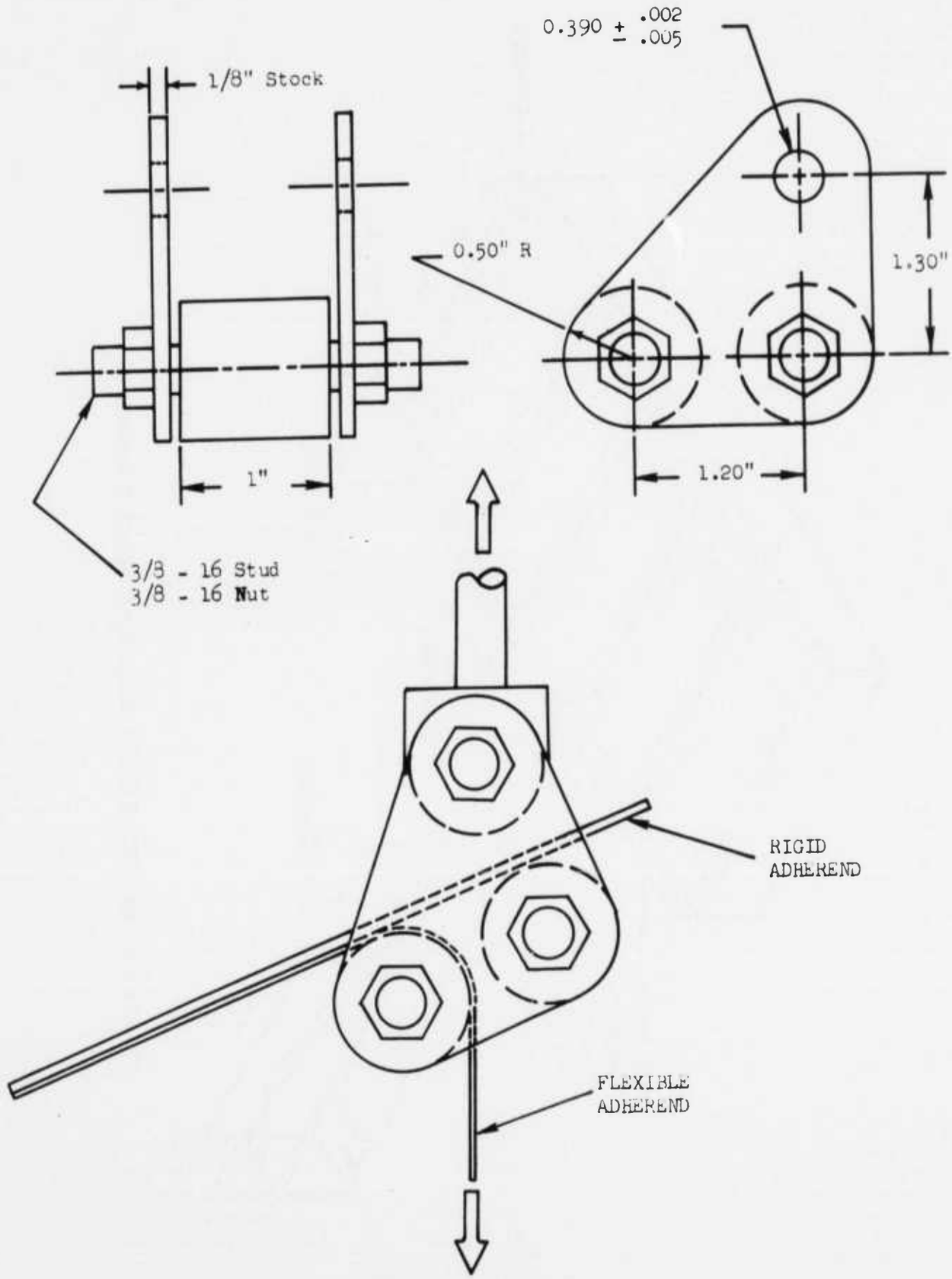

FIGURE A-5 – METAL-TO-METAL TEST FIXTURE

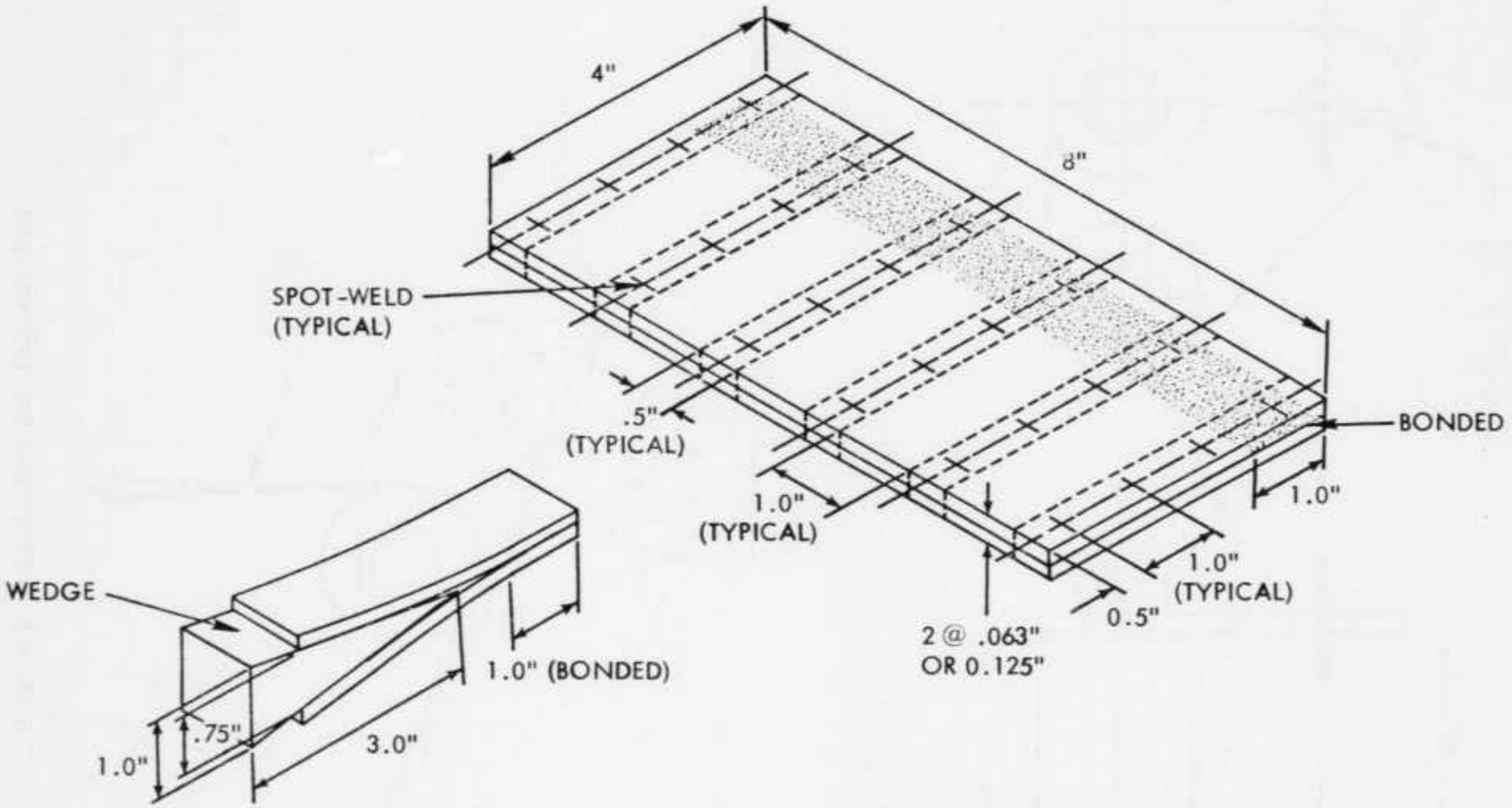

FIGURE A-6 – WELDBOND PANEL, WELDBOND WEDGE SPECIMEN

of approximately one (1) square inch. The test proceeded with the insertion of a wedge between the two adherends at the unbonded end. By this means, the adherends were separated 0.75 inches at the end. The specimens were then suspended in a high humidity environment and time to failure monitored. In addition to time to failure, failure mode and specimen geometry were also recorded.

A.2 Weldbond Joint, Tension-Shear Interaction, and Peel Tests

During the second task of this program, element tests involving static and fatigue loading of weldbond joint specimens and tension-shear interaction tests were conducted along with metal-to-metal peel tests of weldbonded specimens. These tests addressed weldbonding in its final cured state with no elimination of spot-welds as in previous testing.

A.2.1 Weldbond Joint Static Specimen and Test

Single overlap butt lap shear specimens as shown in Figure A7 were fabricated using the finalized weldbond process. These specimens were made individually from three (3) inch wide sheet and, within the program, contained thirty-six (36) separate combinations of spot-weld pattern, adherend overlap and alloy, and adherend thickness. While low temperature (-67^{o}F) test specimens were pin-loaded through doubler reinforced ends, the room temperature and elevated temperature (160^{o}F or 200^{o}F) test specimens were loaded through spherically seated tension grips. The load rate was 50,000 pounds per minute per square inch of weldbond joint area. Ultimate joint shear strength and the mode of failure were recorded for each test.

A.2.2 Weldbond Joint Fatigue Specimen and Test

Specimens similar to those used in joint static testing were fabricated and tested under a fatigue environment during this program. Joint geometries for these specimens were identical to those tested statically. These specimens were lengthened with respect to the static specimens to accommodate testing facilities. Support plates were used during these tests to restrict lateral deflection at the joint while offering no restriction to axial deformations. These tests were conducted in Lockheed-Georgia Company designed tuning-fork fatigue machines having a static capacity of 15,000 pounds and a dynamic capacity of ± 10,000 pounds. Specimen load was applied with a hydraulic actuator and was kept constant during the test by an automatic follow-up system that eliminated any load drop which might have resulted from permanent defomation in the joint. Sinusoidal loading was applied at approximately thirty (30) cycles per second by a variable eccentric wheel attached to one arm of the machine. A mechanical counter attached to the shaft of the wheel recorded the number of cycles applied. An automatic cut-off device stopped the machine upon specimen failure. In addition to cycles to failure, specimen geometry, applied load and mode of failure were recorded for each test.

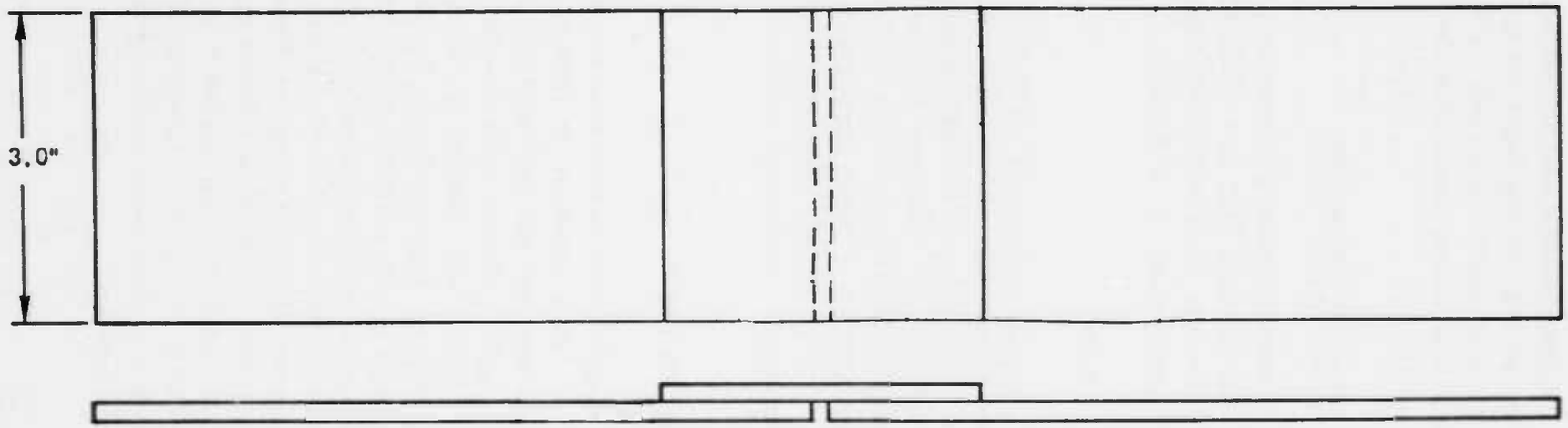

FIGURE A-7 – CENTERED ROW WELD PATTERN SPECIMEN (4 WELD SPACING)

A.2.3 Tension – Shear Interaction

Specimens as shown in Figure A8 were fabricated and tested in order to develop basic tension-shear interaction data. These specimens were tested both statically and in fatigue. Following adhesive cure, these specimens were loaded in tension through one of the four load points to produce a predetermined ratio of tensile to shear stress. For the statically loaded specimens, specimen dimensions, failing load and failure mode were recorded. For the specimens subjected to a fatigue environment, specimen dimensions, load angle, applied load, cycles to failure and failure mode were documented.

A.2.4 Metal-to-Metal Peel – Weldbond

Panels as shown in Figure A9 were fabricated and specimens were removed from these panels. The metal-to-metal peel test procedure was identical to that used for similar "adhesive only" tests described above. It should be noted that specimens tested under this program exhibited premature failures at the first or second weld nugget by tearing of the 0.025-inch thick skin was commonly experienced. Furthermore, using a constant deflection test machine for loading, a fictitiously low peel strength of the adhesive was recorded immediately following the high-energy weld release. Consequently, it is recommended that adjustments to this method be made prior to future weldbond metal-to-metal peel testing.

A.3 Test Environment

During all of the above tests, standard controls and records of temperature, humidity and general environment were maintained. Extreme temperature were controlled to within $\pm 5^{o}F$ of the nominal temperature. Room temperature testing during this program was conducted in the temperature range $70^{o}F$ to $84^{o}F$. Specialized environments addressed under this program are defined below.

A.3.1 High Humidity

The high-humidity environment for this program was defined as 95-100 percent relative humidity at a temperature of $120^{o}F$.

A.3.2 Salt Spray

The salt spray environment for this program was in accordance with Method 811.1 of Federal Test Method Standard 151 as modified by MMM-A-132. The salt concentration used was four (4) to six (6) percent.

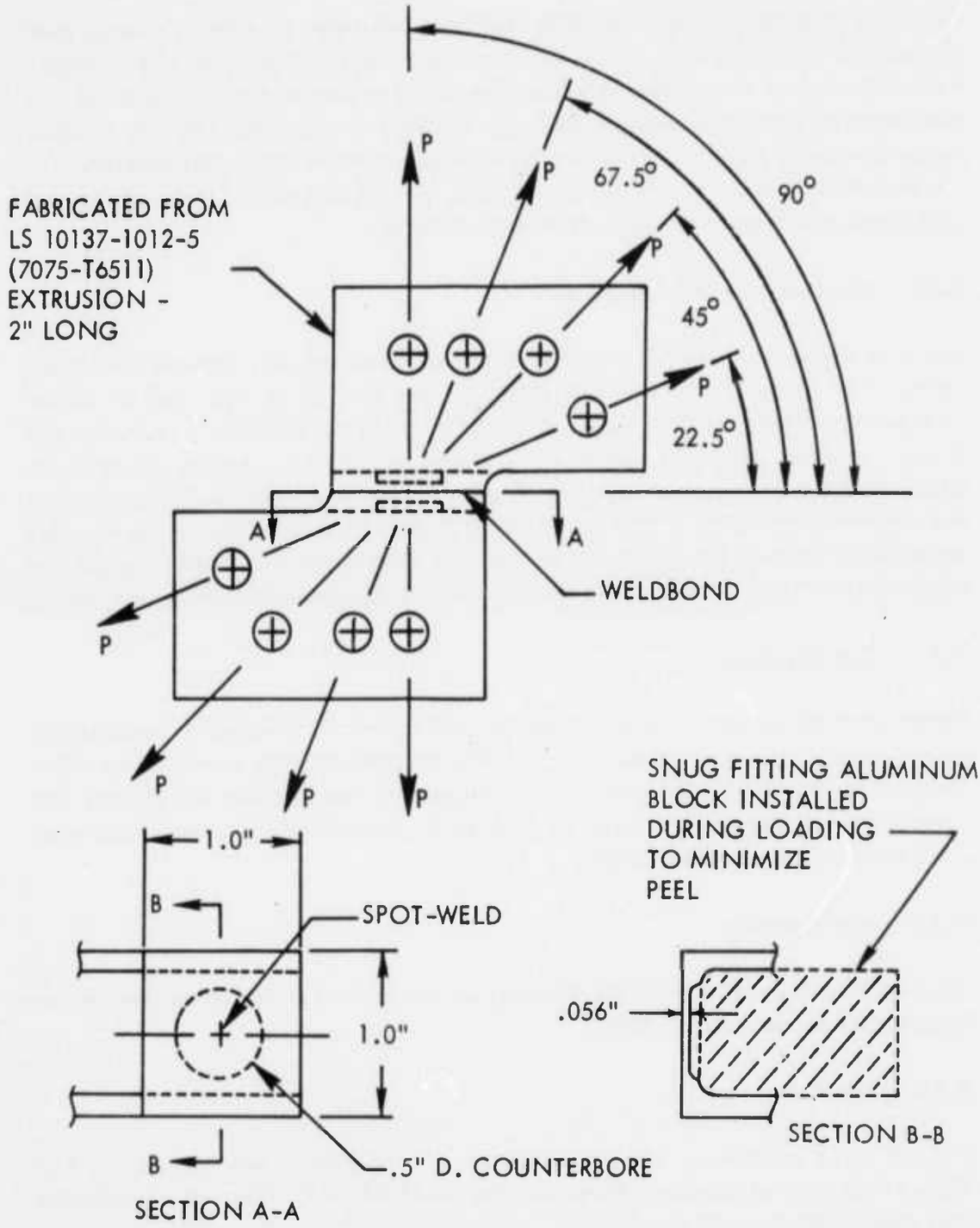

FIGURE A-8 – TENSION-SHEAR INTERACTION SPECIMEN

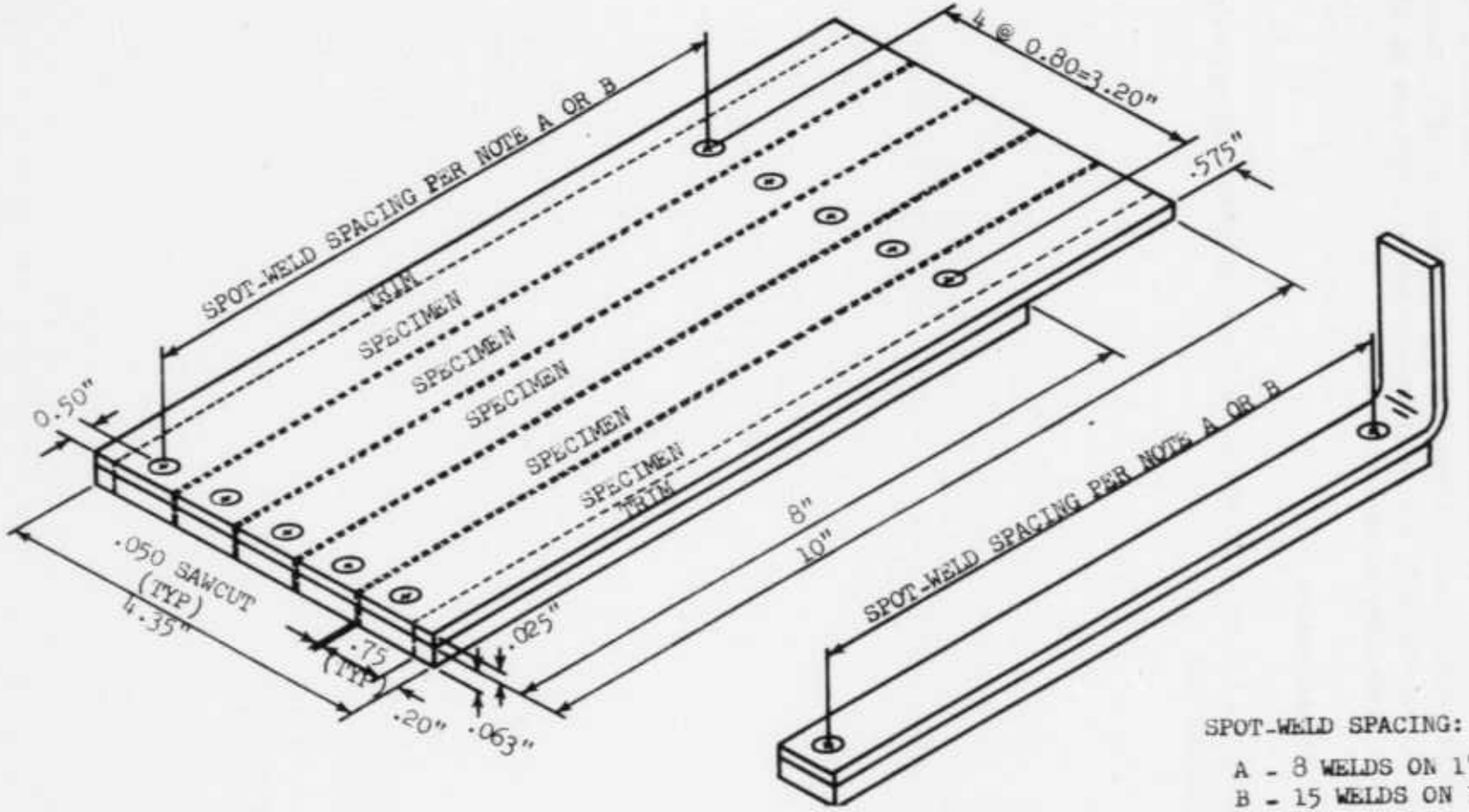

SPOT-WELD SPACING:

A - 8 WELDS ON 1" CTRS.
B - 15 WELDS ON 1/2" CTRS.

ALUMINUM ALLOY - 7075-T6

FIGURE A-9 – "BELL" PEEL TEST PANEL AND SPECIMEN (WELDS IN TESTED BONDLINE)

A.3.3 Temperature – Humidity Cycles

For this program, each cycle consisted of approximately sixteen (16) hours at 120°F and 95-100 percent relative humidity followed by eight (8) hours at -67°F. During days in which cycling was impossible, the specimens were held at 120°F and 95-100 relative humidity after which cyling was resumed.

A.3.4 JP-4 Fuel Immersion

Immersion in JP-4 fuel per MIL-J-5624 was conducted per MMM-A-132 for the time period indicated for each test.

APPENDIX B

STANDARD MATERIAL SPECIFICATION

STM30-106, Rev. A

ADHESIVE, WELDBOND, SERVICE RANGE -67°F to 160°F

1. SCOPE

1.1 This specification establishes the requirements for epoxy adhesives to be used in conjunction with a spot-welding operation. The adhesives qualified herein shall have a service temperature range of -67°F to +160°F. The requirements of this specification have proven satisfactory for fabrication of weldbonded aluminum alloy assemblies under Contract Number F33615-71-C-1716.

1.2 Classification

1.2.1 The adhesives specified herein shall be furnished in the following types:

Type I — One Part Paste

2. APPLICABLE DOCUMENTS

2.1 The following documents, of the issue contractually in effect, form part of this specification to the extent specified herein:

SPECIFICATIONS

Federal

O-A-51	Acetone, Technical
O-S-595	Sodium Dichromate, Dihydrate
O-S-598	Sodium Hydroxide, Technical
O-S-801	Sulfuric Acid, Electrolyte, For Storage Batteries
O-T-634	Trichloroethylene, Technical
P-C-436	Cleaning Compound, Alkali, Boiling Vat (Soak) on Hydrosteam
QQ-A-250/12	Aluminum Alloy 7075, Plate and Sheet
TT-M-261	Methyl-ethyl-ketone (For Use In Organic Coatings)
TT-N-95	Naphtha, Aliphatic
TT-T-548	Toluene, Technical
MMM-A-132	Adhesive, Heat Resistant, Airframe Structural, Metal to Metal
PPP-C-96	Can, Metal, 28 Gage and Lighter

Military

MIL-B-131 Barrier Material, Water Vaporproof, Flexible

3. REQUIREMENTS

3.1 Qualifications

3.1.1 The adhesive furnished under this specification shall be a product which has passed the qualification tests specified herein and has been approved by the procuring activity. When a product has been qualified, any change in the constituent materials or method of manufacture shall require either requalification or prior written approval from the procuring activity.

3.2 General Requirements

3.2.1 Adhesives supplied to the requirements of this specification shall be capable of meeting the requirements of MMM-A-132, Type I, Class 2.

3.2.2 The adhesive shall consist of an epoxy resin, modified as necessary to meet the requirements of this specification, and catalyzed in such a manner as to cure at 270 $\pm$ 10°F within 60 to 80 minutes.

3.2.3 Storage – The adhesive shall meet all of the requirements of this specification after storage in its original unopened container for 180 days at a maximum temperature of 0°F.

3.3 Detail Requirements

3.3.1 The adhesive shall comply with the viscosity and solids content requirements listed in Table B-I, when tested in accordance with 4.6.1 and 4.6.2.

TABLE B-I – VISCOSITY AND SOLIDS REQUIREMENTS

TEST	NO. OF DETERMINATIONS OR SPECIMENS REQUIRED	REQUIREMENTS
Viscosity, Centipoises	3 (1)	Report
Solids Content, Percent	3 (2)	Report

NOTES: (1) Three determinations on one specimen.
(2) Three specimens.

3.3.2 Flow – The adhesive shall not flow out of the bondline when the bondline is in a vertical position during the cure cycle.

3.3.3 Mechanical Properties – The adhesive shall conform to all mechanical property requirements listed in Table B-II when tested in accordance with 4.6.3.

TABLE B-II – MECHANICAL PROPERTY REQUIREMENTS (1)

TEST IDENTIFICATION	-67°F	R.T.	160°F	SALT SPRAY	HIGH HUMIDITY	WEATHERING
Lap Shear (L/t = 16) psi	3000	3500	3000	3000	3000	3000
Lap Shear (L/t = 32) psi	2000	2500	2000	2000	–	–
Weldbond (L/t = 16) psi	3000	3500	3000	3000	–	–
Peel Strength; lb/in.	5	10	10	5	5	5
Creep Deflection; in.	–	0.015	0.015	–	–	–

NOTE: (1) Minimum average values for all tests are given. Each property shall be evaluated by testing five specimens.

3.3.4 Weldability – A certified weld schedule shall be established, by the customer, on the qualification lot of each material from each supplier. This schedule shall then become part of this specification for acceptance of subsequent lots. Nonconforming material shall be rejected. Weldability specimens shall conform to the requirements in Table B-III.

3.3.4.1 The requirements for welds made through the adhesive shall be as specified herein.

3.3.4.1.1 External Defects – The following external weld defects in any test specimen shall be cause for rejection of the material: pits larger than 0.01 inch diameter, surface cracks, blown spots, surface flashes, tip pick-up, metal expulsion, edge and bulge cracks, and excessive surface indentation.

3.3.4.1.2 Internal Defects – Internal defects such as cracks, inclusions, porosity, voids, and lack of fusion which exceed the following size and location limits shall be cause for rejection of the material:

(a) 20 percent of the weld nugget interface diameter.
(b) 25 percent of sheet thickness extension into an outer sheet.
(c) Extension within 10 percent (of the nugget diameter) of the boundary of the nugget structure.

3.3.4.1.3 Weldability Strength – The shear strength of the spot-weld shall be as specified in Table B-III.

TABLE B-III – WELDABILITY REQUIREMENTS

TEST DESCRIPTION	NUMBER OF SPECIMENS		REQUIREMENTS
	QUALIFICATION (3)	ACCEPTANCE (4)	
Visual (1)	25	8	3.3.4.1.1
X-Ray (1)	25	–	3.3.4.1.2
Section (2)	5	3	3.3.4.1.2
Shear (1)	20	5	735 lb. min. at RT

NOTES: (1) Uncured adhesive

(2) Adhesive may be cured to facilitate specimen preparation and examination. Specific cure cycle need not be followed.

(3) The total specimen requirement is twenty-five. The tests, as indicated, are conducted on these specimens.

(4) The total specimen requirement is eight. The tests, as indicated, are conducted on these specimens.

4. QUALITY ASSURANCE PROVISIONS

4.1 Responsibility for Inspection

4.1.1 Unless otherwise specified in the contract or purchase order, the supplier is responsible for the performance of all inspection requirements specified herein. Except as otherwise specified, the supplier may utilize his own or any other facility approved by the procuring activity's Quality Assurance Organization for the purpose of conducting acceptance tests. Qualification tests, as specified herein, shall be performed only by a facility approved by the procuring activity's Engineering organization. The right is reserved to perform any or all of the tests or inspections set forth in this specification, if deemed necessary, to ensure compliance with the prescribed requirements.

4.2 Classification of Tests

4.2.1 The inspection and testing requirements specified herein shall be classified as follows:

(a) Qualification Tests: Those tests and inspection requirements which are necessary to establish that the material or product conforms to all requirements.

(b) Acceptance Tests: Those tests to be performed on individual items or lots of items to determine that certain specified requirements, which serve as a basis for acceptance, have been met.

4.3 Conformance Certification

4.3.1 Qualification Test Report – The supplier shall furnish two copies of a certified report of the results of the qualification tests specified herein, performed to determine conformance with the requirements of this specification. The Qualification Test Report shall be submitted upon completion of test.

4.3.2 Acceptance Test Report – Upon request, the supplier shall furnish two copies of a certified report of the results of the acceptance tests specified herein, performed to determine conformance with the requirements of this specification.

4.3.3 Certificate of Conformance – Upon request, the supplier shall furnish two copies of a certificate of conformance confirming that all material or products in the shipment satisfy and comply with the requirements of this specification. The absence of such request shall in no way relieve the supplier of responsibility for furnishing materials or products which satisfy all the requirements specified herein and supporting data for such a certificate shall be retained by the supplier and be available for review.

4.3.4 Conformance Certification Data – Test reports and certificates of conformance furnished in accordance with these requirements shall include the following identifying information, where applicable:

(a) Purchase order number

(b) Material specification number, revision, and type

(c) Date of manufacture

(d) Manufacturer's stock or lot designation

(e) Date and description of tests performed

4.4. Qualification Tests

4.4.1 Qualification Tests for adhesives to be furnished under this specification shall consist of tests as specified in Tables B-I, B-II and B-III, using adherends as applicable for each type.

4.5 Acceptance Tests

4.5.1 Acceptance tests for adhesives furnished under this specification shall consist of the following tests with results conforming to the applicable requirements of Tables B-I, B-II and B-III.

(a) Viscosity

(b) Solids content

(c) Lap shear, L/t = 16, tested at room temperature

(d) Peel strength, tested at -67°F and room temperature

(e) Weldability (Customer Acceptance Only)

4.6 Test Methods

4.6.1 Viscosity – The adhesive viscosity shall be determined with a Brookfield RVT Viscometer, No. 6 Spindle at 10 RPM (or equal equipment) and a 75 $\pm$2°F after stabilization at this temperature for a minimum period of 2 hours. The average of three readings from one sample shall be reported.

4.6.2 Solids Content – Three specimens consisting of approximately 20 grams of thoroughly mixed adhesive shall be tested for solids content after a 20 $\pm$ 2 minute exposure at 250 $\pm$ 5°F. Calculate the solids content as follows: Solids Content, % = $\frac{W_1 - W_2}{W_1} \times 100$, where W_1 is the specimen weight before exposure and W_2 is the specimen weight after exposure. Report the average of the results for the three specimens.

4.6.3 Mechanical Properties – All specimens shall be prepared from QQ-A-250/12, T6 aluminum alloy, cleaned in accordance with 4.6.5.1, spot-welded in accordance with 4.6.5.2, and cured in accordance with 4.6.5.3. The test specimens shall be prepared in accordance with the following and shall conform to 3.3.3:

(a) Lap shear, L/t = 16; (Figure B-1)

(b) Lap shear, L/t = 32; (Figure B-2)

(c) Weldbond, L/t = 16; (Figure B-3)

(d) Creep Deflection, L/t = 16; (Figure B-1)

(e) Weldability, L/t = 16; (Figure B-3)

(f) Peel Strength; (Figure B-4)

4.6.3.1 Lap Shear Tests (Including Weldbond) – Lap shear tests shall be conducted in accordance with 4.5.5.1, 4.5.5.2, 4.5.5.3, and 4.5.5.9 of MMM-A-132.

4.6.3.2 Peel Test – Peel test shall be accomplished by mounting the specimen, as in Figure B-5, and peel testing at a rate of 6 inches per minute.

4.6.3.3 Creep Deflection – Creep deflection tests shall be conducted in accordance with 4.5.5.5 and 4.5.5.6 of MMM-A-132 except that the conditions shall be 1200 pounds per square inch (psi) at 160 ± 5°F in lieu of 800 psi at 180 ± 5°F as referenced in 4.5.5.6 of MMM-A-132.

4.6.4 Weldability Strength – The mechanical evaluation of the adhesive's weldability shall consist of determining the shear strength of the specimen's spot-weld. This test shall be conducted on a tensile loading machine with self-aligning grips. The load rate shall be 1200 to 1400 pounds per minute and the specimens shall be loaded to failure. Conformance to 3.3.4.1.3 shall be demonstrated.

4.6.5 Test Specimen Preparation – Test specimens shall be prepared as follows:

4.6.5.1 Surface Preparation Procedure – The aluminum details shall be prepared in accordance with the sequence and procedures specified herein.

4.6.5.1.1 Degreasing – Parts shall be degreased by hand wiping with a clean cloth saturated with TT-M-261 Methyl-ethyl-ketone, O-A-51 Acetone, TT-T-548 Toluene, TT-N-95 Aliphatic Naphtha or vapor degreased in O-T-634 Trichloroethylene.

4.6.5.1.2 Alkaline Cleaning – Parts shall be alkaline cleaned in accordance with 4.6.5.1.2.1 or 4.6.5.1.2.2.

4.6.5.1.2.1 Parts may be alkaline cleaned by spraying or immersing for 10 to 15 minutes in a solution of Diversey Corp. No. 909, Wyandotte Chemical Corp. Altrex-Low Foaming, Turco 4215 or 4215S, or equal alkaline cleaner, maintaining a concentration of four to eight ounces of cleaner per gallon of tap water and a temperature of 150 to 180°F.

4.6.5.1.2.2 Parts may be alkaline cleaned by spraying or immersing for 10 to 15 minutes in an alkaline cleaner solution of Turco 4215 or 4215S, or equal, maintained at 175 ± 5°F and a concentration of six to eight ounces of cleaner per gallon of tap water, or in a solution of P-C-436B alkaline cleaner maintained at 150 ± 10°F and a concentration of two to five ounces of cleaner per gallon of tap water.

4.6.5.1.3 Rinse – Alkaline cleaned parts shall be rinsed by spraying and/or immersing for a minimum of three minutes each in a clean water, maximum mineral content of 50 parts per million (ppm), having a temperature of 50 to 150°F.

4.6.5.1.4 Acid Etch – Acid etching of parts shall be accomplished by immersion in an aqueous solution for 3 to 5 minutes. The solution shall have a composition of 9 to 12 ounces per gallon (oz/gal) of O-S-801 Sulfuric Acid (1.828 specific gravity), 4.7 to 6.6 oz/gal of O-S-595 Sodium Dichromate, 0.14 to 0.28 oz/gal Technical Grade Ammonium Biflouride and clean water (Maximum mineral content of 50 ppm). The solution shall be operated at ambient temperature.

4.6.5.1.5 Rinse – Etched parts shall be spray and/or immersion rinsed for 3 to 5 minutes in clean water (maximum mineral content of 50 ppm) having a temperature of 50 to 150°F.

4.6.5.1.6 Alkaline Etch – Alkaline etching shall be accomplished by immersion for 4 to 6 minutes in a solution that is at ambient temperature and composed of 1 to 7 oz/gal of O-S-598 Sodium Hydroxide, Technical Grade Sodium Gluconate (added in a ratio of 1 part Sodium Gluconate to 25 parts Sodium Hydroxide) and clear water (Maximum mineral content of 50 ppm).

4.6.5.1.7 Rinse – Rinse the etched details in accordance with the procedure listed in 4.6.5.1.5.

4.6.5.1.8 Acid Etch – The details shall receive a second acid etch in accordance with the procedure outlined in 4.6.5.1.4 except the immersion time shall be 5 to 10 minutes.

4.6.5.1.9 Rinse – The etched details shall be rinsed in accordance with 4.6.5.1.5 procedures except the rinse time shall be 5 to 10 minutes.

4.6.5.1.10 Hot Air Dry – The parts shall be air dried at 150 ± 10°F.

4.6.5.2 Spotwelding Procedure – The test specimen shall be assembled in accordance with Figures B-1, B-2, B-3, or B-4 as applicable, and spot-welded with the weld schedule established in accordance with 3.3.4.

4.6.5.3 Adhesive Cure Cycle – The cure cycle for the adhesives used to prepare the test specimens shall be 60 to 80 minutes at 270 ± 10°F.

4.6.5.4 Test Environmental Conditions

4.6.5.4.1 Environmental exposure conditions shall be conducted in accordance with the following procedures:

(a) -67°F per MMM-A-132, paragraph 4.3.3

(b) Room temperature per MMM-A-132, paragraph 4.3.1

(c) 160°F in lieu of 180°F per MMM-A-132, paragraph 4.3.2

(d) Salt Spray per MMM-A-132, paragraph 4.3.4. Solid panels or individually cut specimens may be subjected to this exposure. In either case, the cut edges shall be sealed prior to exposure.

(e) High humidity per MMM-A-132, paragraph 4.3.5.

4.6.5.4.2 Weathering exposure shall consist of 30 days (30 cycles) at the following conditions:

(a) A temperature of 125 ± 5°F and relative humidity of 95 to 100 percent for 16 ± 1 hours

(b) A temperature of -67 ± 5°F and ambient relative humidity for 8 ± 1 hour. During days, such as weekends and holidays when cycling is impractical, the specimens are to be held at condition (a) until cycling can be resumed.

5. PREPARATION FOR DELIVERY

5.1 Packaging

5.1.1 Packaging and packing shall be in accordance with the supplier's best commercial practice to assure delivery of acceptable material and prevent damage during storage.

5.2 Marking

5.2.1 Each package shall be permanently and legibly marked to give the following information:

Adhesive, Weldbond, Service Range of -67 to 160°F.

Purchase Order No.

Quantity

Manufacturer's Name and Material Identity

Date of Manufacture

Manufacturer's Lot or Batch Designation

6. NOTES

6.1 Approval

6.1.1 Approval of material and subsequent listing of a supplier as a qualified source is contingent upon submittal and approval of the Qualification Test Report for that supplier.

6.2 Equivalency

6.2.1 There is no existing Government material specification which meets the requirements of this specification.

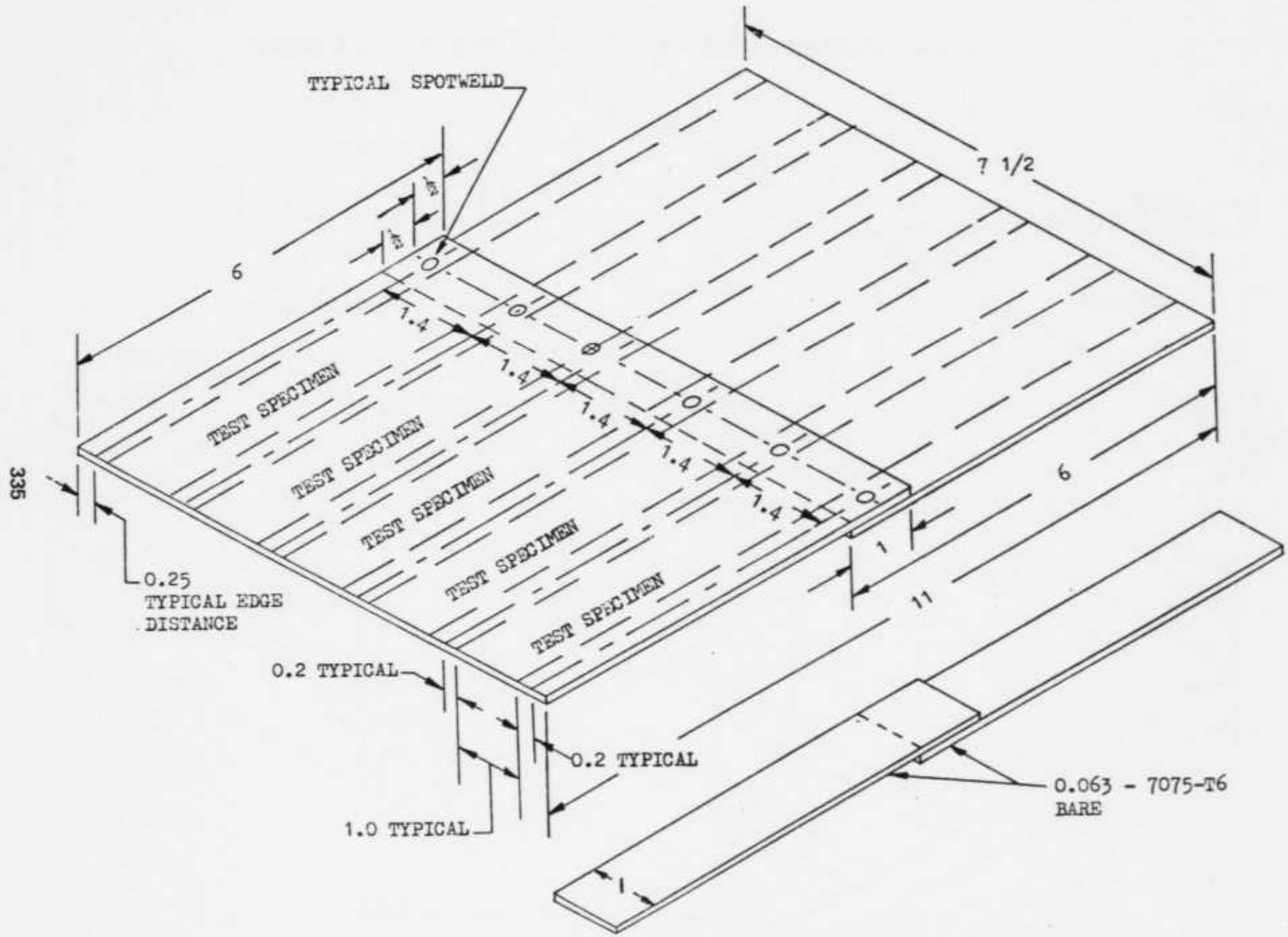

FIGURE B-1 – LAP SHEAR TEST PANEL AND TEST SPECIMEN (L/t = 16)

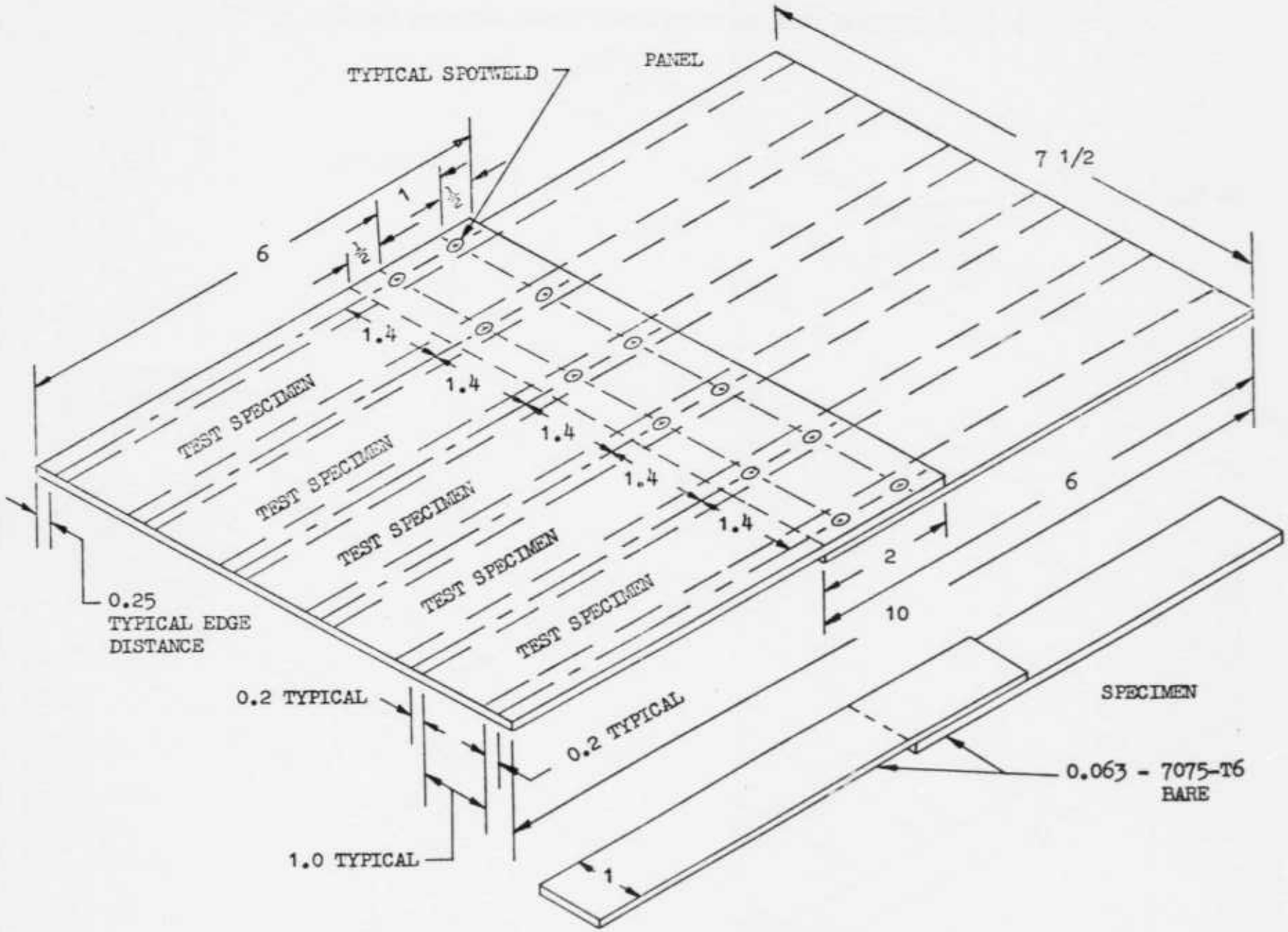

FIGURE B-2 – LAP SHEAR TEST PANEL AND TEST SPECIMEN (L/t = 32)

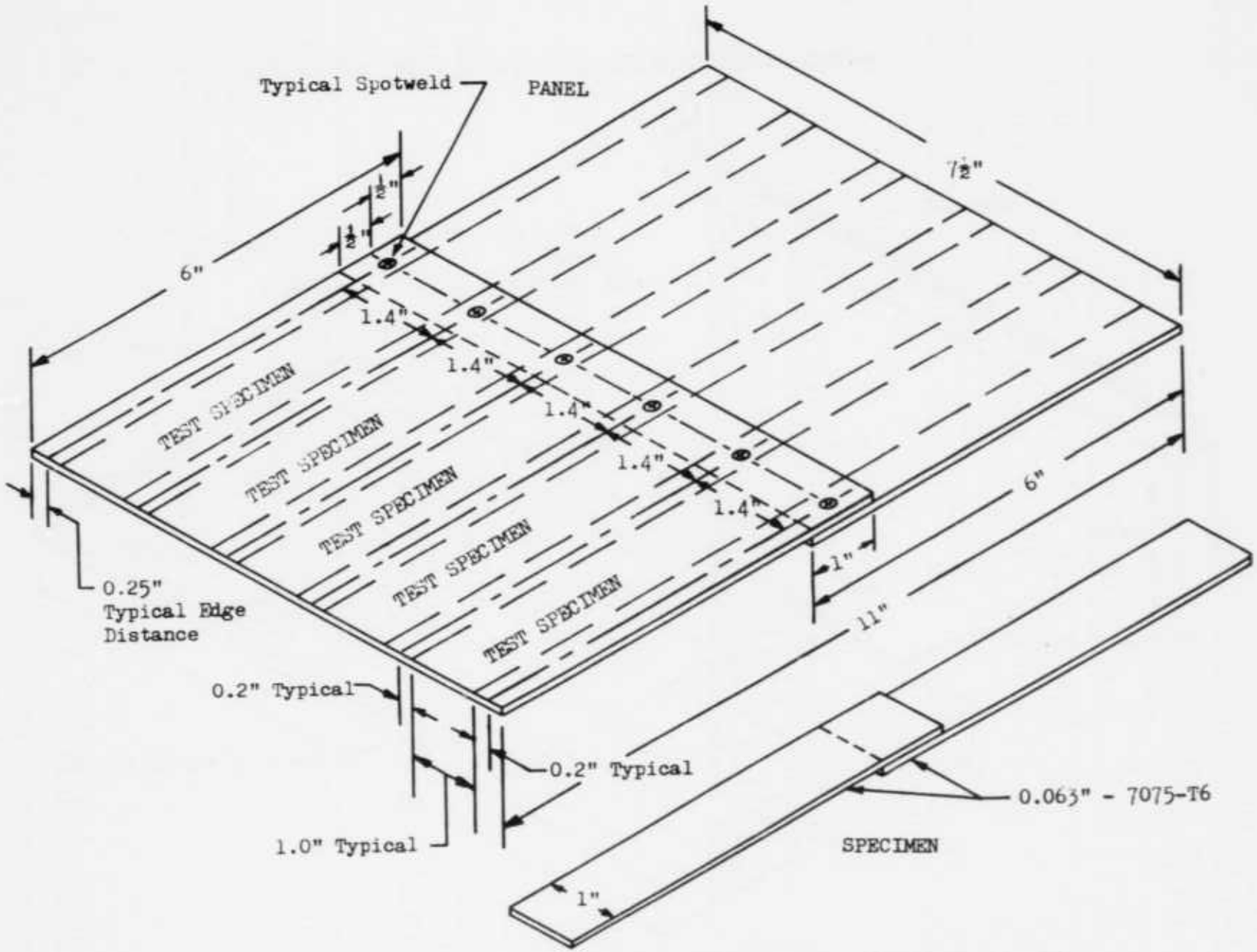

FIGURE B-3 – LAP SHEAR, WELDABILITY AND WELDBOND TEST PANEL AND SPECIMEN (L/t = 16)

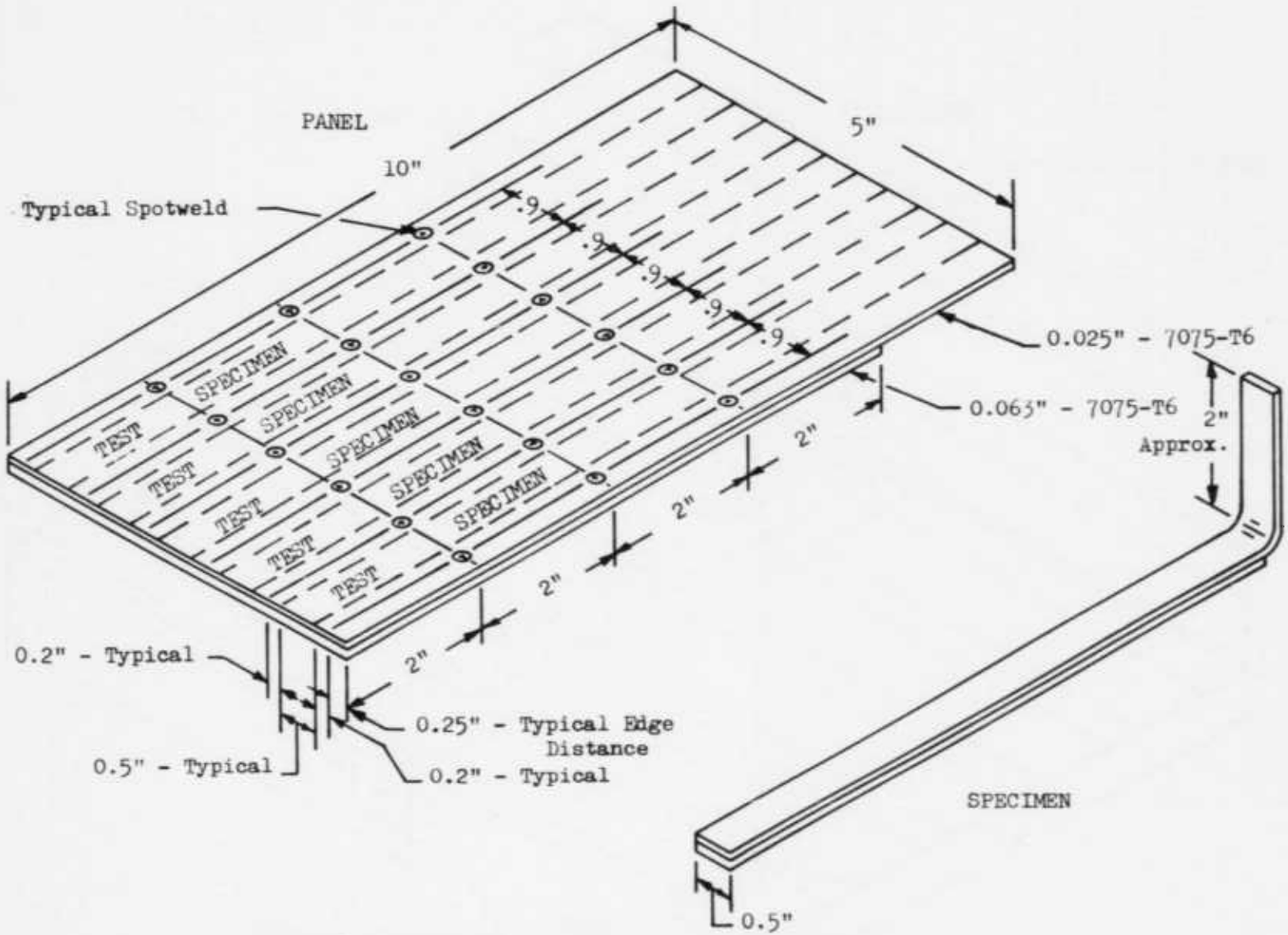

FIGURE B-4 – BELL PEEL TEST PANEL AND TEST SPECIMEN

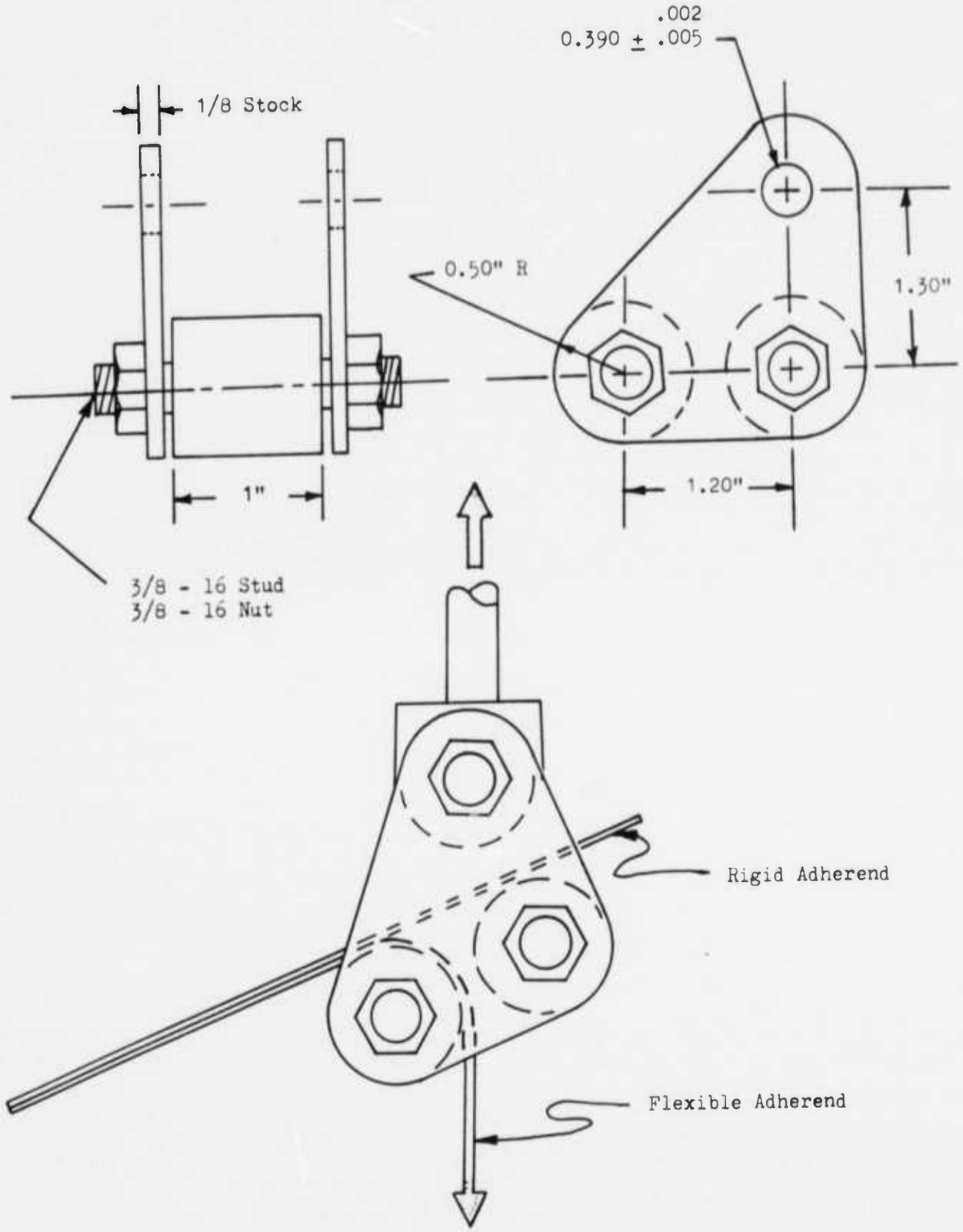

FIGURE B-5 – BELL PEEL TEST FIXTURE

STANDARD PROCESS SPECIFICATION
STP55-001, Rev. B

WELDBONDING OF 2000 AND 7000 SERIES ALUMINUM ALLOYS

1. SCOPE

1.1 This specification establishes the requirements for the weldbonding of 2000 and 7000 series aluminum alloys, 0.020 inch through 0.125 inch thick, in which resistance spot-welds are made in joints containing adhesive at one or more joint interfaces. The requirements of this specification have proven satisfactory for fabrication of weldbonded aluminum alloy assemblies under Contract Number F33615-71-C-1716.

2. APPLICABLE DOCUMENTS

2.1 The following documents, of the latest issue in effect, form part of this specification to the extent specified herein.

SPECIFICATIONS

Federal	
O-T-634	Trichlorethylene, Technical
Military	
MIL-W-6858	Welding, Resistance: Aluminum Magnesium, Non-Hardening Steels or Alloys, Nickel Alloys, Heat Resisting Alloys, and Titanium Alloys; Spot and Seam
Lockheed	
STP57-005	Surface Preparation of Parts for Weldbonding
STM30-106	Adhesive, Weldbond, Service Range -67°F to + 160°F

STANDARDS

Military

MIL-STD-453 Inspection Radiographic

OTHER

Lockheed (Quality Control Procedures QCP)

QCP 14.16 Inspection, Ultrasonic

3. REQUIREMENTS

3.1 Processing Facilities – Weldbonding shall be performed only by those facilities approved by the Procuring Agency.

3.2 Equipment

3.2.1 Welding Machines – The welding machine shall consist of a suitable electrical energy source, water-cooled electrodes, and controls for consistently reproducing output current and electrode force for required time cycles. No current shall flow while electrode force is not being applied. Dressing tools and contour gages shall be provided at each machine.

3.2.1.1 Machine Qualification – Equipment shall be qualified for Class A, Group (a) material in accordance with MIL-W-6858. Except when otherwise required by MIL-W-6858, equipment previously qualified for welding the specified class and group need not be requalified for weldbonding.

3.2.2 Welding Jigs and Fixtures – Weld tooling shall be designed to avoid significant shunting of the weld current. When practicable, tooling which intercepts the welding machine magnetic field shall be made from non-magnetic materials.

3.2.3 Adhesive Application Equipment – Equipment used in application of adhesive to aluminum shall not introduce contaminants which could adversely affect welding or bonding.

3.2.4 Adhesive Curing Oven – Ovens shall be equipped with temperature recorders and shall have working zone thermal profiles not to exceed plus or minus $10^{o}F$ of the control setting within the range of 200 to $300^{o}F$.

3.2.5 Maintenance and Calibration – Welding equipment, mechanical test machines, ovens, temperature recorders and mechanized adhesive application equipment shall be checked and calibrated at intervals acceptable to Quality Assurance. Preventative maintenance schedules shall be established.

3.2.5.1 Welding electrode contour and cleanliness shall be maintained. Damaged or improperly contoured electrodes shall be replaced.

3.3 Materials

3.3.1 Aluminum Alloys – Alloys in the 2000 and 7000 series may be jointed in any combination for which acceptable welding schedules and joint properties can be obtained.

3.3.2 Adhesives – Adhesives shall conform to STM30-106 included herein.

3.3.2.1 Adhesive Weldability Test – When required by the STM or EPS, adhesives shall be tested for weldability in accordance with Table B-IV. Welding shall be performed in accordance with a certified schedule (see 3.8) and production practices.

3.4 Preparation and Protection

3.4.1 Surface Preparation – Parts shall be prepared in accordance with STP57-005, included herein.

3.4.2 Gloves – Except when special instructions exist, such as in chemical cleaning and anodizing operations, parts shall be handled using clean white cotton gloves at all times between initial cleaning and final adhesive curing operations.

3.4.3 Packaging – Parts to be stored or transported within a non-controlled environment shall be protected from contamination by suitable packaging.

3.4.4 Work Areas – All assembly operations associated with weldbonding shall be accomplished in an area where cleanliness is maintained by filtering incoming air; the area shall have its temperature controlled between 65 and 90°F, and its relative humidity shall be controlled between 20 and 65 percent. Cleaned parts shall be stored in the same environment. Cleaned parts or assemblies may be transported through uncontrolled areas provided they are protected against contamination.

3.5 Adhesive Storage and Application

3.5.1 Stock Storage – Adhesive storage temperature and shelf life shall conform to STM30-106. Except when re-qualified by testing in accordance with Table B-IV, outdated adhesive shall not be used. Adhesive requalification shall be valid for 30 days.

3.5.2 Adhesive Distribution – The adhesive shall be disbursed as follows:

3.5.2.1 Each container of adhesive that is removed from refrigerated storage shall be marked with the date and time of removal.

3.5.2.2 The container shall be allowed to warm to within $10^{o}F$ of room temperature before opening.

3.5.2.3 The adhesive shall be dispensed in the original container, or if a complete container is not needed, smaller quantities shall be dispersed in non-contaminating, non-absorbing containers. Containers shall be identified with the specification number and date and time of removal from refrigerated storage. The maximum time out of refrigerated storage shall not exceed 96 hours.

3.5.2.4 Only adhesive that is in the original containers shall be returned for refrigerated storage. The date and time of return to refrigerated storage shall be marked on the container. When the total time out of refrigerated storage exceeds 96 hours, the material shall not be used.

3.5.3 Adhesive Application – Adhesive shall be uniformly applied to the entire joint area by coating one or both members of each interface such that squeeze-out is visible along all bondline edges after welding. The quantity of adhesive applied shall be controlled to avoid extensive cleanup of excess adhesive after welding.

3.5.4 Excess Adhesive – Removal of excess adhesive, if required, shall be accomplished prior to curing. Superficial residues along bondline edges which do not interfere with subsequent finishing or assembly of the part should not be removed.

3.6 Curing – Curing of weldbonded or bonded joints shall be at $270^{o}F \pm 10^{o}F$ for 60 minutes minimum.

3.7 Time Limitations

3.7.1 Processing Time – Adhesive shall be applied and detail parts assembled within 5 days after cleaning of detail parts. Welding shall be completed within 1 week of adhesive application. Curing of the assembly shall be accomplished within 1 week after welding. All details or assemblies being processed through weldbonding operations and prior to curing shall be stored in the controlled area described in 3.4.4.

3.8 Certified Welding Schedules

3.8.1 Extent of Schedule – Welding schedules for spot-welding through adhesive shall be established in accordance with Table B-IV for each welding machine, adhesive type and

metal thickness combination, including the number and stacking arrangement of joint members. Metal thickness shall be measured prior to adhesive application.

3.8.2 Schedule Records – Records shall show the data required by 3.8.1 and shall note all machine settings, welding procedures, auxiliary equipment and tooling. Schedule records shall be located convenient to the welding machine (see 3.16).

3.8.3 Control Adjustment – Settings for each of two parameters may be adjusted within ± 5 percent of the nominal certified setting. When only one parameter is adjusted, a variation of ± 10 percent from nominal is permitted. The same adjustments shall be used for specimens and corresponding production parts. A welding process control specimen set shall be made and tested whenever adjustments are made.

3.8.4 Recertification – A new schedule shall be required when acceptable process control specimens are not produced within the control adjustment limits, or when variations in material or joint thickness exceed the following limits:

a. Variation in the thickness (t) of either outer joint member shall not exceed 0.004 inch or 0.1 t, whichever is greater.

b. Variation in total joint thickness (T) shall not exceed 0.004 inch or 0.1 T, whichever is greater.

3.9 Weld Location

3.9.1 Positional Tolerance – Engineering drawing standard tolerances shall not apply to weld location. When the drawing does not establish specific tolerances, weld location as measured from the center of the electrode impression shall conform to 3.9.1.1 or 3.9.1.2 as applicable. If a tolerance results in an edge distance less then permitted by 3.9.2, the edge distance dimension shall govern.

3.9.1.1 Individually dimensioned weld locations shall be within 1/8 inch of the position indicated by the drawing.

3.9.1.2 Weld positions denoted by a weld symbol or drawing note shall be located within the following limits:

a. Welds in any row shall be within 95 to 105 percent of the number required by the drawing.

b. Welds shall not be displaced in the transverse direction, with respect to the axis of the weld row, by more than 1/8 inch from the calculated correct position.

c. Welds shall not be displaced in the longitudinal (pitchwise) direction by more than 3/16 inch from the calculated correct position.

3.9.2 Edge Distance – The edge distance of each weld as measured from the center of the electrode impression to the nearest edge of the member shall not be less than 2.5t plus 0.1 inches (t = thickness of thinner outer member).

TABLE B-IV – SUMMARY OF TESTS AND INSPECTION REQUIREMENTS

Purpose of Test	Requirement (para)	Joint Type	Type of Test and Inspection	Test (2) (7) Specimens Per Set	Test Procedure	Acceptance Requirements	Fabrication & Test Spec. (Fig. & (Notes))
Weld Schedule Certification	3.8	Weldbond Uncured (3)	Shear	15	4.3.1	3.10	B-6 or B-7 (6)
			Cross-section	5	4.3.2	3.12.4: 3.12.5	
			X-Ray	20	4.3.3	3.13.5	
			Visual	20	4.6	3.12.2: 3.13.2: 3.13.4	
		Weldbond Cured	Shear	15	4.3.1	3.11	B-6 or B-7 (6)
			Visual	15	4.6.1	3.14.1.2: 3.12.2: 3.13.2: 3.13.4	
Welding Process Control	4.4	Weldbond Uncured (3)	Shear	6	4.3.1	3.10	B-6 or B-7 (6)
			Section	4	4.3.2	3.12.4: 3.13.5	
			Visual	10	4.6	3.12.2: 3.13.2: 3.12.4	
Bonding Process Control	4.4	Adhesive Bond	Shear	5	4.3.1	3.11	STM 30-106, 1
			Visual	10	4.6.1	3.14.1.1	STM 30-106, 1 & 4
			Peel	5	4.3.4	3.11	STM 30-106, 4 & 5
Production Qual. and First Article Inspection	3.18 4.7	Prod. Part	X-Ray	–	4.3.3	3.13.6.1	N/A
			Ultrasonic	–	4.3.5	3.14	
			Visual	–	4.6	3.13.3	
Adhesive Weldability Qual. and Acceptance	3.3.2.1	(4)	(4)	(4)	(4)	(4)	(4)
Requalification of Outdated Adhesive	3.5.1	(5)	(5)	(5)	(5)	(5)	(5)

NOTES TO TABLE B-IV

(1) For qualification of welding machines see 3.2.1.1.

(2) For testing of joints having three or more members, a specimen set shall be made and tested for each interface.

(3) Cross section specimens may be cured to facilitate examination. Curing for this purpose need not conform to this specification.

(4) Perform in accordance with the adhesive material specification.

(5) Perform acceptance tests in accordance with the adhesive material specification. Only lap-shear, peel and weldability specimens shall be required. Testing shall be at room temperature, and the L/t ratio for shear tests shall be 16.

(6) Figure B-6 applies to joining of two adherends. Figure B-7 applies to joining of three adherends.

(7) Within the confines of the purpose of test and feasibility: visual, x-ray, shear, cross section, and peel tests may be performed on the same specimens; e.g., a total of 20 uncured and 15 cured weldbond specimens are required for weld schedule certification in accordance with 3.8.

3.10 Weld Mechanical Properties

3.10.1 Welds Made Through Adhesive – The mechanical properties of welds made through adhesive shall be determined in accordance with the schedule established in Table B-IV. Weld strengths shall be in accordance with Table B-V, and shear strength distirbution shall conform to Table B-VI.

3.10.2 Unequal Member Strength – In joints between members of unequal thickness, the required spot strength shall be derived from the weaker member.

TABLE B-V – SPOT-WELD SHEAR STRENGTH

Nominal Thickness of Thinner Sheet, Inch	Pounds Per Weld		Nominal Thickness of Thinner Sheet, Inch	Pounds Per Weld	
	Minimum Individual	Minimum Average		Minimum Individual	Minimum Average
0.020	120	155	0.056	490	610
0.022	145	175	0.063	590	735
0.025	164	205	0.071	725	905
0.028	185	235	0.080	900	1125
0.032	230	285	0.090	1105	1380
0.036	270	335	0.100	1300	1620
0.040	300	380	0.112	1550	1935
0.045	355	445	0.125	1845	2300
0.050	405	510			

TABLE B-VI – SHEAR TEST VALUE DISTRIBUTION

Test Purpose	Requirement
Machine Qualification; Schedule Certification; Adhesive Weld Performance Check	90 percent of test results within ± 15 percent of the actual average and the remainder within ±35 percent of the actual average (1)
Process Control	$\frac{\text{Max. Test Value} - \text{Min. Test Value}}{\text{Average Test Value}} \leqslant 0.35$

NOTE (1) ±20 percent of actual average shall be permissible for 90 percent of test results for joints containing three or more members.

3.10.3 Multi-Layer Joints – When more than two members are present in any joint, strength requirements shall apply separately to each weld between each pair of adjacent members.

3.11 Weldbond and Adhesive Bond Mechanical Properties

3.11.1 Strength – Adhesive bond only specimens shall be made and tested in accordance with Table B-IV. The shear strength shall meet the requirements of Table B-VII.

TABLE B-VII – TEST SPECIMEN MECHANICAL PROPERTIES (1)

Joint Type	Shear Strength (psi) (2)		Peel Strength (lbs/in)
	Minimum Individual	Minimum Average	Minimum Average
Weldbond	2500	2700	
Adhesive Bond	2500	2700	
Peel			10

Notes: (1) Room temperature properties.
(2) L/t = 16, see 6.2.2

3.12 Weld Configuration

3.12.1 Configuration requirements for welds made through an adhesive shall be as specified herein.

3.12.2 Contour – The outline of the electrode impression shall be generally regular in shape. Ovality is permitted provided that the ovality ratio is not greater than 1.30 (see 6.2.1).

3.12.3 Nugget Diameter – When approved by Engineering for production control purposes, nugget diameter measurements may be used in lieu of shear testing. Production Control by nugget diameter shall not be used when electrode impression ovality ratio exceeds 1.15 (see 6.2.1).

3.12.3.1 Nugget diameter values shall be determined during weld schedule certification. The average nugget diameter of a process control specimen set shall not be less than 90 percent of the certification average.

3.12.4 Weld Penetration – The nugget penetration into an outer sheet shall not be less than (a) or (b) below when surveyed over 70 percent of the nugget diameter for two thickness combinations, or 60 percent of the diameter for multiple thickness combinations. Penetration measurements shall be based on sheet thickness before welding.

(a) Outer sheet equal thickness combinations – Penetration shall be at least 20 percent of the sheet thickness.

(b) Outer sheet unequal thickness combinations – Penetration into the thinner member shall be at least 10 percent of its thickness. Penetration Into the thicker member shall be:

(1) For two thickness combinations: at least 10 percent of the thinner member thickness.

(2) For multiple thickness combination: at least 10 percent of the thicker member thickness; or, if less, the sum of the inner sheet thickness(es) plus 10 percent of the thinner outer sheet thickness.

3.13 Weld Quality

3.13.1 Quality requirements for welds made through an adhesive shall be as specified herein. The requirements for conventionally performed welds, e.g., tack welds, shall be in accordance with MIL-W-6858, Class B.

3.13.2 External Weld Defects in Test Specimens – The following defects are not permitted in any test specimen: pits larger than 0.01 inch diameter, surface cracks, blown spots, surface flashes, tip pick-up, metal expulsion, edge and bulge cracks, and excessive surface indentation.

3.13.3 External Weld Defects in Production Parts – Surface cracks, blown spots, metal expulsion, edge cracks, and bulge cracks are not permitted in any production part. The following external defects are permitted within the limits specified.

(a) Pits less than 1/32 inch diameter, surface flashes and tip pick-up.

(1) The number of surface defects of each permissible type shall not exceed 5 percent of the total welds.

(2) The sum of the surface defects of all types, excluding surface indentation, shall not exceed 10 percent of the total welds.

3.13.3.1 Permissible external defects shall be randomly distributed. At least one externally sound weld shall separate each defective weld, in any row.

3.13.4 Surface Indentation – Surface indentation in test specimens and production parts shall not exceed the following values except as noted in 3.13.4.1. Requirements shall be based on the nominal thickness of the member in which indentation occurs:

Aerodynamic Surfaces; 0.004 inch

All Other Surfaces; 0.006 inch for thicknesses in the range 0.020 to 0.040 inch, and 15 percent of thickness for materials thicker than 0.040 inch.

3.13.4.1 Excessive surface indentation shall be permissible in 10 percent of the total of production assembly welds, provided that the indentation defects are randomly distributed.

3.13.5 Internal Weld Defects in Test Specimens – Cracks, inclusions, porosity, voids and lack of fusion shall not exceed the following size and location limits (see 6.2.3):

(a) 20 percent of the weld nugget interface diameter.

(b) 25 percent of sheet thickness extension into an outer sheet.

(c) Extension within 10 percent (of the nugget diameter) of the boundary of the nugget structure.

3.13.5.1 Incipient melting shall not extend within 10 percent (of outer sheet thickness) of the surface of an outer sheet.

3.13.6 Internal Weld Defects in Production Parts – Except when specified in 3.18 for assembly qualification, inspection of production parts for internal weld defects will not normally be required.

3.13.6.1 When specified, internal weld defects in production welds, as determined by radiography, shall not exceed the following limits (see 6.2.3):

(a) 35 percent of the nugget interface diameter.

(b) Cracks, sharp porosity and sharp inclusions shall not extend within 10 percent (of the nugget diameter) of the boundary of the nugget structure.

(c) Voids, lack of fusion, porosity and inclusions may disrupt the nugget boundary provided that:

(1) The defects are smooth.

(2) 75 percent of the regular nugget circumference is intact.

(3) No sharp defect, such as a crack, is evident in the nugget.

(4) The sum of all defects does not reduce the regular nugget area by more than 20 percent.

3.13.6.2 A maximum of 6 percent of welds exceeding the allowable defect limits established in 3.13.6.1 are acceptable without repair. The sum of defects of all types shall not exceed 6 percent.

3.14 Adhesive Bond Quality

3.14.1 Permissible Defects in Test Specimens and Production Parts – Defects in the adhesive bond shall not exceed the following limits.

3.14.1.1 The maximum void in the bondline shall not have an area greater than 0.16 square inches. The maximum aggregate void content between any two weld nuggets shall be 0.16 square inches. The maximum permissible void or dis-bond area within an assembly shall not exceed 5 percent of the total bonded area within the assembly. No voids shall be within 0.13 inches of any edge.

3.14.1.2 Burned adhesive which is in the immediate vicinity and extends around the periphery of the weld nugget shall not extend more than 0.13 inch beyond the periphery of the weld nugget. A maximum of 5 percent of such discontinuities exceeding this requirement is permissible, provided the burned adhesive does not extend within 0.13 inch of the joint edge and does not occur in adjacent weld zones.

3.15 Test Specimens

3.15.1 Material – Material for test specimens shall be truly representative of the materials used in production. For bonding process control, material and shear specimens shall represent the most difficult to clean material in the production batch.

3.15.2 Cleaning – Specimen material for bonding process control shall be cleaned with each batch of detail parts. For clad one side material, the surfaces at the production joint interface(s) shall govern.

3.15.3 Fabrication – Fabrication shall be as specified in Table B-IV for:

(a) joint type

(b) test specimens (or welds) per set

(c) details of fabrication specimen

(d) details of test specimen

3.16 Process Records

3.16.1 Process records shall be maintained and shall be availalbe for examination by an authorized inspector at any time. Records shall include all pertinent process variables and the results of all testing and inspection performed in establishing compliance with the requirements of this specification. The following information shall be recorded for each assembly on the retained part record:

(a) Assembly part number

(b) Date and time details were cleaned

(c) Date and time of adhesive application

(d) Spot-weld schedule used

(e) Date and time of completion of spot-welding

(f) Date and time of initiation of adhesive cure

(g) Cure cycle details; time and temperature

(h) Adhesive batch used

(i) Results of all process control tests

(j) Inspection methods used

3.17 Workmanship

3.17.1 Personnel – Personnel performing resistance welding in accordance with this specification shall have previously demonstrated proficiency adequate to ensure compliance with the requirements herein. Qualified personnel shall be responsible for the control of machine settings and all welding schedules.

3.18 Production Qualification

3.18.1 Weldbond Assembly Qualification – Unless otherwise specified on the Engineering drawing, the first assembly and one assembly selected at random between each 95th and 105th assembly thereafter shall be radiographically inspected for spot-weld quality and ultrasonically inspected for bondline quality. The inspection requirements and acceptance criteria shall be as specified in Table B-IV. The inspection frequency and procedures shall apply for each structural configuration/weld schedule combination.

3.18.2 Requalification -- Any change made in materials, processing, or equipment which results in a weld schedule change will require requalification of the first production part produced for each structural configuration/weld schedule combination.

3.18.3 Assembly Failure – Failure of the assembly to meet all inspection requirements shall be cause for rejection of the assembly. Upon rejection of an assembly, cause of the discrepancy shall be determined and corrected prior to processing of the next assembly. Correction verification shall be accomplished by conducting qualification inspection procdures.

4. QUALITY ASSURANCE PROVISIONS

4.1 An effective quality control system shall be provided to ensure compliance with the requirements of this specification. Details of the inspection system and techniques employed by subcontractors shall be submitted to the customers' Quality Assurance organization for review and approval.

4.2 Specimens – Specimen configurations shall be as noted in Table B-IV. Test specimens shall be made from fabrication specimens. Process control specimen thicknesses shall be representative of the assembly joint member thicknesses.

4.3 Test Methods

4.3.1 Shear Testing – Shear testing shall be performed in accordance with STM30-106. For welded shear specimens, the initial and final welds in each row shall be tested but shall not be considered in calculating weld shear strength distribution.

4.3.2 Cross-Section – Cross-sections shall be taken within 1/32 inch of the center of the electrode impression. Specimens shall be examined at 5X to 10X magnification.

4.3.3 Radiography – Radiographic inspection shall be in accordance with MIL-STD-453.

4.3.4 Peel Testing – Peel testing shall be accomplished in accordance with STM30-106. Spot-welding of the peel test specimen panel may be performed on a separate welding machine to preclude changing the machine settings for performing the test panel welds. If the welds in the peel test panel is accomplished on the welding machine on which the assembly is to be welded, any resulting poor nugget quality may be disregarded provided the poor nugget quality does not affect the bond quality for the peel test specimens.

4.3.5 Ultrasonic Inspection – Ultrasonic inspection shall be in accordance with Lockheed-Georgia Company Quality Control Procedure No. 14.16.

4.4 Frequency of Testing – Fabrication and testing of specimens in accordance with Table B-IV shall be performed at the following minimum intervals during production, except that process control tests pertaining to a schedule not yet in use may be delayed until that schedule is required to be set on the welding machine.

4.4.1 Welding Process Control – For each welding machine, specimen sets shall be tested as follows:

(a) At the start of each production run

(b) At the start of each subsequent shift

(c) Upon replacement of welding electrodes

(d) Whenever a new lot of adhesive is used

(e) At intervals not to exceed two hours of production welding

(f) Whenever control adjustments are made (see 3.8.3)

When unacceptable test results are obtained for any of the specimens, previously made production welds represented by those specimens shall be subject to rejection.

4.4.2 Bonding Process Control – Specimen sets conforming to Table B-IV shall be tested as follows: one set for each batch of parts cleaned and one set for each adhesive lot shall be cured with each oven load of production parts.

4.4.2.1 Unacceptable test results shall be cause for rejection of the parts represented.

4.4.2.2 Sufficient records shall be maintained to provide correlation between test results and the production parts represented.

4.5 Fit-up Surveillance – Surveillance shall be performed during weldbonding production to ensure proper fit up of details and assemblies.

4.6 Visual Inspection – Visual inspection shall be performed at all stages of preparation, assembly, and processing to ensure conformance to the requirements herein.

4.6.1 The joint surfaces of destructively tested specimens shall be examined for conformance to 3.11 and 3.14.

4.7 First Article Inspection – The first part of any production run shall be visually ultrasonically and radiographically inspected.

5. HANDLING AND TRANSPORTATION

5.1 Parts shall be handled and transported in a manner which will ensure that the required physical characteristics and properties are preserved (see 3.4.4).

6. NOTES

6.1 There is no Government process specification that meets the requirements of this specification.

6.2 Definitions

6.2.1 Ovality Ratio – The major diameter divided by the minor diameter.

6.2.2 L/t = 16. The overlap ratio where L is the length and t is the thinnest adherend thickness.

6.2.3 Discontinuity Measurement – The size of a crack, pore, inclusion, or other discontinuity shall be the greatest linear distance between its extremeties. For a star or crow's foot crack, the size shall be the diameter of the circumscribing circle.

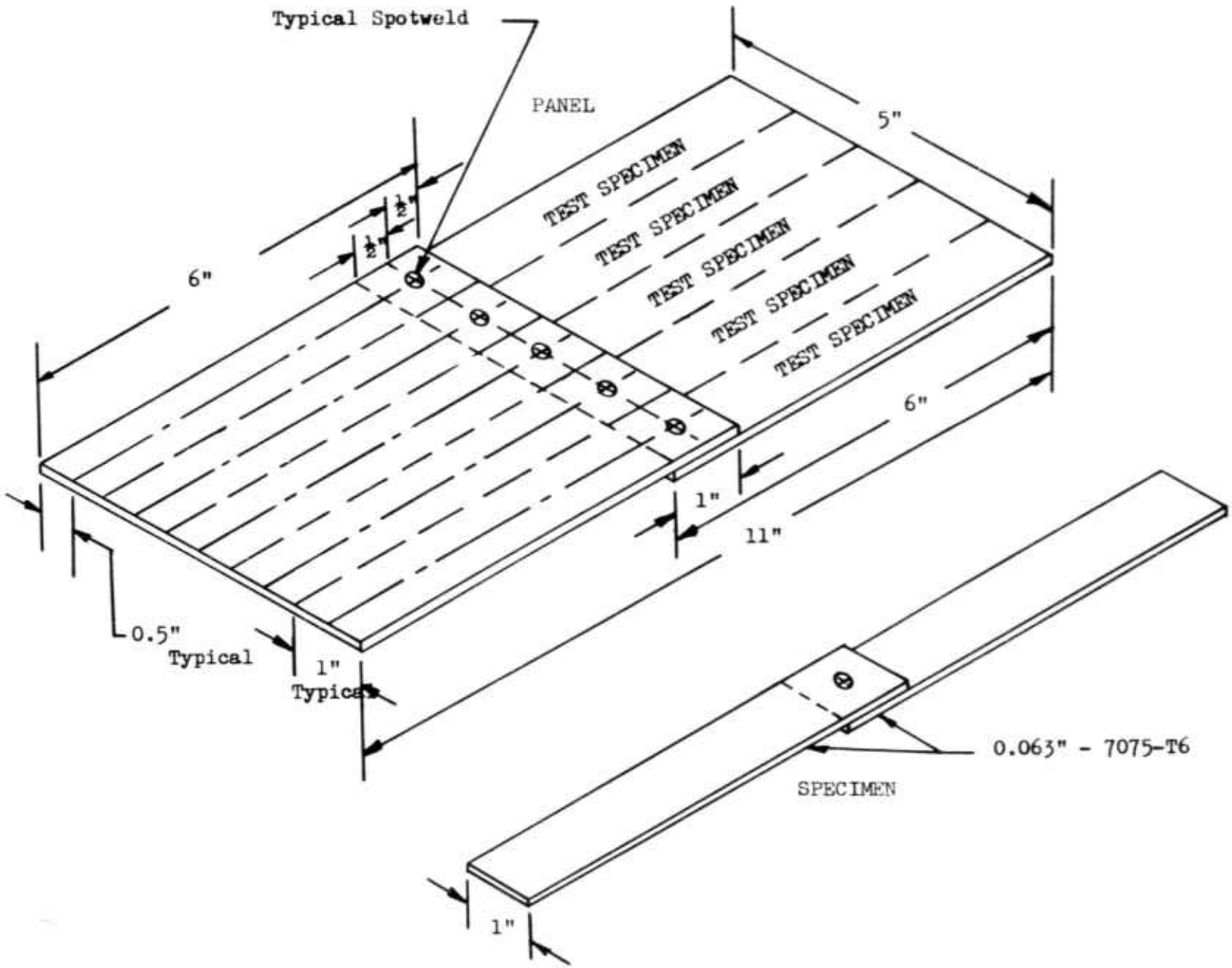

FIGURE B-6 – LAP SHEAR (WITH SPOT-WELDS) TEST PANEL AND TEST SPECIMEN

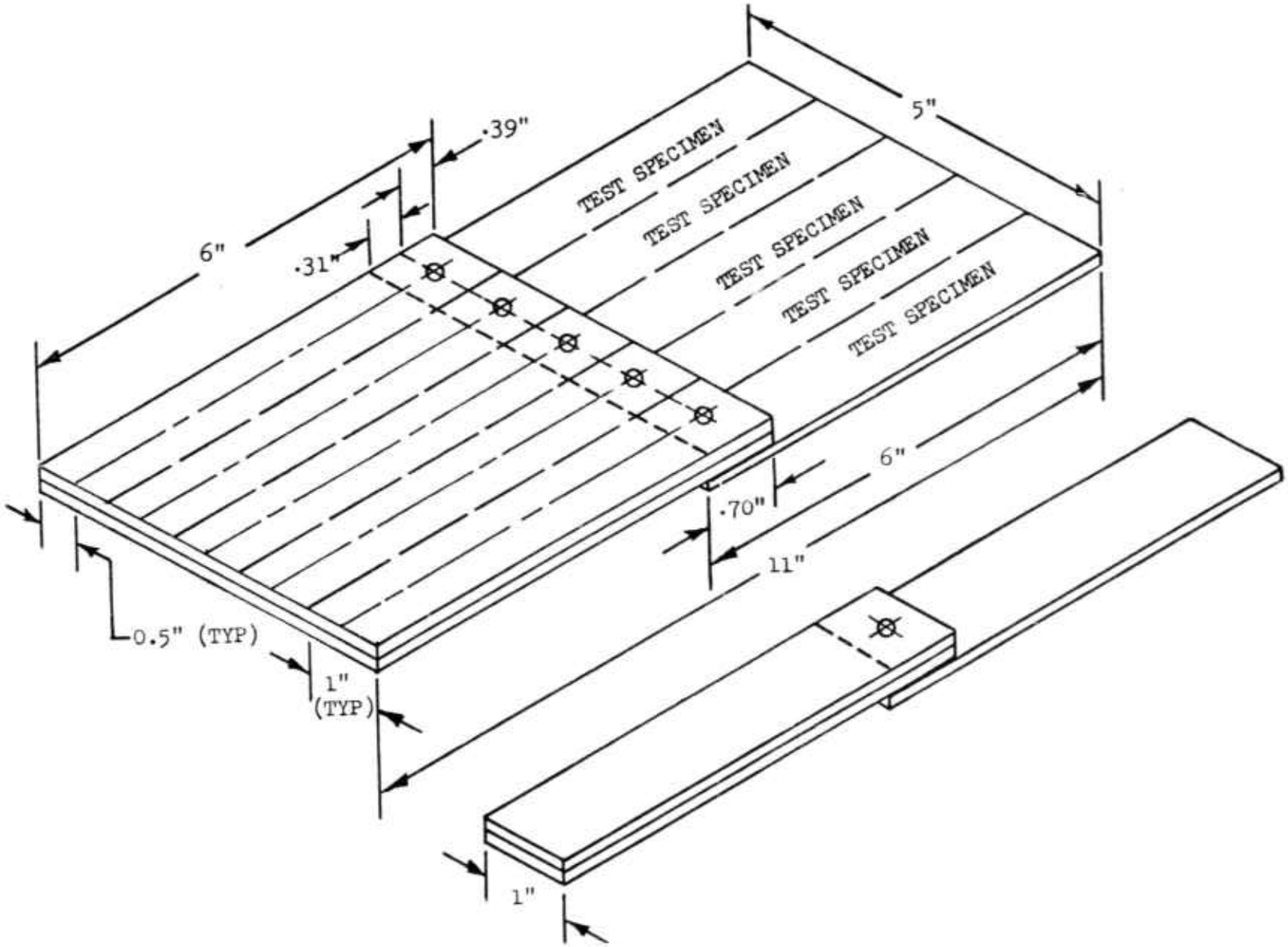

FIGURE B-7 – MULTI-PLY LAP SHEAR TEST PANEL AND TEST SPECIMEN

STANDARD PROCESS SPECIFICATION
STP57-005, REV. A

SURFACE PREPARATION OF PARTS FOR WELDBONDING

1. SCOPE

1.1 This specification establishes the requirements for surface preparation of parts for weldbonding. The requirements of this specification have proven satisfactory for fabrication of weldbonded aluminum alloy assemblies under Contract F33615-71-C-1716.

2. APPLICABLE DOCUMENTS

2.1 The following documents, of the issue contractually in effect, form part of this specification to the extent specified herein:

SPECIFICATIONS

Federal

O-A-51	Acetone, Technical
O-S-595	Sodium Dichromate, Dihydrate, Technical
O-S-598	Sodium Hydroxide, Technical
O-S-801	Sulfuric Acid, Electrolyte, For Storage Batteries
O-T-634	Trichloroethylene, Technical
P-C-436	Cleaning Compound, Alkali, Boiling Vat (Soak) On Hydrostream
TT-M-261	Methyl-ethyl-ketone (For Use in Organic Coatings)
TT-N-95	Naphtha, Aliphatic
TT-T-548	Toluene, Technical

3. REQUIREMENTS

3.1 Materials

3.1.1 Only those materials specified herein shall be used in the process covered by this specification.

3.2 General Requirements

3.2.1 Handling – After cleaning, parts to be weldbonded shall be handled only by personnel wearing clean white gloves. Cleaned parts shall not be touched with bare hands. Touching of bond surfaces with gloved hands shall be avoided whenever practicable.

3.2.2 Solution Control – The chemical balance of processing solutions shall be verified daily when in use. When the processing solutions have not been used for a period exceeding two days, the chemical balance shall be verified prior to use.

3.2.3 Storage – Cleaned parts shall be stored in a controlled environment, or protected to preclude contamination, immediately after cleaning.

3.3 Detail Requirements

3.3.1 Surface Preparation – Aluminum details to be weldbonded shall be prepared in accordance with the sequence and procedures specified herein. All parts, except clad exterior skins, shall be prepared in accordance with 3.3.2. Clad exterior skins shall be prepared in accordance with 3.3.3.

3.3.2 Standard Weldbond Etch Process

3.3.2.1 Degreasing – Details shall be degreased by hand wiping with a clean cloth saturated with TT-M-261 Methyl-ethyl-ketone, O-A-51 Acetone, TT-T-548 Toluene, TT-N-95 Naphtha, or by vapor degreasing with O-T-634 Trichloroethylene.

3.3.2.2 Alkaline Cleaning – Parts shall be alkaline cleaned in accordance with either 3.3.2.2.1 or 3.3.2.2.2.

3.3.2.2.1 Parts may be alkaline cleaned by spraying or immersing for 5 to 20 minutes in a solution of Diversey Corp. No. 909, Wyandotte Chemical Corp. Altrex-Low Foaming, Turco 4215, Turco 4215S, or equal, maintaining a concentration of 4 to 8 ounces of cleaner per gallon of tap water and a temperature of 150 to 180°F.

3.3.2.2.2 Parts may be alkaline cleaned by spraying or immersing for 5 to 20 minutes in an alkaline cleaner solution of Turco 4215 or 4215S, or equal, maintained at 175 ± 5°F and 6 to 8 ounces of cleaner per gallon of tap water or in a solution of P-C-436 Alkaline Cleaner maintained at 150 ± 10°F and 2 to 5 ounces of cleaner per gallon of tap water.

3.3.2.2.3 Rinse – Alkaline cleaned parts shall be rinsed by spraying and/or immersing a minimum of 3 minutes for each rinse method used in a clean water which has a maximum mineral content of 50 parts per million (ppm) and a temperature within the range of 50 to 150°F.

3.3.2.3 Acid Etch – Acid etching of parts shall be accomplished by immersion in an aqueous solution for 3 to 5 minutes. The solution shall have a composition of 9 to 12 ounces per gallon of 0-S-801 Sulfuric Acid (1.828 specific gravity), 4.7 to 6.6 ounces per gallon of 0-S-595 Sodium Dichromate, 0.14 to 0.28 ounces per gallon of Technical Grade Ammonium Bifluoride and water with maximum mineral content of 50 ppm. The solution shall be operated at ambient temperature.

3.3.2.3.1 Rinse – The etched details shall be rinsed by spraying and/or immersing at ambient temperature, for 3 to 5 minutes for each rinse method used, in rinse water which has a maximum mineral content of 50 ppm.

3.3.2.4 Alkaline Etch – Alkaline etching of parts shall be accomplished by immersion in a solution at ambient temperature, composed of 1 of 7 ounces per gallon of 0-S-598 Sodium Hydroxide, Technical Grade Sodium Gluconate (added in a ratio of 1 part Sodium Gluconate to 25 parts Sodium Hydroxide) and clear water (maximum mineral content of 50 ppm).

(a) This process shall not be used on clad exterior skins. Clad skins shall be etched in accordance with 3.3.3.

(b) Clad parts, except exterior skins, shall be limited to a 3 minute maximum etch time.

(c) Parts, except items (a) and (b), shall receive a 5 to 10 minute etch.

3.3.2.4.1 Rinse – The etched details shall be rinsed in accordance with 3.3.2.3.1.

3.3.2.5 Acid Etch – The details shall receive a second acid etch in accordance with the precedure outlined in 3.3.2.3, except the immersion time shall be 5 to 10 minutes.

3.3.2.5.1 Rinse – The etched details shall be rinsed in accordance with the procedure listed in 3.3.2.3.1, except the rinse time shall be 5 to 10 minutes.

3.3.2.6 Hot Air Dry – The parts shall be air dried at $150 \pm 10^{o}F$.

3.3.3 Mild Weldbond Etch Process – Clad exterior skins shall be prepared in accordance with the sequence and procedures specified herein.

3.3.3.1 Degrease – The details shall be degreased in accordance with 3.3.2.1.

3.3.3.2 Alkaline Cleaning – The details shall be alkaline cleaned in accordance with 3.3.2.2.

3.3.3.2.1 Rinse – The alkaline cleaned parts shall be rinsed in accordance with 3.3.2.2.3.

3.3.3.3 Acid Etch – Acid etching of the details shall be accomplished in accordance with 3.3.2.3, except the etch time shall be 10 to 20 minutes.

3.3.3.3.1 Rinse – After acid etching, the details shall be rinsed in accordance with 3.3.2.2.3, except the rinse time shall be 5 to 10 minutes.

3.3.3.4 Hot Air Dry – The parts shall be air dried at 150 ± 10°F.

3.4 Weldability

3.4.1 Weldability tests used for process controls shall be performed prior to subsequent processing.

3.4.2 Weldability tests shall consist of a visual examination of the nuggets for both external and internal defects, plus determination of the shear strength of uncured weldbonded specimens. The weldability requirements shall be as follows:

3.4.2.1 External Defects – The following external weld defects on any test specimen shall be cause for rejection of the material: pits larger than 0.01 inch diameter, surface cracks, blown spots, surface flashes, tip pick-up, metal expulsion, edge cracks, and bulge cracks.

3.4.2.2 Internal Defects – Internal defects in any nugget such as cracks, inclusions, porosity, voids, and lack of fusion, which exceed the following size and location limits, shall be cause for rejection of the load of cleaned parts:

(a) 20 percent of the weld nugget interface diameter.

(b) 25 percent of sheet thickness extension into an outer sheet.

(c) Extension within 10 percent (of the nugget diameter) of the boundary of the nugget structure.

The test specimens which will be sectioned for metallurgical examination may be cured. Any convenient cure cycle may be used.

3.4.2.3 Nugget Strength – The shear strength of the spot-weld shall be 735 pounds minimum.

3.4.2.4 After surface preparation, the details shall be stored in an area where cleanliness is maintained by filtering all incoming air; the area shall have its temperature controlled between 65 and 90°F, and its relative humidity shall be controlled between 20 and 65 percent. Cleaned parts may be transported through uncontrolled areas provided they are protected against contamination.

4. QUALITY ASSURANCE PROVISIONS

4.1 An effective quality control system shall be provided to ensure compliance with the requirements of this specification. The inspection system employed by subcontractors shall be approved by the procuring activity's Quality Assurance.

4.2 Process Control

4.2.1 Test Specimens – Sufficient panel details for the preparation of two panels conforming to Figure B-8, shall be processed for cleaning with each load of parts.

4.2.2 Specimen Preparation – Two panels representing each load of cleaned parts shall be prepared and checked for conformance to the requirements of 3.4. The panels shall be processed with a certified weld schedule, using adhesive which is approved for production use.

4.2.3 Testing – Both panels shall be visually inspected for conformance to the requirements of 3.4.2.1. The one panel, containing 5 nuggets shall be sectioned, and checked for conformance to the requirements of 3.4.2.2. The other panel shall be cut into 5 specimens in accordance with Figure B-8 and tested for conformance to 3.4.2.3.

5. HANDLING AND TRANSPORTATION

5.1 Parts shall be handled and transported in such a manner as to ensure that the required physical characteristics and properties are preserved.

6. NOTES

6.1 Equivalency

6.1.1 There is no existing Government document which meets the requirements of this specification.

6.2 Definitions

6.2.1 Clean Water – Water having a maximum mineral content of 50 parts per million.

6.2.2 Load – All of the metal parts cleaned in a single cleaning operation.

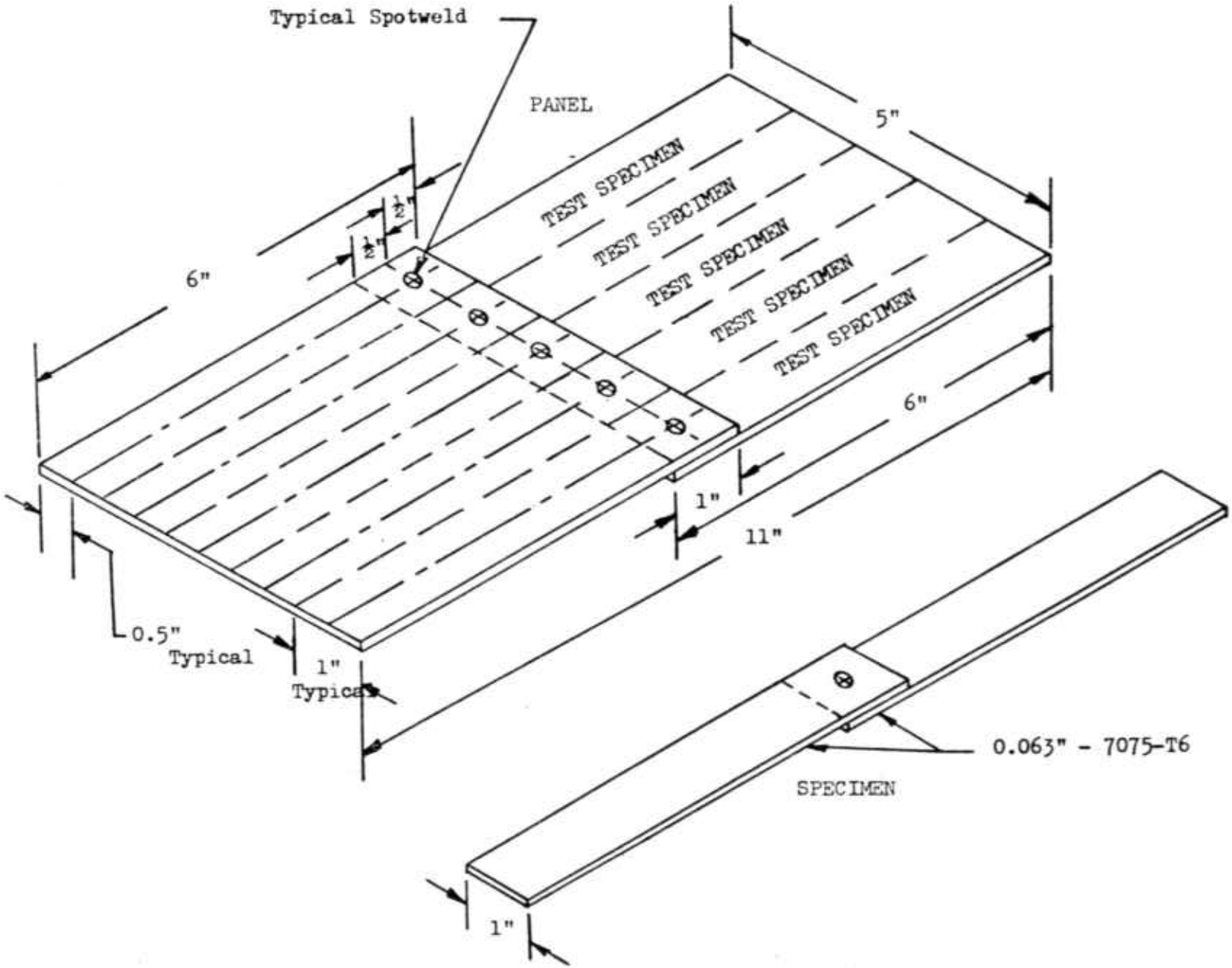

FIGURE B-8 – LAP SHEAR, WELDABILITY AND WELDBOND TEST PANEL AND SPECIMEN (L/t = 16)

REFERENCES

1. STP55-001, "Weldbonding of 2000 and 7000 Series Aluminum Alloys"

2. AFFDL-TR-67-156, "Refinement of Sonic Fatigue Structural Design Criteria", January 1968

3. Dow, N.F., Hickman, W.A., and Rosen, B.W.; NACA TN 3064, "Data on the Compressive Strength of Skin-Stringer Panels of Various Materials", January, 1954

4. Dickson, J.N., "Analysis of Bonded Joints in Laminated Composte Materials With Linear Stress-Strain Behavior", Lockheed-Georgia Company ER-10584, November 1970

5. AFML-TR-70-227, "Resistance Spot Weld-Adhesive Bonding Process", November 1970

6. Wilcox, R.E. and Vennel, W.W.; Structural Design Criteria – C-130E Airplane", Lockheed-Georgia Company ER/P-6588, January 1964

7. Atkinson, L.M., "Mid Fuselage Stress Analysis of the C-130B and C-130E Airplanes", Lockheed-Gerogia Company ER-3067, October 1958

8. Braswell, J.V. and Ray, J.H.; "C-130 Damage Analysis in Rapid Time Computer Program Report", Lockheed-Gerogia Company ER-10984, December 1970

9. Castellon, P.F. and Freyre, O.L.; "Correlation of the C-130B Test to the Safe Life Analysis of the Model C-130B Airplane", Lockheed-Georgia Comapny ER-5347, November 1963

10. Mueller, F.M., "Fail-Safe Criteria -- Ultimate Strength Determination of Damaged Structures", Lockheed-California Company LR 11080, February 1957

UNCLASSIFIED

SECURITY CLASSIFICATION OF THIS PAGE (When Data Entered)

REPORT DOCUMENTATION PAGE		READ INSTRUCTIONS BEFORE COMPLETING FORM
1. REPORT NUMBER AFML-TR-74-179/AFFDL-TR-74-106	2. GOVT ACCESSION NO.	3. RECIPIENT'S CATALOG NUMBER
4. TITLE (and Subtitle) WELDBOND FLIGHT COMPONENT DESIGN/ MANUFACTURING PROGRAM		5. TYPE OF REPORT & PERIDO COVERED Final 7-15-71 to 7-15-74 6. PERFORMING ORG. REPORT NUMBER LG74ER0178
7. AUTHOR(s) Grosko, John J. Kizer, Judson A.		8. CONTRACT OR GRANT NUMBER(s) F33615-71-C-1716
9. PERFORMING ORGANIZATION NAME AND ADDRESS Lockheed-Georgia Company Marietta, Georgia 30063		10. PROGRAM ELEMENT, PROJECT, TASK AREA & WORK UNIT NUMBERS AFML Project No. 834-1 & AFFDL Project No. 1368, Task 136802
11. CONTROLLING OFFICE NAME AND ADDRESS Air Force Materials Laboratory & Air Force Flight Dynamics Laboratory Wright - Patterson AFB, Ohio 45433		12. REPORT DATE December 1974 13. NUMBER OF PAGES 365
14. MONITORING AGENCY NAME & ADDRESS (if different from Controlling Office)		15. SECURITY CLASS. (of this report) Unclassified 15a. DECLASSIFICATION DOWNGRADING SCHEDULE

16. DISTRIBUTION STATEMENT (of this Report)

Distribution limited to U.S. Government Agencies and designated recipients only since this report contains test and evaluation information directly applicable to military hardware. Other requests must be referred to Metals Branch, AFML, or Structural Development Branch, AFFDL, Wright-Patterson AFB, Ohio 45433.

17. DISTRIBUTION STATEMENT (of the abstract entered in Block 20, if different from Report)

18. SUPPLEMENTARY NOTES

19. KEY WORDS (Continue on reverse side if necessary and identify by block number)

Weldbonding
Adhesive Bonding
Spot-Welding
Surface Preparation
Epoxy Adhesive
Overlap Tensile Shear Strength
Tensile Shear Fatigue

20. ABSTRACT (Continue on reverse side if necessary and identify by block number)

This report describes the weldbond process developments, component analyses, and tests that led to the design and manufacture of a C-130H weldbonded fuselage component. The weldbonded fuselage component was installed on C-130H Serial No. AF73-01592 for flight evaluation. This development program was accomplished in five tasks; namely, process development, engineering data development and component design, component fabrication, structural testing and qualification, and component installation. During the course of the program, thirteen candidate surface preparations and eighteen candidate adhesives were

DD FORM 1 JAN 73 1473 EDITION OF 1 NOV 65 IS OBSOLETE

UNCLASSIFIED

SECURITY CLASSIFICATION OF THIS PAGE (When Data Entered)

20. ABSTRACT

evaluated for selection of the weldbond process used in fabrication of test specimens, test components, and the flight component. Weldbonded elemental specimens and sub-scale components were fabricated and tested for establishment of joint static strength, fatigue strength, residual strength after environmental exposure, crippling strength, shear and compression stability, and sonic fatigue. In addition, a full-scale weldbonded fuselage component assembled into a test specimen in conjunction with two standard production fuselage components was comparative strength tested. Also, nondestructive inspection methods for weldbonded joints and cost data were developed.